



Green Process Engineering

**From Concepts to
Industrial Applications**

Editors: **Martine Poux • Patrick Cognet
Christophe Gourdon**

 **CRC Press**
Taylor & Francis Group
A SCIENCE PUBLISHERS BOOK

Green Process Engineering

From Concepts to Industrial Applications

Green Process Engineering

From Concepts to Industrial Applications

Editors

Martine Poux

Laboratoire de Génie Chimique - INP-ENSIACET
Toulouse Cedex
France

Patrick Cognet

Laboratoire de Génie Chimique - INP-ENSIACET
Toulouse Cedex
France

Christophe Gourdon

Laboratoire de Génie Chimique - INP-ENSIACET
Toulouse Cedex
France



CRC Press

Taylor & Francis Group

Boca Raton London New York

CRC Press is an imprint of the
Taylor & Francis Group, an **informa** business

A SCIENCE PUBLISHERS BOOK

Published by arrangement with Dunod, Paris, France

Translation of: Poux, Martine, Patrick Cognet and Christophe Gourdon. 2010. Génie des procédés durables: Du concept à la concrétisation industrielle.

Dunod éditions. Paris, 492 p.

French edition: © Dunod, Paris, 2010

ISBN: 978-2-10-051605-6

CRC Press
Taylor & Francis Group
6000 Broken Sound Parkway NW, Suite 300
Boca Raton, FL 33487-2742

© 2015 by Taylor & Francis Group, LLC
CRC Press is an imprint of Taylor & Francis Group, an Informa business

No claim to original U.S. Government works
Version Date: 20150515

International Standard Book Number-13: 978-1-4822-0818-4 (eBook - PDF)

This book contains information obtained from authentic and highly regarded sources. Reasonable efforts have been made to publish reliable data and information, but the author and publisher cannot assume responsibility for the validity of all materials or the consequences of their use. The authors and publishers have attempted to trace the copyright holders of all material reproduced in this publication and apologize to copyright holders if permission to publish in this form has not been obtained. If any copyright material has not been acknowledged please write and let us know so we may rectify in any future reprint.

Except as permitted under U.S. Copyright Law, no part of this book may be reprinted, reproduced, transmitted, or utilized in any form by any electronic, mechanical, or other means, now known or hereafter invented, including photocopying, microfilming, and recording, or in any information storage or retrieval system, without written permission from the publishers.

For permission to photocopy or use material electronically from this work, please access www.copyright.com (<http://www.copyright.com/>) or contact the Copyright Clearance Center, Inc. (CCC), 222 Rosewood Drive, Danvers, MA 01923, 978-750-8400. CCC is a not-for-profit organization that provides licenses and registration for a variety of users. For organizations that have been granted a photocopy license by the CCC, a separate system of payment has been arranged.

Trademark Notice: Product or corporate names may be trademarks or registered trademarks, and are used only for identification and explanation without intent to infringe.

Visit the Taylor & Francis Web site at
<http://www.taylorandfrancis.com>

and the CRC Press Web site at
<http://www.crcpress.com>

Preface

For over a decade now, the industrial world has been moving towards a greener, safer, cleaner industry that is more environmentally friendly. This movement has been principally driven by an increasing awareness of environmental issues by the society worldwide, initially stimulated by the concept of *sustainable development*.

Indeed in 1980, the International Union for Conservation of Nature (IUCN) introduced the term *sustainable development* for the first time. It was employed again in 1987 in Mrs. Brundtland's report (entitled 'Our Common Future') when she was Prime Minister of Norway and Chair of the United Nations World Commission on Environment and Development (WCED). She defined the concept of *sustainable development* as "development that meets the needs of the present without compromising the ability of future generations to meet their own needs." Since then, the concept of sustainable development has been adopted worldwide.

Although this approach towards sustainability was initiated in the process industries in the 1990s, the increasing environmental, health and safety regulations, and REACH in particular, have more recently triggered profound changes in industry, which are linked to an increased social awareness and attitude, as well as the integration of risks.

Reconciling the industrial and economic progress, whilst preserving and respecting the natural balance of the planet has indeed become a challenge.

In this area, chemical engineering is involved at the utmost level. There is an urgent need for methods and chemical engineering routes that respect the environment and this has been one of the objectives in chemical engineering in recent years.

This trend is named "Green Process Engineering" and implies a change in the traditional concepts of process efficiency, which in addition to conventional reaction performance, takes into account the economic value of wastes (by reusing and recycling), the elimination of wastes at the source and the non-use of toxic or hazardous substances. In this context, the principles of "green chemistry" support the prevention of pollution instead of waste disposal.

The key to the development of acceptable processing methods, in terms of environmental protection, lays in the extensive substitution of old technologies and processes by the use of innovative reaction media and new activation techniques for reactions whereby catalysis is of prime importance. The emergence of new tools for chemical synthesis is of course accompanied by the evolution of chemical processes

but also the implementation of innovative processing equipment and how they are operated.

It is therefore essential to educate and to inform engineers and technicians of the tools available to promote the use of sustainable processes in their professional career.

By including Green Process Engineering in education, students will receive and spread their knowledge around them, which will naturally cause industry to evolve. These reasons led us to publish this book, which is the first such work written in English. It was originally published in French in 2010 (Dunod) and awarded the Roberval Prize in France in 2011.

This book is addressed to researchers and academic staff, students, engineers and technicians. It can also be used as a support for training courses. Written by researchers and academic staff who work in close partnership with industry, this book provides the keys for the successful implementation of green processes in the process industries. Three different but complementary approaches are described in the three parts of this book. They appear in increasing order of process complexity, starting from the improvement of the existing methods and processes, then by considering a change of technology, and finally to the implementation of new synthesis routes.

Jean-Claude Charpentier, who is a worldwide expert in the field of chemical engineering, has honorably written the introduction and through this, he has given his global vision on modern chemical engineering today.

The first part of this book, which is entitled “Tools for green process engineering”, includes three chapters dealing with the available tools and methods for implementing green processes. They focus on how to: i) better integrate social and environmental criteria, in addition to technical and economic criteria, in the design and development of processes; ii) optimize the processes; iii) model processes with computer-aided process engineering tools that offer higher flexibility to incorporate new technological devices.

This is an overall approach at the level of the production chain.

In the second part of the book “Technologies and innovative methods for intensification”, the technical aspects of process intensification are introduced. Chapters on Miniaturization and Multifunctional reactors describe i) the miniaturized systems that offer improvements in production quality by the significant decrease in the size/capacity ratio, low energy consumption and a decrease in the amount of waste products, and ii) multifunctional reactors, which are an efficient equipment due to the synergetic integration of multiple functions, respectively. The following chapters are then devoted to the intensification of the chemical reaction itself and of transport phenomena. They cover the implementation of ultrasounds and microwaves to improve the performance and/or selectivity of reactions and specific operations such as extraction, as well as the use of formulation-based approaches, in particular by implementing microemulsions as novel reaction media.

The third part of the book focuses on “a new generation of processes”, although some of them are not really recent. In the latter, conventional operations are substantially modified with the prime objective of creating sustainable processes. The first three chapters in this section deal with new media: supercritical fluids used as a solvent or as a reaction medium, ionic liquids, as well as water and solvent-

free reactions. These chapters are significantly chemistry-oriented, one of the base-disciplines of the chemical engineer. They present the latest scientific advances on the development of new generation processes. Most conventional branches of chemical engineering, such as electrochemistry, catalysis, photocatalysis, biocatalysis and biotechnology are based core disciplines and that have been redirected towards new applications to take into account current environmental needs. In each of these chapters, the reader will find theoretical concepts and many examples of applications.

It is hoped that amongst the different independent chapters of this book, the reader will find concepts, insights and ideas ... for the design and development of the production processes of tomorrow. Green and sustainable process engineering is an emerging and evolving discipline. It offers solutions that meet the economic, societal and environmental needs of the planet.

Martine Poux
Patrick Cognet
Christophe Gourdon

Contents

<i>Preface</i>	v
<i>List of Contributors</i>	xi
<i>Introduction</i> <i>Jean-Claude Charpentier</i>	xvii

Part 1: Tools for Green Process Engineering

1. Green Process Engineering Design Methodology: A Multicriteria Approach <i>Catherine Azzaro-Pantel</i>	3
2. Process Optimization Strategies <i>Jean-Pierre Corriou and Catherine Azzaro-Pantel</i>	27
3. Representation and Modelling of Processes <i>Christian Jallut, Françoise Couenne and Bernhard Maschke</i>	49

Part 2: Technologies and Innovative Methods for Intensification

4. Process Intensification by Miniaturization <i>Joelle Aubin, Jean-Marc Commenge, Laurent Falk and Laurent Prat</i>	77
5. Multifunctional Reactors <i>Xuan Meyer, Christophe Gourdon, Michel Cabassud and Michel Meyer</i>	109
6. Ultrasound in Process Engineering: New Look at Old Problems <i>Sergey I. Nikitenko and Farid Chemat</i>	145
7. Microwaves: A Potential Technology for Green Process Development <i>Martine Poux</i>	166
8. Intensification by Means of Formulation <i>Patrick Cognet, Isabelle Rico-Lattes and Armand Lattes</i>	207

Part 3: A New Generation of Processes

- | | |
|---|------------|
| 9. Supercritical CO₂, the Key Solvent for Sustainable Processes | 239 |
| <i>Danielle Barth, Séverine Camy and Jean-Stéphane Condoret</i> | |
| 10. Ionic Liquids | 267 |
| <i>Hélène Guerrand, Mathieu Pucheault and Michel Vaultier</i> | |
| 11. Water as Solvent and Solvent-free Reactions | 292 |
| <i>Emilie Genin and Véronique Michelet</i> | |
| 12. Electrochemical Processes for a Sustainable Development | 325 |
| <i>André Savall and François Lopicque</i> | |
| 13. Photocatalytic Engineering | 364 |
| <i>Jean-Marie Herrmann and Eric Puzenat</i> | |
| 14. Biocatalysis and Bioprocesses | 396 |
| <i>Jean-Marc Engasser</i> | |
| 15. Catalysis Contribution to a Sustainable Chemistry | 422 |
| <i>Philippe Kalck and Philippe Serp</i> | |

List of Contributors

Joelle Aubin

Laboratoire de Génie Chimique – UMR CNRS/INP/UPS, Toulouse – France.

<http://lgc.inp-toulouse.fr>

Email: Joelle.Aubin@ensiacet.fr

Catherine Azzaro-Pantel

Laboratoire de Génie Chimique – UMR CNRS/INP/UPS, ENSIACET, Toulouse – France.

<http://lgc.inp-toulouse.fr>

Email: Catherine.AzzaroPantel@ensiacet.fr

Danielle Barth

Laboratoire de Réactions et Génie des Procédés – UPR CNRS, EEIGM, Nancy – France.

<http://www.ensic.inpl-nancy.fr/LRGP>

Email: danielle.barth@univ-lorraine.fr

Michel Cabassud

Laboratoire de Génie Chimique – UMR CNRS/INP/UPS, Toulouse – France.

<http://lgc.inp-toulouse.fr>

Email: Michel.Cabassud@ensiacet.fr

Séverine Camy

Laboratoire de Génie Chimique – UMR CNRS/INP/UPS, ENSIACET, Toulouse – France.

<http://lgc.inp-toulouse.fr>

Email: Severine.Camy@ensiacet.fr

Jean-Claude Charpentier

Laboratoire de Réactions et Génie des Procédés – UPR CNRS, ENSIC, Nancy – France.

<http://www.ensic.inpl-nancy.fr/LRGP>

Email: jean-claude.charpentier@univ-lorraine.fr

Farid Chemat

Sécurité et Qualité des produits d'origine végétale – UMR INRA/UAPV, Avignon – France.

<http://green.univ-avignon.fr/>

Email: Farid.Chemat@univ-avignon.fr

Patrick Cagnet

Laboratoire de Génie Chimique – UMR CNRS/INP/UPS, ENSIACET, Toulouse.

<http://lgc.inp-toulouse.fr>

Email: Patrick.Cagnet@ensiacet.fr

Jean-Marc Commenge

Laboratoire de Réactions et Génie des Procédés – UPR CNRS, ENSIC, Nancy – France.

<http://www.ensic.inpl-nancy.fr/LRGP>

Email: jean-marc.commenge@univ-lorraine.fr

Jean-Stéphane Condoret

Laboratoire de Génie Chimique – UMR CNRS/INP/UPS, ENSIACET, Toulouse – France.

<http://lgc.inp-toulouse.fr>

Email: JeanStephane.Condoret@ensiacet.fr

Jean-Pierre Corriou

Laboratoire de Réactions et Génie des Procédés – UPR CNRS, ENSIC, Nancy – France.

<http://www.ensic.inpl-nancy.fr/LRGP>

Email: jean-pierre.corriou@univ-lorraine.fr

Françoise Couenne

Claude Bernard Lyon 1 University and CNRS – Laboratoire d'Automatique et de Génie des Procédés – ESCPE, Villeurbanne – France.

<http://www.lagep.univ-lyon1.fr/>

Email: couenne@lagep.univ-lyon1.fr

Jean-Marc Engasser

Laboratoire d'ingénierie de Biomolécules, ENSAIA, Vandoeuvre-les-Nancy – France.

<http://www.ensaia.inpl-nancy.fr>

Email: jean-marc.engasser@univ-lorraine.fr

Laurent Falk

Laboratoire de Réactions et Génie des Procédés – UPR CNRS, Nancy – France.

<http://www.ensic.inpl-nancy.fr/LRGP>

Email: laurent.falk@univ-lorraine.fr

Emilie Genin

Chimie et Photonique moléculaires – UMR CNRS/Université de Rennes 1, Rennes.

<http://www.umr6510.univ-rennes1.fr>

Email: emilie.genin@univ-rennes1.fr

Christophe Gourdon

Laboratoire de Génie Chimique – UMR CNRS/INP/UPS, ENSIACET, Toulouse – France.

<http://lgc.inp-toulouse.fr>

Email: Christophe.Gourdon@ensiacet.fr

Hélène Guerrand

Institut des Sciences Moléculaires, Université de Bordeaux- Talence – France.

<http://www.ism.u-bordeaux1.fr>

Email: h.guerrand@ism.u-bordeaux1.fr

Jean-Marie Herrmann

Institut de Recherches sur la Catalyse et l'Environnement de Lyon, UMR CNRS/ Université Lyon 1, Lyon – France.

<http://www.ircelyon.univ-lyon1.fr>

Email: jean-marie.herrmann@ircelyon.univ-lyon1.fr

Christian Jallut

Claude Bernard Lyon 1 University and CNRS – Laboratoire d'Automatique et de Génie des Procédés – ESCPE, Villeurbanne – France.

<http://www.lagep.univ-lyon1.fr/>

Email: jallut@lagep.univ-lyon1.fr

Philippe Kalck

Laboratoire de Chimie de Coordination – UPR CNRS, INP-ENSIACET, Toulouse – France.

<http://www.lcc-toulouse.fr>

Email: Philippe.Kalck@ensiacet.fr

François Lapicque

Laboratoire de Réactions et Génie des Procédés – UPR CNRS, Nancy – France.

<http://www.ensic.inpl-nancy.fr/LRGP>

Email: francois.lapicque@univ-lorraine.fr

Armand Lattes

Laboratoire des Interactions Moléculaires et Réactivité Chimique et Photochimique, UMR CNRS/UPS, Toulouse – France.

<http://imrcp.ups-tlse.fr>

Email: lattes@chimie.ups-tlse.fr

Bernhard Maschke

Claude Bernard Lyon 1 University and CNRS – Laboratoire d’Automatique et de Génie des Procédés – ESCPE, Villeurbanne – France.

<http://www.lagep.univ-lyon1.fr/>

Email: Maschke@lagep.univ-lyon1.fr

Michel Meyer

Laboratoire de Génie Chimique – UMR CNRS/INP/UPS, ENSIACET, Toulouse – France.

<http://lgc.inp-toulouse.fr>

Email: Michel.Meyer@ensiacet.fr

Xuan Meyer

Laboratoire de Génie Chimique – UMR CNRS/INP/UPS, ENSIACET, Toulouse – France.

<http://lgc.inp-toulouse.fr>

Email: Xuan.Meyer@ensiacet.fr

Véronique Michelet

Laboratoire Charles Friedel – UMR CNRS/ENSCP, Paris – France.

<http://www.enscp.fr/>

Email: Veronique-Michelet@chimie-paristech.fr

Sergey I. Nikitenko

Institut de Chimie Séparative de Marcoule, Centre de Marcoule – Bagnols-sur-Cèze – France.

Email: serguei.nikitenko@cea.fr

Martine Poux

Laboratoire de Génie Chimique – UMR CNRS/INP/UPS, Toulouse – France.

<http://lgc.inp-toulouse.fr>

Email: Martine.Poux@ensiacet.fr

Laurent Prat

Laboratoire de Génie Chimique – UMR CNRS/INP/UPS, ENSIACET, Toulouse – France.

<http://lgc.inp-toulouse.fr>

Email: Laurent.Prat@ensiacet.fr

Mathieu Pucheault

Institut des Sciences Moléculaires, Université de Bordeaux- Talence – France.

<http://www.ism.u-bordeaux1.fr/>

Email: m.pucheault@ism.u-bordeaux1.fr

Eric Puzenat

Institut de Recherches sur la Catalyse et l’Environnement de Lyon – UMR CNRS/ Université Lyon 1 – Villeurbanne cedex – France.

<http://www.ircelyon.univ-lyon1.fr>

Email: eric.puzenat@ircelyon.univ-lyon1.fr

Isabelle Rico-Lattes

Laboratoire des Interactions Moléculaires et Réactivité Chimique et Photochimique, UMR CNRS/UPS, Toulouse – France.

<http://imrcp.ups-tlse.fr>

Email: rico@chimie.ups-tlse.fr

André Savall

Laboratoire de Génie Chimique – UMR CNRS/INP/UPS, Toulouse – France.

<http://lgc.inp-toulouse.fr>

Email: Savall@chimie.ups-tlse.fr

Philippe Serp

Laboratoire de Chimie de Coordination – UPR CNRS, INP-ENSIACET, Toulouse – France.

<http://www.lcc-toulouse.fr>

Email: Philippe.Serp@ensiacet.fr

Michel Vaultier

Institut des Sciences Moléculaires, Université de Bordeaux- Talence – France.

<http://www.ism.u-bordeaux1.fr>

Email: m.vaultier@ism.u-bordeaux1.fr

The Institut National Polytechnique of Toulouse - Engineering University situated in the South-West of France - has actively supported and promoted the production of this book.

www.inp-toulouse.fr

Introduction

Jean-Claude Charpentier

At the dawn of this new century, the chemical industry and related industries (petrochemical, healthcare industries, cosmetics, food, environment, textile, paper, glass, asphalt, steel, nuclear, construction materials, electronics) face requirements and constraints unprecedented tooth. Meanwhile, the chemical knowledge is growing so quickly and the discovery rate is increasing every day. Today chemistry is associated with the life sciences, information science and communication science and instrumentation and hence the chemical engineering and process must meet two requirements: produce more while consuming much less and produce more sustainable. But how?

Globalization and Social Conscience: Two Major Issues for Process Engineering

Faced with the globalization of markets, the acceleration of partnerships and innovation, knowing products and processes that will be competitive in the new global economy is one of the first requirements aimed at the process engineering research. Indeed, if at the early 70s, the half-life of product innovation (time-to-market) was in about 10 years, today, a year is often seen as a long time as a result of increasing competition that exists on the market. Besides, more than 14 million chemical compounds can be synthesized, 100,000 can be found on the market, but only a small number of them are found in nature and therefore most to be deliberately designed, formulated, synthesized and manufactured to meet the needs of mankind. Indeed a large number of applications are related to the development of biomaterials, the preparation of nanoparticles, the drug delivery, bionanotechnology, biomass conversion, the manufacturing of microreactors for selective multiphase reactions.

All these demands are clearly focused on societal demands, such as CO₂ sequestration, synthesis of biodiesel or hydrogen production. Most of these subjects are listed in “roadmaps”, published last ten years, such as the 12 principles of green chemistry (Anastas and Warner 1998), the 12 principles of green process engineering (Anastas and Zimmerman 2003), 12 major engineering challenges set by the National American Engineering Academy (NAE USA 2008), the roadmap of the 21st Century IChemE (IChemE roadmap 2007), or even the European roadmap for process intensification. These roadmaps draw attention to a comprehensive global concern

where process engineering will play a crucial role: sustainability, health, safety and environment, energy, water, food and beverage, bio engineering systems, solar energy, nuclear fusion, etc. And finally these roadmaps are campaigning to change the chemical engineering to a modern process engineering voluntarily involved in sustainable development (Bertrand and Mavros 2005; Garcia-Serna et al. 2007). So it seems obvious that the existing methods and new processes will be progressively adjusted to the principles of “green chemistry”.

The second requirement is directly related to a changing demand of the market which leads to a double challenge. In the developing countries where labor is cheap, local stresses in the regulation of production are lower. Industrialized countries are facing a growing rapidly in customer demand for products targeted use properties and at the same time constraints from the public and the media about the processes in the areas of safety and environment, combined with regulatory tools such as analysis of product life cycle analysis (LCA), “cradle-to-the-grave” (see for example REACH, the European standard for chemicals Regulation, Evaluation, Authorization of Chemicals).

To answer such a societal demand for sustainable development and make a contribution to the fight against environmental destruction and unsustainable behavior of a current world production, chemistry and chemical engineering and more generally engineering processes are now facing new challenges on complex systems, particularly at the levels of molecules, products and processes as well.

The challenge is to produce huge quantities at low cost. Indeed do not forget that the global production capacity should increase by a factor of 6 till 2050 if the rate of growth of the world economy by 4% per year is assumed. This requires an integrated approach able to adjust the structure, architecture and process equipment to the terms of physico-(bio) chemical transformations rather than adapting chemistry and operating conditions to the existing equipment and their limitations of use (see IMPULSE, the European project Integrated Multiscale Process Units with Locally Structured Elements) whose goal is to get a radical improvement of the design of large-scale productions (Jenck et al. 2004; Matlosz 2008).

Besides, the consumer does no longer generally appreciate a product only to its technical specifications, but rather for its quality criteria (shape, color, chemical and biological stability, therapeutic activity, sensorial properties such as taste, juiciness, fragrance, smell, roughness, handling, friability, etc.) and functions (adhesion, washing, sanitary requirements, ...). Controlling these values of product quality in the process design, continuous adjustment to changing consumer demands and the speed of reaction and response to market conditions are the dominant elements that must be taken into account by the modern methods of process engineering. The key factor, challenge for the production of pharmaceutical and cosmetic products is not the cost, but the time-to-market, i.e., the speed of discovery and production of these products. These high added value customerized products require the development of polyvalent equipment, with an easy cleaning and maintenance, flexible as well.

The above considerations on the application and design of the desired products and their production processes must be taken into account in the definition and scientific evolution of the modern process engineering.

Sustainable Development, a Driver for the Modern Green Process Engineering

At the crossroad of chemistry and sustainable development, to meet the new challenges and taking into account methodological and technological advances, four main objectives, parallel and simultaneous, are involved and are the subject of intensive research and methodological developments and technological as well (Charpentier 2007a).

The Multi-scale Management of Process for Increasing the Selectivity and Productivity

This aspect requires the intensification of operations and the use of nano and micro tools. For example, in molecular engineering, instead of using porous supports for the heterogeneous catalysis, functional materials with targeted properties are now designed and manufactured. Indeed, the simultaneous control of the composition and functionality of a catalyst is imperative for the success of a catalytic process. And the ability to control its microstructure and chemical composition allows to manage with the activity, the selectivity and the stability of the catalyst. Thus, by controlling, via synthesis of nano-structures, the pore size of the crystallinities and manipulating the stoichiometry and chemical composition, there is now the possibility of producing new structures at the molecular and supramolecular scales.

Moreover, at the micro- and meso-scale level, the control of the local temperatures and compositions by managing the feedings and heat exchanges lead to a greater selectivity and a higher productivity than in the classical approach involving larger volumes. But, finding the ways to bring energy at the right place in order to improve the process by providing an appropriate activation (ultrasound, UV, micro-waves, ...) still remains a challenge and opens many prospects in the near future (Stankiewicz 2006).

Process Intensification

Process intensification promotes sophisticated technologies that replace traditional equipment made of large, energy-intensive, expensive and polluting devices by combining multiple operations into a single apparatus (multifunctional) or by more efficient technologies smaller, cheaper, more secure and less polluting. Process intensification claims a reduction in raw materials, energy and wastes. It can also lead to a reduction in investment and operational expenditures (CAPEX and OPEX).

The objective is clearly to **produce much more** (and better) **using much less**. This means producing more and better in smaller volumes, with greater efficiency and greater selectivity, using less energy and raw materials, less solvent and with reduced transport costs. It fits typically the sustainable development approach.

These benefits can be obtained by using multifunctional reactors that couple or decouple in the same equipment (transfer–reaction–separation) to increase productivity or selectivity and to facilitate the separation of undesirable by-products (e.g., catalytic distillation, extraction or reactive absorption, reactive crystallization, membrane reactors, monolithic, structured catalytic packings, etc...). The resulting

reduction in the number of units leads to a reduction of investment costs and to a better use of energy. In addition, the improvement of the selectivity led to a reduction in the consumption of raw materials and hence in the operational costs. However the use of these hybrid technologies is currently hindered by the problems of process controllability and simulation and lead to interesting challenges in dynamic modelling and in control of strongly non linear processes.

Process intensification can also be obtained either by new methods of production (reverse flow reactor, transient operations, pulsatile flow reactors, extreme conditions of temperature or/and pressure, energy activated reactors, ...), or by operating with new reaction media also based on scientific principles (supercritical fluids, ionic liquids, fluorinated liquids, water, ...).

Besides, process intensification may lead to equipment miniaturization: micro engineering and micro technology. The use of micro-reactors, micro-mixers, micro separators, micro heat exchangers and micro-analysers starts growing significantly in various fields of chemistry and chemical engineering (Hessel et al. 2004, 2005, 2008; Stankiewicz and Moulijn 2004). There are some applications in combinatorial chemistry, screening and high throughput experimentation to quickly test the catalysts and in analytical measurements. Indeed the experiments in larger conventional equipment are limited by the cost of reactants or safety problems that are not encountered with smaller volumes used.

Batch-to-continuous is also a way of process intensification at the industrial scale. Indeed micro mixers and micro or macro-structured millireactors, with specific architectures as interdigital parallel microchannels or layered platelets that facilitate mixing and transport phenomena, are now also used as industrial production tools. Allowing a wide range of fluid flow rates from a few L/hr (typically encountered in the fine-pharma sector for the synthesis of specialty products or for generating creams, foams or emulsions), to several tens of m³/hr, for the petchem sector.

However, several major obstacles must still be overcome before process intensification becomes widespread. It will be proved that such maturity and economic competitiveness of these new technologies are comparable with conventional technologies. Therefore instead of its benefits expected, the potential use of hybrid separation processes is hardly exploited at an industrial scale. In many cases, the cause is the lack of a general design methodology and a detailed “know-how” of the process involved. Also conservatism of companies owning batch facilities will not easily accept a solution for the continuous production offered by the use of micro-structured devices, although miniaturization is a promising approach to achieve this goal!

Formulation and Product Engineering with a Focus on Complex Fluids and Solid Management: Product/Green Process Couple (Charpentier 2002)

In response, as we have seen above, the market demand for sophisticated products that combine several functions or properties, the process engineering has to face complex media such as non-Newtonian fluids, gels, water-soluble polymers, colloids, dispersions, emulsions, microemulsions, and suspensions for which the rheology and the interfacial phenomena play a major role. It also includes the design and

manufacture of solid particles and divided solids that are used in 70% of chemical (and para-chemical) industries, which require the creation and control of the distribution of particle sizes in unit operations such as crystallization, precipitation, spray, aerosol and the generation of nanoparticles, but also the control of the morphology and of the final shape of the particles in calcination operations, agglomeration, compaction and encapsulation. These technologies also concern solids that are formulated to perform smart operations like the controlled release of components or active ingredients.

In these areas, the combined costs of manufacturing and R & D constitute 30–35% of the product cost, shared approximately equally between these two positions. Hence the importance of daily collaborations between many industrial companies and academic partners in research and development programs using programs on topics of multidisciplinary research and multi space and time scales. This has led to many advances made in recent years in the field of product formulation using the classical scientific methods of process engineering (modeling and molecular simulation for the property use, simulation, process modeling of the chemical kinetics and transport phenomena and scale-up from the molecular scale to the laboratory scale). Since the properties or use of the formulated structured products can be affected by the method of production from the lab-scales to the industrial unit, it is clear that the production process can not be disconnected from the formulation process. This again highlights the need for concurrent design of product and process for these structured products targeted use value, and from the design at the molecular level (Anastas 2008).

More generally for the design at the molecular level and the manufacturing of the property required of a product, the product engineering (or product design) is now well known. But how operations can be scaled-up from the laboratory scale to the industrial units? Can we get the same product keeping its initial properties? What is the role of equipment design in determining the properties of the product? All of these questions may be answered only through modeling and simulation.

Multi-scale and Multidisciplinary Modeling and Simulation: from the Molecular Scale to the Industrial Unit

The multi-scale and multidisciplinary approach (Charpentier 2009) is illustrated by (Fig. 1).

The computer science and technology has allowed the way to the simulation of physical and molecular properties at nano and microscopic scales (Gerbaud and Joulia 2006). Computer Assisted Molecular Design (CAMD) to make a desired product is a promising way. It provides the optimal solution of the inverse problem, i.e., to find a compound or a mixture having a series of pre-defined properties (Gani 2004). But as there are many degrees of freedom, especially in formulations of the molecular interactions, the computation time quickly becomes excessive. Then by comparing molecular modeling with reality it seems that a consensus is admitted according that simulation and computer-aided techniques for the design of products are useful in a first approach, but experimental measurements are still essential for the final design. And from the combined results of the molecular theory, computer simulation and experimental measurements, a better understanding of the relationship structures/

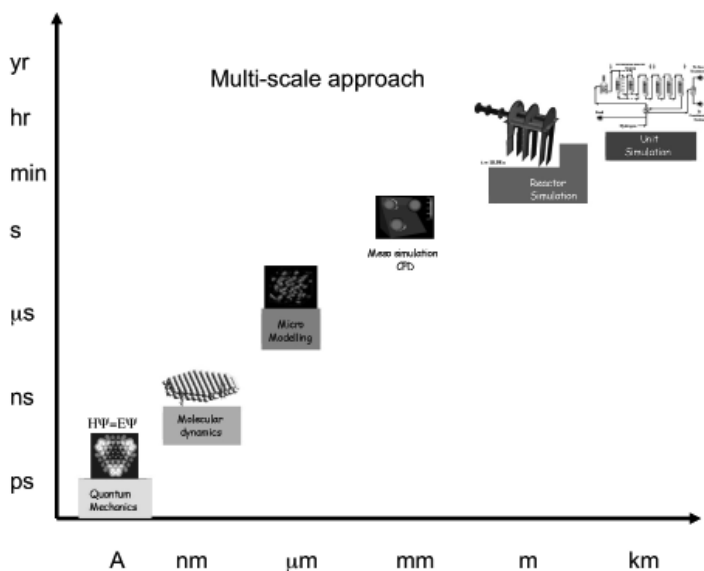


Figure 1. Multi-scale and multidisciplinary approach.

properties is expected, which, coupled with the science of chemical engineering at microscopic scales (hydrodynamics, mass transfer and heat), now form the basis for the design of new materials and processes (Gani 2006; Morales-Rodriguez and Gani 2009).

Besides, at the macroscopic scales, dynamic modeling methods are increasingly developed. The reason is that to be competitive in the production of targeted products, delivered just in time to market to a consumer whose needs are constantly changing, it is required to develop analysis and optimization of the whole production chain. This approach is based on the Computer Aided Process Engineering (CAPE) for the dynamic simulation of events in real time, techniques that take into account the multi-scale approach in space and time as well as compatibility and interconnection of/and corresponding simulation softwares from different origins. For instance, one can cite the CAPE-OPEN European program entitled “Next generation computer aided process engineering simulation open environment” that led to the creation of a network of European laboratories working with this integrated approach with standardized trade simulation models for the various scales of time and space all along the whole chain of chemical production (CAPE-OPEN Laboratories Network, CO-LaN Consortium www.colan.org).

Conclusion: from the Chemical Engineering to the Green Process Engineering

We have seen in this introduction that the chemical and related industries and consequently the process engineering are faced with many challenges in the context of market globalization and sustainable development.

For “driven process industries” such as bulk chemicals and chemical intermediates industries, it is necessary to continue research on process intensification for innovative processes, non-polluting, energy-saving, intrinsically safe and producing virtually zero defect products. For the others, producing specialty chemicals, pharmaceuticals, food and highly specialized materials, dominated by the synthesis and control of a product property, the technologies to be developed have to include both simultaneously the product design and its manufacturing process that are not only moving rapidly, but must be well synchronized as mutually dependent for a chance of a successful production as “first product on the market”. In this case, process intensification concerns simultaneously the formulation and the production while not forgetting safe and environmental issues (Life Cycle Analysis of the product, “from-cradle-to-grave”).

So today, the modern process engineering, namely Green Process Engineering, is completely included in the objective: “to transform molecules into money” (Charpentier 2007b), i.e., shorten the time-to-market: a fundamental for the creation of wealth in the context of globalization and sustainability. This creates new opportunities through product design and/or innovative processes and equipment.

At the origin of this book, originally published in french (Poux et al. 2010), are the conferences organized by M. Poux and P. Cognet in the targeted area of Green Process Engineering held successively in Toulouse (GPE1 2007), Venice (GPE2 2009), Kuala Lumpur (GPE3 2011) and Sevilla (GPE4 2014) at the intention of chemists, biologists, physicists and specialists in engineering involved in green chemistry and new technological applications for sustainable development.

The structure, headings and content of the chapters of the book are an obvious and detailed illustration of this modern approach of process engineering as described above. Indeed, the chapters focus successively on the design methodology and strategies for modeling and optimization of sustainable processes, the process intensification by using multifunctional reactors, miniaturization of processes or techniques of activation by ultrasound and microwave, electrochemical processes and catalytic engineering including biocatalysis and bioprocess, the use of “green solvents” (supercritical fluids, ionic liquids, water as solvent and contributions of catalysis for sustainable chemistry), and finally on the multi-scale product-design process assisted by computer.

So with the successive presentation of tools for sustainable engineering processes, technologies and innovative methods of intensification, new generations of processes and some promising tracks, reading this book shows that modern research in process engineering, based on the couple product/green processes concerns an essential contribution to the environmental, societal and economic progress, contributing to sustainability and to improving the quality of life.

References

- Anastas, P.T. 2008. Fusing green chemistry and green engineering: Design build at the molecular level. *Green Chem.* 10: 607.
- Anastas, P.T. and J.C. Warner. 1998. *Green Chemistry: Theory and Practice*. Oxford University Press, New York.

- Anastas, P.T. and J.B. Zimmerman. 2003. Design of green engineering, through the 12 principles. *Environ. Sci. Technol.* 37(5): 94A–101A.
- Bertrand, J. and P. Mavros. 2005. The changing face of chemical engineering research. *Chem. Eng. Res. Des.* 83: 1–6.
- Charpentier, J.C. 2002. The triplet molecular process-product-process engineering: The future of chemical engineering? *Chem. Eng. Sci.* 57: 4667–4690.
- Charpentier, J.C. 2007a. Modern chemical engineering in the framework of globalization, sustainability, and technical innovation. *Ind. Eng. Chem. Res.* 46: 3465–3485.
- Charpentier, J.C. 2007b. In the frame of globalization and sustainability, process intensification, a path to the future of process and chemical engineering (molecules into money). *Chem. Eng. J.* 134: 84–92.
- Charpentier, J.C. 2009. Perspective on multiscale methodology for product design and engineering. *Comput. Chem. Eng.* 33: 936–946.
- Gani, R. 2004. Chemical product design: challenges and opportunities. *Comput. Chem. Eng.* 28: 2441–2457.
- Gani, R. 2006. Integrated chemical-product-process design: CAPE perspectives. pp. 647–666. *In: G. Heyen and L. Puigjaner (eds.). Computer Aided Process and Product Engineering.* Wiley-VCH, Weinheim.
- Garcia-Serna, J., L. Perrez-Barrigon and M.J. Cocero. 2007. New trends for design towards sustainability in chemical engineering: Green engineering. *Chem. Eng. J.* 133: 7–30.
- Gerbaud, V. and X. Joulia. 2006. Molecular modeling for physical property prediction. pp. 107–136. *In: G. Heyen and L. Puigjaner (eds.). Computer Aided Process and Product Engineering.* Wiley-VCH, Weinheim.
- Hessel, V., S. Hardt and H. Löwe. 2004. *Chemical Micro Process Engineering-Fundamentals, Modeling and Reactions.* Wiley-VCH, Weinheim.
- Hessel, V., H. Löwe and G. Kolb. 2005. *Chemical Micro Process Engineering-Processing and Plants.* Wiley-VCH, Weinheim.
- Hessel, V., C. Knobloch and H. Löwe. 2008. Review on patents in microreactors and micro process engineering. *Recent Patents Chem. Eng.* 1: 1–16.
- Jenck, J., F. Agerberg and M.J. Droscher. 2004. Product and processes for a sustainable chemical industry: A review of achievements and prospects. *Green Chem.* 6: 544–556.
- Matlosz, M. 2008. Microprocess engineering, process intensification and multiscale design. *VDI Berichte* 2039: 77–84.
- Morales-Rodriguez, R. and R. Gani. 2009. Multiscale modelling framework for chemical product-process design. *Comput. Aided Chem. Eng.* 26: 495–500.
- Poux, M., C. Gourdon and P. Cognet. 2010. *Génie des Procédés Durables: du concept à la concrétisation industrielle.* Ed. Dunod.
- Stankiewicz, A.I. 2006. Energy matters: alternative sources and forms of energy for intensification of chemical and biochemical processes. *Chem. Eng. Res. Des.* 84: 511–521.
- Stankiewicz, A.I. and J.A. Moulijn. 2004. *Reengineering the Process Plant: Process Intensification.* Marcel Dekker, New York.

PART 1

**Tools for Green Process
Engineering**

1

Green Process Engineering Design Methodology

A Multicriteria Approach

Catherine Azzaro-Pantel

Sustainable Development in Chemical Process Engineering

The concept of sustainable development is based on the creation of products and goods using processes and non-polluting systems, which preserve energy resources and raw materials while being economically viable. The process industry has a unique position since it transforms raw material feedstock into intermediate and end-user products and thus sits at the core of almost all industrial value chains and uses. From this position, the industry empowers organizations to improve competitiveness while drastically reducing resource and energy inefficiency as well as the environmental footprint of the industrial activities. It is now widely recognized that all the major components in the process industry holistic value chain have to be considered to include raw materials, feedstocks and their source, conversion processes, intermediate and/or end-user needs and also waste streams. The era of “eco-efficiency”, which aims to promote a more “efficient” use of raw materials and energy in order to reduce the economic costs and the environmental impact of production must simultaneously be followed by an era of “eco-design”, where environmental parameters are taken into consideration right from the design of the product and process. “Eco-design” thus appears to be the operational contribution of sustainable development.

Process engineering must play an important role in this “eco-efficiency”. On the one hand, the production induced by this type of industry, which contributes significantly to national revenue, is essential for modern companies: the development of the company depends on the chemical industry and vice versa. On the other hand, a large number of environmental issues are either directly related to such processes or to the use of chemical products through impacts on water, air and soil.

The chemical industry develops the products for multiple consumer markets, which have to be manufactured, used, and recycled using specific, safe and economically viable processes. It is therefore necessary to improve the existing processes and to invent new processes that avoid waste production from the beginning, rather than collecting and treating waste products, thus transitioning from a curative approach to a preventive approach.

This vision, which takes into account the product–process life cycle and expands the scope of investigation, involves a systemic approach based on the concept of the so-called “chemical supply chain”. This vision forms part of the concerns of the “roadmaps” published over the last 15 years and explained in the 12 principles of green chemistry (Anastas and Warner 1998), 12 principles of green engineering (Anastas and Zimmerman 2003), challenges for engineering outlined by the American National Academy of Engineering, or the roadmap of the IChemE, 21st Century Chemical engineering (IChemE roadmap 2013) (Azapagic et al. 2006a,b).

The goal is to improve the decision-making process at different levels, from the extraction of raw materials, to design, operation, process control and supervision as well as to product design and distribution, multisite management, including impact evaluation, with antagonist criteria (see Fig. 1). This chapter is mainly focused on the process design scope.

Some environmental criteria (related, for instance, to emissions) or some social criteria (related, for instance, to safety) have already been integrated into process simulators such as CHEMCAD (Chemstations 2003) with a view to evaluating environmental impacts such as Global Warming Potential, ozone layer depletion and acidification. Yet, this step is generally carried out once the technical and economic components have been achieved. Such an approach can thus lead to a sub-optimal solution since these design choices turn out to be more limited in the subsequent

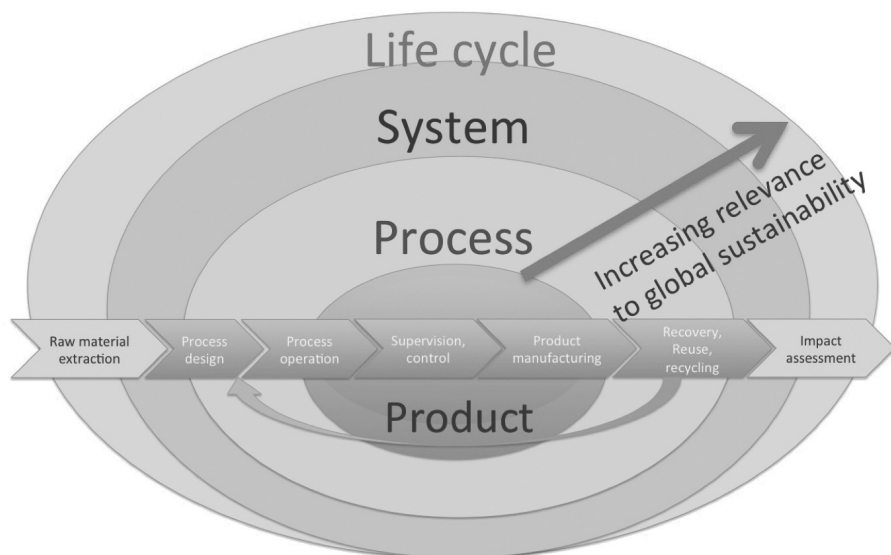


Figure 1. New frontiers in Chemical Process Engineering.

process design stages, which may hamper the design of more sustainable processes as far as the environmental component is concerned. Very often, environmental concerns are treated as constraints to an economic optimization problem, where the constraints are imposed by regulations. Minimizing the amount of waste or pollutants generated within a process is a more sound way to incorporate environmental considerations into process design.

Moreover, even if some environmental criteria are integrated at the level imposed by regulations, it must be highlighted that they exclusively concern the direct contributions of the production unit without considering the upstream and downstream impacts. This explains why the resulting flowsheet may reduce the environmental impacts of a given process locally but lead to an increase in the downstream impact (for instance through a particular choice in raw materials and/or energy sources).

This chapter shows what the new frontiers of the studied system are when tackling the sustainable design of processes and at which stage the different selection criteria need to be taken into account and how they can be quantified. It is based on a methodological order, with a view to assisting the decision-maker. Copious amounts of literature have been dedicated to the sustainable development issue and its applications in chemical and process engineering (Azapagic et al. 2006b; Dewulf and Van Langenhove 2006; Abraham 2006; Allen and Shonnard 2002).

Frontiers of the System

Process engineers are familiar with the systemic approach involved in process design. The process to be studied is defined as a system delimited by a frontier comprising all the items and their interconnections. It must be said that the design stage is generally focused on the items that will be relative to process operation and does not take into account the dismantling phase of the process, which may also have a non negligible impact on economics, environment and society, so that the evaluation of the criteria involved may be misevaluated. New frontiers must now be considered (see Fig. 2).

Let us consider, for explanation purposes, the case of hydrogen, which is considered as a “clean fuel”. If a “gate-to-gate” approach is considered, which means that the boundary of the system studied involves the process, a fuel cell fed with hydrogen has a relatively moderate efficiency (with a 50–60% order of magnitude) but is attractive as hydrogen fuel cell emissions contain harmless by-products: hydrogen fuel cell vehicles emit only water vapor and warm air, which are not problematic in terms of air quality. However, hydrogen production requires a substantial amount of energy: steam methane reforming (SMR) has been the leading technology for hydrogen production in refining and petrochemical complexes and uses metallic catalysts and temperatures in excess of 800°C. This explains why the hydrogen production pathway must be integrated into the frontiers of the system to be considered as a sustainable energy carrier in a “cradle-to-gate” vision (Azapagic 1999; Azapagic and Clift 1999; Azapagic et al. 2006a,b).

It must be highlighted that an integrated approach for pollution reduction, which aims at preventing emissions into air, water and soil is increasingly a regulation

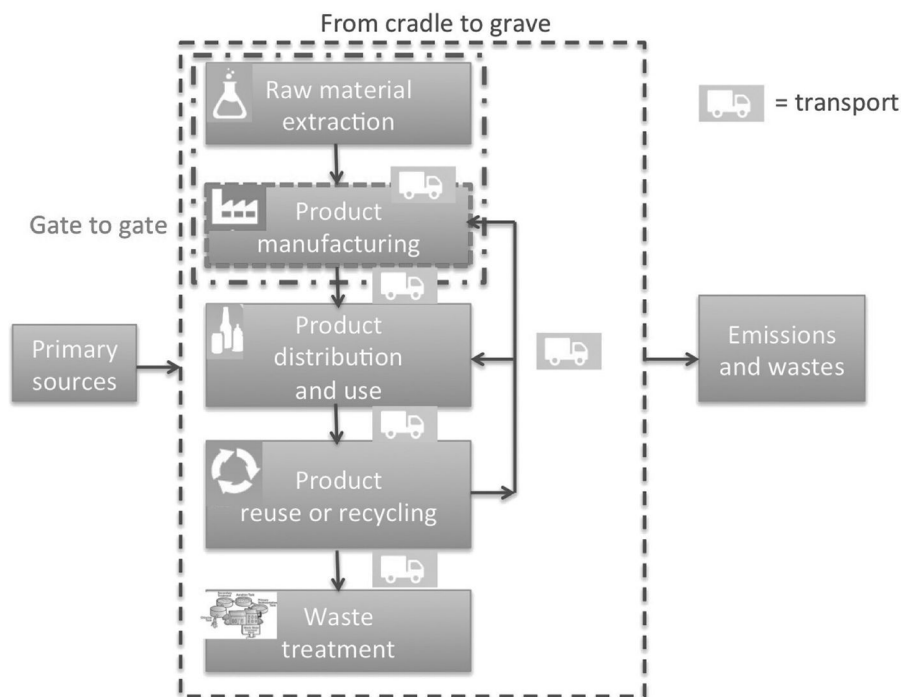


Figure 2. Steps involved in a product life cycle.

requirement. This is a major concern for the largest industrial process units, which account for a considerable share of total emissions of key atmospheric pollutants and also have other significant environmental impacts. Emissions from industrial installations have therefore been subject to EU-wide legislation for some time. In that context, the IPPC directive (the original IPPC directive was adopted as Directive 96/61/EC), concerning integrated pollution prevention and control, sets out the main principles for permitting and controlling installations based on an integrated approach and the application of best available techniques (BAT), which are the most effective techniques to achieve a high level of environmental protection, taking into account costs and benefits. This kind of assessment, applied to the life cycle of a process, involves the design, operation and decommissioning of the plant (see Fig. 3).

Process Design for Sustainability

Stages in Sustainable Process Design

A chemical process project involves several steps as it has long been recognized in the chemical engineering curriculum (Ulrich 1984; Douglas 1988; Biegler et al. 1997). Additional stages have been proposed by Azapagic et al. (2006b) in process design for sustainability (PDFS): (i) Project initiation; (ii) Preliminary design; (iii) Detailed design; and (iv) Final design. Compared to traditional process design stages,

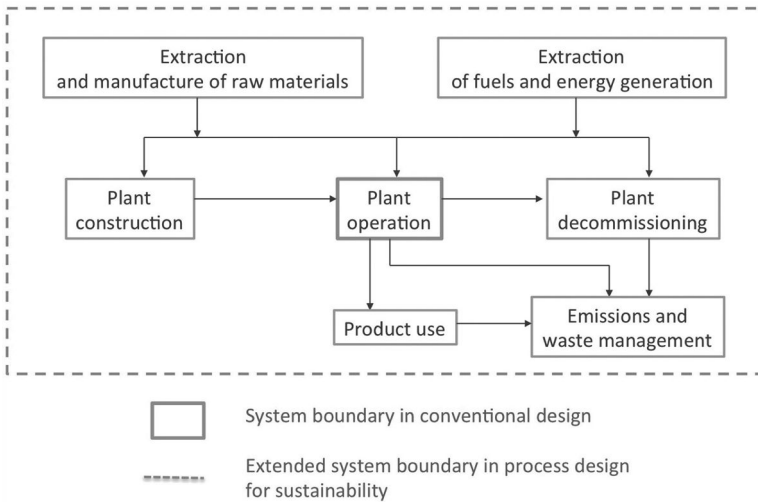


Figure 3. Systemic approach in conventional design and in process design for sustainability (adapted from Azapagic et al. (2006b)).

before preliminary design stage, there is a project initiation stage that includes initial identification of sustainability design criteria and relevant stakeholders as well as the identification and evaluation of alternatives to sustainability criteria. Design criteria established in project initiation will be the basis for alternative assessment in later stages. In the preliminary design stage, the preliminary assessment of sustainability is conducted. A full assessment of sustainability is then carried out in the detailed design stages. The methodology for PDfS includes the evaluation of both the process and product life cycle. This can be summarized in Fig. 4.

Some of the sustainability criteria (see Fig. 5) that are taken into account have been routinely considered in classical design, such as micro-economic indicators (e.g., cost and profit), environmental criteria (e.g., energy and water consumption) or social criteria (e.g., safety criteria). At the initiation project stage, these criteria must

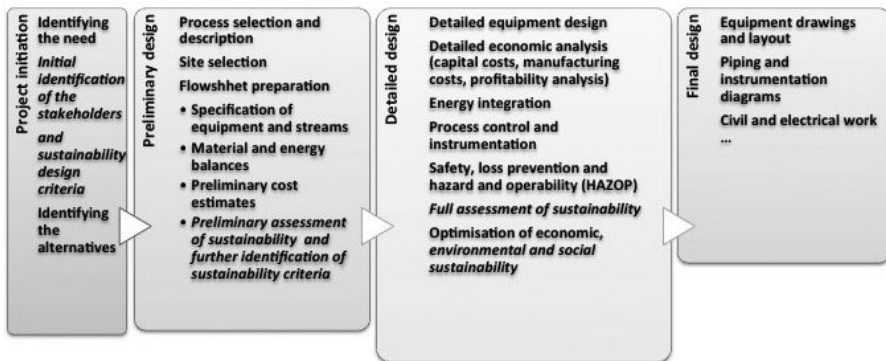


Figure 4. Stages in Sustainable Process Design adapted from Azapagic et al. (2006b): the additional steps to account for sustainability are in italics.

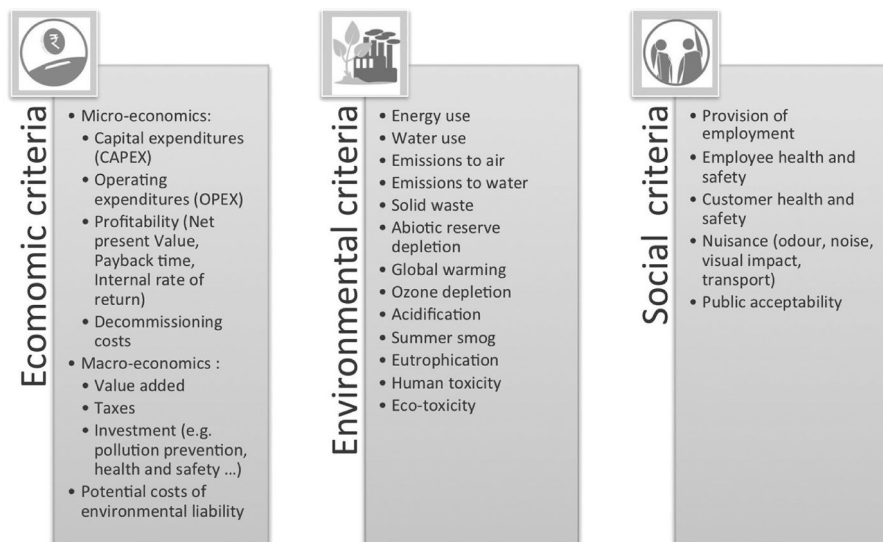


Figure 5. Criteria for PDFS adapted from Azapagic et al. (2006b).

be evaluated qualitatively by identifying the respective advantages and drawbacks of the possible options relative to these criteria. They will be quantitatively evaluated at the preliminary design stage. A very useful illustration is provided in Azapagic et al. (2006b) for vinyl chloride monomer (VCM).

It must be highlighted that the quantification of emissions and wastes has long been considered as a major concern in design due to the constraints imposed on chemical companies through legislation. Yet, emissions and waste are now evaluated in terms of impact. For instance, many environmental effects are associated with energy consumption. Fossil fuel combustion releases large quantities of carbon dioxide into the atmosphere. During the extensive time it remains in the atmosphere, CO₂ readily absorbs infrared radiation, contributing to global warming. Some of the environmental criteria are classics in Life Cycle Assessment (LCA) (Joliet et al. 2005). This initial choice of criteria is not yet fixed and can be adjusted during the design project, according to the project needs and the relevant stakeholders.

In order to analyze the sustainability of a process, the two metrics developed by the AIChE (1D) and IChemE (3D) can be mentioned initially. They consider indicators that are particularly adapted to the process engineering field and to a production system. They are based on eco-efficiency measures defined by some ratios, considering resource uses or environmental impact as the numerator and value creation as the denominator or vice versa.

AIChE Metrics

Following these principles, the eco-efficiency metrics are refined for application at the operational level by the American Institute of Chemical Engineers (AIChE)¹ in

¹ <http://www.aiche.org/ifs>

collaboration with a non-profit organization, BRIDGES to Sustainability Institute (formerly known as BRIDGES to Sustainability). The metrics, proposed in terms of eco-efficiency, include:

- material consumption: the use of materials, non-renewable materials, and in particular, materials with finite resources, affects the availability of resources and leads to environmental degradation relative to raw material extraction and during conversion as discharges;
- energy consumption: apart from the aspects related to its availability and use as a resource, the use of energy leads to varied environmental impacts. For example, the burning of fossil fuels impacts global warming, oxidation of photochemical ozone and acidification;
- water consumption: fresh water is essential for life and for almost all economic activities. As there is an increase in anthropogenic demands and depletion of water resources in some regions of the world, water consumption is a key factor;
- emission of polluting products;
- solid waste;
- land use: soil is considered to be a finite resource that provides varied ecological and socio-economic services. However, the definition of an indicator seems to be complicated and does not appear explicitly in the basic metrics.

The choice of ratios to express the metrics facilitates the comparison between several options and, consequently, the choice of the process during the decision-making phase. The lower the indicator, the weaker the impact generated per unit of value created. Heuristics and decision rules were developed and tested on more than 50 industrial pilot projects involving more than 50 processes of the chemical industry from the data of the Process Economic Program (PEP) at SRI International (Menlo Park, California) (Schwarz et al. 2002). The indicator values were calculated for standard flowsheets.

IChemE Metrics

Significant efforts to establish the metrics for sustainable development have also been made under the aegis of the IChemE (UK), by adding the economic and societal metrics to the metrics focused on environmental aspects (see Fig. 6). The indicators are specifically grouped into environmental, economic, and social categories. The list is particularly suitable for a production site. The environmental indicators are related to the resources or categories of environmental impacts. The metrics involve two types of quantitative indicators, which are the environmental burdens and the impacts. The first group includes the use of material and energy, emissions in air and water and the amount of solid waste. It is obtained from material and energy balances. The information obtained from the burdens can then be used to calculate the environmental impacts.

As mentioned above, most of the indicators of the metrics are calculated as ratios to provide a measurement of the impact, regardless of the scale of the operation. They

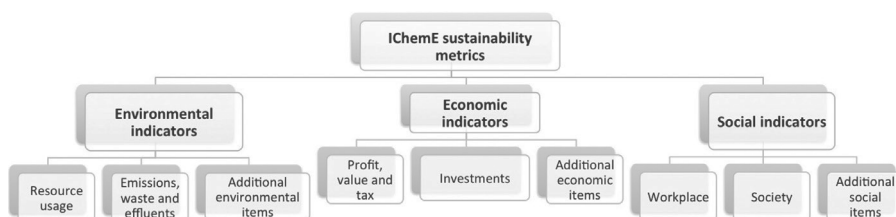


Figure 6. IChemE metrics.

are based on a simple rule: the lower the indicator, the more efficient the process. They involve both the process inputs (use of resources) and outputs (emissions, effluents, discharges, products, and services). They involve a subset of the impact factors used in environmental science, the most significant involve the process industries, for the calculation of environmental burdens. The environmental burden (EB), caused by the emission of a range of substances, is calculated by adding the weighted emissions of each substance. The potential factor of the impact is identified as the impact factor of each substance. A substance may contribute differently to different environmental burdens and may have different impact factors:

$$FE_i = \sum M_N FP_{i,N}$$

The EB are determined with respect to a reference substance (e.g., SO₂ for air acidification). This approach involves a total of 49 indicators. However, the life of the chemical products in various media is not taken into account. In addition, the indicator on human health (normalized with respect to benzene) is limited to carcinogenic effects.

Using Metrics for Sustainable Development

The metrics for sustainable development can be used at different levels in the process of decision-making: (i) evaluation of technical (variety of raw materials, options of process improvements, etc.) or financial (variety of suppliers, etc.) alternatives; (ii) comparison of industrial units; (iii) identification of environmental impacts of an industrial unit.

They can also be used for communication with the stakeholders. It must be emphasized that the metrics of sustainable development are becoming more and more complex in terms of both content and methodology (Tanzil and Beloff 2006). The examples of the previous two metrics show that the choice of appropriate indicators depends on the specifications of the industrial sector concerned or even the product types. According to Lapkin et al. (2004), the indicators should reflect the by-products, discharges, and emissions characterizing the process or the product, and also the resources necessary to provide a service. It is therefore difficult to provide a universal list of indicators. It seems more appropriate to analyze and explain the choice of indicators in a number of typical situations. Two examples reported in other texts can be mentioned here:

- example of GlaxoSmithKline (GSK): the use of sustainable development metrics within this pharmaceutical company is described in Constable et al. (2005). In order to adapt the metrics for its own requirements, GSK has developed specific “green” metrics, including indicators related to atom efficiency, carbon efficiency (CE), and reaction mass efficiency (RME) or the unavoidable energy of solvents. The CE indicator takes into account the efficiency and amount of carbon in the reactants, which is incorporated in the final product. RME takes into account the efficiency, molar amount of reactants and atom efficiency. Examples of calculation are proposed in Constable et al. (2002).
- example of BASF: an eco-efficiency analysis developed at BASF is described in detail in Saling and Kicherer (2002) and Schwanhold (2005). Based on the life cycle assessment method, the approach used the metrics based on the usage of resources and calculations of environmental impacts, health and safety. The use of normalization and weighting methods to generate an environmental performance index were illustrated using examples (particularly the production of indigo or ibuprofen). The approach was extended to cover “socio-effectiveness” aspects, by including the social aspects of sustainable development (Schmidt et al. 2004) and by developing a software tool SEEbalanceTM. The methodology was applied initially during the phases of product and process development. It was then implemented for the development of industrial and communication strategies towards industrial customers and other partners in the value chain.

Potential Environmental Impact Index (Waste Reduction Algorithm, WAR)

As it was difficult to provide all the information required for calculating the indicators of a metric at the preliminary design stage of a process, a number of studies were directed toward the development of an environmental balance. A method, commonly cited in literature and identified by the term waste reduction algorithm (WAR), is based on the concept of environmental balance, similar to material and energy balances (Fig. 7). This is not a tool for life cycle assessment, as the approach is essentially based on the process and generation of utilities associated with the life cycle of the product and does not include the other phases: raw material acquisition, distribution, usage, and recycling of the product.

This method is used in the design phase of a process and uses the process information (flow rates and mass fractions) as well as the toxicological data to calculate the environmental impact of a process. It requires the use of flowsheeting software. This American method was developed in the EPA (Environmental Protection Agency, National Risk Management Research Laboratory), taking environmental aspects into account right from the design phase of the process. The approach is based on the calculation of the potential environmental impact (PEI) of a process, which is the result of an environmental report. This type of balance must be carried out during the design phase of a process, similar to the material and energy balances. The result of the PEI balance is the calculation of an impact index (I) that provides a quantitative measure of the impact of the discharge of a process. The objective of the methodology is to minimize the PEI for a process rather than minimizing the amount

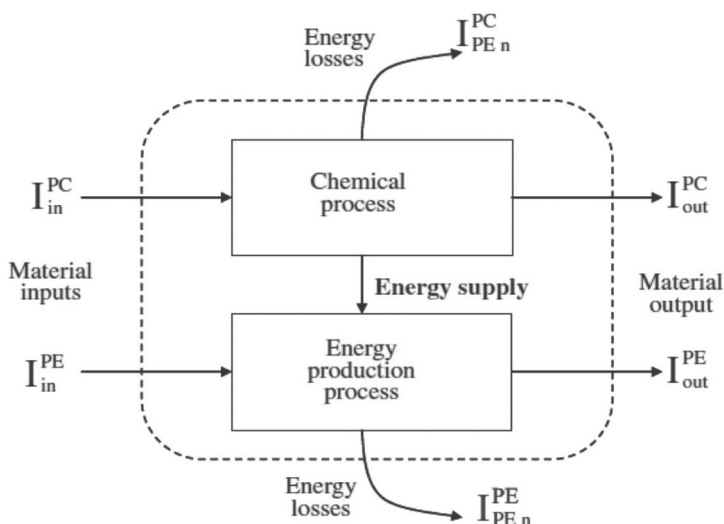


Figure 7. Inclusion of energy in the WAR algorithm (according to Young et al. 2000).

of waste generated by the process. The concept of potential environmental impact of the WAR algorithm is based on the traditional mass and energy balances. The method is presented in Cabezas et al. (1999).

The purpose of the WAR algorithm is to provide a means for comparing the potential environmental impact between the process design alternatives: the lower the index, the more environmental friendly the process.

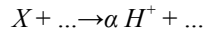
Categories of Environmental Impact Potential in the WAR Method

The toxicological data is arranged into eight environmental impact categories: global warming potential, acidification potential, ozone depletion potential, photochemical oxidation or smog formation potential, human toxicity potential by ingestion and by inhalation and aquatic and terrestrial toxicity potentials. The classification of these impact categories is based on a study in Heijungs et al. (1992). These categories have been proposed to highlight the most representative indicators in relation to the design of a process. These indicators can be classified into two domains: the global atmospheric domain and the local toxicity domain. A brief description of these impact categories is provided below.

The global warming potential (GWP) is an index that compares the contribution of greenhouse gas emissions to global warming with that of carbon dioxide (CO_2) (called reference substance, $GWP_{CO_2} = 1$). The GWP takes into account the measurement of radiation force (amount of infrared that a substance can absorb, a_i in Wm^{-2}) induced by a molecule with concentration C_i in the atmosphere in ppm. This is followed by the integration of the radiation force over a given period of time (usually 100 years):

$$GWP_i = \frac{\int_0^n a_i C_i dt}{\int_0^n a_{CO_2} C_{CO_2} dt}$$

The Acidification Potential (AP) of a compound is related to the number of moles of H^+ created per number of moles of compound X according to the reaction:



X denotes the chemical substance initiating the acidification, and the molar stoichiometric ratio α represents the ratio of the number of moles of H^+ per mole of X. Acidification is usually expressed in terms of mass (η_i , mole H^+ /kg):

$$\eta_i = \frac{\alpha_i}{M_i}$$

where M_i denotes the molecular weight of X (kg *i*/mole *i*). As mentioned before, a reference compound SO_2 is used to express the acidification potential:

$$AP_i = \frac{\eta_i}{\eta_{SO_2}}$$

Ozone depletion potential (ODP) in the stratosphere is based on the calculation of the variation in time and space of O_3 concentration ($\delta [O_3]$) due to the emission of a specific gas with respect to the same amount for a reference compound, trichlorofluoromethane (CFC-11, CCl_3F).

The photochemical oxidation potential or smog-forming potential (Photochemical Oxidation Potential, PCOP) quantifies the contribution to the smog phenomenon (photochemical oxidation of certain gases which produces ozone). It is expressed in equivalent ethylene, C_2H_4 .

These four indicators (GWP, AP, ODP and PCOP) depend on the global or regional atmospheric domain (see Table 1).

The Human Toxicity Potential by Ingestion (HTPI), Human Toxicity Potential by either inhalation or dermal Exposure (HTPE), Aquatic Toxicity Potential (ATP) and Terrestrial Toxicity Potential (TTP) are related to the local toxicological domain. As a first approximation, the lethal dose 50 (LD50) or LC50 (lethal concentration 50) is used to estimate HTPI. This indicator measures the dose of substance causing

Table 1. Environmental impact categories used in the WAR algorithm.

Local toxicological		Global atmospheric impact	Regional atmospheric impact
Impact on man	Ecological		
Human toxicity potential by ingestion (HTPI)	Aquatic toxicity potential (ATP)	Global warming potential (GWP)	Acidification potential (AP)
Human toxicity potential by inhalation or dermal exposure (HTPE)	Terrestrial toxicity potential (TTP)	Ozone depletion potential (ODP)	Photochemical oxidation potential or "smog"-forming potential (PCOP)

the death of 50% of a given animal population (often mice or rats) under specific experimental conditions. ATP is estimated from the study of the effects on the “fathead minnow” (*Pimephales promelas*). Data are expressed in the form of a concentration causing death (LC50) for 50% of the organisms exposed to a substance for a given limited duration.

Application of the WAR Algorithm

The WAR algorithm has been used on many processes and the application process is well illustrated in process test cases (such as the works in Hilaly and Sikdar (1995); Diwekar and Small (2002) on penicillin or benzene by toluene hydrodealkylation production processes).

SP (Sustainable Process Index)

Another approach to analyzing the sustainability of a process is based on the calculation of an aggregate indicator proposed by Krotscheck and Narodoslowsky (1996), the SPI (Sustainable Process Index), which is an expression of the ecological footprint concept for a process that measures the total environmental impact of various human activities. The SPI calculation is based on the mass and energy balances of the process. It is independent of legal standards, which can vary over time, making it particularly attractive. The aim of the SPI is to compare the mass and energy flows generated by human activities to natural material flows, on a global and local scale. In this approach, the planet is seen as a thermodynamically “open” system, i.e., open to the flow of solar radiations toward its surface and which emits energy in the universe. Solar radiations are the only natural driving forces for all the environmental processes and those resulting from human activities. They constitute a limited flow, although available indefinitely, which is received by the planet’s surface. This means that all natural processes or those induced by human activities require some part of this limited flow and a certain surface: in other words, technological processes compete with each other and with the natural processes for this surface, which is a limited resource. Human activities impact the environment in several ways: any process considered in a “cradle to grave” analysis requires raw materials, energy, facilities, staff and produces waste or emissions into the environment. The total area to integrate a specific process in the ecosphere in a sustainable manner is then reached by:

$$A_{\text{tot}} = A_{\text{MP}} + A_{\text{E}} + A_{\text{I}} + A_{\text{S}} + A_{\text{D}} \text{ [m}^2\text{]}$$

where A_{MP} represents the area for the extraction of raw materials, A_{E} denotes the area relative to the energy resource, A_{I} denotes the area relative to facilities, A_{S} denotes the area relative to staff and A_{D} denotes the area to discharge all waste and emissions. Processes produce services or goods. The impact per unit of a good or service is represented by a specific area a_{tot} :

$$a_{\text{tot}} = \frac{A_{\text{tot}}}{N_{\text{p}}}$$

where N_p represents the number of goods or services produced by the process, such as the kilowatts per hour produced by a specific energy system. The reference period is generally one year. Finally, this specific area, for the production of a certain good or service, is related to the statistically available area per person to provide goods or services in a sustainable manner. The following ratio defines SPI as:

$$SPI = \frac{a_{tot}}{a_{in}}$$

where a_{in} is the available surface relative to the annual supply of goods and energy per person. It is usually estimated by dividing the total area of a region by the annual number of its inhabitants. Actually, the SPI indicates how much of the area, which is theoretically available per person to ensure their livelihood under sustainable conditions, is used for the production of the service in question: as the SPI (or a_{tot}) gets lower, the impact on the ecosphere to provide the good or service also becomes lower. A key point of the SPI assessment is the ability to specify and compare the different impacts of a technology. A detailed description of the SPI calculation and application would go beyond the scope of this chapter. Readers may refer to the articles by Narodoslowsky and Krotscheck (1995), and Krotscheck and Narodoslowsky (1996) which illustrate this approach. The authors propose correlations to determine the different areas (Narodoslowsky and Niederl 2006). An interesting case study of this indicator is proposed in Steffens et al. (1999) for the case of a bioprocess (penicillin production).

In order to provide a more comprehensive analysis of the interaction of environmental burdens and financial costs, an environmental performance strategic map has been proposed, based on the combination of different footprints (De Benedetto and Klemeš 2009), carbon footprint (Huijbregts et al. 2008; Wiedmann and Lenzen 2007), water footprint (Hoekstra and Hung 2002) energy footprint (renewable, non-renewable) (Stögllehner 2003) and footprint due to emissions (air, water, and soil) (Sandholzer and Narodoslowsky 2007).

Exergy as a Thermodynamic Base for Sustainable Development Metrics

Another way to define a sustainable development indicator is to use exergy. An introduction to all the concepts has been provided in two parts in Wall and Gong (2001), and Gong and Wall (2001). The use of exergy (Dewulf and Van Langenhove 2008) makes it possible to quantify, on the whole, the resources consumed and the emissions released into the environment, to the extent that it is a physical magnitude that can integrate mass and energy transfers. Exergy analysis is based on the combination of the first (energy conservation) and second principle (development of entropy, consideration of irreversibilities and energy degradation) of thermodynamics (Ahern 1980; Bejan et al. 1995). Due to the generation of entropy, the energy available in the outgoing products (exergy of outgoing products) is lower than the one available in the resources. This deterioration in quality is quantifiable by exergy destruction and is involved in physico-chemical processes, either in the natural ecosystem (biomass production, for example) or in the industrial ecosystem (production, consumption, etc.).

The first applications of exergy analysis in the 1980s mostly focused on the analysis of industrial systems. The research in this area includes both methodological developments and applications to specific industrial processes and to their supply chain. Let us note that many studies have been conducted on the combination of exergy analysis and “pinch” methods, e.g., Feng and Zhu (1997) and Sorin and Paris (1999). Cumulative exergy consumption (CExC) extends the exergy analysis beyond the simple process to consider all the processes from natural resource extraction up to the final product. Here again, the major interest of this overall analysis is to provide guidelines for the improvement of one of the processes involved and to compare several approaches (Morris 1991).

Decision support systems and techniques based on the combination of exergy and economic analysis concepts have also been developed, thereby leading to an exergy cost. Exergy analysis was applied to various energy conversion and chemical processes, particularly comparing different energy sectors (Dewulf et al. 2005; Dewulf and Van Langenhove 2006). This is particularly interesting for cogeneration systems (Gomez et al. 2009; Kanoglu and Dincer 2009).

Indicators from Life Cycle Assessment

Life Cycle Assessment (LCA) is an environmental management tool that allows for identification and quantification of the environmental impact of a product, a service or activity from the “cradle to the grave”, i.e., from the extraction of raw materials up to its end of life processing (waste, discharge, incineration, recycling, etc.). An excellent summary of the use of LCA and its potential is provided in Guinée et al. (2011). LCA is a technique that aims to assess the environmental impact of a product throughout its lifetime, including the production process of raw materials used, which is a “cradle to grave” analysis. The LCA framework includes four phases: goal and scope definition, life cycle inventory (LCI) analysis, life cycle impact assessment (LCIA) and interpretation of results (Fig. 8).

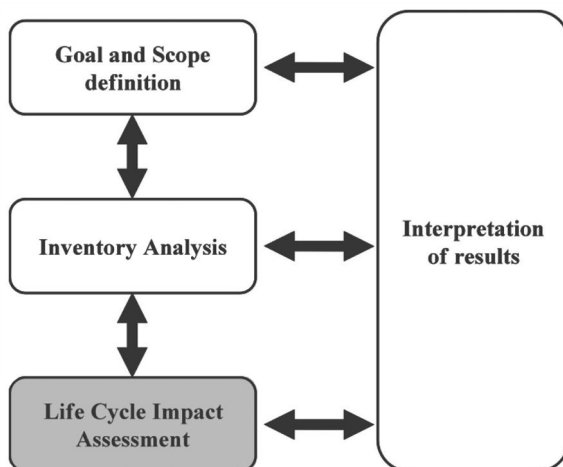


Figure 8. Life Cycle Assessment framework.

Goal and Scope Definition

The objectives and scope of the study are described and a functional unit in which emissions and extractions are reported is established. The system boundaries are fixed.

Inventory Analysis

It involves creating an inventory of flows from and to nature. Inventory flows include inputs of water, energy and raw materials as well as emissions to air, water and soil. The input and output data needed for the construction of the inventory are collected for all activities within the system boundary.

Impact Assessment

Evaluation of potential environmental impacts based on inventory flows made in the previous phase.

Interpretation of Results

Based on the results of the impact assessment, it is possible to establish a set of conclusions and recommendations for the study.

In short, the “goal and scope” defines the limits of the study, the “inventory” includes a full listing and categorization of the different elements involved in the cycle, the “impact assessment” describes and quantifies the impacts and the “improvement assessment” is the basis for improving the existing cycle.

The LCA can be viewed from two main perspectives: as a conceptual process that guides the selection of design options and, methodologically, as a way to build a quantitative and qualitative inventory of environmental burdens or releases, to evaluate these impacts and to identify alternatives to improve environmental performance.

Generally, two types of LCA can be distinguished, either attributional or consequential. In attributional LCA studies, the impacts are attributed to the considered system based on the input and output flows. In consequential LCA studies, the question is to determine how the input and output flows of the system would change as a result of the potential decisions.

Main Methods of Impact Categories

There are various methods used to translate the inventory results into environmental impact indicators at different levels. There are generally classified into two broad categories based on their position on the continuum of the cause and effect chain,

the “mid-point” methods on the one hand, and the “end-point” methods on the other hand:

- “mid-point” methods, the most recognized and currently used methods, are used to characterize the inventoried flows into potential impact indicators (or mid-point indicators), of which there are roughly a dozen. They model the impact relatively closer to the environmental flow and hence consider only part of the environmental mechanism. Their advantage is to reduce uncertainty. Mid-point methods include: the CML 2001 baseline method of the Leiden University in the Netherlands (Heijungs et al. 1992) which has a broad consensus, or the EDIP 97 or 2003 method (Hauschild and Wenzel 1998). This method, commonly used in Scandinavia, models the impacts corresponding to higher-order effects. It enables improved communication but is more uncertain because of the many hypotheses that it involves. The impact categories commonly considered in mid-point methods generally involve global warming, ozone layer depletion, tropospheric ozone formation, acidification, eutrophication, toxicity, ecotoxicity, resource depletion and land use;
- “end-point” methods model the impacts relatively far in the environmental mechanism, i.e., impacts which directly damage human health, ecosystems and resources. These indicators are more relevant in terms of communication and are therefore more simple to use, but their modeling is more uncertain due to the complexity of the mechanism and difficulties to completely model it. Typical methods are the EPS and Eco-Indicator 99 methods (Jolliet et al. 2005). The damage types concern human health, biotic and abiotic natural environments and resources, and the human environment;
- mid-point and end-point methods: some methods model the impacts both in terms of mid-point and end-point (Impact 2002 + method) (Jolliet et al. 2005).

The advantages and disadvantages of the methods of impact categories and indicators have been discussed at length (Azapagic 2006). Some users prefer mid-point indicators because they describe the impacts in the cause and effect mechanism earlier and prevent the accumulation of uncertainties when modeling the indicators to the closest end point (Pennington et al. 2004).

Toward a Sustainable Life Cycle Assessment

In an aforementioned review article on the past, present, and future of LCA (Guinée et al. 2011), it is specified that the development of the LCA has undergone various phases, which eventually include the method as a decisional tool for environmental management, in order to design sustainable products, processes, and systems:

- past of LCA (1970–2000): there were two periods. Initially, method design from 1970 to 1990 often differed in terms of approach, terminologies, or even results, thus showing the absence of scientific discussions and exchange platforms regarding this method. This was followed by a decade of standardization with efforts in terms of scientific activity and coordination of activities

(works of the SETAC², definition of standardization activities: especially ISO 14040 Environmental management—life cycle assessment—principles and framework);

- current LCA (2000–2010): this period is characterized as the decade of development of the methodology.

However, the LCA method, as mentioned clearly, is interested only in the environmental component of the life cycle assessment. The current challenge is clearly the extension of the methodology to other components of sustainable development (LCSA, Life Cycle Sustainable Analysis).

Design Methods for Sustainable Processes and Systems

Several Roads to More Sustainable Processes and Systems

Several techniques have been used for improving sustainability as well as value chain interaction, such as industrial ecology, life-cycle assessment (LCA), green chemistry/engineering and waste minimization. These techniques are not mutually exclusive but each seeks to improve the sustainability of a plant from a different perspective.

Industrial Ecology

At a geographical cluster level, the concept of industrial ecology tends to improve the environmental impact of a plant by favoring waste exchange, recycling and reuse with other plants (Boix et al. 2012; Ehrenfeld and Gertler 1997) nearby. The determination of the conditions that underpin industrial symbiosis and associated framework conditions, as well as how different actors within value chains establish and maintain inter-organizational relationships to develop processes for industrial symbiosis, i.e., optimizing waste valorization within and between sectors, are receiving increasing attention. One example of the successful implementation of this industrial symbiosis is the Kalundborg industrial park in Denmark (Chertow 2000) where an oil refinery, power station, gypsum board facility, pharmaceutical plant and the city itself, share water, steam, and electricity resources, and also exchange a variety of wastes. This leads to a 25% reduction of the fresh water usage, 2.9 million tons of material recycling, and energy for heating 5000 homes.

Life Cycle Assessment

In the previous section, only the environmental metrics associated with LCA have been considered. Here, LCA is viewed as an environmental system-based management tool that can be used for elucidating the environmental burdens over the entire life cycle of the product, starting from raw material extraction to production process, point of use and final disposal. It must be recognized that LCA initially

² Society of Environmental Toxicology and Chemistry (SETAC), <https://www.setac.org/>

and traditionally focuses on products and their impacts on the environment. It has also been applied as a decision-making tool during process design (Azapagic 1999), where its strong interest has been highlighted.

Green Chemistry/Green Engineering, Process Intensification and Waste Management

While industrial ecology and LCA focus outwards from the process and plant, green chemistry/green engineering and waste minimization look inwards. The production process can be made inherently benign through green chemistry and green engineering, which involves designing new processes or products (such as catalysts) that eliminate or reduce the use and generation of hazardous substances (see the twelve principles of Green Chemistry according to Anastas and Warner (1998), and more specifically the Twelve Principles of Green Engineering). Let us recall that:

- Green Chemistry is the design of chemical products and processes that reduce or eliminate the use and generation of hazardous substances.
- Green Engineering is the development and commercialization of industrial processes that are economically feasible and reduce the risk to human health and the environment.

Process intensification is another cornerstone to improve sustainability. It is well recognized that process intensification can lead to large efficiency increases in the pharmaceutical and fine chemicals sectors and will start to become implemented in initial bulk chemical production (Crittenden and Kolaczowski 1995).

Besides, waste minimization is a manufacturing-centric activity, which avoids, eliminates or reduces waste at its source, or allows reuse or recycling of the waste within a plant (Crittenden and Kolaczowski 1995). It is thus suited for initial process design as well as the retrofit situation, where different modifications can be proposed to the base case design and operation in order to improve environmental performance.

Eco-design Approaches

The analysis above shows that the recognition of sustainability criteria in the process design phase is not an easy task and that many scientific challenges are still open. Due to the central position of the chemical industries along the value chain, a major concern is related to the process design stage, which is at the core of the system, and to its connection to the raw material and energy extraction phase, within the boundaries of the so-called cradle to gate system.

In general, process simulators are used to determine the material and energy flow on a boundary related to the process. Cost models combined with these performance models are used to study the process profitability. Simulation and modeling tools have been used mainly to minimize an economic criterion under environmental constraints.

Over the last 15 years, a substantial number of works in the PSE (Process Systems Engineering) domain dedicated to these themes is reported in the literature. The available methods can be classified into two categories, either qualitative or quantitative methods. The qualitative methods include summary techniques based on the Douglas hierarchical procedure model (Douglas 1988), the onion diagram (Smith 1995) or environmental optimization ENVOP (Isalski 1995) which can be applied to identify the solutions for minimizing the potential discharges of a process. Quantitative methods include the pinch technology (Linnhoff 1995), mass exchange networks (El-Halwagi 1997), superstructure optimization (Dantus and High 1996) or simulation. All these methods can be used to better integrate the process and/or its utility network.

The process simulator has become a standard tool for process engineers. Its main advantage is the ability to easily evaluate process changes using commercial software (Aspen Plus, CHEMCAD, gPROMS, HYSYS, PRO/II, ProSimPlus, etc.) in a rather short time period without using difficult and expensive experiments or a pilot test. Such simulators have also been used for environmental studies. The Aspen Plus simulator was coupled with an optimizer to determine the optimal superstructure, thereby reducing waste generation and energy consumption while satisfying a profitability criterion. The CHEMCAD simulator coupled with the WAR algorithm was used in Cabezas et al. (1999) to compare the environmental impacts caused by changes in the production unit. The goal was to reduce environmental impact by recycling in a methyl ethyl ketone unit and an ammonia unit. Another study (Fu et al. 2000) combined the Aspen Plus simulator with multiobjective methods to reduce environmental impact and maximize profitability. The methodology was illustrated in the process of benzene production by toluene hydrodealkylation (HDA process). The HYSYS simulator was used with an optimization module to evaluate the design alternatives for a maleic anhydride process (Chen and Shonnard 2004). More recently, several design choices relative to a biodiesel production processes have been studied by combining the Aspen Plus simulator and multiobjective decision support tools (Othman et al. 2010).

Another approach to sustainable design is adopted in Carvalho et al. (2013), based on a *SustainPro* indicator, to identify, screen and evaluate the design alternatives. *SustainPro* uses the process information in the form of mass and energy balances from a simulator and applies a set of mass and energy indicators. The methodology is based on a reverse design method, where target values are assigned to the indicators and where the most sensitive variables towards indicators are identified. The development of a software tool (*SustainPro*) and its application to chemical processes operating in batch or continuous modes is presented in Carvalho et al. (2009). The software tool is based on the implementation of an extended systematic methodology for sustainable process design using process information/data such as the process flowsheet, the associated mass/energy balance data and the cost data. *SustainPro* guides the user through the necessary steps the methodology implemented. The final design alternatives are evaluated using environmental impact assessment tools and safety indices. The extended features of the methodology incorporate life cycle

assessment analysis and economic analysis. The application and the main features of *SustainPro* are illustrated in a case study of β -galactosidase production. Yet, *SustainPro* does not encompass a multiobjective optimization framework.

A very interesting contribution presented in Halim and Srinivasan (2011) proposes a framework for conducting a sustainability study implemented in the *ENVOPExpert* design support system. Different process system engineering methodologies are combined—the knowledge based approach for identifying the root cause of waste generation, the hierarchical design method for generating alternative designs, sustainability metrics, and multi-objective optimization—into one coherent simulation-optimization framework. This is implemented as a decision-support system using Gensym's G2 and the HYSYS process simulator. The framework involves the following elements: (i) process information representation; (ii) waste source diagnosis; (iii) knowledge-based alternative generation; (iv) quantitative assessment of alternatives, and (v) multi-objective optimization based on Simulated Annealing. Even if this contribution is particularly interesting, the environmental criteria are based on the output flows of the process and are not evaluated as environmental impacts. The approach is only restricted to a gate-to-gate system and no decision aid method is implemented to provide a valuable solution to the decision maker.

A study based on the combination of a simulator coupling the process and the utilities producing unit with a multi-objective optimizer of genetic algorithm type is proposed in Ouattara et al. (2010, 2012). A key point concerns the use of the Ariane ProSim software, a simulator dedicated to the production of utilities (steam, electricity, process water), to calculate the needs in primary energy and quantify emissions of pollutants, which come from the energy production unit. Among the set of optimal solutions in the Pareto front, it is important to determine the one(s) that correspond(s) to the best choices, in order to guide decision-makers in these final tasks. A method for decision support has thus been used to establish the best compromise between the criteria (TOPSIS (Technique for Order Preference by Similarity to Ideal Solution) (Hwang and Yoon 1981)). The fundamental idea of this method is to choose a solution as close to the ideal solution (optimal for all criteria) as possible and as far from the negative-ideal solution (which is negative for all the criteria) as possible. The general framework is illustrated in Fig. 9.

Conclusions

In this chapter, a review of the various indicators and metrics recommended in the design or the evaluation phase of processes and sustainable systems has been provided. It demonstrates the rich literature in the field and the different ways of defining indicators or metrics, with the use of (AIChE, IChemE) metrics, a potential environmental impact, an SPI, which can be viewed as a process sustainable footprint and an energy approach or an approach based on life cycle assessment, etc. The design of processes and sustainable systems involves extremely varied fields or methods, affects key products and processes and requires a completely new approach for process engineers. The literature review highlights the need to

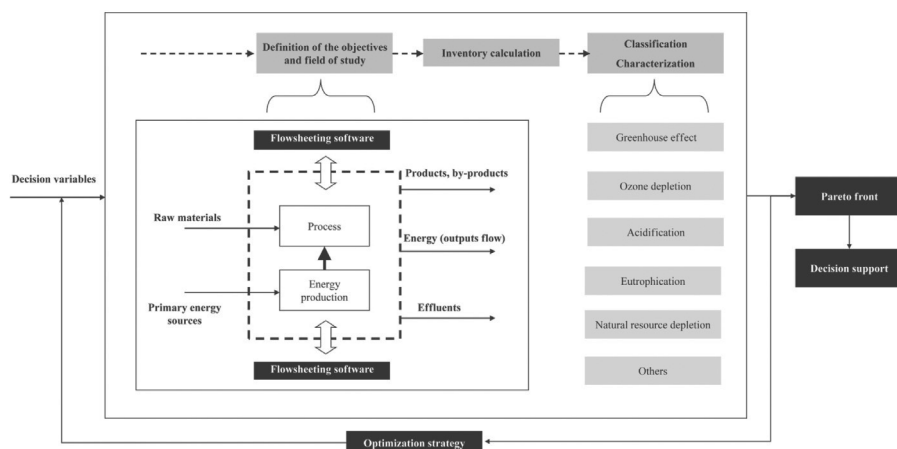


Figure 9. General framework for eco-design proposed in Ouattara et al. (2010, 2012).

couple process simulators, tools for quantification of environmental impacts (life cycle assessment for instance) and the design optimization methods, in order to reach a generally acceptable solution. Due to the conflicting nature of the criteria involved, multiobjective optimization, as well as uncertainty analysis, methods are an interesting field of investigation. They will be presented in the next chapter.

References

- Abraham, M.A. 2006. Sustainability Science and Engineering, Defining Principles, Volume 1, Elsevier, The Netherlands.
- Ahern, J.E. 1980. Method of Energy Systems Analysis. John Wiley & Sons, New York.
- Allen, D.T. and D.R. Shonnard. 2002. Green Engineering: Environmentally Conscious Design of Chemical Processes. Upper Saddle River, NJ.
- Anastas, P.T. and J.C. Warner. 1998. Green Chemistry, Theory and Practice. Oxford University Press, New York.
- Anastas, P.T. and J.B. Zimmerman. 2003. Design through the 12 principles of green engineering. Environ. Sci. Technol. 37(5): 94A–101A.
- Azapagic, A. 1999. Life cycle assessment and its application to process selection, design and optimisation. Chem. Eng. J. 73: 1–21.
- Azapagic, A. 2006. Life cycle assessment as an environmental sustainability tool. pp. 87–109. In: J. Dewulf and H. Van Langenhove (eds.). Renewables-Based Technology. John Wiley & Sons, Ltd., Chichester, UK.
- Azapagic, A. and R. Clift. 1999. The application of life cycle assessment to process optimisation. Comput. Chem. Eng. 23: 1509–1526.
- Azapagic, A., A. Millington and A. Collett. 2006a. A methodology for integrating sustainability considerations into process design. Chem. Eng. Res. Des. 84: 439–452.
- Azapagic, A., S. Perdan and R. Clift. 2006b. Sustainable Development in Practice—Case Studies for Engineers and Scientists. John Wiley & Sons, Chichester.
- Bejan, A., G. Tsatsaronis and M. Moran. 1995. Thermal Design and Optimization. John Wiley & Sons, Inc., USA.
- Biegler, L.T., I.E. Grossmann and A.W. Westerberg. 1997. Systematic Methods of Chemical Process Design. Prentice Hall, New Jersey.
- Boix, M., L. Pibouleau, L. Montastruc, C. Azzaro-Pantel and S. Domenech. 2012. Minimizing water and energy consumptions in water and heat exchange networks. Appl. Therm. Eng. 36: 442–455.

- Cabezas, H., J.C. Bare and S.K. Mallick. 1999. Pollution prevention with chemical process simulators: the generalized waste reduction (WAR) algorithm—full version. *Comput. Chem. Eng.* 23: 4–5, 623–634.
- Cano-Ruiz, J.A. and G.J. McRae. 1998. Environmentally conscious chemical process design. *Annu. Rev. Energy Environ.* 23: 499–536.
- Carvalho, A., H. Matos and R. Gani. 2009. Analysis and generation of sustainable alternatives: Continuous and batch processes using Sustainpro Package. *Proc. Seventh Int. Conf. Found. Comput. Process Des.* 243–251.
- Carvalho, A., H.A. Matos and R. Gani. 2013. SustainPro—A tool for systematic process analysis, generation and evaluation of sustainable design alternatives. *Comput. Chem. Eng.* 50: 8–27.
- Chemstations, CHEMCAD, Chemstations Inc., <http://www.chemstations.net>.
- Chen, H. and D.R. Shonnard. 2004. Systematic framework for environmentally conscious chemical process design: early and detailed design stages. *Ind. Eng. Chem. Res.* 43: 535–552.
- Chertow, M.R. 2000. Industrial symbiosis: literature and taxonomy. *Annu. Rev. Energy Environ.* 25: 313–337.
- Constable, D.J.C., A.D. Curzons and V.L. Cunningham. 2002. Metrics to ‘green’ chemistry—which are the best? *Green Chem.* 4: 521–527.
- Constable, D.J.C., A. Curzons, A. Duncan, C. Jiménez-González and V.L. Cunningham. 2005. The GSK approach to metrics for sustainability. pp. 163–197. *In: B. Beloff, M. Lines and D. Tanzi (eds.). Transforming Sustainability Strategy into Action: The Chemical Industry.* John Wiley & Sons, Inc., Hoboken, NJ, USA.
- Constable, D.J.C., A. Curzons, A. Duncan, C. Jiménez-González and V.L. Cunningham. 2005. The GSK approach to sustainable development and the GSK approach to metrics for sustainability. Chapter 8.7 and Section 6.1.2. *In: Beth Beloff (ed.). Transforming Sustainability Strategy into Action: The Chemical Industry,* 568 pp., Wiley & Sons, Oct 2005.
- Crittenden, B. and S. Kolaczowski. 1995. Waste minimization: a practical guide. *Dev. Chem. Eng. Miner. Process.* 3: 82–93.
- Dantus, M. and K. High. 1996. Economic evaluation for the retrofit of chemical processes through waste minimization and process integration. *Ind. Eng. Chem. Res.* 35: 4566–4578.
- De Benedetto, L. and J. Klemeš. 2009. The environmental performance strategy map: an integrated LCA approach to support the strategic decision-making process. *J. Clean. Prod.* 17: 900–906.
- Dewulf, J. and H. Van Langenhove (eds.). 2006. *Renewables-Based Technology.* John Wiley & Sons, Ltd., Chichester, UK.
- Dewulf, J. and H. Van Langenhove. 2008. Exergy: its potential and limitations in environmental science and technology. *Environ. Sci. Technol.* 42: 2221–2232.
- Dewulf, J., H. Van Langenhove and B. Van De Velde. 2005. Exergy-based efficiency and renewability assessment of biofuel production. *Environ. Sci. Technol.* 39: 3878–3882.
- Diwekar, U. and M.J. Small. 2002. Process analysis approach to industrial ecology. pp. 114–137. *In: R.U. Ayres and L.W. Ayres (eds.). A Handbook of Industrial Ecology.* Edward Elgar Publishing Limited, Cheltenham, UK.
- Douglas, J.M. 1988. *Conceptual Design of Chemical Processes.* McGraw Hill, New York.
- Ehrenfeld, J. and N. Gertler. 1997. Industrial ecology in practice: the evolution of interdependence at Kalundborg. *J. Ind. Ecol.* 1: 67–79.
- El-Halwagi, M.M. 1997. *Pollution Prevention through Process Integration.* Academic Press, San Diego, USA.
- Feng, X. and X. Zhu. 1997. Combining pinch and exergy analysis for process modifications. *Appl. Therm. Eng.* 17: 249–261.
- Fu, Y., U.M. Diwekar, D. Young and H. Cabezas. 2000. Process design for the environment: A multi-objective framework under uncertainty. *Clean Prod. Process.* 2: 92–107.
- Gomez, A., C. Azzaro-Pantel, S. Domenech, L. Pibouleau, C. Latgé, D. Haubensack and P. Dumaz. 2009. Exergy analysis for Generation IV nuclear plant optimization. *Int. J. Energy Res.* 34: 609–625.
- Gong, M. and G. Wall. 2001. On exergy and sustainable development—Part 2: Indicators and methods. *Exergy an Int. J.* 1: 217–233.
- Guinée, J.B., R. Heijungs, G. Huppes, A. Zamagni, P. Masoni, R. Buonamici, T. Ekvall and T. Rydberg. 2011. Life cycle assessment: past, present, and future. *Environ. Sci. Technol.* 45: 90–96.

- Halim, I. and R. Srinivasan. 2011. A knowledge-based simulation-optimization framework and system for sustainable process operations. *Comput. Chem. Eng.* 35: 92–105.
- Hauschild, M.Z. and H. Wenzel. 1998. *Environmental Assessment of Products*. Vol. 2—Scientific background. Chapman & Hall, United Kingdom, 1998, ISBN 0-412-80810-2.
- Heijungs, R., J.B. Guinée, G. Huppes, R.M. Lankreijer, H.A. Udo De Haes, A. Wegener Sleswijk, A.M.M. Ansems, P.G. Eggels, R. van Duin and H.P. de Goede. 1992. *Environmental life cycle assessment of products: guide and backgrounds (Part 1)* CML, Leiden, the Netherlands.
- Hilaly, A.K. and S.K. Sikdar. 1995. Pollution balance method and the demonstration of its application to minimizing waste in a biochemical process. *Ind. Eng. Chem. Res.* 34: 2051–2059.
- Hoekstra, A.Y. and P.Q. Hung. 2002. Virtual water trade: a quantification of virtual water flows between nations in relation to international crop trade. Delft, Netherlands.
- Huibregts, M.A.J., S. Hellweg, R. Frischknecht, K. Hungerbühler and A.J. Hendriks. 2008. Ecological footprint accounting in the life cycle assessment of product. *Ecol. Econ.* 64: 798–807.
- Hwang, C.-L. and K. Yoon. 1981. *Multiple Attribute Decision Making: Methods and Applications: A State-of-the-Art Survey*. Springer-Verlag, Berlin Heidelberg. 186: 259.
- ICHEME, *Chemical Engineering Matters, A review of ICHEME's technical strategy*, 2013.
- ICHEME, *The Sustainability Metrics: Sustainable Development Progress Metrics Recommended for the Use in Process Industries*, Institution of Chemical Engineers, 2013. [Online]. Available: <http://www.icheme.org/sustainability/>.
- Isalski, H. 1995. ENVOP for Waste Minimization in Speciality Conference on Environmental Issues in the Petroleum and Petrochemical Industries. pp. 276–286.
- Jolliet, O., M. Saadé and P. Crettaz. 2005. *Analyse du Cycle de vie, Comprendre et Réaliser un Écobilan*, Presses Polytechniques et Universitaires Romandes.
- Kanoglu, M. and I. Dincer. 2009. Performance assessment of cogeneration plants. *Energy Convers. Manag.* 50: 76–81.
- Krotscheck, C. and M. Narodoslawsky. 1996. The Sustainable Process Index a new dimension in ecological evaluation. *Ecol. Eng.* 6: 241–258.
- Lapkin M., L. Joyce and B. Crittenden. 2004. Framework for evaluating the 'greenness' of chemical processes: case studies for a novel VOC recovery technology. *Environ. Sci. Technol.* 38: 5815–23.
- Linnhoff, B. 1995. Pinch analysis in pollution prevention. pp. 53–67. *In*: A.P. Rossite (ed.). *Waste Minimization through Process Design*. McGraw-Hill, New York.
- Morris, D. 1991. Exergy analysis and cumulative exergy consumption of complex chemical processes: the industrial chlor-alkali processes. *Chem. Eng. Sci.* 46: 459–465.
- Narodoslawsky, M. and C. Krotscheck. 1995. The sustainable process index (SPI): evaluating processes according to environmental compatibility. *J. Hazard. Mater.* 41: 383–397.
- Narodoslawsky, M. and A. Niederl. 2006. The Sustainable Process Index (SPI). pp. 159–172. *In*: J. Dewulf and H. Van Langenhove (eds.). *Renewables-Based Technology: Sustainability Assessment*. John Wiley & Sons, Ltd., Chichester, UK.
- Othman, M.R., J.-U. Repke, G. Wozny and Y. Huang. 2010. A modular approach to sustainability assessment and decision support in chemical process design. *Ind. Eng. Chem. Res.* 49: 7870–7881.
- Ouattara, A., C. Azzaro-Pantel, L. Pibouleau, S. Domenech, P. Baudet and B. Yao. 2010. Eco-efficiency analysis for chemical process design. *Comput. Aided Chem. Eng.* 28: 1249–1254.
- Ouattara, A., L. Pibouleau, C. Azzaro-Pantel, S. Domenech, P. Baudet and B. Yao. 2012. Economic and environmental strategies for process design. *Comput. Chem. Eng.* 36: 174–188.
- Pennington, D.W., J. Potting, G. Finnveden, E. Lindeijer, O. Jolliet, T. Rydberg and G. Rebitzer. 2004. Life cycle assessment part 2: current impact assessment practice. *Environ. Int.* 30: 721–739.
- Saling, P. and A. Kicherer. 2002. Eco-efficiency analysis by BASF: the method. *Int. J. Life Cycle Assess.* 7: 203–218.
- Sandholzer, D. and M. Narodoslawsky. 2007. SPIonExcel—Fast and easy calculation of the Sustainable Process Index via computer, *Resour. Conserv. Recycl.* 50: 130–142.
- Schmidt, I., M. Meurer, P. Saling, A. Kicherer, W. Reuter and C. Gensch. 2004. SEEBalance—Managing sustainability of products and processes with the socio-eco-efficiency analysis by BASF. *Greener Manag. Int.* 45: 79–94.
- Schwarz, J., B. Beloff and E. Beaver. 2002. Use sustainability metrics to guide decision-making. *Chem. Eng. July*: 58–63.

- Smith, R. 1995. *Chemical Process Design*. McGraw-Hill, New York.
- Sorin, M. and J. Paris. 1999. Integrated exergy load distribution method and pinch analysis. *Comput. Chem. Eng.* 23: 497–507.
- Steffens, M.A., E.S. Fraga and I.D.L. Bogle. 1999. Multicriteria process synthesis for generating sustainable and economic bioprocesses. *Comput. Chem. Eng.* 23: 1455–1467.
- Stöglehner, G. 2003. Ecological footprint—a tool for assessing sustainable energy supplies. *J. Clean. Prod.* 11: 267–277.
- Tanzil, D. and B.R. Beloff. 2006. Assessing impacts: overview on sustainability indicators and metrics. *Environ. Qual. Manag.* 15: 41–56.
- Ulrich, G. 1984. *A Guide to Chemical Engineering Process Design and Economics*. John Wiley & Sons, Inc., Somerset, New Jersey, USA.
- Wall, G. and M. Gong. 2001. On exergy and sustainable development, Part I: conditions and concepts. *Exergy An International Journal*, Vol. 1: 128–145.
- Wiedmann, T. and M. Lenzen. 2007. On the conversion between local and global hectares in Ecological Footprint analysis. *Ecol. Econ.* 60: 673–677.
- Young, D., R. Scharp and H. Cabezas. 2000. The waste reduction (WAR) algorithm: environmental impacts, energy consumption, and engineering economics. *Waste Manag.* 20: 605–615.

2

Process Optimization Strategies

Jean-Pierre Corriou and Catherine Azzaro-Pantel

Introduction

Many authors have taken an interest in the design of chemical processes as they became conscious about the environment and numerous methodologies have been proposed (Cano-Ruiz and McRae 1999). An important conclusion of their review is that the adoption of a strategy that considers aggressions against the environment as a design objective and not simply as a constraint on the operations allows us to imagine alternative processes that are efficient both at the economic and environmental levels. Firstly, system optimization was expanded to incorporate environmental objectives such as the minimization of waste and pollutant emissions (SO₂, NO_x, COVs ...). However, the drawback of these techniques is that they are concentrated on emissions coming only from the plant, without considering other aspects of the life cycle, so that it is then possible to reduce plant emissions together with the increase of environmental impact. Among the most general methods, life cycle assessment (Azapagic 1999; Heijungs and Suh 2002) plays an important role and is the most cited as a multi-attribute interdisciplinary analysis. As a tool to support decisions at the environmental level, its use must be combined with social, political, economic and technical considerations. From the point of view of optimization, multi-objective optimization (Miettinen 1999) seems unavoidable.

Chen et al. (2002) provides a guide for process design based on economic and environmental considerations. In their review, they cite several different approaches apart from the life cycle assessment, the WAR algorithm of waste reduction, the methodology of minimization of environmental impact, the evaluation of future and environmental risk. These approaches will be detailed in the following in relation to optimization. Chen et al. (2002) shows that the design of processes concerned with environment presents two aspects: a) methodologies, analysis tools making process synthesis and evaluation to reduce pollution easier, b) return from detailed analysis and optimization under the form of heuristics with regard to economic and environmental design performance with this second aspect being less developed.

Among optimization methods that will be frequently cited, please note the following abbreviations:

- LP (Linear Programming)
- NLP (Non Linear Programming)
- MILP (Mixed Integer Linear Programming)
- MINLP (Mixed Integer Non Linear Programming)

These methods will be more detailed in section 2.3.

Study Cases and Resulting Optimization Types

Studies Related to Energy

Giannantoni et al. (2005) performed an important study about a cogeneration system with the possibility to undertake a transformation of the unit to pass from the vapour cycle to the combined cycle. The following items are mentioned in this order:

- Energetic analyses (mass and energy balances on the system or the subsystems, energetic yield according to the first principle of thermodynamics, conversion coefficient of raw energy), exergetic (exergetic yield, measuring the efficiency of the transformation and having an effect on the subsystems presenting large exergy losses) and thermoeconomic (the exergy quantifies each product from the point of view of the user value). Several thermoeconomic indicators can be used: the cost of exergy destruction, the cost increase due to irreversibilities and the investment cost of the component, the relative cost increase that is the ratio of the cost increase to the exergetic cost, the thermoeconomic factor compares the increase of the monetary cost due to irreversibilities to that due to the subsystem purchase. These analyses are related to the process at the local scale and are related to the system design stage from the subsystems.
- The methods for environmental evaluation: evaluation of the impact considering the environment as a sink, energetic synthesis considering the environment as an information and resource source. The environmental impact factor gives a measurement of the relative importance of each polluting emission. Energy is the total quantity of exergy of a given type (in general, solar) directly or indirectly required to create a new product (Odum 1995).
- Economic methods: micro- and macro-economic and externality evaluations. The micro-economic evaluation is related to the evaluation of the economic performance of the studied energetic systems. Among the indicators, we mainly find the net updated value, the profit index, the internal profitability rate and the investment payback time. The macro-economic analysis uses the raw internal product as an indicator which can be criticized as the natural patrimony and capital should be taken into account in order to avoid the scenario that the more one pollutes, the more the raw internal product increases.

These different aspects lead these authors to propose that optimization should be conducted by considering various design levels implying an iterative procedure, rather than performing a traditional optimization.

Diwekar et al. (1992) published many articles dealing with optimal designs of process flowsheets with an application to environmental control of an IGCC (Integrated Gasification Combined Cycle to generate electric power), in particular sulfur elimination. The problem is formulated as an MINLP optimization problem making use of the selection of an optimal process configuration and optimum design parameters for the selected configuration. The process flowsheet is formulated in a superstructure that includes several possible flowsheets and the superstructure is modelled as an MINLP problem. The continuous variables represent flow rates, operating conditions and design variables. The binary variables take into account the existence or not of process units and hence of its configuration. The same problem was then solved by considering uncertainties (Diwekar et al. 1997) and NO_x control (refer to the stochastic optimization in the same chapter).

Thurston and Srinivasan (2003) give an application for electricity generation in Illinois by using the theory of utility functions. Tables give the environmental impact of different energy sources. The optimization problem is expressed under the recommended form. Improvement propositions are provided with respect to the existing situation by means of a Figure similar to type 1.

Polluting Gas Emission

Life cycle analysis was used by Golonka and Brennan (1996, 1997) to evaluate and compare SO₂ emissions to avoid acidification from blast furnaces in Australia. Four different desulfurization processes were compared. Among the environmental impacts, acidification, global warming, solid waste generation and decreasing resources could be found. Azapagic (1999) uses the best option for the environment (British recommendation in 1997) and life cycle assessment to compare the three more common processes of desulfurization: the wet limestone-gypsum process, the wet double alkali process (calcium carbonate and sodium carbonate) and the sodium carbonate dry process. The analysis deals with an electricity power station. The extraction of raw materials, production and transport were taken into account. The life cycle of CaCO₃ was also considered which revealed that the attempt to reduce acidification had a consequence on global warming. The gypsum wet process produces the least environmental impact whereas the dry process is the most disastrous. Chen et al. (2002) studies the recovering and recycling of COVs (toluene and ethyl acetate) by absorption-distillation. It should be noted that this process formerly required a solvent selected on economic and environmental criteria. The impact evaluation methodology included estimating the process waste stream, the future of pollutant and transport calculation, assessing the exposition potential and relative risk. Seven environmental impact indexes were used, from human toxicity to global warming. In that study, the economic and environmental objectives were aggregated by using a hierarchical structure. The process was optimized by comparing simulations performed with simple process parameter variations. The life

cycle impacts were estimated with a different tool. The final result is a compromise between the solvent flow rate and the absorption temperature.

An American study (Burgess and Brennan 2001) shows that a very high percentage (70–90%) of COV emission comes from fugitive emissions related to equipment leaks in the plants. Some studies consider that aspect.

Studies Related to Environmental Impact During Optimal Design and Batch Process Scheduling

Stefanis et al. (1997) introduce a methodology of minimum environmental impact that incorporates the principles of life cycle assessment. Methods such as mass pinch (El-Halwagi and Manousiouthakis 1989) which designs optimal networks with regard to mass exchange and minimization of generated waste water (Wang and Smith 1994) are involved. Life cycle assessment then takes into account waste associated with the process inlets, as well as the outlets, and emphasizes the environmental impact rather than on actual emissions. Its main steps are the definition of a system frontier, the evaluation of environmental impact through an adequate quantification (for air and water pollution, solid wastes, fossil energy consumption, global warming, acidification, eutrophication, formation of photochemical oxidant and ozone decrease), the incorporation of explicit environmental impact criteria as process design objectives as well as economy in a multi-objective optimization. With continuous processes (Stefanis et al. 1995), batch processes present waste generation peculiarities depending on time-varying design and scheduling. The global objective will be to obtain an optimal cost, a structured design and operating recipes minimizing the environmental impact. The traditional frontier of the process is enlarged to include all the processes associated with raw material extraction and to energy generation. For example, cold water used in the milk industry processes can be produced by ammoniac refrigeration whose design makes use of nitrogen obtained by air separation and of hydrogen coming from NaCl electrolysis and salt mining extraction process. The resulting optimization problem can belong to the class of MINLP formulation. The Pareto lines represent the compromise between the cost and pollution measurement. The definition of the Pareto concept will be introduced in the presentation of multi-objective methods.

Generation of Alternative Reaction Paths

Buxton et al. (1997) describe a systematic procedure for a reaction path in organic chemistry in which the environmental impact considerations are taken into account to reduce waste. For a given final product, Buxton proposed a methodology following different steps, successively:

- Selecting groups of co-materials without mechanism providing a set of possible stoichiometries making use of base material, the product and the co-products.
- Determining a set of co-materials using functional group based molecular design techniques (through additions, substitutions and eliminations). Three sets of groups are distinguished according to the desired chemistry: acyclic, cyclic

and aromatic. Some groups are rejected because they violate the environmental restrictions, for example the chloro groups.

- Identifying a set of possible stoichiometries according to a logical representation and an optimization procedure.
- Generating corresponding mechanisms.
- Assessing the steps with the environmental impact methodology as a selection tool.

The group based design rather than atom based reduces the combinatory aspect, moreover it leads to structurally and chemically like molecules by decreasing the sorting phase. Lastly, the thermodynamic and environmental molecules are obtained according to group contribution methods.

The resulting optimization problem is based on an MINLP formulation and includes two steps:

- The determination of stoichiometry according to a linear formulation (minimize the sum of the absolute values of stoichiometric coefficients with an upper limit on the number of molecules considered in the stoichiometries).
- The evaluation of stoichiometry, a nonlinear programming problem whose objective is the minimization of the environmental impact associated with each stoichiometry, submitted to cost and thermodynamic constraints.

Lastly, the stoichiometries are classified according to the economic and environmental impact. Buxton et al. (1997) give the example of a pesticide production: 1-naphtalenyl methyl carbamate.

Solvent Problems

Optimal Solvent Design

Pistikopoulos and Stefanis (1998) propose a systematic procedure for solvent selection in processes where the separation agents play an important role to take into account environmental interactions, either at the source in the unit, or after the outlet. Solvents are used in many operations like the storage of raw materials, a reactive medium, recipient washing, product separation, ... Methods such as group contributions (Joback and Reid 1987) predicted the physico-chemical and environmental properties. Besides, computer-aided design took into account the property and performance specifications from the design (Odele and Macchietto 1993; Pretel et al. 1994; Vaidyanathan and El-Halwagi 1996). A solvent that is an excellent reactive agent can be undesirable for downstream operations. For that reason, Pistikopoulos and Stefanis (1998) propose an optimal design methodology taking into account the evaluation and the minimization of the environmental impact based on life cycle and risk assessment principles. Four specifications are desired for solvents, which deal with the operation type, environment, safety, health. According to the minimization methodology of environmental impact recommended by Pistikopoulos and Stefanis (1998), the following steps are considered:

- Definition of the system frontier.
- Emission balance of gaseous, liquid or solid waste towards the environment from the process.
- Environmental evaluation of usual emissions. It leads to a classification according to environmental effects, at short term (measurement of the critical quantity of air or water to decrease pollution below a given concentration) or at long term by environment modification (greenhouse effect related to CO₂, decrease of the stratospheric ozone layer related to CFC) or by influence on human health (lethal concentration).
- The synthesis of a benign process with respect to environment.

Practically, the following procedure in three steps is proposed:

- Identification of operations based on the solvent agent and on performance specifications (constraints) for each separation. Group contribution models are used to provide the physical, equilibrium and environmental properties. Constraints of structural feasibility (valence, bond rules) are necessary to obtain chemically possible structures. These rules reduce the problem size.
- At the separation level, determination of possible solvents satisfying the process and environmental constraints.
- At the process level, selection of an optimal solvent from a list of possible solvents while following process and environmental constraints at the plant scale.

According to Pistikopoulos and Stefanis (1998), as this problem includes several objectives, i.e., the minimization of economic and environmental criteria, a multi-objective optimization of MINLP type results which can only be solved by obtaining the Pareto space of optimal parametric solutions with respect to the cost and to different components of environmental impact. The optimization variables are either continuous like the process variables (flow rates, temperatures, mass fractions), or integer (number of groups constituting each molecule). The objective functions are environmental metrics such as the air or water critical mass. The constraints are limits to the lethal concentration, mass and energy balances, definitions of phase equilibrium, direction of driving forces, molecular performance, and predictions of physical and environmental properties. The generation step of a set of potential solvent molecules is followed by a generation step to validate the molecules, to examine if the solvents will not induce pollution on a larger scale, and estimate the operating cost. The objectives are then economic and environmental impact criteria submitted to mass and energy balances, to process specifications, to feasibility constraints, to alternative solvents or topologies, or to inlet-outlet relations with the other processes. Pistikopoulos and Stefanis (1998) apply that method on one side to gas treatment of an acrylic fibre plant, and on another side to acetaldehyde recuperation.

Sinha et al. (1999) set the problem of computer aided molecular design of a solvent that has desired properties in global optimization opposite to the optimization methods which lead to local multiple solutions. These difficulties frequently appear when the problems of computer aided molecular design use an algorithm of external

approximation, which consists in a sequence of iterations of MILP subproblems and of master problems. The NLP subproblem can find itself blocked in a local solution in non-convex problems. Another difficulty is related to the problem uncertainty. Interval analysis is a global approach presently used for reduced size problems. The authors have designed a specific algorithm. The main models for solvent design take into account the solubility parameter, thermodynamic and transport properties and health and safety requirements properties such as the bioconcentration factor, toxicity, flammability. The computer aided molecular design problem can be formulated as $\min_U f(U, \theta)$ submitted to:

$$f_k^{\text{inf}} \leq f_k(U, \theta) \leq f_k^{\text{sup}}$$

$$h_j(U, \theta) = 0$$

where U is a vector of variables which defines the molecular structure, θ a vector of group contribution parameters, f an undesired property to be minimized, f_k the concerned properties included between lower and upper bounds, h_j constraints in general related to structural requirements.

This is an MINLP problem for which a branch and bound solution algorithm of global optimization is proposed. In a classical branch and bound algorithm, a domain is divided into subdomains T_k such that:

$$T_k = \{x, y : x^{\text{inf}(k)} \leq x \leq x^{\text{sup}(k)}; y^{\text{inf}(k)} \leq y \leq y^{\text{sup}(k)}\}$$

In the proposed algorithm, each domain T_k defined by its lower and upper bounds is divided into two subdomains by using an underestimator and an overestimator by means of linear partition functions.

Solvent Recovering and Recycling

Ahmad and Barton (1999) published several articles about the generation of batch distillation process flowsheets with integrated solvent recovering and recycling. The idea is that solvent mixtures that cannot be recycled become toxic waste. The question is to design how, using batch distillation, a maximum recovery is possible from a series of streams and simultaneously minimum waste is generated. The design is based on residue curve maps in batch distillation of homogeneous multicomponent mixtures. The batch distillation feed is constituted by the batch reaction products between the entering, recycled solvents and reactants. The process is thus constituted by reaction and separation tasks, which constitute a superstructure to be optimized. Environment is both a source for incoming mass streams and a sink for the outgoing waste. The optimization problem is formulated as a double problem where an internal optimization problem constrains the external problem:

$$\min \sum_i m_{i,rec}$$

$$\text{submitted to } \min \sum_i c_i m_i$$

$m_{i,rec}$ is the quantity of the pure component i that can be recycled, m_i the quantity of the component i that will become a waste and c_i a weight, representing for example the noxious degree of i or the treatment cost. The external problem deals with the minimization of the recycled streams. This type of problem is difficult to solve and can be solved by a sequential approach where firstly, the minimum degree of waste emitted into the environment is determined by weight factors, then secondly, the recycle flow rates are minimized with respect to the minimum quantity of waste. In a multi-objective perspective, the solution would be the Pareto optimal surface. Finally, the optimization problem is reformulated as:

$$\min \sum_d \sum_i F_{d,i}^{in}$$

$$\text{submitted to } \min \sum_d \sum_j c_j F_{d,j}^{out}$$

where $F_{d,i}^{in}$ is the flow rate of component i entering in task d , $F_{d,j}^{out}$ the flow rate of composition j exiting from task d through the system frontiers. The sum on index d refers to all the tasks. The constraints are the mass balances and design parameters: stoichiometry of reactions, solvation of reactions, reachable selectivity ... and as far as the constraints are formulated in a linear way, the problem is a MILP type. The problem solution involves the compositions, the stream flow rates, the reaction conversions, the chosen solvents and entrainers as well as the recycling structure. By modifying the constraints, the authors obtain different optimum process flowsheets, which are then evaluated according to other criteria not taken into account in the program such as reaction rates and safety.

Hostrup et al. (1999) solve a similar problem where a component A must be removed from a stream containing other components, for example B, and moreover a binary azeotrope exists between A and B. In this case, a third component, separation agent or solvent is used to separate A from B. The objective in this case is to determine the optimal process flowsheet with respect to the separation efficiency, the energy cost, related components and environmental constraints. The optimization problem is an MINLP type with a superstructure that encloses all the possible process flowsheet configurations. However, Hostrup et al. 1999 propose a hybrid method which only solves the NLP optimization problems for each problem with binary variables, i.e., integer ones, as far as the problem is not too combinatorial.

Long Term Planning and Design of Supply Chain Networks

This type of problem is formulated by Hugo and Pistikopoulos (2005) as follows:

Being given a set of markets (distributors or consumers) and their demands on a given horizon, a set of plants capable of producing the desired products, a set of possible geographical locations for these plants, the availability of the resource and utility suppliers, the question is to design the supply chain network that would satisfy the demand on the whole horizon in such a way that the investment net value at the end of the horizon be maximized and that the impact of all the network on environment be minimized. This latter aspect is the only one that makes a difference between a traditional planning problem and the problem which takes into account

the environment of the whole supply chain mainly from the point of view of human health, ecosystem quality, and resource decrease. This is a multi-objective MILP optimization problem.

Maintenance-based Strategies for Environmental Risk Minimization

Environmental risk is associated with events unpredicted by probability and consequences that must be minimized. The consequences are related to the physico-chemical characteristics of process design and operation whereas the probability of unpredicted events depends on the impact of quality and operability on the process design and operation. Many methods of impact treatment and environmental risk are qualitative (using control lists or hazard identification methods like HAZOP). Nevertheless, Vassiliadis and Pistikopoulos (2000) propose applying the methodology of environmental impact minimization developed by Pistikopoulos and Stefanis (1998), by developing a framework taking into account considerations for environmental impact and interactions between the various operability characteristics, such as flexibility, quality and maintenance. The occurrence probability for each state is expressed with respect to maintenance variables, which implies an identification of the reliability and maintenance characteristics. The final problem is a multi-criteria optimization. This study is less convincing than those already cited concerning (Pistikopoulos and Stefanis 1998).

Heat Exchanger Network Design

Traditionally, the pinch method of Linhoff and Flower (1978a,b) based on the minimum temperature difference ΔT_{min} between the hot and cold streams, is associated with the inlet information related to the streams and the utilities to determine the minimum external energy load charge by linear programming. Then, the number of heat exchangers is minimized. Global optimization can be performed to solve the MILP problem. The environmental assessment mainly related to the purchase and the installation of the heat exchangers, and the related fluids, that can be added by using life cycle assessment (Chen et al. 2002). The magnitude order of ΔT_{min} remains close to that determined in the absence of an environmental study.

Optimization Methods

Different Formulations of the Optimization Problem

The most general problem of Mixed Integer Non-Linear Programming (MINLP) can be written as:

$$\max F = f(x, y)$$

submitted to:

$$h(\mathbf{x}) = 0,$$

$$g^{\text{inf}} \leq g(x) \leq g^{\text{sup}},$$

where x is the vector of continuous variables and y is the vector of binary (integer) variables.

Frequently the MINLP problem can be written under a slightly different form:

$$\max F = C^T y + f(x)$$

submitted to:

$$h(x) = 0,$$

$$g^{\text{inf}} \leq g(x) \leq g^{\text{sup}},$$

$$b^{\text{inf}} \leq By + Cx \leq b^{\text{sup}}$$

The typical solution method to an MINLP problem consists in an external loop where a master MILP problem is solved and an internal loop where an NLP sub-problem is solved. In the NLP problem, nonlinear equations are solved with respect to the continuous variables x at fixed binary variables. In the external loop, in the neighbourhood of the NLP optimum x^* , the nonlinear equations are linearized and an MILP problem is solved in order to generate new values for the binary variables y . In an MINLP solution program, the NLP problem is solved by means of a process simulator having optimization possibilities and an interface communicates between the external and internal loops. When the number of binary variables is reduced, the MILP master problem can be simplified by sweeping all the possible sets of integer variables.

Where the objective function is linear, where the constraints are linear, and where there are no integer variables, but only continuous variables, the optimization problem is reduced to a linear programming (LP) problem often denoted as simplex.

If the objective function is linear and the constraints are linear and when both integer and continuous variables exist, the optimization problem involves a Mixed Integer Linear Programming (MILP) formulation. Where the objective function is nonlinear, where the constraints are nonlinear and where no integer variables exist, except continuous variables; the optimization problem is reduced to a Non Linear Programming (NLP).

Life Cycle Assessment and Multi-objective Optimization

Life cycle assessment is an often cited method (Azapagic 1999; Azapagic and Clift 1999; Burgess and Brennan 1999, 2001) when it deals with the study of the environmental influence on the life cycle of a product, a process or an activity by identifying and quantifying energy, raw material consumption and waste release. The latter must be considered as a whole, exceeding the sole direct impact of the plant, and including indirect release, the consumption of raw materials and waste destruction. Process design-based life cycle must allow for technological innovations. The four steps of the life cycle assessment are: defining the goal and the limits of the system, analysing the balances, assessing the impact and improving the impact. Life cycle assessment should be coupled to multi-objective optimization to allow for process design, simultaneously including the environmental, technical and economic

criteria. Figure 1 shows how optimization interferes with the life cycle assessment that constitutes the first step where the mass and energy balances are performed and the loads and the environmental impacts are quantified. The quantification of raw materials and waste is the most controlled part in a life cycle assessment. By contrast, more important difficulties appear in the application of the other steps. The allocation rules consist of defining the proportion of environmental impacts to attribute to the products. An option to define the system frontiers is to consider that if the effect of a process or an activity has an influence on the life cycle assessment, it must be included in the analysis. On another side, determining the frontiers depends on the goals and the extent of the study. The quality of data is another problem source. Furthermore, the time and space aspects are not considered, as the environmental effects are assumed to be non-varying in respect to time, and the spatial definition (global, national, regional, at the company scale) of the system should be taken into account in defining the goal of the life cycle assessment. Finally, interpreting the impact assessment results is difficult. It not only depends on the evaluators, but also on the weighting obtained from bases or from political and scientific rules. There exists no standard methodology of impact evaluation and the weighting of the impact of different types requires compromise between the various environmental problems. Using a panel of experts to establish a qualitative weighting is in itself questionable and less recommended than a quantitative evaluation. Moreover, these weight factors are only valid at the epoch when they were decided. The comparison between the different studies is of course very difficult in the absence of a structured approach for impact evaluation.

In a general way, the problem is expressed as:

$$\min \mathbf{f}(\mathbf{x}, \mathbf{y}) = [f_1, \dots, f_m]$$

submitted to: $\mathbf{h}(\mathbf{x}, \mathbf{y}) = 0, \mathbf{g}(\mathbf{x}, \mathbf{y}) \leq 0, \mathbf{x} \in X \subseteq \mathbb{R}^n, \mathbf{y} \in Y \subseteq Z^p$ (Azapagic 1999),

where \mathbf{f} is a vector of economic and environmental functions, \mathbf{h} and \mathbf{g} are vectors of equality constraints (mass and energy balances) and inequality (material availability,

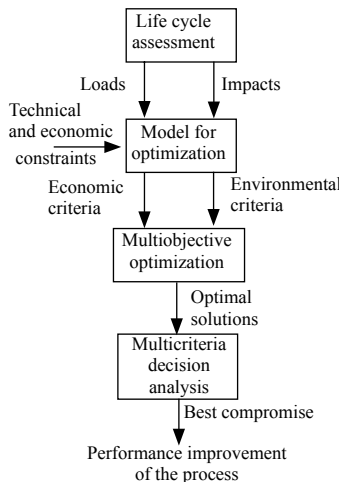


Figure 1. Multi-objective optimization from life cycle assessment (Azapagic 1999).

thermal requirements, capacities, ...), \mathbf{x} and \mathbf{y} are vectors of continuous variables (mass and energy flow rates, pressures, compositions, dimensions of the units, ...) and integer (alternative material or technologies). If there are no integer variables, if the constraints and the objective functions are linear, the problem is Linear Programming (LP). If the constraints and the objective functions are nonlinear, the problem is Non Linear Programming (NLP). Moreover if integer variables are present, the problem is Mixed Integer Non Linear Programming (MINLP). The optimal solutions will belong to Pareto surfaces or curves.

Multi-objective Optimization Methods

Multi-objective optimization has permeated all engineering fields and has been developing at a rapidly increasing speed, particularly during the two last decades in chemical engineering and process design. A review is presented in Bhaskar et al. (2000).

Problem Formulation

A multi-objective optimization problem (MOOP) can be expressed as follows:
Find the decision vector $\bar{\mathbf{x}} \in \mathfrak{R}^n$

$$\bar{\mathbf{x}} = (x_1, x_2, \dots, x_n)^T$$

which satisfies the m inequality constraints:

$$g_i(\bar{\mathbf{x}}) > 0, i = 1, 2, \dots, m$$

the p equality constraints

$$h_i(\bar{\mathbf{x}}) = 0, i = 1, 2, \dots, p$$

and optimizes the vector function:

$$\vec{f}(\bar{\mathbf{x}}) = (f_1(\bar{\mathbf{x}}), f_2(\bar{\mathbf{x}}), \dots, f_k(\bar{\mathbf{x}}))^T$$

A solution that satisfies all the constraints is called a feasible solution. Due to the competing objectives, there is no single solution to the MOOP problem, but more a set of alternative solutions.

Candidate solutions to multi-objective problem are necessarily not dominated. The Pareto set consists of solutions that are not dominated by any other solutions. A solution $\bar{\mathbf{x}}$ dominates $\bar{\mathbf{y}}$ if $\bar{\mathbf{x}}$ is better or equal to $\bar{\mathbf{y}}$ in all criteria, and strictly better in at least one attribute. Considering a minimization problem and two solution vectors of the solution space S ($\bar{\mathbf{x}} = (x_1, x_2, \dots, x_n)^T$ and $\bar{\mathbf{y}} = (y_1, y_2, \dots, y_n)^T$), $\bar{\mathbf{x}}$ is said to dominate $\bar{\mathbf{y}}$ if:

$$\forall_i \in \{1, 2, \dots, k\} : f_i(\bar{\mathbf{x}}) \leq f_i(\bar{\mathbf{y}}) \text{ and } \exists_j \in \{1, 2, \dots, k\} : f_j(\bar{\mathbf{x}}) < f_j(\bar{\mathbf{y}})$$

The space formed by the objective vectors of Pareto optimal solutions is known as the Pareto optimal frontier P . If the final solution is selected from the Pareto optimal set solutions, there would not be any solutions that are better in all attributes. The Pareto front can be viewed as an equilibrium curve composed of good solutions

for the MOOP, i.e., the set of problem solutions among which the decision maker has to make his choice. Each objective function maps the input decision vector (point in the m-dimensional decision space) to the target vector in the n-dimensional objective space.

General Multi-objective Optimization Methods

The multi-objective optimization methods that have first been developed tend to transform the multi-objective problem into a mono-objective formulation. Some significant methods based on this approach are proposed in the following:

Weighted-sum Method (WS)

Historically, the first method for solving MOOPs is the WS method. The method transforms multiple objectives into an aggregated single objective function by multiplying each objective function by a weighting factor and summing up all weighted objective functions.

$$\text{Min } f_{eq}(\vec{x}) = \sum_{i=1}^k w_i f_i(\vec{x})$$

with $\vec{g}(\vec{x}) \leq 0$ (*m inequality type constraints*)

and $\vec{h}(\vec{x}) = 0$ (*p equality type constraints*)

$$\vec{x} \in \mathfrak{R}^n, \vec{g}(\vec{x}) \in \mathfrak{R}^m \text{ et } \vec{h}(\vec{x}) \in \mathfrak{R}^p$$

where w_i represents the relative importance of each criterion in the problem. Generally,

$$w_i \geq 0 \text{ for all } i \in \{1, \dots, k\}$$

and

$$\sum_{i=1}^k w_i = 1$$

Each single objective optimization determines one particular optimal solution point on the Pareto front. The WS method then changes the weights systematically, and each different single objective optimization determines a different optimal solution. The obtained solutions constitute the Pareto front. Some drawbacks can be highlighted:

- i) This intuitive and easy method turns out to be inefficient when the problem is not convex.
- ii) Uniformly distributed set of weights does not guarantee a uniformly distributed set of Pareto-optimal solutions.
- iii) Two different sets of weight vectors do not necessarily lead to two different Pareto-optimal solutions.

Goal Attainment Method

The basic principle of this method is to minimize the deviation from an initial objective function, i.e., a target value to be achieved for each criterion.

An initial vector of objective functions $F \in \mathfrak{R}^k$ and a set of coefficients $\omega_i, i \in \{1, \dots, k\}$ have to be chosen and λ is a scalar to be minimized. The problem can be thus expressed as follows:

$$\min \lambda$$

with

$$f_1(\bar{x}) - \omega_1 \lambda \leq F_1$$

....

$$f_k(\bar{x}) - \omega_k \lambda \leq F_k$$

$$\bar{g}(\bar{x}) \leq 0$$

$$\bar{h}(\bar{x}) = 0$$

$$\bar{x} \in \mathfrak{R}^n, \bar{g}(\bar{x}) \in \mathfrak{R}^m \text{ et } \bar{h}(\bar{x}) \in \mathfrak{R}^p$$

The search direction is fixed by the values of the coefficients. To reach the compromise surface, several search directions must be taken and even several vectors of different initial objective functions must be chosen. This technique turns out to be efficient for non-convex spaces and reaches the Pareto front when varying the search direction initial objective vectors without guaranteeing a uniform distribution for solutions due to difficult scaling.

ε -Constraint Method (ε -C)

In the ε -C method, one of the objective functions is minimized while all the other objective functions are upper-bounded by introducing additional constraints. Thus, the initial problem is transformed into the following one:

$$\min f_1(\bar{x})$$

$$\varepsilon_i, i \in \{1, \dots, k\}, \varepsilon_i \geq 0.$$

$$f_2(\bar{x}) \leq \varepsilon_2$$

....

$$f_k(\bar{x}) \leq \varepsilon_k$$

$$\bar{g}(\bar{x}) \leq 0$$

$$\bar{h}(\bar{x}) = 0$$

$$\bar{x} \in \mathfrak{R}^n, \bar{g}(\bar{x}) \in \mathfrak{R}^m \text{ and } \bar{h}(\bar{x}) \in \mathfrak{R}^p$$

By parametric variation in the Right-Hand-Side (RHS) of the constrained objective functions, the efficient solutions of the problem can be obtained. In practical applications, it may be very difficult to select the initial design values inside the feasible region. Thus, in many works, the optimization is conducted successively: the previous optimization results are used as initial values for the current optimization.

Even if it gained popularity due to an easy implementation, the ε -C method is computationally intensive and difficult to solve with a huge number of constraints.

In this context, the so-called *a posteriori* methods that directly lead to the entire Pareto front with elimination of the scaling phase of the involved criteria are particularly attractive. Among these methods, Genetic Algorithms have received a lot of attention mainly due to their implicit parallelism. While local search-based metaheuristics typically work with one solution at a time, population-based methods, such as evolutionary and Genetic Algorithms maintain a whole set of solutions (the population) and try to evolve the population towards the Pareto set. Many different techniques have been developed to evaluate the so-called fitness of individual solutions in a multi-objective context and guarantee enough diversity to achieve a uniform distribution of solutions over the whole Pareto set. Their basic principle is briefly recalled before treating the multi-objective aspect.

Basic Principles of Genetic Algorithms

Genetic algorithms (GAs) and the closely related evolutionary strategies are a class of non-gradient methods. They have grown in popularity ever since the works of Holland (1975) and Goldberg (1989). The basic idea of GAs is the mechanics of natural selection. Each optimization parameter, (x_i), is coded into a gene, for example as a real number or string of bits. The corresponding genes for all parameters, x_1, \dots, x_n , form a chromosome, which describes each individual. A chromosome could be an array of real numbers, a binary string, and a list of components in a database, all depending on the specific problem. Each individual represents a possible solution, and a set of individuals forms a population. In a population, the fittest are selected for mating. Mating is performed by combining genes from different parents to produce children (crossover operator). Finally, the children are inserted into the population where some mutations are randomly performed, and the procedure starts over again, thus representing an artificial Darwinian environment. The optimization process continues until the population has converged (non-evolution of statistical parameters like means, standard deviations, or domination ranks) or until a maximum number of generations is reached.

The popularity of genetic algorithms has grown tremendously under recent years and they have been applied to a wide range of engineering problems and several variants are available. All the various GAs have different features to solve various types of problems.

Multi-objective Genetic Algorithms

Multi-objective genetic algorithms are generally divided into non-Pareto and Pareto based approaches:

Non-Pareto based approaches. The first multi-objective genetic algorithm was VEGA (Vector Evaluating Genetic Algorithm) developed by Schaffer (1984). VEGA

uses the selection mechanism of the GA to produce non-dominated individuals. Each individual objective is designated as the selection metric for a portion of the population. However, it is reported that the method tends to crowd results at the extremes of the solution space, often yielding poor coverage of the Pareto frontier.

Pareto based approaches (Goldberg, 1989) introduced non-dominated sorting to rank a search population according to Pareto optimality. First, non-dominated individuals in the population are identified. They are given the rank 1 and are removed from the population. Then the non-dominated individuals in the reduced population are identified, given the rank 2, and then they are also removed from the population. This procedure of identifying non-dominated sets of individuals is repeated until the whole population has been ranked. Goldberg also discusses using niching methods and speciation to promote diversity so that the entire Pareto frontier is covered.

In the multi-objective GA (MOGA) presented by Fonseca and Fleming (1995) each individual is ranked according to a degree of dominance. The more numerous population members that dominate an individual, the higher ranking the individual is given. The individuals on the Pareto front that have a rank of 1 are non-dominated. The rankings are then scaled to score individuals in the population. In MOGA, both sharing and mating restrictions are used in order to maintain population diversity.

The niched Pareto GA (NPGA) by Horn and Nafpliotis (1993) is Pareto-based but does not use ranking methods. Instead Pareto domination tournaments are used to select individuals for the next generation. In binary tournaments, a subset of the population is used as a basis to assess the dominance of the two contestants. If one contestant is dominated by a member in the subset while the other is not, the non-dominated one is selected to survive. If both or neither is dominated, the selection is based on the niche count of similar individuals in the attribute space. An individual with a low niche count is preferred to an individual with a high count to help maintain population diversity.

Zitzler and Thiele (1999) developed a multi-objective genetic algorithm called the Strength Pareto Evolutionary Algorithm (SPEA). SPEA uses two populations, P and P' . Throughout the process, copies of all non-dominated individuals are stored in P' . Each individual is given a fitness value, f_i , based on Pareto dominance. The fitness of the members of P' is calculated as a function of how many individuals in P they dominate. The individuals in P are assigned their fitness according to the sum of the fitness values for each individual in P' that dominate them, plus one. Lower scores are better and ensure that the individual spawns a larger number of offspring in the next generation. Selection is performed using binary tournaments from both populations until the mating pool is filled. In this algorithm, fitness assignment has a built-in sharing mechanism. The fitness formulation ensures that non-dominated individuals always get the best fitness values and that fitness reflects the crowdedness of the surroundings.

The non-dominated sorting GA (NSGA) of Srinivas and Deb (1995) implements Goldberg's concepts about the application of niching methods. In NSGA, non-dominated individuals in the population are identified, given a high initial individual score and then removed from the population. These individuals are considered to be of the same rank. The score is then reduced using sharing techniques between

individuals with the same ranking. Thereafter, the non-dominated individuals in the remaining population are identified and scored lower than the lowest one of the previously ranked individuals. Sharing is then applied to this second set of non-dominated individuals and the procedure continues until the whole population is ranked.

Sharing is performed in the parameter space rather than in the attribute space. This means that the score of an individual is reduced according to how many individuals there are with similar parameters, regardless of how different or similar they might be based on objective attributes. Over the years, the main criticisms of the NSGA approach have been as follows:

- i) High computational complexity of non-dominated sorting.
- ii) Lack of elitism.
- iii) Need for specifying the sharing parameter.

All of these issues have been addressed in the improved version of NSGA, called NSGA II. From the analysis of some difficult test problems, it has been found that NSGA II outperforms the performance of NSGA in terms of finding a varied set of solutions and in converging near the true Pareto-optimal set. Its principles are recalled below.

Initially, a random parent population P_0 of size N is created. The population is sorted based on the non-domination principle. Each solution is assigned a fitness (or rank) equal to its non-domination level (1 is the best level, 2 is the next-best level, and so on). Thus, maximization of fitness is assumed. At first, the usual binary tournament selection, recombination, and mutation operators are used to create an offspring population Q_0 of size N . Since elitism is introduced by comparing the current population with the previous best found non-dominated solutions and the procedure is different after the initial generation.

The step-by-step procedure illustrated in Fig. 2 illustrates the NSGA II algorithm. First, a combined population $R_t = P_t \cup Q_t$ is formed. The population R_t is of size $2N$. Then, the population is sorted according to non-domination. If the size of F_1 is lower than N , all members of the set F_1 are definitely chosen for the new population P_{t+1} . The remaining members of the population P_{t+1} are chosen from subsequent non-dominated fronts in the order of their ranking. Thus, solutions from the set F_2 are chosen next, followed by solutions from the set F_3 , and so on. This procedure is continued until no more sets can be formed. Let us say that the set F_{LND} is the last non-dominated set beyond which no other set can be accommodated. In general, the number of solutions in all sets from F_1 to F_{LND} is superior to the population size. To choose exactly the population members, the solutions of the last front are sorted using the crowded comparison operator in descending order and the best solutions needed to fill all the population slots are chosen. The new population P_{t+1} of size N is now used for selection, crossover, and mutation to create a new population Q_{t+1} of size N . It must be highlighted that even if a binary tournament selection operator was used, the selection criterion is now based on the crowded-comparison operator. Since this operator requires both the rank and crowded distance of each solution in the population, these quantities are calculated while forming the population P_{t+1} .

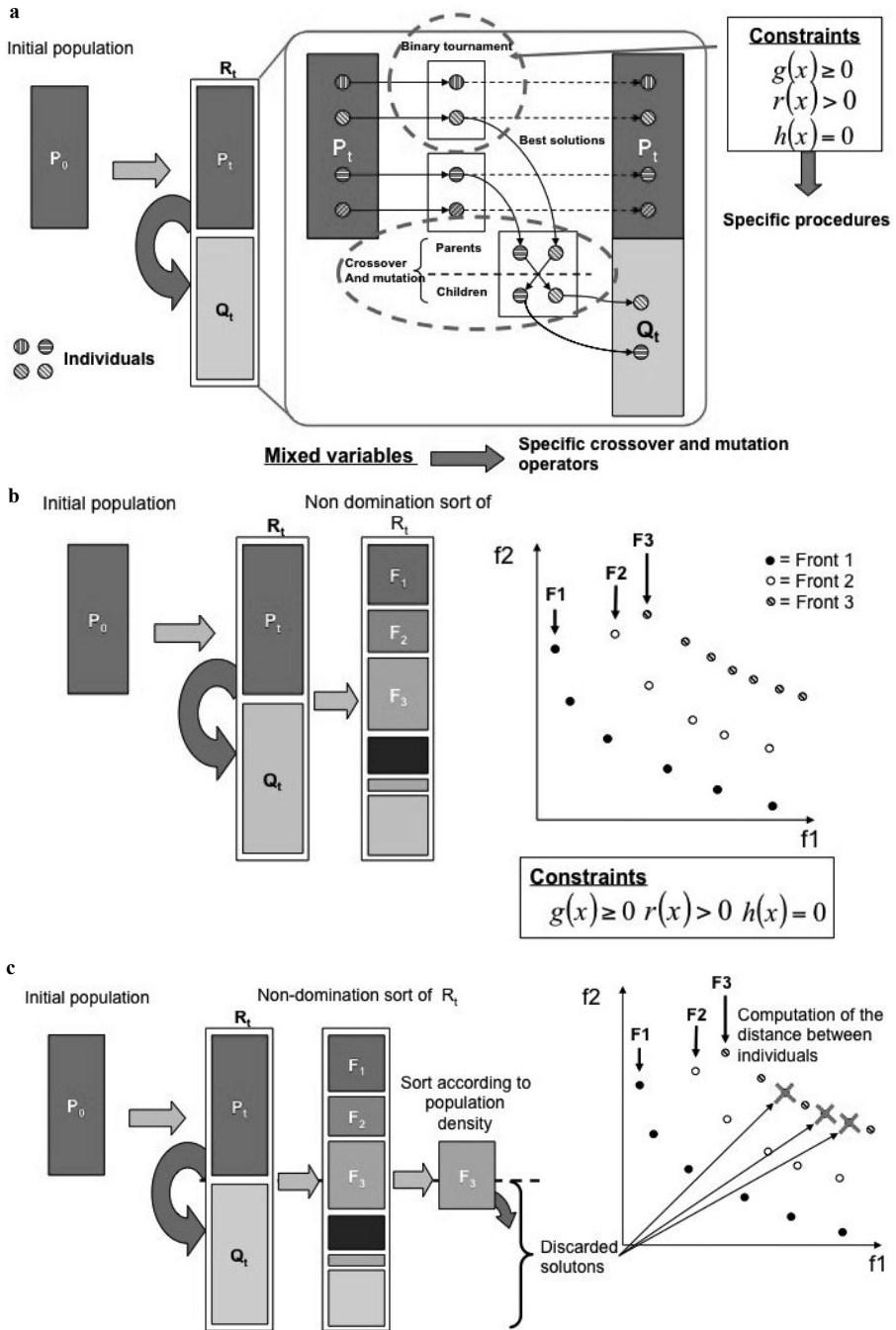


Figure 2. Principles of NSGA II.

Utility Function-based Optimization

Thurston and Srinivasan (2003) propose an approach different from optimization to solve the design compromise problems between the cost and the environmental impact. Figure 3 shows the optimal Pareto frontier.

The designs below that frontier correspond to cases where the cost or the impact is improved, but necessarily, the other factor is damaged, and which is not acceptable, the designs over Pareto curve are under-optimal. The problem to find the optimal point on the Pareto curve can be solved by considering the iso-responses of the utility function curves and by retaining the point where the utility function is maximal. The relations between quality, cost and engineering decisions can be expressed according to a matrix representation where the rows correspond to product performance attributes x_i (cost, quality, weight, environmental impact, ...) whereas the columns correspond to decision variables y_i (material and process choice, process tuning, ...) that the engineer can control to improve the attributes x_i . From the optimization point of view, constraints are equality constraints which represent the model between the product performance vector \mathbf{x} and the decision vector \mathbf{y} , under the form: $\mathbf{x} = \mathbf{h}(\mathbf{y})$, and inequality constraints of the form $x_{k,min} < h_k(\mathbf{y}) < x_{k,max}$ dealing with cost, quality, environmental impact. The objective function is the maximization of utility function, see utility theory in Keeney and Raiffa (1993), with multiple attributes:

$$\max_{U(\mathbf{y})} 1/K [[\prod_{i=1}^n (K k_i U_i [h_i (y_i \dots, y_m)] + 1)] - 1]$$

Each function with a unique attribute $U_i(h_i(\mathbf{y}))$ represents the appreciation of the designer of each attribute i and the risk consideration. They often are in the form:

$$U_i(x_i) = b_i + a_i \exp(-c_i x_i)$$

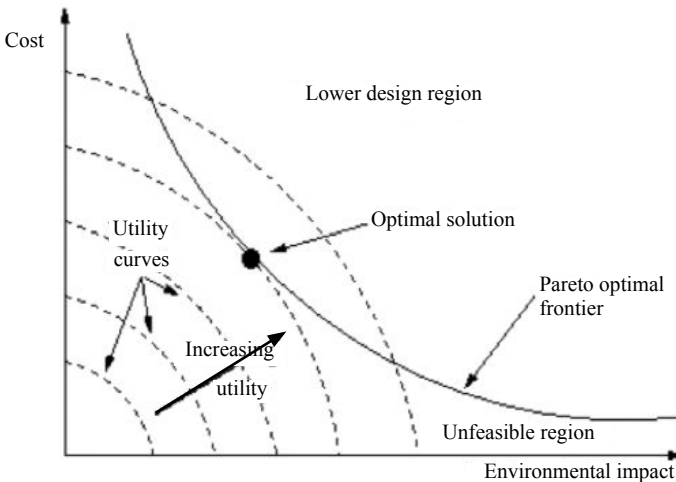


Figure 3. Pareto curve in the environmental impact-cost diagram with the iso-responses of utility curves.

where c_i represents the risk fear degree, a_i and b_i are calculated so that $U_i(x_i)$ be included between 0 and 1.

Uncertainty Consideration in the Optimization Framework

The consideration of uncertainties in the methodologies is very important because the value of environmental impacts cannot be precisely predicted. The uncertainties can be of different types: related to modelling, to the model parameters, to the process fluctuations, to external factors like price modifications, to discrete random events. Thus Chen et al. (2002) developed a mainly statistical study of toxicity evaluation for chemical process design taking into account the uncertainties of the physico-chemical parameters. Diwekar et al. (1997) performed an optimal design of an IGCC process (Integrated Gasification Combined Cycle to generate electric power) in an uncertain framework by using an ASPEN process simulator with the stochastic process module. To be more realistic and consequently acceptable, the optimization techniques, without any doubt, should incorporate the uncertainties present on many levels using from the start, stochastic modelling. In stochastic optimization, the model is treated as stochastic (Diwekar and Rubin 1991) by using distribution functions and optimization takes place as a loop above the uncertain model. However, stochastic programming differs from stochastic optimization as it implies deterministic decisions at each step or random measure, which amounts to solving a sequence of deterministic problems.

References

- Ahmad, B.S. and P.I. Barton. 1999. Process-wide integration of solvent mixtures. *Comp. Chem. Engng.* 23: 1365–1380.
- Azapagic, A. 1999. Life cycle assessment and its application to process selection, design and optimization. *Chem. Engng. J.* 73: 1–21.
- Azapagic, A. and R. Clift. 1999. The application of life cycle assessment to process optimization. *Comp. Chem. Engng.* 23: 1509–1526.
- Bhaskar, V., S.K. Gupta and A.K. Ray. 2000. Applications of multi-objective optimization in chemical engineering. *Rev. Chem. Eng.* 16: 1–54.
- Burgess, A.A. and D.J. Brennan. 1999. The application of life cycle assessment to process optimization. *Comp. Chem. Engng.* 23: 1509–1526.
- Burgess, A.A. and D.J. Brennan. 2001. Application of life cycle assessment to chemical processes. *Chem. Eng. Sci.* 56: 2589–2604.
- Buxton, A., A.G. Livingston and E.N. Pistikopoulos. 1997. Reaction path synthesis for environmental impact minimization. *Comp. Chem. Engng.* 21: s959–964.
- Cano-Ruiz, J. and G. McRae. 1999. Environmentally conscious chemical process design. *Rev. Energ. Env.* 23: 499–536.
- Chen, H., Y. Wen, M.D. Waters and D.R. Shonnard. 2002. Design guidance for chemical processes using environmental and economic assessments. *Ind. Eng. Chem. Res.* 41: 4503–4513.
- Diwekar, U.M. and E.S. Rubin. 1991. Stochastic modelling of chemical processes. *Comp. Chem. Engng.* 15(2): 105–114.
- Diwekar, U.M., H.C. Frey and E.S. Rubin. 1992. Synthesizing optimal flowsheets: applications to IGCC system environmental control. *Ind. Eng. Chem. Res.* 31(8): 1927–2011.
- Diwekar, U.M., E.S. Rubin and H.C. Frey. 1997. Optimal design of advanced power systems under uncertainty. *Energ. Convers. Manage.* 38(15-17): 1725–1735.

- El-Halwagi, M.M. and V. Manousiouthakis. 1989. Synthesis of mass exchange networks. *AIChE J.* 35(8): 1233–1250.
- Fonseca, C.M. and P.J. Fleming. 1995. An overview of evolutionary algorithms in multi-objective optimization. *Evol. Comput.* 3: 1–18.
- Giannantonio, C., A. Lazzaretto, A. Macor, A. Mirandola, A. Stoppato, S. Tonon and S. Ulgiati. 2005. Multicriteria approach for the improvement of energy systems design. *Energy* 30: 1829–2016.
- Goldberg, D.E. 1989. *Genetic Algorithms in Search Optimisation and Machine Learning*. Addison-Wesley Publishing Co., Boston, MA, USA.
- Golonka, K. and D.J. Brennan. 1996. Application of life cycle assessment to process selection for pollutant treatment: a case study of sulphur dioxide emissions from Australian metallurgical smelters. *Trans. IChemE. Part B* 74: 105–119.
- Golonka, K. and D.J. Brennan. 1997. Costs and environmental impacts in pollutant treatment: a case study of sulphur dioxide emissions from metallurgical smelters. *Trans. IChemE. Part B* 75: 232–244.
- Heijungs, R. and S. Suh. 2002. *The Computational Structure of Life Cycle Assessment*. Kluwer Academic publishers, Dordrecht.
- Holland, J. 1975. *Adaptation in Natural and Artificial Systems*, Mit. Press, Cambridge, MA.
- Horn, J. and N. Nafpliotis. 1993. Multi-objective optimization using the niched Pareto genetic algorithm. Technical report, Illinois Genetic Algorithm Laboratory, Dept. of General Engineering, University of Illinois at Urbana-Champaign, Urbana, USA.
- Hostrup, M., R. Gani, Z. Kravanja, A. Sorsak and I. Grossmann. 1999. Integration of thermodynamic insights and MINLP optimization for the synthesis, design and analysis of process flowsheets. *Comput. Chem. Eng.* 23: Supplement, 1 S23–S26.
- Hugo, A. and E.N. Pistikopoulos. 2005. Environmentally conscious long-range planning and design of supply chain networks. *J. of Cleaner Production* 13: 1471–1491.
- Joback, K.G. and R.C. Reid. 1987. Estimation of pure component properties from group-contributions. *Chem. Eng. Comm.* 57: 233–243.
- Keeney, R.L. and H. Raiffa. 1993. *Decisions with Multiple Objectives: Preferences and Value Tradeoffs*. Cambridge University Press, Cambridge.
- Linhoff, B. and J.R. Flower. 1978a. Synthesis of heat exchanger networks : I. Systematic generation of energy optimal networks. *AIChE J.* 24: 633–641.
- Linhoff, B. and J.R. Flower. 1978b. Synthesis of heat exchanger networks : II. Evolutionary generation of networks with various criteria of optimality. *AIChE J.* 24: 642–654.
- Miettinen, K. 1999. *Nonlinear Multi-objective Optimization*. Kluwer Academic Publishers, Dordrecht.
- Odele, O. and S. Macchietto. 1993. Computer aided molecular design: a novel method for optimal solvent selection. *Fluid Phase Equilibria.* 82: 47–54.
- Odum, H.T. 1995. *Environmental Accounting. Emergy and Decision-Making*. Wiley, New York.
- Pareto, V. 1896. *Cours d'économie politique*. Rouge, Lausanne, Switzerland.
- Pistikopoulos, E.N. and S.K. Stefanis. 1998. Optimal solvent design for environmental impact minimization. *Comp. Chem. Engng.* 22(6): 717–733.
- Pretel, E.J., P.A. Lopez, S.B. Bottini and E.A. Brignole. 1994. Computer-aided molecular design of solvents for separation processes. *AIChE J.* 40(8): 1349–1360.
- Schaffer, J.D. 1984. Multiple objective optimisations with vector evaluated genetic algorithms. *Proceedings of the first international conference on genetic algorithms and their applications*. Lawrence Erlbaum Associates Inc. 93–100.
- Sinha, M., L.E.K. Achenie and G.M. Ostrovsky. 1999. Environmentally benign solvent design by global optimization. *Comp. Chem. Engng.* 23: 1381–1394.
- Srinivas, N. and K. Deb. 1995. Multi-objective function optimisation using non-dominated sorting genetic algorithms. *Evol. Comput.* 2: 221–248.
- Stefanis, S.K., A.G. Livingston and E.N. Pistikopoulos. 1995. Minimizing the environmental impact of process plants: a process systems methodology. *Comp. Chem. Eng.* 19(1): s39–44.
- Stefanis, S.K., A.G. Livingston and E.N. Pistikopoulos. 1997. Environmental impact considerations in the optimal design and scheduling of batch processes. *Comp. Chem. Engng.* 21(10): 1073–1094.
- Thurston, D.L. and S. Srinivasan. 2003. Constrained optimization for green engineering decision-making. *Environ. Sci. Technol.* 37: 5389–5397.

- Vaidyanathan, R. and M. El-Halwagi. 1996. Computer aided synthesis of polymers and blends using target properties. *Ind. Eng. Chem. Res.* 35: 627–640.
- Vassiliadis, C.G. and E.N. Pistikopoulos. 2000. Maintenance-based strategies for environmental risk minimization in the process industries. *J. Hazardous Materials* 71: 481–501.
- Wang, Y.P. and R. Smith. 1994. Wastewater minimization. *Chem. Eng. Sci.* 49(7): 881–1006.
- Zitzler, E. and L. Thiele. 1999. Multi-objective evolutionary algorithms: a comparative case study and the strength Pareto approach. *IEEE Transaction on evolutionary computation* 3: 257–271.

3

Representation and Modelling of Processes

Christian Jallut, Françoise Couenne and Bernhard Maschke

Introduction

Many books are devoted to modelling in chemical engineering. An orderly modelling process is based on the combination of conservation principles and constitutive relations for transport phenomena, thermodynamic properties and chemical or biochemical reaction rates. Some of these books are specifically devoted to dynamic modelling (Friedly 1972; Luyben 1990). General textbooks of chemical engineering (Lieto 2004) or those devoted to more specific subjects like transport phenomena (Bird et al. 2002; Couderc et al. 2008) or chemical reactors (Levenspiel 1972; Villermaux 1993) can be considered as an introduction to modelling activity in chemical engineering.

The question is then: “why should we propose a contribution devoted to modelling in chemical engineering?”

Probably because the occurrence of new, safe, clean, highly intensified and miniaturized processes will impact the computer-aided process modelling activity as well as the production of commercially available simulation packages (Moulijn et al. 2008; Klatt and Marquardt 2009). Two points can be emphasized within the framework of dynamic modelling:

- Highly efficient and intensified processes are based on new systems with respect to their principle and geometry, the activation mode and the coupling between phenomena leading to new modelling tools (Stankiewicz 2006). For example, in order to model a Proton Exchange Membrane Fuel Cell (PEMFC), one has to consider coupling between heat transfer, neutral or charged species transfer as well as electrochemical reactions (Franco et al. 2007). The phenomena occur at different scales and are distributed within highly complex multiphase media. Reactive extrusion is an example of an intensified process since two

operations can be performed within the extruder: a polymer synthesis and its extrusion through the die. In order to model a reactive extrusion process, one has to consider coupling between melt flow, heat transfer, chemical reactions and viscous dissipation (Choulak et al. 2004). Furthermore, all these phenomena have to be described within a non-stationary and distributed domain due to the screw motion.

- Due to the miniaturization tendency of some operations, one can assume that a great number of arrangements of small sub-systems can be suggested to design a new process. We can imagine that in some cases, the chemical engineer will provide complex interconnected systems like an automaker assembling a car from existing elements. As far as the example of the car is concerned, some systems that are basically physico-chemical processes like a fuel cell can be used as one of these existing elements. In order to provide a complete model of the car, a fuel cell model will have to be connected with those of the other elements of the car that are mainly electromechanical systems. This is an example of a multi-physic system. As a consequence, the flexibility of the computer-aided process modelling packages will probably be an increasingly important feature. Firstly, the interconnection of existing sub-models will have to be easier for the user. In particular, the multi-physic character of these sub-models will have to be managed. Secondly, an easier development of new sub-models will be of great importance.

Two approaches can be identified to face these new challenges in computer-aided process modelling:

- A computer science approach organising the way the data and information are transferred between sub-models.
- An approach based on the use of universal physical variables leading to an easier interconnection of sub-models through port variables. Due to the universal character of the physical variables under consideration, the multi-physic character of the models is naturally taken into account.

In this contribution, we emphasize the second approach that is based on a thermodynamic view of physico-chemical phenomena. Such a view is assumed to facilitate the development of highly flexible softwares.

Computer Science Approach

Computer-aided engineering and modelling are now current tools for the economical and safe design of systems and processes. Consequently, the model management and documentation become very important topics related to the separation between modelling methods and software, flexibility and portability of models between various simulation tools and easy reusability of sub-models. As far as we know, no tool able to help the management of a model along a process or system life is now available (Eggersmann et al. 2004).

Mainly in the case of finite dimensional models of processes, many studies have been published in order to propose models structures (Stephanopoulos et al. 1990a;

Ponton and Gawthrop 1991; Perkins et al. 1996; Marquardt 1996; Preisig 1996; Gilles 1998; Mangold et al. 2002, 2005). Many efforts have also been devoted to develop a systematic modelling approach by using dedicated softwares based on:

- The combination of equations.
- The building of networks from predefined elements by using a graphical interface. In order to facilitate the reusability and the model management, complex systems models are built from sub-model libraries.

Softwares such as Omola (Nilsson 1994), MODEL.LA (Stephanopoulos et al. 1990b), gPROMS (Barton and Pantelides 1994), Modelica (Mattsson et al. 1998), Modeller (Westerweele et al. 1999), ModDev (Morales-Rodríguez and Gani 2007), ProMot (Tränkle et al. 2000), ModKit (Bogusch et al. 2001) or 20sim (Broenink 1997) are examples of such approaches. These tools are supposed to be compatible with computer-aided modelling and simulation packages like OM SIM (Mattsson et al. 1993), ModKit (Bogusch et al. 2001) or ProMoT (Tränkle et al. 2000) in order to guarantee model consistency (Cameron and Ingram 2008).

Despite the great number of available tools, the portability problem remains. Two approaches have been considered to solve this problem:

- The CAPE-OPEN project (Belaud et al. 2001; Belaud and Pons 2002; Charpentier 2009; Morales-Rodríguez et al. 2008) allowed various commercially available softwares to be compatible by defining a communication standard for models and thermodynamic data (<http://www.colan.org/index-17.html>). Model portability is greatly improved but a standardisation concerning the choice of variables leading to a universal language for physico-chemical systems representation is missing.
- The object oriented, multi-physic modelling language Modelica® (Otter et al. 2007) has been developed through an international research project (Modelica® is the trade mark of the Modelica Design Group). This software solves interoperability problems occurring when complex system simulations are performed since it allows models and libraries exchanges between commercially available softwares through a generalisation of existing simulation languages. The use of different formalisms is allowed: differential equations systems, algebraic and differential equations systems, Bond Graph, Petri Nets as well as libraries issued from various engineering domains. For example, Dymola or Scicos modelling tools use the Modelica® standard. The latter also allows non-causal modelling so that sub-model reusability is improved.

Another way to solve the problem under consideration is as follows: define a universal language for the representation of physico-chemical systems leading to general computer tools. One no more looks for a compatibilisation of existing softwares but defines a universal language for the description of physico-chemical phenomena that can be easily transformed into simulation softwares. Such a language is already available: the Bond Graph graphical language that is commonly used in mechatronics and electrical engineering (Saisset et al. 2006). In this contribution,

we give a brief description of this language and the way it can be used in chemical engineering through an example.

Bond Graph Representation of Physico-chemical Processes

Bond Graph is a graphical modelling language based on the universal concept of energy and on the representation of the exchange of energy between the subparts of a system (Gawthrop and Smith 1996; Karnopp et al. 2000). It has been mainly used in mechatronics, automatic control, robotics and many commercially available softwares are based on the Bond Graph language (<http://bondgraph.org/software.html>). Bond Graph presents many advantages:

- Energy and information fluxes are separated.
- The system to be modelled is represented by a network of subsystems that are exchanging energy. Such a structural modelling approach allows modifying the model by including new phenomena.
- A Bond Graph is a non-causal structure. Causality is included only when operating or boundary conditions are defined.
- Hybrid systems can be represented by continuous-discrete Bond Graph by including events (Breedveld 1999).

The Bond Graph language is based on energy that is a multi-physic fundamental concept. To each form of energy is associated a physical domain (mechanical domain, electrical domain, thermal domain...). An energy transfer is represented by a semi-arrow or link that is associated with a couple of power-conjugated variables, an effort variable $e(t)$ and a flow variable $f(t)$. Their product is a power or a flow of the corresponding form of energy (Fig. 1). A vectorial link represented by a double-line is also defined and the total power is simply the scalar product $e^T(t) \cdot f(t)$. The link orientation is associated with a sign convention: a flow associated with a link is positive in the link direction.

The remaining Bond Graph elements belong to three classes according to their energetic nature:

- Two active elements provide power: the effort source **Se** and the flow source **Sf**.
- Three elements are passive: the energy accumulation element **C** (we do not use the inertial **I** element that is not really necessary) and the energy dissipation elements **R** and **RS**.
- Four junction elements that are power conservative: the common effort element **0**, the common flow element **1**, the transformer **TF**, and the gyrator **GY**.

$$\begin{array}{c} e(t) \\ \longrightarrow \\ f(t) \end{array} \quad \begin{array}{c} e(t) \\ \overline{\overline{\longrightarrow}} \\ f(t) \end{array}$$

Figure 1. Scalar and vectorial links of a Bond Graph.

The Energy Accumulation Element C

The **C** element is represented in Fig. 2. The form of energy E that is stored in the element is a function of a stored quantity q called energy variable that is related to the flow variable f by the balance equation (1a).

$$\frac{e(t)}{f(t)} \rightarrow \mathbf{C} :: E(q)$$

Figure 2. The **C** accumulation element.

The effort variable e is related to the stored energy as a function of q (see equation (1b)) so that the energy balance equation is included in the constitutive equations of the **C** elements as follows:

$$\left\{ \begin{array}{l} \frac{dq(t)}{dt} = f(t) \quad \text{a)} \\ \frac{dE(t)}{dt} = \frac{dE}{dq} \frac{dq}{dt} = e(t)f(t) \quad \text{b)} \end{array} \right. \quad (1)$$

Effort and Flow Sources Se and Sf

These **Se** and **Sf** elements define independently a given value of the effort or of the flow. If these given values vary with time, the corresponding element is said to be modulated, **MSe** or **MSf** (Fig. 3).

The role of these elements is to define boundary or operating conditions.

$$\mathbf{MSf} \frac{e(t)}{f(t)} \rightarrow \quad \mathbf{MSe} \frac{e(t)}{f(t)} \rightarrow$$

Figure 3. Modulated source elements.

Dissipation Elements **R** or **RS**

The **R** element represents an irreversible energy dissipation phenomenon. According to the first principle of thermodynamics, energy is strictly conservative. In order for a Bond Graph including **R** elements to satisfy this principle and remain a power conservative structure, one has to use the **RS** element (Fig. 4).

The energy flow that is dissipated leads to the irreversible entropy production Σ .

$$\frac{e(t)}{f(t)} \rightarrow \mathbf{R} : \quad \frac{e(t)}{f(t)} \rightarrow \mathbf{RS} : \frac{T(t)}{\Sigma(t)}$$

Figure 4. The **R** and **RS** elements.

The constitutive equations of the **RS** element are then as follows:

$$\begin{cases} R(e, f) = 0 \\ \Sigma(t)T(t) = e(t)f(t) \end{cases} \quad (2)$$

where T is the temperature of the element. The first equation gives a constitutive relation between the effort and flow variables while the second equation represents the energy balance of the **RS** element that is power conservative.

For example, an **R** or **RS** element can represent an electrical resistance, a viscous dissipation in a mechanical system or a chemical reaction in a process. The **R** element is used when the thermal domain is not taken into account.

Junction Structure Elements

These elements describe the elementary interconnection between the other elements. They also satisfy the power or energy flow continuity.

0 and 1 Junctions

When elements subject to the same effort have to be connected, the **0** junction is used. All the links that are connected to a **0** junction have the same effort variable. The junction being power conservative, the sum of the corresponding flow variables has to be null. Conversely, one can couple elements having the same flow variable. In this case, the sum of the corresponding effort variables has to be null to satisfy the

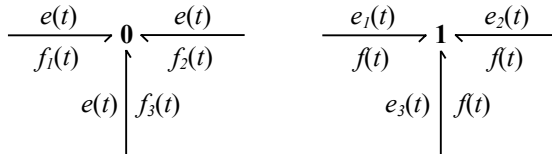


Figure 5. Examples of **0** and **1** junctions where there are three links.

power continuity. **0** and **1** junctions are represented in Fig. 5 where there are three links.

The corresponding constitutive relations of the **0** junction are as follows:

$$\begin{cases} e(t)f_1(t) + e(t)f_2(t) + e(t)f_3(t) = 0 \\ \text{so that} \\ f_1(t) + f_2(t) + f_3(t) = 0 \end{cases} \quad (3)$$

and for the **1** junction:

$$\begin{cases} e_1(t)f(t) + e_2(t)f(t) + e_3(t)f(t) = 0 \\ \text{so that} \\ e_1(t) + e_2(t) + e_3(t) = 0 \end{cases} \quad (4)$$

These elements allow for instance to represent the balance of flow variables for a certain equilibrium of intensive variables.

The Transformer

This **TF** element transforms the values of effort and flow variables without power dissipation (Fig. 6).

The constitutive equations of the **TF** elements are as follows:

$$\begin{cases} e_1(t) = M^T e_2(t) \\ f_2(t) = M f_1(t) \\ e_1^T(t) f_1(t) = e_2^T(t) f_2(t) \end{cases} \quad (5)$$

The transformations can be parameterized by a time-dependent matrix $M(t)$. In this case, the **TF** element becomes a modulated **TF** element **MTF**.

$$\begin{array}{ccc} \begin{array}{c} \xrightarrow{e_1(t)} \\ \xleftarrow{f_1(t)} \end{array} \text{TF} \begin{array}{c} \xrightarrow{e_2(t)} \\ \xleftarrow{f_2(t)} \end{array} & \begin{array}{c} \xrightarrow{e_1(t)} \\ \xleftarrow{f_1(t)} \end{array} \xrightarrow{M(t)} \text{MTF} \begin{array}{c} \xrightarrow{e_2(t)} \\ \xleftarrow{f_2(t)} \end{array} \end{array}$$

Figure 6. The transformer element.

For example, the **TF** element is used to describe the stoichiometry of a chemical reaction (see below).

The Gyrator

The **GY** element transforms the values and the nature of the flow and effort variables by preserving power. The corresponding constitutive equations are functions of the parameter $m(t)$:

$$\begin{cases} e_1(t) = m f_2(t) \\ e_2(t) = m f_1(t) \\ e_1(t) f_1(t) = e_2(t) f_2(t) \end{cases} \quad (6)$$

If the parameter m varies, the element is a Modulated Gyrator **MGY** (Fig. 7).

For electromechanical systems, this element is used to represent the reversible commutation of the conjugated variables between the electrical and the mechanical domain. If $m = 1$, the gyrator is said to be symplectic and is denoted **SGY**: it leads to a simple commutation of the role of the conjugated variables that is common in chemical engineering models (see below).

$$\begin{array}{ccc} \begin{array}{c} \xrightarrow{e_1(t)} \\ \xleftarrow{f_1(t)} \end{array} \text{GY} \begin{array}{c} \xrightarrow{e_2(t)} \\ \xleftarrow{f_2(t)} \end{array} & \begin{array}{c} \xrightarrow{e_1(t)} \\ \xleftarrow{f_1(t)} \end{array} \xrightarrow{m(t)} \text{MGY} \begin{array}{c} \xrightarrow{e_2(t)} \\ \xleftarrow{f_2(t)} \end{array} \end{array}$$

Figure 7. The gyrator element.

Bond Graph Application to Chemical Engineering: Finite Dimensional Systems

The number of state variables describing a finite dimensional system is finite. They are the coordinate of a finite dimensional state vector. In Chemical Engineering, this corresponds to the description of a system by a network of spatially uniform sub-systems. For example, a cascade of theoretical plates frequently represents a distillation column. A chemical reactor can be considered as a network of perfectly mixed continuous tanks. In such situations, the dynamic model of the system is made of ordinary differential equations possibly coupled with some algebraic constraints.

Processes are mainly thermodynamic systems. Using the Bond Graph to process modelling is then based on the definition of the thermodynamic power conjugated variables. We will see below that this transposition of the Bond Graph to thermodynamic systems is very easy since thermodynamic theory is based on the definition of energy and power conjugated variables (Breedveld 1981). In the case of thermodynamic systems like energetic devices or processes, the “true Bond Graph” is not frequently used while the “pseudo Bond Graph” is more common (Karnopp 1979; Ould-Bouamama et al. 2012; Diaz-Zuccarini and Pichardo-Almarza 2011). In this case, the effort and flow variables product is no more a power or energy flow. However, structural and causality properties of this “pseudo Bond Graph” remain the same as the properties of the “true Bond Graph”.

The C Element of a Thermodynamic System

In Chemical Engineering, the total energy of a system includes the matter or internal energy. It is the energy of a collection of elementary particles (atoms, molecules) that is considered macroscopically. In many situations, the internal energy is the only one that is considered since the variations of the other forms can be assumed to be negligible. Recent works have been devoted to the application of Bond Graph to thermodynamic systems as they are encountered in Chemical Engineering (Couenne et al. 2006, 2008a,b). The basic relation is the Gibbs equation (Sandler 1999; Vidal 2003) defined for a multi-component single uniform phase:

$$dU = TdS - PdV + \sum_{i=1}^C \mu_i dN_i \quad (7)$$

In this relation, three couples of energy-conjugated variables are defined: (T, S) , $(-P, V)$ et (μ_i, N_i) . U is the internal energy, S the entropy, T the temperature expressed in Kelvin, V the volume, P the pressure, N_i the mole number of component i , μ_i its chemical potential and C the number of components. Equation (7) is a constitutive equation between thermodynamic properties. It has been established by assuming equilibrium but it can be applied for a complex system far from equilibrium by using the local equilibrium principle. This principle is used to derive the irreversible thermodynamic theory and for processes modelling (De Groot and Mazur 1984). Equation (7) is part of the constitutive equations of a multi-port **C** element (Fig. 8). The model of a thermodynamic system made of a network of interconnected multi-

port C elements will also derive from the balance equations of the corresponding flow variables, entropy, volume (or space) and component i mole number.

This approach based on conservation principles is clearly the basis of the Chemical Engineering modelling activity. The main difference with the Bond Graph approach is that the entropy balance has to be written instead of the energy balance as it is classically performed in Chemical Engineering. The effort variables associated with the thermodynamic flow variables are the ones driving the system toward equilibrium.

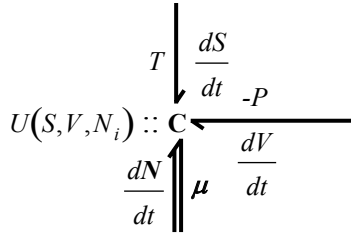


Figure 8. Multi-port C element of an elementary thermodynamic system.

Let us note that, while the principle of a balance is applied to energy, it is not a flow variable since no effort variable is associated with U . This property allows distinguishing the concept of flow variables in Bond Graph theory from the concept of extensive variables in thermodynamic theory.

Example

In order to illustrate the Bond Graph application to Chemical Engineering, we consider the case of a gas phase chemical reactor that is rather new when compared with ordinary chemical reactors (Roestenberg et al. 2010). The principle of this pulsed compression reactor is represented on Fig. 9. It is inspired from piston engines. A piston having a mass M_p moves freely in a vertical cylinder with a velocity v_p . From the chemical point of view, the reactor operates according to a cycle.

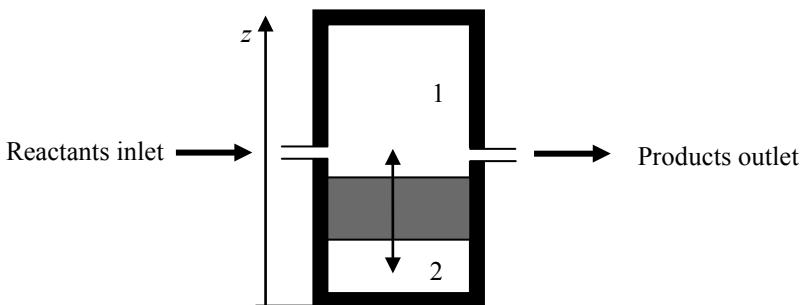


Figure 9. Pulsed compression reactor principle.

When the piston is at the top of the cylinder, the chemical reactions occur at high pressure and temperature in the compartment 1 while the compartment 2 is fed with reactants flow, the reaction products being evacuated. The piston is then pushed downward in order to compress reactants and initiate the chemical reactions in the compartment 2 and so on.

Due to its rather unusual feature, this reactor can be considered as an illustration of these new modelling situations that have been discussed in the Introduction section. The main point is its multi-physics nature since the total energy of the system is the internal energy of the gas in the compartments, the internal energy of the piston (if we do not consider the internal energy of the cylinder wall) and the mechanical energy of the piston.

Since it avoids the use of a catalyst, this reactor is also an intensified one. Let us now show how a Bond Graph model of the reactor can be progressively built in a structured manner by using the port-variables and the Bond Graph symbols. The balance equations equivalent to the Bond Graph will be also given. In the softwares based on the Bond Graph language, these equations are automatically generated.

Bond Graph of the Mechanical Part of the Piston Model

The mechanical energy that is stored in the piston is the sum of its kinetic and gravitational energies:

$$E_m(p_p, z_p) = \frac{p_p^2}{2M_p} + M_p g z_p.$$

A two-port C element is then defined in order to represent the total content of mechanical energy of the piston (Fig. 10). The energy variables associated with the kinetic and gravitational energies are the piston momentum $p_p = M_p v_p$ and its vertical position z_p .

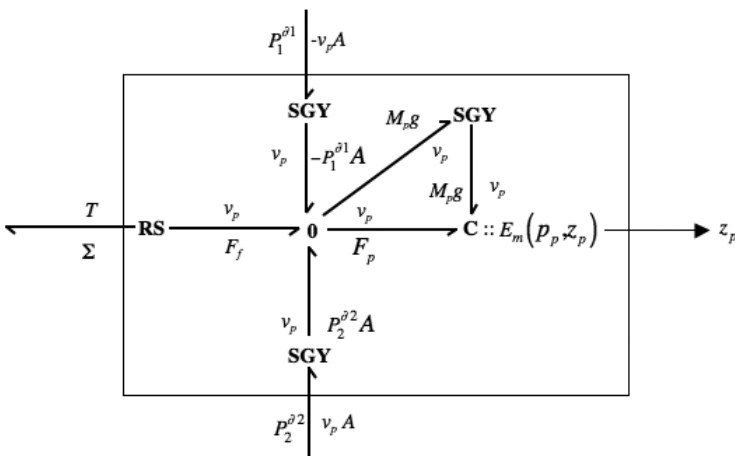


Figure 10. Mechanical model of the piston.

The time variation of the stored mechanical energy in the piston is then:

$$\frac{dE_m}{dt} = v_p \frac{dp_p}{dt} + M_p g \frac{dz_p}{dt} \quad (8)$$

The associated effort variables are the piston velocity v_p and the weight $M_p g$. At the $\mathbf{0}$ -junction connected to the port of the \mathbf{C} element (Fig. 10), one reads the balance equations of the energy variables $p_p = M_p v_p$ and z_p according to the vertical axis z:

$$\left\{ \begin{array}{l} \frac{dp_p}{dt} = F_p = (P_2^{\partial 2} - P_1^{\partial 1})A + F_f - M_p g \quad \text{a)} \\ \frac{dz_p}{dt} = v_p \quad \text{b)} \end{array} \right. \quad (9)$$

F_f is a friction force between the piston and the cylinder wall, A is its surface area, $P_1^{\partial 1}$ and $P_2^{\partial 2}$ are respectively the gas phases pressures applied to the piston boundaries $\partial 1$ and $\partial 2$. The $\mathbf{0}$ junction expresses the sum of the momentum flows as they appear in the momentum balance equation (9a). The \mathbf{SGY} element associated with the $(v_p, M_p g)$ conjugated variables commutes the roles of these variables. The velocity v_p is the effort variable for the kinetic energy $v_p = \frac{\partial E_m}{\partial p_p}$ (see equations (1) and (8)) and becomes the flow variable for the gravitational energy since it expresses what can be named the space balance equation (9b).

With the view of connecting the mechanical model of the piston with the other parts of the reactor model, the port-variables representing the energy transfer with these other parts are defined.

On the one hand, the piston motion is related to the gaseous compartments volume variations by using the corresponding space or volume balances:

$$\frac{dV_1}{dt} = -v_p A \quad \text{a)} \quad (10)$$

$$\frac{dV_2}{dt} = v_p A \quad \text{b)}$$

The velocity v_p is the effort variable associated with the momentum (equation (8)). It now becomes the flow variable associated with compartments volumes. Two others \mathbf{SGY} elements are then used to perform the corresponding change of role (Fig. 10). Let us consider for example the port-variables $(P_1^{\partial 1}, -v_p A)$ associated with the $\partial 1$ boundary. At this point, the effort variable is the pressure $P_1^{\partial 1}$ and the flow variable is the volumetric flow $-v_p A$. The associated power is $-P_1^{\partial 1} v_p A$ which is positive for the piston if it goes downward ($v_p < 0$). On the other side of the \mathbf{SGY} element, the velocity v_p is now the effort variable associated with the kinetic energy of the piston and $-P_1^{\partial 1} A$ is a force, that is to say, a flow of momentum included in the piston momentum balance equation (9a). The \mathbf{SGY} element leads to a power conservative commutation:

$$(P^{\partial 1})(-v_p A) - (v_p)(-P^{\partial 1} A) = 0 \quad (11)$$

The situation is the same for the port-variables associated with the $\partial 2$ boundary.

On the other hand, the friction force F_f leads to mechanical energy dissipation that is transformed into a source term of the entropy balance to be written. This irreversible process is represented by the **RS** junction that is associated with the two couples of conjugated variables (v_p, F_f) and (T, Σ) where T is the temperature of the sub-system where the dissipation occurs and Σ is the entropy production per time unit. The **R** part of the element describes the dissipation process by defining a constitutive relation between the flow variable F_f and the effort variable v_p . The **S** part of the element links the entropy production per time unit Σ to the dissipation process. The **RS** element is power conservative since:

$$T\Sigma = -v_p F_f > 0 \quad (12)$$

In the Bond Graph language, once a flow (or effort) variable is defined, the associated effort (or flow) variable must also be defined. Consequently, a concept of signal variable has been defined. This concept of signal allows transferring numerical data that are not defined as effort or flow variables. Such signal variables are, for example, very important to represent mechanical systems where kinematic relations can depend on the geometric configuration. From the **C** element (Fig. 10), a signal variable z_p is defined by an ordinary arrow. In the sequel, we will see why it is necessary to transfer the piston position to other parts of the model.

Once the port-variables are defined, the mechanical model of the piston can be “encapsulated” according to the boundary that is represented on Fig. 10. Such an “encapsulated” sub-model becomes reusable and connectable to other sub-models through the connection of the port-variables.

Bond Graph of the Thermal Part of the Piston Model

The accumulated energy in the **C** element (Fig. 11) is the piston internal energy $U_p(S_p)$. If the piston temperature T_p is assumed to be uniform, this energy is associated with the energy conjugated-variables couple (T_p, S_p) according to the Gibbs equation (7) where $dN_i = 0$ and dV is neglected:

$$\frac{dU_p}{dt} = T_p \frac{dS_p}{dt} \quad (13)$$

The entropy balance associated with the **C** element is:

$$\frac{dS_p}{dt} = f_s^{p1} + f_s^{p2} + \Sigma_f \quad (14)$$

The **0** junction expresses the entropy balance as a sum of flow variables. The common effort variable is the temperature at which the entropy balance is expressed, in this case, the temperature of the piston.

The entropy created per time unit by the mechanical friction of the piston is calculated by the mechanical model of the piston and is transmitted to the thermal model of the piston through the port-variables (T_p, Σ_f) .

The entropy flows f_s^{p1} and f_s^{p2} are the port-variables associated with the interface models between the piston boundaries and the gaseous compartments. For example,

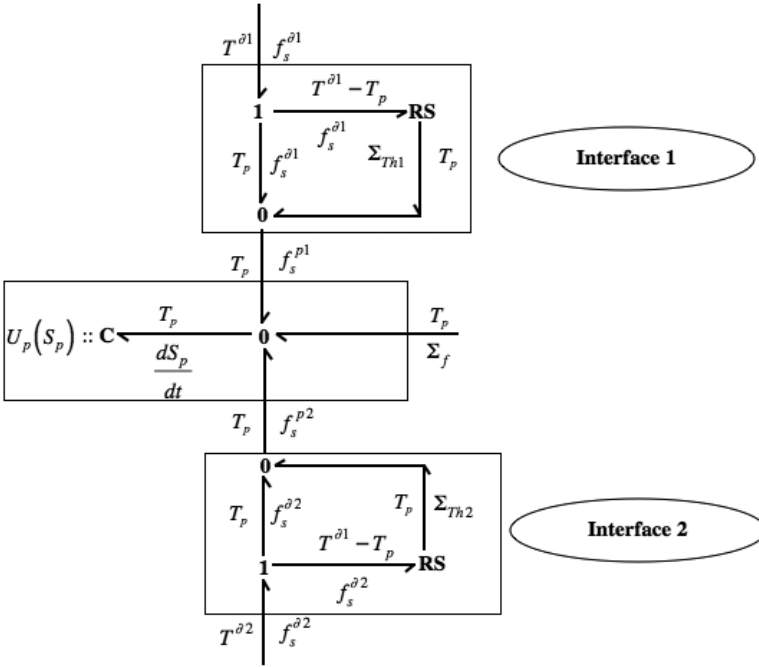


Figure 11. Thermal model of the piston.

let us consider the way the entropy flow f_s^{p1} is built according to the conservative energy flow through the boundary $\partial 1$ as characterized by the power-conjugated variables $(T^{\partial 1}, f_s^{\partial 1})$. The entropy flow $f_s^{\partial 1} = \frac{\Phi^{\partial 1}}{T^{\partial 1}}$ is associated with the heat flow $\Phi^{\partial 1}$ that is exchanged at the boundary $\partial 1$ with the gaseous compartment at a uniform temperature $T^{\partial 1}$. The entropy created per time unit by the heat transfer process between the gas and the piston boundary is given by $\Sigma_{Th1} = \frac{\Phi^{\partial 1}}{T^{\partial 1}} \left(\frac{T^{\partial 1}}{T_p} - 1 \right) > 0$ (De Groot and Mazur 1984). To represent this irreversible process, a common flow **1** junction is used so that the corresponding sum of effort variables is null:

$$T^{\partial 1} - T_p - (T^{\partial 1} - T_p) = 0 \quad (15)$$

The **1** junction allows building the difference $(T^{\partial 1} - T_p)$ that is the driving force for the entropy and heat transfer process. Then, the **R** part of the **RS** element defines a relation between the entropy flow $f_s^{\partial 1}$ and the temperature difference $(T^{\partial 1} - T_p)$ through the use of a heat transfer coefficient for example. The **S** part defines the entropy production due to the irreversible heat transfer process. This definition is power conservative:

$$f_s^{\partial 1} (T^{\partial 1} - T_p) = T_p \Sigma_{Th1} > 0 \quad (16)$$

Finally, the entropy flow f_s^{p1} is given by a **0** junction according to:

$$\begin{cases} f_s^{p1} = f_s^{\partial 1} + \Sigma_{Th1} = \frac{\Phi^{\partial 1}}{T^{\partial 1}} + \frac{\Phi^{\partial 1}}{T^{\partial 1}} \left(\frac{T^{\partial 1}}{T_p} - 1 \right) = \frac{\Phi^{\partial 1}}{T_p} \\ \Phi^{\partial 1} = T_p f_s^{p1} = T^{\partial 1} f_s^{\partial 1} \end{cases} \quad (17)$$

so that the global interface 1 model is power conservative. A similar construction is made for the $\partial 2$ boundary.

Bond Graph of the Piston Model

By encapsulating and connecting the above-described sub-models, one can build a first version of the complete piston model (Fig. 12) based on the assumption that the piston temperature is uniform. The $\mathbf{0}$ junction creates a connection preserving the continuity of the flow and effort port-variables. It does not add any information to the Bond Graph but different notations can be selected for the connected sub-models.

One can check that the global piston model as represented on the Fig. 12 satisfies the first law of Thermodynamics or total energy balance:

$$\begin{cases} \frac{dU_p}{dt} + \frac{dE_m}{dt} = T_p \frac{dS_p}{dt} + v_p \frac{dp_p}{dt} + M_p g \frac{dz_p}{dt} \\ \frac{dU_p}{dt} + \frac{dE_m}{dt} = T^{\partial 1} f_s^{\partial 1} + T^{\partial 2} f_s^{\partial 2} + P^{\partial 2} v_p A - P^{\partial 1} v_p A \end{cases} \quad (18)$$

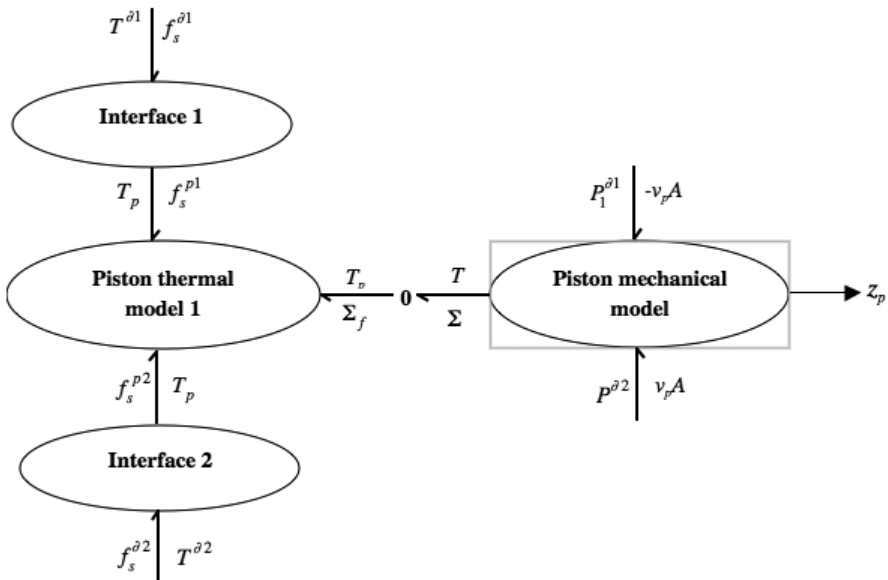


Figure 12. Piston model 1 with its interconnections port-variables.

Let us emphasize an important point concerning the Bond Graph language. We have associated with the piston object two models concerning two energetic domains (mechanical and thermal domains) and two **C** elements. Each of these elements represents the corresponding capacity to store energy and the associated energy variables (entropy, momentum and vertical position). The representation of the irreversible phenomena is also separated. The mechanical dissipation is described in the mechanical model and the thermal dissipation is described in the interface models. The Bond Graph concepts are then more phenomenological than spatial ones. The advantages of this conceptual separation will appear in the sequel: it will allow building a library of more or less detailed sub-models of given phenomena having the same port-variables. Then, they will be easily connectable and reusable according to the assumptions that are made.

Bond Graph of a Gaseous Compartment

The gaseous mixture is assumed to be perfectly mixed. Its energy is the internal energy U_g that satisfies the Gibbs equation:

$$\frac{dU_g}{dt} = T_g \frac{dS_g}{dt} - P_g \frac{dV_g}{dt} + \sum_{i=1}^c \mu_{ig} \frac{dN_{ig}}{dt} \quad (19)$$

The corresponding multi-port **C** element is represented on Fig. 13 and is associated with the three flow variables S_g , V_g and N_{ig} balance equations.

The component i material balance is:

$$\frac{dN_{ig}}{dt} = f_i^{in} + f_i^r - f_i^{out} \quad (20)$$

where $f_i^r = v_i r_v(T_g, \dots, C_k, \dots) V_g$, $r_v(T_g, \dots, C_k, \dots)$ being the volumetric chemical reaction rate and where C_k is the k^{th} component concentration. The four contributions to the i component material balance equation (20) are represented by a four links **0** junction,

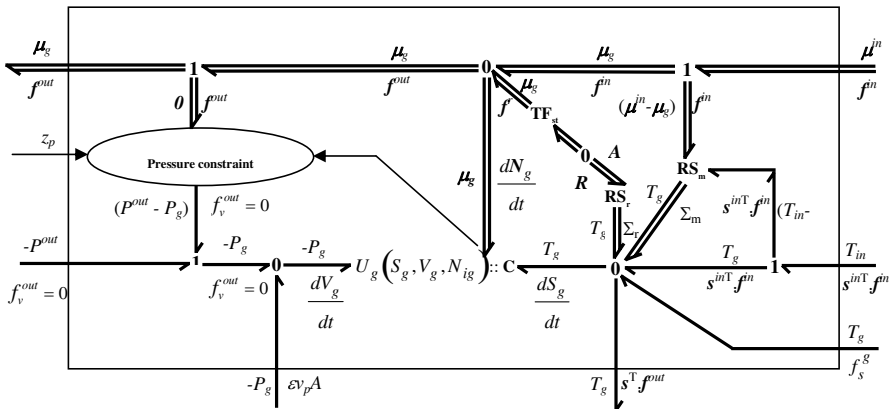


Figure 13. Gaseous compartment model with its port-variables.

the power conjugated-variables of which being respectively $\left(\frac{dN_{ig}}{dt}, \mu_{ig}\right)$, (f_i^{in}, μ_{ig}) , (f_i^r, μ_{ig}) and (f_i^{out}, μ_{ig}) . The chemical reaction stoichiometry is expressed by using direct and reverse positive stoichiometric coefficients, the reactants and products being separated:

$$\sum_i v_i^d R_i = \sum_i v_i^r P_i \quad (21)$$

This notation allows defining the power-conjugated variables associated with the chemical reaction (Oster et al. 1971).

The entropy balance equation is as follows (Couenne et al. 2006):

$$\left\{ \begin{array}{l} \frac{dS_g}{dt} = \sum_i f_i^{in} s_i^{in} - \sum_i f_i^{out} s_i^{out} + f_s^g + \Sigma_g \\ \Sigma_g = \left(\left(-\sum_i v_i \mu_{ig} \right) \frac{r_v V_g}{T_g} + \sum_i \frac{f_i^{in} \left((h_i^{in} - T_g s_i^{in}) - \mu_{ig} \right)}{T_g} \right) = \Sigma_r + \Sigma_m \end{array} \right. \quad (22)$$

On the corresponding five links **0** junction (see Fig. 13), one finds the five contributions to the entropy balance: the storage term, the convected entropy flows associated with the gas inlet and outlet molar flows, the entropy flow due to the heat transfer with the piston and the total irreversible entropy production Σ_g that is made with two contributions.

The first one is the entropy production due to the chemical reaction $\Sigma_r = \frac{1}{T_g} \left(\left(-\sum_i v_i \mu_{ig} \right) r_v V_g \right)$ where $A_f = -\Delta_r G = -\sum_i v_i \mu_i$ is the opposite of the reaction Gibbs free energy or affinity (De Groot and Mazur 1984). This first irreversible process is represented by the **RS_r** element in the Bond Graph. To this end, the affinity A_f is decomposed into direct and reverse affinities that are expressed by using the stoichiometric coefficients according to equation (21) (Oster et al. 1971): A_f

$= A_r - A_d$. Then the **A** vector is defined as follows: $\mathbf{A} = \begin{pmatrix} A_d \\ A_r \end{pmatrix} = \begin{pmatrix} [v^D] \\ [v^R] \end{pmatrix} \begin{pmatrix} \mu_1 \\ \vdots \\ \mu_C \end{pmatrix}$ where

$[v^D]$ and $[v^R]$ contain the direct and reverse stoichiometric coefficients. Similarly, the reaction rate is decomposed into a direct r_v^d and a reverse r_v^r contribution. The direct and reverse affinities $\begin{pmatrix} A_d \\ A_r \end{pmatrix}$ are then the effort variables associated with the flow variables defined as follows: $\mathbf{R} = \begin{pmatrix} +(r_v^d - r_v^r) V_g \\ -(r_v^d - r_v^r) V_g \end{pmatrix}$. The following constitutive equations

of the corresponding transformer **TF_{st}** represented in Fig. 13 are then as follows:

$$\left\{ \begin{array}{l} \begin{pmatrix} A_d \\ A_r \end{pmatrix} = M \begin{pmatrix} \mu_1 \\ \vdots \\ \mu_C \end{pmatrix} \\ \begin{pmatrix} f_1^r \\ \vdots \\ f_C^r \end{pmatrix} = M^T \begin{pmatrix} +(r_v^d - r_v^r)V_g \\ -(r_v^d - r_v^r)V_g \end{pmatrix} \end{array} \right. \quad \text{With } M = \begin{pmatrix} [v^D] \\ [v^R] \end{pmatrix} \quad (23)$$

The second source of entropy production $\Sigma_m = \sum_i \frac{f_i^{in} ((h_i^{in} - T_g s_i^{in}) - \mu_{ig})}{T_g}$ is due to the mixing process between the inlet gas flow and the gaseous compartment content. It is represented by the \mathbf{RS}_m element. This element is unusual since it is a three-port one. As a matter of fact, the entropy production Σ_m is generated from the material domain and the thermal domain. Furthermore, its constitutive relation is not the one of a classical resistive element since it is a function of convective material flows.

Finally, let us consider the coupling between the gaseous compartment model and the piston model as well as the reactor environment. The spatial port $(\varepsilon v_p A, -P_g)$ allows coupling the gaseous compartment model to the piston model in order to generate the gaseous volume or space balance equation:

$$\frac{dV_g}{dt} = \varepsilon v_p A \quad (24)$$

Where $\varepsilon = -1$ for the compartment 1 and $\varepsilon = 1$ for the compartment 2. As far as the associated effort variables are concerned, the continuity is assumed, i.e.:

$$P^o = P_g \quad (25)$$

The pressure in the gaseous compartment being assumed to be uniform, it is the pressure applied to the piston surface. These relations are represented by the $\mathbf{0}$ junction that is connected to the spatial port of the gaseous compartment \mathbf{C} element.

According to the piston position (see Fig. 9), a gaseous compartment is either a closed or an open system. Let us assume an instantaneous transition between the open/closed states characterized by a position level $z_{p,0}$. When a compartment is in the closed state, $f_i^{in} = 0$ and $f_i^{out} = 0$. Otherwise, the inlet molar flow of component i is given by: $f_i^{in} = F^{in} y_i^{in}$ where y_i^{in} is the inlet molar fraction of component i and F^{in} the total molar inlet flow. F^{in} and y_i^{in} are imposed by the reactor environment at the inlet orifice. The outlet molar flows are defined similarly: $f_i^{out} = F^{out} y_i^{out}$. They are calculated by the model. F^{out} is calculated in order the total material balance to be satisfied for a given value of P_g . To this end, a two-port element ‘‘Pressure constraint’’ is introduced to couple the spatial domain $\mathbf{1}$ junction to the $\mathbf{1}$ junction of the material domain. The power-conjugated variables of this two-port element are:

- $f_v^{out} = 0$ is the space flow variable associated with the effort variable $P^{out} - P_g = 0$,
- $f_i^{out} = F^{out} y_i^{out}$, the outlet component i molar flows are associated with a zero effort variable, the gaseous compartment being assumed to be perfectly mixed.

The two-port “Pressure constraint” element is also linked to the signal variable z_p to commute between the two closed/opened situations. If the outlet orifice is closed, $f_i^{out} = 0$. Otherwise, F^{out} is calculated by imposing the pressure constraint $P^{out} - P_g = 0$ where P^{out} is the pressure within the outlet orifice that is also imposed by the reactor environment (Couenne et al. 2006). The constrained volumetric flow $f_v^{out} = 0$ does not modify the space balance equation (25) as it is represented by the $\mathbf{0}$ junction:

$$\frac{dV_g}{dt} = \varepsilon v_p A + f_v^{out} = \varepsilon v_p A \quad (26)$$

This 0 valued flow means that the vertical wall of the cylinder is motionless.

Let us notice that a more realistic model should be to consider a continuous variation of the orifices section between two levels $z_{p+} > z_p$ and a pressure loss law for each of them, $F = F(\Delta P)$ calculating the total inlet and outlet flows according to the corresponding pressure difference. The entropy production due to these viscous losses would have been included in the model. In the Bond Graph model, a three-port “Pressure loss” element would have replaced the two-port “Pressure constraint” one to include in the entropy balance through the corresponding $\mathbf{0}$ junction the entropy production due to viscous dissipation. On the “encapsulated” gaseous compartment Bond Graph (see Fig. 13), the port-variables to be connected to the other sub-models are clearly visible.

Bond Graph of the Reactor

The complete model is obtained by connecting the above-described sub-models through the port-variables according to Fig. 14.

The component i molar flows f_i^{in} and f_i^{out} depend on the piston position as transmitted by the z_p signal. In order to simplify the presentation, we have neglected the internal energy of the cylinder wall. The total energy of the reactor is then:

$$E = U_1 + U_2 + U_p + E_m \quad (27)$$

where U_1 and U_2 are the internal energies of the gaseous compartments 1 and 2, U_p the internal energy of the piston and E_m its total mechanical energy. The total energy accumulation term is then:

$$\frac{dE}{dt} = \frac{dU_1}{dt} + \frac{dU_2}{dt} + \frac{dU_p}{dt} + \frac{dE_m}{dt} \quad (28)$$

One can check that by including the flow variables balance equations in equation (28), the global energy balance of the system is satisfied:

$$\frac{dE}{dt} = \sum_i f_i^{in} h_i^{in} - \sum_i f_i^{out} h_i^{out} \quad (29)$$

As a matter of fact, the reactor has been assumed to be adiabatic, hence only the energy convected by the gaseous inlet and outlet flows is exchanged with the reactor environment.

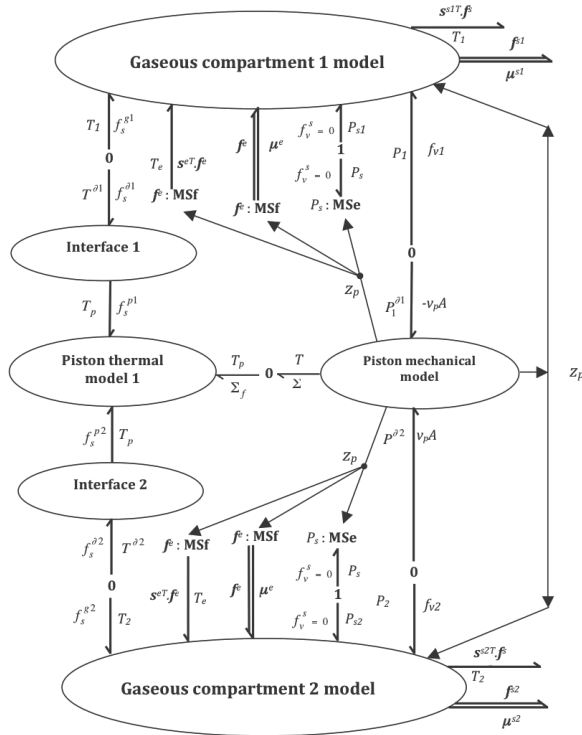


Figure 14. Reactor model with its port variables.

Bond Graph Application to Chemical Engineering: Infinite Dimensional Systems

The state variables of an infinite dimensional system are functions of the spatial coordinates. In such cases, the dynamic models are made of partial differential equations. In Chemical Engineering, such models are obtained from local balances.

The Bond Graph language has been extended to infinite dimensional systems (Maschke and van der Schaft 2001; Baaiu et al. 2008; Franco et al. 2006). As far as thermodynamic systems are concerned, the starting point is the local version of the Gibbs equation (7) that is commonly used in the irreversible thermodynamic theory (De Groot and Mazur 1984; Bird et al. 2002) with respect to mass instead of mole:

$$du = Tds - Pd\upsilon + \sum_{i=1}^C \mu_i d\omega_i \quad (30)$$

u is the internal energy per mass unit. The energy-conjugated variables are $((T, s), (-P, \upsilon), (\mu_i, \omega_i))$: s and υ are the entropy and volume per mass unit while ω_i is the component i mass fraction. The chemical potential μ_i is also expressed for the mass unit of component i . If necessary, other forms of energy can be included to define a generalized Gibbs local equation. For example, if kinetic energy has to be considered in a model, the corresponding energy-conjugated variables (\mathbf{v}, \mathbf{p}) have to

be used where \mathbf{v} is the mass average velocity and \mathbf{p} the momentum per mass unit. The generalized Gibbs equation is then in this case:

$$de = \mathbf{v} \cdot d\mathbf{p} + Tds - Pdv + \sum_{i=1}^C \mu_i d\omega_i \quad (31)$$

where e is the total energy per mass unit. Equation (31) is then assumed to hold for the substantial derivatives $\frac{D}{Dt} = \frac{\partial}{\partial t} + \mathbf{v} \cdot \mathbf{grad}$ of the quantity per mass unit (Bird et al. 2002):

$$\frac{De}{Dt} = \mathbf{v} \cdot \frac{D\mathbf{p}}{Dt} + T \frac{Ds}{Dt} - P \frac{Dv}{Dt} + \sum_{i=1}^C \mu_i \frac{D\omega_i}{Dt} \quad (32)$$

The complete derivation of the transport phenomena dynamic equations in a fluid from equation (32) and the power-conjugated variables concepts has been proposed recently (Jallut 2009). In this contribution, we describe a rather simple example: the heat transfer by conduction in a solid. This example allows illustrating the way a more detailed thermal model of the piston can replace if necessary the thermal model 1 above-described and can be easily inserted in the Bond Graph model of the reactor through the port-variables.

Entropy Balance within the Piston Subject to Conduction Heat Transfer

Let us define \mathbf{j}_q the heat flux within the solid and let us suppose that the solid density ρ_p is constant. The internal energy balance is then (Bird et al. 2002):

$$\rho_p \frac{\partial u_p}{\partial t} = -\mathit{div} \mathbf{j}_q + T_p \sigma_f \quad (33)$$

σ_f is the entropy production per volume unit due to mechanical or electrical dissipative phenomena for example. By using the local Gibbs equation in the case of a motionless isochoric solid, the equation (32) becomes:

$$\rho_p \frac{\partial u_p}{\partial t} = \rho_p T_p \frac{\partial s_p}{\partial t} \quad (34)$$

The entropy balance is then:

$$\begin{aligned} \rho_p \frac{\partial s_p}{\partial t} &= -\frac{1}{T_p} \mathit{div} \mathbf{j}_q + \sigma_f = -\mathit{div} \frac{\mathbf{j}_q}{T_p} + \mathbf{j}_q \cdot \mathbf{grad} \frac{1}{T_p} + \sigma_f \\ \rho_p \frac{\partial s_p}{\partial t} &= -\mathit{div} \mathbf{j}_s + \sigma_{th} + \sigma_f \end{aligned} \quad (35)$$

The entropy flux is then defined as $\mathbf{j}_s = \frac{\mathbf{j}_q}{T_p}$ while a supplementary entropy production term appears due to heat transfer $\sigma_{th} = \mathbf{j}_q \cdot \mathbf{grad} \frac{1}{T_p}$.

The equation (34) is the constitutive equation of a **C** element expressing the capacity of the solid to store energy and entropy. This **C** element appears in the corresponding Bond Graph represented on Fig. 15.

The **DTF** junction element for **Differential Transformer** is the infinite dimensional counterpart of the **TF** transformer. The constitutive equation of the **DTF** when applied to the entropy balance is as follows:

$$\iint_{\partial} T \mathbf{j}_s \mathbf{n} dA = \iiint_V \text{div}(T \mathbf{j}_s) dV = \iiint_V T \text{div}(\mathbf{j}_s) dV + \iiint_V \mathbf{j}_s \cdot \mathbf{grad}(T) dV \quad (36)$$

where \mathbf{n} is an outward normal vector to the solid surface. This integral relation (Stokes formulae) expresses the power continuity. It allows transforming the power-conjugated couple of variables $(T^\partial, \mathbf{j}_s^\partial)$ defined at the domain boundary ∂ into two couples of power-conjugated variables defined within the domain $(T, \text{div}(\mathbf{j}_s))$ and $(\mathbf{j}_s, \mathbf{grad}(T))$.

The couple $(T^\partial, \mathbf{j}_s^\partial)$ defines the boundary conditions and are the port variables of the Bond Graph sub-model. The couple $(T, \text{div}(\mathbf{j}_s))$ expresses the **C** element entropy balance equation (35). Finally, the couple $(\mathbf{j}_s, \mathbf{grad}(T))$ defines a constitutive equation for the **R** part of the **RS** element. In the heat conduction, this relation is derived from the Fourier law (Bird et al. 2002).

In order to simplify the presentation, let us assume that T_p only depends on z (see Fig. 9). The left hand side term in equation (36) is then:

$$\iint_{\partial} T_p \mathbf{j}_s \mathbf{n} dA = (T_p^{\partial 1} j_s^{\partial 1} - T_p^{\partial 2} j_s^{\partial 2}) A = (T_p^{\partial 1} f_{sp}^{\partial 1} - T_p^{\partial 2} f_{sp}^{\partial 2}) \quad (37)$$

The bond Graph represented on Fig. 15 has to be connected to the models of the gaseous compartments and the mechanical part of the piston model. The interface model as defined above is used to connect the gaseous compartments models to the thermal model 2 (Fig. 16).

The connection with the mechanical model of the piston is made through the spatial representation of the mechanical energy dissipation. A continuous power coupling is represented by the ‘‘Coupling’’ element defined as follows:

$$\iiint_V \sigma_f dV = \Sigma_f = \Sigma \quad (38)$$

The equation (38) expresses a scale adaptation or multi-scale coupling between the finite dimensional mechanical model of the piston and the infinite dimensional

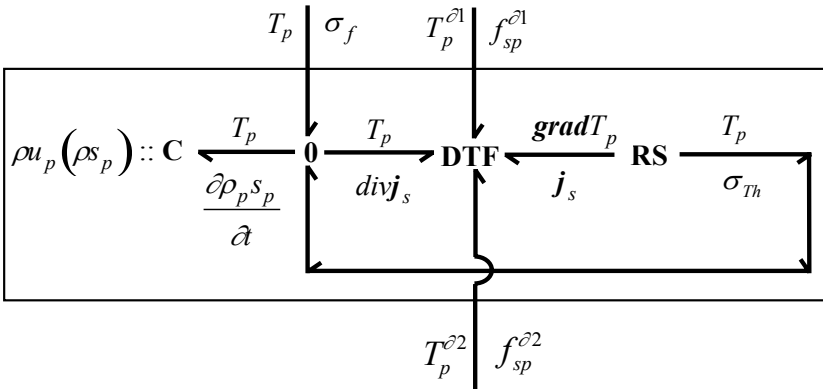


Figure 15. Piston infinite dimensional thermal model 2 and its port-variables.

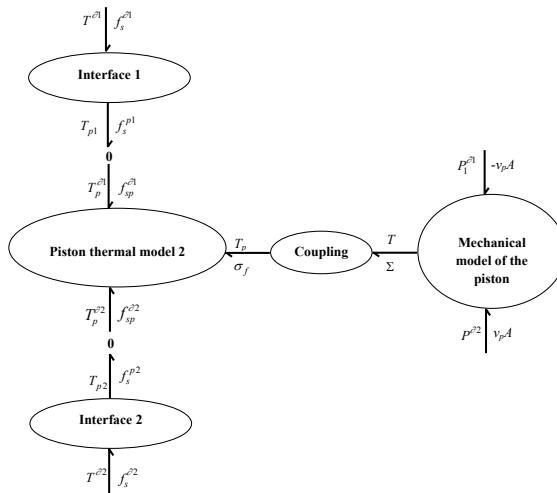


Figure 16. Infinite dimensional piston thermal model 2.

piston thermal model 2 (in Baaiu et al. 2008 is given another example of such a multi-scale coupling in mass transfer modelling).

Numerical Aspect: DTF Spatial Discretization

An infinite dimensional Bond Graph model can be automatically spatially discretized in such a way that the obtained finite dimensional model is also a Bond Graph model. This finite dimensional Bond Graph model is similar to the infinite dimensional original models, only the constitutive relations are modified.

The proposed discretization technique is similar to the mixed finite element method (Bossavit 1998) method adapted to **DTF** and distributed **C** and **RS** elements. These geometrical discretization methods have been presented in Golo et al. (2004) and applied to bidispersed models of adsorption columns (Baaiu et al. 2009). More recently, it has been shown that the collocation methods can also be adapted in order the Bond Graph structure for a model to be preserved (Moulla et al. 2012).

From an infinite dimensional Bond Graph model, it is then possible to generate a similar finite dimensional Bond Graph model for numerical simulation purposes. The port-variables associated with the discretized Bond Graph are simply the projection of the original ones on well-suited basis. Generating numerical models is then performed automatically, leading to a reduction in development costs.

Conclusion

Within the context of Green Process Engineering, chemical engineers will probably have to consider new intensified and highly efficient systems to be integrated into complex processes due to their compactness. To cope with this situation, Computer Aided Process Engineering softwares will probably have to be more and more

flexible. In particular, Model Management during the processes life will have to be improved.

In this contribution, we have presented the graphical Bond Graph language that seems to be adapted to this situation. It allows the design of easily reusable and portable models as well as versatile models of multi-physics and multi-scale systems through the use of energy-conjugated and port variables.

We have given an example of application of this language to a multi-physic and multi-scale chemical process. A model is built from easily connectable sub-models. Only the graphical aspect of the language has been illustrated but different commercially available softwares are based on this language.

Usually these softwares do not include thermodynamic and transport properties calculations that are so important in Chemical Engineering. Furthermore, they are mainly designed for finite dimensional systems. As far as discretization techniques are concerned, we have given some indications on existing techniques that allow the spatial discretization of an infinite dimensional Bond Graph model into a finite dimensional Bond Graph model.

New developments are then necessary to facilitate and promote the use of Bond Graph language in Chemical Engineering. Despite the multiple advantages of the Bond Graph language, its diffusion into the community of Chemical Engineering will heavily depend on using dynamic models in designing innovative processes as well as on integrating softwares dedicated to the numerical models of thermodynamic properties and those dedicated to Bond Graph based dynamical modelling.

References

- Baaiu, A., F. Couenne, Y. Le Gorrec, L. Lefèvre and M. Tayakout. 2008. Port based modelling of a multiscale adsorption column. *Math Comp. Model Dyn.* 14: 195–211.
- Baaiu, A., F. Couenne, Y. Le Gorrec and L. Lefèvre. 2009. Port based discretization of an adsorption process. *J. Process Contr.* 19: 394–404.
- Barton, P.I. and C.C. Pantelides. 1994. Modelling of combined discrete/continuous processes. *AIChE J.* 40: 966–979.
- Belaud, J.P. and M. Pons. 2002. Open software architecture for process simulation. *Comput. Aided Chem. Eng.* 10: 847–852.
- Belaud, J.P., K. Alloula, J.M. Le Lann and X. Joulia. 2001. Open software architecture for numerical solvers. *Comput. Aided Chem. Eng.* 9: 967–972.
- Bird, R.B., W.E. Stewart and E.N. Lightfoot. 2002. *Transport Phenomena*, Second Edition, John Wiley & Sons, New-York.
- Bogusch, R., B. Lohmann and W. Marquardt. 2001. Computer-aided process modelling with ModKit. *Comput. Chem. Eng.* 25: 963–995.
- Bossavit, A. 1998. *Computational Electromagnetism*. Academic Press, New York.
- Breedveld, P.C. 1981. Thermodynamic bond graphs: a new synthesis. *Int. J. Model Simulat.* 1: 57–61.
- Breedveld, P.C. 1999. On state-event constructs in physical system dynamics modelling. *Simul. Model Pract. Th.* 7: 463–480.
- Broenink, J.F. 1997. Modelling, simulation and analysis with 20-sim. *Journal A Special Issue CACSD* 38: 22–25.
- Cameron, I.T. and G.D. Ingram. 2008. A survey of industrial process modelling across the product and process life cycle. *Comput. Chem. Eng.* 32: 420–438.
- Charpentier, J.C. 2009. Perspective on multiscale methodology for product design and engineering. *Comput. Chem. Eng.* 33: 936–946.

- Choulak, S., F. Couenne, Y. Le Gorrec, C. Jallut, P. Cassagnau and A. Michel. 2004. A generic dynamic model for simulation and control of reactive extrusion. *IEC Res.* 43: 7373–7382.
- Couderc, J.P., C. Gourdon and A. Liné. 2008. *Phénomènes de transfert en génie des procédés*. Lavoisier Tec et Doc, Paris.
- Couenne, F., C. Jallut, B. Maschke, P.C. Breedveld and M. Tayakout. 2006. Bond graph modelling for chemical reactors. *Math Comp. Model Dyn.* 12: 159–174.
- Couenne, F., C. Jallut, B. Maschke, M. Tayakout and P.C. Breedveld. 2008a. Structured modelling for processes: a thermodynamical network theory. *Comput. Chem. Eng.* 32: 1128–1142.
- Couenne, F., C. Jallut, B. Maschke, M. Tayakout and P.C. Breedveld. 2008b. Bond Graph for dynamic modelling in chemical engineering. *Chem. Eng. Process.* 47: 1994–2003.
- De Groot, S.R. and P. Mazur. 1984. *Non Equilibrium Thermodynamics*. Dover, New-York.
- Diaz-Zuccarini, V. and C. Pichardo-Almarza. 2011. On the formalization of the multi-scale and multi-science processes for integrative biology. *Interface Focus.* 1: 426–437.
- Eggersmann, M., L. von Wedel and W. Marquardt. 2004. Management and reuse of mathematical models in the industrial design process. *Chem. Eng. Technol.* 27: 13–22.
- Franco, A.A., P. Schott, C. Jallut and B.M. Maschke. 2006. Multi-scale Bond graph model of the electrochemical dynamics in a fuel cell. 5th MATHMOD conference, Vienna, Austria, February 8–10, 2006.
- Franco, A.A., P. Schott, C. Jallut and B. Maschke. 2007. A multi-scale dynamic mechanistic model for the transient analysis of PEMFCs. *Fuel Cells* 2: 99–117.
- Friedly, J.C. 1972. *Dynamic Behaviour of Processes*. Prentice-Hall, Englewoods Cliffs, New Jersey.
- Gawthrop, P. and L. Smith. 1996. *Meta-modelling: Bond Graphs and Dynamic Systems*. Prentice Hall, Hemel.
- Gilles, E.D. 1998. Network theory for chemical processes. *Chem. Eng. Technol.* 21: 121–132.
- Golo, G., V. Talasila, A.J. van der Schaft and B.M. Maschke. 2004. Hamiltonian discretization of boundary control systems. *Automatica* 40: 757–771.
- Jallut, C. 2009. Port-based modelling and irreversible thermodynamics. pp. 172–209. *In: A. Duindam, S. Macchelli, H. Stramigioli and Bruyninckx (eds.). Modelling and Control of Complex Physical Systems. The Port Hamiltonian Approach*. Springer, Berlin.
- Karnopp, D.K. 1979. On the order of a physical system model *Trans. of the ASME, J. of Dyn. Sys. Mea. Control.* 101: 185–186.
- Karnopp, D., D. Margolis and R. Rosenberg. 2000. *Systems Dynamics: A Unified Approach*. John Wiley & Sons, New York.
- Klatt, K.-U. and W. Marquardt. 2009. Perspectives for process systems engineering—Personal views from academia and industry. *Comput. Chem. Eng.* 33: 536–550.
- Levenspiel, O. 1972. *Chemical Reaction Engineering*. Wiley and Sons, New-York.
- Lieto, J. 2004. *Le génie chimique à l’usage des chimistes*. Lavoisier Tec et Doc, Paris.
- Luyben, W.L. 1990. *Process Modelling, Simulation and Control for Chemical Engineers*. Second edition, McGraw-Hill, New-York.
- Mangold, M., S. Motz and E.D. Gilles. 2002. A network theory for the structured modelling of chemical processes. *Chem. Eng. Sci.* 57: 4099–4116.
- Mangold, M., O. Angeles-Palacios, M. Ginkel, A. Kremling, R. Waschler, A. Kienle and E.D. Gilles. 2005. Computer-aided modelling of chemical and biological systems: methods, tools, and applications. *Ind. Eng. Chem. Res.* 44: 2579–2591.
- Marquardt, W. 1996. Trends in computer aided modelling. *Comput. Chem. Eng.* 20: 591–609.
- Maschke, B. and A.J. van der Schaft. 2001. Canonical inter-domain coupling in distributed parameter systems: an extension of the symplectic gyrator. *Proc. Int. Mechanical Engineering Congress and Exposition*, New-York.
- Mattson, S., H. Elmquist and M. Otter. 1998. Physical system modelling with Modelica. *Control Eng. Pract.* 6: 50–510.
- Mattsson, S.E., M. Andersson and K.J. Åström. 1993. Object-oriented modelling and simulation. pp. 31–69. *In: D.A. Linkens (ed.). CAD for Control Systems*. Marcel Dekker Inc., New York.
- Morales-Rodríguez, R. and R. Gani. 2007. Computer-aided multiscale modelling for chemical process engineering. *Computer Aided Chem. Eng.* 24: 207–212.

- Morales-Rodríguez, R., R. Gani, S. Déchelotte, A. Vacher and O. Baudouin. 2008. Use of CAPE-OPEN standards in the interoperability between modelling tools (MoT) and process simulators (Simulis® Thermodynamics and ProSimPlus). *Chem. Eng. Res. Des.* 86: 823–833.
- Moulijn, J.A., A. Stankiewicz, J. Grievink and A. Gorak. 2008. Process intensification and process systems engineering: a friendly symbiosis. *Comput. Chem. Eng.* 32: 3–11.
- Moulla, R., L. Lefèvre and B. Maschke. 2012. Pseudo-spectral methods for the geometric reduction of systems of conservation laws. *Journal of Computational Physics* 231: 1272–1292.
- Nilsson, B. 1994. Dynamic modelling of chemical processes using OMOLA. *Chem. Eng. Res. Des.* 2: 364–370.
- Oster, G., A. Perelson and A. Katchalsky. 1971. Network thermodynamic. *Nature* 234: 393–399.
- Otter, M., H. Elmqvist and S.E. Mattsson. 2007. Multi-domain modelling with modelica. pp. 36.1–36.27. *In: Paul A. Fishwick (ed.). Handbook of Dynamic System Modelling.* Chapman & Hall/CRC, Boca Raton.
- Ould-Bouamama, B., R. El Harabi, M.N. Abdelkrim and M.K. Ben Gayed. 2012. Bond graphs for the diagnosis of chemical processes. *Comput. Chem. Eng.* 36: 301–324.
- Perkins, J., R. Sargent, R. Vazquez-Roman and J. Cho. 1996. Computer generation of process models. *Comput. Chem. Eng.* 20: 635–639.
- Ponton, J. and P. Gawthrop. 1991. Systematic construction of dynamic models for phase equilibrium processes. *Comput. Chem. Eng.* 15: 803–808.
- Preisig, H. 1996. Computer-aided modelling: two paradigms on control. *Comput. Chem. Eng. (Suppl. B):* S981–S986.
- Roestenberg, T., M.J. Glushenkov, A.E. Kronberg, H.J. Krediet and Th H. Van der Meer. 2010. Heat transfer study of the pulsed compression reactor. *Chem. Eng. Sci.* 65: 88–91.
- Saisset, R., G. Fontes, C. Turpin and S. Astier. 2006. Bond Graph model of a PEM fuel cell. *J. Power Sources* 156: 100–107.
- Sandler, S.I. 1999. *Chemical and Engineering Thermodynamics.* John Wiley & Sons, New-York.
- Stankiewicz, A. 2006. Energy matters. Alternative sources and forms of energy for intensification of chemical and biochemical processes. *Chem. Eng. Res. Des.* 84: 511–521.
- Stephanopoulos, G., G. Henning and H. Leone. 1990a. MODEL.LA: a modelling language for process engineering: the formal framework. *Comput. Chem. Eng.* 14: 813–846.
- Stephanopoulos, G., G. Henning and H. Leone. 1990b. MODEL.LA: a modelling language for process engineering: Multifaceted modelling of processing systems. *Comput. Chem. Eng.* 14: 847–869.
- Tränkle, F., M. Zeitz, M. Ginkel and E.D. Gilles. 2000. ProMot: a modelling tool for chemical processes. *Math. Comp. Model. Dyn.* 6: 283–307.
- Vidal, J. 2003. *Thermodynamics. Application in Chemical Engineering and the Petroleum Industry.* Technip, Paris.
- Villiermaux, J. 1993. *Génie de la réaction chimique.* Lavoisier Tec et Doc, Paris.
- Westerweele, M.R., H. Preisig and M. Weiss. 1999. Concept and design of Modeller, a computer-aided modelling tool. *Comput. Chem. Eng. (Suppl.)* 23: S751–S754.

PART 2

**Technologies and
Innovative Methods for
Intensification**

4

Process Intensification by Miniaturization

Joelle Aubin, Jean-Marc Commenge, Laurent Falk and Laurent Prat

Introduction

Fine chemicals and pharmaceuticals industries produce high value-added molecules in discontinuous workshops, mainly comprised of stirred tanks. Whereas the synthesized products result from advanced chemical research, the corresponding production processes are based on poorly efficient devices that may exhibit detrimental drawbacks with respect to the product quality, the environment (through excessive energy or solvent requirements), as well as process safety. The low performance of such equipment, and their accompanying high operating costs, is currently the basis of an awareness of the fine chemicals industry. This is particularly obvious for the production of intermediate products, for which the limitations induced by medium-size and large-size stirred tanks cause product losses by their low selectivity. Indeed, stirred vessels possess low thermal management capacities. For this reason, exothermic reactions are often performed in fed batch reactors or require appropriate dilution of the reactants. This can increase the amount of impurities and the need for additional downstream separation steps. The use of solvents is also detrimental for several reasons. Firstly, the use of solvents that cannot be fully refined and recycled induces direct and indirect environmental wastes. Secondly, additional separation units, as well as waste treatment and solvent recycling steps require large amounts of energy, and these expenses increase with the quantity of solvent involved in the process. Furthermore since the reaction rates are directly related to the concentration of reactants, the above-mentioned dilution contributes to a decrease in reaction rates. This results in an increase in the synthesis times, which induces an increase in the operating costs and the energy consumption, as well as a decrease in the productivity per unit volume. Finally, scale-up from the laboratory scale to the production scale is critical, especially for new added-value molecules. The use of

low-performance and difficultly scalable equipment lengthens the development steps before industrialization and the time to market. The corresponding costs can be particularly penalizing in the current context of strong economic competition.

Over recent years, an alternative to batch reactors has been made available through the development of intensified processes and microstructured reactors. The opportunity consists in converting the discontinuous operation of the reactions into a continuous operation in low-inventory intensified reactors, where operating conditions are finely controlled. The intensification provided by process miniaturization offers various advantages that allow the development of much more efficient processes in terms of energy consumption, raw materials and solvents. The dramatic decrease in residence times enables higher selectivity to be reached by avoiding the formation of secondary products. These low residence times and the possibility to precisely control the flow of reactants also provide the possibility to operate at higher temperatures despite the unfavorable activation effect of secondary reactions. Improved control of heat transfer also prevents thermal runaway of the reactions, as well as the detrimental impact of thermally-activated secondary reactions. For many reactions usually performed at low temperatures, it is even possible to suppress energy-consuming cryogenic cooling systems. The high-performance heat transfer also offers the opportunity to operate with highly-concentrated media, which helps reduce the required amounts of solvents. Micromixers, coupled or not with heat exchangers, are also very effective in increasing mixing efficiency and phase transfer, and contribute in many cases to the improvement of the yield and selectivity of reactions.

In this chapter, the main principles of intensification by miniaturization are presented. This approach is based on a simple analysis of characteristic times and demonstrates how the characteristic dimensions of the devices influence the acceleration of chemical and physical phenomena. The comparative study of these characteristic times not only enables the limitations of a given system to be identified, but it also shows how a process can be selectively enhanced by adjusting the dimensions of the system. Examples of different technologies and applications are also presented for three types of devices: mixers, contactors and heat exchangers.

Technical Principles of Intensification by Miniaturization

One of the main characteristics of chemical processes resides in the fact that their overall performance results from the coupling of diverse fundamental physical and chemical phenomena. Depending on the different coupled phenomena and the relative importance of each, one of them may be limiting with respect to the others. This then allows reactive systems to be operated in different ways; for example, when the reaction is coupled to mass transfer, it can be operated in either the chemical regime or in the diffusion regime.

The basis of process intensification by miniaturization consists in decreasing the characteristic dimension of the system in order to change the relative influence of the phenomena involved by modifying their relative rates. In fact, the following section shows that the process characteristics depend on different time-scales, and that it is possible to change the order in which the phenomena occur by adapting the characteristic dimension to guide the overall performance to a particular purpose.

Relationship Between Process Performance and Characteristic Times

Let us define the performance of a unit operation or a specific device, i.e., a reactor, a heat exchanger or a mass transfer column by its efficiency η . For instance, the efficiency of a heat exchanger is usually defined as the ratio of the transferred heat flux to the maximal heat flux that could be transferred. For chemical reactors, efficiency is the ratio of the number of moles (batch mode) or the molar flux (continuous mode), which is transformed into the maximum number of moles or molar flux that can react and is then equivalent to a conversion. In both cases, the quantity of heat and mass transferred in the exchanger and the quantity of moles transformed in the chemical reactor are defined as the extensity of interest. Similar definitions can be used for any other operation or physico-chemical process and even for hydrodynamic phenomenon, such as capillary ascension where the efficiency is defined as the ratio of the height of the meniscus at time t to the equilibrium height. In the following paragraphs, the term 'operation' is used as a generic term, which represents either a physico-chemical process or an operation in a device.

In simple cases, where the rate of transformation (chemical reactor) or the flux of transfer (heat and mass transfer) is linear to the extensity (first-order process), the operation efficiency can be related to the ratio of the space-time τ in the device to the characteristic time of the operation t_{op} . The space-time is defined as the ratio of the volume V of fluid in the device to the volumetric flow rate Q at the inlet of the device. The characteristic time of the operation can be defined as a magnitude that represents the speed or the ease of the operation. The smaller the characteristic time, the easier or the faster the operation is. The notion of characteristic time is directly related to the concept of intensification, which can be defined here as the means implemented to decrease this characteristic time.

For plug-flow conditions, this relation between efficiency and the characteristic time of the operation can be written as:

$$\eta = 1 - \exp\left(-\frac{\tau}{t_{op}}\right) \quad (1)$$

For perfectly-mixed flow conditions, it becomes:

$$\eta = \frac{\frac{\tau}{t_{op}}}{1 + \frac{\tau}{t_{op}}} \quad (2)$$

The ratio of the space-time of the fluid in the device to the global characteristic time of the operation carried out in this device can be defined as the Number of Operation Units (*NOU*), which is an extension of the concept of the Number of mass Transfer Units and heat Transfer Units (*NTU*) that is well known in chemical engineering. For chemical reactors, this ratio is named the Damköhler number:

$$NOU = \frac{\tau}{t_{op}} \quad (3)$$

Indeed, these simple relationships illustrate the inter-dependency of the efficiency of the operation and the *NOU*, and follow the same trend where the efficiency tends

towards unity for high values of the Number of Operation Units. The example of the heat exchanger illustrates the physical significance of these relations. If the space-time is low compared with the heat transfer time t_{heat} , the resulting efficiency of the operation is poor because the fluid does not stay sufficiently long in the device to exchange enough heat. On the other hand, if the fluid remains in the device a sufficiently long time compared with the characteristic time of heat exchange, the efficiency of the heat exchange is close to unity.

Let us illustrate the simple cases of a heat exchanger and a first order homogeneous chemical reaction in a plug-flow system. In both cases, the variation of extensity is a function of the space-time and is proportional to the extensity itself:

$$\frac{dC}{d\tau} = -kC \text{ and } \frac{dT}{d\tau} = -\frac{H \cdot S}{\rho \cdot V \cdot C_p}(T - T_{ext}) \quad (4)$$

where C is the molar concentration of reactant [mol/m^3], τ the space-time [s], k the kinetics constant of the first-order rate law [s^{-1}], T the temperature [K], H the heat transfer coefficient [$\text{W}/\text{m}^2/\text{K}$], S the heat transfer area [m^2], ρ the fluid density [kg/m^3], V the volume of fluid in the device [m^3], C_p the heat capacity [$\text{J}/\text{kg}/\text{K}$] and T_{ext} the constant external temperature [K].

For these two examples, the analytical solution of the differential equations leads to the following expressions for the characteristic operation time, i.e., the characteristic time of the homogeneous reaction and the characteristic time for heat exchange:

$$t_{op} = t_{hom} = \frac{1}{k} \text{ and } t_{op} = t_{heat} = \frac{\rho \cdot V \cdot C_p}{H \cdot S} \quad (5)$$

For more complex systems, where no linear relationship between the rate of transformation or the flux of transfer can be written, more complex relationships can be derived from the heat and mass balance on the device. However, in any case, the asymptotic behavior of the efficiency with the Number of Operation Unit is conserved. Examples are not presented here and can be found in Commenge and Falk (2009).

Relationship Between the Volume of the Device and the Characteristic Operating Time

Combination of relationships (1) and (2) with the definition of the space-time leads to the following linear expressions of the volume of the device V with the characteristic time of the operation and the volumetric flow rate Q :

Plug-flow device:
$$V = t_{op} Q \text{Ln}\left(\frac{1}{1-\eta}\right) \quad (6)$$

Perfectly mixed flow device:
$$V = t_{op} Q \left(\frac{\eta}{1-\eta}\right) \quad (7)$$

These expressions show an important feature: the volume of the device is directly proportional to the characteristic time of the operation, despite the flow in the device. This means that process intensification, which consists in the reduction of the characteristic time, results in three different consequences: (i) the direct miniaturization of the device, (ii) the increase of the processed flow rate, and

(iii) the increase of the efficiency of the operation. Several strategies for process intensification can be identified, amongst which the principle of microstructuration is one of the most efficient, as illustrated in the following sections.

Relationship Between the Geometrical Dimension and the Characteristic Time

The concept of characteristic times is well known in chemical engineering; common examples are the space-time, the mean residence time and the contact time. As presented previously, the characteristic time of the operation can be seen as a magnitude that represents the speed or the ease of the operation. Mathematically, the characteristic time of a chemical or a physical phenomenon is proportional to the time taken by a system governed by this phenomenon to reach its equilibrium state after a perturbation. Practically, it can also be defined as the ratio of the quantity of extensity, which is transferred or transformed to the initial rate of transfer or transformation of this extensity. For instance, a characteristic reaction time is the ratio of the initial molar concentration of a species in mol/m^3 divided by the initial rate of reaction in $\text{mol/m}^3/\text{s}$. This definition is very similar to (but not equal to) the half-time of reaction used in chemistry that is the time required for consumption of the half quantity of the species. Table 1 collects expressions for characteristic times of different phenomena that are frequently used in chemical engineering.

In Table 1 it can be seen that the characteristic time for homogeneous reactions does not exhibit any dependency on the internal dimension of the device denoted by R , whereas the other characteristic times are strongly dependent on this dimension. This is particularly true for heat and mass transfer for which the characteristic time is proportional to the square of the characteristic dimension. As a consequence, operation in small devices or channels will intensify mass transfer much faster than other phenomena such as heterogeneous reactions or homogeneous reactions, enabling heat and mass-transfer limitations to be suppressed. Other effects such as

Table 1. Expressions of various elementary characteristic times.

Phenomenon	Characteristic time expression	Dependency with respect to dimension R
Nth-order homogeneous reaction	$t_{\text{hom}} = \frac{C_0}{r_0} = \frac{1}{k \cdot C_0^{n-1}}$	0
Apparent first-order heterogeneous reaction	$t_{\text{het},1} = \frac{R}{2k_s}$	1
Diffusive mass transfer	$t_{\text{diff}} = \frac{R^2}{D_m}$	2
Convective mass transfer at constant Sherwood number	$t_{\text{mat}} = \frac{R^2}{Sh \cdot D_m}$	2
Heat conduction	$t_{\text{cond}} = \frac{\rho \cdot Cp \cdot R^2}{\lambda}$	2
Convective heat transfer at constant Nusselt number	$t_{\text{conv}} = \frac{\rho \cdot Cp \cdot R^2}{\lambda \cdot Nu}$	2

gravity and surface tension present intermediate behavior with power-law relations, demonstrating that the hydrodynamics of two-phase flow in microstructured systems can be significantly different compared with that in conventional equipment (Commence and Falk 2009). Heterogeneous reactions are a particular type of phenomenon due to the complexity of their kinetic mechanisms: this usually makes the extraction of a single characteristic time impossible, except in very particular operating conditions. These systems require particular attention.

The non-exhaustive list of expressions given in Table 1 shows that these characteristic times depend differently on the characteristic geometrical dimension. This dependency highlights the impact of the geometrical dimension and the effect of operating conditions on the coupled phenomena. For instance, the determination of the kinetics of a homogeneous exothermic reaction in a reactor requires consideration of the intrinsic chemical reaction rate and the heat transfer. Both phenomena can be described by a characteristic time that exhibits a different relationship with respect to the geometrical dimension. In a conventional macro-scale reactor, heat transfer limitations can lead to non-isothermal behavior and biased reaction rates; a microreactor, on the other hand, provides intensive heat transfer that enables perfect isothermal conditions to be reached and the intrinsic kinetics to be obtained. In fact, the phenomena are very often coupled to one another and several characteristic times need to be considered. In the following section, it will be shown that a unique characteristic time can be defined and related to the efficiency of the operation.

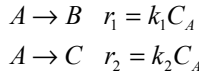
Coupled Phenomena

Unit operations in chemical engineering are very often based on coupled phenomena, principally heat or mass transfer with chemical reactions. The previously presented characteristic time approach focused on a single phenomenon and showed the relationship between the efficiency of a process and the Number of Operation Units. This approach can be extended to more complex and multiple phenomena, where a global characteristic time is considered and defined as a combination of the elementary characteristic times.

The most common way to couple phenomena is in series and in parallel, as illustrated in the following examples:

- A reactant A involved in two simultaneous homogeneous reactions leading respectively to B and C ($A \rightarrow B$ and $A \rightarrow C$): the conversion of A is governed by a global characteristic time that results from the parallel coupling of the two reactions,
- A reactant A involved in a heterogeneous reaction requiring the transport of reactant A from the fluid phase to the catalytic wall: the conversion of A illustrates the serial coupling of reaction and mass transfer. The case of consecutive homogeneous reactions ($A \rightarrow B \rightarrow C$) is also, from the point of view of product C , phenomena coupled in series.

Considering the first case, assuming first-order reactions:



the overall consumption rate of reactant A can be written $r_A = (k_1 + k_2)C_A$. By definition of the characteristic reaction time, the global reaction time with respect to reactant A is:

$$t_{global} = \frac{1}{(k_1 + k_2)} = \frac{1}{(1/t_{hom1} + 1/t_{hom2})}$$

For two basic phenomena with characteristic times t_1 and t_2 , the general expression of the global operation time for phenomena coupled in parallel is:

$$\frac{1}{t_{global}} = \frac{1}{t_1} + \frac{1}{t_2} \quad (8)$$

In the case of a heterogeneous reaction coupled with a mass-transfer phenomenon, the equality between the mass-transfer flux J_A between the fluid phase and the catalytic surface, and the reaction rate leads to:

$$J_A = k_g (C_A^g - C_A^s) = r_s = k_s C_A^s \quad (9)$$

where k_g denotes the mass-transfer coefficient, C_A^g the concentration of reactant A in the fluid phase, C_A^s the concentration of A at the wall, k_s the apparent first-order reaction rate constant. The concentration of A at the solid surface is then:

$$C_A^s = \frac{k_g}{(k_g + k_s)} C_A^g \quad (10)$$

The expression of the rate of consumption of reactant A per unit volume is then given by:

$$P_A = \frac{k_g k_s a_s}{(k_g + k_s)} C_A^g \quad (11)$$

where a_s represents the specific area of the catalyst and where the expression of the global characteristic time appears as:

$$t_{global} = \frac{(k_g + k_s)}{(k_g k_s) a_s} = \frac{1}{a_s k_g} + \frac{1}{a_s k_s} = t_{het,1} + t_{mass}$$

The general expression of the global operation for phenomena coupled in series is the sum of the characteristic times of the basic phenomena with times t_1 and t_2 :

$$t_{global} = t_1 + t_2 \quad (12)$$

In the case of phenomena coupled in parallel, the global operation time is dominated by the smallest elementary time, that is to say the fastest phenomenon. In the case of two parallel reactions, the fastest reaction therefore governs the conversion of the reactant and the selectivity of the system. On the other hand, in the case of phenomena that are coupled in series, the slowest phenomenon dominates: the global time is close to the largest characteristic time. In the case of mass transfer coupled with a heterogeneous reaction, the conversion rate of A is ruled by the slowest step. In the case of a system composed of consecutive homogeneous reactions, the rate

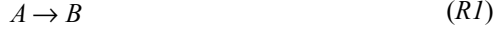
of formation of C is imposed by the kinetics of the slowest reaction. In practice, phenomena coupled in series and parallel are the most common, but phenomena may be coupled in more complex ways that require a more detailed analysis, particularly when events deviate from first order (Zlokarnik 2002). As a result, the intensification strategy is closely related to the way the involved phenomena are coupled. While the characteristic times of elementary phenomena depend on the characteristic dimension of the system, the way the phenomena are coupled is an invariant: when the phenomena are coupled in series, the slowest of the characteristic times always imposes its value as the global operation time, regardless of the absolute values of the individual characteristic times. For this reason, changing the order of importance of phenomena by properly sizing the system enables the phenomenon that govern the overall performance of the system to be selected and imposed.

Intensification by Microstructuration

Process intensification by microstructuration consists in reducing the characteristic dimension of the flow volume in order to reach a significant improvement in the process yield or device compactness. For heat transfer through a straight cylindrical channel under laminar flow conditions with a constant wall temperature boundary condition, the fully-developed Nusselt number is equal to 3.66 and does not depend on the characteristic dimension of the channel. A decrease in the channel dimension then induces a simultaneous increase in the specific heat transfer area and in the heat transfer coefficient, since both these features are inversely proportional to the channel radius R . These combined effects explain why the characteristic time of the operation evolves with the square of the channel dimension, as indicated in Table 1. In this case, a ten-fold decrease in the dimension R implies an intensification of the heat transfer (i.e., a decrease in the corresponding characteristic time) by a factor 100. If the heat transfer efficiency is maintained, which requires the Number of Operation Units to be maintained constant as well, equation (6) shows that the space-time through a heat exchanger, with channels that are 10 times smaller, is reduced by a factor of 100. Simultaneously, the heat exchanger volume is reduced by a factor of 10. Unfortunately, this remarkable gain in compactness is synonymous of a drastic increase in the pressure drop that can become a major drawback for microreactors and microstructured reactors in general. Assuming laminar flow in the channels, the Poiseuille law shows that the pressure drop is inversely proportional to the channel radius R to the power of four. In practice, the decrease in the operation time enables shorter channels to be used, thereby significantly reducing the pressure drop. The solution with the most impact resides in the subdivision of the main flow into numerous sub-flows to feed the mini- or microchannels in parallel, which enables prohibitive pressure drop to be avoided whilst maintaining the high compactness of the device. This flow parallelization is therefore the main geometric specificity of microstructured reactors and exchangers.

Application: Impact of the Intensification of Transport Phenomena on Reaction Selectivity

Let us consider the case of two parallel heterogeneous reactions coupled to potentially limiting mass transfer between the flowing gas phase and the catalytic wall:



The reaction kinetics are given by:

$$r_1 = k_1(C_A^s)^{m_1} \text{ and } r_2 = k_2(C_A^s)^{m_2}$$

where m_1 and m_2 respectively denote the orders of reactions (R1) and (R2), and C_A^s is the concentration of reactant at the catalytic surface. This example corresponds to a typical case of two parallel reactions coupled to a serial mass transfer phenomenon. The combination rules that give access to the global operation time as a function of the coupled elementary times then enable the global conversion time to be expressed with respect to the three phenomena:

$$t_{global} = t_{transfer} + t_{mass} = t_{mass} + \frac{1}{(1/t_{r_1} + 1/t_{r_2})} \quad (13)$$

with

$$\begin{aligned} t_{r_1} &= \frac{1}{a_s k_{1s} (C_{A,0}^s)^{m_1-1}} \\ t_{r_2} &= \frac{1}{a_s k_{2s} (C_{A,0}^s)^{m_2-1}} \\ t_{mass} &= \frac{1}{a_s k_g} \end{aligned} \quad (14)$$

The conversion of reactant A can then be written as:

$$X_A = 1 - \exp\left(-\frac{\tau}{t_{global}}\right) \quad (15)$$

According to equation (13), the global time of the operation is the sum of the mass transfer time and the combined reaction times, which demonstrates that the mass transfer slows down the time evolution of conversion. This limiting effect is even more pronounced when the mass transfer is slow compared with the reaction rates, which corresponds to the usual mass-transfer limitation. In addition to the above-mentioned effect of this limitation on the conversion, its impact on the selectivity is also interesting. The selectivity towards product B compared with that towards product C is defined as the ratio of both reaction rates. This selectivity can be expressed as:

$$S_{B/C} = \left[\frac{k_1}{k_2} (C_A)^{(m_2-m_1)} \right] F_{mass} \quad (16)$$

In equation (16), the term in square brackets is the classical term and F_{mass} is related to mass transfer as:

$$F_{mass} = \left[1 + \frac{t_{mass}}{t_{r1}} + \frac{t_{mass}}{t_{r2}} \right]^{(m_2 - m_1)} = K^{(m_2 - m_1)} \quad (17)$$

Note that the derivation of this expression, which is given in the “additional reading” section, is not necessary for the comprehension of the following sections. Expression (16) of the selectivity includes the product of two terms. The first is the ratio of the reaction rates, and is also found in the classical expressions of the selectivity when mass transfer limitations can be neglected (Villiermaux 1993). The second term specifically describes the impact of the mass transfer limitation on the reaction selectivity.

Additional Reading

The selectivity towards product B with respect to product C can be expressed as the ratio of the production rates of both species:

$$S_{B/C} = \frac{k_{1s}(C_A^s)^{m_1}}{k_{2s}(C_A^s)^{m_2}} = \frac{k_{1s}}{k_{2s}}(C_A^s)^{(m_1 - m_2)} \quad (i)$$

This expression depends on the concentration of reactant A at the surface of the catalyst C_A^s . This concentration is not explicitly known but is related to the concentration of reactant A in the bulk fluid. This relation can be written by equating the reaction rate and the mass-transfer flux between the fluid and the surface:

$$J_A a_s = \frac{(C_A - C_A^s)}{t_{mass}} = \left(\frac{1}{t_{r1}} + \frac{1}{t_{r2}} \right) C_A^s \quad (ii)$$

from which the explicit expression of the surface concentration of reactant A can be obtained as:

$$C_A^s = \left[\frac{t_{r1} t_{r2}}{t_{r1} t_{r2} + t_{mass}(t_{r1} + t_{r2})} \right] C_A \quad (iii)$$

Substituting this expression in equation (i) yields to the final expression of the selectivity (equation (16)).

It can be seen from equations (16) and (17) that, regardless of the values of the reaction time and mass transfer time, the parameter K is always larger than unity. It is even greater when the mass transfer is slow compared with reaction rates ($t_{mass} > t_{r1}$ and $t_{mass} > t_{r2}$). The influence of the order of the reactions can then be studied to predict the impact of the operating conditions on the selectivity. Equation (16) not only enables the classical recommendations concerning the operating concentrations (Villiermaux 1993) to be confirmed, but also allows the influence of the mass transfer rate on the selectivity to be quantified as follows:

- If $m_1 > m_2$, then:
 - the selectivity increases with the concentration of reactant A (classical term),
 - the mass transfer limitation tends to reduce the selectivity $K^{(m_2 - m_1)} < 1$.

- If $m_1 < m_2$, then:
 - the selectivity decreases when the concentration of reactant A increases (classical term),
 - the mass transfer limitation tends to improve to selectivity $K^{(m_2-m_1)} > 1$.

These effects have been highlighted by Hickman and Schmidt (1992) and can be generalized to any reactive system with limitations due to mass transfer or mixing. Many experimental studies have demonstrated that the improvement of mixing conditions generally induces a significant improvement of the reaction yield and selectivity. On the other hand, some studies showed that this improvement in mixing can also result in the reduction of selectivity, as explained by the previous relations.

Example

To properly illustrate the impact of process miniaturization on coupled transport phenomena, the influence of the diameter on the performance of a tubular reactor can be analyzed. Let us consider the flow of a reacting gas in a tube of radius R , whose walls have been coated with a catalyst. As a first approximation, the Sherwood number is assumed to be equal to 3.66. The mass transfer characteristic time and the mass transfer coefficient are given by:

$$t_{mass} = \frac{1}{a_s k_g} \text{ with } a_s = \frac{2}{R} \text{ and } k_g = \frac{Sh \cdot D_m}{2R}$$

Therefore:

$$t_{mass} = \frac{R^2}{2Sh \cdot D_m} = \frac{R^2}{7 \cdot 10^{-5}} \text{ with } Sh = 3.66 \text{ and } D_m = 10^{-5} \text{ m}^2/\text{s}$$

Using equation (16), the influence of the characteristic dimension R on the factor F_{mass} can be studied:

$$F_{mass} = \left[1 + \frac{t_{mass}}{t_{r1}} \left(1 + \frac{t_{r1}}{t_{r2}} \right) \right]^{(m_2-m_1)} = \left[1 + \frac{R^2}{7 \cdot 10^{-5} t_{r1}} \left(1 + \frac{t_{r1}}{t_{r2}} \right) \right]^{(m_2-m_1)}$$

Figure 1 presents the evolution of the factor F_{mass} as a function of the tube radius for different values of $m_1 - m_2$ (the difference in reaction orders) for a given ratio of the reaction times. For small characteristic channel dimensions, the mass transfer rate is increased with respect to reaction rates ($t_{mass} < t_{r1}, t_{r2}$) and the mass transfer factor tends towards unity, indicating that the selectivity solely results from the chemical competition between both reactions. In the present case, where the main reaction runs ten times faster than the secondary reaction, the impact of the mass transfer limitation on the selectivity is very pronounced since a decrease in the tube radius from 3 centimeters down to 3 millimeters enables the overall selectivity to be increased by a factor of five.

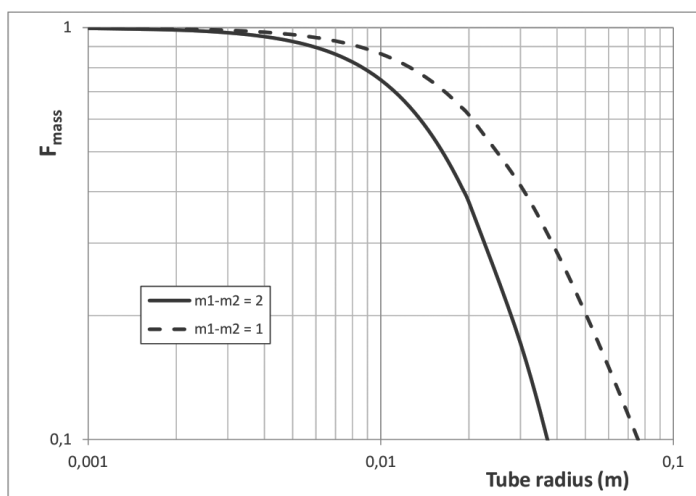


Figure 1. Influence of the tube radius on the selectivity of a heterogeneous reaction (equation (17)) (with $t_{r1}/t_{r2} = 0.1$, $t_{r1} = 10\text{s}$).

Micromixers, Fluid Contactors and Heat Exchangers

Micromixers and miniaturized fluid contactors have an important role in micro chemical processing for both miscible and immiscible fluids. They are employed to promote very fast mixing, mass transfer and/or reaction and can be associated with heat exchange devices, enabling further process intensification. They are also highly adapted to the generation of dispersions and particles with tightly specified properties.

The geometry of the device and the type of fluid contacting mechanism used strongly influences the outcome of the operation (e.g., mixing, reaction, mass or heat transfer) and therefore the process performance. For example, mixing time is directly related to the characteristic length-scale of the system, which is generally determined by the geometry and dimensions of the channels within the device; in the case of immiscible fluid contacting, the flow regime and the bubble or drop size are controlled, in part, by the characteristic dimensions of the contactor.

Fluid Contacting Mechanisms

Micromixer and fluid contactor geometries are designed to stretch fluid interfaces and significantly reduce the time required for mixing by molecular diffusion or for mass transfer. A number of different fluid contacting mechanisms exist for assisting mixing and transport processes or for creating multiphase dispersions in micro processing equipment. Most mechanisms rely on the energy of the flow (e.g., pressure gradients generated by pumping or hydrostatic differences) and the geometry of the micromixer or contactor; others use an external source of energy, such as ultrasound, electro-kinetic instabilities and periodic flow perturbations.

T- and Y-Type Contacting

These mixers are very simple geometries and relatively efficient if correctly designed and operated. At low Reynolds numbers ($Re < 40$), the streamlines in these mixers are parallel and no secondary flows are created to assist mixing; the mixing process is thus controlled by molecular diffusion and mixing time is proportional to the square of the microchannel diameter. At higher Reynolds numbers ($Re > 150$), unstable vortex structures are created, stretching and folding the fluids and decreasing the time for the diffusive mixing process. In the case of immiscible fluid contacting in these geometries, monodisperse drops or bubbles can easily be generated. The bubble and drop sizes depend largely on the characteristic dimensions of the micromixer but also on the physical properties of the fluids and surface effects, such as wettability.

Multilamination

Multilamination is based on the interdigital contacting of multiple fluid streams. The mixing mechanism is purely diffusive and therefore the mixing time depends on the width of fluid streams, which is determined by the dimensions of the microchannels in the mixer. Multilamination mixers are also well adapted for creating gas-liquid and liquid-liquid dispersions; the continuous phase streams squeeze and pinch-off bubbles or drops from the dispersed phase streams.

Hydrodynamic Focusing

These mixer types rely on a decrease in the diffusional path perpendicular to the flow such that diffusional mixing is enhanced. Practically, the width or diameter of the microchannel is progressively or abruptly decreased to generate thinner fluid streams. This mechanism is also very often used in conjunction with multilamination, thereby enabling very fast diffusive mixing or the generation of small monodisperse drops or bubbles.

Split-and-Recombine (SAR) Mixing

The split-and-recombine mechanism repeatedly stretches, splits, folds and recombines the fluid streams such that the interfacial area between the fluids is significantly increased and the characteristic path for diffusion is decreased. *SAR* mixers often generate chaotic flow, providing very fast and energy efficient mixing.

Chaotic Mixing

Chaotic mixing mechanisms provide fast efficient mixing by stretching and folding fluid streams and inducing exponential growth of the fluid interface. They are generated by imposing either periodic time- or space- perturbations to the flow by using either an external source of energy (e.g., a pulsing injection of fluid streams or periodic flow switching with non-uniform electric potentials) or a repeating three-dimensional geometrical structure in the mixer.

Mixing Time

The flow in micromixers and contactors is most often laminar due to the small characteristic size of the channels. In the laminar flow regime, molecular diffusion controls the mixing process and this mechanism is very slow compared with the convective mechanism that dominates in turbulent flows. Diffusional transport processes follow Fick's law, which can be used to show that diffusional mixing time is proportional to a characteristic distance l and the diffusion coefficient D_m :

$$t_{diff} \propto \frac{l^2}{D_m} \quad (18)$$

From this it can be seen that the time required for mixing is strongly dependent on the width of fluid streams, typically determined by the dimensions of the microchannels within the mixer. For simple mixer geometries—such as T-mixers—operating at low Reynolds numbers (where streamlines are parallel), the width of fluid streams is directly controlled by the micromixer dimensions and equation (18) provides a relatively good estimation of mixing time. However, most micromixers are based on more complex contacting mechanisms that stretch the fluid interface and decrease the width of the fluid streams from their original characteristic size at different rates. As a result, estimation of the length scale in equation (18) and consequently the mixing time is rather difficult. In order to characterise the mixing time of such equipment, a number of different optical techniques, as well as test reactions can be employed (Aubin et al. 2010). Analysis of literature data evaluating the mixing performance of various micromixer geometries using the Villermaux-Dushman test reaction (Commenge and Falk 2011) shows that the mixing time t_m is a power-law function of specific power dissipation (Falk and Commenge 2010):

$$t_m \approx 0.15\varepsilon^{-0.45} \quad (19)$$

where ε is the specific power dissipation (W/kg). The advantage of such micro technology is that very high values of power dissipation can be achieved, resulting in very short mixing times (< 1 ms), which is not possible in conventional mixers in turbulent flow.

Note. Specific power dissipation can be determined via pressure drop measurements using the following relationship:

$$\varepsilon = \frac{\Delta P \cdot Q}{V}$$

where Q is the volumetric flow rate and V is the volume of the liquid associated with the pressure drop, ΔP .

Multiphase Mixing

In addition to fast single phase mixing, micromixers are very well adapted for multiphase applications, such as liquid–liquid and gas–liquid contacting, as well as the generation of solids. Due to the small characteristic dimensions of micromixers, small and highly monodisperse drops and bubbles can be created, leading to

extremely high interfacial areas, high mass transfer rates and fast mixing in drops and slugs. However, controlling the multiphase flow regime and the characteristic size of the drops or bubbles is not necessarily simple. Indeed, the flow characteristics depend on a number of parameters, including the physical properties of the fluids (viscosity, density and surface tension), the operating conditions (total flow rate and ratio of phases), the geometry of the mixer, as well as the properties of the mixer walls (wettability, surface roughness. ...).

Liquid–liquid Dispersions

Slug flow is probably the most commonly encountered flow regime in micromixer devices since it enables droplets to be manipulated individually in a controlled manner, which means that all droplets experience exactly the same conditions throughout the process. Drop size is highly dependent on operating conditions (including flow rates and fluid properties), as well as the geometrical characteristics of the micromixer or contactor. Typically, it is decreased by increasing the continuous to dispersed phase flow rate ratio, by increasing the total flow rate or by decreasing the characteristic dimension of the micromixer. Indeed, like for the mixing time, it has been shown that the mean drop size generated in micromixers is inversely proportional to the specific energy dissipation (Löb et al. 2006). However, the type of liquid–liquid dispersion created (i.e., oil-in-water or water-in-oil) depends principally on the wettability of the micromixer walls by the fluids. Due to the very high surface to volume ratio of miniaturized equipment, the surface effects and fluid-material interactions are amplified compared with macro scale equipment. As a result, if the micromixer walls are hydrophobic, it is extremely difficult to create oil-in-water dispersions (Kobayashi and Nakajima 2006).

The controlled processing conditions provided by micromixers allow the generation of liquid–liquid dispersions with tailored properties. Indeed emulsions with very small droplets and high monodispersity, as well as double, triple and quadruple emulsions with specific properties (Chu et al. 2007) can be formed. Such precise product characteristics are not achievable in conventional mixing equipment. A further outcome of small monodisperse droplet emulsions is the increased stability of the dispersion, which enables the amount of surfactant required for product stability to be reduced (Haverkamp et al. 1999). For applications involving mass transfer and chemical reaction, transport phenomena are intensified due to the high interfacial area and the efficient liquid recirculation within each drop, allowing sub-millisecond mixing times.

Gas-liquid Dispersions

Gas-liquid applications involving mass transfer with or without reaction require a high interfacial area between the phases, as well as constant interface renewal, such that there is a continual driving force for mass transfer. In micromixers and contactors, a number of different gas-liquid flow regimes can be obtained, depending mainly on the gas and liquid flow rates, but also the fluid properties and the geometrical characteristics of the mixer. Bubbly flow is characterised by the formation of bubbles

that are much smaller than the diameter of the microchannel and occurs when the liquid flow rate is significantly greater than the gas flow rate. When the gas flow rate is much greater than the liquid flow rate, however, annular flow occurs; in this case, a central core of gas fills the channel and is separated from the wall by a thin film of liquid. At both high gas and liquid flow rates, instabilities in the gas-liquid interface cause churn flow where bubbles are ripped from the gas core into the liquid film. Taylor (or slug) flow, which characterised by regular-sized bubbles and liquid slugs, is probably the most common flow regime encountered in micro devices due to the fact that it occurs for a wide range of low to average gas and liquid flow rates. This flow regime is particularly attractive because it provides tightly controlled processing conditions, very high interfacial area and recirculation in the gas bubbles and liquid slugs (in a frame of reference moving with the bubbles) that allows interfacial renewal and intensified mass transport.

Mass Transfer

The design of systems for mass transfer between two dispersed phases depends mainly on the mass flux prediction. This flux can be calculated from the Sherwood number value. Heat transfer and mass transfer in microchannels directly benefits from scale reduction (Table 1). However, these phenomena are affected by the laminar flow regime. To overcome this problem, slug flow is often implemented for liquid-liquid or gas-liquid systems. Indeed, this flow regime has interesting hydrodynamic properties as it generates internal circulation loops (Thulasidas et al. 1995; Kreutzer et al. 2005; Kashid et al. 2005; Sarrazin et al. 2006; Taha and Cui 2006).

The flow pattern is characterized by three volumes (Fig. 2):

- Dispersed phase (drops or bubbles), characterized by recirculation loops (in frame of reference of the dispersed phase) due to forced convection;
- A continuous film which wets the walls;
- The liquid between two dispersed volumes. The streamlines in this volume are similar to those in the dispersed phase, i.e., characterized by recirculating loops.

The intensity of the recirculation velocity is more important in microchannel compared with larger scale equipment. This is due to the confinement of the dispersed phase that generates substantial velocity gradients between the wall of the channel

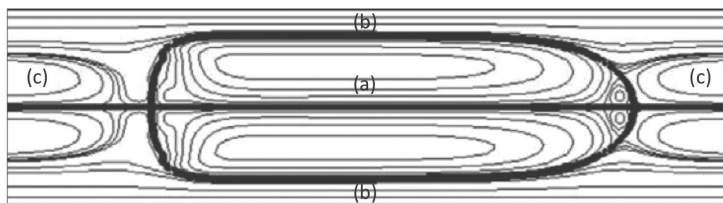


Figure 2. The liquid-liquid and gas-liquid flows can be characterized by three volumes: (a) the dispersed phase volume (drops or bubbles), (b) liquid film between the dispersion and the wall and (c) the continuous liquid phase between two dispersions.

(no slip condition) and the central axis of the dispersion. The convection within the drop has a major impact on the characteristic time of the mass transfer.

Gas-liquid Mass Transfer

Gas-liquid mass transfer in microchannels has often been studied through the implementation of catalyzed gas-liquid reactions. Due to the control of thermal effects, the implementation of these often highly exothermic reactions allows an increase in selectivity and safer conditions (Jähnisch et al. 2004; Hessel et al. 2005). Some correlations are proposed from these studies to estimate the transfer coefficients.

Bercic and Pintar (1997) worked on the adsorption of methane in water. They proposed a correlation to estimate $k_L a$:

$$k_L a = \frac{0.111.U_b^{1.19}}{((1-\varepsilon_G).L_{UC})^{0.57}} \tag{20}$$

where ε_G is the holdup of the gas phase, U_b , the gas velocity and L_{UC} is the flow pattern length.

Vandu et al. (2005) made experimental measurements of $k_L a$ from oxygen absorption in water and incorporated in their correlation the channel characteristic dimension. In addition, they worked with small values of the flow period and low speed, considering that the values of these parameters are crucial to model the transfer process between the two phases. They based their analysis on the simulations from (van Baten and Krishna 2004) and assumed that for large values of L_{UC} and low rates of bubbles, the liquid film will quickly saturate. In such conditions, the film behavior has a dominant effect on mass transfer as it reduces the “active” area for the mass transfer.

The current trend, initially suggested by (Irandoost et al. 1992), adopts a more fundamental approach to model gas-liquid transfer in microchannels. It takes two contributions into account (Kreutzer et al. 2005; van Baten and Krishna 2004): the solute transfer from the gas phase to the liquid through the gas cap $k_{Lcap}.a_{cap}$, and the gas transfer in the liquid film $k_{Lfilm}.a_{film}$.

$$k_L a = k_{Lcap}.a_{cap} + k_{Lfilm}.a_{film}$$

k_{Lcap} is estimated by the Higbie model. The exposure time used in this model is obtained by considering that an element of fluid follows the interface on half of the cap length (distance AB shown in Fig. 3).

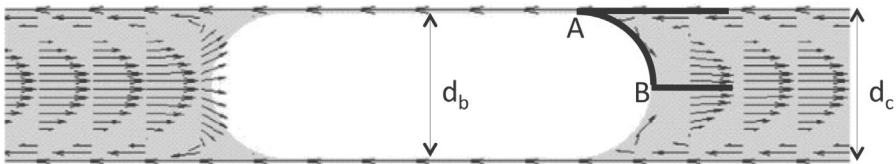


Figure 3. Illustration of the contact length at the ends of the bubble.

In the case of circular capillaries (diameter d_c), the contact length is ($\pi.d_b = 4$), where d_b is the diameter of the cylindrical part of the bubble. Each element of the liquid following a film streamline will be in contact with the gas phase twice (as the liquid is surrounded by two gas bubbles). Thus, assuming that the film has the same mean velocity as the bubble, one can deduce the exposure time, and express the contributions to the transfer:

$$k_{L,cap} a_{cap} = \frac{8}{L_{UC}} \cdot \sqrt{\frac{2.D.U_b}{\pi.d_b}} \quad (21)$$

$$k_{L,film} = \frac{Q_{film}}{\pi.d_c.L_{film}} \cdot \text{Ln}(1/\Lambda) \quad (22)$$

Q_{film} which is the volumetric flow rate and Λ is a dimensionless number which is function of the Fourier number (Fo) as follow:

$$\Lambda = 0,7857.e^{-5,121.Fo} + 0,1001.e^{-39,21.Fo} + 0,036.e^{-105,6.Fo} + \dots$$

Recall that Fo compares the film saturation time (t_{sat} , estimated as the square of the film thickness over the diffusion coefficient) and the exposure time:

$$Fo = \frac{D}{t_{ex,film} \cdot \delta_{film}^2} \quad (23)$$

Thus, the Fourier number is a criterion that can be used to check the film saturation (Pohorecki 2007). Indeed, two extreme cases can be identified:

- for short contact times ($Fo < 0.1$), $k_{L,film}$ film can be written as:

$$k_{L,film} = 2 \cdot \sqrt{\frac{D}{\pi.t_{ex,film}}} \cdot \frac{\text{Ln}(1/\Lambda)}{(1-\Lambda)} \quad (24)$$

- for long contact times ($Fo > 1$), the film saturates very quickly. Thus, in the case of dispersed microchannel flow under such conditions, the contribution of the film transfer can become negligible compared with the transfer through the caps of the bubble.

$$k_{L,film} = 3.41 \cdot \frac{D}{\delta_{film}} \quad (25)$$

The mass transfer coefficient is then multiplied by the interfacial area in order to obtain its contribution to the mass transfer process.

Modeling the gas-liquid mass transfer as the sum of the film and cap mass transfer is relevant with respect to van Baten and Krishna (2004) and Vandu et al. (2005) studies. Indeed, it can generally predict the evolution of the mass transfer coefficient $k_L a$ for different flow parameters and channel geometry.

Other types of intensified gas-liquid contactors have also been developed to enlarge the application domain of these new technologies. One of them, the falling-film microreactor (FFMR), developed by IMM (Institut für Mikrotechnik Mainz GmbH), has even become very famous since it first enabled to demonstrate the potentials of these intensified contactors for safe operation of hazardous syntheses, such as the direct fluorination of aromatics (Jähnisch et al. 2000). A few studies

experimentally determined the mass transfer coefficients on the liquid side and on the gas side in these devices (Claudel et al. 2005; Zhang et al. 2009; Sobieszuk et al. 2010; Sobieszuk and Pohorecki 2010; Commenge et al. 2011). By operating with various chemical systems, such as the reactive absorption of carbon dioxide or sulfur dioxide in sodium hydroxide solutions, these studies enabled typical orders of magnitude of the mass transfer coefficients in the FFMR to be determined. Concerning the liquid-side mass-transfer coefficient, k_L , most values range between 5×10^{-5} and 1.4×10^{-4} m/s with some specific values as high as 10^{-3} m/s. The values of the gas-side mass-transfer coefficients, k_G , still exhibit larger variations depending on the experimental studies, since reported values may range from 5×10^{-7} up to 1.3×10^{-5} mole/(m².s.Pa). These variations can partially be explained by the flow hydrodynamics in the falling-film microreactor. Indeed, whereas the liquid flow is precisely controlled by the surface microstructuring, the hydrodynamics in the gas phase may exhibit much more variability as a function of the gas flow and the specific geometry of the gas manifold. Numerical simulations demonstrated the impact of these parameters on the gas phase behavior and its impact on the overall mass transfer performance (Commenge et al. 2006).

To conclude, Kumar and Nigam (2012) presented a comparison of the mass-transfer performances of various gas-liquid contactors based on either conventional contacting modes (stirred tank, bubble column, etc.) or on intensified technologies (micro packed bed, spinning disc reactor, etc.). This performance comparison, coupled with the comparison of the specific mechanical energy input required, demonstrates the interest of tailor-designed structured contactors that enable to reach high mass transfer capacities while requiring acceptable energy inputs.

Liquid-liquid Mass Transfer

Few works have focused on experimental mass transfer with liquid-liquid slug flow in microchannels using reactive (with instantaneous reactions) or non-reactive systems. Burns and Ramshaw (2001), Harries et al. (2003), Xu et al. (2008) conducted experiments through acid/base reactions. Dummann et al. (2003) carried out the nitration of single ring aromatics and Ghaini et al. (2010) used the alkaline hydrolysis of ester in n-butylformate. Dessimoz et al. (2008) worked in rectangular microchannels and carried out the instantaneous neutralisation of trichloroacetic acid by NaOH in toluene or hexane. Assmann and von Rohr (2011) studied the extraction of vanillin in water with toluene with or without adding an inert gas.

These studies showed the increase of the mass transfer coefficient with the droplet velocity. The influence of other flow parameters, such as the channel diameter and the droplet size, were not clearly identified. Xu et al. (2008) highlighted the coefficient $k_L \cdot a$ increases with decreasing droplet size. However, this effect is mainly due to the increase in interfacial area and does not show the impact of confinement on the droplet transfer coefficient k_L . Di Miceli et al. (2008), on the basis of direct numerical simulations, proposed a correlation to calculate Sherwood number. This correlation depends on ϵ_d , the dispersed phase holdup, the Reynolds number, the

capillary number and a shape factor (w_c is the channel characteristic dimension and d_d the dispersion width):

$$Sh = A \varepsilon_d^{0.17} \cdot Re^{0.7} \cdot Ca^{-0.1} \cdot (w_c / d_d)^{0.75} \quad (26)$$

In addition, Di Miceli et al. (2008, 2014) experimentally validate the simulation and conclude on the impact of the confinement of droplets on mass transfer; a significant acceleration compared with non-confined droplets of the same size is observed.

Conclusion

Mass transfer significantly increases in micro-scale channels due to the increase in the surface/volume ratio. In addition, local hydrodynamics also have a very strong impact for two reasons: (i) The confinement between the dispersed phase and the liquid film wetting the wall generates an considerable velocity gradient in the film; (ii) the presence of recirculation loops in the dispersions and in the volume between two dispersions accelerate the global homogeneity of these volumes. These local hydrodynamic considerations explain why global correlations cannot currently be obtained from apparent operating parameters but they require precise knowledge of local variables (including geometry). Finally, when mass transfer is coupled with complex reaction schemes where competitive reactions take place, the information of the local behavior can become crucial.

Miniaturized Exchangers and Heat Exchanger Reactors

As indicated previously, miniaturized exchangers and heat exchanger reactors exhibit very high heat transfer performances that open new perspectives in sustainable development. The fast evacuation of the thermal fluxes generated by exothermic reactions firstly enables processes to be operated under safer conditions. Furthermore, this feature makes it possible to reduce the amount of solvent required whilst maintaining appropriate operating conditions; this reduces the energy requirements of the downstream separation units and also avoids wasting the solvent.

Geometry of Microstructured Heat Exchangers

The first important feature of microstructured systems lies in their large specific area that is a significant advantage for heat transfer applications. Depending on the operation, the internal diameter of the flow channels may range anywhere between 10 micrometers and a few millimeters. Assuming that the flowing fluid exchanges heat with all the surrounding channel walls, the specific area for heat transfer (defined as the heat transfer area per unit volume (m^2/m^3)) is inversely proportional to the channel diameter. Thus, for channels with a hydraulic diameter around 100 micrometers, the specific area for heat transfer is around $40000 \text{ m}^2/\text{m}^3$.

Performance of Microstructured Heat Exchangers: Heat Transfer Coefficient

The local heat transfer coefficient, h , between the flowing fluid and the wall is given by the following classical expression:

$$h = Nu \left(\frac{\lambda}{d} \right) \quad (27)$$

where Nu is the Nusselt number, λ is the fluid thermal conductivity and d is the hydraulic diameter of the channel. This equation shows that the heat transfer coefficient is inversely proportional to the hydraulic diameter of the channel. A decrease in the characteristic dimension therefore has simultaneous impact on the specific area for heat transfer and the heat transfer coefficient. Heat transfer is therefore drastically intensified by a reduction in the channel diameter.

In laminar flow, which is very common in microchannel systems, the Nusselt number for fully-developed hydrodynamic flow conditions and developing temperature profiles in smooth tubes can be calculated by the following classical correlation (Sieder and Tate 1936): $Nu = 1.86 Gz^{1/3}$ where the Graetz number is defined as $Gz = Re.Pr(d/L)$. For fully-developed hydrodynamic and thermal profiles, the Nusselt number is analytically demonstrated to equal a constant value. Under constant-temperature wall boundary conditions, the Nusselt number is equal to 3.657, whereas for constant heat flux at the wall its value equals 4.364.

Many studies have investigated heat transfer in microchannels and determined the Nusselt number experimentally as a function of the Reynolds number, Re , and the Prandtl number, Pr . Figure 4 presents the results obtained by several studies that

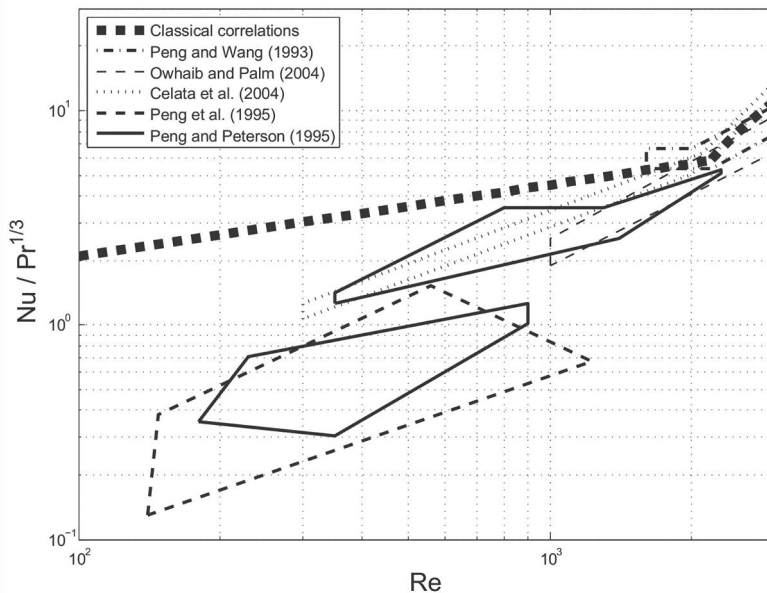


Figure 4. Comparison of the ratio $Nu/Pr^{1/3}$ measured with liquids in microchannels and the values predicted by classical correlations, as a function of the Reynolds number under laminar flow conditions. The polygonal shapes represent the border of the experimental points of each study.

observed Nusselt number values below the classical estimations. This observation may be attributed to the effects of heat conduction that may occur in the channel walls, particularly in the longitudinal flow direction. This heat conduction effect tends to diminish thermal gradients and artificially reduces the values of the observed Nusselt number. Particular attention should therefore be paid to such effects in microstructured heat exchangers.

Characteristic Time for Heat Transfer

The characteristic time for heat transfer presented in Table 2 is the main parameter of interest for quantifying the potential of microstructured heat exchangers, more so than the heat transfer coefficient and the specific area available for heat transfer:

$$t_{heat} = \frac{\rho.Cp}{h} \left(\frac{V}{A} \right) = \frac{\rho.Cp}{\lambda} \frac{R^2}{Nu} \quad (28)$$

Table 2. Comparison of the characteristic times for heat transfer in microstructured heat exchanger reactors and jacketed stirred tanks.

Microstructured heat exchanger reactor		Jacketed stirred tank	
$R = 100 \mu\text{m}$	$t_{heat} = 0.019 \text{ s}$	$V = 100 \text{ L}$	$t_{heat} = 38 \text{ min}$
$R = 1 \text{ mm}$	$t_{heat} = 1.9 \text{ s}$	$V = 1 \text{ m}^3$	$t_{heat} = 1.35 \text{ hr}$
$R = 10 \text{ mm}$	$t_{heat} = 190 \text{ s}$	$V = 6 \text{ m}^3$	$t_{heat} = 2.45 \text{ hr}$

Numerical Application

To illustrate the high heat management capacity of microstructured reactors, the characteristic time for heat transfer for different channel sizes is compared with the classical value obtained in jacketed stirred tanks. For this application, the properties of water are considered for the fluid ($\lambda = 0.6 \text{ W/m/K}$; $Cp = 4186 \text{ J/kg/K}$).

Table 2 summarizes the values of characteristic times for heat transfer obtained for various characteristic dimensions in both technologies. In the microstructured heat exchanger, the characteristic dimension ranges from 100 micrometers to 10 mm. For a Nusselt number equal to 3.66, the corresponding characteristic time ranges from 0.02 s to more than 3 min. In the case of the jacketed stirred tank, the heat transfer coefficient depends on the stirring conditions and a complete analysis is not possible here, but an average value of this coefficient can be considered equal to $200 \text{ W/m}^2/\text{K}$. According to equation (28), estimation of the characteristic time requires an estimation of the surface-to-volume ratio of the equipment. For the most commonly used tank shapes, this ratio is related to the tank volume as:

$$\frac{A}{V} = 4.3V^{-1/3} \quad (29)$$

For stirred tanks, the volumes considered in Table 2 range from 100 liters to 6 m^3 and the corresponding heat transfer time ranges from 38 min to 2.45 hr. This comparison demonstrates that the heat transfer capacities of microstructured

reactors and stirred tanks are radically different: their values differ by three orders of magnitude.

As a result of this high heat transfer capacity, microstructured heat exchangers possess specific features:

- Compactness: the large surface-to-volume ratio enables the volume of these devices to be drastically reduced whilst the transferred heat flux is maintained. The decrease in the volume induces a decrease in the corresponding capital expenditure and installation costs. Furthermore, the reduction of the internal volume of these devices directly improves the process safety. This gain in safety further contributes to the reduction of the operating costs of industrial sites.
- Potential intensification of operating conditions: with appropriate geometry, microstructured heat exchangers may exhibit very high heat fluxes per unit volume (as high as several kW/cm³). In addition, the relatively small channel dimensions with respect to thickness of channel walls compared with conventional heat exchangers enables the microstructured heat exchanger to be operated under more demanding conditions and particularly under high pressure. These features make microstructured heat exchangers interesting for use as heat exchanger reactors operating under high pressure. Indeed, for numerous gas-liquid systems, an increase in pressure results in a significant intensification of multiphase mass transfer, and hence improves the reaction conditions. For single-phase liquid systems, high operating pressures enable the process to be carried out at higher temperatures whilst avoiding solvent boiling; these intensified temperature conditions directly increase the reaction rate through the Arrhenius law, as well as the volume productivity.

Application: Reduction of Solvent Consumption via Implementation of a Heat Exchanger Reactor

The following example presents how the intensification of the heat transfer capacities may induce a decrease in the quantity of solvent required by implementation of a heat exchanger reactor. To facilitate the comparison between a microstructured heat exchanger reactor and a continuous stirred tank, both systems are assumed to behave as an ideal continuous stirred tank. The reaction rate obeys a first-order law with respect to the main reactant A . Under these assumptions, the simplified heat balance over the reactor can be written as:

$$\rho C_p Q (T_e - T_s) - \Delta_r H r V = h S (T_s - T_{ex})$$

Furthermore, assuming that the reactor operates under isothermal conditions, the inlet and outlet temperatures are equal and the heat balance then becomes:

$$(-\Delta_r H) r V = h S \Delta T_{ref}$$

where $\Delta T_{ref} = (T_s - T_{ex})$ denotes the temperature difference between the reactor and the heat exchange fluid. This equation can also be written as:

$$\frac{(-\Delta_r H) C_{A,0}}{\rho C_p} k \frac{C_A}{C_{A,0}} = \frac{h S}{\rho C_p V} \Delta T_{ref}$$

From this, the following definitions are then introduced:

- the adiabatic temperature rise: $\Delta T_{ad,pure} = \frac{(-\Delta_r H)C_{A,pure,0}}{\rho C_p}$
- the characteristic time for heat transfer: $t_{heat} = \frac{\rho C_p V}{hS}$
- the characteristic reaction time: $t_r = 1/k$
- the dilution factor F : $C_{A,0} = C_{A,pure,0}/F$
- the reactant conversion X_A : $C_A = C_{A,0}(1 - X_A)$

From the previous heat balance, the expression of the dilution factor F as a function of the operating conditions and the ratio of the characteristic times for reaction and heat transfer can be written as:

$$F = \left[(1 - X_A) \frac{\Delta T_{ad,pure}}{\Delta T_{ref}} \right] \frac{t_{heat}}{t_r}$$

From this it can be seen that two different reactors, both operating under isothermal conditions and equal conversions, only differ in their dilution factors and their characteristic times for heat transfer. Thus, if a conventional jacketed stirred tank is compared with a microstructured heat exchanger reactor, the ratio of their dilution factors equals the reciprocal ratio of their characteristic heat transfer times:

$$\frac{F_{micro}}{F_{tank}} = \frac{(t_{heat})_{micro}}{(t_{heat})_{tank}}$$

In the previous application example dedicated to the estimation of heat transfer characteristic times, a difference of several orders of magnitude between a stirred tank and a microstructured heat exchanger reactor has been demonstrated. This result shows that it is possible to work with almost no solvent in a microstructured reactor, if the operating conditions allow it. In practice, this problem is slightly different since fine chemical industry usually employs stirred tanks in semi-batch mode whereby a reactant is fed into the tank at an appropriate rate that enables the heat generated by chemical reactions to be evacuated. In this case, solvents are not necessarily diluted a lot. However, for highly exothermic reactions, the fed-batch operation may require very slow feeds since stirred tanks have poor heat transfer capacity and this will significantly increase the operation time and may be detrimental to the overall productivity.

Commercial Equipment

Since the mid-1990s there has been huge development in the area of microreaction technologies for continuous processing. The number of microreactor patent families reached a maximum of 80–100 patents per year in the period 2004–2007 (Hessel et al. 2008; Dencic et al. 2012). Since, the annual number of patents on such equipment has decreased and it is expected to level off in coming years. Future patent applications concerning microreaction technology will no doubt focus on methods of implementing specific reactions rather than the geometry and operation

of the equipment. Amongst the top-15 device patent owners are large worldwide chemical companies (e.g., Merck, Fuji, BASF, Degussa (now Evonik Industries), Bayer, Clariant), research institutes (e.g., Batelle, IMVT at Karlsruhe Institute of Technology, IMM) and equipment manufacturers (e.g., Velocys, Corning).

A vast number of commercial micromixers, contactors, heat exchangers and reactor-heat exchangers are available and some examples are given in Fig. 5 and Fig. 6. These devices are for use in both research and development, as well as in industrial production. Some application specific devices also exist, such as falling film microreactors (Fig. 5) and micro bubble columns (Dencic et al. 2012). Although the concept of ‘numbering-up’ (multiplication of microreactors) has been successfully applied for small capacity production (e.g., Braune et al. 2009; Togashi et al. 2009), viable industrial solutions for increasing throughput capacity are leaning towards microstructured reactors composed of multiple channels (i.e., internal numbering-up) of simple or more complex geometry (e.g., Deshmukh et al. 2010; Kirschneck and Tekautz 2007), and plate microreactors that integrate one or more operations (e.g., mixing, heat transfer, residence time) (e.g., Roberge et al. 2009). The characteristic dimensions of such equipment are typically on the millimeter-scale and are sized according to the characteristic times of the reaction or operation. Examples are the large stack falling film microreactor commercialised by IMM and the Fischer-Tropsch microchannel reactor by Velocys, shown in Fig. 5 and Fig. 6, respectively. Another industrial trend for continuous processing is the concept of modular container-based factories, which has been developed in the European F³ Factory Project (F3Factory) and demonstrated in the INVITE Research Center (Leverkusen, Germany; www.invite-research.com). These ‘plug and play’ modular chemical production units involve continuous process intensification equipment, including microstructured reactors, allowing flexible and sustainable chemical production.

The material of construction of microstructured reactors can be varied (including glass, stainless steel and other alloys) and depends on both the application and the compatibility of the fabrication technique with the complexity of the geometry. Glass reactors may be preferred for biological applications, whilst metal alloys are typically best suited to harsh chemical environments and applications where heat transfer is important. The manufacturers of micro-reaction technology are typically small-medium enterprises or research institutes who specialise in the domain, such as IMM, IMVT at Karlsruhe Institute of Technology, Ehrfeld BTS, Mikroglas Chemtech, Micronit Microfluidics, Corning, Velocys, Syrris and The Little Things Company GmbH.

Industrial Examples

Since the birth of micro-reaction technology in the 1990s there has been increasing use of microstructured reactors for both research and development and production of specialty chemicals, fine chemicals and pharmaceuticals. The majority of users include chemical manufacturers, such as Clariant, Sigma-Aldrich, BASF, Evonik Industries, DSM, Solvay, Arkema and DuPont, and pharmaceutical companies, such as GlaxoSmithKline, Astra Zeneca, Novartis and Sanofi, as well as contracting

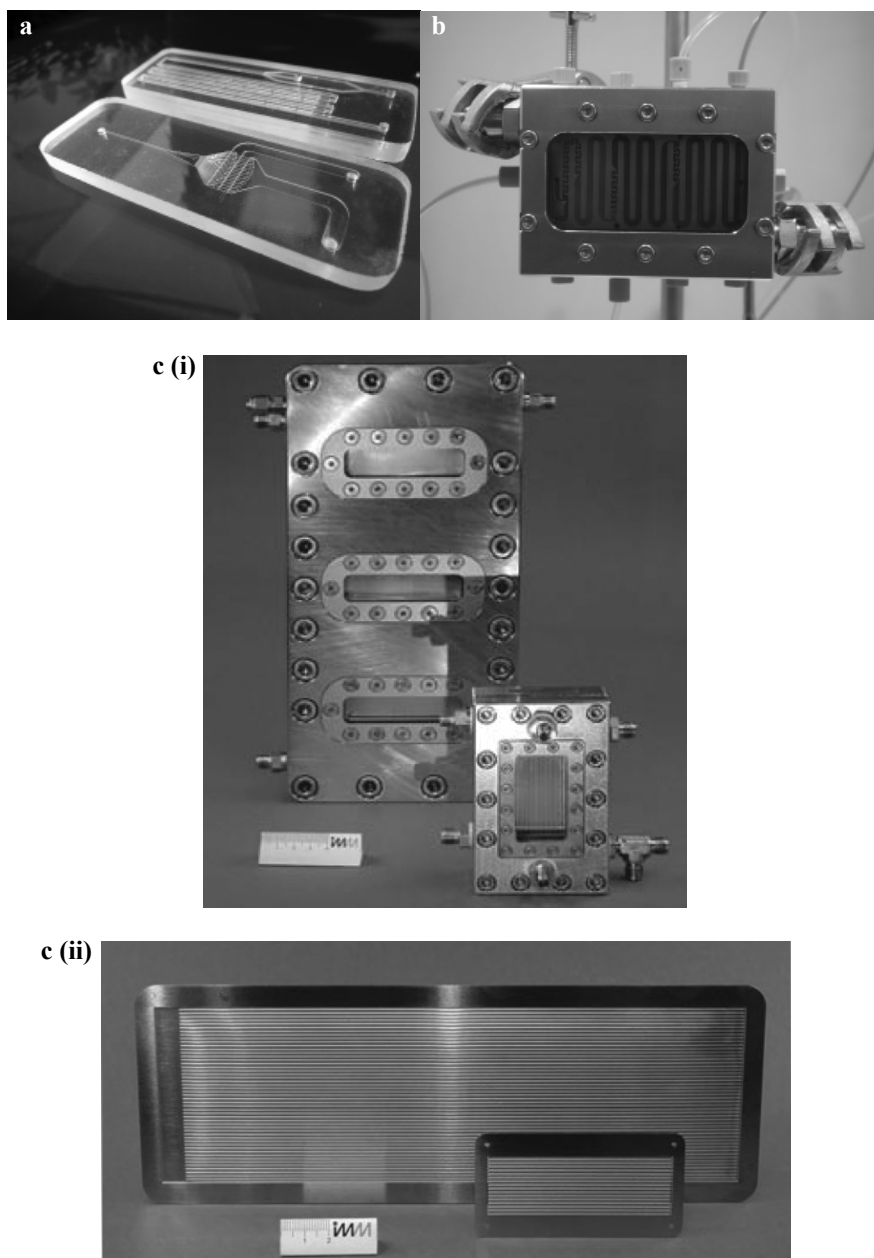


Figure 5. Miniaturized mixers and fluid contactors. (a) Interdigital glass micromixer based on multilamination and hydrodynamic convergence mixing mechanisms (photo courtesy of Mikroglas Chemtech). (b) Lonza FlowPlate® Lab Microreactor (photo courtesy of Ehrfeld Mikrotechnik BTS). (c) i) Large and standard Falling Film Microreactors for gas-liquid applications; ii) Reaction plates for large and standard Falling Film Microreactors comprising up to 50 parallel channels (photos courtesy of IMM).

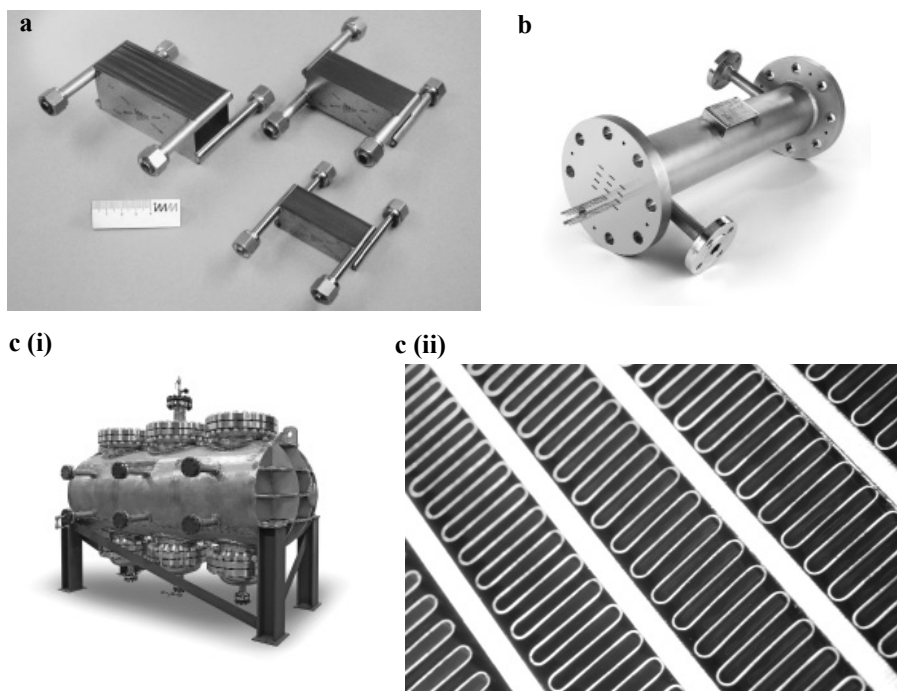


Figure 6. Miniaturized heat exchangers and heat exchanger reactors. (a) Microstructured plate heat exchanger and reactor for liquid-liquid, gas-liquid and gas-gas applications using a counter- or co-current flow scheme (photos courtesy of IMM). (b) Miprowa® high performance reactor/heat exchanger for pilot scale applications (pressures up to 150 bar, temperatures up to 250°C) (photo courtesy of Ehrfeld Mikrotechnik BTS). (c) i) 3-core Fischer-Tropsch (FT) microchannel reactor and ii) close up of the channels in the FT reactor (photos courtesy of Velocys).

manufacturers like Lonza. There are also interests in large-scale production activities, such as the production of consumer products (e.g., Procter and Gamble) and fuels (e.g., GreenSky London, Calumet).

The current industrial applications of microstructured reactors are in both research and development and production. In research and development, micro-reaction technology is particularly interesting for process development using only small quantities of reagents for trials, determining chemical kinetics of reactions, and correctly sizing and designing micro-structured geometries. Lonza, for example, has developed FlowPlate® microreactors of different sizes, the smallest being used for pre-clinical trials of Active Pharmaceutical Ingredient (API) production and the design of microstructures, and the larger microstructured plates enabling process scale-up (to the pilot plant scale) without internal parallelisation and numbering-up (Roberge et al. 2009; Roberge 2012). In their intensified mini-plant, which allows processing at >1 kg/day, the microreactors are currently being used for the reaction part in order to ensure high yields and selectivity. Example applications include the ozone-mediated conversion of chrysanthemic acid at a throughput of 0.5 t/day (Roberge 2012).

In chemical production, micro-reaction technology provides a means of performing highly exothermic reactions and dangerous chemistries under safe and controlled conditions, with improved selectivity and a faster time to market. One example is the pilot plant with modular parallelized micro-structured reactors developed by DSM and Corning for selective nitration under current good manufacturing practice (cGMP) conditions. In just nine months, DSM went from a 1 kg laboratory process of this hazardous reaction to a pilot campaign under cGMP conditions enabling more than 25 metric tons of fluids to be processed in safe conditions and more than 0.5 tons of quality product to be produced in four weeks (Braune et al. 2009). The pilot-plant led to the development of a large-scale microreactor production plant, which can process nearly 600 tons of fluids in seven weeks (Poechlauer and Brune 2010). Another example is the use of a mini continuous flow reactor for phosgenation reactions at La Mesta Chimie Fine (AET Group, www.la-mesta.com), a custom manufacturer of fine chemicals. AET Group has developed the RAPTOR continuous flow reactor that provides fast mixing and efficient heat transfer with an integrated system for *in situ* phosgene generation. Once the phosgene is produced, it reacts immediately to form phosgenated products, thereby avoiding storage or transport of this hazardous reactant. The current system generates around 4 kg of phosgene per hour, equivalent to more than 20 tons per year.

Other outcomes of using micro-reaction technology are increased production capacity in shorter processing times and with reduced energy requirements. This has been clearly demonstrated by the integration of a microstructured reactor in an existing process line for fine chemicals production (Kirschneck and Tekautz 2007). The original process was carried out in a single batch reactor and consisted of a highly exothermic reaction, which needed to be cooled lasting 4 hours, followed by an endothermic reaction, which required heating for several hours. To improve process performance a continuous microstructured reactor was integrated into the process line just before the batch reactor in order to carry out the first exothermic reaction. The high surface area to volume and the continuous nature of the reactor enabled the first reaction to be completed in a few minutes without any cooling. The warm products were fed directly to the batch reactor, thereby requiring less time and energy to heat the reactants for the second reaction. Overall, the new process allowed the original production capacity to be almost doubled with less time and energy.

Conclusions and Outlooks

Over recent years micro-reaction technology and microstructured reactors have been shown to be highly efficient for both process intensification and process safety in chemical production, particularly for specialty chemicals, fine chemicals and pharmaceuticals. The decrease in the characteristic dimensions of the equipment results in a decrease in the characteristic times of the process, which leads to a significant increase in heat and mass transfer coefficients. As a result, miniaturized processes use less energy, reactants and solvents than conventional processes and have equivalent or, in many cases, improved process performance. They also allow for process flexibility and a faster time to market. Indeed, industrial examples have

clearly demonstrated that process miniaturization and the use of microstructured reactors are a means to developing green and sustainable processes.

The industrial applications up until now have shown that microstructured equipment are particularly well adapted to process development and small to medium scale chemical production, which is well suited to many fine chemical and pharmaceutical applications. Although recent advances in miniaturized process design have shown very encouraging results in terms of production capacity, their application for large-scale production still needs development. There are a number of challenges that need to be dealt with, including:

- **Solids handling:** solids may be required by the reaction (e.g., catalyst) or be formed during the reaction. The small characteristic dimensions and increased surface effects of miniaturized equipment leads to clogging of the equipment.
- **Life and robustness of miniaturized equipment.** Industrial experience with long-term operation of microstructured equipment is limited. Long term effects of processing on possible corrosion and scaling, as well as reactor performance are still unknown.
- **Scale-up and numbering-up** for increasing production capacity. Although numbering-up of microreactors has been successfully implemented in some industrial applications, the multiplication of the number of reactors required directly increases process investment costs, which may oppose the benefits of the intensification achieved with the microstructured technology. Scale-up to the 'pertinent' characteristic size of the process avoids the problems associated with the parallelization of reactors, however generic design rules and methodologies for such an approach still require development.

The concept of process units or modular chemical plants, which have gained increased significance in the last few years, follows from the compactness (via miniaturization) of the intensified equipment associated with the possibility of parallelization. The development of these units is motivated by a combination of factors such as the difficulties associated with very strong international competitiveness, reduced product lifecycle (between launch and decline) and the high volatility of markets, as well as an excessive rise in energy costs, which lead to particularly poor economic forecasts (Falk 2012). In this difficult context, the plant of the future therefore needs to become more flexible to better adapt itself to the market demand. To fully benefit from the modular plant concept, flexible and interchangeable modules need to be developed. Indeed, the main objective of the European project F³Factory (F3Factory) was to design and develop such modules, based on intensified and automated equipment, assembled on a backbone facility that delivers utilities from a dedicated platform. The advantage of this multi-partner platform is to share the investment and operating costs.

Indeed, if we are going to reindustrialise the process industries for a sustainable future, micro-reaction technology and continuous flow miniaturized equipment need to be integrated universally into a wide range of processes and applications. It is therefore essential that this technology be developed further for large-scale production and adapted for diverse operating conditions (e.g., solids handling,

viscous fluids). This process development should also be accompanied by generic design rules and methodologies that will be diffused broadly in industry and taught to the up-coming generations.

References

- Assmann, N. and P.R. von Rohr. 2011. Extraction in microreactors: intensification by adding an inert gas phase. *Chem. Eng. Proc.: Proc. Int.* 50: 822–827.
- Aubin, J., M. Ferrando and V. Jiricny. 2010. Current methods for characterising mixing and flow in microchannels. *Chem. Eng. Sci.* 65: 2065–2093.
- Bercic, G. and A. Pintar. 1997. The role of gas bubbles and liquid slug lengths on mass transport in the Taylor flow through capillaries. *Chem. Eng. Sci.* 52 (21–22): 3709–3719.
- Braune, S., P. Pöchlauer, R. Reintjens, S. Steinhofner, M. Winter, O. Lobet, R. Guidat, P. Woehl and C. Guermeur. 2009. Selective nitration in a microreactor for pharmaceutical production under cGMP conditions. *Chimica Oggi Chemistry Today* 27: 26–29.
- Burns, J.R. and C. Ramshaw. 2001. The intensification of rapid reactions in multiphase systems using slug flow in capillaries. *Lab Chip* 1: 10–15.
- Chu, Y.-L., A.S. Utada, R.K. Shah, J.-W. Kim and D.A. Weitz. 2007. Controllable monodisperse multiple emulsions. *Angew. Chem. Int. Ed.* 46: 8970–8974.
- Claudel, S., C. Nikitine, C. Boyer and P. Font. 2005. Gas-liquid mass transfer in a micro-structured falling-film reactor. Proceedings of the Eight International Conference on Microreaction Technology IMRET 8, Atlanta, USA, April 10–14.
- Commonge, J.-M. and L. Falk. 2009. Reaction and process system analysis, miniaturization and intensification strategies. pp. 23–42. *In: V. Hessel, A. Renken, J.C. Schouten and J.-I. Yoshida (eds.). Micro Process Engineering—A Comprehensive Handbook—Volume 3: System, Process and Plant Engineering.* Wiley-VCH Verlag, Weinheim.
- Commonge, J.-M. and L. Falk. 2011. Villermaux–Dushman protocol for experimental characterization of micromixers. *Chem. Eng. Proc.* 50: 979–990.
- Commonge, J.-M., T. Obein, G. Genin, X. Framboisier, S. Rode, V. Schanen, P. Pitiot and M. Matlosz. 2006. Gas-phase residence time distribution in a falling-film microreactor. *Chem. Eng. Sci.* 61: 597–604.
- Commonge, J.-M., T. Obein, X. Framboisier, S. Rode, P. Pitiot and M. Matlosz. 2011. Gas-phase mass-transfer measurements in a falling-film microreactor. *Chem. Eng. Sci.* 66: 1212–1218.
- Dencic, I., V. Hessel, M.H.J.M. de Croon, J. Meuldijk, C.W.J. van der Doelen and K. Koch. 2012. Recent changes in patenting behavior in microprocess technology and its possible use for gas-liquid reactions and the oxidation of glucose. *ChemSusChem* 5: 232–245.
- Deshmukh, S.R., A.L.Y. Tonkovich, K.T. Jarosc, L. Schrader, S.P. Fitzgerald, D.R. Kilanowski, J.J. Lerou and T.J. Mazanec. 2010. Scale-up of microchannel reactors for Fischer-Tropsch synthesis. *Ind. Eng. Chem. Res.* 49: 10883–10888.
- Dessimoz, A.L., L. Cavin, A. Renken and L. Kiwi-Minsker. 2008. Liquid–liquid two-phase flow patterns and mass transfer characteristics in rectangular glass microreactors. *Chem. Eng. Sci.* 63: 4035–4044.
- Di Miceli Raimondi, N., L. Prat, C. Gourdon and P. Cognet. 2008. Direct numerical simulations of mass transfer in square microchannels for liquid–liquid slug flow. *Chem. Eng. Sci.* 63(22): 5522–5530.
- Di Miceli Raimondi, N., L. Prat, C. Gourdon and J. Tasselli. 2014. Experiments of mass transfer with liquid–liquid slug flow in square microchannels. *Chem. Eng. Sci.* 105: 169–178.
- Dummann, G., U. Quittmann, L. Gröschel, D.W. Agar, O. Wörz and K. Morgenschweis. 2003. The capillary-microreactor: a new concept for the intensification of heat and mass transfer in liquid–liquid reactions. *Cat. Today* 79–80: 433–439.
- F3Factory. 2013. <http://www.f3factory.com/scripts/pages/en/home.php>.
- Falk, L. 2012. The place of intensified processes in the plant of the future. pp. 401–435. *In: J.-P. Dal Pont (ed.). Process Engineering and Industrial Management.* John Wiley & Sons Inc., Hoboken NJ and ISTE Ltd., London.
- Falk, L. and J.-M. Commonge. 2010. Performance comparison of micromixers. *Chem. Eng. Sci.* 65: 405–411.

- Ghaini, A., M.N. Kashid and D.W. Agar. 2010. Effective interfacial area for mass transfer in the liquid-liquid slug flow capillary microreactors. *Chem. Eng. Proc.: Proc. Int.* 49: 358–366.
- Harries, N., J.R. Burns, D.A. Barrow and C. Ramshaw. 2003. A numerical model for segmented flow in a microreactor. *Int. J. of Heat and Mass Trans.* 46: 3313–3322.
- Haverkamp, V., W. Ehrfeld, K. Gebauer, V. Hessel, H. Löwe, T. Richter and C. Wille. 1999. The potential of micromixers for contacting of disperse liquid phases. *Fresenius J. Anal. Chem.* 617–624.
- Hessel, V., P. Angeli, A. Gavrilidis and H. Löwe. 2005. Gas-liquid and gas-liquid-solid microstructured reactors: contacting principles and applications. *Ind. and Eng. Chem. Res.* 44: 9750–9769.
- Hessel, V., C. Knobloch and H. Löwe. 2008. Review on patents in microreactor and micro process engineering. *Rec. Patents in Chem. Eng.* 1: 1–16.
- Hickman, D.A. and L.D Schmidt. 1992. The role of boundary layer mass transfer in partial oxidation selectivity. *J. Catal.* 136: 300–308.
- Irandoost, S., S. Ertlé and B. Andersson. 1992. Gas-liquid mass transfer in Taylor flow through a capillary. *Can. J. Chem. Eng.* 70: 115–119.
- Jähnisch, K., M. Baerns, V. Hessel, W. Ehrfeld, V. Haverkamp, H. Löwe, C. Wille and A. Guber. 2000. Direct fluorination using elemental fluorine in gas/liquid micro-reactors. *J. Fluorine Chem.* 105: 117–128.
- Jähnisch, K., V. Hessel, H. Löwe and M. Baerns. 2004. Chemistry in microstructured reactors. *Ang. Chem. Int. Ed.* 43: 406–446.
- Kashid, M.N., I. Gerlach, S. Goetz, J. Franzke, J.F. Acker, F. Platte, D.W. Agar and S. Turek. 2005. Internal circulation within the liquid slugs of a liquid-liquid slug-flow capillary microreactor. *Ind. and Eng. Chem. Res.* 44: 5003–5010.
- Kirschneck, D. and G. Tekautz. 2007. Integration of a microreactor in an existing production plant. *Chem. Eng. Technol.* 30: 305–308.
- Kobayashi, I. and M. Nakajima. 2006. Generation and multiphase flow of emulsions in microchannels. chapter 5, pp. 149–172. *In: N. Kockmann (ed.). Advanced Micro and Nanosystems Vol. 5. Micro Process Engineering.* Wiley-VCH Verlag GmbH & Co. KGaA, Weinheim.
- Kreutzer, M.T., F. Kapteijn, J.A. Moulijn and J.J. Heiszwolf. 2005. Multiphase monolith reactors: chemical reaction engineering of segmented flow in microchannels. *Chem. Eng. Sci.* 60: 5895–5916.
- Kumar, V. and K.D.P. Nigam. 2012. Process intensification in green synthesis. *Green Process. Synth.* 1: 79–107.
- Löb, P., H. Pennemann, V. Hessel and Y. Men. 2006. Impact of fluid path geometry on operating parameters on I/I-dispersion in interdigital micromixers. *Chem. Eng. Sci.* 61: 2959–2967.
- Poehlauer, P. and S. Brune. 2010. Process intensification in development and efficient production of pharmaceuticals. 2nd Symposium on Continuous Flow Reactor Technology for Industrial Applications. Oct. 4–5. Paris.
- Pohorecki, R. 2007. Effectiveness of interfacial area for mass transfer in two-phase flow in microreactors. *Chem. Eng. Sci.* 62: 6495–6498.
- Roberge, D. 2012. Lonza—hazardous flow chemistry for streamlined large-scale synthesis. *Green Process Synth.* 1: 129–130.
- Roberge, D.M., M. Gottspöner, M. Eyholzer and N. Kockmann. 2009. Industrial design, scale-up and use of microreactors. *Chimica Oggi Chemistry Today* 27: 8–11.
- Sarrazin, F., K. Loubière, L. Prat, C. Gourdon, T. Bonometti and J. Magnaudet. 2006. Experimental and numerical study of droplets hydrodynamics in microchannels. *AIChE Journal* 52(12): 4061–4070.
- Sieder, E.N. and G.E. Tate. 1936. Heat transfer and pressure drop of liquids in tubes. *Ind. Eng. Chem.* 28: 1429–1435.
- Sobieszuk, P. and R. Pohorecki. 2010. Gas-side mass transfer coefficients in a falling film microreactor. *Chem. Eng. Processes.* 49: 820–824.
- Sobieszuk, P., R. Pohorecki, P. Cyganski, M. Kraut and F. Olschewski. 2010. Marangoni effect in a falling film microreactor. *Chem. Eng. J.* 164: 10–15.
- Taha, T. and Z.F. Cui. 2006. CFD modelling of slug flow inside square capillaries. *Chem. Eng. Sci.* 61: 665–675.
- Thulasidas, T.C., M.A. Abraham and R.L. Cerro. 1995. Bubbletrain flow in capillaries of circular and square cross section. *Chem. Eng. Sci.* 50(2): 183–199.

- Togashi, S., T. Miyamoto, T. Sano and M. Suzuki. 2009. Microreactor synthesis using the concept of numbering-up. pp. 678–681. *In*: F.G. Zhuang and J.C. Li (eds.). *New Trends in Fluid Mechanics Research*. Springer, Berlin Heidelberg.
- van Baten, J.M. and R. Krishna. 2004. CFD simulations of mass transfer from Taylor bubbles rising in circular capillaries. *Chem. Eng. Sci.* 59: 2535–2545.
- Vandu, C.O., H. Liu and R. Krishna. 2005. Mass transfer from Taylor bubbles rising in single capillaries. *Chem. Eng. Sci.* 60: 6430–6437.
- Villermaux, J. 1993. *Génie de la réaction chimique conception et fonctionnement des réacteurs*. Lavoisier, Paris.
- Xu, J.H., J. Tan, S.W. Li and G.S. Luo. 2008. Enhancement of mass transfer performance of liquid–liquid system by droplet flow in microchannels. *Chem. Eng. J.* 141: 242–249.
- Zhang, H., G. Chen, J. Yue and Q. Yuan. 2009. Hydrodynamics and mass transfer of gas-liquid flow in a falling film microreactor. *AIChE Journal* 55(5):1110–1120.
- Zlokarnik, M. 2002. *Scale-up in Chemical Engineering*. Wiley-VCH, Weinheim.

5

Multifunctional Reactors

*Xuan Meyer, Christophe Gourdon, Michel Cabassud and
Michel Meyer*

Introduction

Process Intensification

In the introduction of this book, the concept of process intensification (PI) in the context of Sustainable Process Engineering has been presented. Clearly, PI, which aims “to produce much more and better using much less”, definitely fits the famous 3P triangle (Planet, People, Profit) from the Brundtland report (Fig. 1), and appears to be one of the main issues for sustainable development (Ramshaw 1995).

Figure 2 shows a non-exhaustive list of equipments and methods which concern process intensification (Stankiewicz and Moulijn 2000). This classification serves to underline the considerable scope of this topic.

The concept of multifunctional reactors is featuring high in this classification. This term, as it has been pointed out in the introduction to the book, integrates the

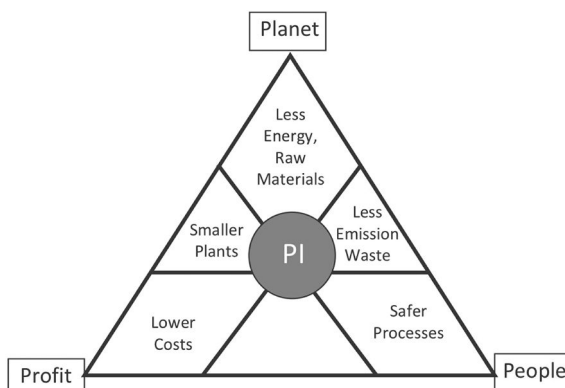


Figure 1. 3P Triangle for Sustainable Development.

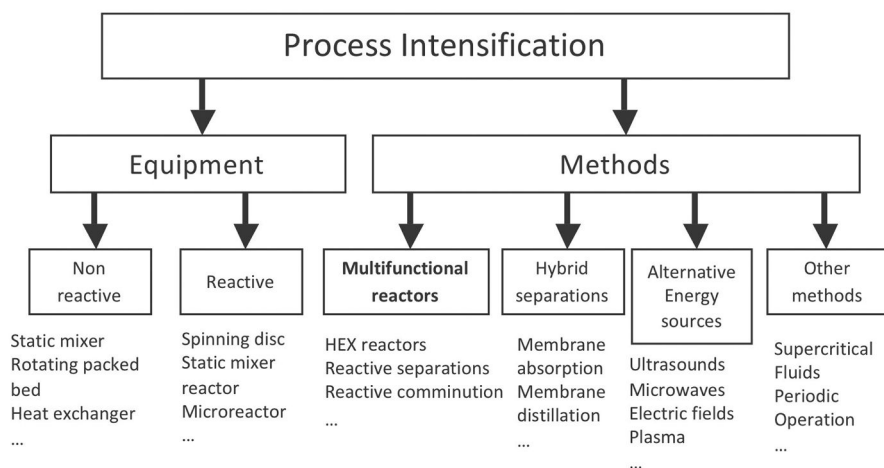


Figure 2. Classification of specific methods and equipments relative to PI.

principle of “at least pair operations in one apparatus”, transport phenomena-reaction-separation, in order to give rise to synergetic effects, to increase productivity and/or selectivity, and/or to facilitate separation of the side products. In practice, this led to the emergence of technologies such as:

- intensified reactors (heat-exchanger reactors, membrane reactors, spinning disc reactor),
- reactive separation techniques (distillation, extraction, absorption, adsorption),
- reactive mechanical operations (extrusion, comminution, filtration).

One will focus in what follows on two specific and emblematic concepts: the intensified reactors and the reactive separations.

Concept of Intensified Reactors

Intensifying reactors means first to implement some principles of multifunctionality:

- either by coupling the unit operations of reaction and separation, such as in membrane reactor (naturally a strong analogy with the concept of reactive separation developed in the next paragraph, knowing that here it is the reaction which is the main objective);
- or by integrating a number of functions, such as conversion and mixing in the static mixer reactor or such as heat exchange and reaction with the heat exchanger reactor;
- or by enhancing a particular mechanism (transfer or reaction), like in the spinning disc reactor or reactors under specific activation (ultrasound, microwave, photo-excitation, ...).

Beyond multifunctionality, an intensified reactor generally accompanies the promotion of continuous operations, allowing miniaturization of equipment, leading both to the acceleration of transport phenomena and to the increase of process safety. This miniaturization can go in some cases down to micro-scales described in Chapter *Process Intensification by Miniaturization*, in this case the reactors are called microreactors. In this chapter, the millimetric or centimetric scales, which are more adapted to the compliance of the optimal compromise between productivity and energy consumption (pressure drop) is preferred. Here, the reactors are milli-reactors.

For the design of these intensified technologies, four important parameters are traditionally considered:

- the heat transfer performance;
- the flow characteristics (plug flow, mixing);
- the reactor dynamics;
- the residence time.

One will focus specifically on the heat exchanger reactors (HEX-reactors), while detailing the methods used to characterize them as regards the previous design parameters and reviewing a number of devices, either commercial or under development.

Reactive Separation Concepts

The principle of a reactive separation is based on the use of a multifunctional reactor in which reactions take place in addition to the at least one additional separation step. The aim of this approach is to reduce the number of unit operations as shown in Fig. 3.

In the simplest case, reaction and separation are equivalent to each other so that no one of both phenomena predominates over the other one; however two operating modes may be distinguished:

- the one where separation is used in the service of the reaction, the principle being further detailed for a particular application: the reactive distillation;
- the other one where the reaction is used to improve the separation, including for example the case of mixtures (isomers) impossible to separate in a conventional way. In this case a reagent is generally added.

Integrating reaction and separation in one device generally requires the addition of at least one phase to the reaction system or energy for heating or cooling the mixture. The system studied is at least biphasic in nature, whereas the reaction phase has the residence time required for the reaction and at least the additional phase is used for the mass transfer (reactants, products, by-products, inert ...). The difference in physico-chemical properties of the components of the system will favor one or another type of separation, and indeed a whole family of reactive separations is then possible. Table 1 summarizes the various possible operations, depending on the physical state of the phases (reaction and transport phases).

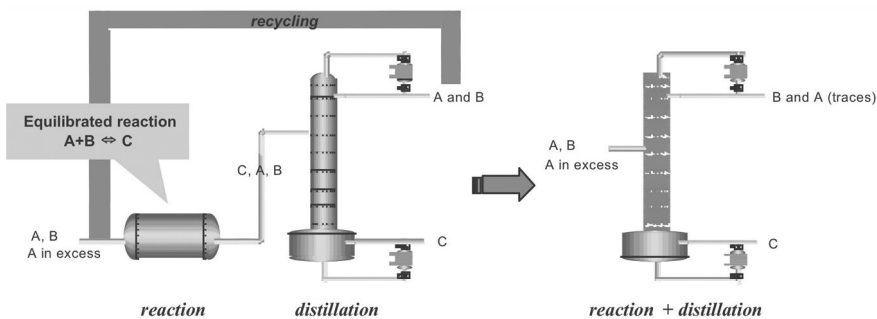


Figure 3. Comparison of conventional process versus multifunctional process.

Table 1. Overview of reactive separations.

Physical phase state			Separation properties	Reactive separation
Reaction	Transp. 1	Transp. 2		
Liquid	Vapor		Volatility	Reactive distillation
Liquid	Vapor		Volatility	Reactive stripping
Liquid	Vapor		Permeability	Reactive pervaporation
Liquid	Vapor	Solid	Solubility/Volatility	Precipitation/ reactive evaporation
Liquid	Liquid		Solubility	Reactive extraction
Liquid	Liquid		Permeability	Reactive membrane process
Liquid	Solid		Solubility	Reactive crystallization
Liquid	Solid		Affinity	Reactive adsorption
Gas	Liquid		Volatility	Reactive condensation
Gas	Liquid		Solubility	Reactive absorption
Gas	Solid		Affinity	Reactive adsorption

In most cases, the additional phase is used to remove the products of the reaction from the reaction zone. So the concentration of the component in the reaction zone decreases, and according to the law of Le Chatelier, the chemical equilibrium imposes an increase in the conversion which leads sometimes to a total conversion. The transport phase can also be used as a controlled reactive feed flow. Slow or controlled transport of reagents in the reaction phase is possible without diluting the reagent or using an intermediate feed. This is particularly advantageous for systems with side reactions. The selectivity of the main reaction can thus be increased. The major example is the reactive distillation.

Heat-Exchanger/Reactors

Heat-exchanger/reactors (HEX-reactors) play an important role in process intensification since many chemical reactions are temperature dependent. The

principle of a heat-exchanger/reactor consists in combining a reactor and a heat exchanger in only one unit.

Design Parameters

The principle of design of a heat-exchanger/reactor is based on a combination of elements in which the reaction medium is flowing and modules relative to the utility fluid flow. Usually, the device consists in an alternating arrangement of plates as shown in the drawing below (Fig. 4).

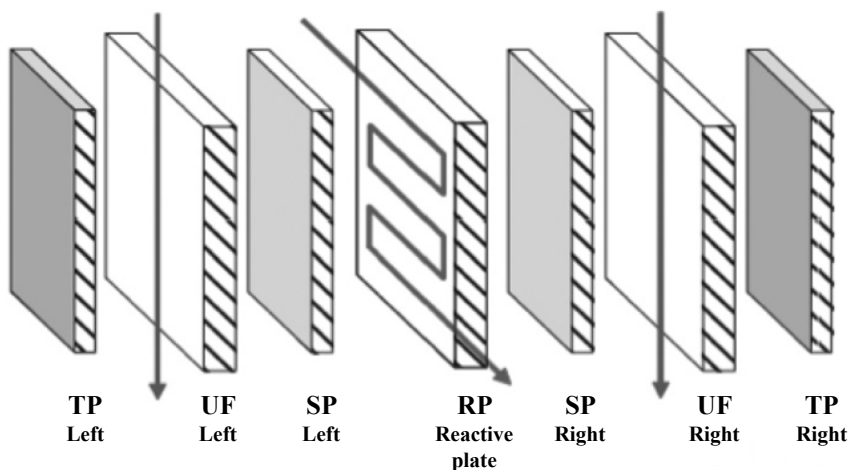





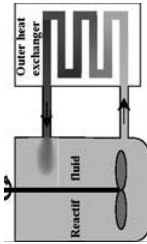
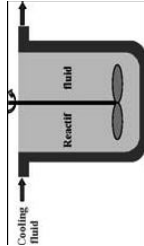
Figure 4. HEX-reactor design principle. UF, SP and RP are respectively the Utility, Separation (“sandwich”) and Reactive Plates. TP are the Terminal (boundary) Plates.

The distinctions between the different technologies arise from the plates drawing, the plates assembling methods (welding, brazing, sealing ...), the nature of materials, the methods of connection, etc. In what follows, the main parameters guiding the design of a heat-exchanger/reactor are reviewed.

Heat Exchange Intensification

During a reaction operation, control of the temperature is a key issue for obvious reasons such as safety (thermal runaway) and product quality (reduction of side reactions). In agitated batch reactors, typically implemented solutions for the thermal control like jacket, internal or external coil loop are rarely sufficient to face the exothermicity encountered, which generally leads to operate in degraded conditions (reagent feeding, dilution, less efficient catalyst). From this point of view, the heat-exchanger/reactor appears as a very attractive technology, as it combines the high performances of a heat-exchanger to those of a reactor. Table 2 presents the expected

Table 2. Heat transfer performances of different technologies.

Process	Plate Heat Exchanger configuration		Shell-and-tube configuration	Loop configuration	Jacketed batch reactor
	Offset Strip Fins Re = 2000	Metallic foams Re = 1000			
Schematic diagram					
Specific Area, S/V (m ² .m ⁻³)	800	400	400	10	2.5
Global heat transfer coeff., U (W.m ⁻² .K ⁻¹)	5000	3500	500	1000	400
US/V (kW.m ⁻³ .K ⁻¹)	4000	1400	200	10	1

performances of different equipments and illustrates the interest of heat-exchanger/reactors.

Specific surface area, or compactness factor, is defined as the ratio of the area available for the heat exchange (S) to the reaction volume (V). The thermal performances, or intensification factor, are evaluated as the product of this compactness factor multiplied by the overall heat transfer coefficient (U).

Flow Regime

The flow regime should be as close as possible to a plug flow, in such a way to prevent short-circuit or dead zone and to ensure flow uniformity. It is also the best way to transpose pure batch to continuous, batch operation time being formally equivalent to the mean residence time in this case. In addition, it is necessary to intensify mixing of reagents, from then macroscopic scales to the micro ones (Nilsson and Sveider 2000; Ferrouillat et al. 2006a,b). The major difficulty comes from the hydraulic regime that is often laminar, rarely turbulent, due to the miniaturization of intensified reactors. Therefore a particular attention has to be paid to the design of the heat-exchanger/reactor to approach these flow criteria.

Reactor Dynamics

The dynamics of the reactor relative to transport phenomena is an important feature, especially with respect to safety and quality issues. Indeed, in many processes, transitional stages (responses to disturbances or changes in operating conditions) may be problematic, as well as procedures for start-up and shutdown. In that case, the interest of a continuous operating mode involving a more compact device, in which the inventory is smaller than in batch process is evident. Moreover, these processes offer flexibility and characteristics regime set times are shorter. In this field, we will see later the importance of the choice of materials for heat-exchanger/reactors.

Residence Time

The residence time in an intensified continuous reactor (from minutes to hour) is naturally shorter than in a batch reactor for which it is theoretically unlimited. This is undoubtedly the most important limitation for this type of technology. However, the experience shows that a continuous intensified mode significantly reduces the reaction times, allowing to operate under conditions leading to a higher reactivity (higher temperatures and/or pressures, with more active catalysts, at higher concentrations).

According to these four design features, a wide variety of technological solutions of heat-exchanger reactors, made of various materials (glass, stainless steel, hastelloy, PEEK, silicon carbide ...) are nowadays available. For more details, the reader can refer to the review article (Anxionnaz et al. 2008).

In the next section, some emblematic heat-exchanger reactors are presented: Open-Plate Reactor Alfa-Laval (now marketed under the name ART for Advanced Reactor Technology™), the reactor ShimTec® Chart Industries, the Corning reactors (Advanced-Flow™ Glass Reactors) and a prototype from our lab.

Some Examples of HEX-reactors

The Alfa-Laval Reactor

The Alfa-Laval ART[®] Plate Reactor combines the properties of a continuous chemical reactor with those of a plate heat exchanger. It contains flow-directing reactor plates that are sandwiched between heat transfer plates, held together by pressure plates to create a modular reactor unit. Ports along the reaction channel provide access to the reaction mixture for measurement, sampling and reactant addition. The plate reactor can be disassembled and reassembled quickly allowing easy cleaning.

Alfa-Laval claims several advantages with this technology. The high heat transfer of a plate heat exchanger is combined with efficient mixing producing reliable reaction control in one unit. This allows users to improve existing processes and develop new products.

The mechanical design of the reactor allows for reaction at elevated temperature and pressure. There are different sizes of frames for ART Plate Reactors and within each frame model there are different sizes of plates. This means that the ART Plate Reactors can be used for a large range of throughputs. Due to the similar fluid dynamics in different sizes, the scale-up effect is reduced and only minor work is needed to go from lab-scale to large-scale production. Therefore, the product range has capacities from 0.25 L/hr up to 1 m³/hr covering all steps from laboratory scale R&D to full production.

The ShimTec Reactor (Chart)

Chart Energy and Chemicals, a world leader in the design and manufacture of aluminum plate fin heat exchangers, has developed two types of compact heat exchange reactors, ShimTec[®] and FinTec[™]. Each type provides compact multi-channel construction incorporating unique design features and high heat transfer capabilities utilizing a variety of materials, including aluminium, stainless steel and nickel alloys. Chart Reactors can address the full range of processing volumes required in the chemical industry. Applications include a variety of chemical processes requiring close temperature control.

Both ShimTec[®] and FinTec[™] reactors are constructed with reactant and utility streams layered within the structure, ensuring there is only a short heat path between adjacent streams. In this way, heat is readily added or removed from where the duty is most required. Individual reactors can include three or more streams as the process may require.

The flexibility of the design creates options for controlled chemical additions into bulk streams through intermediate layers and channels. The specific injection arrangement matches the process requirements, thereby limiting the potential for hot spots to form when operating very exothermic reactions.

Let us notice that it is claimed that there are several options for catalyst incorporation within the reactor structure: coated onto internal surfaces to facilitate heat transfer; packed for ease of removal and replacement; incorporated within a removable insert; injected along the reaction path.

The ShimTec reactor from Chart Industries (Enache et al. 2007; Plucinski et al. 2005) is an example of heat exchanger reactor with diffusion bounded plates. Swagelok fittings are used for all connections.

The geometrical data and characteristic sizes of the heat exchanger reactor studied in our lab are detailed in Table 3. But, many other geometries are available (CHART Industries).

Table 3. Characteristics of a ShimTec reactor.

Details	Process stream	Utility stream
Number of parallel channels	2	70
Number of layers of each stream	1	2
Individual channel width (mm)	2.0	1.05
Individual channel depth (mm)	2.0	3.0
Average flow area per channel (mm ²)	4.0	2.61
Individual channel length, L (mm)	1855	125
Hydraulic diameter, d _h (mm)	2.0	1.141
Total fluid volume, V (mm ³)	14836	45712
Total surface area, A (mm ²)	29673	160209
Thickness of the metal between streams (upper bound), e (mm)	1.2	

The Corning® Advanced-Flow™ Glass Reactor

The Corning reactors are based on glass technology, this material offering chemical compatibility with a wide range of chemicals and one of the highest corrosion resistance with almost all chemicals. The heat exchanger reactor integrates thermal management capabilities in the form of one or more high-flow buffer fluid passages or layers. The device includes a unitary mixer, i.e., a mixing passage through which all of at least one reactant to be mixed is made to pass, the mixing passage being structured so as to promote efficient mixing. The reaction and heat exchange volumes are for instance about 5 mL, and 16 mL respectively. Typical dimensions for the reactor channels are in the millimeter and sub-millimeter range.

Recently, Corning has developed a high flow rate reactor for chemical production that retains the outstanding mixing and heat exchange performance of its lower-scale Advanced-Flow™ glass reactors while also providing large internal volume, high flexibility, metal-free reaction path and scalability from G1 to high-flow G3 with a throughput factor increase > 20.

A Prototype in our Lab

In the frame of collaborative projects with other partners, our lab has developed a prototype which has been constructed either in SiC or in stainless steel.

The heat-exchanger reactor made of ceramic (SiC) has been developed in the frame of a collaboration between BOOSTEC and our lab (Elgue et al. 2007).

BOOSTEC is a french innovative SME, specialized in high-performance all-silicon carbide components and systems. The sintered silicon carbide provides a unique combination of key advantages for the production of high performance components or systems:

- nearly pure SiC, no secondary phase (to avoid interaction between the material and the reactive medium),
- isotropic physical properties (that guarantee a good homogeneity of the reactor channels),
- high mechanical strength and stiffness, insensitivity to mechanical fatigue,
- high thermal conductivity,
- high stability in time and ability to handle corrosive media.

From a PI viewpoint, the use of ceramic allows strong corrosion resistance, high heat transfer capacity and temperature stability. Consequently, such a reactor appears particularly suited to PI of highly exothermic and/or strongly corrosive applications that are frequently carried out in pharmaceutical and fine chemical industry. In fact, intensification allows reactions to be improved (increase of reactants concentration, of catalyst amount, etc.) and then leads to the use of more aggressive and more corrosive products in an environment where thermal exchanges are enhanced. Moreover, the reactor also offers promising perspectives in the fields of safety (reduction of reactive medium amount, minimisation of thermal runaway risk), of energy efficiency (high thermal transfer performances), of productivity (possibility to increase reactants concentration) and of environmental impact (reduction of solvent consumption and therefore of separation steps).

The concept of the reactor is based on a modular structure built by the alternative stacking of reaction plates and of utility plates containing the thermal fluid. Reaction

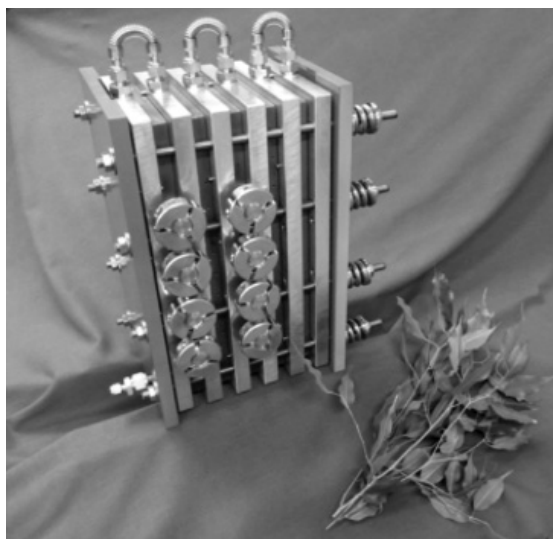


Figure 5. Silicon carbide plate heat exchanger.

Table 4. SiC reactor characteristics according to flow rate.

Flow rate (L/hr)	Reynolds number (-)	Peclet number (-)	Residence time (s)	Pressure drop (bar)	Compactness factor (m ² .m ⁻³)	Thermal performances (kW.m ⁻³ .K ⁻¹)
2	300	> 100	60	0.4	2,000	9,600
5	760		25	0.7		20,000

and utility plates are made of SiC, end plates are made of stainless steel to facilitate the connection with the feed lines and the outlets.

The reactor has been designed for a nominal range of flow rates from 1 to 10 L/hr. In such a range, the reactor offers interesting performances gathered in Table 4.

Remind that the thermal performances are as usual estimated from the product between the compactness factor and the global heat transfer coefficient. Consequently, due to the large value of this factor combined with the conductivity performances of the SiC material, the heat exchange performances are expected to be very high, as it can be noticed in the last column of this table.

Methodology of Characterization

Given the wide variety of technologies, particularly in the range of heat exchanger reactors, the user needs to be guided in his choice depending on the intended application, with criteria as objective as possible. Standard procedures are beginning to emerge in order to establish a form of “benchmark” of intensified technologies.

This echoes the long-standing process engineering concerns, when, for example, in the 80’s, one had been led to define liquid-liquid test systems to help in the selection of equipment in solvent extraction. Without being exhaustive, one presents below some of the methods that are recommended to characterize heat exchanger reactors. The methods will be illustrated by some performance results of some of the devices described above, in terms of:

- residence time distribution;
- pressure drop;
- mixing;
- heat transfer.

Residence Time Distribution

Characterization of residence time distributions (RTD) is now part of the standard arsenal of characterization techniques of process hydrodynamic regimes in chemical engineering (Villiermaux 1996). What particularly distinguishes the case of heat exchanger reactors is their relatively short residence time, which requires special care in both the positioning of injections and tracer detections (the closer the inputs and outputs of the device) and in the choice of detection sensors (resolution time as small as possible). In addition, given the difficulty of achieving a perfect Dirac

pulse, it is strongly recommended to use numerical techniques of signal treatment (deconvolution, CFD ...).

In practice, a spectrophotometric UV technology has been used, with a typical acquisition time of approximately 0.12 s. For example, Fig. 6 shows a typical result obtained with the DTS Shimtec Chart reactor at a given rate (17.6 L/hr) with water at 20°C, the abscissa corresponding to the reduced time. Here it is clear that the behavior is close to plug flow.

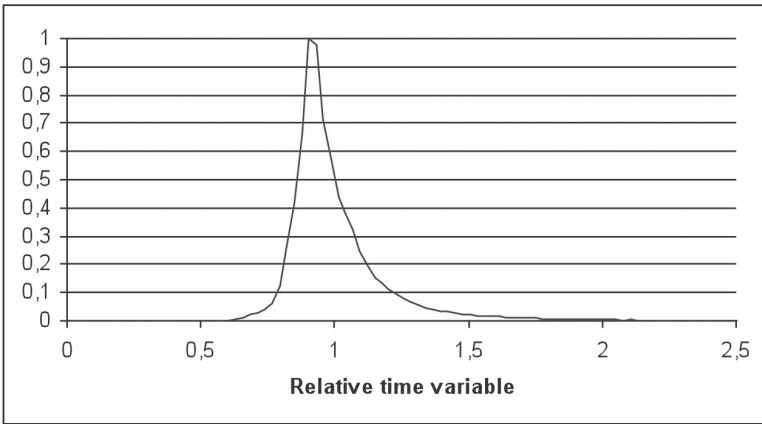


Figure 6. Typical RTD curve (Shimtec reactor).

Pressure Drop

The pressure drops (linear and singular) are also a key parameter for the characterization of devices. The measurement does not cause any particular difficulty. For example, Fig. 7 reports the results obtained with the Corning reactor for different fluids (water and glucose solutions) in the range from 2 to 10 L/hr and for different temperatures.

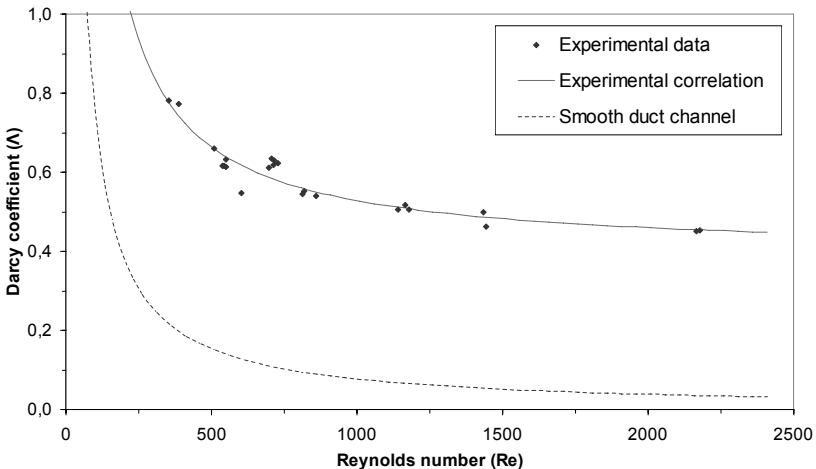


Figure 7. Darcy coefficient versus Reynolds number (pressure drop in a Corning reactor).

The results are typically presented in the form of a Darcy coefficient depending on the Reynolds number (Bird et al. 2002). Naturally, pressure drops are larger than in a smooth tube. Indeed, the contribution related to the design of channels (singularities) is included into this coefficient.

Mixing

Mixing is a subject extensively discussed in the literature, where databases are still relevant on both theoretical and experimental aspects, including micromixing. Our intention here is very limited and we will only evoke very quickly a simple way to characterize the mixture in a transparent device, such as Corning reactor for example. A visualization technique is used, whose main merit is its simplicity of implementation and operation. For example, we opted for a bleaching reaction of iodine with sodium thiosulfate in a homogeneous medium, reaction known to be instantaneous according to the following scheme:

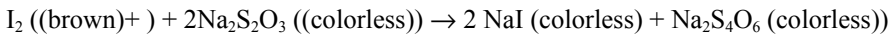


Figure 8 reports mixing times obtained as a function of Reynolds number in transparent mock-ups built for various channels geometries (Anxionnaz-Minvielle et al. 2013). One can notice that, as expected, the mixing time decreases with the Reynolds number (Re) and for lower Re, the mixing time may be close to 10 s.

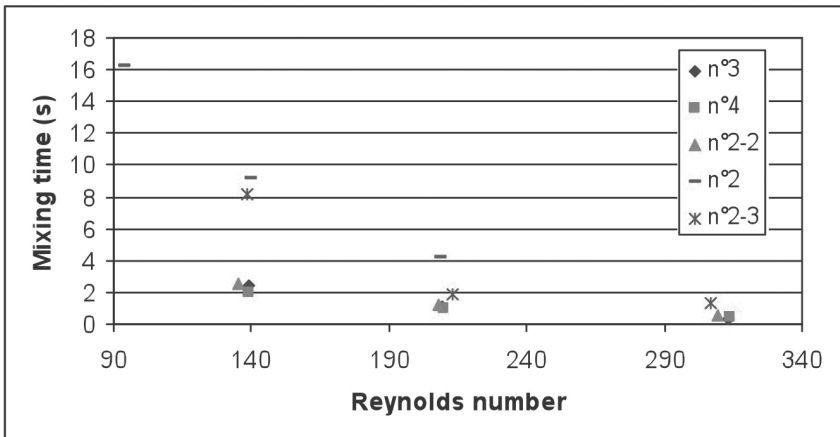


Figure 8. Mixing times versus Reynolds number according to different channel geometries (Anxionnaz-Minvielle et al. 2013).

Heat Exchange

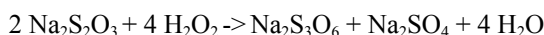
For the characterization of heat exchange performances, two complementary methods may be used, to be performed in a successive way:

- cooling hot process water with a cold utility, in steady and unsteady states, in order to understand the dynamic nature of the heat exchanger reactor;

- implementation of a rapid, highly exothermic reaction, for which all data are available and have been validated. A simple heat balance is then used in all cases to access to the global heat exchange coefficient (U) (Cabassud and Gourdon 2010).

In the first case, the aim is to verify the ability of the device to exchange heat, to estimate heat losses and to evaluate the dynamics of the device, before carrying out the test reaction.

In the second case, the aim is to test the capabilities of the device to operate in a different operating window than for a batch or a semi-batch reactor (with a given reactive feeding rate). As a test reaction, the oxydation of sodium thiosulfate ($\text{Na}_2\text{S}_2\text{O}_3$) by hydrogen peroxide (H_2O_2) has been chosen (Benaïssa et al. 2008a,b; Prat et al. 2005). It reacts according to the following stoichiometric scheme (Lo and Cholette 1972):



As illustration, for a given experiment in a Shimtec reactor, Fig. 9 shows the time evolution of the input and output temperatures for the reaction medium side ($T_{p,in}$ and $T_{p,out}$) and the utility side ($T_{u,in}$ and $T_{u,out}$). The reactants are introduced at $t = 700$ s,

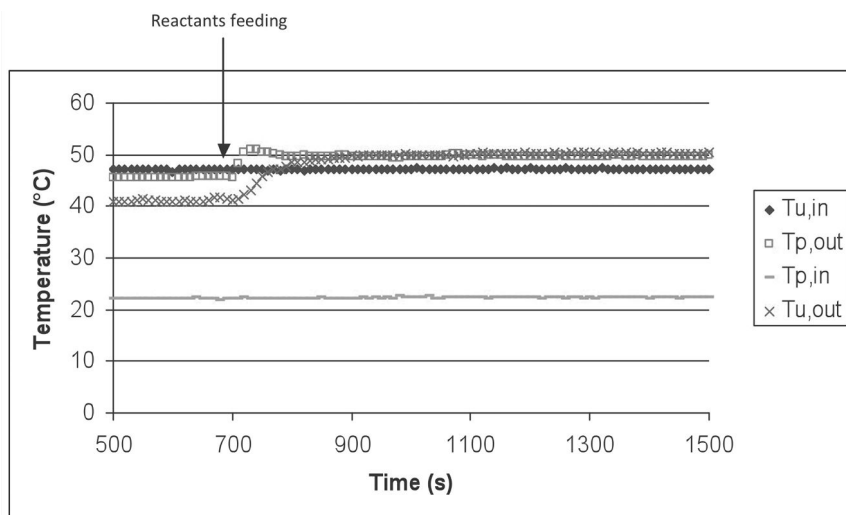


Figure 9. Inlet and outlet temperatures evolution of a Shimtec reactor (process and utility sides).

Influence of Material and Compactness Factor

As a preliminary comparison, Table 5 gives the performance-related characteristics of different heat-exchanger/reactors presented above.

The choice of material primarily required by the nature of the reagents involved and the issues of corrosion resistance has also an influence on the reactor dynamics.

Table 5. Comparison of heat transfer performances according to the HEX-reactor type and material.

Reactor	SiC HEX reactor (Boostec)	Haynes HEX reactor (Chart)	Glass HEX reactor (Corning)	Stainless steel HEX reactor (Alfa Laval)	Batch reactor
Heat transfer coefficient ($W.m^{-2}.K^{-1}$)	7500	1500	600	2500	400
Residence time	Few minutes	Few minutes	Few minutes	Few minutes	Few hours
Ratio of surface/volume ($m^2.m^{-3}$)	2000	2000	2750	400	2.5
Heat exchange capacity ($kW.m^{-3}.K^{-1}$)	15000	3000	1650	1000	1

Indeed, an important parameter in heat exchange is linked to the material effusivity b which is related to the material, defined by:

$$b = \sqrt{\lambda \cdot \rho \cdot C_p}$$

and which appears in the unsteady conduction equation as follows (t is the time):

$$b = \sqrt{t} \approx const.$$

ρ and C_p being respectively the density ($kg.m^{-3}$) and the specific heat at constant pressure ($J.kg^{-1}.K^{-1}$). In terms of the dynamic response of the reactor, the larger effusivity b is, the larger the material imposes its temperature to the reaction medium. Some effusivity values of the various materials used in heat-exchanger/reactors are summarized in Table 6, the data naturally favor the silicon carbide (SiC).

Table 6. Effusivity values according to the HEX-reactor material.

	SiC	Stainless steel	Glass
λ (20°C) $W.m^{-1}.K^{-1}$	180	16	1
C_p (20°C) $J.kg^{-1}.K^{-1}$	680	500	800
ρ ($kg.m^{-3}$)	3210	7900	2600
Effusivity $b = (\lambda \cdot C_p \cdot \rho)^{1/2}$	20000	8000	1500

The Reactive Distillation

Introduction

The reactive distillation can be defined as the simultaneous implementation, inside one apparatus, of chemical reactions and a multistage distillation. Its basic principle is based on the theory of chemical equilibria set in 1884 by Le Chatelier, “when external changes to a physico-chemical system in equilibrium causes a shift to a new equilibrium state, this evolution is opposed to the external changes and moderates the effect”. An endothermic reaction, for example, is favored by a higher temperature because increasing the temperature leads to a shift of the reaction equilibrium in the forward direction, and similarly, the removal of a reaction product of the reaction

phase leads to a shift of the reaction into the direction of forming this product. It is precisely this latter case which is the basement of the reactive distillation: gradually as the reaction proceeds, a component is separated from the mixture by distillation in such a way that starting from a stoichiometric mixture the reagents are completely converted to product. But the increase in conversion is not the only advantage of the reactive distillation, it is also expected:

- an increased selectivity: the rapid removal of reaction products from the reactive phase allows an increase in the selectivity of the reaction;
- energy integration: if the reaction is exothermic, the reaction heat contributes to the separation of the mixture;
- an improved quality of production: products are heated once so reducing the risk of thermal degradation;
- scale-down economy: the process equipment (pumps, valves, sensors ...), which may represent a significant share of the cost of the process is reduced;
- catalysis: the temperature at any point is limited by the bubble temperature, the risk of degradation of the catalyst is removed simultaneously with the risk of formation of hot spots.

One of the emblematic examples of reactive distillation industrial success is undoubtedly the case of esterification of methanol to methyl acetate (Agreda et al. 1990). Figure 10 shows the process developed by Eastman Chemicals claiming an energy saving of around 85% compared to the traditional process. The Amberlyst constituting the fixed catalyst bed is also used as adsorber. Sulphonic groups catalyze the esterification reaction and the polymer preferentially adsorbs water. One

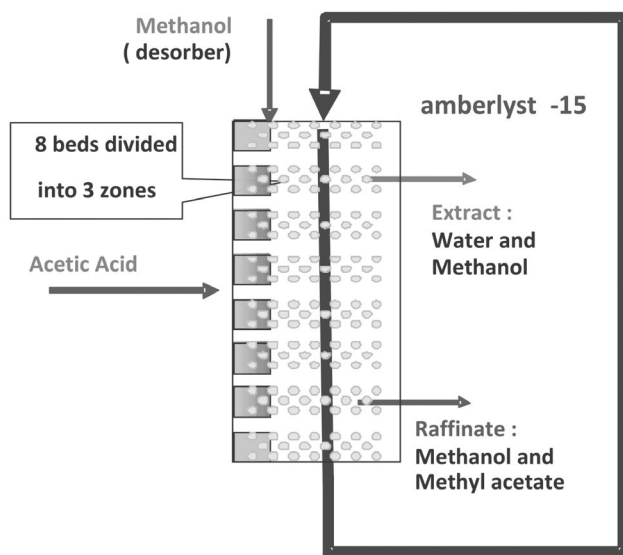


Figure 10. Illustration of reactive distillation applied to methanol esterification.

feed is acetic acid and the other pure methanol which serves as a reagent and as desorbent. Acetic acid is fed to the center of the reactor where it intersects a down flow containing methanol. In the presence of Amberlyst-15, the reaction takes place to form methyl acetate and water. The Amberlyst preferentially adsorbs water and transports acetate upwardly. The separation of the methyl acetate and water leads to complete conversion of the acetic acid. Gradually as the adsorbent moves upwardly, it crosses the stream of methanol which desorbs water. The methanol/water mixture is removed from the apparatus. The adsorbent leaving the top of the reactor is substantially free of water which minimizes the risk of reverse reaction. The raffinate stream contains mainly methanol and methyl acetate. This method allows obtaining 100% conversion of the acid.

However combining reaction and separation is not always advantageous. A number of favorable conditions must be met in order to claim its applicability in reactive distillation:

- reactive distillation is more particularly appropriate to equilibrated reactions;
- the operating temperature ranges for the reaction and separation must be compatible with each other and with that of the catalyst;
- the reaction should be sufficiently fast to minimize hold-up volume, thereby limiting the size of the column;
- if the catalyst is a solid, its lifetime must be sufficient to not jeopardize the economic viability of the process.

Referring to the 12 principles of green chemistry outlined by Anastas and Zimmerman (Anastas and Zimmerman 2003) and to the 12 principles of Green Process Engineering (Malone et al. 2003), the positive and negative aspects of the reactive distillation have been assessed (Table 7). It follows that many aspects of the intensified reactive distillation take account inherently the Green Process design principles.

Design Method

The dissemination of this type of process in the industrial field is dependent on innovative design methods which are able to answer quickly and cheaply the issues of feasibility and preliminary design of the equipment. Consequently, one will describe in this section a methodology developed in the early 2000's that integrates the results of a decade of research (They et al. 2005).

General Principle of the Design Methodology

The general principle of the proposed approach for the feasibility analysis, synthesis and design of reactive distillation processes, is shown schematically on Fig. 11. The

Table 7. Positive and negative aspects of reactive distillation (from Malone et al. 2003).

Principles	Reduced number of process units	More specialized equipment	Complex design & control	Enhance overall rates	Overcome unfavorable equilibria	Avoid difficult separations	Improve selectivity	Reduce energy	Reduce solvent
1			-						
2					+		+		+
3					+	+			+
4				+	+	+	+	+	+
5					+				
6	+		-						
7		-							
8	+			+					
9			-						
10	+	+						+	
11	+	-							
12	+								

- Principle 1: inherent rather than circumstantial
- Principle 2: prevention instead of treatment
- Principle 3: design for separation
- Principle 4: maximize efficiency
- Principle 5: output-pulled vs. input-pushed
- Principle 6: conserve complexity
- Principle 7: durability rather than immortality
- Principle 8: meet need, minimize excess
- Principle 9: minimize material diversity
- Principle 10: integrate local material & energy flows
- Principle 11: design for a commercial afterlife
- Principle 12: renewable rather than depleting

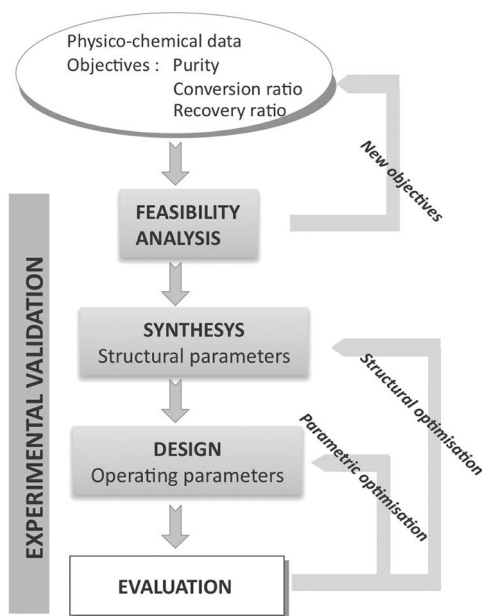


Figure 11. Proposed methodology for feasibility analysis, synthesis and design of reactive distillation.

major advantage of this approach lies in the fact that through a gradual introduction of the complexity, a lot of informations about the process are provided, such as:

- the thermodynamic properties of the system;
- data on the chemical reaction (stoichiometry, value of the equilibrium constant, ...);
- the objectives in terms of purity, recovery or conversion ratio.

As shown on Fig. 11, this procedure relies on four major steps.

The feasibility analysis is to ensure that the specifications are thermodynamically feasible. If necessary, this step can also determine a set of available distillate and residue compositions corresponding to specifications of purity, recovery and conversion ratio. Otherwise, the process targets are adjusted on the basis of the previous observations.

The synthesis step is based on a more detailed analysis of the phenomena involved. This analysis is first of all concerned with the structural aspects of the process. Synthesis allows to confirm (or refute) the results obtained after the first step, and then, to determine a column configuration to achieve the goals initially set.

The actual **design step** allows determining the operating parameters of the process. After these three steps, a column configuration to achieve the goals initially set by the designer is available.

The fourth step is to **evaluate the value** of the process in terms of cost (investment and operation) and environmental impact (effluent, energy consumption ...). To complete

this step, a sensitivity analysis of the process with respect to various configuration settings and operating parameter of the process can be considered, or optimization procedures can be implemented:

- a parametric optimization of the operating variables of the process;
- a structural optimization of the column configuration. Finally, let's note that all along the design process, the methodology recommends a pilot experiment to validate the results obtained by calculations especially at the step 3, the so-called "design".

In this chapter, we are primarily interested in the first three steps of this procedure. To clearly highlight their complementarity and the evolution of the complexity of the adopted models, Fig. 11 is briefly discussed. The next sections will summarize in detail each step of the procedure.

To initiate the feasibility study, the generation and the analysis of the **reactive residue curves** are used. This step is an essential part of the feasibility analysis of a reactive distillation process, because it provides a simple and very illustrative tool with a graphical visualization to analyze the coupling between reaction and separation. This approach allows:

- locating the singular points of the system (reactive azeotrope, unreactive azeotropes);
- determining the nature of the singular points (stable node, unstable node, saddle point, etc.);
- building the distillation boundaries generated by these singular points. Viewing and analyzing distillation boundaries can provide information concerning potential barriers to achieving a given objective.

Following this analysis, the conditions required to obtain the desired product can be defined. These conditions are related to the feed composition or to the structure of the column (need to introduce pure separation sections, need for a double feed ...).

Finally, the **steady-state analysis** based on the approach proposed by Giessler et al. (Giessler et al. 1999) is used to:

- analyze the phenomena which govern the behavior of the system in any non-reactive section;
- provide a set of available distillate and residue compositions corresponding to specifications formulated in terms of purity, conversion or recovery ratio ...

The analyzes presented in the context of the feasibility analysis are subject to numerous assumptions that are far from being valid in reality (total reflux in the case of the analysis of residue curves, flow rates of liquid and vapor phases infinite in the case of the analysis of steady state, ...). In this sense, the feasibility analysis proposed here can answer the question of feasibility of the objectives by considering only the thermodynamic limits.

For the synthesis step, the design method based on **boundary value method**, introduced by Barbosa and Doherty (Barbosa and Doherty 1988) for fully reactive

and extended to hybrid processes by Espinosa et al. (Espinosa et al. 1996), seems the most appropriate. Although based too on simplifying assumptions (in fact the whole thermal effects occurring in the column are neglected), this approach, using a more rigorous model (liquid and vapor flow rates and reflux have finite values) allows to confirm or refute the results of the first step. Then, using data obtained at the end of the feasibility analysis (compositions accessible to the distillate and residue products, favorable proportions of reactants, etc.), it provides more accurate information about the process configuration that either fully reactive or hybrid with pure separation zones. These informations are as follows:

- the minimum and maximum reflux ratio; and, for a given reflux ratio:
- the position of the reactive zone;
- the number of theoretical stages;
- the location of the feed stage.

In that sense, it can be compared to a ShortCut method (FUG equations) used in the case of multicomponent system for a conventional distillation.

Finally, a simulation step enables to carry out the design step itself. Knowing the configuration of the desired column, this step determines the operating parameters required to achieve an objective formulated in terms of purity and (or) quantity of the desired product. Unlike the design stage is based solely on the resolution of mass balance equations and thus neglects the whole thermal effects likely to occur in the column (phenomena due to non-constant heat of vaporization or high heat of reaction, ...), the simulation itself is based on the resolution of all equations: material balances, liquid-vapor equilibrium equations and chemical equilibrium equations, summation and enthalpy balances (MESH equations). If it is needed to introduce some technological data in the simulation, it will then move towards advanced models called “transfer models” (rate based approach, Non Equilibrium models) which allow to take into account the kinetics of mass transfer in these multicomponent mixtures based on the diffusivity laws like Maxwell-Stefan, Fick or Nernst-Planck (Rouzineau et al. 2002).

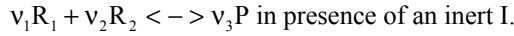
After this last step, a column configuration to achieve the objectives set at the beginning of the procedure has been achieved.

Analysis of Reactive Residues Curves

In this section, the principle of reactive residues curve analysis is briefly presented. For more details, let's refer to (Thery 2002). Similarly to the feasibility condition set for non-reactive distillation processes, the following necessary condition for feasibility can be formulated as:

A reactive distillation operation is possible at total reflux, if in the space of reactive compositions, the representative points of the distillate and residue belong to the same reactive residue curve, and representative points of the feed, distillate and residue are aligned.

Case Study # 1. Applying this rule to the feasibility analysis of a reactive distillation process involving a reaction type:



The residue curves map for this system is shown on Fig. 12. For this system, all residue curves start from the same point (the inert I) and reach the same stable node formed here by the reactive azeotrope. There is therefore no boundary distillation. Two cases can occur:

- Case 1: **direct separation**, the objective of a direct separation is to recover the lightest component (unstable node) in the distillate. Here, it is the component I. It is then possible to determine the composition of the product available at the residue (point B1) by drawing the mass balance line passing through the point I and the feed point F.
- Case 2: **indirect separation**, the goal of an indirect separation is to recover the heaviest (stable node) at the residue. Here it is the reactive azeotrope (point quoted “Az”). The product is available at the distillate obtained similarly to the case of the direct separation and corresponds to the point D₂.

Figure 13 shows schematically both configurations of reactive columns resulting from the study of the system considered. As we can see, none of these simple structures directly reaches the pure product P. The latter cannot exist alone in the chemical equilibrium. Indeed, it appears necessary to introduce a pure separation zone at the column to separate the heavy product P from the residual reactants R₁ and R₂. To generalize this observation, we can formulate the following rule:

If it is necessary to separate a product which is not represented on the hypersurface of the chemical equilibrium, then a pure separation section is required.

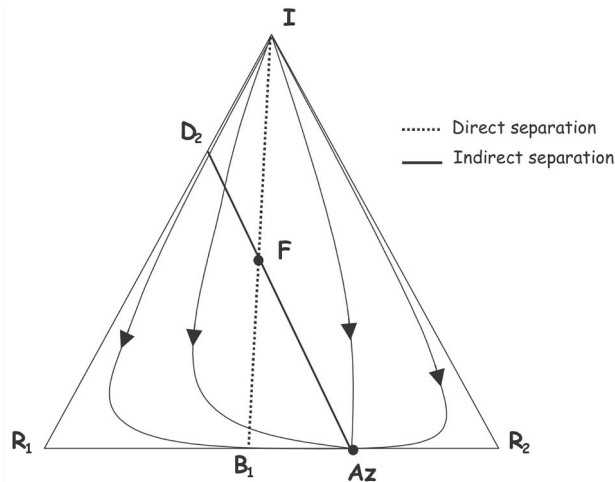


Figure 12. Reactive residues curves for the system $v_1R_1 + v_2R_2 \leftrightarrow v_3P$ in presence of an inert I.

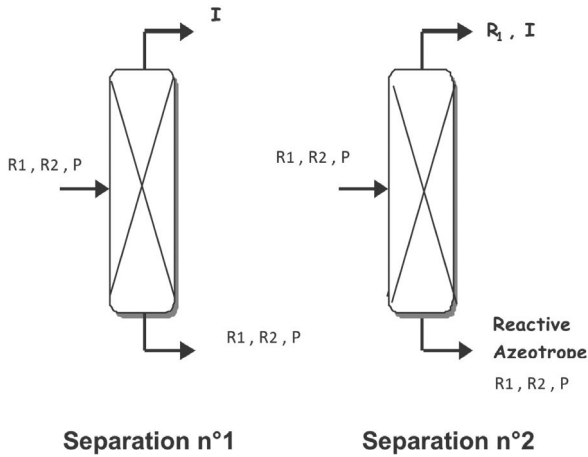
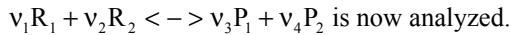


Figure 13. Column configurations for the system shown on Fig. 12.

Let's notice, however, that although the reactive residues curve analysis allows identifying whether or not introducing pure separation trays, it does not allow a rigorous analysis of the feasibility of reactive distillation combining the reactive zones and pure separation zones. Reactive residue curves map is limited here to the analysis of entire reactive distillation.

Case Study # 2. The residue curves of a system involving an equilibrium reaction of the type:



The shape of the reactive residue curves is highly dependent on the relative volatilities of the components. Therefore, we consider two separate rankings of the components, according to the increasing volatility: $P_1 - R_2 - R_1 - P_2$ (Fig. 14a), $P_1 - P_2 - R_1 - R_2$ (Fig. 14b).

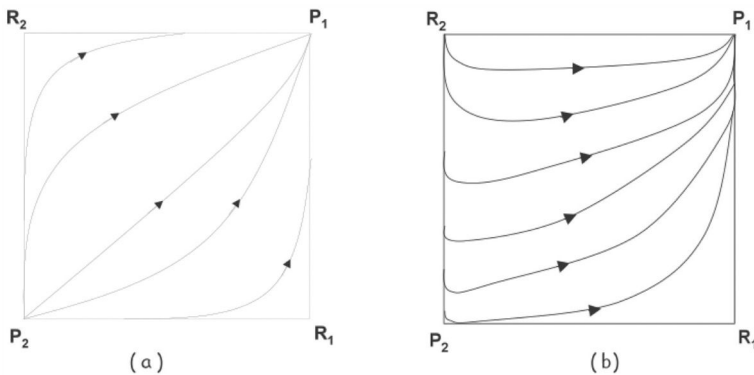


Figure 14. Reactive residues curves for the system $n_1R_1 + n_2R_2 \rightleftharpoons n_3P_1 + v_4P_2$ at different increasing volatilities: a) $P_1 - R_2 - R_1 - P_2$; b) $P_1 - P_2 - R_1 - R_2$.

In the first case, temperatures of the reactants and intermediate bubbles products P_1 and P_2 are respectively the heavy component and the components the most volatile. All residue curves are derived from product P_2 and ending at the product P_1 . The reactants are saddle points and products nodes. In this case, it is quite possible to obtain both, products P_1 and P_2 produced in a single reactive distillation column.

In the second case, the stable and unstable nodes are respectively product P_1 and the reactant R_2 . Furthermore, as the product P_2 is a saddle point, no residue curve binds the component P_2 to the component P_1 . The necessary feasibility condition mentioned above is not satisfied, and it seems, therefore, impossible to design a column to recover, both P_1 and P_2 as pure products. Bessling et al. (Bessling et al. 1997) propose the following rule:

The distillation process is favorable if the two products are stable and unstable nodes interconnected by a residue curve, and if the bubble points are sufficiently different.

However, in the case where one of the products (or both) is a saddle point, then it is possible to make the separation by implementing a column having a double feed.

Synthesis Step: Design from the Boundaries Values Method

After having determined the most convenient feed conditions, the designer has to determine the crucial parameters for the design and control of the process. It is the objective of the second step. To this aim, the design method based on Boundary Value Method Design is recommended (Barbosa and Doherty 1988).

The proposed method is based on the following assumptions:

- feed is at the boiling point,
- the column is adiabatic,
- reaction heat is neglected,
- heats of vaporisation of each component are equal.

This allows us to decouple material balance and energy balance and to consider the vapor molar flow rate as being constant in the column, the liquid molar flow variation being exclusively due to the chemical reaction.

In addition:

- Reaction is supposed instantaneously equilibrated,
- Each stage is at the thermodynamic equilibrium.

The principle of the method is as follows: knowing the desired and feasible compositions of the residue and distillate products, mass balances are written starting on one hand from the top to the bottom and on the other hand from bottom to top.

It leads to two profiles (stripping and rectifying) whose are depending on the reflux ratio. A feasible separation is obtained when both profiles intersect, and a reactive bubble point calculation on each tray is used to locate the reactive section.

Figure 15 is a representation of a reactive distillation process with a pure separation section.

Let's remind briefly thereafter the equations to represent each of the column section.

Pure stripping section (without chemical reaction). This section covers all the trays beneath the first reactive stage. Balance between the bottom of the column and any stage of pure stripping section zone:

$$X_{j,s-1} = \frac{s}{s+1} Y_{j,s} + \frac{1}{s+1} X_{j,B}$$

for $j = 1, N_c$ and $s = 1, N_{\text{stripping}}$

$$\text{with } s = \frac{V}{B}$$

The profile is then generated in the stripping section and a test is performed on each tray to detect the intersection of this profile with the reactive surface: it is a set of liquid compositions, vapor composition and a temperature for which the chemical equilibrium and physical equilibrium are simultaneously satisfied. Once this condition is satisfied, it must then be switched to the reactive stripping zone.

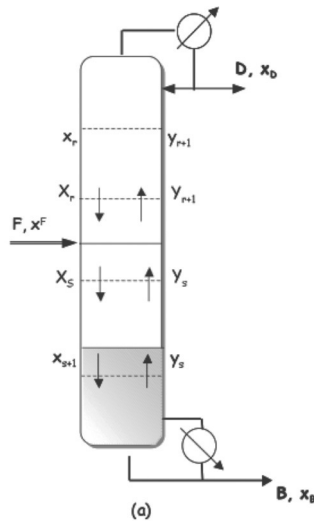


Figure 15. Reactive distillation column with pure stripping section.

Reactive stripping section. This section covers the zone above the first reactive stage and below the feed tray. The presence of the chemical equilibrium reaction now permits the use of reactive compositions.

Balance between the bottom of the column and any stage of the reactive stripping section zone:

$$X_{j,n-1} = \frac{s_s^*}{s_s^* + 1} Y_{j,n} + \frac{1}{s_s^* + 1} X_{j,B}$$

for $j = 1, N_c; j \neq k$ and $n = N_{stripping}, N_{feed}$

$$\text{with } S_n^* = s^* \frac{V_k - V_t y_{k,n}}{V_k - V_t x_{k,B}}$$

Reactive rectifying section. This last section covers the zone above the feed stage. Balances from the column head and any of the reactive rectifying stage:

$$Y_{j,r+1} = \frac{r_r^*}{r_r^* + 1} X_{j,r} + \frac{1}{r_r^* + 1} X_{j,D}$$

for $j = 1, N_c; j \neq k$ and $r = 1, N_{feed}$

$$\text{with } r_r^* + 1 = \frac{V_k - V_T y_{k,r+1}}{V_k - V_T x_{k,D}} (r + 1) \text{ and } r = \frac{L_N}{D}$$

The equations to design a column with a non-reactive section at the bottom of column have been presented. But, a general procedure to design the whole column configurations (Table 8) exists.

Table 8. Different column configurations (reactive distillation).

	Reactive column	1 pure stripping section	1 pure rectifying section	1 pure stripping section 1 pure rectifying section
1 feed				
2 feeds				

Given the degree of freedom of the system, the user needs to provide:

- the composition of the feed stream;
- the operating pressure;
- the head and bottom compositions: in fact, for a mixture of four components, only three independent transformed compositions are needed, others are derived from a mass balance on the column;

- the reflux ratio, it is the latter parameter on which we will have to act to get the intersection of the two profiles (stripping and rectifying, see Fig. 16).

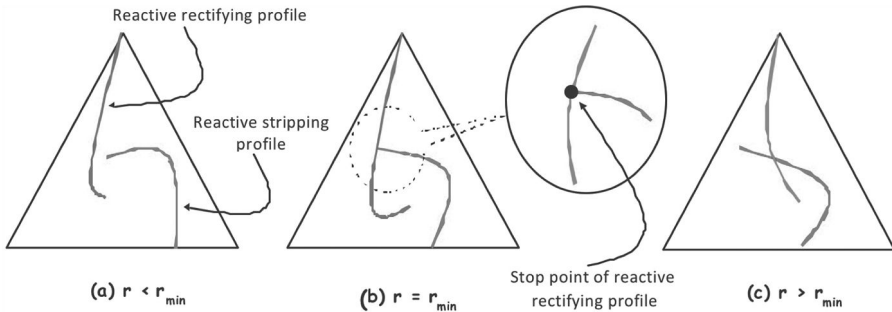


Figure 16. Influence of reflux ratio on the composition profiles.

The operating pressure and the feed composition are often well-known by the designer. The compositions of the products obtained at the top and bottom of the column are obtained by following the results of the first feasibility analysis step.

Thus, at the end of this procedure, the designer gets the following results:

- validation (or not) of the feasibility of a given separation and, when appropriate,
- value of the minimum reflux ratio, it is the value of the reflux for one of both profiles which reached its stationary point (point beyond which the liquid and vapor compositions do no longer change) at the intersection point with the other profile.

Finally, for a reflux ratio above the minimum reflux:

- the number of theoretical stages required, in fact, the composition profiles being generated stage by stage, one has just to count the number of stages required;
- the location of the reactive zone;
- the location of the feed tray.

From these results, the steps of simulation and experimental validation can be now considered.

Technology Issues

Once the design step of the reactive distillation column is completed, the issue of the technological choice raises, particularly with regard to the nature of the column internals. This choice differs from the case of classical non-reactive column due to constraints related to the reaction:

- the residence time of the chemical species in the reactive section should be important to get a decent conversion rate. It must therefore have a significant liquid hold-up in the reactive zone;

- it is necessary to maximize the catalyst -liquid contact for promoting the reaction.

In addition to the conventional distillation constraints:

- ensure a good mass transfer between gas and liquid;
- limit pressure drop and flooding.

Furthermore, depending on the type of catalyst, homogeneous or heterogeneous, the technology used will be different.

Homogeneous Catalysis

Practically, the easiest way to make a distillation column “reactive” is to place at the top of the column a liquid catalyst feed (often this catalyst is non-volatile), in the case of homogeneous catalysis. To promote hold-up, the most effective technology is to use bubble-cap tray internals. The use of packed column (random or structured) is also possible if the reaction rate is fast enough such that the retention is sufficient. However, the implementation of a homogeneous catalyst has some drawbacks:

- the use of a homogeneous catalyst allows the introduction of pure separation sections above the catalyst feed, resulting in a limited modularity that can prevent the practical realization of the designed column;
- the use of a homogeneous catalyst increases the operating costs of the unit;
- the presence of a homogeneous catalyst can cause corrosion problems if the materials chosen for the equipment is not suitable;
- the risk of side reactions between the catalyst and any of the species cannot be excluded.

Heterogeneous Catalysis

The disadvantages previously mentioned for the homogeneous catalysis have led scientists and industrials to develop a new type of heterogeneously catalyst, based on the use of solid particles:

- ability to adjust as much as possible, the location of the reaction;
- ability to control the amount of catalyst at any point in the column;
- substantial savings if the lifetime of the catalyst is sufficient and if it is possible to regenerate the catalyst;
- the output streams, free of catalyst, require no additional treatment;
- easy and safe handling.

Heterogeneous catalytic column internals can be of three types:

- catalytic beds: arranged in the plates (Fig. 17a), allowing the reaction of the liquid phase while allowing the plates available for the separation;

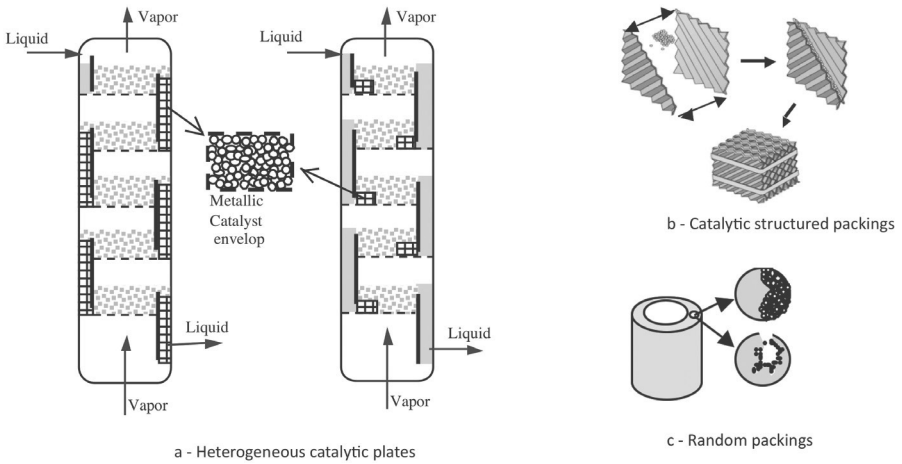


Figure 17. Different types of catalytic internals. (a) heterogeneous catalytic plates, (b) catalytic structured packing, (c) random packings.

- catalytic structured packing: in order to avoid catalyst particles losses in the column, the particles being contained between two metal sheets assembled in cube or cylinder (Fig. 17b);
- random packing activated: Figure 17c shows a sectional view of a conventional Raschig ring made active by means of catalyst particles, the material of the ring must therefore be porous to allow the diffusion of components.

To date, only the catalytic structured packings have been widely studied and developed by the scientific community. They now exist in mainly two commercial forms, the Katapak Sulzer (<http://www.sulzerchemtech.com>) and Multipak society Montz (<http://www.montz.de>). Both packings are based on the same principle: catalytic baskets alternating with corrugated metal sheets (Figs. 18a,b,c), the latter being identical to the elements of traditional non-reactive structured packing.

Studies on these packings (Kołodziej et al. 2001; Kołodziej et al. 2004a,b; Olujic et al. 2003; Götze et al. 2001; Ellenberger and Krishna 1999; Ratheesh and Kannan 2004) show preliminary good capabilities in terms of pressure drop and flooding and also in terms of mass transfer. This seems logical since the structure corrugated sheet is equivalent to traditional packings.

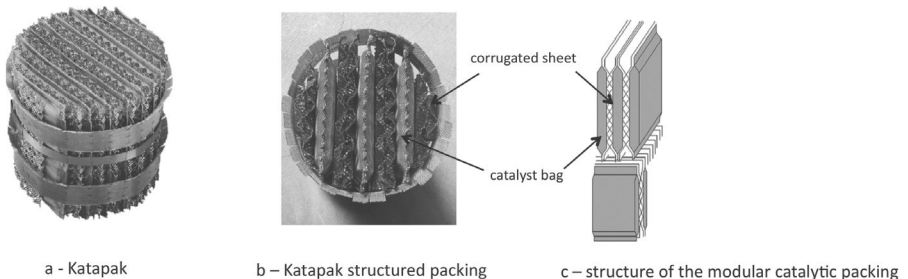


Figure 18. Structured catalytic Katapak packings. (a) Katapak, (b) structure Katapak, (c) stacking.

Tests have also been made in the case of the reactive distillation (Kołodziej et al. 2001). The results show two major disadvantages of this packing technology:

- the conversion rate seems low given the amount of catalyst present in the packing. This suggests that the contact between the liquid and the catalyst is only partial. A recent study of tomography on the liquid distribution of this packing confirms this analysis (Toye et al. 2005). Figure 19 shows a superimposed picture: distribution of solid in gray and in black liquid distribution. This distribution of liquid is distributed to 75.8% on the separation zone and 23.3% on the tray 2 and 0.1% on the tray 1 and 3 of the reaction zone. This clearly shows that the catalyst sees only partially the liquid;
- when the catalyst is at the end of life, the packing has to be changed. It results in a significant operating cost.

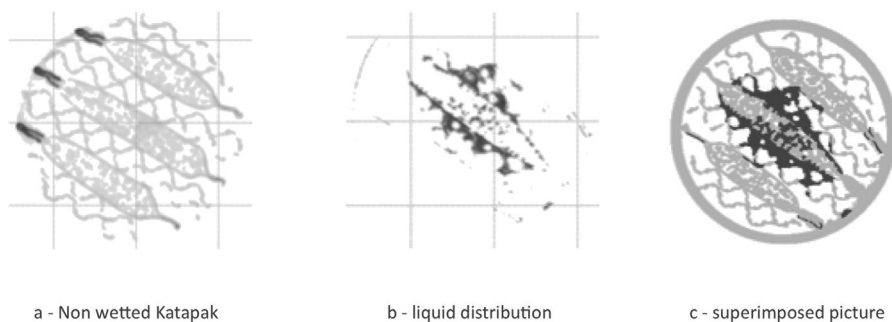


Figure 19. Liquid distribution on a Katapak packing. (a) Non wetted Katapak, (b) liquid distribution, (c) superimposed picture.

To date, only few catalytic packings exist for reactive distillation. The technology consists of using conventional structured packing and inserts catalysts inside. This technology is satisfactory from a separation viewpoint but suboptimal from a reaction viewpoint because of the large amount of catalyst to be used related to the problem of liquid distribution over the catalyst. Alternative and innovative solutions are now being researched (Leveque et al. 2009), it is to coat the catalyst on the structure of the packing directly.

Some Achievements

Some very comprehensive reviews on potentially applicable mixtures to the reactive distillation of major industrial interest have been published in the last decade (Hiwale et al. 2004; Malone and Doherty 2000; Sharma and Mahajani 2003). They affect about one hundred reactions gathered within fifteen different classes. Esterification reactions are probably the most studied for reactive distillation:

- the n-propyl acetate: Bart et al. 1996; Okasinski and Doherty 2000; Brehelin et al. 2007.
- the n-butyl acetate: Steinigeweg and Gmehling 2002; Grob and Hasse 2005.

- the amyl-acetate: Lee et al. 2000; Okasinski and Doherty 2000.
- methyl formate: Tischmeyer and Arlt 2004.
- the n-butyl acrylate: Chen et al. 1999; Schwarzer and Hoffmann 2002.
- fatty esters: Omota et al. 2003; Steinigeweg and Gmehling 2003.

Other families of reactions have been investigated in reactive distillation including transesterification (Bonet 2007; Nishihira et al. 2000; Shaerfl et al. 2000; Lyuben et al. 2004), whose applications are increasing in the field of green solvents and biodiesel. The etherification reactions are also a large pool of applications for the reactive distillation as the synthesis of MTBE (Ryu and Gelbein 2002), TAME (Kołodziej et al. 2004b) or ETBE; hydration reactions such as hydration of ethylene oxide (Steyer et al. 2002) or the dehydration of tertiary butyl alcohol (Abella et al. 1999). In their book, Lyuben and Yu (Lyuben and Yu 2008) present an inventory of over 200 reactions studied in reactive distillation.

Production of Methyl acetate by Reactive Distillation

The synthesis of methyl acetate from methanol and acetic acid may be described by the following reaction:



This reaction is usually catalyzed by a strong acid, for example sulfuric acid in a homogeneous phase or by an ion exchange resin such as Amberlyst. The equilibrium constant of this reaction is equal to 5.2 and is relatively independent of temperature. From the point of view of phase equilibrium, the system is a diphasic liquid-vapor system and has the following characteristics in terms of boiling point at 1 atm:

Azeotrope MeOH/MeAc:	53.6°C
Azeotrope MeAc/H ₂ O:	56.4°C
MeAc:	57°C
MeOH:	64.5°C
H ₂ O:	100°C
AcAc:	118°C

From these physico-chemical data, one can plot reactive Residue Curve Map (rRCM). Figure 20 shows the shape of the rRCM. Pure substances are located at the corner and the edges are non-reactive binary. The desired products (MeAc and H₂O) are saddle points, so the reactive column must have two feeds.

Therefore, the flowsheet of the column is given on Fig. 21. The methanol is fed down while the acetic acid is fed above. The heaviest product of the reaction is withdrawn at the bottom of the column while MeAc is the lightest product obtained at the distillate.

The study of such a column shows a different behavior from that of a conventional distillation. In fact, the temperature profile in the column is not necessarily monotonous (Lyuben and Yu 2008) and the effect on the purity of the reflux head is not monotonous, which generates the concept of maximum reflux or

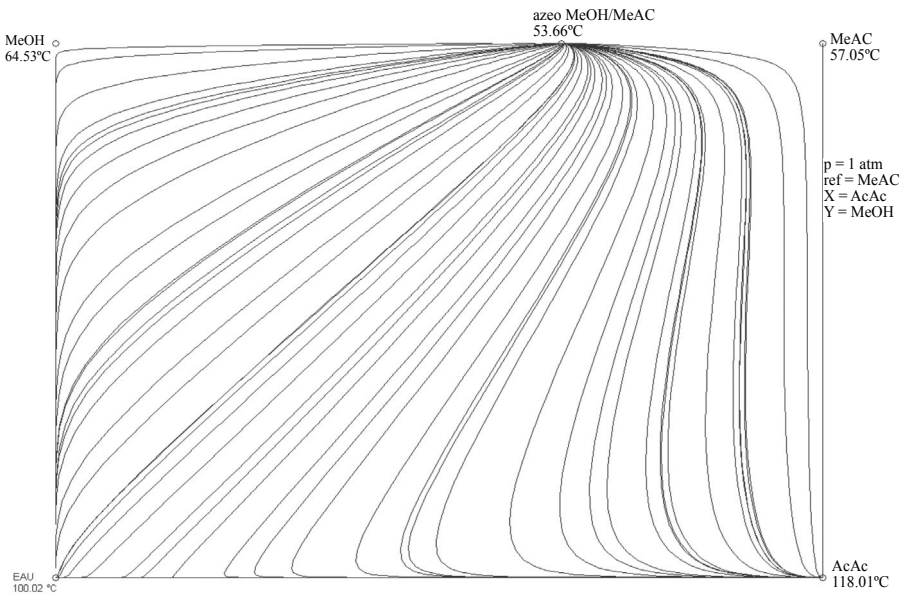


Figure 20. rRCM for methyl acetate.

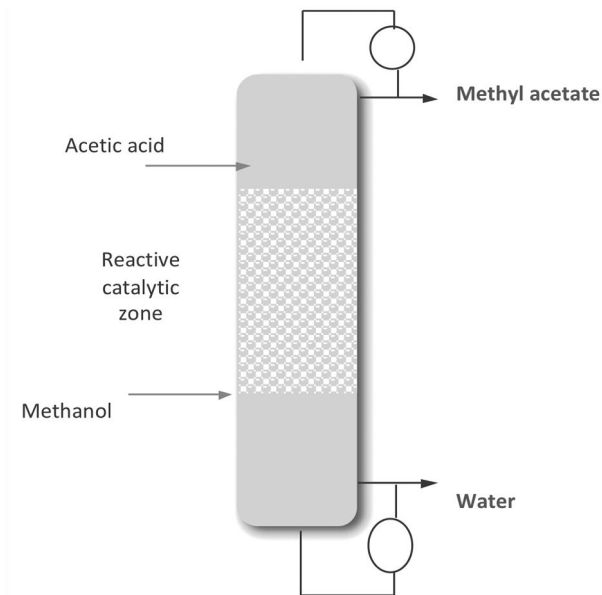


Figure 21. Reactive distillation with two feed streams.

optimal reflux (Fig. 22). These both unexpected effects for a specialist in separation are related to the chemical reaction.

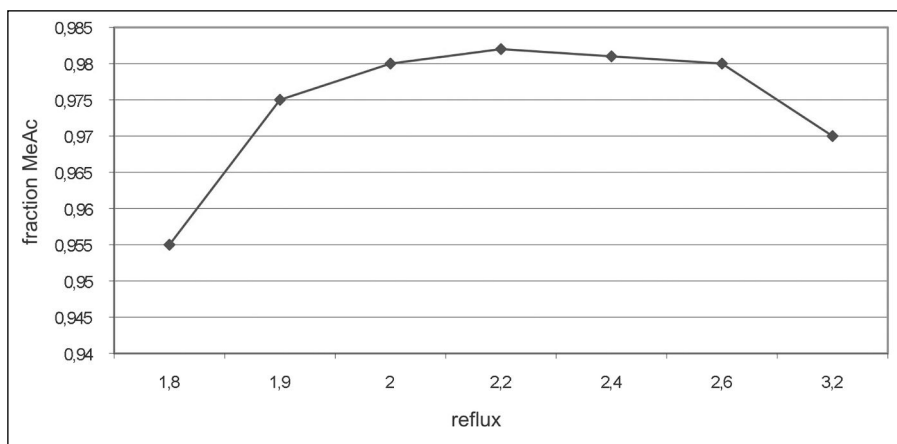


Figure 22. Sensitivity to reflux ratio.

Conclusion

Multifunctionality is an important part of process intensification strategy in a goal of producing more and better by consuming less (raw materials, energy). We have in this chapter explored two complementary tracks, the HEX reactor coupling reaction and heat exchange and the reactive distillation coupling reaction and separation. In the first case, we saw that a large number of technological solutions are now available, and in the second case, we have seen the interest of this approach for the equilibrium reactions such as esterification.

It remains that even today the implementation of these operations in industry is still limited. But, there are well known reasons to this situation. Include primarily the difficulty of investing money in innovative technologies for which we do not yet have enough feedback. One also has to face some technico-economical objections, which hinder large diffusion in the industrial world: investment cost, lack of versatility or flexibility of technologies, susceptibility to corrosion and difficulties cleaning, etc.

Nevertheless, efforts are undertaken around the world to demonstrate the interest of these new technologies and to try to limit risk-taking inherent in the introduction of a disruptive technology. In fact, facing the challenges of reducing costs, including operating, of reducing amounts of solvent, of risk mitigation and environmental impacts, of increasing the complexity and quality of manufactured products, we believe that in the very next year, there is place for an active research and large dissemination through the industry of these intensified technologies.

Acknowledgments

A major part of the experimental facilities were supported by the ANR, FNADT, Grand Toulouse, Préfecture Midi-Pyrénées and FEDER fundings.

References

- Abella, L.C., P.D. Gasparillo, H. Itoh and S. Goto. 1999. Dehydration of ter-butyl alcohol in reactive distillation. *J. Chem. Eng. Jap.* 32: 742–746.
- Agreda, V.H., L.R. Partin and W.H. Heise. 1990. High-purity methyl acetate via reactive distillation. *Chem. Eng. Prog.* 86(2): 40–46.
- ALFA LAVAL, available at: www.alfalaval.com/campaigns/stepintoart/Pages/default.aspx.
- Anastas, P.T. and J.B. Zimmerman. 2003. Design through the twelve principles of green engineering. *Env. Sci. and Tech.* 37(5): 95–101.
- Anxionnaz, Z., M. Cabassud, C. Gourdon and P. Tochon. 2008. Heat exchanger/reactors (HEX Reactors): concepts, technologies: state-of-the-art. *Chem. Eng. Process.* 47: 2029–2050.
- Anxionnaz-Minvielle, Z., M. Cabassud, C. Gourdon and P. Tochon. 2013. Influence of the meandering channel geometry on the thermo-hydraulic performances of an intensified heat exchanger/reactor. *Chem. Eng. Process.* 73: 67–80.
- Barbosa, D. and M.F. Doherty. 1988. Design and minimum reflux calculation for single feed multicomponent reactive distillation columns. *Chem. Eng. Sci.* 43(7): 1523–1537.
- Bart, H.J., W. Kaltenbrunner and H. Landschutzer. 1996. Kinetics of esterification of acetic acid with propyl acetate by heterogeneous catalysis. *Int. J. Chem. Kinet.* 28: 649–656.
- Benaïssa, W., S. Elgue, N. Gabas, M. Cabassud, C. Douglas and M. Demissy. 2008a. Dynamic behaviour of a continuous heat exchanger/reactor after flow failure. *Int. J. Chem. React. Eng.* 6(A23).
- Benaïssa, W., N. Gabas, M. Cabassud, D. Carson, S. Elgue and M. Demissy. 2008b. Evaluation of an intensified continuous heat-exchanger reactor for inherently safer characteristics. *J. Loss Prev. Process Ind.* 21(5): 528–536.
- Bessling, B., J.M. Ioning, A. Ohlgschlager, G. Schembecker and K. Sundmacher. 1997. Design of processes with reactive distillation line diagrams. *Ind. Eng. Chem. Res.* 36: 3032–3042.
- Bird, R.B., W.E. Stewart and E.N. Lightfoot. 2002. *Transport Phenomena*. John Wiley & Sons, New York, 2nd ed.: 178–184.
- Bonet, J. 2007. Contribution à l'étude de la transestérification de l'acétate de méthyle par distillation reactive. PhD Thesis. Institut National Polytechnique de Toulouse—Univ Barcelone.
- Brehelin, M., D. Rouzineau, X. Meyer, F. Former, J.U. Repke and M. Meyer. 2007. Production of n-propyl acetate by reactive distillation: experimental and theoretical study. *Chem. Eng. Res. Des.* 85A: 109–117.
- Cabassud, M. and C. Gourdon. 2010. Intensification of heat transfer in chemical reactors: heat exchanger reactors. pp. 261–285. *In: J. Moulijn and A. Stankiewicz (eds.). Novel Concepts in Catalysis and Chemical Reactors*. Wiley-VCH, Weinheim.
- Chart Industries, Compact Heat Exchange Reactors, www.chart-ind.com/app_ec_reactortech.cfm.
- Chen, X., Z. Xu and T. Okuhara. 1999. Liquid phase esterification of acrylic acid with 1-butanol catalysed by solid acid catalyst. *Applied Catalysis A: Gen.* 180: 261–269.
- CORNING, Reactor Technologies: Corning® Advanced-Flow™ Glass Reactors, available at www.corning.com/r_d/emerging_technologies/reactors.aspx.
- Elgue, S., M. Ferrato, M. Momas, P. Chereau, L. Prat, C. Gourdon and M. Cabassud. 2007. Silicon carbide equipments for process intensification: first steps of an innovation. *Proc. 1st congress on Green Process Engineering*, Toulouse.
- Ellenberger, J. and R. Krishna. 1999. Counter-current operation of structured catalytically packed distillation columns: pressure drop, holdup and mixing. *Chem. Eng. Sci.* 54: 1339–1345.
- Enache, D.I., W. Thiam, D. Dumas, S. Ellwood, G.J. Hutchings, S.H. Taylor and E.H. Stitt. 2007. Intensification of the solvent-free catalytic hydroformylation of cyclododecatriene: comparison of a stirred batch reactor and a heat-exchange reactor. *Catal. Today* 128(1-2): 18–25.
- Espinosa, J., P. Aguirre and G. Pérez. 1996. Some aspects in the design of multicomponent reactive distillation columns with a reactive core: mixtures containing inerts. *Ind. Eng. Chem. Res.* 35: 4537–4549.
- Ferrouillat, S., P. Tochon, D. Della Valle and H. Peerhossaini. 2006a. Open loop thermal control of exothermal chemical reactions in multifunctional heat exchangers. *Int. J. Heat Mass Transfer* 49(15-16): 2479–2490.

- Ferrouillat, S., P. Tochon and H. Peerhossaini. 2006b. Micromixing enhancement by turbulence: application to multifunctional heat exchangers. *Chem. Eng. Process.* 45(8): 633–640.
- Giessler, S., R.Y. Danilov, R. Pisarenko, L.A. Serafimov, S. Hasebe and I. Hashimoto. 1999. Design and synthesis of feasible reactive distillation processes. *Comput. Chem. Eng. Sup.* S811–S814.
- Götze, I., O. Bailer, P. Moritz and C. von Scala. 2001. Reactive distillation with KATAPAK[®]. *Catal. Today* 69: 201–208.
- Grob, S. and H. Hasse. 2005. Thermodynamics of phase and chemical equilibrium in a strongly nonideal esterification system. *J. Chem. Eng. Data* 50: 92–101.
- Hiwale, E.S., N.V. Bhate, Y.S. Mahajan and S.M. Mahajani. 2004. Industrial applications of reactive distillation: recent trends. *Int. J. Chem. React. Eng.* 2(R1): 1–53.
- Kołodziej, A., M. Jaroszynski, A. Hoffmann and A. Górak. 2001. Determination of catalytic packing characteristics for reactive distillation. *Catal. Today* 69: 75–85.
- Kołodziej, A., M. Jaroszynski and I. Bylica. 2004a. Mass transfer and hydraulics for KATAPAK-S. *Chem. Eng. Process.* 43: 457–464.
- Kołodziej, A., M. Jaroszynski, W. Salacki, W. Orlikowski, K. Fraczek, M. Kloker, E.Y. Kenig and A. Gorak. 2004b. Catalytic distillation for TAME synthesis with structured catalytic packings. *Chem. Eng. Res. Des.* 82: 175–184.
- Lee, M.J., H.T. Wu and H.M. Lin. 2000. Kinetics of catalytic esterification of acetic acid and amyl alcohol over Domex. *Ind. Eng. Chem. Res.* 39: 4094–4099.
- Leveque, J., D. Rouzineau, M. Prévost and M. Meyer. 2009. Hydrodynamic and mass transfer efficiency of ceramic foam packing applied to distillation. *Chem. Eng. Sci.* 64: 2607–2616.
- Lo, S.N. and A. Cholette. 1972. Experimental study on the optimum performance of an adiabatic MT reactor. *Can. J. Chem. Eng.* 50(1): 71–80.
- Lyuben, W.L. and C.C. Yu. 2008. *Reactive Distillation Design and Control*, Ed. John Wiley & Sons, Hoboken, New Jersey.
- Lyuben, W.L., K.M. Pszalgoeski, R.M. Schaefer and C. Siddons. 2004. Design and control of conventional and reactive distillation processes for the production of butyl acetate. *Ind. Eng. Chem. Res.* 43: 8014–8025.
- Malone, M.F. and M.F. Doherty. 2000. Reactive distillation. *Ind. Eng. Chem. Res.* 39(11): 3953–3957.
- Malone, M.F., R.S. Huss and M.F. Doherty. 2003. Green chemical engineering aspects of reactive distillation. *Env. Sci. Tech.* 37(3): 5325–5329.
- Nilsson, J. and F. Sveider. 2000. Characterising mixing in a HEX reactor using a model chemical reaction. www.chemeng.lth.se/exjobb/002.pdf, Department of Chemical Engineering II, Lund, Sweden.
- Nishihira, K., S. Tanaka, Y. Nishihida and S. Fujitsu. 2000. Process for producing a diaryl oxalate. U.S. patent 6,018,072.
- Okasinski, M.J. and M.F. Doherty. 2000. Prediction of heterogeneous reactive azeotropes in esterification systems. *Chem. Eng. Sci.* 55: 5263–5271.
- Olujic, Z., B. Seibert, H. Kaibel, T. Jansen, T. Rietfor and E. Zich. 2003. Performance characteristics of a new high capacity structured Packing. *Chem. Eng. Process.* 42: 55–60.
- Omota, F., A.C. Dimian and A. Bliet. 2003. Fatty Acid esterification by reactive distillation. Part 1: Equilibrium-based design. *Chem. Eng. Sci.* 58: 3159–3174.
- Plucinski, P., D. Bavykin, S. Kolaczowski and A. Lapkin. 2005. Liquid phase oxidation of organic feedstock in a compact multichannel reactor. *Ind. Eng. Chem. Res.* 44: 9683–9690.
- Prat, L., A. Devatine, P. Cognet, M. Cabassud, C. Gourdon, S. Elgue and F. Chopard. 2005. Performance evaluation of a novel concept “open plate reactor” applied to highly exothermic reactions. *Chem. Eng. Technol.* 28(9): 1028–1034.
- Ramshaw, C. 1995. The incentive of process intensification. *Proceeding of the 1st International Conference on Process Intensification for chemical industry*. BHR Group, London.
- Ratheesh, S. and A. Kannan. 2004. Holdup and pressure drop studies in structured packings with catalysts. *Chem. Eng. J.* 104: 45–54.
- Rouzineau, D., F. Druart, J.M. Reneaume and M. Meyer. 2002. Catalytic distillation modelling. *Comput. Aided Chem. Eng.* 10: 181–186.
- Ryu, J.Y. and A.P. Gelbein. 2002. Process and catalyst for making dialkyl carbonates. U.S. Patent 6,392,078.

- Schwarzer, S. and U. Hoffmann. 2002. Experimental reaction equilibrium and kinetics of the liquid-phase butyl acrylate synthesis applied to reactive distillation simulations. *Chem. Eng. Technol.* 25(10): 975–980.
- Shaerfl, R.A., M.J. Day, S.P. Piecuch and R.R. Tellier. 2000. Preparation of substituted hydroxyhydrocinnamate esters by continuous transesterification using reactive distillation. US Patent 6,291,703.
- Sharma, M.M. and S.M. Mahajani. 2003. Industrial applications of reactive distillation. pp. 3–29. *In*: K. Sundmacher and A. Kienle (eds.). *Reactive Distillation*. Wiley-VCH, Weinheim.
- Stankiewicz, A.I. and J.A. Moulijn. 2000. Process intensification: transforming chemical engineering. *Chem. Eng. Prog.* 22: 24–34.
- Steinigeweg, S. and J. Gmehling. 2002. n-Butyl Acetate synthesis via reactive distillation: thermodynamic aspects, reaction kinetics, pilot-plant experiments and simulation studies. *Ind. Eng. Chem. Res.* 41: 5483–5490.
- Steinigeweg, S. and J. Gmehling. 2003. Esterification of fatty acid by reactive distillation. *Ind. Eng. Chem. Res.* 42: 3612–3619.
- Steyer, F., Z. Qi and K. Sundmacher. 2002. Synthesis of cyclohexanol by three-phase reactive distillation: influence of kinetics on phase equilibria. *Chem. Eng. Sci.* 57: 1511–1520.
- Thery, R. 2002. Analyse de faisabilité, synthèse et conception de procédés de distillation réactive, Ph.D. Thesis, Institut National Polytechnique de Toulouse.
- Thery, R., X. Meyer, X. Joulia and M. Meyer. 2005. Preliminary design of reactive distillation columns. *Chem. Eng. Res. Des.* 83(4): 379–400.
- Tischmeyer, M. and W. Arlt. 2004. Determination of binary vapor liquid equilibria (VLE) of three fast reacting esterification systems. *Chem. Eng. Proc.* 43: 357–367.
- Toye, D., M. Crine and P. Marchot. 2005. Imaging of liquid distribution in reactive distillation packings with a new high-energy x-ray tomography. *Meas. Sci. Technol.* 16: 2213–2220.
- Villiermaux, J. 1996. Réacteurs chimiques—Principes. *Techniques de l'Ingénieur, Traité Génie des procédés*, J4 010.

6

Ultrasound in Process Engineering

New Look at Old Problems

Sergey I. Nikitenko and Farid Chemat

Introduction

When studying the action of 100–500 kHz ultrasound on aqueous solutions, Richards and Loomis (1927) discovered that the ultrasonic waves accelerate the hydrolysis of dimethylsulfate and the reduction of potassium iodate by sulfurous acid (iodine “clock” reaction). Two years later, Schmitt et al. (1929) reported the oxidation of iodide ions in aqueous solutions under the effect of 750 kHz ultrasound. These seminal works have introduced a new field of chemistry, referred to as “sonochemistry” by Neppiras in 1980. Large amounts of research papers and detailed critical reviews have been published since that time describing different ultrasonic processes, such as cleaning and degassing (Mason and Lorimer 2002), extraction of biologically active compounds (Chemat 2011), food processing (Ashokkumar et al. 2008; Feng et al. 2011), advanced oxidation processes (Adewuyi 2001; Mahamuni and Adewuyi 2010), synthesis of nanostructured materials (Bang and Suslick 2010) and redox reactions of actinide ions (Nikitenko et al. 2010).

Ultrasound spans the frequencies of roughly 15 kHz to 1 GHz. As a rule, the sonochemical effects are observed in the range of 15 kHz–2 MHz. The ultrasound of higher frequency is used for medical and material diagnostics (Mason and Lorimer 2002). The acoustic wavelengths of chemically active ultrasound ($10\text{--}10^{-4}$ cm) are much higher than the molecule size. Therefore, the sonochemistry arises not from a direct action of ultrasonic waves on molecules, but rather from the acoustic cavitation. Simply put, cavitation is a set of consequent events: nucleation, growth and violent collapse of microbubbles in liquids submitted to ultrasonic vibrations. There is a

general consensus that the chemical and physical effects of power ultrasound are related to extremely rapid implosion of the cavitation bubbles.

The acoustic cavitation leads not only to the chemical phenomena, but also to the light emission, known as sonoluminescence (SL). In 1933 Marinesco and Trillat have accidentally observed the darkening of photographic plates submitted to ultrasound in water. They attributed this finding to the ultrasonic acceleration of Ag^+ chemical reduction at the surface of plates. However, Frenzel and Schultes (1934) shown that photographic plate darkening is due to the light emission from sonicated water rather than from chemical reaction. In modern literature two different types of SL can be distinguished: light emission from a cloud of bubbles (multibubble sonoluminescence, MBSL) and light emission from a single cavitation bubble trapped in a standing acoustic wave of relatively weak pressure (single bubble sonoluminescence, SBSL). For the first time SBSL was reported by Yosioka and Omura (1962). Eight years later Temple (1970) described the same phenomenon in his MS thesis. However, neither observation attracted the attention of the scientific community and as recently as 1990, Gaitan and Crum independently re-discovered and studied the SBSL in water/glycerin mixtures in more detail. In degassed water, the SBSL was bright enough to be visible to the naked eye. The experiments demonstrated the unique properties of this system: the light emission occurs every acoustic cycle at the final stage of collapse and the pulse duration of the light flash is below 200 ps (Barber and Putterman 1991; Barber et al. 1997; Putterman and Weninger 2000). It is noteworthy that single collapsing bubbles can be produced in liquids also by focused laser beam (Lauterborn 1974), but the sonoluminescence of these kinds of bubbles are less frequently studied than that of ultrasonic bubbles. In the years since SBSL was discovered, more than one thousand papers have been published on this topic. The most significant results in sonoluminescence obtained before 2005 have been summarized in the monograph of Young (2005).

Herein, we will focus on more recent results in sonoluminescence and sonochemistry which provided new insights into the origin of the processes occurring during acoustic cavitation. We will also present a complete picture of current knowledge on industrial reactors and applications of ultrasound in process engineering: treatment, preservation and extraction.

Sonoluminescence as a Probe of Intrabubble Conditions

The nonlinear oscillations of a bubble driven in liquids by acoustic waves are generally described by Rayleigh-Plesset equation (Plesset 1949; Plesset and Hsieh 1960; Leighton 1994; Moss 1997):

$$R \ddot{R} + \frac{3}{2} \dot{R}^2 = \frac{1}{\rho} \left[\left(P_0 + \frac{2\sigma}{R_0} \right) \left(\frac{R_0}{R} \right)^{3\gamma} - \frac{2\sigma}{R} - \frac{4\mu \dot{R}}{R} + P_\infty \right], \quad (1)$$

where R is the bubble radius, \dot{R} and \ddot{R} are the bubble wall velocity and the acceleration respectively, R_0 is the equilibrium bubble radius at ambient pressure P_0 , γ is the polytropic index, ρ is the bulk density, σ is the surface tension, μ is the viscosity, and P_∞ is the far-field acoustic pressure. Numerous studies of bubble dynamics reviewed

recently by Lauterborn and Kurtz (2010) indicate that the Rayleigh-Plesset equation works well over most of the range of bubble radius. However, this equation fails at the final stage of bubble implosion where the density of compressed gas inside the bubble is comparable to that of the bulk liquid (Suslick and Flannigan 2008). It is noteworthy that the SL flash occurs only in the last stage of collapse. Consequently, the theoretical description of conditions required for SL, based on the Rayleigh-Plesset equation, becomes somewhat uncertain. Despite this limitation, the Eq. 1 is very useful for calculations of several practically important parameters of cavitation bubbles. For example, Table 1 summarizes the calculated values of maximal bubble radius (R_m) and the time of total collapse (τ) as a function of ultrasonic frequency, in accordance with Minnaert's acoustic resonance conditions (Minnaert 1933). One can see that the bubbles are much smaller and their implosion is much more rapid at higher ultrasonic frequency. It should be emphasized that the distribution of the cavitation field is also different between low and high frequency ultrasound. A 20 kHz horn system yields a limited conical cavitation zone near the horn tip, while high frequencies (≥ 100 kHz) tend to give a more diffuse, widely distributed zone of cavitation (Mason and Lorimer 2002). Therefore, at high frequency, a larger volume of solution is directly submitted to ultrasonic irradiation compared to 20 kHz ultrasound. On the other hand, as the frequency increases, the generation of cavitation bubbles becomes more difficult to achieve in the time available and greater sound intensity is required in order to provide bubble formation.

In the revolutionary work on acoustic cavitation, Rayleigh (1917) suggested that the rapid bubble implosion should lead to adiabatic heating of the gas inside the cavity. This idea was further developed by Noltingk and Neppiras (1950) and later by Flynn (1975). Using the Rayleigh-Plesset equation and presuming adiabatic conditions during bubble implosion, they calculated the temperature and the pressure within the bubble at the moment of total collapse. For nitrogen-filled bubbles in water, their calculations provided 4200 K and 975 atm respectively. Note here that this calculation does not take into account electronic and vibrational excitation of N_2 molecules or their possible high temperature dissociation. Despite the numerous contradicting points (Margulis 2006), the adiabatic heating model based on simple physical principles was quite rapidly accepted by sonochemists since it allowed for an easy explanation of the majority of sonochemical phenomena in terms of thermal flame-like processes.

Spectroscopic studies of sonoluminescence offer a powerful experimental tool to probe the intrabubble conditions and to confirm or to improve the theoretical models of cavitation. The SBSL spectra of degassed water did not reveal any structures as

Table 1. The values of maximal bubble radius (R_m) and its collapse time (τ), as a function of ultrasonic frequency (f) in air-saturated water and at ultrasonic intensity of $10 \text{ W} \cdot \text{cm}^{-2}$.

f , kHz	R_m , μm	τ , μsec
20	150	5
205	17.5	1.6
358	10.0	0.9
618	5.8	0.5
1071	3.3	0.3

lines and bands. Early SBSL studied attributed these spectra to black body emission which is in line with adiabatic heating model. However, Gompf et al. (1997), Hiller et al. (1998) and Moran and Sweider (1998) have not found any significant difference between the pulse width in the UV part of SBSL spectrum (300–400 nm) and in the red part (590–650 nm). This contradicts a thermal model which suggests that the red pulse of the black body emission should be about twice as long as the UV part. Moreover, the intensity of the pulse predicted by the black body model is about two orders of magnitude larger than the experimental values for the experimental parameters studied (Brenner et al. 2002). Today, many researches believe that the featureless SBSL spectra originated from bremsstrahlung rather than from black body emission (Young 2005; Brenner et al. 2002). Bremsstrahlung emission produced by the deceleration of an electron by an atomic nucleus in plasma. Plasma formation in the single cavitation bubble was observed in concentrated H_2SO_4 , pre-equilibrated with 50 mbar of argon at the driven frequency of 20 kHz (Flannigan and Suslick 2005a). Spectral analysis revealed light emission from excited Ar atoms and ionized oxygen O_2^+ . Formation of O_2^+ species is inconsistent with any thermal process. The ionization energy of O_2 molecules is more than twice its bond dissociation energy. Therefore, the strong heat should lead to O_2 homolytic dissociation rather than to ionization. By contrast, the O_2^+ species can be formed by electron impact in plasma (Fridman 2008). Furthermore, the SBSL spectra in sulfuric acid in the presence of noble gases show emission lines from Xe^+ , Kr^+ and Ar^+ with the energies ranging from 26.0 eV to 34.2 eV (Flannigan and Suslick 2005b). On the other hand, the effective gas temperature calculated from Ar^* line widths under the same conditions is only about 1 eV (ca. 11000 K). Such a discrepancy cannot be understood by presuming only adiabatic heating during bubble collapse. The time-resolved spectra of SBSL in H_2SO_4 pre-equilibrated with Kr measured using a streak camera revealed the spectrum evolution with the time of collapse (Chen et al. 2008). At 0.5 ns the SBSL spectrum exhibits line emission from excited Kr atoms centered at 810 nm (5s-5p). With evolution of time, the lines of Kr^* disappear, the central wavelength moves from infrared to ultraviolet monotonously, and at 8.5 ns the spectrum shows featureless emission in the UV range. Emission from excited Kr ($E \sim 9.9$ eV) at the early stage of collapse is incompatible with the adiabatic heating model as a possible mechanism of SBSL.

In contrast to SBSL, the MBSL spectra in different solvents exhibit molecular line emissions under a wide range of conditions. Spectroscopic analysis of C_2^* emission bands (Swan band $d^3\Pi_g - a^3\Pi_u$) during sonolysis at 20 kHz of argon-saturated silicon oil gives the effective cavitation temperature of about 5000 K (Flint and Suslick 1991). However, the interpretation of this spectroscopic temperature is not without complications since C_2^* is the product of a set of chemical reactions, and the relative band intensities might reflect the kinetics of these reactions rather than the intrabubble temperature. The MBSL spectra of H_2SO_4 at 20 kHz in the presence of argon revealed the emission lines from excited Ar atoms (Eddingsaas and Suslick 2007). However, as in the case of SBSL, the calculated effective gas temperature (~ 8000 K) was much lower than the energy of Ar^* species (~ 13 eV or ~ 143000 K).

The MBSL spectra of pure water pre-equilibrated with Ar, Kr, and Xe are composed of the emission lines of excited OH[•] radicals in A²Σ⁺ and C²Σ⁺ states and a broad continuum ranging from UV to near-infrared spectral range, which probably results from the superposition of several emission bands: H+OH[•] recombination, water molecule de-excitation, and OH(B²Σ⁺-A²Σ) emission (Pflieger et al. 2010; Ndiaye et al. 2012). Figure 1 shows the experimental SL spectra in argon measured at different ultrasonic frequencies normalized on the most intense OH(A²Σ⁺-X²Π_i) (0-0) transition. In the spectral range of 280–350 nm, the vibrational bands (0-0), (0-1), (1-0), (1-1), (2-1), (2-2), (3-2), and (4-3) of the OH(A-X) system can be identified. These spectra clearly demonstrate the dramatic effect of ultrasonic frequency on the relative populations of vibrational levels. In addition, for high frequency ultrasound, OH(C²Σ⁺-A²Σ⁺) emission can be seen around 250 nm. The OH(C²Σ⁺) state cannot be populated by any thermal process since excited water molecule required for formation of such species must possess an excitation energy of at least 16.1 eV. The most probable mechanism of OH(C²Σ⁺) species production involves electron impact of water molecules. It was concluded that the observation of OH(C²Σ⁺-A²Σ⁺) emission indicates the formation of a nonthermal plasma inside the cavitation bubble (Pflieger et al. 2010). Spectroscopic analysis of OH(A²Σ⁺-X²Π_i) vibrational transitions supports this hypothesis (Ndiaye et al. 2012). The relative populations of OH(A²Σ⁺) v' = 1–4 vibrational states have been calculated using an optical thin plasma model. Figure 2 show that, in contrast to a thermalized system, the relative population distribution obtained from MBSL spectra deviates strongly from the equilibrium Boltzmann distribution. At 20 kHz, the vibrational population distribution of OH(A²Σ⁺) state appears to follow a Brau distribution function typical for weak vibrational excitation. At higher ultrasonic frequencies it follows a Treanor distribution function which describes strong vibrational excitation. It is

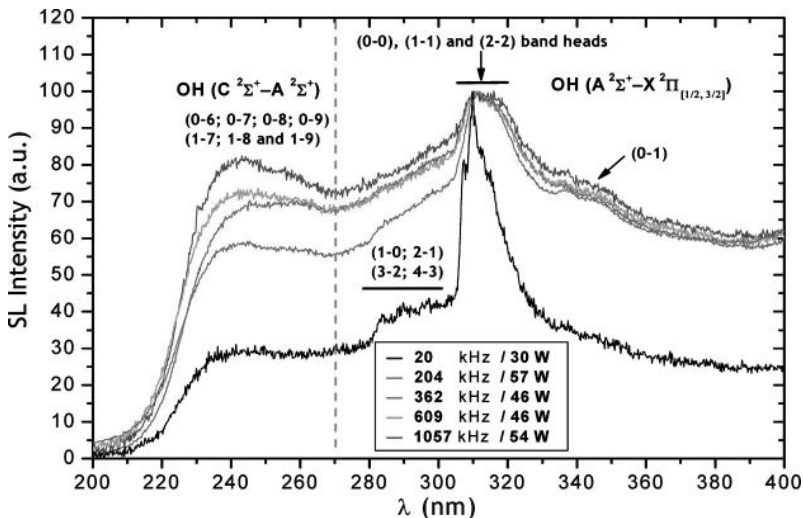


Figure 1. Normalized MBSL spectra of water sparged with argon at 10–11°C for different ultrasonic frequencies. Reproduced with permission from Ndiaye et al. 2012.

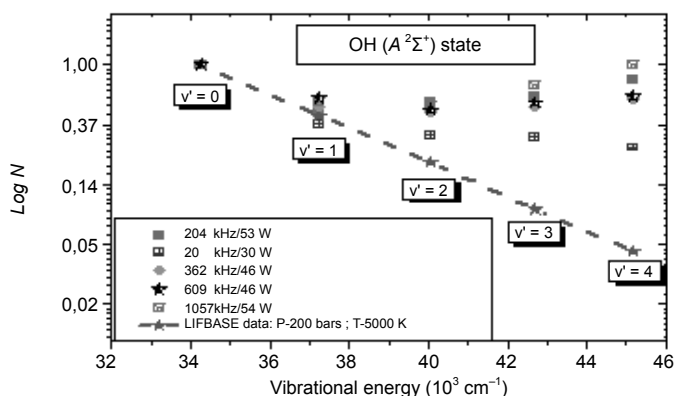


Figure 2. Relative vibrational population distribution of the OH($A^2\Sigma^+$) state as a function of vibrational energy for different ultrasonic frequencies. The green line demonstrates Boltzmann equilibrium distribution at $T = 5000$ K, calculated using the Libase database. Reproduced with permission from Ndiaye et al. 2012.

noteworthy that the spectroscopic analysis based on the determination of the relative vibrational level populations of excited species does not depend on total intensity of sonoluminescence. Consequently, this method is sensitive to intrabubble conditions rather than to the total number of light emitting bubbles.

Obviously, plasma far from equilibrium cannot be characterized by average gas temperature around 5000 K usually referred for multibubble cavitation (Suslick and Flannigan 2008). This kind of plasma is described by multiple temperatures related to different plasma particles and different degrees of freedom. The electron temperature (T_e) often significantly exceeds the vibrational (T_v), rotational (T_r), and translational (T_0) temperatures: $T_e > T_v > T_r \approx T_0$ (Fridman 2008). Table 2 summarizes the optimized values of T_e and T_v estimated from the simulated MBSL spectra (Ndiaye et al. 2012). It shows that the nonequilibrium plasma generated during the sonolysis of water sparged with argon obeys the classical inequality $T_e > T_v$. The T_e value increases with the ultrasonic frequency from ~ 8000 K (~ 0.7 eV) at 20 kHz to ~ 12000 K (~ 1 eV) at 1057 kHz. This data clearly indicates that the acoustic collapse creates more drastic conditions at higher ultrasonic frequency. Another interesting phenomenon described in the text is that the shape of the OH \cdot radical SBSL spectrum obtained in water pre-equilibrated with 70 mbar of Ar is very similar to that observed in MBSL spectra of argon-saturated water at 20 kHz, indicating the strong similarity

Table 2. Estimated vibronic temperatures of intrabubble plasma versus ultrasonic frequency in argon-saturated water at 10–12°C (Ndiaye et al. 2012).

f, kHz	T_e , K	T_v , K
20	8000	5000
204	9500	7600
362	10000	8450
609	11000	9050
1057	12000	9800

of intrabubble conditions for SBSL and MBSL under certain experimental conditions (Schneider et al. 2011).

The MBSL is strongly influenced by saturating noble gas. In xenon, the vibrational population distribution for OH• radicals exhibits strong vibrational (Treanor) behavior even at low ultrasonic frequency. Moreover, the MBSL spectra of water exhibit much stronger OH($C^2\Sigma^+ - A^2\Sigma^+$) emission bands in the presence of Xe compared to those in Ar (Ndiaye et al. 2013). In terms of the nonequilibrium plasma model, the higher vibronic temperatures in Xe are the result of lower ionization potential of Xe compared to Ar (12.13 eV for Xe, 15.76 eV for Ar). Lower ionization potential provides a plasma with higher electron density, or in other words, with higher electron temperature.

The formation of nonequilibrium plasma inside the cavitation bubble is in strong correlation with the isotope effects in MBSL spectra of heavy and light water observed recently by Ndiaye et al. (2013). Despite the very small variation in physico-chemical properties of H₂O and D₂O, their MBSL spectra exhibit a striking difference, regardless of the ultrasonic frequency. The OH/OD($A^2\Sigma^+ - X^2\Pi_i$) emission bands exhibit not only the isotope shift but also the spectral profile modifications, indicating differences in the populations of the OH/OD($A^2\Sigma^+$) vibrational levels. The strong emission from the OH($C^2\Sigma^+$) excited state observed in light water is dramatically reduced in heavy water. The spectroscopic analysis of OH/OD($A^2\Sigma^+ - X^2\Pi_i$) transitions revealed overpopulation of both OH• and OD• vibrational levels compared to Boltzmann equilibrium distribution. Moreover, the isotope effect for relative OD/OH($A^2\Sigma^+$) vibrational populations ($\alpha = \frac{N_v^{OD}}{N_v^{OH}}$) does not follow an exponential Boltzmann function. The trend followed by $\ln\alpha$ can be explained by the formation of “hotter” nonequilibrium plasma in D₂O than in H₂O. Finally, the nonequilibrium model can contribute to an understanding of SBSL in sulfuric acid. Actually, the electron temperature is an average energy of the electrons in plasma (Fridman 2008). The electron energy distribution function (EEDF) in nonequilibrium plasma is quite different from the quasi-equilibrium Boltzmann distribution. Usually, the EEDF is described by Maxwellian or by Druyvesteyn distributions (Fridman 2008). In both cases, for $T_e \sim 1$ eV nonequilibrium plasma can contain the electrons with an energy of tens eV. This would explain the emission bands of highly energetic ionized and excited species in SBSL spectra of H₂SO₄. In water, these species are quenched with H₂O molecules.

Activating Molecules, Ions, and Solids with Acoustic Cavitation

The finding of nonequilibrium plasma formation during acoustic cavitation represents a paradigm shift in sonochemistry. Instead of a simplistic adiabatic heating model, the sonochemical processes can be considered in terms of a more sophisticated plasma chemical approach, allowing for an explanation of the new effects in sonochemistry as well as in sonoluminescence. One of these processes is a carbon isotope effect during sonochemical carbon monoxide disproportionation in water (Nikitenko et al. 2009). The prolonged sonication of water with 20 kHz ultrasound in the presence of 20% CO/Ar gas mixture yields a tiny amount of solid carbon-containing product. It

was found that the composition of this product has some similarity with poly(carbon suboxide) which is known to be formed during CO disproportionation in plasma (Fridman 2008). Moreover, the product of sonolysis was enriched with the ^{13}C isotope ($\alpha = 1.053\text{--}1.055$). This effect is inconsistent with the equilibrium isotope effects described by Bigeleisen-Mayer theory which predicts the enrichment of reaction products with light isotopes (Bigeleisen and Mayer 1947). By contrast, vibrational excitation of CO molecules in nonequilibrium plasma leads to reverse isotope effect (Fridman 2008). The population of highly vibrational states of CO molecule occurs through an anharmonic vibration-to-vibration pumping mechanism, known as Treanor effect. It is noteworthy that the nonequilibrium vibrational excitation of OH \cdot radicals discussed above is related to the same phenomena. One can conclude that the isotope effect observed clearly indicates that the nonequilibrium plasma inside the cavitation bubbles can influence not only the MBSL spectra but the sonochemical reactions too.

In theory, each cavitation bubble can be considered as a plasmochemical microreactor providing highly energetic processes of the bulk solution at almost room temperature. The photons and the “hot” particles produced inside the bubble enable excitation of the non-volatile species in solutions, thus increasing their chemical reactivity. For example, power ultrasound enables excitation of the ions of lanthanides (Sharipov et al. 2003; Pflieger et al. 2013) and uranyl UO_2^{2+} (Pflieger et al. 2012) in aqueous acidic solutions. The mechanism of excitation involves two stages: sonophotoluminescence (excitation with photons emitted by collapsing bubble) dominates in diluted solutions, and collisional excitation with “hot” particles would add its contribution at higher metal ions concentration. It should be emphasized that the nonradiative de-excitation pathways play a more important role in MBSL of Ln(III) and U(VI) ions compared to photoluminescence due to quenching with sonolytical products (H_2O_2 , H_2 , etc.).

Oxidizing properties of power ultrasound in aqueous solutions related to the sonochemical production of OH \cdot radicals and hydrogen peroxide are known for a long time (Adewuyi 2001). The sonochemical reduction processes are less common. Recently, the reduction of Pt(IV) under the action of 20 kHz ultrasound in pure water has been reported (Chave et al. 2012). In the presence of argon, reduction occurs by hydrogen issued from hemolytic water molecule split. However, Pt(IV) ion reduction appears to be slow under these conditions due to the formation of oxidizing species (OH \cdot , H_2O_2) leading to reoxidation of intermediate Pt(II) ions. Sonochemical reduction is accelerated manifold in the presence of formic acid or CO/Ar gas mixture. Both CO and HCOOH act as OH \cdot radical scavengers and reducing agents. Sonolysis of Pt(IV) in aqueous solutions provides an innovative synthetic route to obtain monodispersed Pt nanoparticles without any templates or capping agents. The sonochemical process with CO/Ar gas mixture in pure water yields Pt nanoparticles within the range of 2–3 nm highly stable towards sedimentation (Fig. 3). It is noteworthy that the high efficiency of the reduction process at low frequency ultrasonic irradiation is a further advantage for the controllable Pt nanoparticles deposition on various specific supports, even on thermosensitive materials like polymer beads (Chave et al. 2013). The sonochemical reduction of

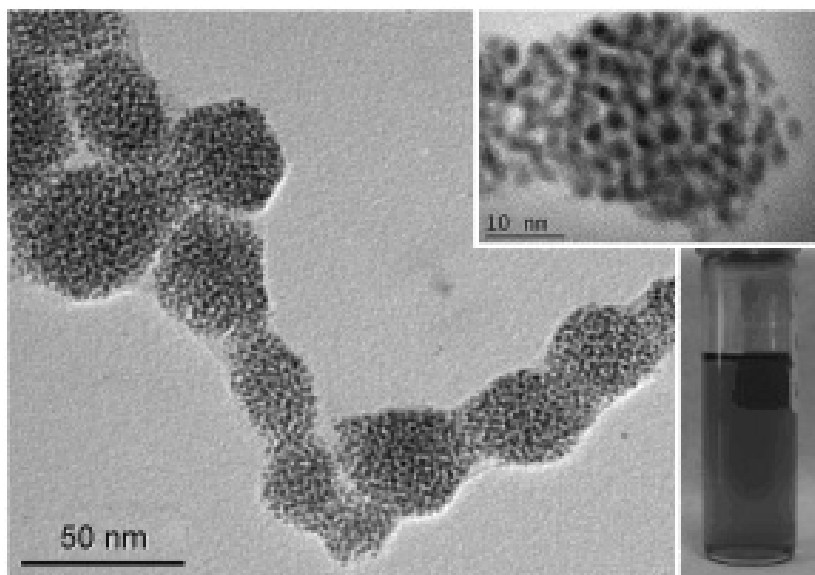


Figure 3. TEM image of Pt nanoparticles obtained under ultrasonic irradiation in pure water with Ar/CO atmosphere. Picture of brown colloid obtained is shown as an inset. Reproduced with permission from Chave et al. 2012.

Au(III) ions to Au⁰ in argon-saturated water also has been observed by Caruso et al. (2002).

The acoustic cavitation is accompanied not only by the generation of chemically active species but also by strong shear forces which arise around violently imploding bubbles. Ultrasonic chain scission of polymers in solutions under the effect of these forces occurs for an extensive period (Basedow and Ebert 1977). Recently the ultrasonic activation of homogeneous latent catalysts has been reported (Piermattei et al. 2009; Jakobs and Sijbesma 2012). It was shown that the mechanochemical scission of a metal-ligand bond triggered with low-frequency ultrasound may be used to release the innate catalytic activity of either the ligand or the metal.

Actually, the mechanical forces generated by cavitation play a much more important role in heterogeneous systems than in homogeneous solutions. The first observation of cavitation erosion was reported by Thornycroft and Barnaby (1895), much earlier than any data on sonochemistry or sonoluminescence. They observed that the propeller of a torpedo-boat destroyer became pitted and eroded over a relatively short operation period. This phenomenon is explained by asymmetric bubble collapse near the interface which generates microjets and shock waves proving intense pressure and temperature gradients in the local vicinity. Today, the use of power ultrasound to enhance the reactivity of solids has become a routine technique in heterogeneous catalysis and various cleaning methods.

Mason and Lorimer (2002) and extraction (Feng et al. 2011) processes. In general, the mechanical effects of ultrasound are much stronger at low frequency ultrasounds compared to high ultrasonic frequency, which is related to the decrease

of bubble size with the increase of ultrasonic frequency. It was recently established that the light emitted by an acoustically driven cloud of cavitation bubbles enables excitation of Tb(III) contained in a $(\text{Ce},\text{Tb})\text{PO}_4$ solid extended matrix (Virot et al. 2011). The MBSL spectrum shown in Fig. 4 demonstrates the Tb(III) light emission resulting from ${}^5\text{D}_4$ - ${}^7\text{F}_j$ f-f transitions along with OH(A-X) and continuum emission typical for MBSL in water saturated with argon. Finally, the strong luminescence and even soft X-Ray emission (0.7–1.2 keV) has been recently reported during cavitation generated by high-pressure spindle oil jet at $P \geq 80$ –90 bar using narrow dielectric channels (Kornilova et al. 2009). Detailed studies of this phenomenon led to the conclusion that the X-Ray emission originates from the excitation of the jet surface atoms by the cavitation-induced shock waves.

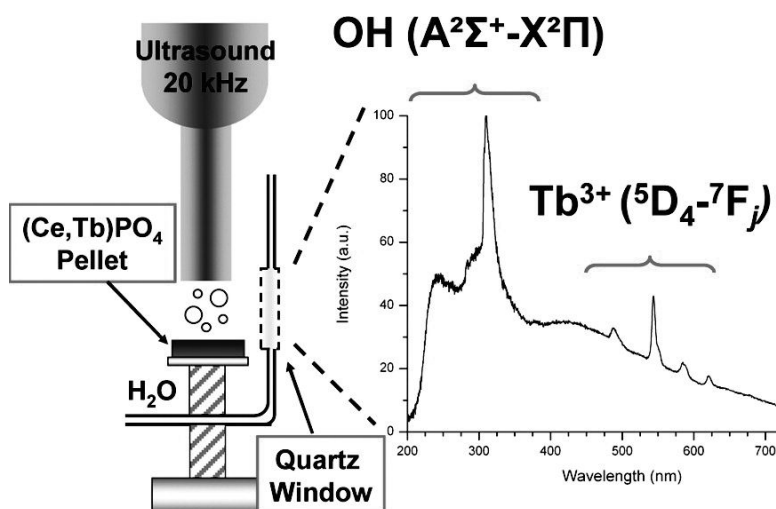


Figure 4. Simplified representation of the experimental setup and MBSL spectrum obtained for the sonication of $(\text{Ce}_{0.9}\text{Tb}_{0.1})\text{PO}_4$ pellet with optimized horn-sample distance and focusing near the ultrasonic horn (9°C , Ar, $f = 20$ kHz, $I = 18$ $\text{W} \cdot \text{cm}^{-2}$). Reproduced with permission from Virot et al. 2011.

Ultrasound Reactors for Green Process Engineering

Two different types of ultrasound equipments are commonly used in laboratory. The first one is the ultrasonic cleaning bath which is commonly used for solid dispersion into solvent (ultrasounds will dramatically reduce the size of the solid particles, which will enhance its solubility), for degassing solutions or even for cleaning small material by immersion of the glassware into the bath. The ultrasonic baths are less commonly used for chemical reactions even if they are easy to handle and economically advantageous because the reproducibility of the reaction is low. In fact, the delivered intensity is low and is highly attenuated by the water contained in the bath and the walls of the glassware used for the experiment. The second one, the ultrasonic probe or horn system, is much more powerful because the ultrasonic intensity is delivered on a small surface (only the tip of the probe) compared to the ultrasonic bath. Another change is that the probe is directly immersed into the

reaction flask so less attenuation can happen. This probe system is widely used for sonication of small volumes of the sample but special care has to be taken because of the fast rise of the temperature in the sample.

Both probe and bath systems are used industrially, depending on the application. Several types of ultrasonic devices have been developed for industrial uses or scale-up laboratory experiments by a large number of companies such as Hielscher (Germany), Branson (Switzerland), Vibracell (USA) and REUS (France), among others. The disposition of the ultrasound transducer varies upon the device and in some cases an agitation system is also added.

REUS has developed reactors from 30 to 1000 L to which pump systems are coupled in order to fill the ultrasonic bath, to stir the mixture and to empty the system at the end of the procedure (Fig. 5). Most of the compounds extracted on an industrial

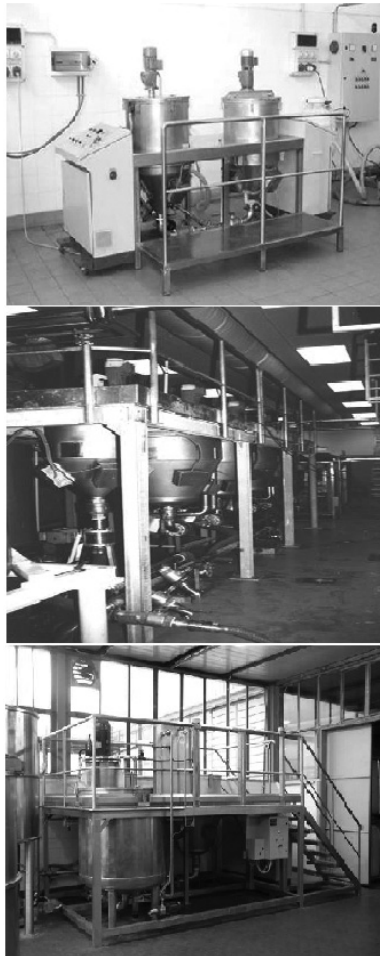


Figure 5. Industrial ultrasonic equipments: 50, 500 and 1000 liters (with permission of www.etsreus.com).

scale by ultrasound have immediate use (for instance in alcohol liquor production) or can be used as food and cosmetic additives (in the case of essential oil and molecules with special activity). GMC (G. Mariani & C. Spa) is an Italian company specialized in aromatic herbs extraction that adapts their ultrasound extraction system depending on the characteristics of the herbs. GIOTTI is an Italian company that uses ultrasound assistance in extracting food, pharmaceutical additives and producing alcoholic drinks. This company works with four batch systems equipped with ultrasound on each side of the tank and an agitation system.

The price of industrial ultrasound reactors vary between 10,000 euros (5 L in batch or 5 L/h in continuous mode) and 200,000 euros (1000 L in batch or 1000 L/h in continuous mode). The choice of implementing an ultrasound reactor in the existing process represents only about 25% more than the initial investment compared to a conventional extraction reactor. However, if we consider that the ultrasound use divides the total time of the procedure by a factor of 10 to 100, together with a decrease of consumed energy and pollution by a factor of 10, the procedures using ultrasound assistance have a production cost and a functioning cost which is much lower than the costs for conventional procedures.

Ultrasound in Process Engineering

Ultrasound can be used depending on the target effect, mechanical or chemical, for processing, preservation or extraction of food or non food products. The applications in the food and fine chemistry industries can be summarized in Table 3 below.

Table 3. Applications of ultrasounds in food industry.

Mechanical effects	Chemical and biochemical effects
Freezing	Oxidation and aging
Crystallization of sugars and lipids	Deactivation of enzymes
Degassing and cutting	Microbial effect
Mixing and homogenisation	Treatment of wastewater
Extraction of aromas	Deactivation of bacteria and yeasts
Filtration and drying	Sterilisation of equipments

Ultrasound as Treatment Technology

The principle aims of ultrasound technology are to reduce the processing time, save energy and improve the shelf life and quality of food products. Ultrasound technology is a novel technology which has the potential to produce high-quality and safe food products. However, current limitations such as high investment costs, full control of variables associated with the process operation, lack of regulatory approval and importantly consumer acceptance have been delaying wider implementation of these technologies on an industrial scale. There are a large number of potential applications of high intensity ultrasound in food processing: cooking, freezing, crystallization, drying, pickling, marinating, degassing, filtration, de-moulding, de-foaming, emulsification, oxidation, cutting, etc.

One of the successes of combining ultrasound with conventional food processing, and especially separation and extraction, is acoustically aided filtration. The need to remove suspensions of solids from liquids is common in the dairy industry. This separation can either be for the production of solid-free liquid or to produce a solid isolated from its mother liquor. Conventionally, membranes of various sorts are employed, ranging from simple semi-permeable osmotic type membranes to size-exclusion principle types for purification. Unfortunately, conventional methodologies often lead to ‘clogged’ filters and, consequently, a need to replace filters on a regular basis.

There are two specific effects of ultrasonic irradiation which can be harnessed to improve the filtration technique. Sonication will cause the agglomeration of fine particles (i.e., more rapid filtration), and at the same time, will supply sufficient vibration energy to the system to keep the particles partly suspended and therefore leave more free ‘channels’ for solvent elution (Fig. 6). The combined influence of these effects has been successfully employed to enhance the filtration of industrial dairy products, which are particularly time consuming and difficult to process (Muthukumarana et al. 2005). The application of ultrasound to filtration, known as ‘acoustic filtration’, suggests that the use of ultrasound acts in such a way as to lower the compressibility of both the initial protein deposit and the growing cake. Ultrasonic irradiation significantly enhances the permeate flux with an enhancement factor of 50%. The use of this combination can lead to a doubling in the permeate flux, the potential for this process is clearly enormous. Improvements on the acoustic method use an electrical potential which is applied across the slurry mixture while acoustic filtration is performed (Muralidhara et al. 1985). The filter itself is made to be the cathode while the anode, on the top of the slurry, functions as a source of attraction for the predominantly negatively charged particulate material. The



Figure 6. Acoustically aided filtration.

additional mobility introduced by the electric charge increases the drying efficiency of a 50% coal slurry by a further 10%. When applied to fruit extracts and drinks this technique has been used to increase the quantity of apple juice extracted from the pulp. Where conventional belt vacuum filtration achieves a reduction in moisture content from an initial value of 85% to 50%, electro-acoustic technology achieved a significantly lower percentage of 38% (Mason et al. 1996).

Ultrasound as Preservation Technology

Destruction of micro-organisms by power ultrasound has been of considerable interest since the 1920s when the first work by Harway and Loomis was reported and the argument of ultrasonic inactivation and destroying cells was born. Research studies have focussed on different experimental procedures, approaches, experimental designs, techniques and biological systems to study inactivation effect of ultrasound.

Saccharomyces cerevisiae and *Escherichia coli* are the most frequently studied micro-organisms, not only in the field of power ultrasound, but also among other methods of food preservation. Other relevant micro-organisms inactivated using ultrasound include gram-negative pathogens *Salmonella typhimurium*, *Salmonella enteridis*, and *Escherichia coli*; the gram-positive *Staphylococcus aureus* and *Listeria monocytogenes*; the spores forming pathogens *Bacillus cereus* and *Bacillus subtilis*; and nonpathogenic spoilage flora *Pseudomonas fluorescens*. Further research on spore-formers *Bacillus coagulans* has been inactivated by ultrasound. In general, gram-negative bacteria are more sensitive than gram-positive bacteria. Cell shape (i.e., rod, spherical) and size also seem to play an important role in the effect of ultrasonic treatment (Chemat et al. 2011).

The inactivation effect of ultrasound is attributed to intracellular cavitation, that is, micro-mechanical shocks that disrupt cellular structural and functional components up to the point of cell lysis. Figure 7 represents a proposed mechanism of ultrasound-induced cell damage. Cavitation is the formation, growth and, sometimes, the implosion of micro-bubbles created in a liquid when ultrasound waves propagate through it. The collapse of the bubbles leads to energy accumulation in hotspots where temperatures of above 5000°C and pressures of approximately 500 MPa have been measured. This phenomenon can cause enzyme inactivation through three

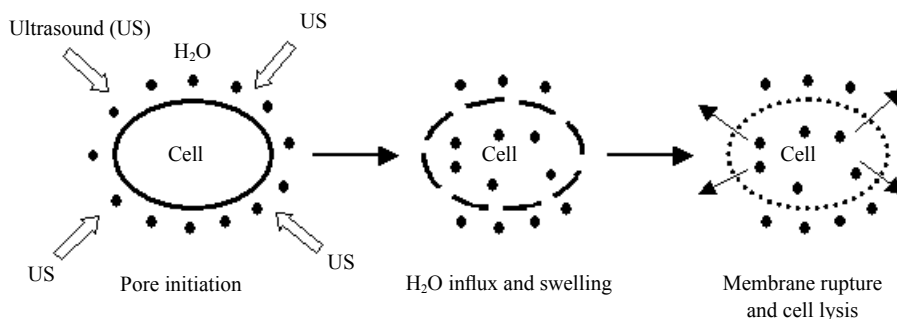


Figure 7. Mechanism of ultrasound-induced cell damage.

mechanisms, which can act alone or together. The first one is purely thermal, due to the enormous temperatures achieved during cavitation. The second one is due to free radicals generated by water sonolysis, and the third one is due to the mechanical forces (shear forces) created by micro-streaming and shock waves.

The increased effectiveness of ultrasound preservation in combination with heat and pressure opens new possibilities. The combination of heat and ultrasound irradiation under moderate pressure is called manothermosonication (MTS). MTS treatments allow for the inactivation of several enzymes at lower temperatures and/or in a shorter time than thermal treatments at the same temperatures for similar reactions. Figure 4 shows the strengths and weaknesses of ultrasound as a preservation technology. At the moment MTS is laboratory or pilot scale, but may well have potential as an alternative pasteurization or sterilization method for liquid foods in the future. Use on solid foods is less likely because of the difficulty of delivering sufficiently high ultrasonic intensities into solid substrates economically (Mason and Lorimer 2002).

Ultrasound as Extraction Technology

Flavor and fragrances are complex mixtures of volatile compounds usually present in low concentrations. They are present in varieties of aromatic plants, either in the roots, stems, seeds, leaves, flowers or fruits. Their amounts are plant dependent (different varieties will have different amount of volatile substances) and plant part dependent (volatiles are not distributed at the same rate into the different parts of the plant). The molecules responsible for the flavor of the aromatic plant can be extracted and used in the food industry, medicine or the perfume industry. The first aroma extractions are difficult to date precisely. Old testimonies lead to the conclusion that the Hindus controlled fermentation and obtained odorant oils starting from rudimentary distilling apparatuses. At the beginning of the fourteenth century, the distilling apparatuses made their appearance in the medical and alchemical laboratories but were very sophisticated and distillates were strongly alcoholised. As yet, there was no concept of essential oils. In the past few years, many improvements in the extraction processes have been done. These new processes were directed towards few targets: improvement of the yield of extraction, reducing time and energy costs and non destruction of the volatile compounds. One of these improving processes is the coupling of the distillation procedure with ultrasounds or even the development of new ultrasound-assisted extraction (UAE). A non-exhaustive list of these applications is provided in Table 4.

The composition of wine depends on several factors: production area, soil, climate, varieties of fruits, practices used to make wine, etc. Wines and alcohol beverages contain a lot of volatile compounds which play an important role in organoleptic characteristics. Ultrasound assisted extraction of volatile compounds of wine and aged brandies. UAE has been compared to other types of recent extraction procedures such as solid-phase extraction or direct immersion solid phase extraction. Other authors have set up new experiments assisted by ultrasounds. UAE allowed better yields and a shorter extraction time compared to conventional method and up to 37 volatile compounds could be satisfactorily quantified. Alcohols and acids

Table 4. Ultrasound assisted extraction of aromas and essential oils.

Matrix	Analyte	Extraction conditions	References
Caraway seeds	carvone and limonene	US, 20 kHz, 150W, 20°C, <i>n</i> -hexane, 60 min	Chemat et al. 2004
Vanilla	vanillin	US, 20kHz, 750w, 25°C, Et ₂ O, 2min	Hardcastle et al. 2001
Mint	menthol	US, 40kHz, 22°C, H ₂ O, agitation, 60 min,	Shotipruk et al. 2001
Safran	safranal	US, 35kHz, 25°C, H ₂ O:Et ₂ O, 10 min	Kanakis et al. 2004
Old Brandy and red wine	aromas	US, 20°C, CH ₂ CH ₂ , agitation: 3 x 10 min	Caldeira et al. 2004

have been identified as the predominant volatiles in wine and are mostly issued from fermentation (Chemat 2011).

UAE has also been developed for essential oils from aromatic plants such as peppermint leaves, artemisia and lavender, or from other vegetal matrices such as garlic and citrus flowers. Except the work on citrus flowers, authors have compared different procedures of essential oil extraction in their publications: hydrodistillation, microwave assisted extraction, supercritical CO₂ and UAE. Increased yields of essential oil were found for peppermint leaves (up to 12%) and for artemisia when using UAE, and increase by 2 to 3 fold of the main compounds of lavandula essential oil when comparing UAE to conventional distillation. Moreover, UAE not only improved yields but as a method is fast and runs at a low temperature, the final product usually showed less thermal degradation than traditional or microwave assisted methods. This is especially important in the case of food or cosmetics because in these two fields, essential oils have to be of high quality and good flavor (Mason et al. 1996).

Several studies have been performed on extraction of the main aroma compounds from spices. For example, vanillin was extracted from vanilla pods carvone from caraway seeds and safranal from Greek saffron. Yields of vanillin were comparable after one hour by UAE vs. 8 hours with conventional extraction. Another publication showed that 80% of the pure vanillin was obtained after only 120 sec of ultrasounds

(ultrasonic probe) whilst it took 24 hours with the conventional method to obtain 100%. In both cases, vanillin was obtained in lower amounts than in the conventional method, but the extract was pure and obtained in much shorter processing times. For carvone extraction, the UAE method was compared to the Soxhlet. Unwanted fatty materials were extracted by Soxhlet extraction while the extract with UAE was of better quality and richer in carvone than in limonene. In the case of saffron, safranal was extracted from Greek saffron either by microsimultaneous hydro-distillation (MSDE) or by UAE. The mean value of safranal content extracted by UAE was lower than by MSDE but on the other hand, higher HTCC (4-Hydroxy-2,6,6-trimethyl-1-cyclohexene-1-carboxaldehyde, a precursor of safranal) concentrations were found. Authors explained this difference by the lower temperatures used for UAE, which could mean that MSDE overestimate safranal concentrations (safranal is produced from HTCC during extraction) (Chemat et al. 2011).

Every medium has a critical molecular distance: below this critical value, the liquid remains intact, but above this distance, the liquid would break down and voids can be generated into the liquid. In the case of ultrasounds, if the rarefaction cycle is strong enough, the distance (d) between contiguous molecules can reach or even exceed the critical molecular distance of the liquid. The voids created in the medium are the cavitation bubbles which are responsible for the ultrasonic effect. In fact, these cavitation bubbles are able to grow during rarefaction phases and decrease in size during compression cycles. When the size of these bubbles reach a critical point they collapse during a compression cycle and release large amounts of energy. The temperature and the pressure at the moment of collapse have been estimated to be up to 5000°K and 5000 atmospheres in an ultrasonic bath at room temperature. This creates hotspots that are able to dramatically accelerate the chemical reactivity in the medium. When these bubbles collapse onto the surface of a solid material, the high pressure and temperature released generate microjets directed towards the solid surface. These microjets are responsible for the degreasing effect of ultrasounds on metallic surfaces which is widely used for cleaning materials. Another application of microjets in the food industry is the extraction of vegetal compounds. As shown in Fig. 8, a cavitation bubble can be generated close to the plant material surface (a), then during a compression cycle, this bubble collapse (b) and a microjet directed toward the plant matrix is created (b and c). The high pressure and temperature involved in this process will destroy the cell walls of the plant matrix and its content can be released into the medium (d). This is a very interesting tool for extracting ingredients from natural products.

Future Trends

Ultrasound in process engineering is increasingly efficient at directly transferring knowledge into technology for commercial development. Ultrasound makes use of physical and chemical phenomena that are fundamentally different from those applied in conventional techniques. This innovative process can treat, process, preserve, or extract materials under a concentrated form (low volumes of solvent) and free from any contaminants or artefacts. The new systems developed to date clearly indicate

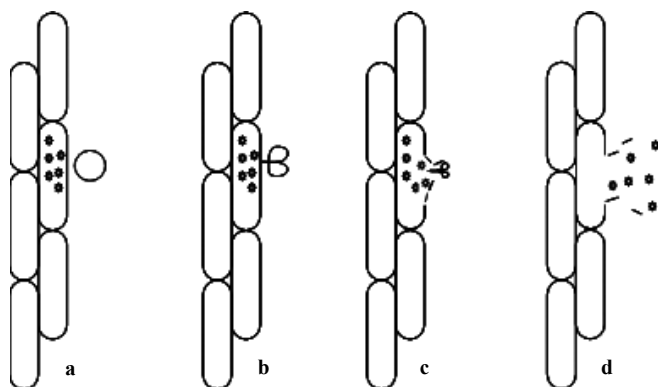


Figure 8. Cavitation bubble collapse and plant material releasing.

that ultrasound offers net advantages in terms of yield, selectivity, operating time, energy input and preservation of thermo-labile compounds.

References

- Adewuyi, Y.G. 2001. Sonochemistry: environmental science and engineering applications. *Ind. Eng. Chem. Res.* 40: 4681–4715.
- Ashokkumar, M., D. Sunatorio, S. Kentish, R. Mawson, L. Simons, K. Vilku and C. Versteeg. 2008. Modification of food ingredients by ultrasound to improve functionality: a preliminary study on a model system. *Innov. Food Sci. Emerg. Technol.* 9: 155–160.
- Bang, J.H.B. and K.S. Suslick. 2010. Applications of ultrasound to the synthesis of nanostructured materials. *Adv. Mater.* 22: 1039–1059.
- Barber, B.P. and S.J. Putterman. 1991. Observation of synchronous picoseconds sonoluminescence. *Nature* 352: 318–320.
- Barber, B.P., R.A. Hiller, R. Löfstedt, S.J. Putterman and K.R. Weninger. 1997. Defining the unknowns of sonoluminescence. *Phys. Rep.* 281: 65–143.
- Basedow, A.M. and K.H. Ebert. 1977. Ultrasonic degradation of polymer in solution. *Adv. Polym. Sci.* 22: 83–148.
- Bigeleisen, J. and M.G. Mayer. 1947. Calculation of equilibrium constants for isotopic exchange reactions. *J. Chem. Phys.* 15: 261–267.
- Brenner, M., S. Hilgenfeldt and D. Lohse. 2002. Single-bubble sonoluminescence. *Rev. Mod. Phys.* 74: 425–483.
- Caldeira, I., R. Pereira, M. Climaco and A. Belchior. 2004. Improved method for extraction of aroma compounds in aged brandies and aqueous alcoholic wood extracts using ultrasound. *Ana. Chim. Acta.* 513: 125–134.
- Caruso, R.A., M. Ashokkumar and F. Grieser. 2002. Sonochemical formation of gold sols. *Langmuir.* 18: 7831–7836.
- Chave, T., N.M. Navarro, S. Nitsche and S.I. Nikitenko. 2012. Mechanism of Pt(IV) sonochemical reduction in formic acid media and pure water. *Chem. Eur. J.* 18: 3879–3885.
- Chave, T., A. Grunewald, A. Ayrat, P. Lacroix-Desmazes and S.I. Nikitenko. 2013. Sonochemical deposition of platinum nanoparticles on polymer beads and their transfer on the pore surface of silica matrix. *J. Colloid Interface Sci.* 395: 81–84.
- Chemat, F. (ed.). 2011. *Éco-extraction du végétal*. Dunod, Paris.
- Chemat, F., H. Zille and M. Khan. 2011. Applications of ultrasound in food technology. *Ultrason. Sonochem.* 18: 813–835.

- Chemat, S., A. Lagha, H. AitAmar, P.V. Bartels and F. Chemat. 2004. Comparison of conventional and ultrasound-assisted extraction of carvone and limonene from caraway seeds. *Flav. Frag. J.* 19: 188–192.
- Chen, W., W. Huang, Y. Liang, X. Gao and W. Cui. 2008. Time-resolved spectra of single-bubble sonoluminescence in sulfuric acid with a streak camera. *Phys. Rev. E.* 78: 035301(R).
- Eddingsaas, N.C. and K.S. Suslick. 2007. Evidence for a plasma core during multibubble sonoluminescence in sulfuric acid. *J. Am. Chem. Soc.* 129: 3838–3839.
- Feng, H., G.V. Barbosa-Cánovas and J. Weiss. 2011. *Ultrasound Technologies for Food and Bioprocessing*. Springer, New York.
- Flannigan, D.J. and K.S. Suslick. 2005a. Plasma formation and temperature measurement during single-bubble cavitation. *Nature* 434: 52–55.
- Flannigan, D.J. and K.S. Suslick. 2005b. Plasma line-emission during single-bubble cavitation. *Phys. Rev. Lett.* 95: 044301.
- Flint, E.B. and K.S. Suslick. 1991. The temperature of cavitation. *Science.* 253: 5026. 1397–1399.
- Flynn, H. 1975. Cavitation dynamics. Free pulsations and models for cavitation bubbles. *J. Acoust. Soc. Am.* 58: 1160–1170.
- Frenzel, H. and H. Schultes. 1934. Luminescence in water carrying supersonic waves. *Z. Phys. Chem.* 27: B421–B424.
- Fridman, A. 2008. *Plasma Chemistry*. Cambridge University Press, Cambridge.
- Gaitan, D.F. and L.A. Crum. 1990a. Observation of sonoluminescence from a single, stable cavitation bubble in a water/glycerin mixture. *Frontiers of nonlinear acoustics*. pp. 459–463. *In: M. Hamilton and D.T. Blackstock (eds.)*. *Frontiers of Nonlinear Acoustics: Proceedings of 12th ISNA*. Elsevier App. Sci., New York.
- Gaitan, D.F. and L.A. Crum. 1990b. Sonoluminescence from single bubbles. *J. Acoust. Soc. Am. Suppl.* 1. 87: S141.
- Gompf, B., R. Gunther, G. Nick, R. Pecha and W. Eisenmenger. 1997. Resolving sonoluminescence pulse width with time-correlated single photon counting. *Phys. Rev. Lett.* 79: 1405–1408.
- Hardcastle, J.L., C.J. Paterson and R.J. Compton. 2001. Biphasic sono-electroanalysis: Simultaneous extraction from, and determination of vanillin in food flavoring. *Electroanalysis* 13: 899–905.
- Harway, E. and A. Loomis. 1929. The denaturation of Luminous bacteria by high frequency sound waves. *J. Bact.* 17: 373–379.
- Hiller, R.A., S.J. Putterman and K.R. Weninger. 1998. Time-resolved spectra of sonoluminescence. *Phys. Rev. Lett.* 80: 1090–1093.
- Jakobs, R.T.M. and R.P. Sijbesma. 2012. Mechanical activation of a latent olefin metathesis catalyst and persistence of its active species in ROMP. *31: 2476–2481*.
- Kanakakis, C.D., D.J. Daferera, P.A. Tarantilis and M.G. Polissiou. 2004. Qualitative determination of volatile compounds and quantitative evaluation of safranal and 4-hydroxy-2,6,6-trimethyl-cyclohexene-1-carboxaldehyde (HTCC) in Greek saffron. *J. Agri. Food Chem.* 52: 4515–4521.
- Kornilova, A.A., V.I. Vysotskii, N.N. Sysoev and A.V. Desyatov. 2009. Generation of X-Rays at bubble cavitation in a fast liquid jet in dielectric channels. *J. Surf. Invest. X-Ray Synchro. Neutro. Techn.* 3: 275–283.
- Lauterborn, W. 1974. Cavitation by laser light. *Acustica* 31: 51–78.
- Lauterborn, W. and T. Kurz. 2010. *Physics of bubble oscillations*. Rep. Prog. Phys. 73: 106501–106589.
- Leighton, T.G. 1994. *The Acoustic Bubble*. Academic Press, London.
- Mahamuni, N.N. and Y.G. Adewuyi. 2010. Advanced oxidation processes (AOPs) involving ultrasound for waste water treatment: a review with emphasis on cost estimation. *Ultrason. Sonochem.* 17: 990–1003.
- Margulis, M.A. 2006. On the mechanism of multibubble cavitation. *Russ. J. Phys. Chem.* 80: 1908–1913.
- Marinresco, N. and J.J. Trillat. 1933. Action des ultrasons sur les plaques photographiques. *Proc. R. Acad. Sci. Amsterdam* 196: 858–860.
- Mason, T.J. and J.P. Lorimer. 2002. *Applied Sonochemistry: The Uses of Power Ultrasound in Chemistry and Processing*. Wiley-VCH, Weinheim.
- Mason, T.J., L. Paniwnyk and J.P. Lorimer. 1996. The use of ultrasound in food technology. *Ultras. Sonochem.* 3: 253–260.
- Minnaert, M. 1933. On musical air-bubbles and the sound of running water. *Phil. Mag.* 16: 235–248.

- Moran, M.J. and D. Sweider. 1998. Measurements of sonoluminescence temporal pulse shape. *Phys. Rev. Lett.* 80: 4987–4990.
- Moss, W.C. 1997. Understanding the periodic driving pressure in the Rayleigh-Plesset equation. *J. Acoust. Soc. Am.* 101: 1187–1190.
- Muralidhara, H., B. Parekh and N. Senapati. 1985. Solid-liquid separation process for fine particles suspensions by an electric and ultrasonic field. United States Patent 4561953.
- Muthukumarana, S., S.E. Kentish, M. Ashokkumarb and G.W. Stevens. 2005. Mechanisms for the ultrasonic enhancement of dairy whey ultrafiltration. *J. Mem. Sci.* 258: 106–114.
- Ndiaye, A.A., R. Pflieger, B. Siboulet, J. Molina, J.F. Dufreche and S.I. Nikitenko. 2012. Nonequilibrium vibrational excitation of OH radicals generated during multibubble cavitation in water. *J. Phys. Chem. A.* 116: 4860–4867.
- Ndiaye, A.A., R. Pflieger, B. Siboulet and S.I. Nikitenko. 2013. The origin of isotope effects in sonoluminescence spectra of heavy and light water. *Angew. Chem. Int. Ed.* 52: 2478–2481.
- Neppiras, E.A. 1980. Acoustic cavitation. *Phys. Rep.* 61: 159–251.
- Nikitenko, S.I., P. Martinez, T. Chave and I. Billy. 2009. Sonochemical disproportionation of carbon monoxide in water: evidence for Treanor effect during multibubble cavitation. *Angew. Chem.* 48: 9529–9532.
- Nikitenko, S.I., L. Venault, R. Pflieger, T. Chave, I. Biesel and P. Moisy. 2010. Potential applications of sonochemistry in spent nuclear fuel reprocessing: a short review. *Ultrason. Sonochem.* 17: 1033–1040.
- Noltingk, B.E. and E.A. Neppiras. 1950. Cavitation produced by ultrasonics. *Proc. Phys. Soc.* 63B: 674–685.
- Pflieger, R., H.P. Brau and S.I. Nikitenko. 2010. Sonoluminescence from $\text{OH}(\text{C}^2\Sigma^+)$ and $\text{OH}(\text{A}^2\Sigma^+)$ radicals in water: evidence for plasma formation during multibubble cavitation. *Chem. Eur. J.* 16: 11801–11803.
- Pflieger, R., V. Cousin, N. Barré, P. Moisy and S.I. Nikitenko. 2012. Sonoluminescence of uranyl ions in aqueous solutions. *Chem. Eur. J.* 18: 410–414.
- Pflieger, R., J. Schneider, B. Siboulet, H. Möhwald and S.I. Nikitenko. 2013. Luminescence of trivalent lanthanide ions excited by single-bubble and multibubble cavitations. *J. Phys. Chem. B.* 117: 2979–2984.
- Piermattei, A., S. Karthikeyan and R.P. Sijbesma. 2009. Activating catalysts with mechanical force. *Nature Chem.* 1: 133–137.
- Plesset, M.S. 1949. The dynamics of cavitation bubbles. *J. Appl. Mech.* 16: 277–282.
- Plesset, M.S. and D.Y. Hsieh. 1960. Theory of gas bubble dynamics in oscillating pressure fields. *Phys. Fluids* 3: 882–892.
- Putterman, S.J. and K.R. Weninger. 2000. Sonoluminescence: how bubbles turn sound into light. *Annu. Rev. Fluid Mech.* 32: 445–476.
- Rayleigh, L. 1917. On the pressure developed in a liquid during the collapse of a spherical cavity. *Phil. Mag.* 34: 94–98.
- Richards, W.T. and A.L. Loomis. 1927. The chemical effects of high frequency sound waves. I. A preliminary survey. *J. Amer. Chem. Soc.* 49: 3086–3100.
- Schmitt, F.O., C.H. Johnson and A.R. Olson. 1929. Oxidation promoted by ultrasonic radiation. *J. Amer. Chem. Soc.* 51: 370–375.
- Schneider, J., R. Pflieger, S.I. Nikitenko, D. Shchukin and H. Möhwald. 2011. Line emission of sodium and hydroxyl radicals in single-bubble sonoluminescence. *J. Phys. Chem. A.* 115: 136–140.
- Sharipov, G.L., R.K. Gainetdinov and A.M. Abdrakhmanov. 2003. Sonoluminescence of aqueous solutions of lanthanide salts. *Russ. Chem. Bull. Int. Ed.* 52: 1969–1973.
- Shotipruk, A., P.B. Kaufman and H.Y. Wang. 2001. Feasibility study of repeated harvesting of menthol from biologically viable *Mentha piperata* using ultrasonic extraction. *Biotech. Prog.* 17: 924–928.
- Suslick, K.S. and D.J. Flannigan. 2008. Inside a collapsing bubble: sonoluminescence and the conditions during cavitation. *Annu. Rev. Phys. Chem.* 59: 659–683.
- Temple, P.R. 1970. Sonoluminescence from the gas in a single bubble. MS thesis, University of Vermont, USA (cross reference from Young 2005).
- Thornycroft, J. and S.W. Barnaby. 1895. Torpedo-boat destroyers. *Inst. Civil Eng.* 122: 51–55.

- Virost, M., R. Pflieger, J. Ravaux and S.I. Nikitenko. 2011. Sonoluminescence of Tb(III) at the extended solid-liquid interface. *J. Phys. Chem. C*. 115: 10752–10756.
- Yosioka, K. and A. Omura. 1962. The light emission from a single bubble driven by ultrasound and the spectra of acoustic oscillations. *Proc. Annu. Meet. Acoust. Soc. Jpn.* 125–126 (in Japanese).
- Young, F.R. 2005. *Sonoluminescence*. CRC Press, Middlesex, UK.

7

Microwaves A Potential Technology for Green Process Development

Martine Poux

Introduction

Microwaves first appeared in the chemistry and process research fields almost thirty years ago, saw a boom in interest, and then were more or less forgotten until now, with a renewed enthusiasm for them among the scientific community. Environmental constraints, standards limiting or even prohibiting the use of certain solvents, safety-related constraints—all these relatively recent measures have implications for processes. The use of microwaves as a means of heating may enable more sustainable synthesis or extraction processes meeting these demands to be proposed. In this chapter, we will cover microwave-based processes from this perspective by showing their advantages, their limits and their potential for integration in the industry.

Fundamentals of Microwaves

It is unthinkable for a process engineer to envisage the use of microwaves in a process without addressing the subject of ‘microwave physics’. This is an essential step in understanding the complexity of microwave heating, which is different from conventional heating techniques. It is clear that in many cases, whether in terms of interpretation of results or of implementation on an industrial scale, considering microwaves as a ‘black box’ is one of the causes of failure or dissatisfaction. This section presents the preliminary information required by any engineer to use or design a microwave-based process.

Microwaves in the Electromagnetic Spectrum

Microwaves are non-ionizing electromagnetic waves composed of an electric and a magnetic field. Microwave frequencies (also called hyper-frequencies) are located in the radio frequency range of 300 MHz–300 GHz, which corresponds to wavelengths of between 1 m and 1 mm (Fig. 1). To avoid any interference problems, the International Telecommunications Union defines the frequency bands authorized for scientific, industrial and medical (ISM) purposes: 433.99, 915, 2450 and 5800 MHz; the 2450 MHz band being the most widely used (it is the frequency used in domestic microwave ovens) (Osepchuk 2002). The 915 MHz band, used in France for a few specific applications, especially in the agri-food sector, requires special authorization. In the electromagnetic spectrum shown below, microwaves are situated between the wavelengths used for broadcasting and the infra-red wavelengths.

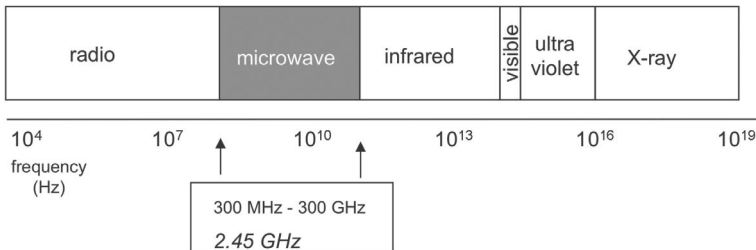


Figure 1. Microwaves in the electromagnetic spectrum.

Microwave Propagation Characteristics

Electromagnetic waves result from the instantaneous propagation of associated oscillating electric and magnetic fields. These fields are perpendicular to each other, perpendicular to the direction of propagation, and vary over time. Microwaves are thus characterized by two alternating vectors: vector E, the electric field (in V.m⁻¹) and vector H, the magnetic field (in A.m⁻¹).

Electromagnetic Field Fundamentals

An electromagnetic wave can be described by Maxwell’s equations—the basic electromagnetic equations (derived from Gauss’s theorem and Faraday’s law). The theory is based on the fact that a variable electric field produces a magnetic field for reasons of symmetry.

$$\begin{aligned}
 \text{rot} \vec{E} &= -\frac{\partial \vec{B}}{\partial t} \\
 \text{div} \vec{D} &= \rho \\
 \text{rot} \vec{H} &= \frac{\partial \vec{D}}{\partial t} + \vec{j} \\
 \text{div} \vec{B} &= 0
 \end{aligned}
 \tag{1}$$

E and H are the electric and magnetic fields (E in V.m^{-1} and H in A.m^{-1})

D and B are the electric and magnetic induced fields (D in C.m^{-2} or A.s.m^{-2} and B in Tesla or Wb.m^{-2} or $\text{kg}/(\text{A.s}^2)$)

J is the electric current density (A.m^{-2})

ρ is the current density (C.m^{-3})

Maxwell's equations must be completed by equations that account for the properties of the material; if the medium is isotropic, these equations are as follows:

$$\begin{aligned}\vec{D} &= \epsilon \cdot \vec{E} \\ \vec{B} &= \mu \cdot \vec{H} \\ \vec{J} &= \sigma \cdot \vec{E}\end{aligned}\quad (2)$$

where:

ϵ = electric permittivity (F.m^{-1} , F: Farads)

μ = magnetic permeability (H.m^{-1} , H: Henrys)

σ = electric conductivity (S.m^{-1} , S: Siemens)

Wave Propagation

Propagation equations for the E and H vectors, called Helmholtz equations, are derived from Maxwell's equations. In a steady sinusoidal state and in a vacuum (in fact, in air), these equations are expressed by the following formulae (where μ_0 is the magnetic permeability of the vacuum, ϵ_0 the electric permittivity of the vacuum, and ω the wave pulse ($= 2\pi f$, f being the wave frequency)). In a dielectric material, these equations are identical, with μ_0 and ϵ_0 being replaced with μ and ϵ .

$$\begin{aligned}\Delta \vec{E} + \omega^2 \mu_0 \epsilon_0 \vec{E} &= 0 \\ \Delta \vec{H} + \omega^2 \mu_0 \epsilon_0 \vec{H} &= 0\end{aligned}\quad (3)$$

Far from the sources and in an infinite medium, the simplest configuration in which electromagnetic energy can propagate is a plane wave; a plane wave is a TEM (Transverse Electro-Magnetic) wave with sinusoidal variation of the electric field, E, a vector polarized (for example) in the vertical direction, and with a horizontally-polarized magnetic field, H, varying sinusoidally in phase with the electric field, as shown in Fig. 2 below:

The two components E and H are in the same plane and the direction of field propagation is perpendicular to this plane.

Plane waves are the simplest solution to the propagation equations, but do not exist in reality; they only constitute a limit case or local approximation.

In practice, the devices used to transport electromagnetic fields use metal conductors to transmit the waves from the generator to the load. In this case, the fields are considered to be a superposition of several plane waves with different propagation directions.

At the microscopic scale, in analogous manner to optics, the incident electromagnetic wave is partially reflected at the surface of the material, the remainder being absorbed by the material and thus heating it. Moreover, when an electromagnetic field enters a medium with different dielectric characteristics, its

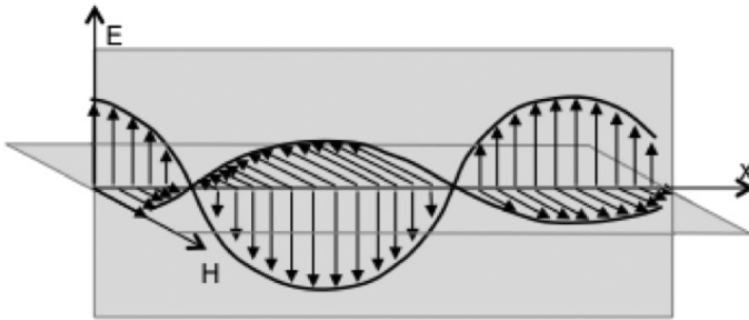


Figure 2. Configuration of an electromagnetic wave in a vacuum.

amplitude, phase and polarization may then be modified. The conditions at the boundaries of the electromagnetic fields at the interface of the two media dictate the law of reflection and are deduced from Maxwell's equations.

A waveguide is the device used to convey and guide electromagnetic waves from the generator to the applicator in which the product to be heated will be placed. It is a metal tube, usually of rectangular section, but may be cylindrical or a coaxial guide.

In a rectangular waveguide, the fields are broken down into a transverse component (straight section of the guide) and a longitudinal component (the axis of propagation, z); depending on the configuration of these components, the propagation modes in the guide may be of two types:

- transverse magnetic mode (TM)–($H_z = 0$)
- transverse electric mode (TE)–($E_z = 0$)

Using Maxwell's equations, the generating functions of the TM_{mn} and TE_{mn} modes may be established, the indices m and n respectively indicate the number of maxima of the sinusoidal variations of the E field in the x and y axes.

The first mode propagating in a guide is called the dominant mode, TE_{10} .

It is characterized by a single component of the electric field normal to the axis (z) and to the largest side of the guide (x axis). The amplitude of the electric field is greatest at the centre of the guide, zero on the vertical walls and constant in the axis (y), as shown in Fig. 3. The geometrical dimensions of a waveguide are computed so that the guide remains single mode and to minimize current maxima on the walls. Waveguide dimensions for the different frequency bands of the microwave spectrum have been standardized.

Wave-matter Interaction

Microwave Heating Principle

Unlike conventional heating techniques which use a combination of convection, conduction and thermal radiation to transfer energy to a material, microwave heating results from the conversion of electromagnetic wave energy into heat within the material itself.

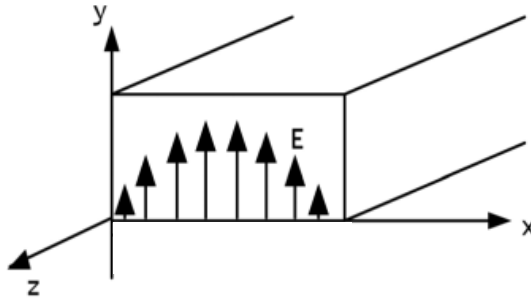


Figure 3. Propagation in dominant mode in a waveguide.

A material sensitive to microwaves is a lossy dielectric material, i.e., that absorbs or attenuates electromagnetic waves.

In a lossy medium, two types of mechanism are the source of heating, the first is related to the presence of free charges, the second to the polar nature of the molecules.

In the first case, the free electric charges (ions) subject to an electric field, E , will migrate in the direction of the field and give rise to a conduction current, j_c . This is the *ionic conduction* mechanism:

$$\vec{j}_c = \sigma \cdot \vec{E} \tag{4}$$

where

- j_c = conduction current
- σ = electric conductivity
- E = electric field

On polar molecules at the macroscopic level, the effect of the electric field is to orientate the dipoles in the direction of the field: this phenomenon is called *dipolar orientation polarization*. If the field is a high-frequency alternating field, the dipoles are oriented in the direction of the field for a half-cycle, disoriented when the field is cancelled, and re-oriented in the other direction during the second half-cycle. The interactions between dipoles cause heating of the material and a disturbance during the rapid changes in orientation. This results in a delay between the appearance of the field and the orientation of the dipoles and also between cancellation of the field and depolarization. The dipoles thus rotate but with a latency time which results in the general motion becoming disorderly and transformed into a Brownian motion. This time is called the electric relaxation time and depends on the viscosity of the medium, the temperature, and the frequency of the applied field. There is thus a phase difference with respect to the incident field, which is expressed by the permittivity equation as a complex number, as is shown by equation 5. These two mechanisms are shown in Fig. 4

At this point, it is legitimate to ask the following question—the answer to which will conclude much debate on the action of microwaves on matter: “Can microwave energy break chemical bonds?” To answer this, it is simply necessary to compare microwave energy with the energy of the main chemical bonds.

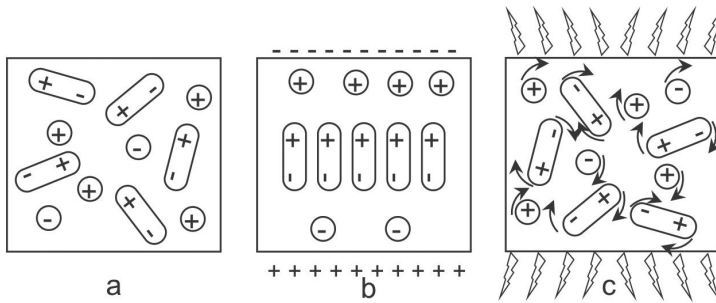


Figure 4. Influence of an electric field on dipolar molecules and charges ((a) with no electric field, (b) with an electric field, (c) with an alternating electric field).

Microwave energy (in J) is calculated using the following formula:

$$W = h f$$

where h = Planck's constant (6.626×10^{-34} J.s) and f = frequency (Hz).

In the microwave range, extending from 300 MHz to 300 GHz, the energy range is from 2×10^{-25} J to 2×10^{-22} J, i.e., 1.24×10^{-6} eV to 1.24×10^{-3} eV.

These values are much lower than those for the ionization energy of the basic atoms (C, H, N, O), the values of which vary from 11.26 eV to 14.53 eV respectively. Concerning the comparison with the chemical bonding energy (e.g., OH bond, CC bond, CO bond, hydrogen bond—that are of the order of 2 to 10 eV), the microwave energy is, again, much lower.

In conclusion, microwave energy is not strong enough to ionize atoms and break chemical bonds.

Dielectric properties

As we have already seen, some materials are sensitive to microwaves, others not. To use such a method of heating in a material transformation process, it is important to identify and understand the factors allowing product behavior with respect to microwaves to be characterized.

The property that describes the behavior of a dielectric subjected to an electromagnetic field is complex permittivity, ϵ ($F.m^{-1}$), which is defined by the following equation:

$$\epsilon = \epsilon' - j\epsilon'' = \epsilon_0(\epsilon_r' - j\epsilon_r'') \tag{5}$$

where

- Permittivity = ϵ' ($F.m^{-1}$) (real part)
- Dielectric loss factor = ϵ'' ($F.m^{-1}$) (imaginary part)

or again, by introducing vacuum permittivity ϵ_0 ($\epsilon_0 = 8,854187 \times 10^{-12} F.m^{-1}$)

- The real part of the relative permittivity $\epsilon_r' = \epsilon'/\epsilon_0$
- The imaginary part of the relative permittivity $\epsilon_r'' = \epsilon''/\epsilon_0$

The **dielectric loss factor ϵ''** expresses the capacity of the material to transform electromagnetic energy into heat; it is the material absorption term which corresponds to the dissipative component of the permittivity.

Products with a loss factor greater than 1 are particular in that they are heated well by microwaves; this is the case of liquid water, aqueous products and polar solvents such as alcohol.

If the loss factor is between 0.1 and 1, as is the case of relatively non-polar solvents such as ethyl acetate, the products are somewhat difficult to heat.

Gases, non-polar molecules, metals (which reflect the waves) and materials which cannot be polarized, such as quartz and Teflon, are insensitive to microwaves and their loss factor is almost zero.

The **relative permittivity ϵ_r'** also referred to as the **dielectric constant**, indicates the faculty of the material to be polarized, i.e., to be oriented under the effect of an electric field. This term corresponds to the non-dissipative component of the permittivity.

This relationship between these two parameters, **$\tan\delta : \epsilon''/\epsilon'$** , called the loss angle tangent, is often used and expresses the phase difference induced on the orientation of the dipoles after application of the electric field.

Important note: The values of these parameters for a same material vary according to the temperature and application frequency (see, for example, the graphs for water in Fig. 5). Knowing how the loss factor changes with temperature is essential for process management, particularly to prevent thermal runaway during reactions. Some values of these parameters are shown in Table 6.8.

In the case of mixtures, for example, to perform a chemical reaction in a medium with no solvent, it is, of course, necessary to ensure that the reagents are sensitive to microwaves and that this is also the case for the products of the reaction as, otherwise, the temperature will fall over time, thus stopping the reaction.

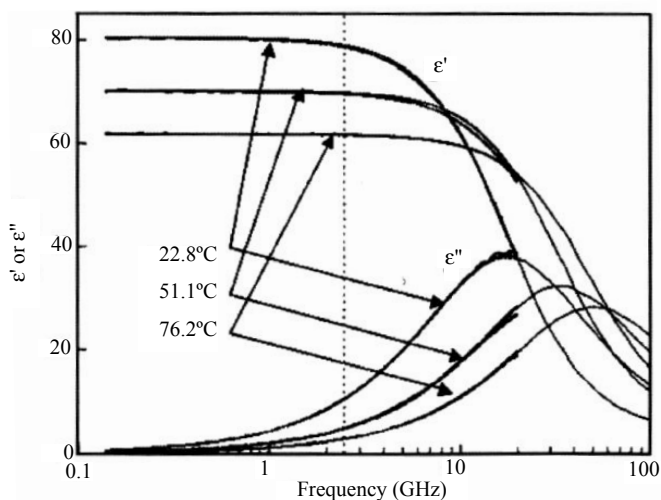


Figure 5. Variation in the electrical properties of water according to temperature (Kappe et al. 2009).

Table 1. Some loss factor and dielectric constant values (from Gabriel et al. 1998; Roussy et al. 2003; Kappe et al. 2009).

	ϵ'_{r}	ϵ''_{r}
acetone	20,7	0,87
CCl4	2,24	0,0009
chloroform	5	–
DMF	37	–
water (ice-12°C)	3,2	0,00288
water (25°C)	78,4	13
water (85°C)	56	3
ethanol (20°C)	7,49	6,46
glycerol (20°C)	6,33	3,42
hexane	1,88	–
heptane	1,9	0,0002
methanol (20°C)	20,06	11,77
propanol (20°C)	7,94	3,41
quartz	3,78	0,0008
teflon	2,05	0,0003
glass	6,8	0,07

Microwave heating may also be caused by magnetic losses in the propagation medium when it is more sensitive to the magnetic field than the electric field; this is not common to the materials used in chemical processes. In this case, the property of the material with respect to the magnetic field is given by the complex permeability ($\mu = \mu' - j\mu''$).

Electromagnetic Energy Density

The energy density transferred by an electromagnetic wave is given by the intensity of the Poynting vector. The energy released by the wave, i.e., absorbed by the material is expressed as follows (in $W.m^{-3}$):

$$P_t = 2\pi f \epsilon_0 \epsilon_r'' |E|^2 = \pi f \epsilon_0 \epsilon_r' tg \delta |E|^2 \tag{6}$$

where

f = frequency (s^{-1})

E = intensity of the electric field ($V.m^{-1}$)

ϵ_0 = vacuum permittivity ($F.m^{-1}$)

ϵ_r'' = relative loss factor of the medium ($= \epsilon''/\epsilon_0$)

This equation enables the influence of the loss factor on the absorbed power to be evaluated. It is also interesting to note that, due to the variation of $\tan \delta$ with frequency, f, the power is doubly dependent on this parameter.

The product, $f\epsilon_r''$, is called the absorption coefficient.

The difficulty in calculating the dissipated power lies in determining the distribution and amplitude of the electric field throughout the entire volume of the material (which can be obtained from Maxwell's equations, equations, 1 and 3). It should be noted that this equation is valid for a dielectrically homogeneous material and that, when dealing with a mixture, the loss factor must be per volume fraction of each component, provided that there is no interaction between components (hydrogen bond for example, solvation, etc.) (Estel et al. 2003). The complexity created when a chemical reaction takes place is seen here.

This transmitted power, P_t , is thus different to the incident power and is related to this latter by the following equation:

$$P_t = (1 - R^2)P_i \quad (7)$$

In the case of an incident wave on water, the R modulus is 0.97. This means that a large part of the wave is reflected and thus that the transmitted power is low, around 5% of the incident power. To increase power transmission efficiency, means of adaptation which consist in rendering the wave reflected by the load (product to be treated) as low as possible are used. These consist of capacitive or inductive components (screws, pillars, irises) placed at certain locations on the line, adjustable short circuits, additional metal parts in the cavity.

Penetration Depth

An important concept in the use of microwaves heating is penetration depth. This is because when an electromagnetic wave enters a material, part of the wave is reflected at the surface while the remainder penetrates the material. The energy of the wave is transformed into thermal energy and diminishes as the wave progressively penetrates the material. The penetration depth corresponds to the distance from the surface at which the microwave power is equal to the transmitted power at the surface multiplied by the factor e^{-1} (63% of the initial power has then been transferred to the material). The penetration depth, d_p (expressed in meters) is calculated based on the dielectric characteristics of the material using the following approximation:

$$d_p \approx \frac{\lambda_r \sqrt{\epsilon_r'}}{2\pi\epsilon_r''} \quad (8)$$

where:

λ_r = wavelength (meters) in the dielectric medium (at 2450 MHz, the wavelength in air is 0.12 m)

The wavelength is expressed according to the dielectric characteristics of the medium by the relative permittivity and the wavelength in a vacuum λ_0 ($= c/f$, where c is the propagation speed of the wave in air—the speed of light, and f is the frequency of the wave)

$$\lambda_r = \frac{\lambda_0}{\sqrt{\epsilon_r'}} \quad (9)$$

This shows that in order to study the interactions of electromagnetic waves with a material, it is necessary to look at the relationship between its geometrical dimensions and the wavelength in the medium. It is therefore a fundamental parameter to be considered for the development of microwave heating processes.

Hence, a material that is not very sensitive to microwaves will have a high penetration depth, whereas for an absorbent product the penetration depth will be low (for example, at 25°C and at a frequency of 2450 MHz, d_p for water is 3.4 cm, for ethylene glycol d_p is 1.3 cm). We should also note that the value of this parameter will change according to temperature due to the dielectric characteristics. Hence, for water, penetration depth increases from 2.7 cm at 15°C to 14 cm at 95°C.

Wave penetration in the material depends on the type of material (Fig. 6). A product is classified as being:

- A perfect insulator, when ϵ''_r is around 0. Almost the entire electromagnetic wave penetrates the material and propagates through the material without attenuation. This is the type of material (which can be described as “transparent” to electromagnetic waves) that must be used as the container to perform a transformation in a process. Thus glass, with a loss factor of $\epsilon''_r = 0.026$ is to be avoided; quartz is recommended ($\epsilon''_r = 0.0008$) as are Teflon and PTFE (polytetrafluoroethylene) ($\epsilon''_r = 0.0003$).
- A lossy insulator, when ϵ''_r is positive and ϵ'_r is greater than 1. The electromagnetic wave penetrates the medium and its amplitude decreases as it penetrates further into the medium.
- A conductive material, when the permittivity is high. The wave hardly penetrates the medium but is reflected. This is the case with metals.

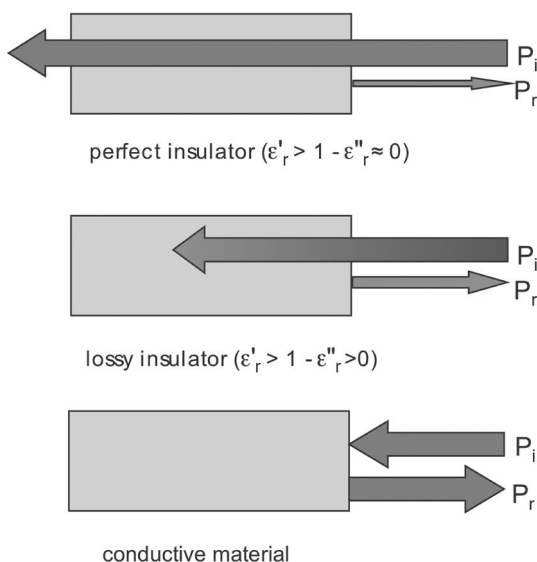


Figure 6. Interactions of microwaves with different types of materials (P_i : incident power; P_r : reflected power).

Equations, Specific Features and Complexity of Microwave Heating

Heat Transfer Equation

The heat transfer equation expresses the change in temperature at a point according to the power and the thermal constants of the medium, such as the thermal conductivity, k , of the medium (assumed to be constant here) and the specific heat, C_p . It is expressed in the standard form of the thermal conduction equation (Fourier's law):

$$k\Delta T - \rho C_p(T) \frac{\partial T}{\partial t} = -P_T \quad (10)$$

Here, P_T represents the total power that is the sum of various powers (related to the transformation of the medium and a state change or chemical reaction) and the microwave power defined by the microwave source term. This latter is expressed, as already mentioned, as a function of the intensity of the local electric field, which is obtained using Maxwell's equations.

Non-homogeneous Microwave Heating

The information presented above shows that microwave heating is unquestionably of a non-homogeneous nature. This is due to the fact that the temperature field in a material depends on:

- The field applied locally, that is itself non-homogeneous due to the presence of standing waves, and the attenuation of the waves penetrating the material.
- The thermal conductivity of the material that determines the quality of thermal transfer. The rapid speed of microwave heating generates temperature differences within the material as thermal equilibrium is more difficult to achieve.
- Thermal losses at the surface and walls. It should be noticed here that, due to the particular nature of microwaves, the coldest parts are located at the surface and walls, unlike with conventional heating techniques, where the walls are the hottest areas (see Fig. 7).

Moreover, if the product to be heated is heterogeneous by nature, e.g., comprises two phases, a liquid and a solid phase for example, the differences between the dielectric properties of the solid and liquid will result in higher temperature areas; this is often the case for chemical reactions with a solid catalyst.

Interactions between Different Parameters

The parameters that dictate the behavior of a system subjected to microwave radiation are multiple and interdependent. Let's take a look at the interactions between these parameters that influence the amplitude of the electric field at a point in the product to be heated, referred to here as the "load". The distribution of the field in the load depends on factors related to the microwave generator, the applicator and the load itself. This triangular combination of generator-applicator-load changes over time (due to the thermal treatment), as the properties of the load change with temperature.

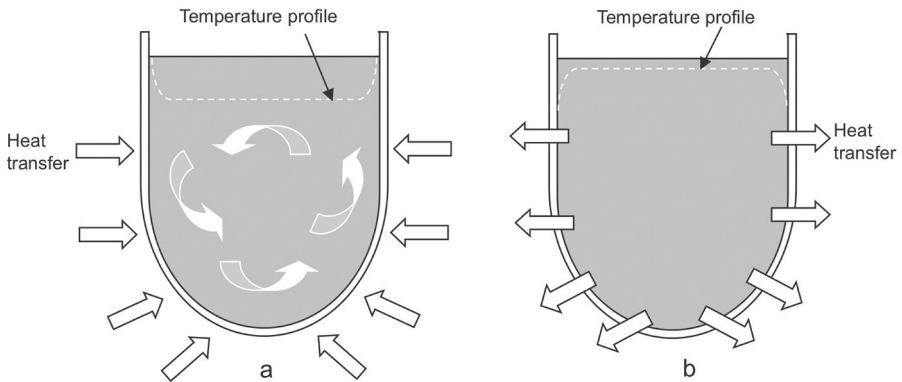


Figure 7. Temperature profiles in a reactor generated with a) conventional heating and b) microwave heating.

The diagram (Fig. 8) shows the full complexity of microwave heating in process implementation.

From a general point of view, a microwave heating problem is solved by resolving the system of coupled equations:

- Heat equation
- Electromagnetic field propagation equation
- Equation expressing the response of the medium

In the diagram (Fig. 8), an initial area (1) that represents the action of the heat source (originating from an electromagnetic wave) on the product is to be distinguished—this is, in fact, the same as when dealing with a conventional heating problem. The actions caused by the temperature rise of the product are more or less

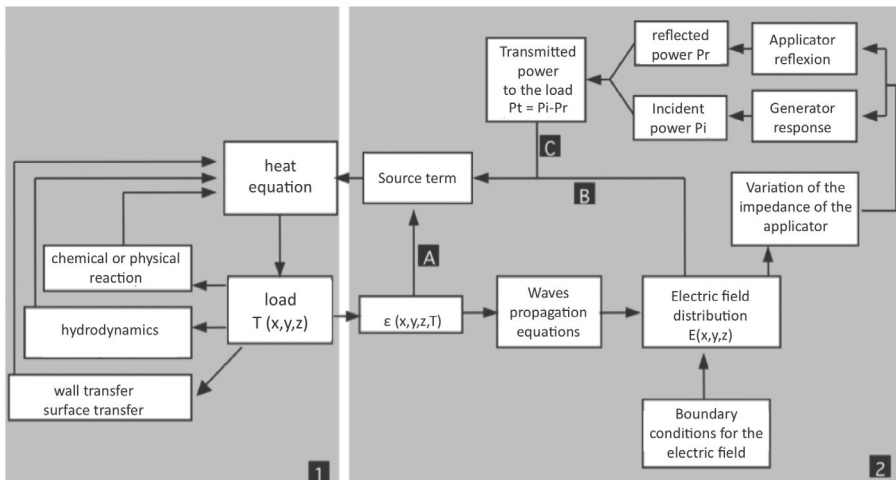


Figure 8. Complexity of microwave heating.

complex according to the desired operation. For example, in the case of heating of a liquid, different levels of difficulty may be envisaged depending on whether a global or local approach is taken, i.e., performing a simple thermal balance by evaluating the global losses at the walls and surface or an in-depth study of the hydrodynamics of the system by taking convection movements into account. If, rather than a simple liquid, a reaction mixture is considered, then the enthalpy of the reaction and change in composition of the mixture must also be considered. Each type of transformation means that the appropriate state changes must be taken into account, for example state changes such as those for drying, defrosting, etc. For example, for a microwave application in organic synthesis, the system of equations that describes heating in a reactor in which a chemical reaction is performed is as follows:

- Wave equation
- Heat equation (with a source term related to the endothermic or exothermic chemical reaction)
- Chemical kinetic equation
- Continuity equation
- Momentum equations

Changes in the medium (whether thermal and/or chemical) that induce a variation in the dielectric properties will modify the distribution of the electromagnetic field and its environment (zone 2).

The temperature obtained by solving the heat equation depends on the power dissipated locally, which is represented by the microwave source term. This source term involves the characteristics of the medium (A) which are, of course, related to the temperature, but also to the amplitude of the electric field (B). The distribution of the electric field is obtained using the wave equation, which is also dependent on the dielectric properties.

In addition, it is necessary to take into account the consequences of applicator reflection and generator response on the power transmitted to the product and thus on the source term (C). This part essentially refers to wave propagation and generator operation concepts.

Hence, the distribution of fields in a load placed in an applicator at a given time is extremely difficult to determine. There are calculation codes based on solving Maxwell's equations (e.g., COMSOL), but these codes are of limited use owing to the number of simplifying assumptions made. Moreover, the complexity increases when the characteristics of the load vary over time.

Microwave Equipment

Main Components

Any microwave heating system is composed of three parts:

- The wave generator, which produces electromagnetic waves.

- The waveguide, the function of which is to transfer the electromagnetic waves from the generator to the application enclosure.
- The applicator (also called the cavity), in which the product to be treated is placed.

Microwave Generator

The magnetron is the most widely used type of generator for the production of electromagnetic waves.

The magnetron is a circular vacuum tube comprising a central cathode heated by a filament and a concentric anode composed of resonant cavities of different shapes according to the type of magnetron. Two types of field co-exist:

- An axial magnetic field produced by two magnets located at the end of the tube.
- An electric field generated between the anode and the cathode and which is perpendicular to the magnetic field.

A very high voltage (several kV) is applied in an extremely small space of a few millimeters between the anode and the cathode, thus resulting in the production of electrons. The electric field increases their kinetic energy and the magnetic field bends their path. The electrons thus accelerated radiate energy in the form of electromagnetic waves. The anode unit is cooled by air or, in high-power magnetrons, by a water cooling system.

The powers available range from several kW up to around 15 kW at 2.45 GHz; magnetrons of up to 25 kW should soon be commercially available (Osepchuk 2002).

Waveguide

The waveguide is a metal component that transports waves from the generator to the applicator. It is a rectangular hollow travelling wave tube of precise dimensions. Its dimensions determine electromagnetic wave propagation mode. To obtain a single propagation mode, the dimensions required for a frequency of 2.45 GHz are 86.5 mm x 43.5 mm.

Applicator

The applicator is a closed cavity that transfers electromagnetic energy from the waveguide outlet to the product to be treated.

There are two basic types of applicator architecture according to the propagation mode used: single mode or multi-mode (Fig. 9).

An applicator is said to be single mode when its geometrical dimensions allow a single mode of propagation, and thus a single field configuration. This type of applicator gives precise control of the electric field, but is reserved for treatment of products with a small volume, the product is then placed in the waveguide.

In a multimode cavity, the electromagnetic waves are reflected on the walls and a network of standing waves develops (a standing wave oscillates without moving

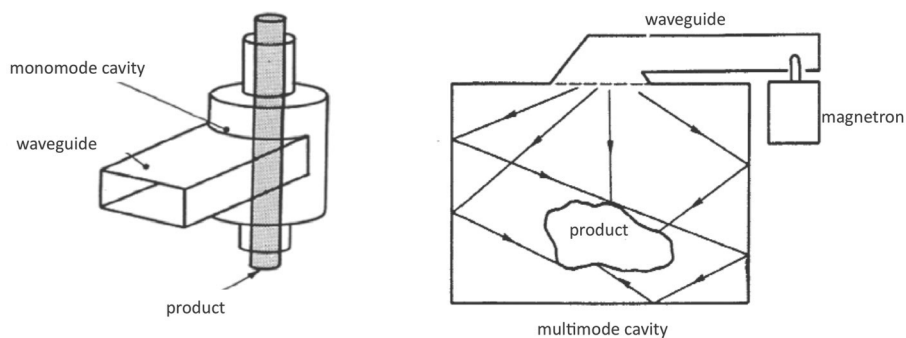


Figure 9. Different types of applicators.

and has points with no displacement (nodes) and points of maximum displacement (antinodes) fixed in space). This is called a resonant cavity. There are thus several field configurations with a variable distribution. A larger quantity of product can be treated in such a cavity than in a single mode cavity, but it is difficult to control the distribution of the field and steep temperature gradients may develop in the product. To remedy this problem, a widely used technical solution is to use wave stirrers or turntables (as in domestic ovens).

Commercial Systems

Over the past few years, a number of manufacturers have produced sophisticated systems, thus contributing to rendering experiments at laboratory scale more relevant and reproducible.

Three major commercial manufacturers offer a wide range of systems, of sizes ranging from a few millimeters to perform rapid synthesis for research on new medicinal products, for example, up to several liters for analytical purposes. These are CEM, Anton Paar and Milestone in the microwave-assisted chemistry field; Biotage, a company specializing in the life sciences field, should also be mentioned.

The systems available all have temperature control, pressure measurement and a stirring system when required by reactor size, thus enabling good reproducibility of experiments to be achieved. Most of these systems are multimode type.

CEM has several product ranges: Discover, intended for laboratory synthesis, with a volume of a few milliliters up to a maximum of 50–125 mL, depending on the model, and operating at atmospheric pressure or under pressure; Explorer, a synthesis system that can treat up to 96 samples simultaneously (volume treated: 4–35 mL), and lastly, Voyager and Mars, recommended for synthesis of volumes of up to a kilogram and delivering a power of 1600 W.

Anton Paar has developed the Synthos 3000 system for high pressure and high temperature reactions. Different reactor models allowing a large number of reactions to be performed simultaneously are available.

Milestone specializes in higher production capacities (3.5 L maximum) and offers a continuous flow system. Of note is the innovative MultiSYNTH system, a hybrid system that combines single- and multi-mode technologies, thus rendering it

extremely versatile as it can be used with a single reactor or with a system composed of several small reactors. The BatchSYNTH (batch) and FlowSYNTH (continuous flow) devices should also be mentioned. These are equipped with internal temperature sensors and offer a wide operating range (up to 230°C and 30 bar) for a treatment capacity of 300 mL. The UltraCLAVE has a 3.5-L reactor, a power of 1000 W and can operate at pressures up to 200 bar.

All these systems have accessory kits intended to best facilitate chemical synthesis. There are, for example, various models of multi-plate rotors and multi-reactors to be placed in the oven and intended to perform a large number of simultaneous reactions and open or closed reactors made of different materials such as PTFE, glass, quartz, etc.

Figure 10 shows some commercially-available microwave systems and Table 2 shows their main features.

In recent years, the problem of scaling-up has begun to be tackled using commercial microwave systems. Some publications thus include the term “scale-up” in their title, but it should be made clear that the volume treated remains very low from a process engineer’s point of view (from a few mL to several hundred mL—a liter being the maximum). The variation in the volume treated is obtained by using the various modules provided by the manufacturers—by using reactors in a parallel configuration, for example.

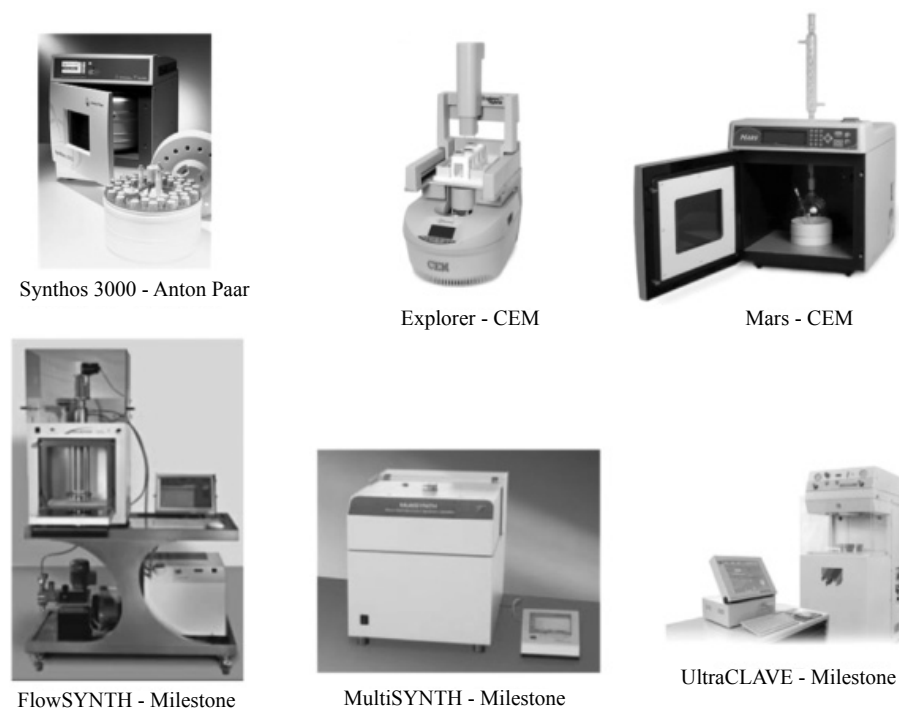


Figure 10. Some commercial microwave systems.

Table 2. Characteristics of some commercial microwave systems.

Manufacturer	CEM	CEM	CEM	Anton Paar	Milestone	Milestone	Milestone
Model	Discover	Voyager SF	Mars	Synthos 3000	MultiSYNTH	BathSYNTH FlowSYNTH	UltraCLAVE
Waveguide and cavity	Single mode	Single mode	Multimode	Multimode	Single mode and multimode	Multimode	Multimode
Max. power (W)	300	300	1600	1400 (2 magnetrons)	400 or 800		1000
Max. temperature (°C)	300	220	300	300	250	230	280
Max. pressure (bar)	20	14	55	80	20	30	200
Reactor volume	4–125 ml	80 ml	Carousel or reactor of up to 5 L	Depending on accessory selected 96x3 ml–8x60 ml	Different volumes from 2.5 ml–1L	250 ml from 12 to 100 ml/min	3 L or 77 reactors
Temperature measurement	Infra-red + optical fiber	Optical fiber	Infra-red + optical fiber	Infra-red + internal thermometer	Infra-red + internal thermometer	Infra-red + internal thermometer	Internal thermometer
Stirring	Magnetic	Magnetic	Magnetic	Magnetic	Magnetic + vibration	Magnetic Screw for FlowSynth	Magnetic

It is therefore of interest to note that some work has been performed recently to compare the various commercially-available systems based on such criteria as the efficiency of one or more chemical reactions and product purity (Lehmann and LaVecchia 2005; Moseley et al. 2008; Bowman et al. 2008a) by varying the quantity treated. Work on pressurized systems has also been reported by Bowman et al. 2008b, demonstrating successful scaling up in the range of 10 mL–350 mL.

Using Microwaves for Chemical Synthesis

In a reactor, substituting microwave energy for the energy conventionally supplied by a heat transfer medium circulating in either a jacket or an immersed coil is a relatively recent approach that was first used in the 90's. Organic chemists were the first community to show an interest in microwave heating. Publications by Gedye et al. (1986) and Giguere et al. (1986) may be cited as reference publications and were, doubtless, the origin of chemists' enthusiasm for this new mode of heating. Since that time, the amount of literature published in this field has not ceased to grow (there are currently more than 5000 references), with many papers noting that microwave heating increases the speed of synthesis by a factor of 100 to 1000 compared to conventional heating.

The use of microwaves in chemistry now covers a large field: organic synthesis, organometallic synthesis (Kumar Gupta et al. 2013), inorganic synthesis, etc. There are a number of books describing such work, which may be referred to for precise descriptions of the reactions (Loupy 2006; Kappe et al. 2009; de la Hoz and Loupy 2013). The reader may also refer to the review articles by Caddick 1995, Lidström et al. 2001, and Baig and Varma 2012, that cite large numbers of reference works and papers. We give only a broad outline here.

State of the Art

Microwave assisted chemistry has experienced considerable growth in recent years with the arrival on the market of systems specifically designed for synthesis. Initial work was performed in domestic microwave ovens adapted for the purpose and without reliable temperature or power measurement instrumentation. Moreover, as we have seen, such systems have a multimode cavity, resulting in temperature inhomogeneities. In such conditions, it is difficult to perform a valid comparison between a chemical reaction performed with microwave heating and a reaction with conventional heating equipment. A large number of results reporting a specific microwave heating effect have thus been published, but have not really been validated.

Of course, to demonstrate a microwave heating effect, comparisons with conventional heating must be based on heating performed in *identical temperature and pressure conditions*. This thus implies the use of appropriate equipment with continuous monitoring of temperature and absorbed power. There is now a wide choice of equipment with such features intended for laboratory tests. Such systems offer temperature control and ramp programming and measurement is often performed by an internal wall-mounted infra-red sensor. It is therefore assumed that

the temperature in the reactor is the same as that of the wall, which is not always the case (Kappe 2013; Mazubert et al. 2014). For more accurate measurement, it is preferable to use optical fiber probes placed directly in the reactor when the operating range allows (300°C max.). A suitable stirring system is also highly recommended, a simple magnetic bar stirrer rarely being effective to homogenize the contents of a reactor, even when the reactor is small (Herrero et al. 2008; Obermayer et al. 2013).

The appearance of such equipment between 1998 and 2000 has rendered research work simpler and more relevant. Promising effects have recently been demonstrated (Kappe et al. 2013).

Effects and Advantages of Microwave Heating

The specific features of microwave heating described in the “Fundamentals of microwaves” section result in advantageous effects for processes, such as:

- The rapid temperature rise (which may be as fast as 10°C/s).
- No overheating of the wall.
- Selective heating of the products.

The consequences of this type of heating on chemical synthesis are a reduced reaction time (and thus reduced power consumption), no formation (or reduced formation) of by-products, and an increase in reaction yield—all advantages that position microwaves as a technology capable of rendering processes greener and more sustainable.

The scientific community has attempted to provide an explanation for the latter point, and there are currently three hypotheses:

A Thermal Kinetic Effect

It is now known that, in most cases, the increase in yield and selectivity observed is the result of a purely thermal effect. This is due to the rapid temperature rise—such a temperature ramp (greater than 10°C/s) cannot be achieved with conventional heating—the effect of which is to minimize secondary reactions and the formation of by-products. It should also be remembered that the comparisons of results in many studies are out of date due to the lack of equivalence between experiments performed with conventional heating and with microwave heating (often related to temperature measurement).

A Specific Effect

Probably one of the most important effects of microwaves results from selective heating of the product, e.g., the heating of catalysts that are highly absorbent of electromagnetic waves (Pd/C, etc.) immersed in an organic solvent that is not very absorbent. The temperature at the catalyst grain surface is then much higher than the mass temperature, resulting in a significant increase in yield, the actual temperature to be considered for calculations then being difficult to obtain.

Advantage can be taken of this specific feature to heat solutions with zero or little sensitivity to microwaves: it is then simply a matter of adding to the medium compounds that are highly receptive to microwaves—susceptors—and that are chemically inert to achieve heating of the entire solution by conduction and convection (Chemat et al. 1996b).

Another phenomenon that has been observed is liquid superheating. The boiling points recorded for solvents heated with microwaves at atmospheric pressure are between several degrees to several tens of degrees higher than conventional boiling points. The reversed temperature gradients—that result in the walls being colder than the solution—are the origin of this phenomenon, which disappears if pumice stone is introduced or the incident power reduced.

An Athermal Effect

The athermal effect may result from a direct interaction between the electric field and the reaction medium. The orientation of the dipoles may induce a variation of the pre-exponential factor in the Arrhenius equation or the activation energy via entropy. It has also been postulated that, in the case of a polar reaction mechanism, the polar molecules are stabilized when the transition state of the reaction is more polar than the initial state—which may result in a decrease in the activation energy.

According to the same line of thought, it would seem that there is an athermal effect for reactions with a high reaction enthalpy and a late transition state.

These approaches are still much debated today and remain controversial (Kappe et al. 2013).

Solvent-free Reactions

The use of solvent-free reactions in an integral aspect of one of the objectives of chemistry for sustainable development. It is, moreover, with this type of reaction that most of the significant effects of microwaves have been observed. This is because the absence of solvent allows microwaves to interact directly with the reaction medium. Extremely short reaction times, often just a few minutes, associated with extremely high temperatures, sometimes under pressure, mean that the products are extremely pure and that the yields are high. A list of examples of solvent-free reactions may be found in articles by Loupy (1999, 2004) and Varma (1999).

Solvent-free reactions are used for:

1. Reactions on Solid Mineral Substrates

Mineral oxides (Al_2O_3 , MnO_2 , KSF, etc.), although extremely poor conductors of heat, are sensitive to microwaves.

The substrate is impregnated with reagents such as clay, aluminum oxide or silica. To achieve extremely high temperatures, graphite is used—enabling a temperature of 1000°C to be reached with less than a minute of irradiation. Such a substrate can also be doped with catalyst (Laporterie et al. 2002). The products are

extracted by elution at the end of the reaction. N-alkylations and S-alkylations are among the types of reaction that have been performed with microwaves. The recent review by Heravi and Moghimi 2013, provides a summary of reactions performed on mineral substrates using microwaves.

2. Catalysis by Phase Transfer

Whether in solid-liquid or liquid-liquid systems, phase transfer catalyst reactions involve ionic reagents and a transfer agent such as quaternary ammonium salt. The presence of these charged compounds renders such reactions extremely responsive to microwaves—and even more so when they are performed on a solid substrate. Examples: O-alkylations, N-alkylations, oxidations, Knoevenagel condensations.

3. Dry Reactions (using neat reagents)

The reagents are directly placed in contact without using a solvent or substrate. In the case of a heterogeneous system—solid-liquid—there is either solubilization of the solid in the liquid or adsorption of the liquid in the solid, which produces a reaction at the interface. If they are heated poorly or not at all by microwaves, one method of overcoming this problem consists in adding a few drops of polar solvent in order to initiate the reaction. Nucleophile aromatic substitution and deacetylation may be cited as examples of this method.

Pressure Reactions

Microwave synthesis can be performed under pressure. This type of synthesis has expanded significantly with the commercialization of systems enabling operating conditions to be controlled and extremely high pressures of up to 200 bar to be achieved. The main advantage is to be able to work at extremely high temperatures beyond the boiling point of the solvent, without having to recourse to the use of solvents with high boiling points to speed up the reaction. Indeed, for organic synthesis, it can be said that reaction time is reduced by half for a temperature increase of 10°C. This approximation shows that a reaction time of 18 hours at 80°C can be reduced to 16 seconds at 200°C, provided that the compounds can withstand such a temperature!

It is thus extremely simple, under pressure, to perform a reaction at high temperature by using such a solvent as methanol, the boiling point of which is increased by 100°C by passing from atmospheric pressure to a pressure of around 15 bars.

However, attention must be paid to the dielectric properties of the solvent, which may change radically with temperature. In his review, Strauss 2009, lists a series of reactions and demonstrates the advantages of working with microwaves and under pressure.

Microwave synthesis under pressure (and thus at high temperature) appears to be a promising avenue for intensifying reactions, provided that only limited volumes are used for safety reasons. It is for this reason that it is also performed

with miniaturized systems. There is a section dedicated to this technology at the end of this chapter. It will surely enable new and previously impractical avenues of synthesis to be discovered.

Solid-liquid Extraction with Microwaves

Microwaves were first used for extraction at the same time as for chemical synthesis, in 1986, by Ganzler et al. and Lane and Jekins. There are currently some 600 articles on the subject and over the past few years, due to new standards stipulating reduced volumes of solvent and even prohibiting the use of certain solvents (the REACH regulation), there has been a new interest in this process which fully meets green process requirements. It is in the field of plant product extraction that this new technique is developing to the greatest extent, but the applications, of course, extend well beyond this field (Jain et al. 2009). The same techniques can thus be applied for analytical purposes such as the extraction of organic compounds and are used in many analysis laboratories (Letellier and Budzinski 1999).

There are chapters of books and entire works specifically devoted to this topic which can be referred to for in-depth study (Paré and Bélanger 1997; Chemat and Lucchesi 2006; Chemat and Cravotto 2013; Destandau et al. 2013); only an overview will be given here.

Microwave-assisted extraction processes are classified in three categories:

- Microwave-Assisted Solvent Extraction, MASE.
- Microwave-Assisted Distillation, MAD.
- Microwave Hydrodiffusion and Gravity, MHG.

Microwave-assisted solvent extraction (MASE)

In this technique (MASE), also called MAE (Microwave Assisted Extraction), introduced by Paré and Bélanger in 1990, the solid matrix is immersed in a solvent heated by microwaves. The behavior of the matrix/solvent is determined by the polarity of the solvent: if the solvent is sensitive to microwaves then the matrix is heated by conduction via the solvent which, once heated to its boiling point, will solubilize the solute. This process is identical to that used in a conventional extraction process, the only advantage is the reduced heating time. This is due to the fact that there is no thermal inertia and the solvent temperature rise is rapid.

With a solvent that is not very sensitive to microwaves (such as hexane or toluene), the water-rich matrix is heated preferentially, which results in an extremely rapid release of the substrates. The temperature of the water in the cell rises and the internal pressure then rises until the membrane breaks, thus releasing the required substances more easily.

If the matrix does not contain much water, the extraction mechanism is related to the existence of a reverse temperature gradient which increases the diffusion of the microwave-sensitive solute to the outer surface of the membrane.

The result of microwave heating in this example is a reduction in extraction time from one hour to several minutes and a reduction in the quantity of solvent required—

the yield usually remaining comparable to that obtained with a conventional method. One of the first companies to apply this process industrially was the French company Phytotex, with a MASE pilot built by Micro-ondes Energie Systèmes (MES) based on a Thermo-Star applicator capable of continuous processing of 50 to 100 kg of raw material per hour (Bousquet 1997).

Microwave Assisted Distillation (MAD)

Intended for the extraction of essential oils from plants, this technique, based on steam distillation, can be used under pressure or under vacuum and is performed with different protocols:

1. Compressed Air Microwave Distillation

This process, first proposed in 1989 by Craveiro et al., is based on the conventional principle of steam distillation and uses compressed air instead of steam to extract the volatile compounds. The matrix is heated directly by microwaves. Compressed air is injected into the reactor to draw off the essential oil. The extract is recovered in a few minutes and is of identical quality to that obtained with a conventional process—which would take more than an hour. This method requires a significant energy input to enable extraction.

2. Vacuum Microwave Hydrodistillation

Patented by the Archimex company (Mengal and Mompon 1994), this extraction process is performed in two stages: the plant matrix is first heated with microwaves (a certain amount of water is added if the matrix is dry), then placed in a vacuum (of around 100 to 200 mbar) thus allowing azeotropic distillation of the water-oil mixture at a temperature of less than 100°C, the main advantage of this being that thermal degradation of sensitive compounds is avoided. This sequence can be repeated over several cycles (see Fig. 11).

As well as the aforementioned advantage, this technique also reduces operating time (by a factor of 10) and power consumption. The recommended incident power is around 0.2 to 1 kW per kilogram of raw material.

3. Solvent-free Microwave Hydrodistillation

This is a recent extraction process (Chemat et al. 2004a), performed at atmospheric pressure and which does not require any solvent provided that the initial material contains enough water. Under the effect of microwaves, the cells of the plant material explode, thus releasing the essential oil which evaporates with the water in the plant matrix. The distillate is continuously condensed outside the system and the water is re-injected into the matrix to enable the operation to continue (see Fig. 12).

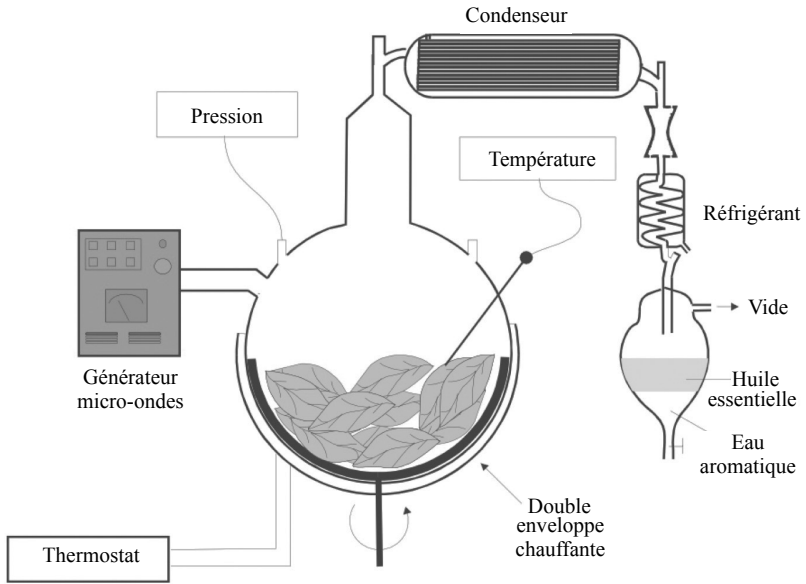


Figure 11. Vacuum microwave hydrodistillation (from Anizon et al. 2003).

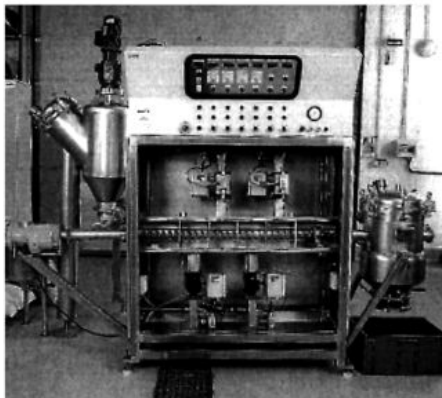
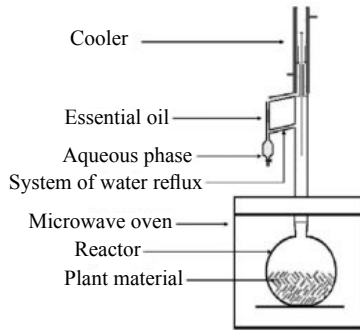


Figure 12. Solvent-free microwave hydrodistillation (from Lucchesi et al. 2004).

Microwave Hydrodiffusion and Gravity

The originality of this process lies in its simplicity as it uses gravity to remove the aqueous and oily phases from the matrix once they have been extracted from the plants under the action of microwaves and without using solvents (Abert-Vian et al. 2008). The principle is of the same type as that used for solvent-free hydrodistillation, but separation is performed after condensing in a container called a 'florentine flask' (see Fig. 13). The advantage of this method is that extraction and distillation are combined, thus rendering the process a single-stage process which, as well as being time saving, offers the additional benefits of power savings and ease of implementation.

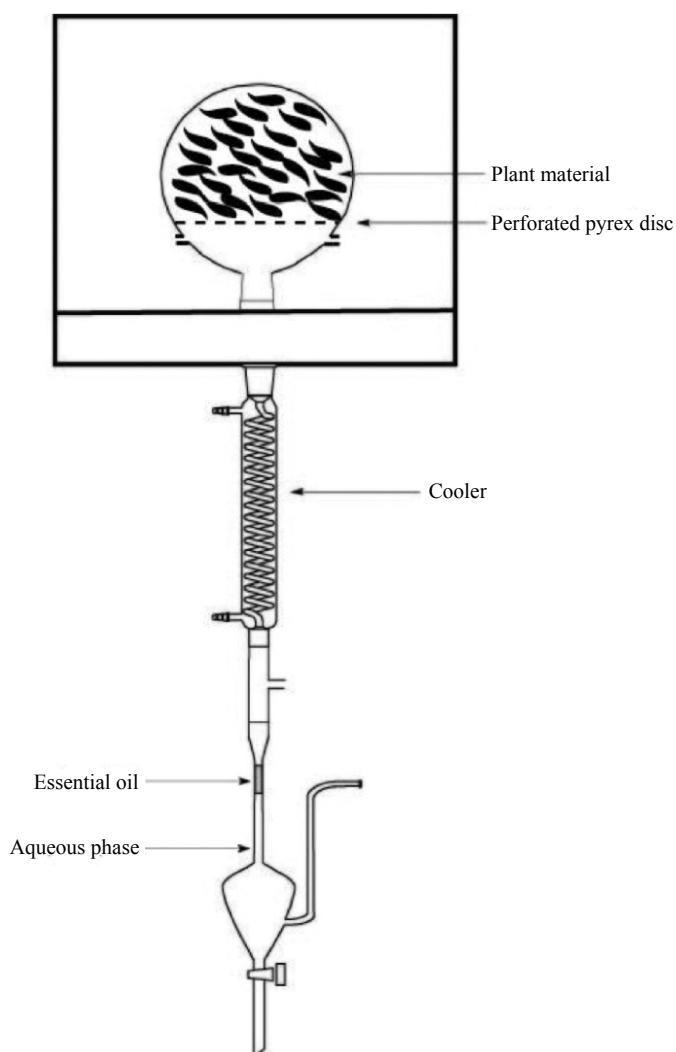


Figure 13. Microwave hydrodiffusion and gravity system (from Abert-Vian et al. 2008).

Microwaves in Industry

Industrial Sectors Concerned

Today, the microwave heating process is widely used on an industrial scale in many sectors, including the food, timber pharmaceutical and chemical (polymers, materials, fine chemistry, etc.) industries.

The food sector pioneered this technology with applications such as drying and vacuum drying, cooking, pasteurization and sterilization, tempering and defrosting (Chandrasekaran et al. 2013). The technology used is specific to the field. The product to be processed is transferred on a conveyor belt through a tunnel irradiated with microwaves. Such tunnels can be equipped with hot air blowers. This type of heating is essential to evaporate the water which accumulates at the surface and which, due to its high sensitivity to microwaves, could result in local heating and even a deterioration of the product. For pasty and viscous products, a tube that is transparent to microwaves is used, through which the product is moved by screw conveyor.

In the timber industry, high-frequencies are used for gluing.

Applications in the pharmaceutical industry are similar to those in fine chemistry. For new medicinal product research goals, the use of specific laboratory systems offers the possibility of performing a large number of reactions simultaneously, with reduced consumption of reagents and reduced reaction times. In this case, the technique is used in research laboratories and not in the production sector.

It is certainly in the chemical industry that the most varied and recent applications are used:

- The rubber, plastics and polymer thermoforming (vulcanization, polymerization) industries (Estel et al. 2008).
- Materials: the use of microwaves to sinter metal powders and ceramics is of value because of the rapid temperature rise to high temperatures (up to 1800°C) thus reducing synthesis time from around thirty hours to a few hours. This technique also opens up promising paths for the production of new materials (www.industrialheating.com) such as, for example, the production of fiber-reinforced composites (Feher and Thumm 2004).
- Digestion: for analytical purposes, extremely rapid sample preparation for analysis. There are laboratory systems developed specifically for this application.
- Extraction.
- Synthetic chemistry.

However, in these latter sectors, application on production sites still remains extremely limited.

Problems in Microwave Synthesis Scale-up

Although the feasibility of a large number of protocols has been demonstrated at laboratory scale, there is still a lack of technologies capable of overcoming the hurdle of industrial production and this poses a real problem.

In recent years, impressive progress has been made in moving from the scale of a gram to a scale of around a hundred grams or even a kilogram; such systems can be used for low-volume production, but this does not always correspond to the industrial demand.

In switching to a large scale, the benefits obtained on a small scale (such as rapid temperature rise) are lost; moreover, as regards safety, the drastic operating conditions required on a large scale (300°C/30 bar) to obtain a useful microwave heating effect for certain reactions cannot be maintained. In similar manner, rapid cooling, which can be performed on a small scale to prevent decomposition products forming, is impractical when the volume becomes large.

The depth of penetration of the waves in the medium also hampers the development of high-volume systems. For large objects, only the area near the wall is irradiated and the core is then heated by convection or conduction, which results in a steep temperature gradient. Stirring may somewhat remedy this problem, however the propagation speeds of the electromagnetic field are much higher than the flow rates, which means that a certain temperature gradient subsists.

Lastly, as we saw, the distribution of the electromagnetic field is more uniform and more easily controlled in small cavities. It is therefore obvious that a conventional stirred reactor with a volume ranging from several liters to several hundred liters is not really suitable.

These arguments have therefore resulted in research being oriented towards the development of continuous processes with relatively small-diameter reactors (a few centimeters) and with or without a recycling system depending on the required residence time.

The first continuous systems were created by modifying discontinuous systems. The issue at that time was, first and foremost, to demonstrate the feasibility of transposing chemical reactions from the lab bench scale to that of low production (Cablewski et al. 1994; Chemat et al. 1996b; Marquié et al. 2001).

The technologies have evolved and now systems with tubular reactors ranging from several tens or hundreds of microns to a centimeter are available. The former gave birth to microwave flow chemistry (Bagley et al. 2013), the main advantage of which is strict control of the operating conditions, thus ensuring a certain reproducibility and safety level. Commonly used in the pharmaceutical field, microwave flow chemistry also limits the quantity of products to be used while still allowing sufficient quantities to be obtained for research. Often equipped with on-line analysis capabilities, such systems are commercially available (the manufacturer Mettler Toledo may be cited as an example) and are used in industrial R&D laboratories. There is a section devoted to microsystems at the end of this chapter.

Higher volume systems are regularly studied for larger scale production. A continuously-operating single mode microwave reactor composed of a ceramic tube that is transparent to microwaves of a centimeter in diameter and that can withstand

a maximum pressure and temperature of 60 bars and 310°C respectively has been tested for four reactions that are of industrial interest. With a flow rate of 3.5 to 20 L/h and a power of 0.6 to 6 kW, this system has demonstrated its capacity to meet an industrial production demand (Morschhäuser et al. 2012).

Examples of Industrial Transposition for Microwave Reactors in Fine Chemistry

The transposition of chemical synthesis performed at laboratory scale to production facilities requires study to determine the best technology to use—which depends on the characteristics of the reaction (phases present, viscosity, temperature, reaction time, etc.).

Microwave synthesis reactors are thus often developed according to industrial demand by manufacturers specializing in microwave technology such as CEM, C-Tech, SAIREM, etc.

Synthesis of Laurydone®

The production of Laurydone is the first fine chemistry industrial process to be performed with microwaves on a large scale (1 m³). Laurydone®—the lauric ester of L-pyrrolidone carboxylic acid or L-PCA—is a product that is used in the formulation of many cosmetics as it has moisturizing properties due to its amphiphilic structure and the presence of a fat chain with a 12 carbon atoms resulting in a prolonged release of the acid over time.

This esterification reaction involves S-pyroglyutamic acid and n-decanol. In conventional mode, it takes place at 110°C with toluene as solvent and p-toluene sulfonic acid and sulfuric acid as catalysts.

Under microwave, the reaction takes place without solvent at 150°C and requires no catalyst, which simplifies the purification stage. An 80% reduction in process duration and a 40% reduction in power consumption have thus been observed, solely due to the reduced number of process stages. Indeed, it has been demonstrated that microwave heating does not speed up the reaction (Dressen 2009).

A series of products derived from L-PCA for use in cosmetics (Ceramidone®, Myristidone® and Waxidone®) are produced based on the same principle.

The industrial process is the result of joint work by Bioeurope (the Solabia Group), SAIREM and De Dietrich, and is shown in Fig. 14. It comprises a stirred reactor (with an external recirculation loop) that is placed in the microwave cavity. The microwave generator has a power of 6 kW and the reaction time is 3 hours.

Production of Fatty Acid Esters

The production of fatty acid esters is of major importance in the cosmetic industry. For example, stearyl stearate is an emollient, moisturizing and skin-care product that is easy to apply and that penetrates the skin well. It is synthesized by esterification of fatty alcohols with fatty acids catalyzed by montmorillonite clays (esterification of stearic acid with *stearylic alcohol*). The process may be performed as a dry process to render it more environmentally friendly. The difficulty lies in strictly maintaining

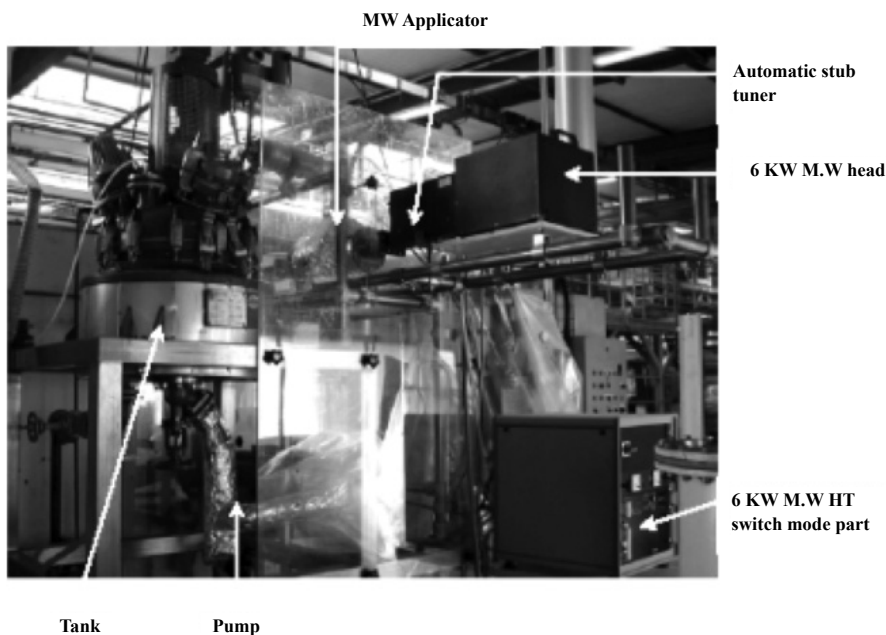


Figure 14. Industrial reactor for Laurydone® production (Dressen 2009).

the temperature at 170°C to prevent the formation of secondary products. The ATO-DLO Group (Wageningen, Netherlands) in collaboration with Unilever (Esveld et al. 2000a, 2000b) has developed a continuous, semi-industrial microwave reactor for this type of reaction with a capacity of 10 to 100 kg/hour. The technical solution adopted is to perform the reaction on a conveyor belt in a suitable microwave enclosure (power: 6 kW; wavelength in the enclosure: 150 cm), the reaction mixture being placed in independent reactors. A schematic diagram is shown in Fig. 15. The system was designed using experimental and numerical thermal data to ensure temperature homogeneity.

It has thus been possible to produce 10 to 100 kg of fatty ester per hour with a yield of 95%. The reaction has proved to be 20 to 30 times faster than in the industrial

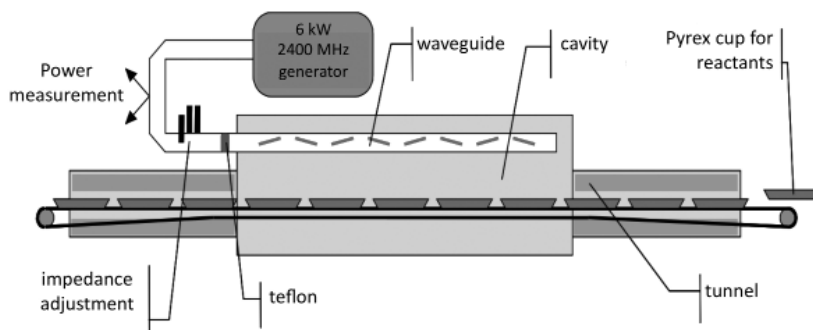


Figure 15. Continuous microwave reactor for “dry” synthesis.

reactors used by Unilever. Measuring the power consumption has shown that the energy efficiency of the system is comparable to that of industrial reactors.

Example of Industrial Transposition for Microwave Reactors in Extraction

Extraction of Natural Bioactive Compounds with Vegetable Oils

Solid/liquid extraction of bioactive compounds for the cosmetic or food industries from raw vegetable material generally requires a heating stage to accelerate the diffusion of the molecules of the solute to be extracted into the solvent. This is because the increase in temperature results in a modification of the solid matrix, denaturation of the proteins and disassembly of the lipoprotein complexes—thus causing destructuring of the membranes and rupture of the walls (Escribano-Bailon and Santos-Buelga 2003). Oleo-eco-extraction is the first patented process for the extraction of vegetable substances using vegetable oil or natural fat with the heating stage performed using a microwave reactor (Rossignol-Castera 2009). Oils are extraction solvents that are transparent to microwaves, which means that only the vegetable matter is heated, thus favoring the passage of bioactive compounds from the plant cells to the solvent. Microwave heating of the plant/oil pair is performed with stirring in a 6 kW–2450 MHz Labotron Extraction™ reactor (SAIREM) with a capacity of 2 to 20 liters, by applying a power of 1600 to 3000 W (Fig. 16). The microwaves are directly delivered by an antenna that guides and focuses them from the generator to the center of the solid/liquid mixture. The extraction parameters are selected according to the plant/oil pair. For example, a mixture of myrtle leaves in sunflower oil may be heated to 200°C in less than 5 minutes. Microwave-assisted



Figure 16. Labotron Extraction™ reactor (SAIREM) for the extraction of phytoactive compounds using vegetable oils.

solid/liquid extraction thus enables much greater yields of bioactive compounds to be obtained than with simple static maceration or convection heating. Moreover, due to the reduced process time and reduced oxygen atmosphere, extraction by microwaves enables oxidative degradation of both the solvent (particularly of its polyunsaturated fatty acids and its native antioxidants) and of the bioactive compounds extracted to be avoided. The Oléos® company (Lunel, France) holds exclusive rights to this patented oleo-eco-extraction process which, since 2010, has enabled it to market innovative oily complexes called “Oléoactifs®” that are rich in phytoactive compounds, notably polar biophenols that are both stabilized and vectorized for topical or oral applications. This process meets both the eco-extraction criteria as no solvents or chemical products are used and the sustainable development criteria as no pollutants, either liquid or gaseous, are generated and energy costs are reduced.

Combining Activation and Intensification Techniques

Microwaves and Ultrasounds

The low energy levels generated by microwave heating, around 10^{-6} eV, are not strong enough to create molecular activation. One solution to activate chemical reactions is to combine this technique with other forms of energy such as ultrasounds, thus enabling energy levels close to those of the chemical bonds to be achieved, i.e., several eV.

Sonochemistry uses the cavitation phenomenon (see Chapter 6) that occurs when a sound wave propagates in a liquid. High temperatures and pressures approaching 5000 K and 2000 atmospheres or intense electrical fields of 10^{11} V/m induce a particular reactivity that favors free radical processes. In heterogeneous media, ultrasounds may play another role as material, heat and movement transfer agents. Combining these two techniques may thus be expected give some interesting results.

From a technological point of view, two types of system have been developed—those with the ultrasonic probe positioned in the microwave cavity and those with the probe outside the microwave cavity. These are referred to as simultaneous or alternating irradiation type systems. An entire chapter in a recent work is devoted to the combination of microwaves with ultrasounds (Cintas et al. 2011).

A first prototype combining microwaves and ultrasounds in an original manner was developed by Maeda and Amemiya 1995 and by Chemat et al. 1996a. The unique design includes a cup-horn type ultrasonic system. Transmission is from the base of the cylinder used to contain the reagents. The metal ultrasonic probe is not placed in direct contact with the reactor and is at a sufficient distance from the electromagnetic field to avoid short circuits (Fig. 17). To allow propagation of the ultrasonic waves from the probe to the reactor, the annular space is filled with a liquid that is inert to microwaves. Decaline was chosen for this because of its low viscosity when hot, resulting in good propagation of ultrasounds, and its inertia to microwaves so as not to disturb the electromagnetic field.

The results showed this combination to be more effective in the case of heterogeneous reactions (Toukoniitty et al. 2005). The microwaves provide selective

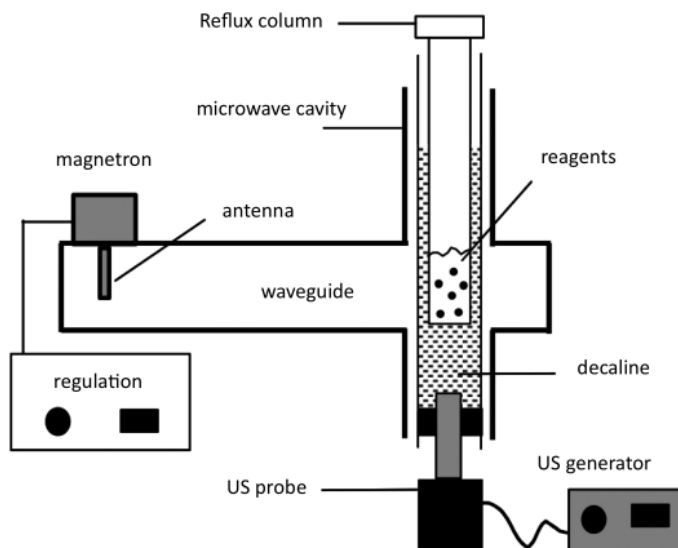


Figure 17. Reactor combining microwaves and ultrasounds (from Chemat et al. 1996a).

heating at the surface of the solid catalyst, thus increasing the intrinsic temperature of the reaction. The ultrasounds increase material transfer at the surface and in the pores of the solid catalyst, thus ensuring cleaning of the reaction surface and efficient degassing for removal of the by-products.

This technique has successfully been used for the esterification of stearic acid with butanol using montmorillonite clay as the catalyst (Chemat et al. 1997) and for the pyrolysis of urea to form cyanuric acid pyrolyse, which are of great industrial importance, with a gain in productivity of up to 20%.

Useful applications have been demonstrated in other chemical fields such as the digestion of food oils to determine the natural copper content and its influence on the rancidity mechanism (Lagha et al. 1999; Chemat et al. 2004b).

Recently, a new type of reactor has been proposed in which the microwaves and ultrasounds are directly transmitted to the medium by a transmitter and probe respectively, thus facilitating implementation (Ragaini et al. 2012). However, the distribution of the electromagnetic field and ultrasonic waves is far from homogeneous with this type of reactor geometry.

Another method is to place the ultrasound probe directly in the microwave cavity, provided that it is rendered insensitive to radiation, i.e., insulated with a tube made of quartz, Pyrex, PTFE or PEEK (Cravotto and Cintas 2007; Hernoux-Villière et al. 2013). Commercial microwave systems may then be used, but scale-up remains a difficult problem.

An alternative method is to sequentially irradiate a reaction medium circulating in a closed loop in two separate cavities, one subject to microwaves and the other to ultrasounds (Cravotto and Cintas 2007). It is thus possible to have different operating temperatures in the two cavities; extremely good results have been obtained in terms

of yields and reaction times, due to the sonochemical activation of the metal catalysts and the microwave heating (Cravotto et al. 2005; Wu et al. 2008). This is not a true combined microwave/ultrasound system, but rather a successive use of the two techniques.

Microwaves and Ionic Liquids

Ionic liquids are liquids that by nature—they are composed only of ions (see Chapter 9)—are highly sensitive to microwaves (heating is by the ionic conduction mechanism). They can be combined with microwaves to achieve three goals:

1. *For their own synthesis:* The synthesis of ionic liquids requires a purification stage that consumes large quantities of solvent. The use of microwaves considerably reduces the amount of solvent used (or even eliminates the need for solvent), increases yield, reduces reaction time and, lastly, enables higher purity to be achieved (Deetlefs and Seddon 2003; Horikoshi et al. 2008).
2. *For use in reactions as a solvent* (Vallin et al. 2002), reagent (Leadbeater et al. 2003) or catalyst (Estager et al. 2006; Arfan et al. 2007; Kantevari et al. 2008). Some very useful effects of combining microwaves with ionic liquids for the treatment of cellulose may be noted, such as, for example, acylation (Gericke et al. 2012). The extreme sensitivity of ionic liquids to microwaves results in a rapid temperature rise of the medium and allows high temperatures to be reached (around 200°C).
3. *For use as ‘convectors’ in media that are not very sensitive to microwaves:* An extremely low concentration of ionic liquid (several per cent) is sufficient to modify the dielectric properties of unreceptive solvents or media, accelerate the temperature rise (temperature ramps greater than 10°C/s can be achieved) and allow high temperatures to be reached (Leadbeater and Torenius 2002; Ley et al. 2001; Marcos et al. 2013).

Microwaves and Microreactors

Microreactors are a recent and important technological advance with advantages for chemical reactions that include enhanced transfer and thus gains in conversion rate and selectivity combined with improved safety conditions, especially when the reactions are highly exothermic.

Combining this method of process intensification with the specific features of microwave heating seems attractive and has many expected advantages (Stankiewicz 2007). Nonetheless, the small diameter of such systems is not favorable to microwave absorption—indeed, it is much less than the depth of wave penetration (that is, it should be remembered, of the order of a few centimeters) and continuous operation implies extremely short residence times in the irradiation area. Over the past few years, there has been an increasing number of articles published reporting reactions performed in such microsystems with microwave radiation.

He et al. 2004 were among the first to propose a miniaturized system. In their system, the lower part of the external surface of a U-shaped capillary tube of diameter 800 μm is covered with a film of gold—this is the location at which the catalyst is placed. The tube is then placed in a single mode CEM oven and the reaction mixture is heated by conduction and not by direct microwave irradiation.

Using simple laboratory capillary tubes (of 200 to 1150 μm in diameter) placed in a Biotage microwave oven and equipped with a reagent pre-mixing module, Comer and Organ (2005a, 2005b) demonstrated the feasibility of performing chemical reactions in parallel, at reduced cost and in short times—a useful procedure for supplying chemical libraries (Fig. 18). The work of Shore et al. (2009) describing a series of chemical reactions performed in microreactors with their internal walls covered with a film of gold deposited on a layer of silver may also be cited.

After these first-generation systems, more sophisticated systems were put forward. A new type of pressurized system with its temperature controlled by automatic monitoring of the resonance frequency in the single mode cavity has been used to synthesize copper nanoparticles. It is equipped with a 1.5-mm diameter quartz tube and can operate up to 10 MPa (Nishioka et al. 2013).

Sauks et al. (2013) present an innovative PCD (Pressure Control Device) which enables high temperatures and pressures of up to 73 bar to be achieved and maintained in a continuous microreactor. It is not easy to maintain high pressures and ensure reproducibility in such systems. Two types of reaction occur in this system—Claisen rearrangement and benzimidazole synthesis—demonstrating its effectiveness.

When highly-absorbent materials are used as certain catalysts, there may be an extremely high temperature rise that is sometimes difficult to control and that may present a certain danger. Microreactors offer the advantage that the surface/volume ratio is extremely high and are thus extremely efficient from a thermal transfer point

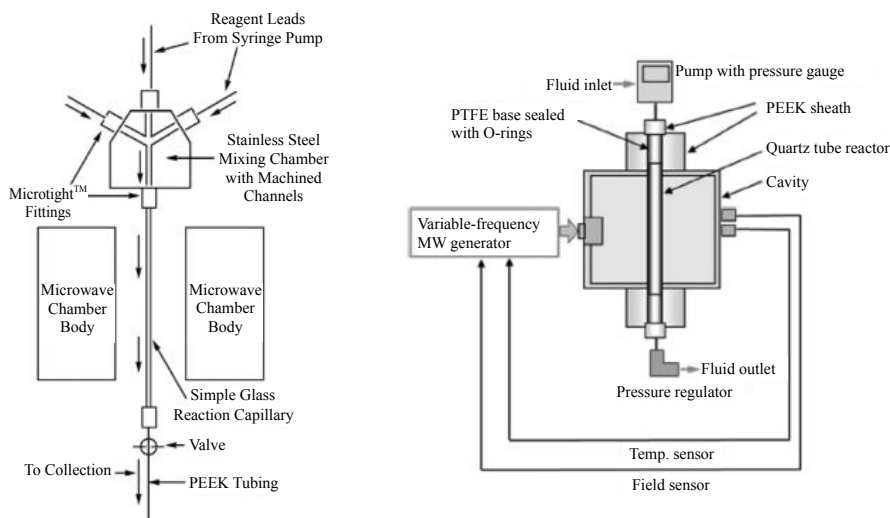


Figure 18. Microreactors operating with microwaves (Comer and Organ 2005a, 2005b; Nishioka et al. 2013).

of view. The COMSOL software has been used to perform temperature field and thermal transfer simulations for a microwave system composed of a microreactor (3-mm tube) equipped with a cooling system in which a liquid transparent to microwaves circulates. It has been used to study esterification with a heterogeneous catalyst. The authors (Patil et al. 2012) state that a production rate of 1 kg/day is possible.

Challenges remain in this innovative field; the combination of microwaves with microreactors offers a promising avenue for work on intensification in which researchers still have much to invest, notably on such aspects as electromagnetic field distribution in these geometries with greatly-reduced dimensions, type of material, etc.—and why not by combining them with another intensification technology such as ionic liquids? (Hessel et al. 2008).

Microwaves and Photochemistry

The combination of photochemistry and microwaves to perform chemical synthesis is not without interest as these two techniques induce different and complementary interactions on matter. Although the energy delivered by microwave radiation is insufficient to break bonds, ultra-violet or infra-red radiation can switch molecules to a metastable, energy-rich, excited state. Simultaneous UV-IR and microwave radiation can affect the course of a reaction by different mechanisms at each transformation step. Assuming that the reaction starts with the creation of a molecule in an excited state, microwaves may or may not have an effect on this latter, and the effect will depend on its lifespan and nature. The mechanism is different if radicals are formed. Klán and Cirkva 2002 discuss these different possibilities in detail.

Although UV electrodeless discharge lamps activated by microwaves have existed since the 80's, it was only around the year 2000 that these two methods of activation were combined to perform chemical synthesis by Klán et al. 2001, who designed the first system of this type. The mercury vapor lamp is directly placed in the reaction medium to allow simultaneous irradiation of the medium by ultra-violet and microwave radiation (Fig. 19).

Another type of system combining microwave and UV radiation in which the lamp is positioned outside the microwave cavity was developed by Chemat et al. 1999.

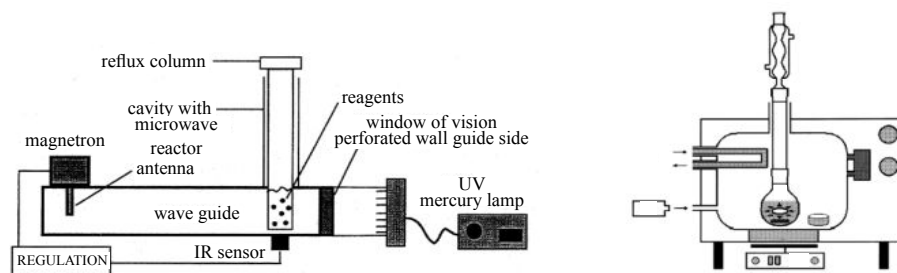


Figure 19. Systems combining microwaves and photochemistry (from Chemat et al. 1999; Klán et al. 2001).

This system (Fig. 18) has been tested on the thermal rearrangement reaction of *o*-aroyloxyacetophenone to 1-(*o*-hydroxyphenyl)-3-phenyl propane-1,3-dione and the degradation of humic substances to carbon dioxide and water to aqueous solution. These reactions are of great importance both for the pharmaceutical industry and the treatment of drinking water. Although the rearrangement reaction takes place as well with microwaves as with ultra-violet radiation, there is an effect of synergy between the two types of radiation that results in a yield of 95% instead of the 70% and 20% respectively obtained with microwaves alone and UV alone, for a reaction time of 90 minutes.

Other types of technology offering different UV transmission sources, which may or may not be located in the microwave cavity, are reported by Horikoshi and Serpone 2009. Examples of reactions in a continuously-operating system are given in Cirkva and Relich 2011.

Other applications—which are somewhat more marginal—should be highlighted, such as photodegradation and thermolysis for the treatment of pollutants and toxic agents in waste water, and sterilization for the continuous destruction of pathogenic agents in biological fluids without altering their biological properties (Chen et al. 2011; Parolin et al. 2013).

Conclusion

In almost 30 years of research, the application of microwaves in processes and, more specifically, to chemical synthesis or extraction, has undergone real but relatively slow progress. The marketing of well-instrumented commercial laboratory systems meeting the requirements of research workers has facilitated their development and allowed their effectiveness in various fields of investigation to be proven, thus demonstrating their feasibility.

Nonetheless, such microwave-assisted processes face the difficult problem of scale-up that is one of the limitations on their industrial use—which is still relatively restricted—especially in the chemical industry in the widest sense. However, it should be noted that, in recent years, a real effort has been made on this point. Obviously, fields in which small quantities are processed are privileged and the manufacturers offer a catalog of potentially suitable systems. However, continuous systems remain the solution in many cases.

Replacing a conventional reactor in a process with a microwave system has important implications, the scope of which must be measured. The entire process may be affected (the separation operations modified, etc.). Other factors to be considered are the energy costs—savings may sometimes need to be proven, and investment costs must also not be forgotten.

Given the complexity of microwave heating, the success of such an operation cannot be guaranteed without the close collaboration of the stakeholders involved: microwave physicists, process engineers and chemists and manufacturers. Simulation must then play an important part in defining the items of equipment and their operating modes so as to achieve a true process/product match in order to ensure the success of the operation.

In any case, progress will only be made by adopting a considered approach which consists in taking advantage of the specific features of microwave heating—which will inevitably lead to protocols that are different to those used today. It is no longer a question of repeating existing transformations, but of performing them in a different way and by proposing processes that are more environmentally friendly and more sustainable.

Acknowledgements

The author wish to thank her colleague Prof. Lionel Estel (LSPC, INSA Rouen, France) for his kind help, as well as the fruitful exchanges and scientific discussion on the content of this chapter.

References

- Abert-Vian, M., X. Fernandez, F. Visinoni and F. Chemat. 2008. Microwave hydrodiffusion and gravity, a new technique for extraction of essential oils. *J. Chromatogra. A.* 1190: 14–17.
- Anizon, J.Y., B. Lemaire and M. Surbled. 2003. Extraction assistée par micro-ondes. *Techniques de l'Ingénieur*, F 3 060: 1–10.
- Arfan, A., L. Paquin and J.P. Bazureau. 2007. Acidic task-specific ionic liquid as catalyst of microwave-assisted solvent-free Biginelli reaction. *Russ. J. Organ. Chem.* 43: 1058–1064.
- Bagley, M.C., V. Fusillo, R.L. Jenkins, M.C. Lubinu and C. Mason. 2013. One-step synthesis of pyridines and dihydropyridines in a continuous flow microwave reactor. *Beilstein J. Org. Chem.* 9: 1957–1968.
- Baig, R.B.N. and R.S. Varma. 2012. Alternative energy input: mechanochemical, microwave and ultrasound-assisted organic synthesis. *Chem. Soc. Rev.* 41: 1559–1584.
- Bonnet, C., L. Estel, A. Ledoux, B. Mazari and A. Louis. 2004. Study of the thermal repartition in a microwave reactor: application to the nitrobenzene hydrogenation. *Chem. Eng. Process.* 43: 1435–1440.
- Bousquet, F. 1997. Nouveaux extraits de plantes, leur procédé de fabrication et leur utilisation dans les produits cosmétiques. Patent FR 2 740 991—Phybiotex SA—WO 1997018283 A1-22 mai 1997.
- Bowman, M.D., J.L. Holcomb, C.M. Kormos, N.E. Leadbeater and V.A. Williams. 2008a. Approaches for scale-up of microwave-promoted reactions. *Org. Process Res. Dev.* 12: 41–57.
- Bowman, M.D., J.R. Schmink, C.M. McGowan, C.M. Kormos and N.E. Leadbeater. 2008b. Scale-up of microwave-promoted reactions to the mutigram level using a sealed-vessel microwave apparatus. *Org. Process Res. Dev.* 12: 1078–1088.
- Cablewski, T., A.F. Faux and C.R. Strauss. 1994. Development and application of a continuous microwave reactor for organic synthesis. *J. Org. Chem.* 59: 3408–3412.
- Caddick, S. 1995. Microwave assisted organic reactions. *Tetrahedron* 51: 10403–10432.
- Chandrasekaran, S., S. Ramanathan and T. Basak. 2013. Microwave food processing—a review. *Food Res. Int.* 52: 243–261.
- Chemat, F. 2009. *Essential Oils: Green Extraction and Applications*. HKB, New Delhi.
- Chemat, F. and M.E. Lucchesi. 2006. Microwave assisted extraction of essential oils. pp. 959–985. *In: A. Loupy (ed.)*. *Microwaves in Organic Synthesis*, Second Edition. Wiley, Weinheim.
- Chemat, F. and G. Cravotto. 2013. *Microwave-assisted Extraction for Bioactive Compounds: Theory and Practice—Vol. 4*. Springer Science U.S.A, New-York.
- Chemat, F., M. Poux, J.L. Dimartino and J. Berlan. 1996a. An original microwave-ultrasound combined reactor suitable for organic synthesis: application to pyrolysis and esterification. *J. Microwave Power E.E.* 3: 19–22.
- Chemat, F., M. Poux, J.L. Dimartino and J. Berlan. 1996b. A new continuous flow recycle microwave reactor for homogeneous and heterogeneous chemical reactions. *Chem. Eng. Technol.* 19: 420–424.
- Chemat, F., M. Poux and S.M. Galema. 1997. Esterification of stearic acid by isomeric forms of butanol in a microwave. *J. Chem. Soc., Perkin Trans. 2*: 2371–2374.

- Chemat, F., M.E. Lucchesi and J. Smadja. 2004a. Extraction sans solvant assistée par micro-ondes de produits naturels. EP Patent 1 439 218 A1.
- Chemat, F., M. Abert-Vian and Y.J. Zill-e-Huma. 2009. Microwave-assisted separations: green chemistry in action. pp. 33–62. *In*: J.T. Pearlman (ed.). Green Chemistry Research Trends. Nova Science Publishers, New York.
- Chemat, S., A. Aouabed, P.V. Bartels, D.C. Esveld and F. Chemat. 1999. An original microwave—ultraviolet combined reactor suitable for organic synthesis and degradation. *J. Microwave Power E.E.* 34: 55–60.
- Chemat, S., A. Lagha, H. Ait Amar and F. Chemat. 2004b. Ultrasound assisted microwave digestion. *Ultrason. Sonochem.* 11: 5–8.
- Chen, H., E. Bramanti, I. Longo, M. Onor and C. Ferrari. 2011. Oxidative decomposition of atrazine in water in the presence of hydrogen peroxide using an innovative microwave photochemical reactor. *J. Hazard. Mater.* 186: 1808–1815.
- Cintas, P., G. Cravotto and A. Canals. 2011. Combined ultrasound-microwave technologies. pp. 659–673. *In*: D. Chen, S.K. Sharma and A. Mudhoo (ed.). Handbook on Applications of Ultrasound, CRC Press, Boca Raton.
- Cirkva, V. and S. Relich. 2011. Microwave photochemistry. Applications in organic synthesis. *Mini-Reviews in Organic Chemistry* 8: 282–293.
- Comer, E. and M.G. Organ. 2005a. A microreactor for microwave-assisted capillary (continuous flow) organic synthesis. *J. Am. Chem. Soc.* 127: 8160–8167.
- Comer, E. and M.G. Organ. 2005b. A microcapillary system for simultaneous, parallel microwave-assisted synthesis. *Chem. Eur. J.* 11: 7223–7227.
- Craveiro, A.A., J.A. Matos, W. Alencar and M.M. Plumel. 1989. Microwave oven extraction of an essential oil. *Flav. Fragr. J.* 4: 43–44.
- Cravotto, G. and P. Cintas. 2007. Combined use of microwaves and ultrasound: improved tools in process chemistry and organic synthesis. *Chem. Eur. J.* 13: 1902–1909.
- Cravotto, G., M. Beggiato, G. Palmisano, A. Penoni, J.M. Lévêque and W. Bonrath. 2005. High-intensity ultrasound and microwave, alone or combined, promote Pd/C-catalyzed aryl-aryl coupling. *Tetrahedron Lett.* 46: 2267–2271.
- de la Hoz, A. and A. Loupy (eds.). 2013. *Microwaves in Organic Synthesis, 2 Volume Set—Vol. 1.* Wiley–VCH, Weinheim.
- Deetlefs, M. and K.R. Seddon. 2003. Improved preparations of ionic liquids using microwave. *Green Chem.* 5: 181–186.
- Destandau, E., T. Michel and C. Elfakir. 2013. Microwave-assisted extraction. pp. 113–156. *In*: Mauricio A. Rostagno and Juliana M. Prado (eds.). *Natural Product Extraction: Principles and Applications.* Royal Society of Chemistry, Cambridge, UK.
- Dressen, M. 2009. Microwave heating in fine chemical applications: role of the heterogeneity. PhD Thesis. Eindhoven University of Technology, Netherlands.
- Escribano-Bailon, M.T. and C. Santos-Buelga. 2003. Polyphenol extraction from foods. pp. 1–16. *In*: C. Santos-Buelga and G. Williamson (eds.). *Methods in Polyphenol Analysis.* Royal Society of Chemistry, Cambridge, UK.
- Estager, J., J.M. Lévêque, R. Turgis and M. Draye. 2006. Solventless and swift benzoin condensation catalyzed by 1-alkyl-3-methylimidazolium ionic liquids under microwave irradiation. *J. Mol. Catal. A: Chem.* 256: 261–264.
- Estel, L., C. Bonnet, M. Delmotte and J.M. Cosmao. 2003. Kinetic analysis via microwave dielectric measurements. *Chem. Eng. Res. Des.* 81: 1212–1216.
- Estel, L., A. Ledoux, P. Lebaudy, C. Bonnet and M. Delmotte. 2008. Microwaves thermal conditioning of preforms. *Chem. Eng. Process.* 47: 390–395.
- Esveld, E., F. Chemat and J. Van Haverin. 2000a. Pilot scale continuous microwave dry media reactor—Part 1: design and modeling. *Chem. Eng. Technol.* 23: 279–283.
- Esveld, E., F. Chemat and J. Van Haverin. 2000b. Pilot scale continuous microwave dry media reactor—Part 2: application to waxy esters production. *Chem. Eng. Technol.* 23: 429–435.
- Feher, L.E. and M.K. Thumm. 2004. Microwave innovation for industrial composite fabrication—the HEPHAISTOS technology. *IEEE Transactions On Plasma Science* 32: 73–79.

- Gabriel, C., S. Gabriel, E.H. Grant, B.S. Halstead and D.M.P. Mingos. 1998. Dielectric parameters relevant to microwave dielectric heating. *Chem. Soc. Rev.* 27: 213–223.
- Ganzler, K., A. Salgo and K. Valko. 1986. Microwave extraction: a novel sample preparation method for chromatography. *J. Chromatogr.* 371: 299–306.
- Gedye, R., F. Smith, K. Westaway, H. Ali, L. Baldisera, L. Laberge and J. Rousell. 1986. The use of microwave ovens for rapid organic synthesis. *Tetrahedron Lett.* 27: 279–282.
- Gericke, M., P. Fardim and T. Heinze. 2012. Ionic liquids—promising but challenging solvents for homogeneous derivatization of cellulose. *Molecules* 17: 7458–7502.
- Giguere, J.R., T.L. Bray, S.M. Duncan and G. Majetich. 1986. Application of commercial microwave ovens to organic synthesis. *Tetrahedron Lett.* 27: 4945–4948.
- He, P., S.J. Haswell and P.D.I. Fletcher. 2004. Microwave heating of heterogeneously catalysed Suzuki reactions in a microreactor. *Lab Chip.* 4: 38–41.
- Heravi, M. and S. Moghimi. 2013. Solid-supported reagents in organic synthesis using microwave irradiation. *Curr. Org. Chem.* 17: 504–527.
- Hernoux-Villière, A., U. Lassi, T. Hu, A. Paquet, G. Cravotto, L. Rinaldi, S. Molina-Boisseau, M.F. Marais and J.M. Leveque. 2013. Simultaneous microwave/ultrasound-assisted hydrolysis of starch-based industrial waste into reducing sugars. *Sustainable Chem. Eng.* 1: 995–1002.
- Herrero, M.A., J.M. Kremsner and C.O. Kappe. 2008. Nonthermal microwave effects revisited: on the importance of internal temperature monitoring and agitation in microwave chemistry. *J. Org. Chem.* 73: 36–47.
- Hessel, V., D. Kralisch and U. Krtischil. 2008. Sustainability through green processing—novel process windows intensify micro and milli process technologies. *Energy Environ. Sci.* 1: 467–478.
- Horikoshi, S. and N. Serpone. 2009. Photochemistry with microwaves: catalysts and environmental applications. *J. Photochem. Photobiol.* 10: 96–110.
- Horikoshi, S., T. Hamamura, M. Kajitani, M. Yoshizawa-Fujita and N. Serpone. 2008. Green chemistry with a novel 5.8-GHz microwave apparatus. Prompt one-pot solvent-free synthesis of a major ionic liquid: The 1-Butyl-3-methylimidazolium tetrafluoroborate system. *Org. Process Res. Dev.* 12: 1089–1093.
- Jain, T., V. Jain, R. Pandey, A. Vyas and S.S. Shukla. 2009. Microwave assisted extraction for phytoconstituents—an overview. *Asian J. Research Chem.* 2: 19–25.
- Kantevari, S., M.V. Chary, A.P.R. Das, S.V.N. Vuppapapati and N. Lingaiah. 2008. Catalysis by anionic liquid: highly efficient solvent-free synthesis of aryl-14H-dibenzo[a,j]xanthenes by molten tetrabutylammonium bromide under conventional and microwave heating. *Catal. Commun.* 9: 1575–1578.
- Kappe, C.O. 2013. How to measure reaction temperature in microwave-heated transformations. *Chem. Soc. Rev.* 42: 4977–4990.
- Kappe, C.O., D. Dallinger and S.S. Murphree. 2009. *Practical Microwave Synthesis for Organic Chemists: Strategies, Instruments and Protocols.* Wiley–VCH, Weinheim.
- Kappe, C.O., B. Pieber and D. Dallinger. 2013. Microwave effects in organic synthesis: myth or reality? *Angewandte Chemie International Edition.* 52: 1088–1094.
- Klán, P. and V. Cirkva. 2002. Microwave photochemistry. pp. 463–486. *In: A. Loupy (ed.). Microwaves in Organic Synthesis.* Wiley–VCH, Weinheim.
- Klán, P., M. Hájek and V. Cirkva. 2001. The electrodeless discharge lamp: a prospective tool for photochemistry—Part 3. The microwave photochemistry reactor. *J. Photochem. Photobiol. A.* 140: 185–189.
- Kumar Gupta, A., N. Singh and K. Nand Singh. 2013. *Microwave Assisted Organic Synthesis: Cross Coupling and Multicomponent Reactions.* *Curr. Org. Chem.* 17: 474–490.
- Lagha, A., S. Chemat, P. Bartels and F. Chemat. 1999. Microwave-ultrasound combined reactor suitable for atmospheric sample preparation procedure of biological and chemical products. *Analisis.* 27: 452–457.
- Lane, D. and S.W.D. Jenkins. 1986. Polynucl. Aromat. hydrocarbons: Chem., Charact. Carcinog., Int. Symp., 9th. 437–449.
- Laporterie, A., J. Marquié and J. Dubac. 2002. Microwave-assisted reactions on graphite. pp. 219–248. *In: Loupy (ed.). Microwave in Organic Synthesis.* Wiley–VCH, Wienheim.

- Leadbeater, N.E. and H.M. Torenus. 2002. A study of the ionic liquid mediated microwave heating of organic solvents. *J. Org. Chem.* 67: 3145–3148.
- Leadbeater, N.E., H.M. Torenus and H. Tye. 2003. Ionic liquids as reagents and solvents in conjunction with microwave heating: rapid synthesis of alkyl halides from alcohols and nitriles from aryl halides. *Tetrahedron* 59: 2253–2258.
- Lehmann, H. and L. LaVecchia. 2005. Evaluation of microwave reactors for pre-scale synthesis in a Kilolab. *J. Lab. Autom.* 10: 412–417.
- Letellier, M. and H. Budzinski. 1999. Microwave assisted extraction of organic compounds. *Analisis.* 27: 259–271.
- Ley, S.V., A.G. Leach and R.I. Storer. 2001. A polymer-supported thionating reagent. *J. Chem. Soc., Perkin Trans. 1*: 358–361.
- Lidström, P., J. Tierney, B. Wathey and J. Westman. 2001. Microwave assisted organic synthesis—a review. *Tetrahedron* 57: 9225–9283.
- Loupy, A. 1999. Solvent-free reactions. *Curr. Chem.* 206: 153–207.
- Loupy, A. 2004. Solvent-free microwave organic synthesis as an efficient procedure for green chemistry. *C.R. Chimie.* 7: 103–112.
- Loupy, A. 2006. *Microwave in Organic Synthesis.* Wiley–VCH, Weinheim.
- Lucchesi, M.E., F. Chemat and J. Smadja. 2004. Solvent-free microwave extraction of essential oil from aromatic herbs: comparison with conventional hydro-distillation. *J. Chromatogr. A.* 1043: 323–327.
- Maeda, M. and H. Amemiya. 1995. Chemical effects under simultaneous irradiation by microwaves and ultrasound. *New J. Chem.* 19: 1023–1028.
- Marcos, A., P. Martins, J. Trindade Filho, G.S. Caleffi, L. Buriol and C. Frizzo. 2013. Ionic liquids as doping agents in microwave assisted reactions. pp. 433–455. *In: Jun-ichi Kadokawa (ed.). Ionic Liquids—New Aspects for the Future, InTech, DOI: 10.5772/51659.*
- Marquié, J., G. Salmoria, M. Poux, A. Laporterie, J. Dubac and N. Roques. 2001. Acylation and related reactions under Microwaves. 5. Development to large laboratory scale with a continuous-flow process. *Ind. Eng. Chem. Res.* 40: 4485–4490.
- Mazubert, A., C. Taylor, J. Aubin and M. Poux. 2014. Key role of temperature in interpretation of MW heating on transesterification and esterification reactions for biodiesel production. *Bioresources Technology.* 161: 270–279.
- Mengal, P. and B. Mompon. 1994. Method and plant for solvent-free microwave extraction of natural products, *WP Pat.* 94/26853.
- Morschhäuser, R., M. Krull, C. Kayser, C. Boberski, R. Bierbaum, P.A. Püschner, T.N. Glasnov and C.O. Kappe. 2012. Microwave-assisted continuous flow synthesis on industrial scale. *Green Process Synth.* 1: 281–290.
- Moseley, J.D., P. Lenden, M. Lockwood, K. Ruda, J.P. Sherlock, A.D. Thomson and J.P. Gilday. 2008. A comparison of commercial microwave reactors for scale-up within process chemistry. *Org. Process Res. Dev.* 12: 30–40.
- Nishioka, M., M. Miyakawa, Y. Daino, H. Kataoka, H. Koda, K. Sato and T.M. Suzuki. 2013. Single-mode microwave reactor used for continuous flow reactions under elevated pressure. *Ind. Eng. Chem. Res.* 52: 4683–4687.
- Obermayer, D., M. Damma and C.O. Kappe. 2013. Design and evaluation of improved magnetic stir bars for single-mode microwave reactors. *Org. Biomol. Chem.* 11: 4949–4956.
- Osepchuk, J.M. 2002. Microwave power applications. *IEEE Trans. Microwave Theory and Techn.* 50: 975–985.
- Paré, J.R.J. and J.M.R. Bélanger. 1990. Extraction de produits naturels assistée par micro-ondes, *Brevet européen, EP 398798.*
- Paré, J.R.J. and J.M.R. Bélanger. 1997. Microwaves-assisted process (MAPTM): principles and applications. pp. 57–79. *In: J.R.J. Paré and J.M.R. Bélanger (eds.). Instrumental Methods in Food Analysis.* Elsevier Sciences BV, Amsterdam.
- Parolin, F., U.M. Nascimento and E.B. Azevedo. 2013. Microwave-enhanced UV/H₂O₂ degradation of an azo dye (tartrazine): optimization, colour removal, mineralization and ecotoxicity. *Environ. Technol.* 34: 1247–1253.

- Patil, N.G., A.I.G. Hermans, F. Benaskar, J. Meuldijk, L.A. Hulshof, V. Hessel, J.C. Schouten and E.V. Rebrov. 2012. Energy efficient and controlled flow processing under microwave heating by using a millireactor–heat exchanger. *AIChE J.* 58: 3144–3155.
- Ragaini, V., C. Pirola, S. Borrelli, C. Ferrari and I. Longo. 2012. Simultaneous ultrasound and microwave new reactor: detailed description and energetic considerations. *Ultrason. Sonochem.* 19: 872–876.
- Rossignol-Castera, A. 2009. Procédé d'extraction de composés non volatils. Patent no.: 2 943 684.
- Roussy, G., J.F. Rochas and C. Oberlin. 2003. Chauffage diélectrique : principes et spécificités D 5 940 in *Techniques de l'Ingénieur*.
- Sauks, J.M., D. Mallik, Y. Lawryshyn, T.P. Bender and M.G. Organ. 2013. A continuous flow microwave reactor for conducting high temperature and high pressure chemical reactions. *Org. Process Res. Dev.* DOI: 10.1021/op400026g.
- Shore, G., M. Tsimmerman and M.G. Organ. 2009. Gold film-catalysed benzannulation by Microwave-Assisted, Continuous Flow Organic Synthesis (MACOS). *Beilstein J. Org. Chem.* 5: no. 35.
- Stankiewicz, A. 2007. On the applications of alternative energy forms and transfer mechanisms in microprocessing systems. *Ind. Eng. Chem. Res.* 46: 4232–4235.
- Strauss, C.R. 2009. A strategic 'green' approach to organic chemistry with microwave assistance and predictive yield optimization as core, enabling technologies. *Aust. J. Chem.* 62: 3–15.
- Toukoniitty, B., J.-P. Mikkola, D. Yu. Murzin and T. Salmi. 2005. Utilization of electromagnetic and acoustic irradiation in enhancing heterogeneous catalytic reactions. *Appl. Catal. A* 279: 1–22.
- Vallin, K.S., P. Emilsson, M. Larhed and A. Hallberg. 2002. High-speed heck reactions in ionic liquid with controlled microwave heating. *The Journal of organic chemistry* 67: 6243–6246.
- Varma, R.S. 1999. Solvent-free organic syntheses. using supported reagents and microwave irradiation. *Green Chem.* 43–55.
- Wu, Z.-L., B. Ondruschka and G. Cravotto. 2008. Degradation of phenol under combined irradiation with microwaves and ultrasound. *Environ. Sci. Technol.* 42: 8083–8087.

8

Intensification by Means of Formulation

Patrick Cognet, Isabelle Rico-Lattes and Armand Lattes

Introduction

Formulation is often regarded as “knowledge and practical operations necessary for mixing, associating or formatting ingredients of natural or synthetic origin, often mutually incompatible, in order to obtain a commercial product characterized by its function use” (Aubry and Schorsch 1999). Some mixtures are formed spontaneously at the molecular level (mixture of two miscible liquids, for example). Others do not spontaneously and require an input of energy, usually in mechanical form (agitation), which is the case, for example, for unstable emulsions. Generally, small parts of one phase are observed, dispersed in another phase (continuous one). The associated phases can be solids, liquids or gases (Table 1).

The advantage of formulation is to confer original properties to the resulting mixture, different from the properties of each phase, separately considered. These properties are derived from the induced coexistence of both phases, and properties are directly related to the interfaces.

This chapter specifically focuses on applications of formulation in chemical synthesis processes. It specifically addresses the case of two liquid phases in presence (emulsion, microemulsion) and the case of a solid phase dispersed in a liquid phase (dispersion).

Table 1. Different types of heterogeneous mixtures (from Cabane 2003).

Continuous phase	Dispersed phase		
	Solid	Liquid	Gas
Solid	Composites	porous	porous
Liquid	Dispersions	Emulsions	foams
Gas	smokes	aerosols	–

After a short description of the physicochemical concepts useful to approach formulation operation, we focus on formulation as a tool for process intensification and give some examples of applications in chemical synthesis.

Physicochemical Concepts of Formulation

When two phases are in contact, the separation surface between both is an area of particular properties, called interface. This is a place of energy and mass transfers and so, an ideal environment for chemical reactions intensification. Let's consider the case of liquid/solid and liquid/liquid interfaces. In the second case, two types of conditions may lead to the creation of liquid/liquid interfaces: emulsions and micellar systems or microemulsions.

Emulsions

Emulsions are heterogeneous systems composed of two or more liquid phases, constituted by a continuous phase in which at least a second liquid is dispersed, in the form of fine liquid droplets. When one phase is water, emulsions can be distinguished:

- Oil in water
- Water in Oil
- Others: multiple emulsions water/oil/water (for example)

Emulsions are thermodynamically unstable preparations. Two immiscible liquids, subjected to mechanical agitation, evaluate towards the dispersion of one liquid in another; when agitation is stopped, both liquids separate again in two phases.

Micellar Solutions and Microemulsions

To stabilize an emulsion, it is necessary to add an active product that will help maintain the dispersed liquid droplets; most of the time, this product is a surfactant or a polymer. Depending on the conditions of formulation, an emulsion or a micellar solution can be obtained:

- In an emulsion, both liquids are distinguished with the eye or, exceptionally, using a simple optical method.
- In a micellar solution, all seems completely homogeneous. In all cases, it is a suspension of very small objects, micelles, whose size allows the observation only by sophisticated physical methods.

Surfactants and Micellar Solutions

A substance is called surfactant when, even at low concentrations, it acts at an interface (e.g., water-oil or water-air) by lowering the interfacial tension. The activity of these substances is related to their chemical structure. A surfactant is an amphiphilic molecule bearing a long chain, composed of two parts:

- One with hydrophobic behaviour, generally one or more long hydrocarbon chains, sometimes having internal units such as aromatic ring, unsaturated hydrocarbon. ...
- The other of hydrophilic nature: the polar head. This may be anionic (e.g., sulfonate—SO₃⁻), cationic (quaternary ammonium), zwitterionic or non ionic (polyoxyethylene or sugars).

Table 2 presents the main structures of surfactants.

A surfactant dissolved in water tends to adsorb at the liquid-air interface. In the bulk solution and at low concentrations, the surfactant molecules are dispersed in water by simple dissolution. When the concentration increases, and if certain conditions are met, molecular aggregates appear: micelles (Fig. 1). These aggregates are in equilibrium with individual surfactant molecules: they appear when a certain concentration of surfactants is attained. This particular concentration is called the critical micelle concentration (CMC).

Table 2. Different structures of surfactants.

Name of the structure	Representation
single-stranded molecule	
double-stranded molecule	
bola amphiphile	
Gemini	

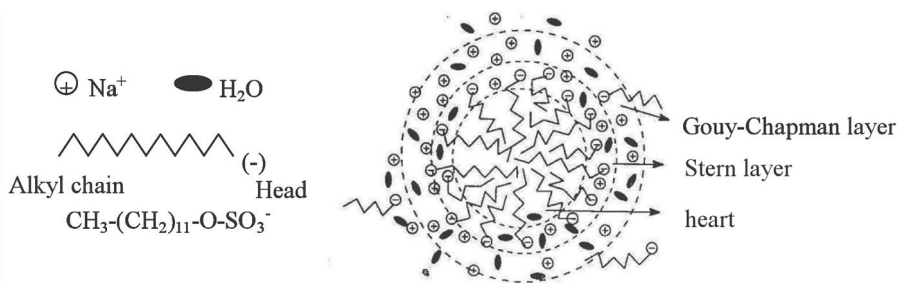


Figure 1. Representation of a direct micelle.

Micellisation Parameters (Lattes and Rico-Lattes 2006)

Critical micelle concentration (CMC). CMC is determined from graphs showing the variation of a physicochemical property of the solution depending on its concentration: a sudden break in the graph reflects a shift by the CMC. Experimental techniques are numerous from physicochemical properties such as conductivity, the measurement of surface tension, viscosity, NMR spectra, etc. ... Care must however be taken with regard to the temperature at which the determinations are carried out.

KRAFFT temperature. Especially for the use of ionic surfactants, there is a minimum temperature, so-called “Krafft point”, which must be achieved to favor micelle formation: only above this temperature can micelles form. This temperature is sometimes interpreted as the melting point of the hydrated surfactant.

Cloud point. It is generally observed for the nonionic surfactants. The evolution of surfactant solutions as a function of temperature shows that, when temperature rises, the solutions become turbid. Micelle formation therefore occurs only above a certain concentration, above the Krafft temperature and below the cloud point.

Table 3. Examples of surfactants and micelle associated parameters.

Surfactants	Abbreviations	CMC (water: 25°C) (mM)
$R_{12}N^+(CH_3)_3, Cl^-$	DAC	20
$R_{16}N^+(CH_3)_3, Cl^-$	HAC	0.9
$R_{12}SO_4^{2-}, 2 Na^+$	SDS	8
$R_{12} R_{12}N^+(CH_3)_2, Cl^-$	DODAC	0.15
$R_{12} (O-CH_2-CH_2)_6OH$	$R_{12}POE_6$	0.09
$R_{12}OCH_2CH(OH)-CH_2\overset{O^-}{\underset{ }{P}}(O)CH_2-CH_2N^+$	$R_{12}PC$	0.70
$R_{16}OCH_2CH(OH)-CH_2\overset{O^-}{\underset{ }{P}}(O)CH_2-CH_2N^+$	$R_{16}PC$	0.007
$R_{16}OCH_2\underset{\underset{O}{ }}{C}H-CH_2\overset{O^-}{\underset{ }{P}}(O)CH_2-CH_2N^+$ $\underset{\underset{O}{ }}{R_{10}}$	$R_{10} R_{10}DPPC$	$5 \cdot 10^{-6}$

Inverse Micelles

Aggregation of molecules into micelles is also observed in apolar solvents. In this case, in contrast to aqueous solutions, so-called “reverse” micelles are obtained. In these micelles, the heart is composed of a small volume of water surrounded by the polar head, while the hydrophobic carbon chains are in contact with the apolar solvent (Fig. 2).

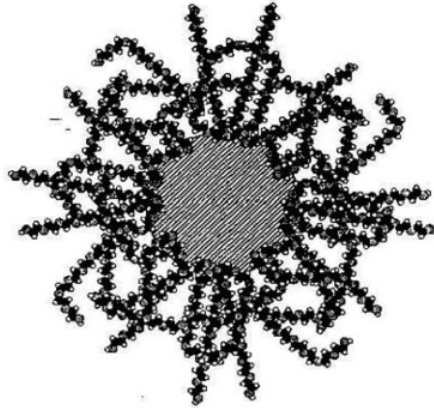


Figure 2. Representation of inverse/reverse micelle.

Liquid Crystals

When the surfactant concentration increases in the aqueous solution, the micelle form is subjected to gradual changes in order to produce more complex structures: cylindrical and combination cylinders to form cubic or hexagonal liquid crystals (Barois 1996), and finally lamellar structures (Fig. 3).

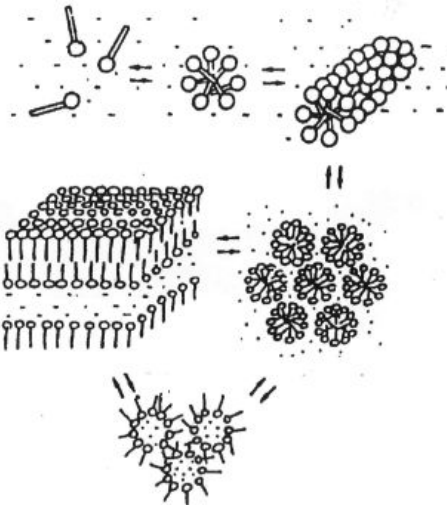


Figure 3. Evolution of aggregate structures depending on the surfactant concentration.

Particular Case of Microemulsions

For both direct and inverse micelles, the major property of micellar solutions is their ability to solubilize products which are originally non soluble in the continuous

phase. This solubilization, as well as other factors later discussed, are of great interest for chemical reactivity. Let's keep in mind however that, in most cases, amounts of solute dissolved in micellar medium remain limited, due to low concentrations of surfactants, thus of micelles and, correspondingly, due to the restricted dimensions of micelles. As such, microemulsions are often more advantageous. Adding hydrocarbon and alcohol to aqueous micellar solutions can lead to different micro-heterogeneous phases. Most of these media, although often showing very different structures, are identified under the term 'microemulsion'. The different types of systems that can be observed are:

1. Microemulsions using four components: surfactant, co-surfactant, water and hydrocarbon. The co-surfactant is a small molecule bearing a polar head but a short chain (e.g., butan-1-ol, $\text{CH}_3\text{CH}_2\text{CH}_2\text{CH}_2\text{OH}$).
2. Is also referred to as microemulsions, three-component systems:
 - Sometimes without co-surfactant (Shinoda 1967)
 - Sometimes without surfactant (Smith et al. 1977)
 - 1) Finally, it is also possible to replace water
 - in systems with four components,
 - by other structured and polar solvents as formamide (Rico and Lattes 1986), ethylene glycol (Friberg and Lapczynska 1975), glycerol (Friberg 1983).

Given the problems of viscosity associated with the use of ethylene glycol or of glycerol, four-component systems (water or formamide, organic compound, surfactant and co-surfactant) are generally used.

Domain of Existence and Phase Diagram of Microemulsions

The region of existence of a microemulsion is determined in the manner of a conventional analytical assay: to a water/hydrocarbon emulsion (for example) is added a calibrated surfactant/co-surfactant mixture solution: the transparency, spontaneously and brutally succeeding the milky emulsion, serves as a criterion to fix the limits of the areas of existence of microemulsions (Cayias et al. 1977). Microemulsions can be made by the method of HLD (Salager et al. 2001).

These areas are represented by a three-dimensional phase diagram (Fig. 4). Indeed, quaternary phase diagrams are not very easy to use and pseudo-ternary diagrams are preferred. For this purpose, the components are grouped so as to form a "pseudo-component" (e.g., surfactant/co-surfactant in a constant ratio).

The main characteristics of microemulsions are:

- in the area rich in oil (B), reverse micelles are formed, dispersed in a continuous medium consisting of organic solvent and co-surfactant;
- in the area rich in water (A) O/W microemulsions, direct micelles are formed, dispersed in water;

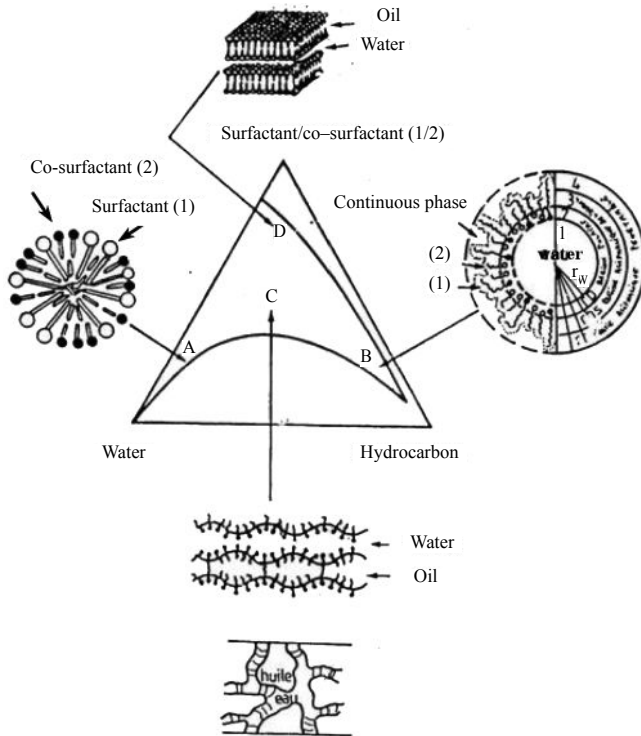


Figure 4. Structure of microemulsions: pseudo-ternary phase diagram.

- the transition of W/O microemulsions to O/W microemulsions reveals a new structure called bi-continuous structure (C): these structures at large spatial extension consist of nested and distinct water and organic compound channels, separated by an interfacial film;
- in the area where there is a lot of surfactant and co-surfactant (D), we observe lyotropic liquid crystals, e.g., lamellar phases. In this area, the viscosity is often very high, making it difficult to use for practical application.

Remarks

Heterogeneous areas of the phase diagram. In areas of demixing, which lie below the lower limit of the microemulsion, there are the differences that have been underlined by the microemulsion region itself. The observed multiphase systems, can form several types of equilibria: microemulsions can exist in equilibrium with an excess of organic solvent, water or both. Winsor (Winsor 1954) described these equilibria using 4 types:

- WINSOR I, in the water-rich region: oil in equilibrium with the microemulsion,
- WINSOR II, in the rich organic solvent zone: water in equilibrium with the microemulsion,

- WINSOR III, below the bicontinuous region: microemulsion in equilibrium with both water and oil.

By extension, the monophasic region is often called WINSOR IV.

Comparison between structural characteristics of micellar solutions and microemulsions. The surfactant concentration is higher in the micellar solution and droplet sizes are larger (100 to 500 Å) for an O/W microemulsion against 40 to 100 Å in an aqueous micellar solution. This results in a higher power for solubilizing the microemulsion. In the case of a microemulsion, it is possible to pass continuously from a system of direct micelles (H/E) to a system of reversed micelles (W/O). It is also possible to “break” a microemulsion by varying one of the parameters of the formulation, or by making a salt effect, or by acting on the temperature. In all cases, it leads to demixing, which facilitates the separation of the phases, therefore the products of a reaction, for example.

Comparison between structural characteristics of emulsions and microemulsions. The physical properties of microemulsions are clearly distinguished from those of emulsions. They are transparent, because of their extreme degree of dispersion: 100–500 Å instead of 2 to 20 microns for emulsions. They have a very low viscosity (excepted in the case of liquid crystals). They are stable over time, in contrast to emulsions. They form spontaneously without mechanical energy.

Interfaces and Reactivity

The existence of two boundary media that may be used in reactivity (emulsions-micellar solutions or microemulsion) highlights the differences between both systems (Lattes and Rico-Lattes 2006). In an emulsion, reagents may be distributed between the two phases and the reaction between them can occur if they can “meet”. This could possibly be:

- at the interface;
- or in one of the two phases, if, by a chemical artifice, they can be solubilized in the same phase. This is the problem of “phase transfer catalysis” and use of transfer agents (so-called phase transfer catalysts) for reversing the solubility properties of a reagent (Lattes and Rico-Lattes 2006).

In a microemulsion, macroscopically homogeneous, but microscopically heterogeneous, there is, for an organic solute, various possible locations.

i) In a direct micelle, it may:

- be inserted into hydrophobic heart,
- enter the micelle in the area of the first hydrophilic groups,
- adsorb at the interface.

ii) In a reverse micelle, it may:

- stay solubilized in the continuous phase,
- enter the micelle and, if it has a polar group, it can occupy the interface between the surfactant head and the heart of the aqueous micelle.

Conversely, a salt or a highly polar solute remains dissolved in the water or, in some cases, remains at the water-organic compound interface. Most organic solutes used in reactivity bear polar functional groups. During their solubilization in a microemulsion, the molecules will be arranged so that the polar groups are oriented towards the aqueous medium. This will result in:

- a local increase in concentration,
- an organization of molecules.

These two factors are favorable to increase the reactivity and thus the reaction rate. Clearly, the effects of a microemulsion reaction process can be:

- a compartmentation of space, which will help separating compounds which could be implied in non desirable side-reactions or otherwise can help concentrating reagents to promote desirable reactions,
- a control of the localisation of the reactants and products,
- an effect of orientation of molecules.

Moreover, interfacial processes take place in environments showing high dielectric constant (water + polar environment of the surfactant), thus favoring most synthetic reactions (Cabaleiro-Lago et al. 2005).

Remarks

1. It is also possible to combine the use of a microemulsion and that of a phase transfer agent. Indeed, we see that the micro-organization of such heterogeneous environments reproduces, at the microscopic scale, a liquid/liquid two phase system. Therefore, in this configuration, the addition of a phase transfer catalyst facilitates the progress of the reaction.
2. Regarding bi-continuous systems, the existence of extended channels would allow to carry out step by step reactions (for example, radical reactions) different from those taking place alone, at the surface of the micelle.

Applications to Reactivity

Reactions in Macroscopically Heterogeneous Environments: Phase Transfer Catalysis

Heterogeneous media can be of two types (Sirovski 1995):

- liquid-liquid: mixture of two immiscible liquids, water and organic solvent, for example;
- liquid-solid: suspension of a solid in a liquid in which it is not soluble.

Chemical Reactions in Liquid-liquid Two-phase Medium

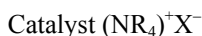
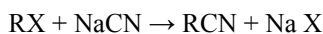
This situation occurs when two reactants soluble in two distinct phases have to react: for example an inorganic salt in water and an organic reagent in the solvent. Two cases can be considered:

- Using a transfer agent, the reagent normally soluble in water is transferred into the organic phase where it can react with the second reagent. This first mechanism implies the use of complexing agents: quaternary ammonium or phosphonium, a complex between a metal cation and a crown ether or cryptand, etc... These complexing agents form ion pairs with the water-soluble reagent, hydrophobic enough to be soluble in the organic solvent.
- An interfacial mechanism takes place. Here, there is no transfer and the catalyst has two functions:
 - To form and stabilize a new salt associating the cation of the complexing agent and the anion of the reagent,
 - To release the anion from the interface and make it react with the second reactant.

Most reactions of organic chemistry have been carried out by phase transfer catalysis. To illustrate, we can mention some well-known reactions:

Basic aqueous phase. Here are some examples:

- Synthesis of nitriles



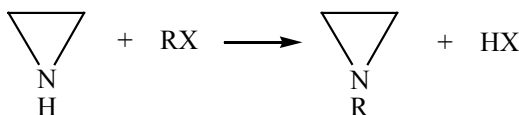
High yield (95%)

- C-alkylation $\text{C}_6\text{H}_5\text{CH}_2\text{CN} + \text{RX} \rightarrow \text{C}_6\text{H}_5\text{CH}(\text{R})\text{CN} + \text{HX}$



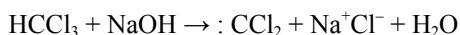
Different yields obtained, according to halides (from 25 to 95%)

- N-alkylation



In this case, catalyst is TEBA chloride and yields rise up to 100%. In this case, the direct alkylation is not possible because the aziridinium salt formed cleaves easily to give a very active carbocation.

- Formation of carbenes:



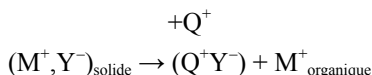
The catalyst is still TEBA chloride and yields may approach 80%.

Many addition, elimination, oxidation and reduction reactions are cited in the literature (Lattes and Rico-Lattes 2006; Sirovski 1995).

Acid aqueous phase. In this case, cations or protons can transfer into the organic phase, enabling reactions such as esters hydrolysis, acid addition to alkenes, synthesis of alkyl halides from alcohols (Caubère 1982).

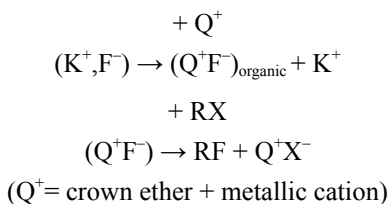
Chemical Reactions in Two phase Liquid-solid Media (Escoula et al. 1989)

The suspension of a mineral salt, or an inorganic base, in an organic solvent will create an interface between the solid and the liquid. The same principle applies for L/S reactions as for L/L reactions. Thus, an ion pair can be formed by taking an ion from the surface of the solid, which complexes the cation of the catalyst allowing it to pass into the organic phase where it reacts with the second reagent (Escoula et al. 1989).

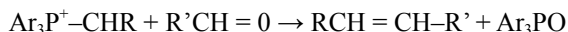


Among the possible reactions, we find:

Halogene-fluor exchange



Wittig reaction



The catalyst used in this case is a crown ether.

Reverse Phase Transfer Catalysis

Less developed than phase transfer catalysis implying reaction in the organic phase, there is also reverse phase transfer catalysis where the reaction takes place in water. The best known example is the synthesis of hippuric acid (Caubère 1982).

Reactions in Microemulsions

Phase transfer catalysis is a remarkable laboratory method but is difficult to implement in industrial processes and that, essentially for two reasons:

1. The difficulties linked to multiphase system stirring,
2. The high price of phase transfer catalysts and/or their environmental impact.

As reactions in simple micellar environments are limited to the use of low concentrations of products, we will only present the case of reactions in microemulsions. In these systems, the essential point is related to the distribution in space, which leads to the compartmentalization of the reactants. If we look at the molecular order which can be observed in different environments, it follows the sequence: crystal > monolayer > micelles, microemulsions > polymer solution > molecular solutions. The term “Organized Molecular System (OMS)” is then used to describe micellar solutions and microemulsions (Lattes and Rico-Lattes 1997).

We have mentioned above some properties of these organized molecular systems: solubilization, location, reagents distribution. This results in significant consequences for reactivity (Rico-Lattes et al. 2001a; Rico-Lattes and Lattes 2003; Robinson and Rogerson 2005):

- Alteration of the concentrations at the microscopic level and preservation of reagents concentration gradients;
- Changing of ionization and redox potentials;
- Modification of some reaction mechanism, and thus reaction rate, by stabilizing reagents, intermediates or products;
- Separation of products and/or electric charges.

Many reactions have been tested in microemulsion (Holmberg 2007). Examples include the solvolysis reactions (Hao 2000; Fernandez et al. 2003; Fernandez et al. 2007; Garcia-Rio et al. 1997), nucleophilic substitution (Haeger et al. 2004), reactions involving Schiff bases (Mishra et al. 2001), photocatalytic reactions (Rico-Lattes and Lattes 1997). The synthesis of fluorinated compounds for biological applications (Rico-Lattes et al. 2001b), as well as the decontamination of mustard gas (Gonzaga et al. 1999, 2001), were also studied.

To illustrate the benefits of these systems, the following examples have been chosen:

- the Wacker process and other olefin oxidation,
- the amidation of olefins,
- the polymerization of norbornenes,
- the synthesis of alkyl glucosides.

Wacker Process (alkenes catalytic oxidation process)

This industrial method is widely developed: it transforms a terminal olefin into ketone, in the presence of water and a catalyst: a palladium salt. The palladium Pd(II) is reduced into Pd(0) during the process. It is then regenerated by either an inorganic oxidant (the Cu(II)/O₂ tandem) or by a quinone.

This reaction process was studied both in homogeneous phase and in heterogeneous medium:

- For the homogeneous catalysis process, palladium salts which are industrially used are complex catalysts, which makes such processes expensive,

- For heterogeneous catalysis process, two-phase media are used, consisting of mixtures of dimethylformamide (DMF), water and palladium chloride: here yields are good, processes are less expensive, but generally slow.

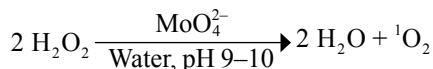
Alandis et al. (Alandis et al. 1994) took advantage of the special qualities of formamide, a good solvent for palladium chloride, to study the reaction in homogeneous monophasic microemulsions involving hydrocarbons and formamide, directly immiscible, by adding a surfactant and a cosurfactant. Since water is necessary in the Wacker process, it is a combined microemulsion system containing both water and formamide. The microemulsion system is selected as follows: water, formamide, hex-1-ene, propan-2-ol, and polyethoxylated nonylphenol as surfactant. Benzoquinone and palladium chloride are then incorporated into the selected media. Observed results compared to conventional systems, are excellent:

1. the reaction in water/DMF two phase system starts only after an induction period of about 100 to 110 minutes;
2. using microemulsion, there is no induction time and the process is accelerated, compared to the water/DMF system: the reaction rate is multiplied by 3.

Oxidation by Singlet Oxygen: Towards Continuous Process

Context. Singlet oxygen $^1\text{O}_2$ is an oxidizing reagent showing a very good selectivity. It is generally obtained by photochemical irradiation of molecular oxygen or generated through chemical reactions. The molecular oxygen photo-oxidation process can not be easily implemented at an industrial scale and it requires the use of photoreactors operating in gas/liquid medium, specially designed for specific applications. From a safety perspective, this type of process presents many hazards, due to the simultaneous presence of organic solvents, light and oxygen; this process is therefore not developed at an industrial scale, and rather concerns small productions. The generation of singlet oxygen by chemical reactions involves the use of inorganic oxidants such as ClO^- or BrO^- , which may cause side reactions, or oxygen organic sources, such as ozonides or endoperoxides, which may require a previous preparation. Moreover, these agents are used in stoichiometric amounts and generate many by-products. These oxidation processes are therefore poorly atom-efficient and lead to difficult product separations.

An alternative way is to use H_2O_2 as singlet oxygen source, combined with a catalyst (molybdate, tungstate...). This synthetic route has the advantage of being able to produce large amounts of $^1\text{O}_2$ at room temperature (quasi-quantitative reaction) without using photochemical apparatus (Aubry et al. 2006).



This reaction works well in an aqueous or hydroalcoholic medium but is, in this case, restricted to hydrophilic substrates or substrates of low molecular weight (1,4-cyclohexadiene derivatives, allylic alcohols, for example). For moderately hydrophobic compounds, a polar organic solvent must be added to solubilize them, such as methanol or DMF. This results in a lower reactivity together with the use of

environmentally hazardous solvents. To overcome these problems, two-phase water/organic solvent were tested: the catalyst system (H_2O_2 , Na_2MoO_4) is present in the aqueous phase while the hydrophobic substrate is dissolved in a water-immiscible organic phase. Unfortunately, the singlet oxygen lifetime (a few microseconds) is too short for it to efficiently transfer from the aqueous phase to the organic phase and react. Therefore, the majority of the oxygen is lost and a large excess of hydrogen peroxide is required to obtain suitable conversion (Aubry et al. 2006).

A promising solution is to use a water in oil microemulsion medium. In this case, the singlet oxygen has time to diffuse from microdroplets of a few nanometers diameter toward the organic phase. Such produced singlet oxygen can then react with an organic substrate having double bonds (alkene, diene, terpene. ...) to give an epoxide or an allylic hydroperoxide (Schenk reaction).

Reaction in water in oil microemulsion. The first tests of reaction in microemulsion media focused on water/ H_2O_2 / Na_2MoO_4 -chlorinated organic solvent (CH_2Cl_2) systems, using SDS as surfactant and n-butanol as co-surfactant (Aubry et al. 2006). Formulation tests have resulted in an oil in water microemulsion, stable during the reaction. Different reactions can be conducted in these media, such as Schenk reaction, [2 + 2] and [2 + 4] cycloadditions or oxidation of sulphides. An illustration of the benefits that can be expected of these particular media is the selective oxidation of allyl alcohols into chiral allylic hydroperoxides. This method allows to obtain high diastereoselectivities and chemoselectivities (up to 97 and 92% respectively) whereas in a homogeneous medium, the main product remains the epoxide. The development of such a reaction system has certain advantages, compared to liquid-liquid two-phase medium or homogeneous medium, but still suffers from several points: the presence of a chlorinated solvent, significant amounts of SDS, the obligation of using a large excess of hydrogen peroxide aqueous solution in the case of poorly reactive substrates, due to a significant loss of singlet oxygen (life time is too short). Ethyl acetate was proposed as a substitute for dichloromethane and microemulsions compositions could then be obtained by optimizing the formulation including the use of the simplex method. An additional step can be taken entirely by eliminating the use of an organic solvent: in this case, the substrate is itself the organic phase.

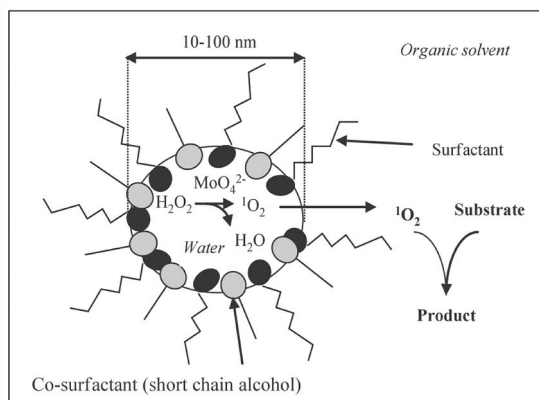


Figure 5. Schematic representation of water in oil microemulsion system used (Aubry et al. 2006).

Microemulsion multiphase system. Obtaining a Winsor IV type microemulsion (single phase), requires the use of high concentrations of surfactants (15–25%). This massive use of surfactants is detrimental to the development of an industrial process: on the one hand due to the difficulty to fully recycle the surfactant and secondly because product recovery is more difficult. It can be clever to work with multiphase media (Winsor I, II or III), to reduce the amount of surfactant needed and facilitate product recovery. Aubry et al. have therefore tested the 4 types of microemulsion for the oxidation of the α -terpinene. The organic solvent used here is toluene. Table 4 presents the results.

Table 4. Influence of the type of microemulsion on the performance of the oxidation of α -terpinene. From Aubry et al. (2006).

Winsor system	Composition		α -terpinene conversion (%)
	$\text{Na}_2\text{MoO}_4, 2 \text{H}_2\text{O}$ (mol kg ⁻¹)	SDS + n-propanol (weight %)	
IV	0.15	25	78
I	0.45	6	65
III	0.54		36
II	0.64		20

Toluene/(water + catalyst) = 1:1 (weight); SDS/n-C₃H₇OH: 1:1 (weight); (α -terpinene) = 0.1 mol kg⁻¹; (H₂O₂)15 mol kg⁻¹. From Aubry et al. 2006.

The worst results for the Winsor II and III systems are due to an excess of aqueous phase. The catalyst is partitioned between the microdroplets of the microemulsion and the aqueous phase macrodroplets. In the latter, singlet oxygen has no time to diffuse and react with the substrate. Winsor I system gives good results with the possibility of recovering the product extracted into the organic phase, which is an advantage from the perspective of a process development.

The major problem of such systems is the production of water, due to the reaction. Indeed, the resulting change in composition can destabilize the microemulsion and lead to demixing, slowing or blocking the chemical transformation. The formation of water also condemns the process to remain discontinuous. To remain in the concentration range of the microemulsion, the continuous water removal can be a solution. Distillation is energy consuming and requires to work at temperatures around 100°C. It can degrade reactants and products: it is therefore prohibited here. So, membrane separation appears as the technique of choice.

Use of a membrane for pervaporation. Using the same catalytic oxidation system by H₂O₂, Caron et al. have developed a semi-continuous oxidation process in microemulsion wherein water is continuously removed from the reaction medium (Caron et al. 2005). This ensures the stability of the microemulsion while avoiding the dilution of reactants and products by produced water. For very reactive substrates such as α -terpinene, reaction is not or little slowed by the dilution of the medium by water.

However, for less reactive substrates, such as β -citronellol, reaction is stopped due to dilution, and the continuous elimination of water can boost conversion. For

this application, and due to the presence of strong oxidants, the authors chose a robust ceramic type hydrophilic membrane. It consists of a hollow cylinder, made of alumina ($\gamma\text{-Al}_2\text{O}_3$) and coated with an outer SiO_2 layer (Fig. 6). The chosen membrane proved to be selective to water but not selective to alcohol (a part of propanol diffuses).

The reaction system chosen by Caron et al. is a two-phase system in which a microemulsion phase and an organic phase co-exist (Winsor I system). This system has been chosen in order to minimize the concentration of surfactants, and the presence of an excess of organic phase, which allows to continuously extract the product. The system finally chosen is: sodium laurate (4%), n-propanol (4%), toluene (46%) and an aqueous solution of sodium molybdate (0.8 M). The experiments were carried out using the installation presented below (Fig. 7).

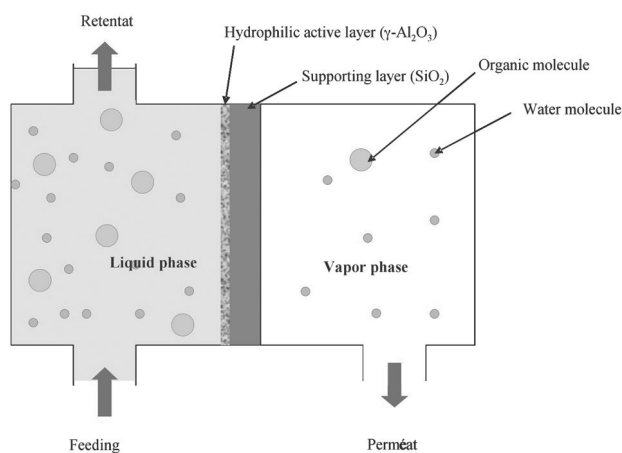


Figure 6. Schematic representation of the membrane process.

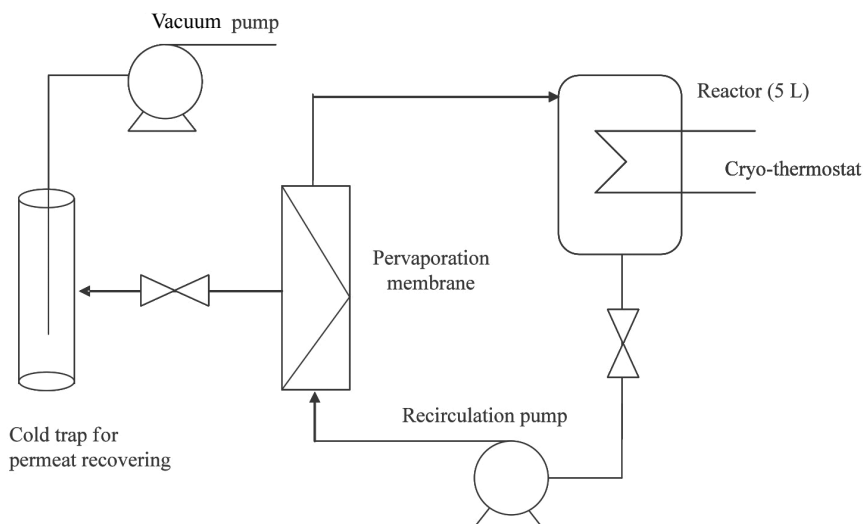


Figure 7. Setup used for the reaction/pervaporation coupling. From Caron 2005.

Substrate concentrations of the order of 1 mol L^{-1} were treated with this device. Unfortunately, the membrane surface area, available to the reaction medium, was too low and this did not permit a sufficient rate of water removal. The operation was thus carried out discontinuously, using successive reaction steps (feeding by an aqueous H_2O_2 solution) and pervaporation steps.

Nevertheless, this example provides the basis for a reaction/separation coupling and opens the way towards the development of a continuous industrial process.

Towards the design of catalysts-surfactants. As we saw earlier, microemulsions are environments that have many advantages for organic synthesis but for which two major drawbacks remain: the difficulty of isolating the products, due to the high concentration of surfactants (around 20%), and demixing after addition of a certain amount of hydrogen peroxide. Two-phase microemulsion/organic phase systems allow the use of less surfactant but are very sensitive to dilution by water formed during the conversion of H_2O_2 . Nardello-Rataj et al. (2008) have developed three-phase water/microemulsion/oil systems, using “catalytic” surfactants. In this case, the catalyst MoO_4^{2-} is linked by electrostatic interaction to the surfactant. Thus, quaternary ammonium surfactants having a double tail (two hydrocarbon chains) can play at the same time the role of surfactant, co-surfactant and catalyst (combination with molybdate). One can thus obtain in this case a three-phase medium with only three components. In this medium (Fig. 8), MoO_4^{2-} is located at the water/oil interface in the microemulsion microdroplets. The organic substrate is divided between the microemulsion phase and the oil phase while H_2O_2 is partitioned between the aqueous phase and the microemulsion.

The generation of singlet oxygen takes place only in the aqueous domain of the microemulsion. Their size is of the order of tens of nanometers, $^1\text{O}_2$ has time to diffuse towards the hydrophobic substrate and react with a good yield. In this case, the oil phase serves as a reservoir of substrate and product and the water phase as a reservoir of H_2O_2 . The reaction is conducted under stirring: the oxidation products are continuously extracted by the organic phase and the water generated by the reaction diffuses to the aqueous phase. Thus, the microemulsion is not destabilized by the formation of water. Stopping stirring leads to immediate separation of the 3 phases.

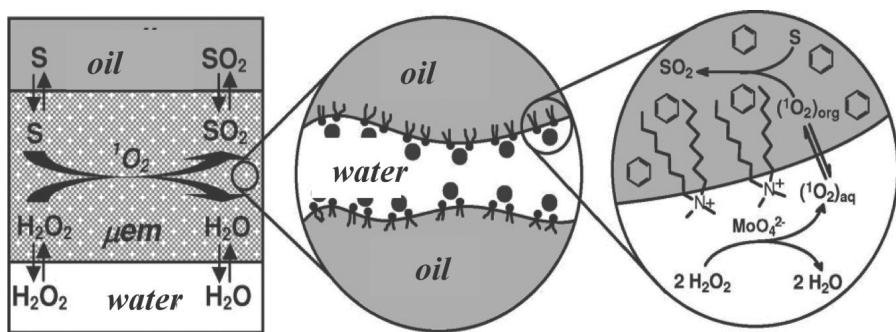


Figure 8. Oxidation of a substrate S in a three-phase system (one microemulsion phase, one organic (oil) phase, one aqueous (water) phase)—catalyst-surfactant: $[(\text{C}_8)_2\text{N}(\text{C}_{12})_2\text{MoO}_4]$. From Nardello-Rataj et al. 2008.

Such a system has been applied to the oxidation of rubrene (5,6,11,12-tétraphénylnaphthacène). This very hydrophobic compound, hindered and poorly soluble in most organic solvents, can react via a [4 + 2] cycloaddition to yield peroxide. The reaction performances were compared in two-phase medium (molybdate system/water/benzene), in phase transfer catalysis conditions using terabutylammonium bromide (PTC 1) or using teraocetylammmonium bromide (PTC 2), in microemulsion, and in the new three-phase system (Table 5).

Table 5. Results obtained by Nardello-Rataj et al. (2008) for rubrene peroxidation by the $\text{H}_2\text{O}_2/\text{X}_2\text{MoO}_4$ system ($\text{X} = \text{Na}^+$ or $(\text{C}_8)_n\text{N}(\text{C}_{1m})_m^+$); $[\text{rubrene}] = 0.02 \text{ mol L}^{-1}$; $T = 25^\circ\text{C}$, see experimental conditions in (Nardello-Rataj et al. 2008).

	Two-phase system	Phase transfer catalysis 1 (PTC 1)	Phase transfer catalysis 2 (PTC 2)	Microemulsion	Three-phase system (surfactant catalyst)
$[\text{H}_2\text{O}_2]$ mol L^{-1}	13	13	0.61	0.080	0.092
Reaction time (heures)	60	60	15	0.5	0.5
Yield (%)	10	13	> 98	> 98	> 98

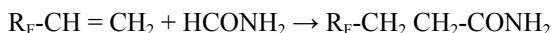
In the case of the two-phase medium, most of generated singlet oxygen is deactivated by reaction with H_2O before being able to transfer to the organic phase. In this case, mechanical stirring generates aqueous phase droplets having a diameter of the order of magnitude of one millimeter. In the presence of a hydrophilic phase transfer (PTC 1), no improvement is obtained since terabutylammonium bromide and molybdate remain in the aqueous phase. However, teraocetylammmonium bromide (PTC 2) is mainly located in the organic phase and is capable of carrying approximately half of the formed oxidation agent (peroxomolybdate) towards the organic phase, where the oxidation reaction takes place. The microemulsion medium (SDS + n-butanol) gives good results with the disadvantages associated with the use of a microemulsion alone. Finally, the three-phase system using a catalyst-surfactant allows to obtain the same performance in terms of yield and reaction time (1/2 hour) as with the microemulsion alone, but using only 1 wt% of surfactant (against 30% (SDS + n-butanol) for the microemulsion. Additionally, products are readily recovered in the organic phase and all the catalyst-surfactant complex remains in the microemulsion middle phase and can be recycled.

This illustrative example was carried out with benzene as solvent. It should of course be replaced by a less toxic and more environmentally friendly solvent.

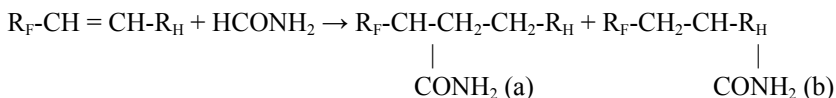
In conclusion, this innovative reaction system combines the advantages of the reactivity of microemulsion (high interfacial area, compartmentalization of reactants in nanosized reactors) and the implementation of phase transfer catalysis (simplicity, easy separation of products). The development of these new systems, used in small amounts and playing the dual role of surfactant and catalyst, simplifies the implementation of the reaction as well as the separation of products and should lead to the emergence of industrially viable synthesis processes.

Amidation of Olefins

The Wacker process example shows one of the disadvantages of the use of microemulsions as reaction media: the large number of components of the system, in this case 7 at the beginning and 8 when ketone is formed! To overcome this drawback, Rico-Lattes et al. proposed to apply the principle of molecular economy (Lattes 1987). The aim is to reduce the number of compounds, using substances with several features, e.g., surfactant and reagent, hydrocarbon and reagent, etc. ... A good illustration of this principle is the application to the amidation of olefins, more particularly of fluorinated olefins (Rico-Lattes et al. 1989). The amidation of terminal olefins of structure $R_F\text{-CH} = \text{CH}_2$ was performed by gamma radiolysis in a microemulsion using formamide, containing the olefin as the organic compound, a perfluorinated carboxylic acid potassium salt as perfluorinated surfactant and an alcohol as co-surfactant. The olefin and the formamide are the reactants and the components of the microemulsion as well.



Here, this free radical reaction is carried out only in the part of the microemulsion having a bicontinuous structure (olefin and formamide interpenetrating channels) and not in direct or reverse micellar system. Photo-amidation of substituted olefins, $R_F\text{-CH} = \text{CH-R}_H$, performed under the same conditions, leads to excellent yields of two positional isomers a and b.



While in a homogeneous solution of tert-butyl alcohol, amidation takes place on the α carbon of the alkyl chain, a reverse regioselectivity is observed in microemulsion (b/a = 7 in tert-butyl alcohol and 0.4 in microemulsion (Gautier et al. 1990)).

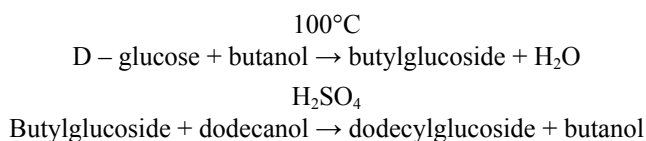
Polymerization of Norbornene (Eycheenne et al. 1993)

Among the methods of polymerization of norbornene, vinyl polymerization in the presence of PdCl_2 has the advantage of resulting in latex. This reaction is generally carried out at high temperature in the absence of solvent and leads to polydisperse polymers with low yields. In an aqueous emulsion prepared with an anionic surfactant (SDS), the Pd^{2+} ions are concentrated at the interface of the micelle, which enables the preparation of latex composed of saturated polymers where the norbornene group is maintained; stable latex is thus obtained in the form of small particles with a homogeneous size (close to 100 nm) and of atactic structure (Lattes 1987). This polymerization process can be extended to derivatives of norbornene: N-methyl norbornylgluconamide and N-methyl norbornyllactobionamide (Puech et al. 2000). In water, in the absence of surfactant (as they are themselves potential amphiphiles), these monomers also lead to stable small particles. The latter show interesting properties as diverse as the DNA compaction or the development of biochemical sensors. This is still an interesting application of the principle of

molecular economy: the reagent is also the surfactant. Other applications in microemulsion polymerization have been described such as the co-polymerisation of methyl méthavrylate with acetonitrile (Reddy et al. 2005) or with styrene (Reddy et al. 2007), the polymerization of styrene (Badran et al. 2000; Yildiz and Capek 2003).

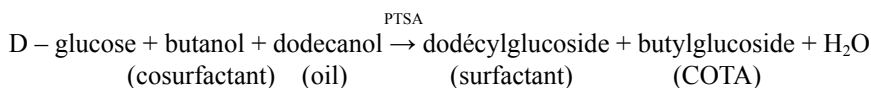
Synthesis of Alkylpolyglucosides (APG)

The same principle has been applied to the synthesis of APG (Perez et al. 1997), nonionic surfactants prepared from sugars and which can be seen as products of the future in the family of “green” surfactants. The industrial process is the Henkel process, composed of two stages:



This process requires to continuously remove water during its formation by vacuum distillation and the obtained final product is yellow.

By working in one step at ambient temperature, a self-emulsification process is favoured:



In this process, the reaction does not require distillation as the water formed is extracted in the heart of reverse micelles and equilibrium is moved in the direction of the formation of the surfactant.

Adipic Acid Synthesis

Adipic acid, $\text{HOOC}(\text{CH}_2)_4\text{COOH}$, is a white crystalline solid used primarily in the manufacture of nylon-6,6 polyamide. In industry, adipic acid is mainly produced by oxidation of cyclohexane with air and nitric acid following a homogeneous two-step route. However, this process leads to the formation of nitrous oxide, a greenhouse gas that has to be decomposed. Recently, a greener process, using cyclohexene as a raw material has been proposed (Blach et al. 2010; Quesada Peñate et al. 2012; Lesage et al. 2012). The process has been studied at pilot scale in order to obtain and recover pure adipic acid, and the evaluation of its industrial practicability was discussed. Adipic acid was synthesized from cyclohexene and hydrogen peroxide in microemulsions with stearyl dimethyl benzyl ammonium chloride as surfactant. The non-polluting catalyst sodium tungstate, which contains no heavy metal, was used and the reaction carried out under mild conditions (85°C, 8 h). Yields of up to 81% were reached at the 0.14 L scale. However at the end of the reaction the catalyst and the surfactant must be separated and recycled for subsequent cycles (Fig. 9). The reuse of the reaction media enabled the conversion to be increased up to 92%

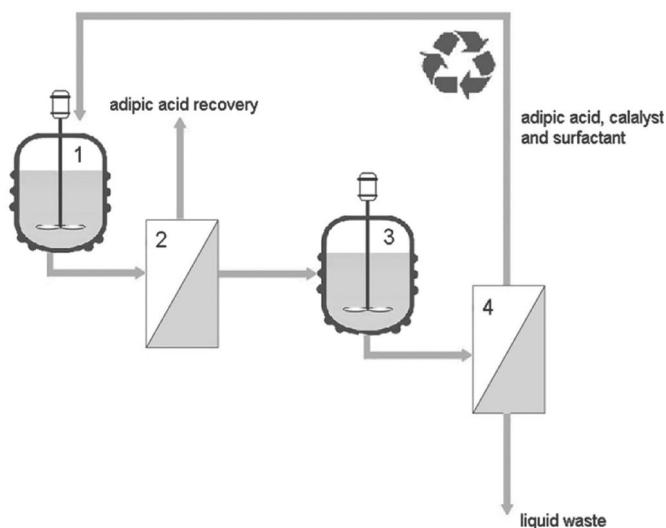


Figure 9. Simplified diagram for adipic acid synthesis in a microemulsion with BenzCl C18. 1: Reaction of cyclohexene oxidation by hydrogen peroxide at 85°C and first adipic acid precipitation at 40°C; 2: Filtration at 40°C; 3: Second precipitation at 20°C (adipic acid, catalyst, possible by-products and surfactant); 4: Filtration at 20°C.

but a loss of surfactant and/or catalyst through the cycles progressively reduced the yields. Yields at the bench scale (1.4 L) increased during the two first cycles and then decreased to conversions of between 60% and 70%. Globally the yield is a little lower at bench scale.

The results obtained show that the synthesis of adipic acid by a heterogeneous one-step oxidation of cyclohexene in the presence of hydrogen peroxide is an attractive route for developing a future green industrial process.

Microemulsions and Biotechnologies

The use of enzymes in organic synthesis is an interesting challenge for organic chemists. However, the differences of solubility between the enzyme and its substrates are an obstacle that limits their use. The use of microemulsions in the portion of the reverse micelle phase diagram can lift this handicap: the aqueous micelle heart dissolves enzymes while the continuous phase acts as a solvent for the substrates (Pastou et al. 2000; Mlejnek et al. 2004).

The choice of surfactant is very important here, because they often denature enzymes, thus limiting their use. By choosing particular surfactants, with polar heads (the bola-amphiphilic or bolaforms), we can avoid this pitfall while constituting dispersing media of choice for organic substrates.

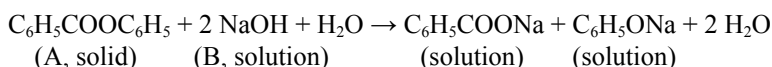
Using bolaform surfactants with two sugar heads, it is possible to carry out enzymatic reactions at preparative scale. Thus, linoleic acid is oxidized with soybean lipoxygenase in excellent conditions. The specific activity of this enzyme is higher than that found in normal micellar solutions; this activity is not disturbed after 60

hours of operation in the presence of bolaform while the same reaction, carried out in Tween 20 solutions, shows a specific activity of only 4% (Brisset et al. 1996).

Microemulsions and Solid-liquid Reactions

Microemulsions may in some cases be very efficient media for the acceleration of solid-liquid reactions (Hasnat and Roy 1998). Among the reactions studied are the alkaline hydrolysis of the esters and the oximation cyclododecanone (Bhagwat and Sharma 1988). Alkaline hydrolysis of esters (or saponification) is widely used to model the liquid-solid heterogeneous reactions. In this case, phenyl benzoate (A) or 2,4-dichlorophenyl (A') can be used in their solid form (particle diameter of about 100 μm), dispersed in an aqueous sodium hydroxide solution. The solubility of the esters in water is $5.1 \cdot 10^{-4} \text{ mol L}^{-1}$ (A) and $4.2 \cdot 10^{-5} \text{ mol L}^{-1}$ (A').

The reaction is as follows:



The ester transfers from the solid phase to the sodium hydroxide solution, where it undergoes hydrolysis. The reaction rate can be limited either by chemical kinetics, or by mass transfer. To model the behavior of the reaction, the double film theory can be used, for a reaction between A and B, taking place in the phase containing B, A transferring into this phase. The following equation has to be solved:

$$D_A \frac{d^2[A]}{dx^2} = k_2[B][A] \quad (1)$$

With:

[A]	:	local concentration of A in the aqueous phase, mol L^{-1}
[B]	:	local concentration of B in the aqueous phase, mol L^{-1}
D_A	:	diffusion coefficient of A in the aqueous phase, $\text{m}^2 \text{ s}^{-1}$
k_2	:	hydrolysis rate constant, $\text{L mol}^{-1} \text{ s}^{-1}$
x	:	distance in the film, $0 \leq x \leq \delta$, m
δ	:	film thickness, m

This equation is valid in the liquid film of thickness δ . If the following condition is satisfied:

$$\left(1 + \frac{[B]_0 D_A}{2[A^*] D_B} \right) \gg \frac{\sqrt{D_A k_2 [B]_0}}{k_{SL}} = \sqrt{Ha} \quad (2)$$

[B] can be replaced by $[B]_0$. Furthermore, transfer resistance in phase A is equal to zero (pure ester).

Notations:

$[A^*]$:	local concentration of A at the interface, mol L ⁻¹
$[B]_0$:	concentration of B in the bulk aqueous phase, mol L ⁻¹
D_B	:	diffusion coefficient of B in aqueous phase, m ² s ⁻¹
k_{SL}	:	solid-liquid mass transfer coefficient, m s ⁻¹

To solve equation (1), the following assumptions can be made:

$$\begin{aligned} x = 0 & \quad [A] = [A^*] \\ x = \delta & \quad [A] = [A]_0 \end{aligned}$$

The continuity equation can be written as follows:

$$R_A a_p = a_p D_A \left(-\frac{d[A]}{dx} \Big|_{x=0} \right) \quad (3)$$

With:

R_A	:	specific reaction rate, mol m ⁻² s ⁻¹
a_p	:	surface area of solid particles, m ⁻¹

More details on equations solving can be found in (Villermaux 1982). Finally, using a large excess of sodium hydroxide ($k_2 [B]_0 \gg k_{sl} a_p$):

If $\sqrt{Ha} < 0.3$, then:

$$R_A a_p = k_{SL} a_p [A^*] \quad (4)$$

If $\sqrt{Ha} > 3$, then:

$$R_A a_p = a_p [A^*] \sqrt{D_A k_2 [B]_0} \quad (5)$$

The diffusion coefficient D_A can be estimated from the Wilke and Chang relation. Its value is estimated at $6.7 \cdot 10^{-10}$ m² s⁻¹ for A, and at $6.0 \cdot 10^{-10}$ m² s⁻¹ for A' at 28°C, in a 0.5 M sodium hydroxide solution. The solid-liquid mass transfer coefficient, k_{SL} , has been experimentally determined to $1.1 \cdot 10^{-5}$ m s⁻¹ for A and $8.5 \cdot 10^{-6}$ m s⁻¹ for A'. This coefficient is determined by measuring the esters hydrolysis rate in an aqueous soda diluted medium. In these conditions, reaction is slightly limited by mass transfer (slow regime, $Ha < 0.3$). In these conditions, the following relation applies:

$$\frac{[A^*]}{R_A a_p} = \frac{1}{k_2 [B]_0} + \frac{1}{k_{SL} a_p} \quad (6)$$

This hydrolysis reaction was carried out in an alkaline medium, without and with surfactant, in the same conditions of concentration and temperature. Under "usual conditions", without surfactant, a finite ester concentration exists in the liquid phase. A Ha number value slightly greater than 0.3, indicates conditions of slow reaction regime. In the presence of sodium lauryl sulfate (SLS), Ha is greater than 3, indicating a shift to the fast reaction regime. In this case, the reaction occurs entirely in the diffusion film. The acceleration of the apparent reaction rate obtained in this

medium is further enhanced by the addition of a co-surfactant: propan-2-ol. The following table gives an example of some results.

Table 6. Alkaline hydrolysis of phenylbenzoate in LSS-butan-1-ol microemulsions (from Bhagwat and Sharma 1988).

Entry	[LSS] mol L ⁻¹	[butan-1-ol] mol L ⁻¹	R _A × 10 ⁶ mol m ⁻² s ⁻¹	φ	k _{2me} L mol ⁻¹ s ⁻¹
1	–	–	4.1	1.0	–
2	0.0173	–	13.3	3.3	2.9
3	0.0173	0.515	22.4	5.7	8.5
4	0.0173	0.644	26.0	6.4	11.7
5	0.0408	0.644	36.0	8.9	22.2

d_p = 95 μm; stirring speed = 20 s⁻¹; solid retention = 33.3 kg m⁻³; [NaOH] = 0.46 mol L⁻¹; a_p = 1590 m⁻¹; Temperature = 301 K.

With:

- d_p : solid ester particle diameter, m
k_{2me} : hydrolysis rate constant in microemulsion, L mol⁻¹ s⁻¹
φ : increase factor of reaction specific rate, dimensionless

Adding LSS to the reaction medium results in the apparition of micelles and multiplies by 3 the apparent hydrolysis rate (entry 2). In the presence of sodium lauryl sulfate, the addition of a co-surfactant (butan-1-ol) enables to generate the microemulsion and leads to a high increase of the rate of reaction (entry 3). By increasing the co-surfactant concentration (entries 4 and 5), an apparent reaction rate, 9 times higher than in the case of “conventional” hydrolysis without surfactant (entry 1), is obtained.

The water-in-oil microemulsion microdrops have a high affinity with respect to non-polar hydrophobic molecules. Ester-type molecules have a polar functional group and a hydrophobic carbon skeleton. These molecules therefore tend to cling to the microdroplets by the hydrophobic part. However, the polar portion has less affinity with the microdrop and will tend to remain at the outside, in the continuous aqueous phase. The ester function can therefore be attacked by nucleophiles such as OH⁻ even though this species is very hydrophilic and can not easily penetrate the microdroplet. The reaction will thus take place near the surface of the microdrop.

The study of this reaction showed that the apparent rate constant is proportional to the concentration of the surfactant introduced into the medium (for a constant average microdrop diameter) and proportional to the microdroplet diameter (at constant surfactant concentration).

In conclusion, the use of a microemulsion medium allows to localize the reaction in the reaction diffusion film. The increase in reaction rates is greater than in the case of using non-microemulsion micellar environments. In the case of nucleophilic attack in microemulsion medium, using an anionic surfactant (e.g., sodium lauryl sulfate), the reaction occurs at the surface of the microdroplets. The nucleophile is repelled by the anionic surfactant heads while being attracted by cationic heads. The rate increase

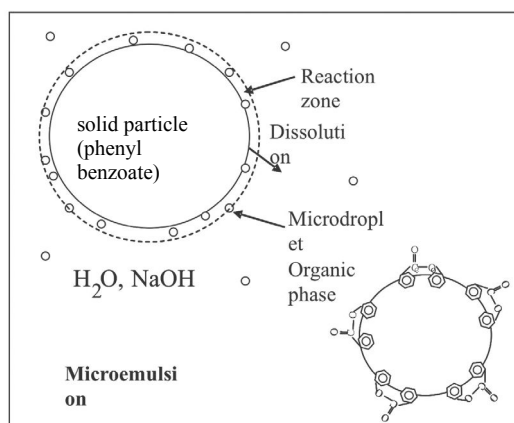


Figure 10. Alkaline hydrolysis of phenylbenzoate: schematic representation of the reaction medium.

is more important in the case of a cationic surfactant as cetyltrimethylammonium bromide than in the case of an anionic surfactant (sodium lauryl sulfate). In the case of cyclododecanone oximation, a multiplicative factor of 600 was observed for the reaction rate, by working in microemulsion medium.

Synthesis of Nanoparticles in Microemulsions

Microemulsions have recently been used for the synthesis of nanoparticles (Gan and Chaw 1995; Mo et al. 2001; Li et al. 2003; Ye and Wai 2003; Cao et al. 2004; Liu et al. 2004; Kosak et al. 2004; Andersson et al. 2007; Fan et al. 2007). Among developed applications, many works have been reported on the synthesis of TiO_2 nanoparticles (Cong et al. 2006; Moriguchi et al. 2004) and on the synthesis of catalysts (Aramendia et al. 2002; Svensson et al. 2006). Finally, an important application relates to the synthesis of multifunctional nanoparticles based on silica (Aubert et al. 2010). They are used as indicators or as magnetic and/or sources of photons and find applications in biotechnology and information technology. These applications require a control of the size and morphology of these new objects and therefore a good understanding of the synthesis parameters in order to control the properties of the final product: size, morphology, shell effects on the heart of the particle.

The water-in-oil microemulsions can be advantageously used for the synthesis of inorganic nanoparticles. They consist of nano-droplets of aqueous phase dispersed in an organic phase and in reverse micelles stabilized spherical size created by adding surfactants. The aqueous phase nano-drops can be regarded as nano-reactors and, controlling the composition of the oil/water/surfactant, it is possible to predetermine both size and shape of the final product. Microemulsions have been used first of all in the 80's to control the synthesis of mono-dispersed SiO_2 nanoparticles. The synthesis requires the use of a silica alkoxide precursor, water and often of a base to catalyze the hydrolysis and condensation steps. The size of the silica particles can be controlled from 10 to 100 nm. Since then, many studies have been published

on the synthesis of functionalized silica nanoparticles with magnetic and/or optical properties of $M@SiO_2$ type...

In most microemulsion processes, nanoparticles are obtained by simple mixing of two water-in-oil microemulsions, one containing a salt or a metal complex and the other one containing the precipitating agent. The disadvantage of this method comes from the effect of the reagents and products on the microemulsion stability domain, in particular the concentration of the metal species.

Some authors (Aubert et al. 2010), to avoid precipitation, proposed an original synthesis process using an aqueous colloidal dispersion instead of the metal salt solution (Fig. 11). This alternative route allows to increase the concentration of metal without destabilizing the microemulsion and allows to avoid the calcination step. This method has been applied to the synthesis of nanoparticles of $M@SiO_2$ type. Finally, these syntheses are based on a two steps sol-gel process, located in the nanodrops of aqueous phase : hydrolysis of the alkoxide precursor and polycondensation of hydrolyzed monomers. The "oil" phase is composed of n-heptane and the aqueous phase of an colloid acid, TEOS and ammonia. The nonionic surfactant used is polyoxyethylene lauryl ether; the co-surfactant is then not necessary. This Process allows the preparation of multifunctional nanocrystals, coated with silica, and showing remarkable catalytic, magnetic or luminescent properties. Examples include $ZnFe_2O_4@SiO_2$, $CeO_2@SiO_2$, $CS_2[Mo_6X_{14}]@SiO_2$ ($X = Cl, Br, I$)...

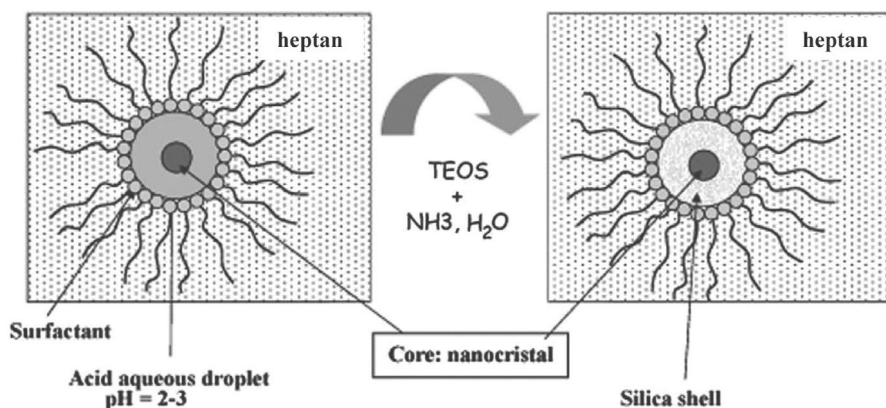


Figure 11. Preparation of nanoparticles of heart-shell by microemulsion water-in-oil. From (Aubert et al. 2010).

Conclusion

Microemulsions can be considered as monophasic and thermodynamically stable media at a macroscopic scale. They can be efficiently used as reactional media, especially to carry out reactions implying non compatible reagents (for example when a hydrophobic reagent has to react with a hydrophilic one). This solution can be an alternative to the use of phase transfer catalysis (two phase medium associated to a phase transfer agent). Mechanisms implied in both cases are very different. In

the case of phase transfer catalysis, one chemical species has to transfer from one phase to the other thanks to the transfer agent whereas, in the case of microemulsion, the main mechanism relies on the contact of both reagents at the interface, which is dramatically increased (Holmberg 2007). Moreover, both mechanisms can be associated. Many reagents can orientate themselves at the interface and the use of microemulsion is also a way to induce regioselectivity. Microemulsions are particularly well adapted to the case of oxidation reactions using H_2O_2 . Use of microemulsions in reactions cover a large number of applications, far beyond organic synthesis, ranging from polymerisation to nanoparticles synthesis. Microemulsions can also be used to accelerate certain types of solid-liquid reactions.

References

- Alandis, N., I. Rico-Lattes and A. Lattes. 1994. Micellar medium improves yield of acetophenone from styrene and hydrogen peroxide catalyzed by palladium chloride. *New J. Chem.* 18(11): 1147–1149.
- Andersson, M., A. Kiselev, L. Oesterlund and A.E.C. Palmqvist. 2007. Microemulsion-mediated room-temperature synthesis of high-surface-area rutile and its photocatalytic performance. *J. Phys. Chem. C* 111(18): 6789–6797.
- Aramendia, M.A., V. Borau, C. Jimenez, J.M. Marinas, F.J. Romero and F.J. Urbano. 2002. Microemulsion-assisted synthesis of catalysts based on aluminium and magnesium phosphates. *J. Mol. Catal. A-Chem.* 182-183: 35–46.
- Aubert, T., F. Grasset, S. Mornet, E. Duguet, O. Cador, S. Cordier, Y. Molard, V. Demange, M. Mortier and H. Haden. 2010. Functional silica nanoparticles synthesized by water-in-oil microemulsion processes. *J. Colloid. Interf. Sci.* 341: 201–208.
- Aubry, J.M. and G. Schorsch. 1999. Formulation, Présentation Générale, Techniques de l'Ingénieur, traité Génie des Procédés J 2 110.
- Aubry, J.M., W. Adam, P.L. Alsters, C. Borde, S. Queste, J. Marko and V. Nardello. 2006. Dark oxygenation of organic substrates in single-phase and multiphase microemulsion systems. *Tetrahedron* 62(46): 10753–10761.
- Badran, A.S., H.E. Nasr, A.E.M. Ali, G.M. El Enany and A.A. El-Hakim. 2000. Microemulsion polymerization of styrene using developer redox initiation system and study of rheological properties of obtained latexes. *J. Appl. Poly. Sci.* 77(6): 1240–1249.
- Barois, P. 1996. Cristaux liquides. Techniques de l'Ingénieur, traité Sciences fondamentales A 1 325: A1325.1–A1325.12.
- Bhagwat, S.S. and M.M. Sharma. 1988. Intensification of solid-liquid reactions: microemulsions. *Chem. Eng. Sci.* 43(2): 195–205.
- Blach, P., Z. Boestrom, S. Franceschi-Messant, A. Lattes, E. Perez and I. Rico-Lattes. 2010. Recyclable process for sustainable adipic acid production in microemulsions. *Tetrahedron* 66(35): 7124–7128.
- Brisset, F., R. Garelli-Calvet, J. Azema, C. Chebli, I. Rico-Lattes and A. Lattes. 1996. Synthesis of new sugar-based bolaamphiphilic compounds physicochemical study of their molecular aggregation in aqueous solution. *New. J. Chem.* 20: 595–605.
- Cabaleiro-Lago, C., L. Garcia-Rio, P. Herves and J. Perez-Juste. 2005. Reactivity of benzoyl chlorides in nonionic microemulsions: potential application as indicators of system properties. *J. Phys. Chem. B* 109(47): 22614–22622.
- Cabane, B. 2003. Formulation des dispersions. Techniques de l'Ingénieur, traité Génie des Procédés J 2185.
- Cao, M., Y. Wang, Y. Qi, C. Guo and C. Hu. 2004. Synthesis and characterization of MgF_2 and KMgF_3 nanorods. *J. Solid State Chem.* 177(6): 2205–2209.
- Caron, L., V. Nardello, J. Mugge, E. Hoving, P.L. Alsters and J.M. Aubry. 2005. Continuous process for singlet oxygenation of hydrophobic substrates in microemulsion using a pervaporation membrane. *J. Colloid. Interface Sci.* 282: 478–485.
- Caubère, P. 1982. Le transfert de phase et son utilisation en chimie organique. Masson.

- Cayias, J.L., R.S. Schechter and W.J.H. Wade. 1977. The utilization of petroleum sulfonates for producing low interfacial tensions between hydrocarbons and water. *J. Colloid Interface Sci.* 59(1): 31–38.
- Cong, Y., F. Chen, J. Zhang and M. Anpo. 2006. Carbon and nitrogen-codoped TiO₂ with high visible light photocatalytic activity. *Chem. Lett.* 35(7): 800–801.
- Escoula, B., I. Rico and A. Lattes. 1989. Formamide, a water substitute in solid-liquid phase transfer: chlorine-fluorine substitution reaction. *Bull. Soc. Chim. Fr.* 2: 256.
- Eychenne, P., E. Perez, I. Rico, M. Bon, A. Lattes and A. Moisand. 1993. First example of lattices synthesis via oligomerization of norbornene in aqueous emulsions, catalyzed by palladium chloride. *Colloid Polym. Sci.* 271: 1049–1054.
- Fan, W., X. Song, S. Sun and X. Zhao. 2007. Microemulsion-mediated hydrothermal synthesis and characterization of zircon-type LaVO₄ nanowires. *J. Solid State Chem.* 180(1): 284–290.
- Fernandez, E., L. Garcia-Rio, A. Godoy and L.R. Leis. 2003. Reactivity in w/o microemulsions. Activation parameters for solvolysis in AOT/isooctane/water systems. *New J. of Chem.* 27(8): 1207–1215.
- Fernandez, E., L. Garcia-Rio, M. Parajo and P. Rodriguez-Dafonte. 2007. Influence of changes in water properties on reactivity in strongly acidic microemulsions. *J. Phys. Chem. B* 111(19): 5193–5203.
- Friberg, S.E. 1983. Microemulsions. *Prog. Coll. Pol. Sci.* 8: 41–47.
- Friberg, S.E. and I. Lapczynska. 1975. Microemulsions and solubilization by nonionic surfactants. *Prog. Coll. Pol. Sci.* 56: 16–20.
- Gan, L.M. and C.H. Chaw. 1995. From microemulsions to nano-structured materials. *Bull. Singapore Natl. Inst. Chem.* 23: 27–46.
- Garcia-Rio, L., J.R. Leis and C. Reigosa. 1997. Reactivity of typical solvolytic reactions in SDS and TTABr water-in-oil microemulsions. *J. Phys. Chem. B.* 101(28): 5514–5520.
- Gautier, M., I. Rico and A. Lattes. 1990. Comparative study of photoamidation of a mixed olefin RFCH:CHRH in homogeneous and microscopically heterogeneous media. *J. Org. Chem.* 55(5): 1500–1503.
- Gonzaga, F., E. Perez, I. Rico-Lattes and A. Lattes. 1999. The role of lipophilicity in oxidation of mustard gas analogues from micellar solutions. *Langmuir* 15(23): 8328–8331.
- Gonzaga, F., E. Perez, I. Rico-Lattes and A. Lattes. 2001. New microemulsions for oxidative decontamination of mustard gas analogues and polymer-thickened. *New J. Chem.* 25(1): 151–155.
- Haeger, M., U. Olsson and K.A. Holmberg. 2004. Nucleophilic substitution performed in different types of self-assembly structures. *Langmuir* 20(15): 6107–6115.
- Hao, J. 2000. Studies on chemical reactions in microemulsion media.(I). Hydrolysis kinetics studies in microemulsion system for CTAB/n-butanol/25% n-octane/water. *J. Disper. Sci. Technol.* 21(1): 19–30.
- Hasnat, A. and S. Roy. 1998. Intensification of instantaneous heterogeneous reaction by simple salts and charged microphase. *AIChE J.* 44(3): 656–666.
- Holmberg, K. 2007. Organic reactions in microemulsions. *Eur. J. Org. Chem.* 2007(5): 731–742.
- Kosak, A., D. Makovec and M. Drofenik. 2004. Microemulsion synthesis of MnZn-ferrite nanoparticles. pp. 219–224. *In: Materials Science Forum, 453–454; Progress in Advanced Materials and Processes.*
- Lattes, A. 1987. Relation structure-réactivité chimique et photochimique en microémulsions, *J. Chim. Phys.* 84: 1061–1069.
- Lattes, A. and I. Rico-Lattes. 1997. Communities of molecules and reactivity in organized molecular systems, *Comptes-Rendus de l'Académie des Sciences, Série IIb : Mécanique, Physique, Chimie, Astronomie* 324(9): 575–587.
- Lattes, A. and I. Rico-Lattes. 2006. Catalyse aux interfaces liquide-liquide, *Techniques de l'Ingénieur, J* 1 230v2.
- Lesage, G., I. Quesada Peñate, P. Cognet and M. Poux. 2012. Green Process for adipic oxidation by hydrogen peroxide in water microemulsions using benzalkonium chloride C12-C14 surfactant, *Int. J. Chem. React. Eng.* 10(A47).
- Li, F., C. Vipulanandan and K.K. Mohanty. 2003. Microemulsion and solution approaches to nanoparticles iron production for degradation of trichloroethylene. *Colloid. Surface. A* 23(1-3): 103–112.
- Liu, Z.L., X. Wang, K.L. Yao, G.H. Du, Q.H. Lu, Z.H. Ding, J. Tao, Q. Ning, X.P. Luo, D.Y. Tian and D. Xi. 2004. Synthesis of magnetite nanoparticles in W/O microemulsion. *J. Mater. Sci.* 39(7): 2633–2636.

- Mishra, B.K., N. Patel, P.K. Dash and G.B. Behera. 2001. Reactions in microemulsion media: Schiff bases with targeting/anchoring module as kinetic sensors to map the polarity pocket of a microemulsion droplet. *Int. J. Chem. Kinet.* 33(8): 458–464.
- Mlejnek, K., B. Seiffert, T. Demberg, M. Kaemper and M. Hoppert. 2004. Temperature optima of enzyme-catalyzed reactions in microemulsion systems. *Appl. Microbiol. Biot.* 64(4): 473–480.
- Mo, X., C. Wang, L. Hao, M. You, Y. Zhu, Z. Chen and Y. Hu. 2001. Convenient microemulsion route to star-shaped cadmium sulphide pattern at room temperature. *Mater. Res. Bull.* 36(11): 1925–1930.
- Moriguchi, I., Y. Katsuki, H. Yamada, T. Kudo and T. Nishimi. 2004. Bicontinuous microemulsion-aided synthesis of mesoporous TiO₂. *Chem. Lett.* 33(9): 1102–1103.
- Nardello-Rataj, V., L. Caron, C. Borde and J.M. Aubry. 2008. Oxidation in three-liquid-phase microemulsion systems using “balanced catalytic surfactants”. *J. Am. Chem. Soc.* 130(45): 14914–14915.
- Pastou, A., H. Stamatis and A. Xenakis. 2000. Microemulsion-based organogels containing lipase: application in the synthesis of esters. *Prog. Coll. Pol. Sci.* 15: 192–195.
- Perez, E., I. Rico-Lattes, A. Lattes and L. Godefroy. 1997. Patent No.: 9708461.
- Puech, L., E. Perez, I. Rico-Lattes, M. Bon and A. Lattes. 2000. New polymer and latex prepared by vinyl polymerization of derivatives of norbornene catalyzed by PdCl₂, or PdCl₂(TPPTS)₂ in water. *Colloid. Surface. A*, 167: 123.
- Quesada Peñate, I., G. Lesage, P. Cagnet and M. Poux. 2012. Clean synthesis of adipic acid from cyclohexene in microemulsions with stearyl dimethyl benzyl ammonium chloride as surfactant: from the laboratory to the bench scale. *Chem. Eng. J.* 200-202: 357–364.
- Reddy, G.V.R., C. Magesh and R. Sriram. 2005. Microemulsion co-polymerization of methyl methacrylate with acrylonitrile. *Des. Monomers Polym.* 8(1): 75–89.
- Reddy, G.V.R., N.G. Devi and J. Panda. 2007. Microemulsion and conventional emulsion copolymerizations of styrene with methyl methacrylate. *Popular Plast. Packag.* 52(4): 117–126.
- Rico, I. and A. Lattes. 1986. *Surfactants in Solutions*. Ed. K.L. Mittal, Plenum Press, N.Y.
- Rico-Lattes, I. and A. Lattes. 1997. Organized media and homogeneous photocatalysis. *Wiley Series in Photoscience and Photoengineering* 2: 309–353.
- Rico-Lattes, I. and A. Lattes. 2003. Systèmes moléculaires organisés et synthèse organique. *Actualité Chimique* 4-5: 77–81.
- Rico-Lattes, I., A. Lattes, K.P. Das and B. Lindman. 1989. Reaction in the bicontinuous phase of a nonaqueous microemulsion: amidation of the olefin C8F17CH=CH₂ by gamma. radiolysis. *J. Am. Chem. Soc.* 111(8): 7266–7267.
- Rico-Lattes, I., B. Guidetti and A. Lattes. 2001a. Molecular organized systems with fluorinated compounds: from synthesis to biological applications. *J. Fluorine Chem.* 107(2): 355–361.
- Rico-Lattes, I., A. Lattes, E. Perez, F. Gonzaga and A.R. Schmitzer. 2001b. Chemical activation in micelles, pseudomicelles, and microemulsions. *Surfactant Science Series* 337–347.
- Robinson, B.H. and M. Rogerson. 2005. Reaction processes in self-assembly systems. pp. 475–507. *In: R. Zana (ed.) Dynamics of Surfactant Self-Assemblies: Micelles, Microemulsions, Vesicles and Lyotropic Phases, Surfactant Science Series*, 125. CRC Press, Boca Raton, Florida.
- Salager, J.M., R. Anton, J.M. Andrez and J.M. Aubry. 2001. Formulation des microémulsions par la méthode du HLD. *Techniques de l'Ingénieur traité génie des procédés J2* 157.
- Shinoda, K. 1967. The correlation between the dissolution state of nonionic surfactant and the type of dispersion stabilized with the surfactant. *J. Colloid. Interface. Sci.* 24(4): 4–9.
- Sirovski, F.S. 1995. Phase-transfer and micellar catalysis in two-phase systems. pp. 68–88. *In: M.E. Halpen (ed.) Phase Transfer Catalysis, ACS Symposium Series*. Washington DC.
- Smith, G.D., C.E. Donelan and R.E. Barden. 1977. Oil-continuous microemulsions composed of hexane, water, and 2-propanol. *J. Colloid. Interf. Sci.* 60(3): 488–496.
- Svensson, E.E., S. Nossos, M. Boutonnet and S.G. Jaeras. 2006. Microemulsion synthesis of MgO-supported LaMnO₃ for catalytic combustion of methane. *Catalysis Today* 117(4): 484–490.
- Villiermaux, J. 1982. *Génie de la réaction chimique conception et fonctionnement des réacteurs, Technique et documentation*, Lavoisier.
- Winsor, P.A. 1954. *Solvent Properties of Amphiphilic Compounds*. Butterworths' Scientific Publication, London.

- Ye, X. and C.M. Wai. 2003. Making nanomaterials in supercritical fluids: a review. *J. Chem. Educ.* 80(2): 198–204.
- Yildiz, U. and I. Capek. 2003. Microemulsion polymerization of styrene in the presence of macroinimer. *Polymer* 44(8): 2193–2200.
- Yu, J.C., L. Wu, J. Lin, P. Li and Q. Li. 2003. Microemulsion-mediated solvothermal synthesis of nanosized CdS-sensitized TiO₂ crystalline photocatalyst. *Chem. Commun.* 13: 1552–1553.

PART 3

**A New Generation of
Processes**

9

Supercritical CO₂, the Key Solvent for Sustainable Processes

Danielle Barth, Séverine Camy and Jean-Stéphane Condoret

Introduction

In processes that transform matter, solvents are very frequently used. A solvent is a liquid that dissolves substances. This is very useful especially when these substances are in a solid state. Also, in the field of chemistry, solvents are essential for carrying out reactions: they allow effective contact of the reactive molecules, adjustment of the viscosity of the reaction system, and may also act as a “thermal buffer” in exothermic reactions. Of course, the omnipresent solvent is liquid water, especially because most biochemical reactions occur in water based mixtures. However, although water is a very powerful solvent, many compounds are poorly soluble in water (lipids for instance) and also water exhibits hydrolytic properties that can be undesirable. In such cases, organic solvents are used and their great variety can provide a solution to almost any case. However, this convenience may result in disadvantages that are now unacceptable in our society: toxicity, often flammability and volatile organic compounds (VOC) emissions, etc. Of course, completely eliminating these solvents would be difficult but concepts of green chemistry give us strong incentives to systematically rethink their use. Among the alternative paths, supercritical fluids and especially supercritical CO₂, can bring about a solution. They can also be the source of new products. All of the interest in these media for proposing novel sustainable processes is elaborated below.

Overview of Supercritical Fluids

Definition of a Supercritical Fluid

A supercritical fluid (SCF) is a fluid whose pressure and temperature are above their critical values (T_c , P_c). The supercritical domain is seen in the schematic description

of Fig. 1 for a pure substance. Generally, this domain corresponds to pressures higher than atmospheric (a minimum of a few tens of bar, see Table 1).

Note, however, that in practice these fluids are often not strictly above their critical point and are therefore termed as near-critical fluids. Below the critical point and when approaching the critical coordinates, a dense gas and an expanded liquid coexist along the vapour-liquid line. These two phases become more and more similar, until they cannot be distinguished, and then the fluid enters the supercritical domain. In this particular domain, the molecules associate into fugitive and very mobile aggregates. Macroscopic density of molecules resembles a liquid one (a few hundreds of kg/m^3 , see Table 2), thus favouring intermolecular interaction and giving to the fluid a solvent power in respect to solutes which are normally in liquid or solid state under these conditions of pressure and temperature. Figure 2 shows a simplified view of the situation of a non-volatile solute present in the different cases: gas, supercritical and liquid. At the microscopic level, the supercritical fluid exhibits

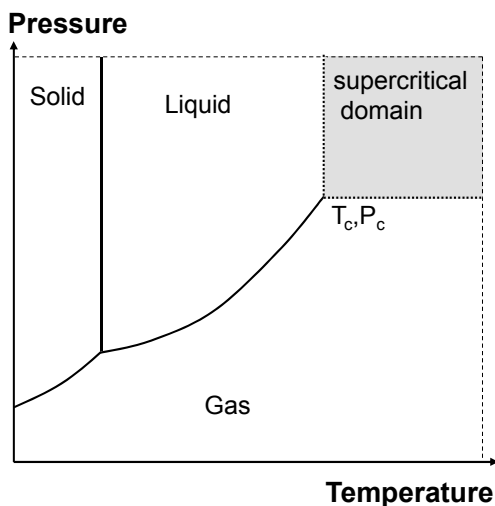


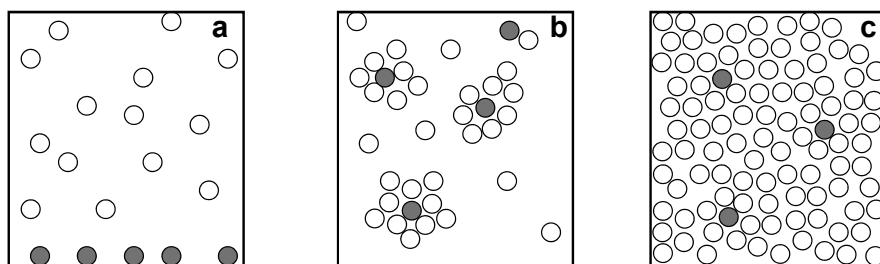
Figure 1. Schematic Pressure-Temperature diagram of a pure substance.

Table 1. Critical coordinates of some common fluids.

Solvent	T_c ($^{\circ}\text{C}$)	P_c (bar)
Water	374	218
CO_2	31	74
Propane	97	42
Ethane	32	48
Butane	152	38
Acetone	235	47
Ethanol	243	63
Pyridine	347	55

Table 2. Typical values for the properties of a supercritical fluid.

	Gas	SCF	Liquid	
Density kg.m ⁻³	1	700	1000	Good solvent power. Tuneable
Viscosity Pa.s	10 ⁻⁵	10 ⁻⁴	10 ⁻³	Good mass transfer properties
Diffusivity m ² .s ⁻¹	10 ⁻⁴	10 ⁻⁷	10 ⁻⁹	
No surface tension effect				Good penetration into porous media

**Figure 2.** Schematic view of the molecular organization of a solvent in the presence of a solute (black dots). (a) with a gas (no solvation), (b) with a supercritical fluid, (c) with a liquid.

a “heterogeneous” nature where the solvent molecules aggregates around molecules of solute forming structures termed “clusters”.

The solvent power of a supercritical fluid depends directly on its density (Chrastil 1982). For instance, the variation of the density of supercritical CO₂ in respect to pressure and temperature is given in Fig. 3 where it is seen that density can be varied continuously from low values (a few tens of kg/m³) to liquid-like values. This allows the solvent power to vary correlatively by simply varying pressure or temperature. This is a key characteristic of a supercritical fluid. For example, a depressurization significantly reduces the solvent power and causes precipitation of products extracted or produced from a reaction step, so that they can be easily recovered. On the other hand, due to this easy modulation of the fluid density, solvent and solute interactions can be adjusted, leading to a possible influence on extraction selectivity or reaction kinetics. This ability to be adjustable is a unique feature of supercritical fluids as compared to traditional solvents. Therefore, taking advantage of the degree of freedom offered by the choice of temperature and pressure, a single fluid can be the equivalent of a family of solvents. Near the critical point, small changes in pressure or temperature result in very large variations of density and compressibility (theoretically, at the critical point, the latter tends to infinity, as well as heat capacity). These phenomena are referred to as critical divergence properties. This domain, extending to about $T/T_c = 1.3$, is certainly interesting from an academic point of view but is not advisable for operating a process, because controlling the properties is too difficult (Carlès 2010).

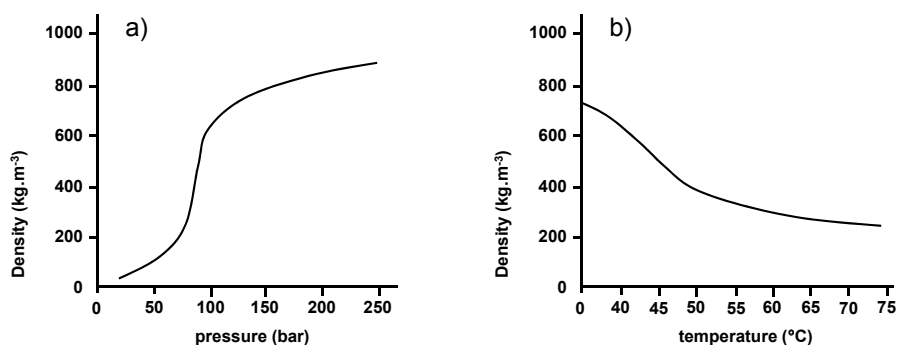


Figure 3. Changes in the density of CO₂: (a) at 40°C, in respect to pressure, (b) at 100 bar in respect to temperature (data from National Institute of Standards and Technology).

Transport Properties

Supercritical fluids are often said to be intermediate between gases and liquids, although their characteristics are closer to liquid ones. When using them in processes, these characteristics result in very interesting transport properties (diffusivity, viscosity, thermal conductivity...), more favourable than those of conventional liquid solvents (see Table 2). For example, although values strongly depend on pressure, dynamic viscosity of a supercritical fluid is significantly lower than those of liquids, and therefore the diffusion coefficients of solutes are higher. Low dynamic viscosity and high density result in a low kinematic viscosity, which favours free convection. All of these characteristics combine to give these fluids very good mass transfer properties, an inestimable quality for industrial processes, which are often impeded by mass transfer (diffusion in large particles in solid extraction, diffusion inside catalytic porous particles in the case of heterogeneous catalysis...). Note also such fluids are exempted of any capillarity or wettability effect for penetration in micro- or mesoporous solids.

Supercritical CO₂, the Relevant Fluid for Sustainable Processes

As can be seen in Table 1, most fluids exhibit relatively high critical pressure (about 74 bar for CO₂) and this constitutes the main obstacle in developing the supercritical fluid technology. In fact, high pressure operation requires significant investments to build the equipment. However, note that using a fluid such as water or CO₂ (which are non-flammable and non-toxic), does not require costly safety constraints such as those needed for organic solvents, which conversely are very often highly flammable or toxic. This is an often misjudged advantage in strategic decisions when benchmarking the various processes. Within the framework of Green Process Engineering, Table 1 readily indicates two candidate fluids: Water and CO₂. However, water has a high critical temperature (374°C) which prohibits

the processing of thermally labile components as well as the majority of organic synthesis reactions. Only reactions of degradation for organic pollutants or reactions of mineral synthesis can be envisaged. In addition, processes using supercritical water are handicapped by the “aggressiveness” of this fluid on materials. Special alloys for equipment have to be used and the lifetime of the equipment becomes a key factor. Because of these restrictions and idiosyncrasies, the technology of supercritical water is not considered here. In fact, water in its simple liquid state is a very useful solvent for many chemical species and remains the preferred solvent for Green Chemistry but cannot cover all the needs. Light hydrocarbons (propane, ethane...), despite their relatively low toxicity and accessible critical coordinates, are not very commonly used because of their high flammability. Finally, CO₂ appears as the most suitable fluid for the development of supercritical processes obeying the principles of Green Chemistry. An important point to be highlighted: from its role in the greenhouse effect, CO₂ has a very poor image in public opinion. This is justified when considering the generation of CO₂ from fossil fuels but when CO₂ is used as a solvent, its extensive use does not participate in the CO₂ overall balance. Most of the CO₂ comes from ammonia or fermentation industrial plants but the use of CO₂ extracted from underground reservoirs acts as anti-sequestration and does not meet the principles of Green Chemistry. Moreover, in a supercritical process, CO₂ is almost entirely recycled thus leading to extremely low CO₂ emissions. Therefore the CO₂ molecule carries the paradox of being a major player in the degradation of our environment and simultaneously offers one of the best alternatives to replace organic solvents which create pollution and hazards in industrial processes. This explains the renewed interest towards applications of supercritical CO₂ which arises more from the “green” aspect of this molecule than from the intrinsic properties of the supercritical state. A comprehensive review of the interest of CO₂ for Green Chemistry can be found in the article by Beckman 2004.

Advantages of the Use of CO₂

- a) CO₂ is relatively inert in respect to many reactive compounds. This is an advantage on a process and environmental point of view because side reactions involving CO₂ are relatively rare. Note, however, that this relative chemical inertness is an important obstacle to the development of processes aimed at consuming CO₂ in chemical reactions.
- b) CO₂ cannot be oxidized which explains its non-flammability. In fact, the CO₂ molecule results from the complete oxidation of organic compounds. In the implementation of oxidation reactions, this non-oxidizable character is a crucial advantage over the majority of organic solvents, which, in contact with an oxidant, generates degradation products. Note that CO₂ shares this advantage only with perfluorinated solvents. For instance, replacing a fluorinated solvent with supercritical CO₂ has been recently proposed for the industrial production of oxidized cellulose for biomedical applications (Camy et al. 2009; Vignon et al. 2006).

- c) CO₂ does not cause contamination to aqueous phases. Usually, when an organic phase is in contact with an aqueous phase, cross-contamination is unavoidable. Thus the aqueous phase, polluted by traces of organic solvent, requires specific treatment before discharge. With using CO₂, the aqueous phase is contaminated with CO₂ but this is not considered as pollution.
- d) Above 31°C, low critical temperature gases (such as H₂, O₂ or CO) are miscible in all proportions with supercritical CO₂. This is an important advantage for the development of chemical processes involving gas-solvent systems because their productivity often limited due to the difficult dissolution of the gas in the solvent. For example, this is the case for hydrogen and oxygen, which are sparingly soluble gases, either in aqueous or organic phases. Using CO₂ as a solvent makes it possible to operate in a single-phase mixture which simultaneously dissolves gas and reactants. Interphase mass transfer limitations are then *de facto* eliminated. Note that operation in a single-phase system is not always required. In fact, when maintaining a pressurized vapour phase containing CO₂ above a liquid, the high solubility of CO₂ in the liquid phase may strongly and favourably modify the liquid properties. In particular the solubility of gases such as hydrogen is greatly enhanced. In this case the presence of high pressure CO₂ has an indirect effect and this constitutes a new field which can be termed as “CO₂ assisted” processes.
- e) CO₂ has a low viscosity. CO₂ can easily penetrate complex solid geometry, much better than liquids. In addition, as indicated in the preceding paragraph, its presence, dissolved at high concentration in a liquid, may significantly decrease the viscosity of this liquid phase and this is often an advantage for the process. For instance, membrane filtration of oils can be improved by reducing oil viscosity. This was proposed for waste oil regeneration (Rodriguez et al. 2002).
- f) CO₂ has a sterilizing effect but this property has seldom been pointed out. Indeed, CO₂ is able to inactivate micro-organisms and most viruses. An extensive review about these properties can be found in Perrut 2012. The mechanisms of inactivation of cells are numerous, mainly based on extra- and intra-cellular pH modification or displacement of the intra-cellular electrolytic balance. More information can be found in Spilimbergo’s works (Garcia-Gonzalez et al. 2007). The influence of CO₂ on pH is looked at more closely in next paragraph. Virus inactivation has been less studied but, for example, has been validated in the production of bone implants (Fages et al. 1998).

Disadvantages of the Use of CO₂

- a) CO₂ is not a very good solvent, particularly in respect to polar compounds. This is due to the low value of its dielectric constant (around 1.5 and slightly influenced by pressure). So, to increase the solvent power, very high pressures are often used or a polar co-solvent is added, such as ethanol, methanol or acetone. Nevertheless, the use of an additional component complicates the process and degrades the “clean process” character. When the co-solvent is water or ethanol, it is a very acceptable solution. Some qualitative rules can be given to assess the solubility of a solute in supercritical CO₂:

- Compounds with moderate and low molecular mass, like aldehydes, ketones, esters, hydrocarbons, alcohols and ethers, are very soluble.
 - Fatty acids are poorly soluble but their esterification significantly increases their solubility.
 - Alkaloids, phenols, carotenoids, proteins, sugars and most anilines have a low solubility (Stahl and Schiltz 1978).
 - Chlorophyll, amino acids have very low solubility (Stahl and Schiltz 1978) and most inorganic salts are insoluble.
 - For compounds of similar chemical properties, the solubility decreases with the molecular mass.
 - Adding a polar group, especially carbonyl and hydroxyl, amine or double bond reduces the solubility (Wong and Johnston 1986).
- b) In contact with an aqueous phase, pressurized CO₂ generates carbonic acid (H₂CO₃) in the latter and pH values can reach 2.85 (Toews et al. 1995). This pH modification may be unfavourable, for example, in the case of biocatalytic reactions because many enzymes are less active in low pH environment. These low pH values are obtained at relatively low pressure (20 to 30 bar). Pressure allows for modulating the value from below 3 to neutral. This acidification is thus reversible by returning to atmospheric pressure. This may be advantageously utilized to acidify an aqueous phase without subsequently the need to use a base for neutralization. This is a very seldom used property while it provides a reversible low-cost acidifying agent which obeys the concept of sustainable development. For instance, based on this pH modulation, a process for fractionation of whey proteins has been proposed (Bonnaillie and Tomasula 2012) and also an improvement in the process for tanning leather (Renner et al. 2012).

The Main Areas of Application

Solvents are widely used in industry (chemistry, cleaning, vegetal or mineral extraction, elaboration of materials...) and this wide spectrum also corresponds to potential applications of supercritical fluids. Their classification in three main areas is shown in Fig. 4.

The use of these fluids as solvents for chemical reactions (including enzymatic and electrochemical reactions) has been the least explored but is very promising in view of developing clean (if CO₂ is used) and intensified chemical processes. The whole process (raw material preparation–reaction–purification) can be designed around the use of a supercritical fluid.

Extraction from Solids and Liquids

Historically, the first area to be developed, up to heavy-duty industrial applications, was extraction from vegetal matter. Nowadays, a significant part of decaffeinated coffee is industrially produced by extracting caffeine using supercritical CO₂ (Zosel 1980).

The supercritical extraction processes can be batch-type, for solid processing, or continuous in the case of liquid processing.

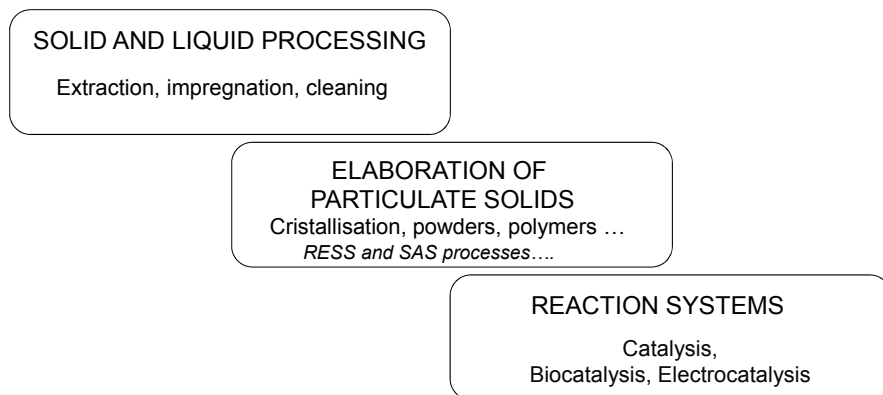


Figure 4. Main areas for SCF applications.

Extraction from Solids

Overview and Economics

Extracting products of interest from solids using supercritical fluids has been developed on an industrial scale for over thirty years in many industrial areas: chemical, food, pharmacy and biotechnology. In the food industry, especially with the use of supercritical carbon dioxide, large scale industrial plants are in operation, such as the decaffeination of coffee (autoclave > 20 m³) (Brunner 2005) and extraction of bitter hop fractions (autoclave ~ 5 m³). The Maxwell Company (USA) is exploiting a patented quasi-continuous process for producing 25,000 tons per year of decaffeinated coffee. On a smaller scale, there are extraction and concentration of essential oils, oleoresins and other value-added products derived from plants and spices as well as the extraction of pesticides from plants.

Other applications (Akgermann and Madras 1994) have been developed in the field of pollution control: Soil remediation, regeneration of adsorbents or catalysts and purification of polymers. These applications are in fact ‘cleaning’ applications rather than extractions. The process is physically the same and is scientifically processed in the same way but the product of interest is the solid residue in the extractor. This makes a great difference when considering the economics of the process because there are two key constraints for economically viable applications of supercritical extraction:

- i) considering a high added value product,
- ii) which is present at a sufficiently high concentration in the raw material. Cleaning applications satisfy *de facto* the second constraint. So for cleaning or purification applications, 1 kg processed = 1 kg of final product. A striking example is the decaffeination of coffee which is really purification of coffee and not extraction

of caffeine, which is in fact only a valuable co-product. Some other industrial examples, such as processing of cork stoppers (Oeneo Bouchage Company) (Lumia et al. 2001) or delipidation of bone implants (Biobank Company) (Fages et al. 1994) can also be quoted.

Another related process is impregnation using supercritical CO₂. Such process uses the same principle as extraction but in the reverse way: the CO₂ dissolves a solute and brings it inside a solid matrix where it is left after changing pressure and temperature conditions. Note, however, that some specificity does not allow direct transposition; especially concerning the deposition step and homogeneity of the processed matter which is crucial in certain applications (dyeing for instance). Impregnation also obeys the above mentioned economic law (1 kg processed = 1 kg of final product) and, for example, impregnation of wood with biocide has reached industrial levels (the SUPERWOOD process, Kjellow and Henriksen 2009). Another example of impregnation concerns the dyeing of textiles where industrialisation started a few years ago, as illustrated by the development of the recent company DyeCoo Textile Systems (The Netherlands). This promising application eliminates large quantities of aqueous effluent which handicap the conventional water process. More information about this new dyeing processes can be found in the works of Bach (Bach et al. 2002).

The economics of supercritical processes is often said to be difficult to evaluate. It is true that it is not easy to give realistic and accurate values to assess the cost of manufacturing (COM) of a supercritical extraction, cleaning or impregnation process. In fact, with vegetal extraction, the COM has to be computed for each product associated with its raw material. Such computations are sometimes done in scientific articles (see for example the numerous works of the of the Meireles team (Meireles 2003; Rosa and Meireles 2005)). For rough estimations, the cost of processing on an industrial scale of 1 kg of raw material has been proposed in the range of 0.5–1 €/kg of raw material (Brunner 2005; Lack and Seidlitz 2001). This value corresponds to semi-continuous processing of the solid and significant reduction is expected if a reliable technological solution for continuous processing of solids is provided. Finally, it is noticeable that small units achieve significantly higher COM than industrial plants, mainly because the cost of labour and the cost of investment are not favourable for small units. For example, Perrut has indicated that the investment cost increases roughly only as the square root of the plant capacity, a situation that obviously disfavors small units (Perrut 2005).

Physical Description of the Extraction Process

The extraction of solutes from the solid matrix depends on several mechanisms:

- Simple dissolution of the solute in the supercritical solvent (no solvent-matrix interaction).
- Presence of solute-matrix interaction: desorption process.
- Possible swelling of the solid phase or change in the texture of the solid.

- Reactive extraction, insoluble solute reacts with the solvent to give soluble compounds.
- Mass transfer phenomena, either inside the solid or at the solid surface.

During the supercritical extraction, the solid matrix is continuously in contact with the supercritical solvent. In most cases the solid is a fixed bed of particles. The process takes place in two stages: extraction of solutes and supercritical solvent-solute separation.

One main characteristic of extracting vegetal matter with supercritical CO₂ is that CO₂ is not a good solvent for most of the targeted solutes. Increasing the pressure (up to 1,000 bar) or adding a co-solvent may significantly increase solubility. For instance, solubility of triglycerides in pure CO₂ varies, depending on the pressure from a few g/L to 20 g/L. Nevertheless, such a solvent would not have been envisaged in a conventional approach of liquid–solid extraction because it implies a high solvent to raw material ratio but all of the previously mentioned advantages of CO₂ compensate for this drawback. As a consequence it is very common that extraction kinetics exhibit (at least at the beginning) a solubility limitation where the CO₂ exiting from the extractor is saturated. In this case pressure and temperature can have a great influence. Conversely, in conventional liquid–solid extraction, kinetics is most of the time limited by diffusion of the solute inside the solid particles.

From a few experiments on a laboratory scale, modelling gives better understanding of the physical phenomena and so provides clues in determining the optimal operating conditions for extraction. Also, a great interest of modelling is to derive adequate extrapolation rules to design an industrial plant. Numerous works have attempted to propose complete modelling of the extraction kinetics and a good overview for oil seeds can be found in Del Valle and De La Fuente 2006. Also note a very useful, simplified approach proposed by Sovova (Sovova 2012).

Purification of Liquids

Supercritical fluids can also be used for purifying liquid similarly to liquid–liquid extraction: the liquid to be processed and the supercritical fluid are counter-currently contacted in a high pressure packed column. Production of polyunsaturated fatty acids is, for example, a prime target for this technology. Especially, (n-3)polyunsaturated fatty acids present in fish oil and in certain plants are now attracting great interest since epidemiological studies have demonstrated a positive correlation between the incidence of cardiovascular diseases, such as atherosclerosis, thrombosis, and daily food intake of fish. However, polyunsaturated fatty acids are thermally or chemically sensitive compounds and soft fractionation conditions must be used. This is why supercritical preparative chromatography (Barth 2004) and supercritical fractionation (Brunner 2009) are good candidates. The suitable supercritical fluid in this case is carbon dioxide because of its lack of toxicity and its solvent properties in respect to fatty acid ethyl esters.

Industrial applications for fractionation of the ethyl esters of n-3 fatty acids have also been developed (Riha and Brunner 2000) as well as for tocopherol enrichment (Fang et al. 2007). There are other potential applications: water-ethanol separation

(Schatz et al. 2008), deterpenation of lemon oils (Danielski et al. 2008), and deacidification of edible oil (Zacchi et al. 2008).

Generation of Particulate Solids

Particulate solids can be obtained using very specific technologies based on the properties of supercritical fluids. Such powders have attracted great interest, especially for drug formulation, because of their unique properties (in terms of size distribution and structure). However, this interest has not really been materialized on an industrial scale, very likely because of the difficulty in handling these powders on a large scale. Technologically speaking, many methods have been proposed and a very good overview can be found in Jung and Perrut (2000). The main principles are given below.

The solvent processes. The principle of the method “Rapid Expansion of Supercritical Solutions” (RESS) is to dissolve the compound of interest in supercritical carbon dioxide and then achieve rapid expansion through a nozzle. Thus, carbon dioxide loses its solvent power and the dissolved compound precipitates. Because of the specific physico-chemical properties (viscosity, diffusivity...), micro- or nanoparticles with a very narrow distribution of sizes can be produced. About a hundred substances have been micronized using this process: caffeine, cholesterol, phytosterols, lecithin, tocopherol, β -carotene, salicylic acid, aspirin, and in the field of polymers, polylactide, polymethylmethacrylate ... The major drawback of this method arises from the very low solubility of many products in supercritical carbon dioxide and this has contributed to the development of complementary methods as described in the next paragraph.

The “anti-solvent” processes. Another method is the “Supercritical Anti-Solvent” process (SAS), which processes solutes that are not soluble in supercritical CO₂. The solute is dissolved in a conventional solvent and the solution is contacted with the supercritical fluid, usually by nozzle pulverization into a vessel containing supercritical CO₂. The supercritical fluid dissolves the conventional solvent droplets and the solute precipitates as nano- or microparticles. There are variants of the anti-solvent process depending essentially on the manner the solvent and anti-solvent are contacted. Despite the complexity, this process has the greatest potential for development on an industrial scale. However, residual solvent elimination from the processed particles is often very difficult, especially when non-volatile solvents are used.

The “Particles from Gas Saturated Solutions” (PGSS) processes. Some substances have the property of being able to dissolve large quantities of supercritical fluid. For instance, certain oils can dissolve about 30% (by weight) of CO₂ at a pressure of about 100 bar. This solution, saturated with the supercritical fluid, is then sprayed through a nozzle into an expansion chamber. About a hundred substances in the food (Weidner 2009) or in the polymer industry (Reverchon et al. 2009) were micronized using this process.

Supercritical Media for Chemical Reaction

Organic solvents are commonly used to perform chemical reactions but there is increased interest in considering their replacement with supercritical CO₂. As already mentioned, it is a “natural” compound whose contact with products is considered as completely safe (while conventional purification steps of reaction products often aim at chasing the last traces of organic solvent, especially in the food and health industry).

Indeed, an adjustable reaction solvent (as was mentioned in Table 2) is very attractive because the so-called “solvent effect” upon a chemical reaction can be easily adjusted. In addition, the “cluster” effect, that we already mentioned (a significant increase of the local density around solute molecules) provides another adjustment tool for kinetics and selectivity of the reactions (Baiker and Wandeler 2000). However, these phenomena are still too poorly understood to be mastered and research studies are still needed in this field. The most interesting effects on the overall productivity of a chemical transformation occur especially when operating with multiphase systems, as when using a catalyst deposited onto a porous solid support. With a supercritical solvent, the diffusion within the porous structure is facilitated. Also, with reactions involving a gas and a liquid, the complete miscibility of the gas can be used to implement a single-phase reaction system in which gas and liquid substrates are dissolved, thereby completely eliminating the gas-liquid transfer limitations. For example, supercritical CO₂ or propane were the first alternative methods proposed for the hydrogenation of oils (Van den Hark et al. 1999; Van den Hark and Härröd 2001).

However, although the first idea was to obtain a single phase reaction medium, recently it was proposed to operate in a biphasic system, involving a “light” CO₂-rich phase and a liquid phase containing a significant proportion of CO₂. Operation in such systems, called GELs (Gas Expanded Liquids, Nunes da Ponte 2009) or CLXs (CO₂ Expanded Liquids, Kerler et al. 2004) can be done at lower pressures and with higher concentrations of reagents. The name “expanded liquid” arises from the fact that, in contact with pressurized CO₂, a dramatic increase of the volume of the liquid phase may be observed (multiplied by 2 or more). The interest then lies in the fact that the amount of CO₂ dissolved in the liquid phase favourably modifies its properties. In particular, the viscosity is reduced, and therefore the diffusion phenomena are favoured. But the main effect, in a gas-liquid reaction, is the large increase of solubility of the gaseous substrate in the expanded liquid phase. These systems do not achieve total removal of the organic solvent in the process, but significantly reduce the involved quantities. In such biphasic systems, it is easy to understand that good knowledge of the phase equilibrium is an important asset in understanding and controlling the reaction. Moreover, the complexity of the phenomenon is increased due to the changing properties of the reaction medium during the course of the reaction (Pereda et al. 2009).

The use of supercritical fluids as a reaction media extends beyond traditional chemistry (with or without a catalyst). Thus, applications have also been proposed in the field of enzymatic synthesis, in particular the use of lipases (Marty et al. 1994; Lozano 2010) where the natural character of the enzyme catalyst combines perfectly

with the use of supercritical CO₂. In the case of enzyme catalysts immobilized on a solid support, it has been shown that the equilibrium distribution of a small amount of water between the supercritical CO₂ and the solid support played a crucial role for the kinetics of these reactions (Condoret et al. 1997). Electrochemical syntheses were also considered (Abbott and Harper 1996) but, with CO₂, such methods are severely handicapped by the low electrical conductivity of supercritical CO₂ and only operating in GELs proved to be effective (Chanfreau et al. 2008) in this case.

General Architecture of a Supercritical Process

Description of the Process and Technology

Described below is the process for extracting solutes from a solid raw material with a supercritical fluid. However, the architecture presented here can also be used for a reaction process or for most processes using a supercritical fluid. In an extraction process from a solid material, the extraction step is carried out in a high-pressure vessel. In fact, the solid to be processed, usually in the form of a fixed bed of particles, is percolated by the supercritical fluid, up to exhausting the compound to be extracted. Then the process is stopped and the vessel is decompressed. After discharge, a load of fresh solid is reinserted into the vessel, which is again pressurised to start a new process. So far, no reliable technology for continuously introducing solid pressure in a high pressure vessel has been proposed, and it is also one of the weaknesses of this technology because it reduces productivity. Nevertheless, the use of several extraction vessels, where one is under pressure while the others are in the discharge or loading step, makes it possible to mimic a continuous process. When several vessels are used, it is possible to operate them according to the concept of simulated moving bed so that CO₂ issuing from the final extractor is almost saturated in all process phases. Moreover, processed feed unloading and fresh feed loading can be operated without stopping the extraction process. In processing a liquid, where counter-current packed columns are generally used, the architecture of the cycle is the same, but they are operated continuously because the liquid to be processed may be easily inserted and removed under pressure in the fluid-liquid contactor using conventional high pressure pumps.

Specific high pressure equipment (up to 700 bar) is available on an industrial scale, ranging from a few litres to several hundred litres. For extraction and reaction, specialized manufacturers offer complete systems, including the recycling of the solvent. In Europe, the main manufacturers are Separex, Uhde, Sitec, Natex and Top Industrie. The complete cycle of the supercritical fluid is shown in Fig. 5 (here is the most common configuration that uses depressurization for separation of the extract). Three zones are identified:

- i) The zone where the fluid is in supercritical state and where the desired operation is carried out (extraction, reaction, impregnation...).
- ii) The separation zone where the products are recovered and almost pure fluid is obtained.

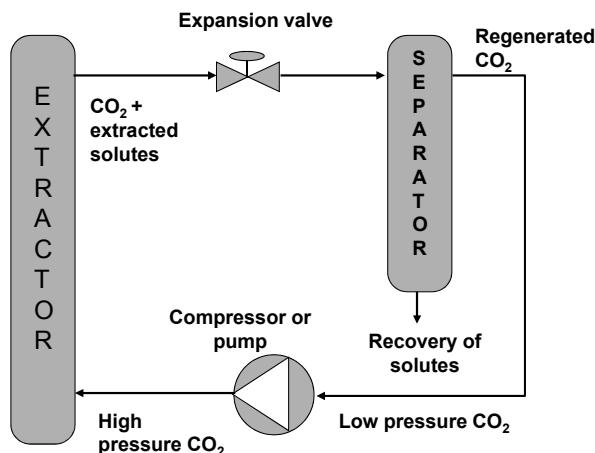


Figure 5. General architecture of a SCF process.

- iii) The recirculation zone where the fluid is delivered in a supercritical state to start a new cycle. In pilot and large scale units, it is necessary to reheat the fluid after the expansion valve.

In the separation zone, the solvent power of the fluid is changed, either by depressurization (Fig. 6a), or by a change in temperature (Fig. 6b), or by using an additional component (Fig. 6c), so as to recover the compound of interest.

In systems using depressurization (Fig. 6a), which are the most common, several depressurization steps can be used. This may allow performing pre-fractionation of complex mixtures issued from the extractor (Marty et al. 1994). Indeed, it is possible, with an optimized choice of temperatures and pressures in the separators, to selectively recover a target compound in each of the separators. In addition, this procedure avoids operating in the two-phase region, i.e., where the presence of liquid CO_2 may be detrimental to the efficiency of the mechanical separation of the two-phase mixture. In the case of a cycle with a single depressurization step (Fig. 7a), or three depressurization steps (Fig. 7b), the thermodynamic path of CO_2 is drawn in the

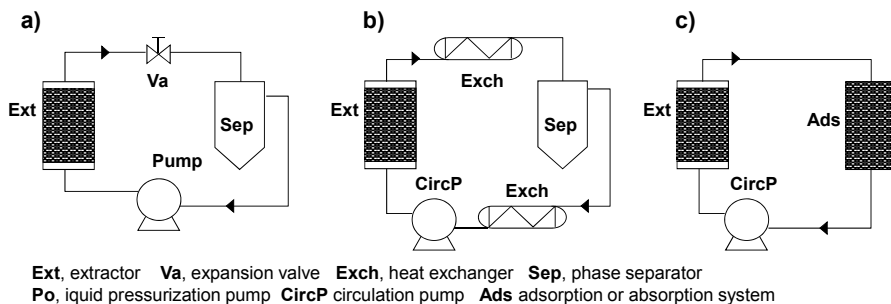


Figure 6. Different principles of operating the separation zone: (a) by depressurization (b) by temperature change (c) by using a solid or liquid additional component (adsorption or absorption).

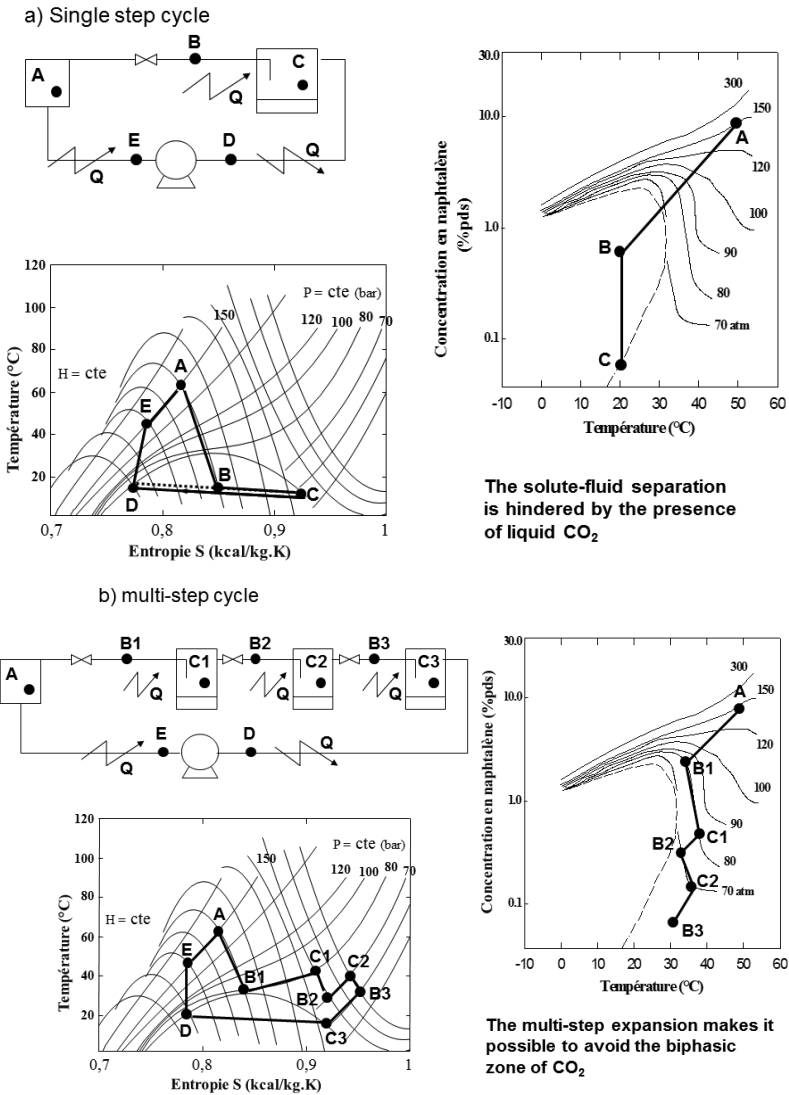


Figure 7. Thermodynamic path of CO₂ in a process with liquid pumping and depressurization/reheating (a) single step cycle (b) multi-step cycle.

Temperature-Entropy diagram. The variation of the solubility of a compound (here, for example, naphthalene) is shown all along the cycle and zones of low solubility where precipitation of solutes in the separators occurs. However, it is often necessary to take into account the imperfect mechanical separation of the two-phase mixture in the separators (Camy and Condoret 2001; Takeuchi et al. 2008) and technologies such as cyclone separators have been proposed to overcome this drawback.

The principle of separation using a temperature change (Fig. 6b) is less frequent. It is usually done by heating the fluid which results in lowering the density and

consequently a drop in solvent power. This behaviour, called “retrograde solubility”, is specific to supercritical fluids and occurs in a well-defined temperature and pressure range which depends on the solute-solvent couple. Its application is not universal.

The separation using an additional component (Fig. 6c) is, for example, used in the extraction of caffeine from green coffee beans. The effluent from the extractor, the supercritical CO₂ containing caffeine, is contacted with water in a high pressure counter-current column to achieve a fluid-liquid extraction. Caffeine, recovered in the aqueous effluent from this column is then separated from the aqueous phase by distillation. For the same application, adsorption on charcoal was also proposed (Zosel 1980). Note that in the case of an additional component, a further separation step for regenerating the additional component is always necessary.

The main interest of these two last principles, temperature changes or using an additional component, is to avoid the re-pressurization step and is recommended. Nevertheless, for small scale operations, the separation by depressurization remains the most convenient one.

In separation by depressurization, after recovering the component of interest in the separation zone, two methods for recycling the fluid are possible:

- i) Condensation of the CO₂ gas phase issued from separators, pressurizing the liquid phase with a pump, then heating the pressurized liquid phase,
- ii) Direct pressurization of the CO₂ gas phase issued from separators, generally followed by cooling up to the targeted extraction temperature.

Pumping the liquid phase is more convenient for small plants because a pump requires less maintenance and investment than a gas compressor. However, in heavy-duty industrial facilities, gas compression systems are often used. From an exergetic analysis of the cycle, Smith et al. 1999 have identified the conditions for pressure and temperature where the optimum recommends either the use of a compressor or a liquid pump (Fig. 8).

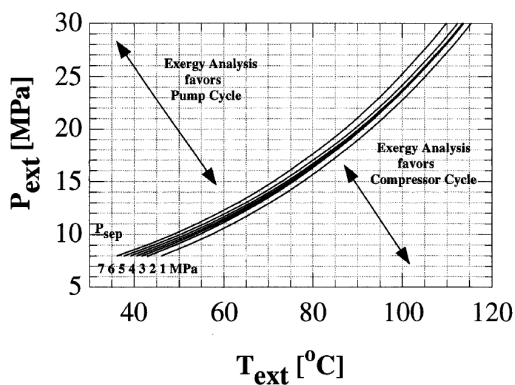


Figure 8. Choice of the technology for pressurization, in terms of exergetic criterion of the solvent cycle. P_{ext} and T_{ext} are the pressure and the temperature of the high-pressure vessel. Computations were done for different separator pressures (from Smith et al. 1999).

Description of the Thermodynamic Cycle and Energy Calculations

Within the framework of sustainable processes, new technology must be assessed in terms of energetic efficiency. For CO₂ as the supercritical fluid, energy calculations can be easily done, in a first approach, by considering the cycle of pure CO₂. In general, solutes are sufficiently dilute and this approach is quite acceptable. A thermodynamic phase diagram can be used (for example, Temperature-Entropy or Enthalpy-Temperature) or more accurate calculations can be done using an equation of state (Peng-Robinson or Redlich-Kwong, for example). Data can also be obtained from the website of the National Institute of Standards and Technology (<http://webbook.nist.gov/chemistry/name-ser.html>).

For the most common cycle, with single step depressurization/reheating and liquid pumping, some values can be given that set the order of magnitude for usual operating conditions. For example (details of the calculation can be found in Clifford 1999) for extraction at 200 bar and 47°C, with 100 kg/h CO₂ flow rate, the energy required for pumping (liquid pressurization at -3°C) is approximately 400 W, and preheating until the temperature of extraction requires a heat power of about 2,400 W. The heat power for maintaining the separator at 47°C is approximately 5,400 W. For condensation and sub-cooling of CO₂ to a temperature of -3°C (to ensure no cavitation at the pump), a cooling power of about 8,700 W is required.

A comparative study of the extraction process of aromatic hop fractions using an organic solvent or supercritical CO₂ was carried out by Sievers and Eggers 1996. These authors have shown that a supercritical CO₂ process where the separation is achieved by depressurization becomes energetically competitive if the refrigeration machine for the CO₂ condensation is adapted as a heat pump operating between the condenser and the process heat exchangers.

Thermodynamics of Mixtures under High Pressure

Successful development of supercritical processes is largely based upon knowledge of solubility of compounds in supercritical solvents or high pressure phase diagram. Such knowledge provides useful information, as, for example, in an extraction process, the solvent capacity of the supercritical fluid together with its evolution with pressure and temperature. Also the number and composition of phases present in a reactor, depending on the operating conditions and conversion rate of the reaction, can be predicted, as well as partitioning a solute between phases in a fractionation process. Although computational methods and predictive thermodynamic models have recently seen significant progress, the need for experimental data is often still compulsory and a great number of high-pressure fluid-phase equilibria have been studied in the last years (Fonseca et al. 2011). So, effort has been made to develop experimental set-up and methods to obtain accurate and reliable data. In many cases, these data are used to adjust parameters of specific thermodynamic models. These models make it possible to extend the range of application and provide more convenient use. Such adapted models are more reliable than purely predictive models.

Experimental Methods

Experimental methods for studying high pressure phase equilibria or solid solubility can be divided into two groups according to the method for determining the composition phases. A complete review of experimental methods is proposed by Dohrn et al. 2012.

Synthetic methods are based on the preparation of a mixture of accurately known composition whose behaviour is observed in a high pressure cell. Required equipment is usually simpler than the one used for analytical methods, especially when simple visual observation is envisaged. As shown in Fig. 9, the set-up generally comprises a variable volume cell fitted with sapphire windows through which phase transitions are visually detected. When the mixture is inside the cell, temperature and pressure are generally adjusted so that the mixture is single phase. Then, temperature or pressure is varied until the occurrence of a second phase. Phase transitions are generally detected visually but various automatic detection methods, based on acoustic or optical measurements have also been developed (Ke et al. 2010). The main challenge of this method is the accurate preparation of the mixture to be introduced inside the cell. Moreover, it is mostly dedicated to the study of binary systems with non-negligible mutual solubility and for which phase diagrams are moderately influenced by composition. Because of the relative simplicity of the method, many types of apparatus have been developed and numerous liquid-fluid mixtures with very different properties and behaviour have been studied, as for example, mixtures of CO₂ and ethyl esters of eicosapentaenoic acid (C20: 5 (n-3)) and acid docosahexaenoic (C22: 6 (n-3)) (Jaubert et al. 2001) or mixtures of CO₂ and NO₂/N₂O₄ (Camy et al. 2011). Such synthetic methods may be suitable to study the solubility of solids, provided that the solubility is significant. Measurements of cloud points of polymers in supercritical CO₂ have also been successfully performed with this method (Stoychev et al. 2012; Girard et al. 2013).

Analytical methods are based on measuring the compositions of the co-existing phases at equilibrium. This can be done by sampling each phase and analysing them

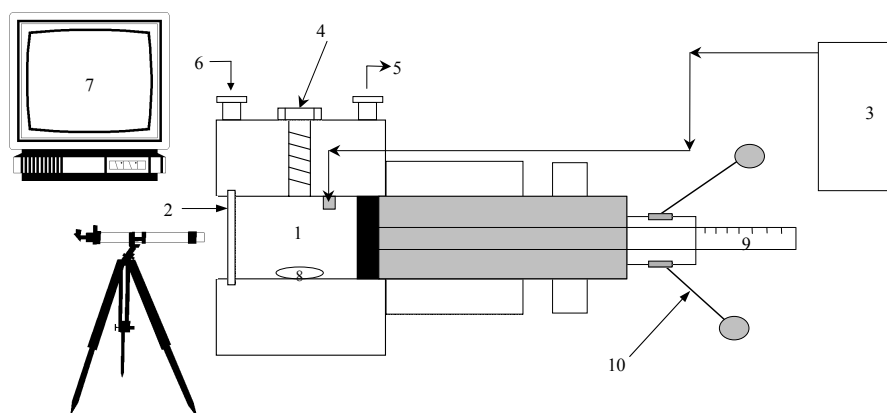


Figure 9. Scheme of the high pressure cell with variable volume (1.7 à 12.4 cm³) from Top Industrie (France). (1) cell; (2) sapphire window; (3) CO₂ tank; (4) closing plug; (5) and (6) heating fluid; (7) screen connected to video camera; (8) magnetic stirrer; (9) graduated piston; (10) piston handles.

outside the equilibrium cell by chromatographic methods (HPLC, gas chromatography or supercritical chromatography) or thanks to *in situ* analytical techniques such as spectroscopy (Raman, UV-vis, IR, NMR). Recirculating phases is sometimes operated to achieve faster equilibration. Analytical methods are particularly useful in a mixture with more than two components (Arenas-Quevedo et al. 2013) but this kind of method is complex to perform and perturbation of the equilibrium is very probable when sampling co-existing phases. In comparison, the advantage of *in situ* spectroscopic assays arises from their rapidity and absence of perturbation because sampling is not required. However, finding a method to accurately quantify the various compounds of the system and calibrating the methods remains a challenge. Medina-Gonzalez et al. (2013) used non-intrusive FT-IR spectroscopy to study mutual solubility of glycerol and CO₂ as a function of pressure in the temperature range from 40 to 200°C, as shown on Fig. 10. In this system with very low mutual solubility, FT-IR spectroscopy was shown to give accurate and reproducible results.

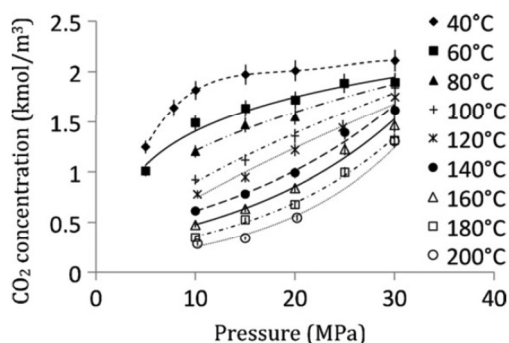


Figure 10. Solubility of CO₂ in glycerol as a function of pressure at T = 40–200°C. Lines have been added to guide the eye. (From Medina-Gonzalez et al. 2013).

The analytical method with an equilibrium cell can be used to determine the solubility of solids (or non-volatile compounds) in supercritical fluids. In this case an excess quantity of solid is put inside the cell in contact with the fluid at a fixed temperature and pressure and the equilibrium fluid phase is sampled for analysis. However, in the case of low solubility solutes, dynamic-type apparatus are generally more adequate. They comprise an equilibrium cell previously filled with the solid to be solubilised and continuously fed with the supercritical solvent. The solute extracted by the solvent is trapped at the cell outlet. Simple computation from the amount collected, the flow-rate and the experiment duration yields the value of solubility. For example, in the context of developing textile dyeing in supercritical CO₂, understanding the solubility of dye molecules is crucial. Based on the method developed by Lin et al. 2001, Kerdoud (Kerdoud 2005) measured the solubility of several dyes using the dynamic method, the solubility being determined by the difference in mass between the load and the residue (gravimetric determination of the solubility). Such measurements are impeded by the very low solubility of dyes. In Fig. 11, the value at the plateau gives the value of the solubility, in that case a molar fraction equal to $3 \cdot 10^{-5}$, which corresponds to a concentration of dye equal to $178 \text{ mg} \cdot \text{L}^{-1}$.

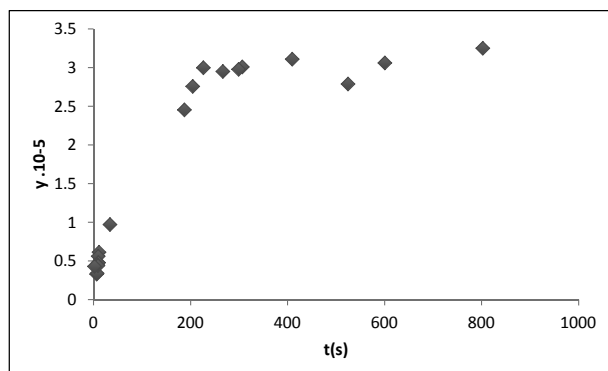


Figure 11. Evolution of the molar fraction of the pure red dye 82 (CI 11140, red Terasil 3BL) in supercritical CO₂ (80°C, 200 bar) in respect to contact time $\tau = m/F$ (m = mass of dye in the extractor, F = CO₂ mass flow rate) from Kerdoud 2005.

The study of the impregnation of salicylic acid into polymethyl methacrylate using supercritical CO₂ has been studied through sampling the supercritical phase in a closed, stirred reactor with (solubility measurement) or without the presence of polymers (impregnation measurement) (Diankov et al. 2007).

Behaviour and Estimation of Solubility of Liquids and Solids in Supercritical CO₂

In supercritical processes, compounds of interest are characterized by their molecular size, vapour pressure and critical properties that are very different from supercritical CO₂ properties. Solubility of these solutes in supercritical CO₂, and also its variation with temperature and pressure, is very important to be understood. However, supercritical systems exhibit complex thermodynamic behaviour that may not obey conventional intuition. Indeed, if the increase in pressure always leads to an increase in the solubility of a compound, an increase in temperature in a given pressure range, may cause a significant decrease of the solubility. This corresponds to the phenomenon called “retrograde solubility” (which was already mentioned in the description of the various methods for recovering extracts) where lowering the density of the solvent is not counter-balanced by the increase of the vapour pressure of the solute. In fact, to understand solubility variation with pressure and temperature, the relevant parameter is the density of the fluid. So when iso-density solubility curves are drawn (corresponding to variable pressure) solubility is always increasing with temperature. This is shown on Fig. 12 for solubility of caffeine in CO₂. Although the solubility of caffeine is low in supercritical carbon dioxide, it could be measured by UV-visible spectroscopy (Ebell and Franck 1984). These measurements were performed in the temperature range 50°C–160°C and pressures range 70 to 200 bar.

Considering the solubility-solvent density log-log linear relationship, specific semi-empirical correlations have been established, in particular by Chrastil 1982. Chrastil showed that the solubility can be related to solvent density by the relation:

$$\ln C = k \ln \rho + \frac{a}{T} + b \quad (1)$$

with:

C	:	concentration of the solid in the supercritical fluid (g/L)
k	:	association number = number of CO ₂ molecules around the solute molecule
ρ	:	density of the supercritical fluid (g/L)
T	:	equilibrium temperature (K)
a and b	:	empirical constants depending on solute

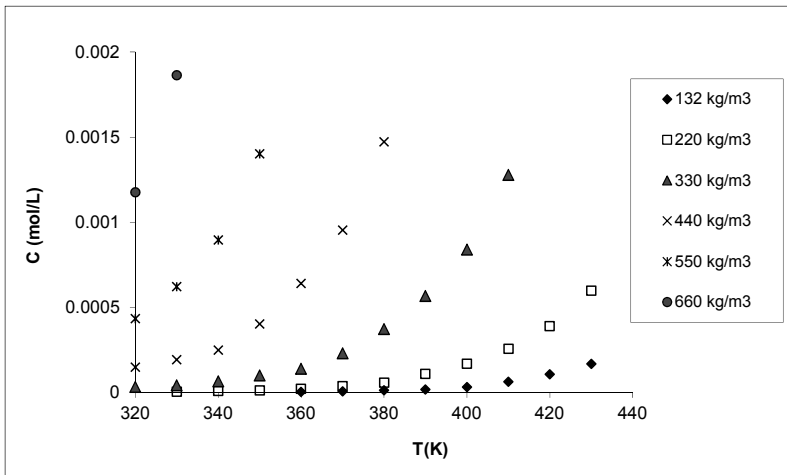


Figure 12. Solubility of caffeine at different densities of supercritical CO₂ (Ebell and Franck 1984).

The parameters k , a and b are obtained by fitting experimental data. Due to its simplicity, a variety of experimental data of solubility in supercritical CO₂ (mainly fatty acids, triglycerides and sterols), have been successfully correlated by the Chrastil's equation or its modified versions.

Although convenient to predict solubility of some compounds, these kind of empirical correlations are not able to predict complete fluid phase equilibria, which are essential data to understand the behaviour of multi-component systems (solid-fluid, liquid-liquid or liquid-liquid-liquid), involved in processes such as chemical reactions or liquid fractionation.

Phase Diagram of Binary Mixtures

Most binary systems can be described using the classification of Van Konynenburg and Scott 1980 which describes five types of behaviour (which are not detailed here). Phase diagrams of type I and II are the simplest where the critical point line is continuous and connects the critical points of pure substances. This configuration is very common, especially when the two components of the mixture have similar volatility. Note that systems can exhibit discontinuous critical point line or that this

line does not connect the critical points of pure substances. A good overview of the thermodynamics of high pressure systems can be found in Brunner 1994.

Modelling of binary and multi-component high pressure fluid phase equilibria and mixture properties is still required for future development of environmental benign processes based on the use of supercritical fluids. Considering the atypical behaviour of mixtures in the vicinity of their critical point, and the possible strong asymmetry of molecules, modelling of phase equilibrium is often complex.

Classically, for vapour liquid systems, the condition of equilibrium at given temperature and pressure is written in terms of equality of fugacities of compounds, f_i , in each phase:

$$f_i^L(T, P, x) = f_i^V(T, P, y) \quad (2)$$

Considering the high pressure, the most common and suitable way to solve this equation is to use a cubic equation of state such as the well-known two parameter Peng-Robinson or Soave-Redlich-Kwong equations of state (EoS) to calculate fugacity coefficients Φ_i^L and Φ_i^V , which corresponds to the generally called Φ - Φ approach. The equation to be solved is thus:

$$x_i \cdot \Phi_i^L(T, P, x) = y_i \cdot \Phi_i^V(T, P, y) \quad (3)$$

When applied for mixtures, cubic equations of state must be used with a proper mixing rule, taking into account parameters of pure components, so that binary interaction parameters represent specific interactions between components. Classical van der Waals one-fluid mixing rules are generally used to calculate the two EoS parameters:

$$a(T) = \sum_{i=1}^n \sum_{j=1}^n z_i z_j \sqrt{a_i a_j} (1 - k_{ij}) \quad (4)$$

$$b = \sum_{i=1}^n z_i b_i \quad (5)$$

One binary interaction parameter (namely k_{ij}) is generally used, although in some specific cases with complex interactions, especially solid-fluid equilibria, a second parameter (l_{ij}) may be introduced for calculating the co-volume (b) in equation 5. Experimental data are necessary to adjust binary interaction parameter(s). Specific predictive approaches have been developed such as the PPR78 model (Predictive Peng Robinson 78) where binary interaction parameters can be obtained using a group contribution method. Experimental data can be successfully represented by this model as shown for example on Fig. 13, for the system CO₂-m-xylene (Vitu 2007).

Note that cubic equation of state with classical mixing rules generally fails when one or several polar compounds are present in the system. In that case, equations of state can be combined with activity coefficient models (such as for example the well-known UNIQUAC, NRTL or UNIFAC models) through specific mixing rules (namely Huron-Vidal, Wong-Sandler, MHV1, MHV2, PSRK,) via the so-called

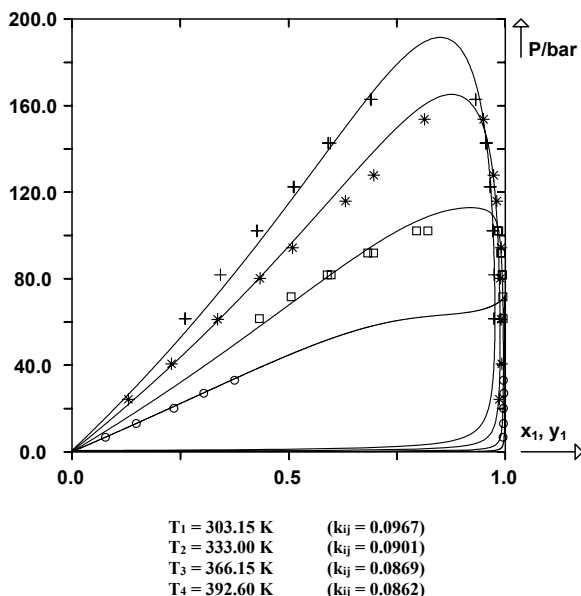


Figure 13. Bubble and dew curves and their modelling using PPR78 for the system CO₂(1) – m-xylene (2) (Vitu 2007).

EoS/G^E approach. For example, with PSRK and MHV2 mixing rules, the mixture parameters are obtained from:

$$q_1 \left(\alpha - \sum_i z_i \alpha_i \right) + q_2 \left(\alpha^2 - \sum_i z_i \alpha_i^2 \right) = \frac{g_0^E}{RT} + \sum_i z_i \ln \left(\frac{b_i}{b} \right) \quad (6)$$

$$\alpha = \frac{a}{bRT} \quad (7)$$

$$\alpha_i = \frac{a_i}{b_i RT} \quad (8)$$

where a_i and b_i are parameters for pure components, obtained from critical coordinates and the acentric factor, and b is obtained from (5). If equation (6) is used with the Peng-Robinson equation of state, then $q_1 = 0.64663$ and $q_2 = 0$ for the PSRK model (explicit calculation of α) and $q_1 = -0.4347$ and $q_2 = -0.003654$ for the MHV2 model (implicit calculation of α). Then a model for activity coefficients has to be chosen to determine the value of the excess Gibbs energy at zero pressure (reference pressure), g_0^E . Using a predictive model for activity coefficients such as UNIFAC leads to a very interesting predictive way to use cubic equations of state. EoS/G^E approach gives very satisfying results for predicting liquid-vapour equilibria of mixtures containing CO₂ and polar compounds, as seen in Fig. 14 for the CO₂+methanol system, where experimental data are quite well represented with the PR equation of state and MHV2 mixing rules with UNIQUAC model for activity coefficients. Most of the above mentioned mixing rules are now available in process simulators such as Aspen or ProSim Plus.

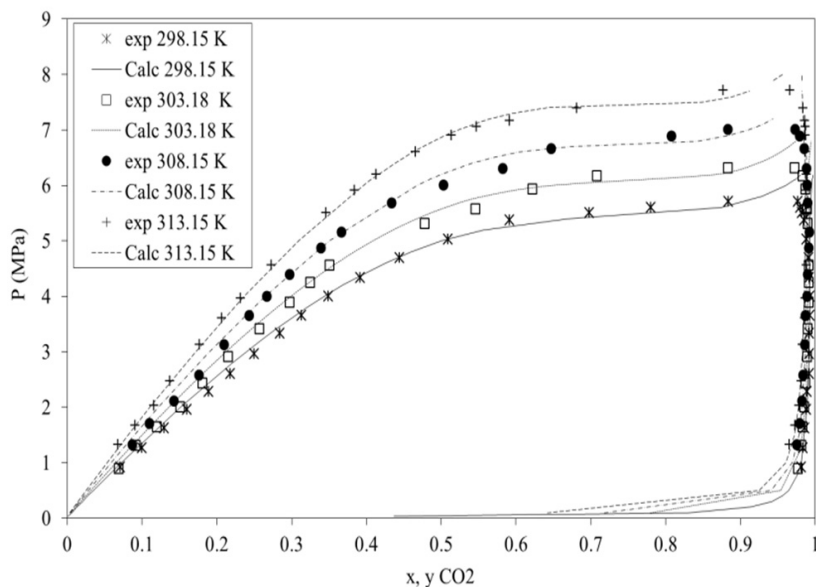


Figure 14. Vapor-liquid equilibria (P - x,y) for the CO_2 -methanol system at different temperatures. Comparison of experimental data (from Chang et al. 1998) and calculated results with PR-MHV2-UNIQUAC model ($A_{\text{CO}_2\text{-methanol}} = 502.12$ cal/mol and $A_{\text{methanol-CO}_2} = 131.71$ cal/mol).

The most recent developments in the domain of thermodynamic models concern the association theories. From these theories, especially from SAFT perturbation theory (Statistical Association Fluid Theory), associating models have been developed that are able to account for associations such as hydrogen bonding in calculating thermodynamic equilibria. Although more complex, such models give interesting results for the mixtures of CO_2 and polar compounds at high pressure. A complete overview of EoS/ G^E mixing rules such as statistical association theories and their range of application can be found in the recent book by Kontogeorgis (Kontogeorgis 2010).

Conclusions and Perspectives

We have shown that the supercritical fluid technology, in the framework of the “Green Process Engineering”, is preferably implemented by using carbon dioxide. This can be confusing because it is sometimes difficult to evaluate if the advantage of this technology arises from the specific properties of the supercritical state or more simply from the properties of CO_2 . Of course the greater advantage is expected from their synergy. But it also means that the use of liquid CO_2 must be systematically considered. Indeed, sometimes it has proved to be more suitable to the problem because liquid CO_2 has the required extraction selectivity, as it is for the decaffeination of roasted coffee beans (Gehring et al. 1984). The same expanded vision must also lead us to envisage the case of two-phase reaction systems (GELs or CLXs as described in paragraph about reaction in SCF) or the possibility of

using a “sustainable development labelled” acidifying agent. Indeed, “CO₂ assisted” processes are ultimately a more universal concept based on the following idea: can we provide an advantage or a solution for a process by introducing a “neutral” component (in the sustainable process sense) such as CO₂? Of course, the price to pay is now to operate the process under pressure, tens to hundreds of bars, but successful examples exist and the list will certainly get longer. The crystallization process by SAS is a prime example, but also the improvement of the membrane process for waste oil regeneration by blending with CO₂ (Rodriguez et al. 2002) as well as extractive reactions coupled with supercritical CO₂ in ionic liquids (Lozano et al. 2006) or glycerol (Delamplé et al. 2010). So, the adventure of “CO₂ assisted” processes, now driven by the need to respect the concepts of sustainable development, has revived the supercritical technology which, after an enthusiastic start in the 80’s, struggled to find its second wind. However, although high pressure technology has nowadays become more accessible in terms of price and convenience, technological developments are still needed. As a final remark, why not dream of a chemical industry where water and CO₂ would be the only solvents in most of the future sustainable processes?

Acknowledgments

The authors would also like to thank Michel Perrut (Separex-France) for his advices and the review of this chapter.

References

- Abbott, A.P. and J.C. Harper. 1996. Electrochemical investigations in supercritical carbon dioxide. *J. Chem. Soc., Faraday Trans.* 92: 3895–3898.
- Akgermann, A. and G. Madras. 1994. Fundamentals of solids extraction by supercritical fluids. *Supercritical Fluids Fundamentals for Application*. Nato. Science Series E. vol. 273. 669–695.
- Arenas-Quevedo, M.G., L.A. Galicia-Luna, O. Elizalde-Solis and J.A. Pérez-Pimienta. 2013. Vapor–liquid equilibrium for the ternary carbon dioxide–ethanol–nonane and decane systems. *Fluid Phase Equilib.* 338: 30–36.
- Bach, E., E. Cleve and E. Shollmeyer. 2002. Past, present and future of supercritical dyeing technology—an overview. *Rev. Prog. Col. Rel. Top.* 32: 88–102.
- Baiker, A. and R. Wandeler. 2000. Supercritical fluids: opportunities in heterogeneous catalysis. *CATTECH.* 4: 128–143.
- Barth, D. 2004. Fractionnement par le dioxyde de carbone supercritique et urée Dossier : Acides gras oméga 3. Sources, extraction, formulation, O.C.L. 11: 131–132.
- Beckman, E.J. 2004. Supercritical and near-critical CO₂ in green chemical synthesis and processing. *J. Supercrit. Fluids.* 28: 121–191.
- Bonnaillie, L. and P. Tomasula. 2012. Fractionation of whey protein isolate with supercritical carbon dioxide to produce enriched α -lactalbumin and β -lactoglobulin food ingredients. *J. Agr. Food Chem.* 60: 5257–5266.
- Brunner, G. 1994. *Gas Extraction*. Springer, New York.
- Brunner, G. 2005. Supercritical fluids: technology and application of food processing. *J. Food Eng.* 67: 21–33.
- Brunner, G. 2009. Counter-current separations. *J. Supercrit. Fluids.* 47: 574–582.
- Camy, S. and J.S. Condoret. 2001. Dynamic modelling of fractionation of a liquid mixture using supercritical CO₂. *Chem. Eng. Process.* 40: 499–509.

- Camy, S., S. Montanari, A. Rattaz, M. Vignon and J.S. Condoret. 2009. Oxidation of cellulose in pressurized carbon dioxide. *J. Supercrit. Fluids*. 51: 188–196.
- Camy, S., J.-J. Letourneau and J.-S. Condoret. 2011. Experimental study of high pressure phase equilibrium of CO₂+NO₂/N₂O₄ mixtures. *J. Chem. Thermodyn.* 43: 1954–1960.
- Carles, P. 2010. A brief review of the thermophysical properties of supercritical fluids. *The Journal of Supercritical Fluids* 53: 2–11.
- Chanfreau, S., P. Cagnet, S. Camy and J.S. Condoret. 2008. Electrocarboxylation in supercritical CO₂ and in CO₂ expanded liquids. *J. Supercrit. Fluids*. 46: 156–162.
- Chang, C.J., K.-L. Chiu and C.-Y. Day. 1998. A new apparatus for the determination of P–x–y diagrams and Henry's constants in high pressure alcohols with critical carbon dioxide. *J. Supercrit. Fluids*. 12: 223–237.
- Chrastil, J. 1982. Solubility of solids and liquids in supercritical gases. *J. Phys. Chem.* 86: 3016–3021.
- Clifford, A. 1999. *Fundamentals of Supercritical Fluids*. Oxford University Press, New York.
- Condoret, J.S., S. Vankan, X. Joulia and A. Marty. 1997. Prediction of water adsorption curves for heterogeneous biocatalysis in organic and supercritical solvents. *Chem. Eng. Sci.* 52: 213–220.
- Danielski, L., G. Brunner, C. Schwänke, C. Zetzl, H. Hense and J. Donoso. 2008. Deterpenation of mandarin (*Citrus reticulata*) peel oils by means of countercurrent multistage extraction and adsorption/desorption with supercritical CO₂. *J. Supercrit. Fluids* 44: 315–324.
- Delample, M., N. Villandier, J.-P. Douliez, S. Camy, J.-S. Condoret, Y. Pouilloux, J. Barrault and F. Jerome. 2010. Glycerol as a cheap, safe and sustainable solvent for the catalytic and regioselective b; b-diarylation of acrylates over palladium nanoparticles. *Green Chem.* 12: 804–808.
- Del Valle, J. and J. De La Fuente. 2006. Supercritical CO₂ extraction of oilseeds: review of kinetics and equilibrium models. *Crit. Rev. Food Sci. Nutr.* 46: 131–160.
- Diankov, S., D. Barth, A. Vega-Gonzalez, L. Pentchev and P. Subra-Paternault. 2007. Impregnation isotherms of hydroxybenzoic acid on PMMA. *J. Supercrit. Fluids*. 41:164–172.
- Dohrn, R., J.M.S. Fonseca and S. Peper. 2012. Experimental Methods for Phase Equilibria at High Pressures, *Annu. Rev. Chem. Biomol. Eng.* 3: 343–367.
- Ebeling, H. and E.U. Franck. 1984. Spectroscopic determination of caffeine solubility in supercritical carbon dioxide. *Ber. Bunsenges. Phys. Chem.* 88: 862–865.
- Fages, J., A. Marty, J.-S. Condoret, D. Combes and P. Frayssinet. 1994. Use of supercritical CO₂ for bone delipidation. *Biomaterials*. 15: 650–656.
- Fages, J., E. Jean, P. Frayssinet, D. Mathon, B. Poirier, A. Autefage and D. Larzul. 1998. Bone allografts and supercritical processing: effects on osteointegration and viral safety. *J. Supercrit. Fluids* 13: 351–356.
- Fang, T., M. Goto, X. Wang, X. Ding, J. Geng, M. Sasaki and T. Hirose. 2007. Separation of natural tocopherols from soybean oil by-product with supercritical carbon dioxide. *J. Supercrit. Fluids*. 40: 50–58.
- Fonseca, J.M.S., R. Dohrn and S. Peper. 2011. High-pressure phase equilibria: experimental methods and systems investigated (2005–2008). *Fluid Phase Equilib.* 300: 1–69.
- Garcia-Gonzalez, L., A.H. Geeraerd, S. Spilimbergo, K. Elst, L. Van Ginneken, J. Deverebe, J.F. Van Impe and F. Devlieghere. 2007. High pressure carbon dioxide inactivation of microorganisms in foods: the past, the present and the future. *Int. J. Food Microbiol.* 117: 1–28.
- Gehring, M., O. Vitzthum and H. Wiengas. 1984. Process for extracting caffeine from ground roasted coffee with CO₂. German Patent. DE 3303679-C2.
- Girard, E., T. Tassaing, S. Camy, J.-S. Condoret, J.-D. Marty and M. Destarac. 2013. Enhancement of poly(vinyl ester) solubility in supercritical CO₂ by partial fluorination: the key role of polymer–polymer interactions. *J. Am. Chem. Soc.* 134: 11920–11923.
- Jaubert, J.N., P. Borg, L. Coniglio and D. Barth. 2001. Phase equilibria measurements of EPA and DHA ethyl esters in supercritical carbon dioxide. *J. Supercrit. Fluids*. 20: 145–155.
- Jung, J. and M. Perrut. 2000. Particle design using supercritical fluids: a patent and literature survey. *J. Supercrit. Fluids* 20: 179–219.
- Ke, J., Y. Sanchez-Vicente, G.R. Akien, A.A. Novitskiy, G. Comak, V.N. Bagratashvili, M.W. George and M. Poliakov. 2010. Detecting phase transitions in supercritical mixtures: an enabling tool for greener chemical reactions. *Proc. R. Soc. A.* 466: 2799–2818.

- Kerdoud, D. 2005. Etude de solubilité des colorants dans le dioxyde de carbone. Application au procédé de teinture en milieu CO₂ supercritique. Thèse INPL-Nancy.
- Kerler, B., R.E. Robinson, A.S. Borovik and B. Subramaniam. 2004. Application of CO₂-expanded solvents in heterogeneous catalysis: a case study. *Appl. Catal.*, B. 49: 91–98.
- Kjellow, A. and O. Henriksen. 2009. Supercritical wood impregnation. *J. Supercrit. Fluids*. 50: 297–304.
- Kontogeorgis, G.M. 2010. Thermodynamic Models for Industrial Applications: From Classical and Advanced Mixing Rules to Association Theories. John Wiley & Sons Ltd., Chichester.
- Lack, E. and H. Seidlitz. 2001. Economics of high pressure processes. pp. 440–443. *In*: A. Bertucco and G. Vetter (eds.). *High Pressure Technology*. Elsevier, Amsterdam.
- Lin, H.M., C.Y. Liu, C.H. Cheng, Y.T. Chen and M.J. Lee. 2001. Solubilities of disperse dyes of blue 79, red 153, and yellow 119 in supercritical carbon dioxide. *J. Supercrit. Fluids* 21: 1–9.
- Lozano, P. 2010. Enzymes in neoteric solvents: from one phase to multiphase systems. *Green Chem.* 12: 555–569.
- Lozano, P., T. De Diego, M. Larnicol, M. Vaultier and J.L. Iborra. 2006. Chemoenzymatic dynamic kinetic resolution of *rac*-1-phenylethanol in ionic liquids and ionic liquids/supercritical carbon dioxide systems. *Biotechnol. Lett.* 28: 1559–1565.
- Lumia, G., C. Perre and J.-M. Aracil. 2001. Method for treating and extracting cork organic compounds, with a dense fluid under pressure. International Patent. WO 2001/023155 A1.
- Marty, A., D. Combes and J.S. Condoret. 1994. Continuous reaction-separation process for enzymatic esterification in supercritical CO₂. *Biotechnol. Bioeng.* 43: 497–504.
- Medina-Gonzalez, Y., T. Tassaing, S. Camy and J.-S. Condoret. 2013. Phase equilibrium of the CO₂/glycerol system: experimental data by *in situ* FT-IR spectroscopy and thermodynamic modelling. *J. Supercrit. Fluids*. 73: 97–107.
- Meireles, A. 2003. Supercritical extraction from solid: process design data (2001–2003). *Curr. Opin. Solid St. M.* 7: 321–330.
- Nunes da Ponte, M. 2009. Phase equilibrium-controlled chemical reaction kinetics in high pressure carbon dioxide. *J. Supercrit. Fluids*. 47: 344–350.
- Pereda, S., E.A. Brignole and S.B. Bottini. 2009. Advances in phase equilibrium engineering of supercritical reactors. *J. Supercrit. Fluids* 47: 336–343.
- Perrut, M. 2005. Supercritical fluids applications: industrial development and economic issues. *Ind. Eng. Chem. Res.* 39: 4531–4535.
- Perrut, M. 2012. Sterilisation and virus inactivation by supercritical fluids (a review). *J. Supercrit. Fluids* 66: 359–371.
- Renner, M., E. Weidner, B. Jochems and H. Geihlsler. 2012. Free of water tanning using CO₂ as process additive. *J. Supercrit. Fluids*. 66: 291–296.
- Reverchon, E., R. Adami, S. Cardea and G. Della Porta. 2009. Supercritical fluids processing of polymers for pharmaceutical and medical applications. *J. Supercrit. Fluids*. 47: 484–492.
- Riha, V. and G. Brunner. 2000. Separation of fish oil ethyl esters with supercritical carbon dioxide. *J. Supercrit. Fluids* 17: 55–64.
- Rodriguez, C., S. Sarrade, L. Schrive, M. Dresch-Bazile, D. Paolucci and G.M. Rios. 2002. Membrane fouling in cross-flow ultrafiltration of mineral oil assisted by pressurized CO₂. *Desalination* 144: 173–178.
- Rosa, P. and A. Meireles. 2005. Rapid estimation of the manufacturing cost of extracts obtained by supercritical fluid extraction. *J. Food Eng.* 67: 235–240.
- Schatz, C., C. Zetzl and G. Brunner. 2008. From plant material to ethanol by means of supercritical fluid technology. *J. Supercrit. Fluids* 46: 299–321.
- Sievers, U. and R. Eggers. 1996. Heat recovery in supercritical fluid extraction process with separation at subcritical pressure. *Chem. Eng. Process* 35: 239–246.
- Smith, R.L. Jr., H. Inomata, M. Kanno and K. Arai. 1999. Energy analysis of supercritical carbon dioxide extraction processes. *J. Supercrit. Fluids* 15: 145–156.
- Sovova, H. 2012. Steps of supercritical fluid extraction of natural products and their characteristic times. *J. Supercrit. Fluids* 66: 73–79.
- Stalh, E. and W. Schilz. 1978. Löslichkeitsverhalten polaren Naturstoffe in Überkritischen Gasen im Druckbereich bis 2500 bar. *Chemie-Ingenieur-Technik*. 50: 535–537.

- Stoychev, I., F. Peters, M. Kleiner, S. Clerc, F. Ganachaud, M. Chirat, B. Fournel, G. Sadowski and P. Lacroix-Desmazes. 2012. Phase behaviour of poly(dimethylsiloxane)-poly(ethylene oxide) amphiphilic block and graft copolymers in compressed carbon dioxide. *Proc. R. Soc. A.* 466: 2799–2818.
- Takeuchi, M., P.F. Leal, R. Favareto, L. Cardozo-Filho, M.L. Corazza, P.L. Rosa and A. Meireles. 2008. Study of the phase equilibrium formed inside the flash tank used at the separation step of a supercritical extraction unit. *J. Supercrit. Fluids* 43: 447–448.
- Toews, K.L., R.M. Shroll, C.M. Wai and N.G. Smart. 1995. pH-defining equilibrium between water and supercritical CO₂. Influence on SFE of organics and metal chelates. *Anal. Chem.* 67: 4040–4043.
- Van den Hark, S. and M. Härröd. 2001. Hydrogenation of oleochemicals at supercritical single-phase conditions: influence of hydrogen and substrate concentrations on the process. *Appl Catal., A.* 210: 207–215.
- Van den Hark, S., M. Härröd and P. Möller. 1999. Hydrogenation of fatty acid methyl esters to fatty alcohols at supercritical conditions. *J. Am. Oil Chem. Soc.* 76: 1363–1370.
- Van Konynenburg, P.H. and R.L. Scott. 1980. Critical lines and phase equilibria in binary Van der Waals mixtures. *Philosophical Transactions of the Royal Society of London Ser. A* 298: 495–540.
- Vignon, M., S. Montanari, D. Samain and J.-S. Condoret. 2006. Method for the controlled oxidation of polysaccharides. International Patent. WO 2006/018552 A1.
- Vitu, S. 2007. Développement d'une méthode de contributions de groupes pour le calcul du coefficient d'interaction binaire de l'équation d'état de Peng-Robinson et mesures d'équilibres liquide-vapeur de systèmes contenant du CO₂. Thèse INPL-Nancy.
- Weidner, E. 2009. High pressure micronization for food applications. *J. Supercrit. Fluids* 47: 556–565.
- Wong, J.M. and K.P. Johnston. 1986. Solubilisation of biomolecules in carbon dioxide based supercritical fluids. *Biotechnol Prog.* 2: 29–38.
- Zacchi, P., C. Bastida, P. Jaeger, M.-J. Cocero and R. Eggers. 2008. Countercurrent de-acidification of vegetable oils using supercritical CO₂: holdup and RTD experiments. *J. Supercrit. Fluids* 45: 238–234.
- Zosel, K. 1980. Separation with supercritical gases. pp. 20–22. *In: Stalh Schneider and Wilke (eds.). Extraction with Supercritical Gases.* VCH Verlagsgesellschaft mbH, Weinheim.

10

Ionic Liquids

Hélène Guerrand, Mathieu Pucheault and Michel Vaultier

Introduction

Since the early 2000s, ionic liquids have become more and more popular in many fields of chemistry (Kadokawa 2013; Kokorin 2011; Plechkova and Seddon 2013; Wasserscheid and Welton 2008). Due to their rapid identification as a new reaction environment, they can substitute volatile solvents. Some years before, the main innovation in this area had to do with water (see chapter in this book), perfluorinated solvents or HMPT, a more outstanding solvent which appeared in the 60s. The physico-chemical properties of these solvents (dielectric constant, electric dipolar moment, hydrophobicity, etc.) initiate the reactivity and the special selectivity observed in these environments. Ionic liquids have gained rapidly in popularity among chemists and are subject to many international groups' research. They are no longer considered only as solvents. The huge diversity of accessible molecules by simple and effective ways allows for the awarding of particular properties, making them technology liquids. Their uses are varied and range from batteries to additive painting. They are also used in solution supported chemistry.

What is an Ionic Liquid?

Onium salts are compounds formed by the combination of an anion and a cation, of which at least one is organic. **Ionic liquids** are onium salts whose melting point is below 100°C (Boon et al. 1986). Many of them are liquids at room temperature and are denominated as Room Temperature Ionic Liquids (RTILs).

The first ionic liquid, ethylammonium nitrate ($\text{EtNH}_2, \text{HNO}_3$), was described in 1914 by Walden (Walden 1914). Its melting point is 12°C. It is easily prepared by reacting nitric acid with ethylamine. Ionic liquid chemistry has its origin in molten salt chemistry, whose melting point is usually very high (825°C for NaCl for example). In order to avoid harsh conditions (heating to high temperatures to

melt salts), Walden conducted experiments to replace them with organic salts. These generally have lower melting points; some of them are liquids at room temperature (John 2007).

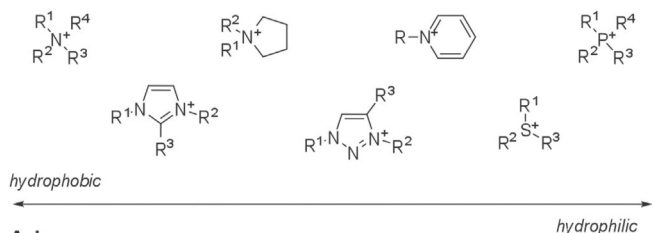
Comment

An ionic liquid is an onium salt whose melting point is less than or equal to 100°C (J. Wilkes) corresponding to the boiling temperature of water. This is arbitrary and is relevant only from a historical perspective.

The first ionic liquids used as solvents were the ammonium chloroaluminates (Robinson and Osteryoung 1979). They were prepared from trichloroaluminium and the corresponding ammonium chlorides. Depending on stoichiometry, aluminum anion complexes are formed $AlCl_4^-$, $Al_2Cl_7^-$, $Al_3Cl_{10}^-$, etc. Unfortunately, these salts are prone to hydrolysis, which limits their uses. In the early 90s, a new family of ionic liquids such as tetrafluoroborates or imidazolium or pyridinium hexafluorophosphates was prepared by Wilkes and Fuller. This new family of ionic liquids were stable in the atmosphere and in the presence of water. This innovative method gave access to a wider range of ionic liquids and made it easy to refine their properties (Fuller et al. 1994; Wilkes and Zaworotko 1992). Therefore, the number of available ionic liquids has grown exponentially and nowadays over a hundred of ILs can be accessed from commercial sources.

However, one of the great advantages of ionic liquids is the ability to tailor their structures depending on the desired properties. They are called “designer solvents” because of the quasi-infinite numbers of possible cation and anion combinations that can be envisioned (Welton 1999). Nowadays, the most widely used ionic liquids have a structure with cations centered on nitrogen (tetraalkylammonium, alkyipyridinium, alkyimidazolium), phosphorous (phosphonium) or sulfur (sulfonium). For stability purposes aimed at the optional addition of base in the reaction medium, protic salts are of limited use. Anions give the wider structural diversity; the most used ones are halide ions, acetate, trifluoroacetate, triflate, bistriflimide, sulfates, sulfonates, tetrafluoroborate, etc. ... (Fig. 1).

Cations :



Anions :

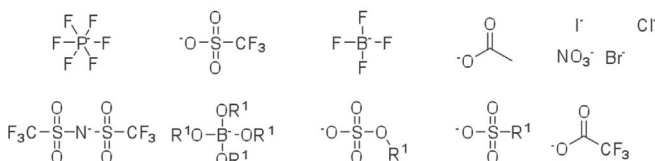


Figure 1. Some common cations and anions used in ionic liquids.

Synthesis

This anion diversity is mainly due to the synthesis methods of onium salts. The anion modification occurs generally in the last step by anion metathesis and can be easily adjusted. On the other hand, cations are mainly synthesized by quaternization of a heteroatom carrying a lone pair (nitrogen, phosphorous, sulfur). The heart of the central cation is often the same. In contrast, the chain diversity which can be attached to it is much greater, apart from alkyl- or aryl-sulfates, sulfonates and carboxylates, anions are usually structurally fixed.

Cation Formation

The most commonly used method for cation synthesis is the alkylation of an atom with a lone pair. The following examples are developed for a nitrogen atom (the most commonly used atom), but the same strategy can be applied for other heteroatoms.

In the presence of alkyl halide in reflux of acetonitrile, amines are converted into ammonium salts with a halide counter-anion. Thus, it is possible to obtain onium salts such as butylmethylimidazolium chloride [bmim]Cl, butylpyridinium bromide [C₄Py]Br or trimethylbutylammonium iodide [N₁₁₁₄]I (Fig. 2).

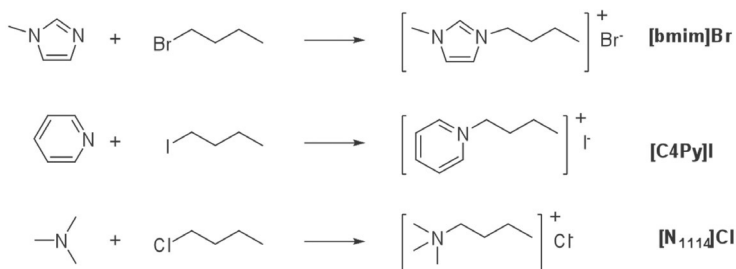


Figure 2. Synthesis of onium halides by alkylation.

Other alkylating agents may be used for the same purpose. Thus, alkyltriflates, dimethyl and diethyl sulfates, dimethyl carbonate and alkyl tosylates can create other onium salts. As part of these methods, the presence of halide is avoided, which can be crucial depending on the following use. In these cases, temperature control is also required to avoid exothermic reactions. When reacting with dimethyl carbonate the corresponding product is unstable, therefore it is trapped as a more stable chloride onium salt, while expelling CO₂ and NH₃ (Fig. 3).

Interestingly, these different methods give access to a wide variety of onium salts bearing mostly hydrophilic ions. On the other hand, most of these compounds are solid at room temperature because the anions are small and hold easily inside a three dimensional crystal structure. Therefore, it appears necessary to develop methods for exchanging anions from these salts, more specifically cheap onium halides with easy access.

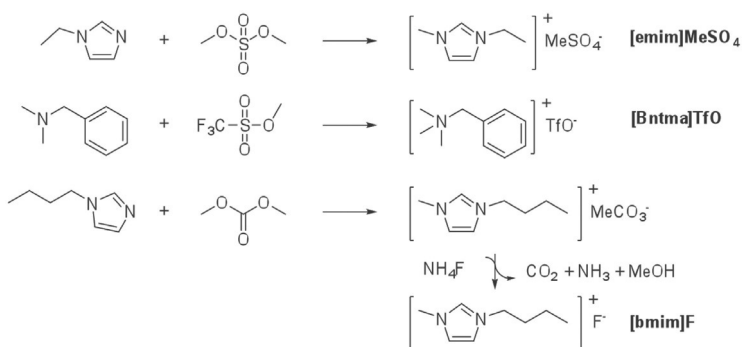


Figure 3. Synthesis of halide free onium salts.

Nomenclature

Ionic liquid nomenclatures differ vastly depending on the communities to which articles are applied to, which can add to the confusion. For cations, generic name abbreviations are used (1-butyl-3-methylimidazolium chloride: [bmim]Cl, trimethylbutylammonium iodide: [tmba]I), others use the carbon number carrying by different alkyl chains following or preceding the cation heart abbreviation (butylpyridinium bromide: [C₄Py]Br, trimethylbutylammonium iodide: [N₁₁₁₄]I). For anions, either abbreviations are (bistrifluorosulfinimide: TFSI, trifluoroacetate: TFA), or actual formula (bistrifluorosulfinimide: NTf₂, trifluoroacetate: CF₃CO₂). Unfortunately, it is common to see several names for the same compound.

Anion Modification

Anionic metathesis. The easiest and most efficient way of changing the anion of the onium salt is based on alkaline/alkaline earth metal ion exchange. Therefore, ions will be associated by relative affinity according to the rules of the HSAB theory and properties of solubility. Thus, the addition of a saturated aqueous solution of lithium N,N-bistriflimidure in a saturated solution of butylmethylimidazolium chloride leads to liquid phase demixing, consisting exclusively of [bmim]NTf₂. Lithium chloride remains in aqueous phase. This method is particularly effective when species possess different physico-chemical properties. In this way, triflates, triflimides, tetrafluoroborates, hexafluorophosphates, trifluoroacetates, etc. can be obtained.

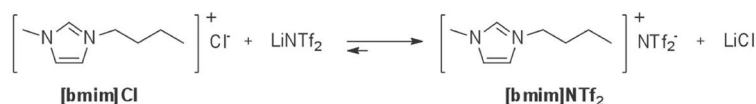
On the other hand, as this is an equilibrium reaction, to make an exchange which results in a structurally similar anion, we must push the equilibrium in the direction of product formation by adding a large excess of the anion or gradually eliminating one of the two products formed. As a result, it is possible to displace the equilibrium by forming insoluble silver salts or by forming gas with strong acids.

The acid used has to be stronger than the conjugate acid of the original onium salt. For example, to remove chlorides, it is possible to use triflic, triflimidic, tetrafluoroboric or hexafluorophosphoric acid. However, adding acetic acid (pK_a = 4.8) or fluorohydric acid (pK_a = 3.2) does not lead to the corresponding acetates

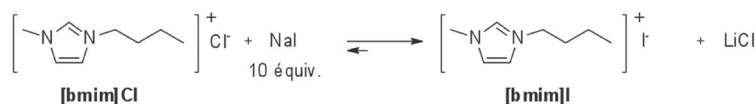
or fluorides. Another method of obtaining the original onium salts is the use of ion exchange resins. Despite the high efficiency of this method, the resins are expensive and their use will be reserved for special cases.

It is also possible to perform reactions directly on anions without proceeding to an exchange. Thus, coordinating ate complex may be formed by adding a stoichiometric amount of Lewis acid. Onium salts bearing ferrates groups (FeCl_4^-), stannates (SnCl_3^-), aluminates (AlCl_4^-) are then obtained. These onium salts, which are water sensitive, may however be attractive for reactions requiring the presence of Lewis acid (Friedel-Crafts). Indeed, ate complexes are in equilibrium with the starting halide and the Lewis acid which can then play its role as a reaction catalyst.

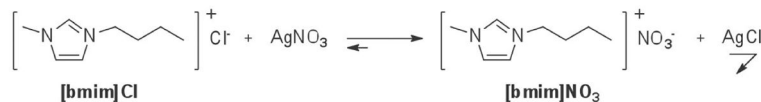
Addition of alkali metal salt



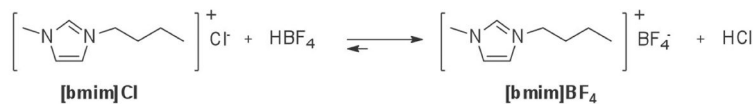
Addition of reagent excess



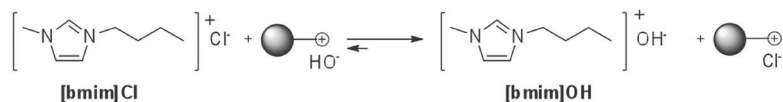
Precipitate formation



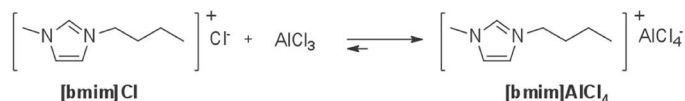
Addition of strong acid



Use of an ion exchange resin



Ate complex formation



Reaction on anion

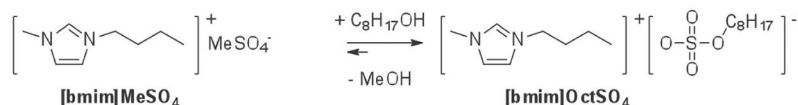


Figure 4. Anionic modifications of onium salts.

Finally, the last possible type of reaction is related to ethyl and methylsulfate ions that can be transesterified by other alcohols in the presence of acid traces to yield to sulfates with longer alkyl chains. These compounds are then much more hydrophobic.

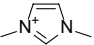
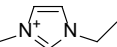
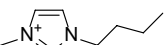
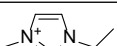
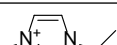
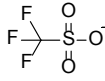
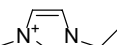
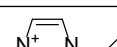
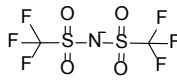
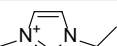
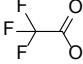
Finally, by applying all of these methods, it is possible to choose the desired cation and anion at will. In this way, combining fifteen cations and twenty commonly used anions, in theory exactly 300 ionic liquids can be prepared with a wide range of physico-chemical properties (Hu and Xu 2006).

Physico-chemical Properties

Onium salts, as their name suggests, are salts. Consequently, their saturation vapor pressure is very low. As a result, these solvents are virtually impossible to evaporate. This has the disadvantage of preventing purification by distillation, but the reaction product can be separated quickly from the solvent instead.

Ionic liquids are rather polar compounds. It is quite difficult to create a general rule about cation and anion influence on the polarity of the solvent. Some ionic liquids are as polar as water, particularly protic ionic liquids which can develop strong hydrogen bonds ($[\text{EtNH}_3][\text{NO}_3]$). Others have a lower intrinsic polarity, despite the presence of an ion pair which is the case of salts bearing long aliphatic chains as $[\text{omim}][\text{NTf}_2]$ whose polarity is similar to the polarity of acetonitrile. Between these two values, the modularity of ionic liquid structure allows access to the entire polarity range. In general, conventionally used onium salts have similar polarity to that of short chain alcohols (ethanol, methanol).

Table 1. Melting points of different onium salts.

Cation	Anion	Melting point (°C)
	Cl^-	125
	Cl^-	87
	Cl^-	65
	NO_3^-	38
		-9
	BF_4^-	6
		-3
		-14

Ionic liquids are also very relevant to electrochemistry. Due to their high conductivity, they are used as background salts and solvents at the same time. Their conductivity values range between 0.5 and 20 $\text{mS}\cdot\text{cm}^{-1}$, but most ionic liquids are between 3 and 7 $\text{mS}\cdot\text{cm}^{-1}$. In addition, ionic liquids generally have a particularly broad electrochemical window. In general, the limit is due to the cation reduction and the anion oxidation, except for the chloroaluminates which generate limiting cathodic reduction. Notably the presence of impurities can significantly affect the electrochemical window limits. In general, the electrochemical window magnitude is 4 to 5V which allows for observation of the original redox phenomena.

Ionic liquid solubility is key when selecting the appropriate ion pair for a given reaction. Low coordinating anions such as bistriflimide (NTf_2^-), hexafluorophosphate (PF_6^-) or anions with long hydrophobic chains such as octylsulfate ($\text{C}_8\text{H}_{17}\text{OSO}_3^-$) or perfluorooctyltrifluoroborate ($\text{C}_8\text{F}_{17}\text{BF}_3^-$) generally form hydrophobic onium salts, which are not very soluble in water but are very soluble in slightly polar solvents such as dichloromethane. On the other hand, when water solubility is required, small anions such as chlorides, bromides or acetate will be preferably used as they can form strong hydrogen bonds with solvents. The tetrafluoroborate ion displays intermediate behavior and the onium salt solubility will mainly be governed by the cation.

For the cation, factors are less dependent on the nature of the cation core and more dependent on its environment. Indeed, small cations with short chains tend to be hydrophilic, while cations bearing long saturated alkyl chains are rather hydrophobic.

Overall, the primary factor influencing the physicochemical properties is the ion size and their ability to interact with each other. The smaller and more symmetrical the ion is, and the quicker it is to make connections, the higher the melting point and viscosity. In contrast to large, asymmetrical and low coordinating ions, the melting point and the viscosity will be low.

Ionic liquids are also chemically and thermally inert. It is possible to heat most of them up to 200–250°C without any degradation. For example, the thermal decomposition of $[\text{N}_{1114}]\text{NTf}_2$ starts at only around 450°C. Obviously, chemical reactivity depends mostly on the structure of the ions used. Sulfonium salts with interesting physicochemical properties are rarely used due to their alkylating reactivity compared to other nucleophilic centered heteroatoms. Some complex ions such as chloroaluminates are sensitive to water, but generally ionic liquids are chemically quite stable. Under very basic conditions, imidazolium salts are deprotonated in 2-position and the corresponding carbenes are formed. It is possible to avoid this reaction using 2-methylimidazolium salts. The most inert ionic liquids are possibly the alkylammonium salts which only give the Hoffman degradation in the presence of a very strong base (tBuOK or organolithium species).

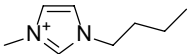
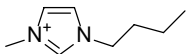
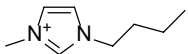
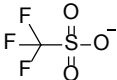
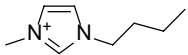
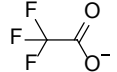
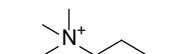
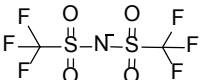
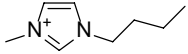
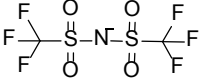
Reminder

Ionic liquids generally have:

- variable melting points, according to the ions selected,
- adjustable (modular) viscosity,
- high thermal stability,

- high chemical stability,
- low saturated vapor pressure,
- large electrochemical window,
- adjustable polarity (between acetonitrile and water),
- adaptable solubility.

Table 2. Viscosity and density of various compounds.

Cation	Anion	Density (g.mL ⁻¹)	Viscosity (cP)
Honey		1,36 (20°C)	2000 (20°C)
	PF ₆ ⁻	1,37 (30°C)	330 (20°C)
	BF ₄ ⁻	1,24 (30°C)	154 (20°C)
		1,29 (20°C)	90 (20°C)
Olive oil		0,92 (20°C)	84 (20°C)
		1,21 (20°C)	73 (20°C)
		1,44 (20°C)	72 (20°C)
		1,43 (20°C)	52 (20°C)
H ₂ O		0,99 (20°C)	1 (20°C)

Ionic Liquid Used as Solvent

Contribution of Ionic Liquids in Organic Synthesis

Due to the variety of their physicochemical properties, ionic liquids have become more and more popular as solvents for organic synthesis over the last decade. Both ionic and polar molecules as well as conventional organic compounds can be solubilized in these liquids. More than 40 articles per day using ionic liquids as solvent and about 150 journals on the subject by year are currently published (Wasserscheid and Welton 2008). As an example, we will illustrate the various advantages of these ionic liquids which include various uses and cannot be restrained thorough.

In recent years, ionic liquids have been named using different adjectives based on commercial and scientific aspects. To say that all ionic liquids are green solvents may be an overstatement. Certainly, due to their low volatility, ionic liquids can be used as interesting alternatives to conventional molecular solvents. The safety

of the process is greatly improved because all the ionic liquids are non-flammable. The impact on the operator's health was significantly improved by decreasing the atmospheric contamination. Nevertheless, while most ionic liquids have low toxicity, salts whose anion is cyanide or mercurate can hardly be called "eco-friendly" (Stolte et al. 2006). As a majority, statements regarding ionic liquids are true, however scientists need to keep a critical point of view and avoid established generalizations.

Volatility

Ionic liquids are solvents with vapor pressure which is negligible at room temperature. This allows for easy recycling of the products by distillation directly from the mixture. However, this saturation vapor pressure is negligible but not zero. In some cases, it is possible to separate ionic liquids by fractional distillation at very low pressures and high temperatures. These cases are extremely rare and most ionic liquids degrade by heating before being distilled.

Due to their polarity and high ionic strength, ionic liquids can have a significant influence on the selectivity of reactions. This is especially true in cases where the transition states and reaction intermediates develop charges.

For example, in condensation reactions leading to the formation of heterocycles from amines and ketones, the intermediate iminiums are stabilized in solvents of a similar structure, such as imidazolium salts. Heterocycles (pyrroles, imidazoles, thiazoles, pyridines, pyrimidines, etc.) can be prepared with greater kinetics than those observed in common solvents such as acetic acid.

For the Diels-Alder reaction, increasing the solvent polarity produces a more compact transition state by hydrophobic compression. On a macroscopic scale, this results in an increase in diastereoselectivity (endo vs. exo). Although this effect is observed with most of the ionic liquids, it is somewhat lower in the case of water, which has a higher polarity and in addition is able to form hydrogen bonds. Therefore, water sensitive reagents may be used in combination with hydrophobic ionic liquids (Fischer et al. 1999). In nucleophilic substitution reactions, transition states are either charged or highly polarized, so it is possible to change the regioselectivity of aromatic alcohol alkylation and minimize the C-alkylation to exclusively form the O-alkylation product. In the nucleophilic substitution of butanediol in the presence of HCl, the reaction selectivity is very poor and results in a mixture of different products such as THF and chlorobutanol. On the other hand, when hydrochloric acid is dissolved in ionic liquid, only 1,4-dichlorobutane is obtained.

It is also possible to benefit from the liquid state of these salts to lead to simpler and more efficient processes. For instance, the BASIL process (Biphasic Acid Scavenging utilizing Ionic Liquids) was initiated in the early 2000s by BASF. Conventionally, hydrochloric acid released into the reaction between dichlorophosphine and ethanol was trapped by a stoichiometric amount of triethylamine. The resulting ammonium hydrochloride created a difficult solid to remove, resulting in a $10 \text{ kg} \cdot \text{m}^{-3} \cdot \text{h}^{-1}$ production rate with 50% yield. By simply substituting triethylamine with *N*-methylimidazole, *N*-methylimidazolium chloride was formed at 75°C and the reaction medium was biphasic. The reaction yield is increased to 98% and productivity is 70,000 times higher.

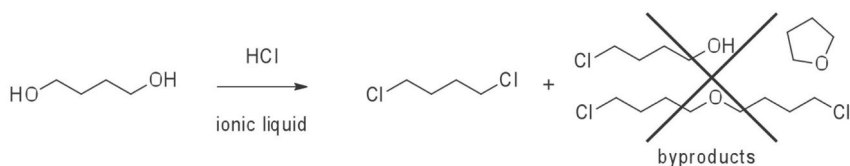


Figure 5. Hydroxyl substitution by hydrochloric acid in the synthesis of 1,4-dichlorobutane.

Acid Catalysis

One of the first uses of ionic liquids was chloroaluminates, used both as solvents and Lewis acid. Indeed, by modifying the stoichiometry (R) between aluminum chloride and onium chloride, it is possible to obtain a basic ($R < 1$), neutral ($R = 1$) or acidic ($R > 1$) ionic liquid. Therefore, the aromatic electrophilic substitution reactions, such as Friedel-Crafts acylations, nitrations and aromatic chlorinations may be achieved without additional Lewis acids. However, by using this method, regioselectivities are quite similar to what can be achieved using more traditional methods. Furthermore, chloroaluminate based ionic liquids remain extremely sensitive to moisture and are difficult to recycle.

Reactions Catalyzed by Transition Metal Complexes

As mentioned previously, ionic liquids are suitable solvents for any charged species. In particular, transition metal complex based catalysts are usually soluble in ionic liquid. The acceleration phenomena are quite similar to those obtained for the nucleophilic substitutions. In many cases, the presence of an ionic liquid can radically affect the nature of the catalyst and therefore the catalytic cycle. For example, when using imidazolium salts, a small amount of base is sufficient to deprotonate the 2-positions of the heterocyclic compound. *N*-heterocyclic carbene may be formed and used as a monodentate ligand by coordinating with the transition metal chosen for the reaction. This metal carbene species then has a very different activity compared to its corresponding precursor. In addition, ammonium salts are known to stabilize transition metal nanoparticles. In the presence of tetrabutylammonium bromide, palladium aggregates to nanoparticles which catalyze coupling reactions with accelerated kinetics. Nevertheless, while modifications of these catalysts can often have a positive impact on the rate and selectivity of reactions on a macroscopical scale, their true nature is often misunderstood.

The different solubility properties of ionic liquids, which demonstrate a wide range of advantages, can be exploited. Indeed, most of them are immiscible with low coordinating solvent such as hexane or diethyl ether. Most salts with small anions are miscible with water and those with hydrophobic anions form two separate phases in its presence. For example, in carbon-carbon bond forming reactions, the use of phosphonium bromide with a long perfluorinated chain allows for easy removal of the ammonium salt formed during the Sonogashira reaction. This reaction between an aromatic halide and an alkyne is traditionally catalyzed by a palladium complex combined with a copper salt. The product is recovered by extraction with hexane

after the reaction while the ammonium bromide formed is removed by backflow washing with water. The palladium complex remains in the ionic liquid phase without significant loss of activity. Nevertheless, in the case of imidazolium salt, the same washing principle can be applied, but the activity decreases, probably as a result of the formation of a palladium carbenoid.

This property allows for processes which involve several distinct phases. The general principals of multiphasic catalysis can be applied to ionic liquids. As a result, phase transition state catalysts can be trapped in ionic liquids. From 1996 to 2004, Eastman Chemical Company developed a tin based catalyst in phosphonium salt to achieve isomerization of 3,4-epoxybutene to 2,5-dihydrofuran with a productivity of 1400 tons per year. Overall, the process was implemented with three mixed continuous reactors, followed by an evaporator and a distillation system. In addition, a continuous backflow extractor ensured the recycling of the catalyst.

Another example of biphasic catalysis using ionic liquids is the Dimersol process, performing dimerization of linear alkenes, typically butene or propene. This reaction, which leads to linked alkenes, is catalyzed by a cationic nickel complex. The reaction is performed between -15°C and 5°C by using an aluminate counter-ion and chloroaluminate as solvent. At these temperatures, the catalyst is in a separate phase and can be easily recycled after a simple phase separation. Significant improvement in activity and selectivity were also observed which allowed for the process to be performed with less reactive olefins. Finally, the reactor size could be reduced as well as compared to homogeneous phase methods which facilitated the control of the reaction.

Several other methods use the concept of differential solubility. For example, hydrosilylation reaction with polysiloxane can be catalyzed by a complex of platonic acid (spyer complex), H_2PtCl_6 . When these complexes dissolve, an ionic liquid matrix is added to a mixture of siloxane and olefin, the reaction leads quickly to an expected alkylsiloxane with excellent conversions ($> 99\%$). Therefore the ILRT/Pt mixture separates from the reaction mixture and can be reused in a new reaction cycle. It turned out that only platonic acid can be immobilized in the ionic liquid phase. In fact $[(\mu\text{-Cl})_2\{\text{PtCl}(\text{cyclohexene})\}_2]$, the complex is globally neutral and easily leached while the PtCl_6^{2-} ion is trapped in the ionic liquid.

Biocatalysis

Biocatalysis is a particularly attractive method because high activity and good levels of stereoselectivity can be achieved when using enzymes. However, enzymes are active only on a limited number of substrates which are soluble in the aqueous medium to be processed. Therefore, many research teams looked at the use of different solvents to perform enzymatic reactions. The first examples of biocatalysis in ionic liquid have emerged in the early 2000s and involved mainly the use of ammonium and imidazolium salts. At the beginning, the main goal was to replace organic solvents by other non-volatile liquids that could be recycled (Dominguez 2012).

Enzymes are biological substances whose activity is closely related to their three-dimensional structure. Indeed, the transformation involved often remains inside the active site, which is both spatially close but distant in the protein sequence.

The conformation is maintained by several inter and intramolecular interactions (disulfide bonds, hydrogen bonds). Therefore, the use of different solvents, such as an ionic liquid may cause denaturation of the protein and subsequently inactivity of the enzyme.

In general, it was found that ionic liquids did not always lead to protein denaturation. The presence of a small amount of water is often required for catalytic activity but there are many cases where an enzyme remains active in an anhydrous ionic liquid. It is also possible to use an ionic liquid mixture with other solvents, such as water or supercritical carbon dioxide. In this case, enzymes are in direct contact with the ionic liquid, which is not necessarily the case if the solvent used is not miscible with the ionic liquid. A sophisticated use of this theory is the combination of homogeneous and heterogeneous catalysis. By coating with acidic ionic liquid, first silica particles act as an acid catalyst, then particles of Novozyme 435, as they can be associated with the same reactor. By using scCO_2 as a solvent, reactions take place only in the ionic liquid phase, and supercritical fluid is used to provide transport between different particles. As a result, incompatible catalysts (acid and enzymatic catalysis) can be combined in the same reactor and achieve a dynamic kinetic resolution of phenylethanol. The enzyme carries out acetylation of one of the phenylethanol enantiomers, acid catalyst accomplishes the racemization of the other enantiomer. This is a competing tandem method of catalysis and the product can be obtained in 78% yield with 97.4% enantiomeric excess (Lozano et al. 2006).

When selecting the ionic liquid used, it is often necessary to use kosmotropic anions and chaotropic cations to stabilize proteins. This is the case with ammoniums, sulfonates and acetates for example. A various screening system is generally required to obtain the most suitable solvent for a given use. Lipases, such as CalB or PclL, were widely studied, but other varied enzymes demonstrated activity in neoteric media. These results differ greatly with different IL/enzyme systems and it is quite difficult to draw a general conclusion. In addition, there is confusion caused by the lack of consideration of the ionic liquid purity in the early studies. In particular, the presence of residual chloride from incomplete anion exchange can lead to complete inactivation of the enzyme.

More recent studies have shown that ionic liquids can stabilize enzymes. Indeed, significant enzymatic activity was maintained at 150°C under 100 MPa (Lozano et al. 2003). Many industrial applications of biocatalysis, which were prohibited because of excessive reaction time, are now possible. Temperature increase is accompanied by a drastic increase in reaction rate, but generally results in an equally rapid inactivation. In the presence of an ionic liquid, enzymes can be stabilized, leading to a significant decrease in reaction time (hours *vs* days).

Finally, a biocatalysis example using entire cells was recently published. The [bmim]PF₆/water biphasic system proved to be more effective than the more commonly used toluene/water system. The transformation concerns an insignificant reduction of nitrile to amine but demonstrates the flexibility and the safety that ionic liquid can offer in a process using biological substrates.

Use as a Technological Liquid

The field of ionic liquids is not limited to chemical synthesis. Ionic liquids can be used in material chemistry (such as in polymer chemistry) as an additive which can easily disperse polymerization catalysts. They are also used as additives in paints to improve details while maintaining optimum drying.

Ionic liquids are also used to dissolve natural polymers such as cellulose. If efficiencies are huge and the recovery rate is around 100%, the regenerated cellulose cannot really be used in conventional fields of stationery because of the loss of its fibrous structure. Nevertheless this recycled application can potentially save tens of billions of tons of used cellulose each year.

The field of e-reactors is currently emerging. The concept is to carry out reactions on very small volumes (a few microliters) with a surface of a printed circuit whose displacement is controlled by a computer. A large number of reactions can be performed during a short time with a small amount of products. Nevertheless, the use of volatile solvents limits uses as one drop of some μL evaporates in less than 5 minutes at room temperature. Therefore, the entire system has to be covered with a fluid (oil) that is immiscible with the drops to prevent evaporation. However, this addition leads to contamination between drops which can be significant if the substrate/reactants mixture is partially soluble in insulating oil. Ionic liquids, due to their low saturated vapor pressure, naturally emerged as a possible alternative to molecular solvents. Problems associated with the higher viscosity of ionic liquid (drops mixture) can be adjusted cleverly by printing a convective motion inside the drop by Marangoni effect or by irradiation with surface acoustic waves. Some promising uses have been made with the real time monitoring of fluorescence (Marchand et al. 2008).

Due to their viscosity, low volatility, and high conductivity, ionic liquids have emerged as an alternative to organic solvents in lithium batteries. Pionics™ introduces over two million battery cells per month, which is a good alternative system for conventional batteries using electrolytes. Although performance decreases slightly (10 to 20%), the “ice system” can guard against accidents due to battery burning.

Finally, Linde™ recently developed a liquid piston system or “ionic compressor”, allowing for the isothermic compression of gas using ionic liquid as a “liquid piston”. This system is applicable to ILs because of their low compressibility. The actual pilot system can produce up to $500 \text{ m}^3 \cdot \text{h}^{-1}$ of compressed gas at 250 bar while reducing the number of moved and voltage mechanical parts by 60.

To resume ionic liquid applications as technological fluids are diverse. They are used as lubricants, as mass spectrometry matrixes, as liquid mirrors in space, as transport agents in photovoltaic cells, as stationary phases in chromatography and as anti-fire agents in polymers. Ionic liquids are not panacea, but with a view to researching alternative processes, they can lead to unique and highly competitive technological solutions.

Task Specific Ionic Liquids (TSIL) and Task Specific Onium Salts (TSOS)

Definition

Task specific ionic liquids are defined as ionic liquids whose cation or anion was amended to give them a particular property (Davis 2004; Pucheault and Vaultier 2009). This function can be chemical, physical, biological, spectroscopic, etc. For example, 3-hydroxypropyltrimethylammonium hexafluorophosphate $[N_{1113OH}][PF_6]$ can be described as an ionic moiety (trimethylammonium, N_{111}) linked to a hydroxyl function *via* a three carbon linker (Fig. 6).

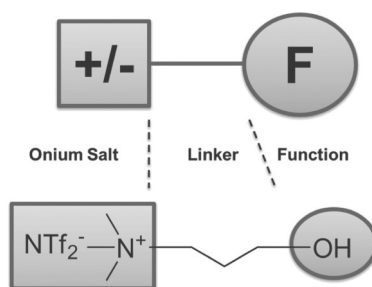


Figure 6. General structure of task specific ionic liquid with $[N_{1113OH}][NTf_2]$ as example.

The main function can either be linked to the cation, the anion or both through a spacer. A modulation of the function's property will generally be observed in terms of special proximity with the ionic head of the onium salt. As mentioned earlier (see § 9.1), there is no real difference between ionic liquid and onium salt, except the melting temperature. In other words, task specific ionic liquids are tasks specific onium salts with a melting point above 100°C.

The majority of functionalized onium salts are solids or very viscous or waxy liquids at room temperature. The increase in the melting point is often connected to the complexity of the functionalization and causes handling difficulties. One of the solutions is to dissolve the onium salt in liquid matrix, in particular a non-functionalized ionic liquid. The resulting binary mixture is named Binary Task Specific Ionic Liquid (BTSIL). These BTSILs have physical properties which are close to the matrices and at the same time maintain the advantageous properties of the starting onium salt.

In particular TSOSs are not very volatile and their solubility can be easily adjusted by modifying the counter-ion structure. We have observed that the side chain of TSOS scan also modify the physicochemical properties, especially in terms of solubility.

Synthesis

The synthesis of TSOSs is analogous to non-functionalized ionic liquids. Synthesis conditions do not have to affect the function supporting the desired property. General

methods have been developed in order to access the TSOSs with alcohol, amine, halide or acid functions in just a few steps. With these different functions, it is easier to attach the molecule which confers a specific property to the TSOS. Quaternization of tertiary amines, phosphines and sulfides with a functionalized alkyl halide affords the corresponding functionalized ammonium, phosphonium and sulfonium. These salts can be modified using the same techniques mentioned above: anionic metathesis, anionic exchange resins or addition of acid. Similar protic salts can be obtained by reacting a strong acid with a tertiary symmetric amine. In most cases, the products obtained possess most of the criteria which enable them to be considered as task specific onium salts. However, they are base-sensitive so are rarely used (Greaves and Drummond 2008).

As an example, condensation between linear chloroalcohol such as 3-chloropropan-1-ol and trimethylamine lead after reaction at 80°C in acetonitrile to ammonium chloride bearing desired hydroxyl function (Fig. 7). Derivatives with the halide group can be prepared from dihalide alkanes. For more complex functions, it is possible, for instance, to transform simple hydroxyl to acrylate by reacting alcohol and acryloyl chloride. Several other reactions can be performed on task specific onium salts.

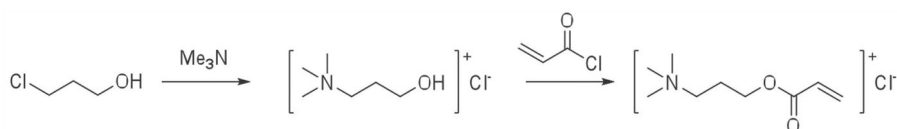


Figure 7. Synthesis of acrylates supported ammonium salt.

TSOSs may alternatively be described as normally functionalized molecules to which an ionic appendix has been grafted. The resulting molecule properties are obviously a combination of properties of onium salt and the molecule itself. These molecules can be used in many different ways. In chemical procedures, they serve mainly in confining a molecule in a different phase from that in which the reaction takes place. Used under pure form or as a solution in a molecular or ionic solvent, the ionic moiety of TSOSs is used as an anchor point to facilitate the separation. Using only simple and cheap operations such as decantation, precipitation/filtration/washing, final molecules can be easily recovered under an analytically pure form.

Based on this unique general theory, the uses appear to be numerous. TSOSs can be used as chelating agents, supported reagents, lubricants, electrolytes, supported catalysts, soluble resin analog for synthesis and more (Lee 2006; Miao and Chan 2006; Vaultier 2008). TSOSs' tasks are not limited to chemical functions, as the first historical example of TSOS for which the molecule was biologically active (miconazole, antifungal) can testify (Davis et al. 1998). Finally TSOSs can be used pure as a solvent. This is the case of chiral ionic liquids which have been used as a chiral solvent with a view to transferring the chiral information to the reaction product. Despite some promising results, inductions remain low (Chen et al. 2008; Ohno and Fukumoto 2007).

TSOSs are mainly used in the immobilization approach, very similar to perfluorated derivatives or chemistry in water (see Chapter 10). Therefore, we should present and compare different methods of immobilization. There are techniques where a reactive entity is physically located in a separate phase from the reagents. This is the case in heterogeneous catalysis, a technique which is widely used in industry as it allows for easy separation of catalysts from products, and in synthesis supported solid resin, which is used for the synthesis of natural oligomers (peptides, oligonucleotides, polysaccharides). Another example is multiphasic catalysis (organoaqueous, perfluorated). Reagents rely on confining the catalyst in one liquid phase while keeping in another. In all these cases, reaction can occur only at the interphase between phases and the strategy to increase the reactivity consists to increase the contact surface by finely dispersing the solid particles, by agitating violently the biphasic liquid mixture or by adding to the system a phase transfer agent (Fig. 8).

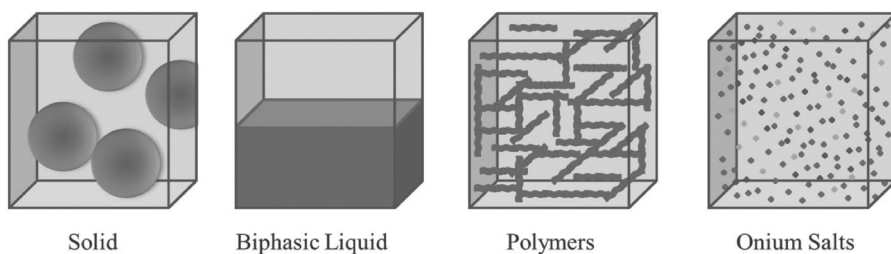


Figure 8. Immobilization of reactive entity (in dark).

Alternatively, the same process of immobilization can be performed with all the reagents in the same phase. Generally speaking, products/reagents/supported catalysts are recovered and recycled after reaction by adding a non-solvent which causes phase separation or precipitation. Multiple links are possible in this case: soluble polymers such as poly(ethylene)glycols (PEGs) or onium salts. The resulting activity is often much better than using conventional techniques. Indeed, reaction occurs in the three dimensional space of the solution in contrast to the use of solid supported substances which present a 2D surfacic reactivity. Onium salt supported methods differ from soluble polymers, meaning that access to the active site which is confined in the polymeric network greatly limits the reactivity by a pseudo-dilution.

TSOSs Benefits Compared to other Immobilization Techniques

- Low molecular weight leading to the use of concentrated solution (0.1M to 1M).
- Highly tunable properties in terms of nature of ions.
- High thermal and chemical stability
- Increased activity.
- Use in a pure form or diluted in molecular or ionic solvent, even in pure water.

TSOSs can be used in all different compartments of reaction conditions:

- As a **solvent**, which is similar, in theory, to the use of a non-functional ionic liquid,
- As a **reagent** or supported **catalyst**, allowing for easy work-up and recovery of products,
- As a **substrate**, allowing for Onium Salt Supported Organic Synthesis (OSSOS).

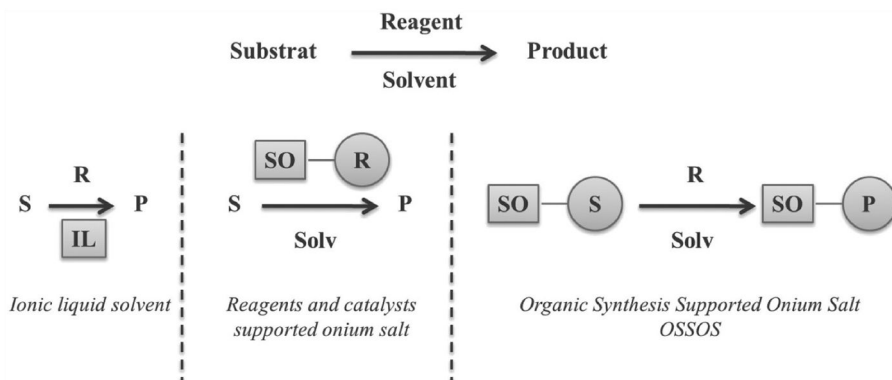


Figure 9. Different uses of onium salts leading to a different concept.

Onium Salt Supported Reagents

The general concept of onium salt supported reagents and catalysts is rather similar to all multiphase systems, where one reagent (catalyst or reagent) is retained in one phase, while substrates and forthcoming products remain in another. In this case, TSOSs are separated between an “ionic phase”, containing only TSOS or a BTSIL, and an immiscible molecular phase, typically with dialkylether, alkanes or water. The ionic phase may then be recycled. This concept may possibly be declined in a version in which onium salts are soluble only in water. This corresponds to the particular case of organoaqueous systems using soluble ionic linker in water. This concept will not be detailed here.

Another system using ionic liquid as an immobilization method is referred to as the supported ionic liquid phase (SILP) (Burguete et al. 2007; Riisager and Fehrmann 2008; Riisager et al. 2008). The general theory is that a TSOS that can be grafted covalently to a particle of silica should be used. The particle can be coated with another non-functional ionic liquid which preferably solubilizes a third TSOS used as a catalyst. This concept has been developed and widely used by P. Wasserscheid from the Technical University of Erlangen, specifically in order to produce a hydroformylation reaction at a gas/solid interface, thus limiting the release of metal (Haumann and Riisager 2008).

If this method could not really lead to a viable process for CO₂ capture, it was used to separate CO₂ from methane with excellent selectivity by cyclic capture and release (Hanioka et al. 2008).

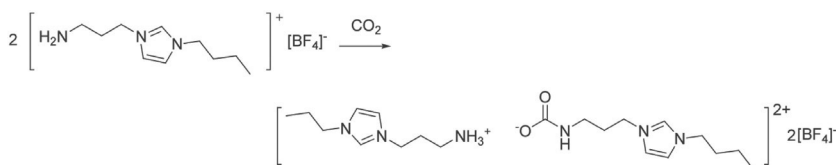


Figure 10. CO₂ capture using an amine supported onium salt.

Another highly relevant use of this method is to specifically coordinate metallic cations which can then be extracted from aqueous media. For transition and toxic metals such as lead, cadmium and mercury, this technique is very attractive. This was achieved by using specific ligands of onium salt supported cations (Fig. 11). It has been observed that the partition coefficient between ionic and water phases could be increased by 100 and lead to almost complete extraction of the relevant ions (Hg²⁺, Cd²⁺) (Kogelnig et al. 2008; Visser et al. 2001). Another use of this theory is to preferentially segregate certain ions in a complex mixture, such as during the reprocessing of nuclear fission products. Thus, it is possible to separate ¹³⁷Cs⁺, ⁹⁰Sr²⁺ or uranyl UO₂⁺ (Luo et al. 2006; Ouadi et al. 2007).

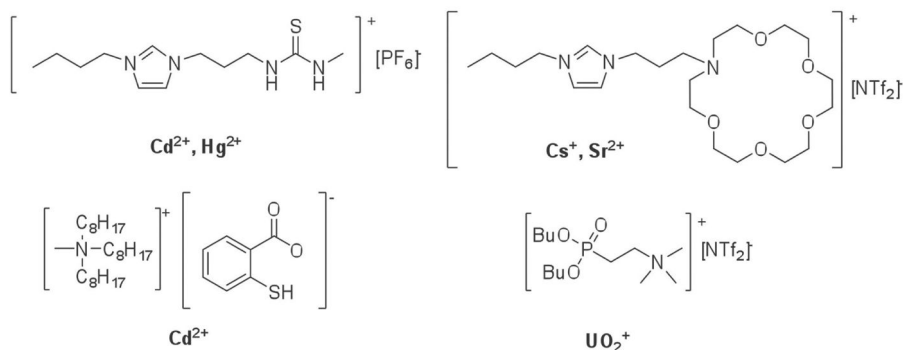


Figure 11. TSOSs used for complexing heavy metal cations.

Finally, TSOSs can be used to perform chemical transformations and facilitate byproduct elimination. For example, in the presence of imidazolium salt supported acid, it is possible to open an epoxide to halohydrin, an internal salt obtained as a by-product can be simply isolated then regenerated using halohydric acid. Alcohol oxidation into ketone with TEMPO leads to a corresponding amine which can be reused in a new reaction cycle after re-oxidation.

Supported Catalysis

When reagents are used in sub-stoichiometric amounts and do not interfere with a chemical equation, it becomes a catalyst. The general theory is very similar to the one described for the onium salt supported reagent.

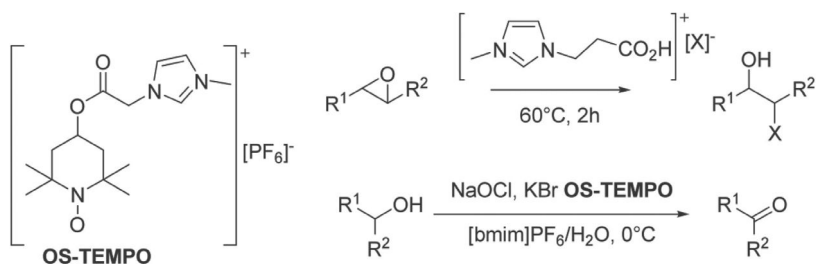


Figure 12. Supported carboxylic acid and TEMPO used as reagents for oxidation of alcohol and epoxide ring opening respectively.

Acid/base Catalysts

Onium salt supported sulfonic acid is the most commonly used catalyst. Now commercial, it can catalyze many reactions (Pechman, esterification, Prins, Biginelli, carbonyls protection and quinoxaline synthesis). In some cases, the reactivity is increased compared to conventional acids, in other cases chemoselectivity is improved. On the other hand, in all cases, acid may be easily recovered and reused in a new reaction cycle. The best strategy is probably to synthesize these products, relying on opening the corresponding sulfone with the relevant amine. The internal salt could then be acidified using a strong acid such as HBF_4 . The product obtained can be used as catalysts of heteroaromatic condensation and form products with high value added, such as porphyrins.

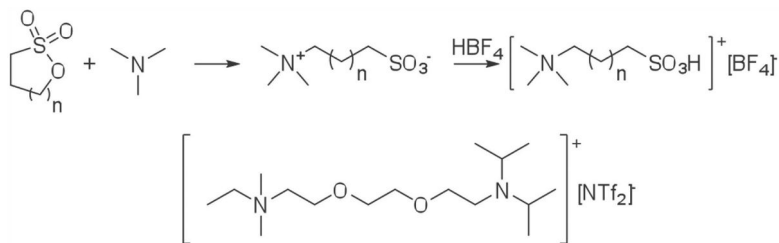


Figure 13. Supported sulfonic acid and Hünig base.

Concerning bases, the supported analog of Hünig base could be prepared. Indeed the nature of the linker between the onium salt part and the base showed an important influence on pK_b of the base. When less than six atoms between nitrogen and onium salt are used, the cation effect is negligible. As an example, these bases were employed as a catalyst in Knoevenagel condensation.

Organometallic Catalysis

Organometallic catalysis is undeniably one of the late 20th century's major advances in organic synthesis. Using transition metals such as platinum, palladium, rhodium, ruthenium, original transformations with high efficiency and with a very small amount

of material can be performed. Nevertheless, for both economic and environmental reasons, it is necessary to recover heavy or precious metals. Catalysts based onium salt supported transition metal can be used. Indeed, if transition metals are preferably soluble in ionic liquid, during the reaction, metal released is often observed, leading to the inactivation of the system. Use of ligands, with one part which coordinates with the metal and the other part being composed of onium salt and scavenges, all in ionic liquid, could be a solution.

After fundamental work on alkene hydroformylation was performed, many research groups have attempted to apply this concept to all conventional organometallic catalysis reactions: reduction (Nobel Prize 2001, Noyori), oxidation (Nobel Prize 2001, Sharpless), metathesis (Nobel Prize 2005), coupling reaction (Heck Suzuki-Miyaura, Sonogashira), etc. Of course, it would be too complicated to write an exhaustive list in this chapter (Parvulescu and Hardacre 2007; Pucheault and Vaultier 2009) and only some examples illustrating the concept will be developed.

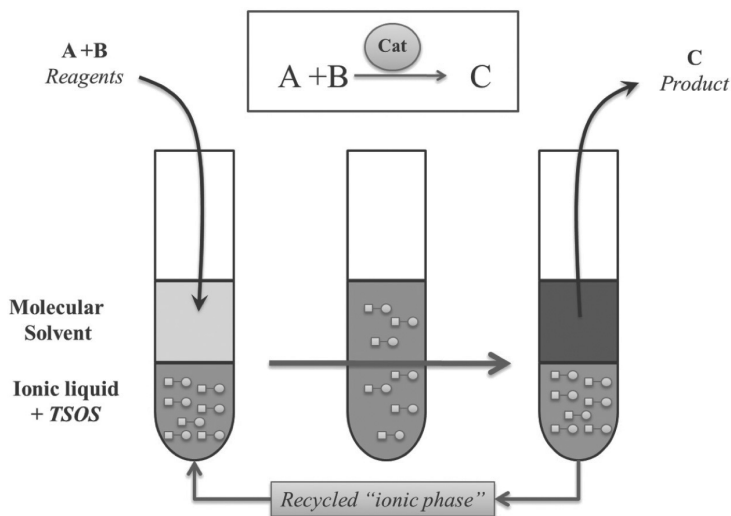


Figure 14. Recycling in biphasic catalysis.

The first ligands tested are derived from the studies of Y. Chauvin, which demonstrated that alkene hydroformylation was particularly efficient in ionic liquid. Phosphines, similar to TPPTS used in Ruhrchemie processes, led to higher activity and selectivity in conventional homogeneous conditions ($\text{TOF} > 800\text{h}^{-1}$, $\text{L/B} > 49$). These phosphines were then used in coupling reactions with palladium. Concerning nitrogen ligands, aldoxime pyridine ether and imidazoles have been efficient in recycling palladium, even in small amounts for several cycles. In these cases the loss of activity due to catalyst deactivation is negligible. Even if the concept is interesting, it is often unprofitable for a process to recycle a catalyst such as palladium. In conventional homogeneous conditions, the order rate of a catalyst is around ten ppm. However, for catalysts used in large quantities, recycling, except from an environmental point of view, can decrease the use of the transition metal

in the process. This is the case of metathesis catalysts, which are not very efficient in less than 1% order rate. A second generation Grubbs-Hoveyda catalyst bearing phenylidene supported imidazolium salt was prepared. Only a very small decrease in activity was observed after ten cycles where unsupported versions of the catalyst showed no activity after the third cycle of recycling.

Another field of application of these concepts concerns enantioselective catalysis. Due to the cost of catalysts and more often the cost of ligands, which are synthesized in several steps and bear the chiral information of the complex, the need for an efficient way to recover the catalysts is still acute. For example diam-BINAP ligand, a functionalized analog of ammonium ion of BINAP included in the Genet catalyst, showed a very good activity in asymmetric hydrogenation. Bisoxazoline supported imidazolium salt was also prepared; Mukaiyama aldolisation reaction or Diels Alder reactions occur with excellent enantioselectivity and with higher activity than unsupported ligands.

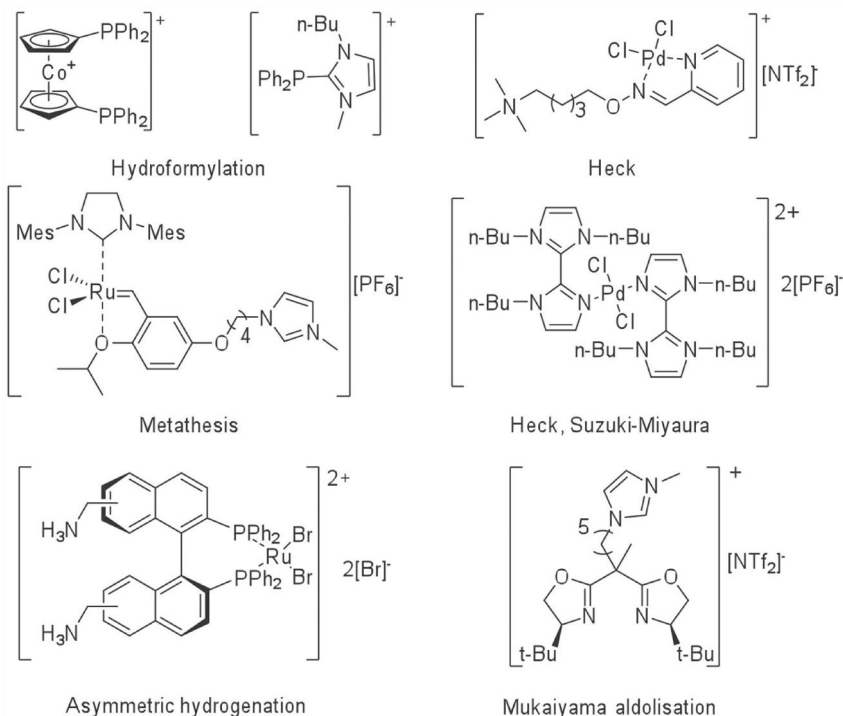


Figure 15. Supported complexes and ligands.

Onium Salt Supported Organic Synthesis (OSSOS)

If TSOSs prove to be very attractive as reagents or as supported catalysts, it is also possible to use them as substrates. This strategy could allow for the realization of one equivalent in homogeneous conditions of synthesis supported solid phase. This

concept was named Onium Salt Supported Organic Synthesis or OSSOS (Vaultier et al. 2003).

Initially, the concept originates from the extension of binary specific task ionic liquids, containing TSOSs which can be modified after being dissolved in ionic liquid matrix. Easy removal of all by-products and reagent excess with simple washes is the main advantage of this method. On the other hand, if adding an ionic liquid matrix enhanced all the physical characteristics of the assembly, it is rather difficult to recover the pure onium salt from the matrix. As a result, it seems to be necessary to extend to the use of molecular solvents which could be removed after reaction under reduced pressure.

Onium salt supported organic synthesis (OSSOS) is a concept which is fairly similar to the solid phase supported synthesis, the only difference being the nature of the anchor point: onium salt instead of a resin. The process can be demonstrated by some key steps (Fig. 16):

1. TSOS-substrate is in solution in a molecular solvent which contain consistent property thereof, as well as compatible with the proposed reaction.
2. Reagents are added in a manner analogous to conventional methods of organic synthesis: same reagents, same temperature, same solvent, same stoichiometry.
3. After transformation, modified TSOS is isolated using simple purification methods (precipitation/filtration, washes, decantation). By-products and reagents excess are eliminated.
4. The TSOS-product is separated from the original support, which may be reused in another reaction cycle, and is then isolated as its pure form.

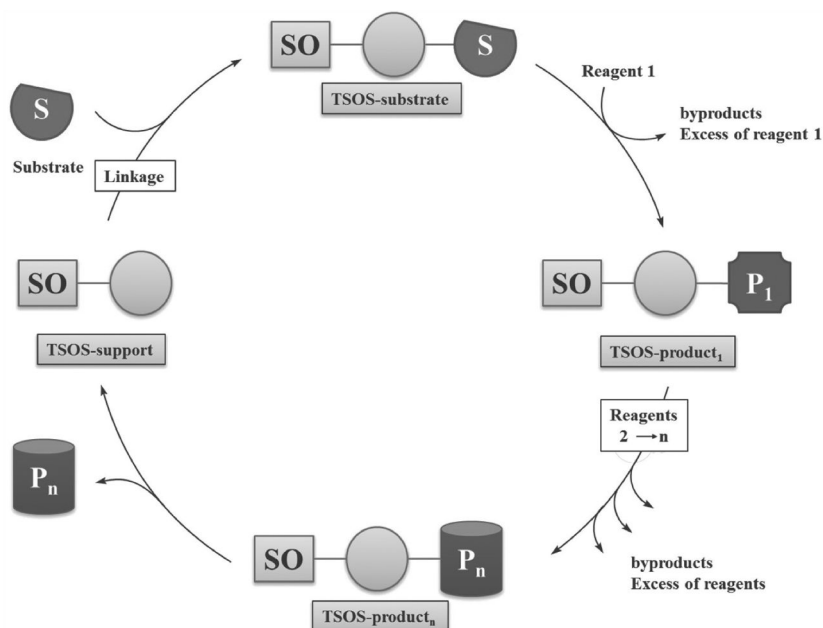


Figure 16. Onium Salt Supported Organic Synthesis.

This method has numerous advantages over conventional supported organic synthesis. First, due to the low molecular weight of the support salt, the loading capacity varies from approximately 2 to 5 mmol.g⁻¹ and can reach up to 12 mmol.g⁻¹ for multivalent onium salts. As a comparison, typical resin hardly reaches 1 mmol.g⁻¹ and a commonly used PEG₅₀₀₀ has a loading capacity of 0.2 mmol.g⁻¹. This low molecular weight subsequently allows for working at conventional concentration (0.1M to 1M). Reaction kinetics are not affected dramatically by the linkage on the ionic support, reaction conditions developed for unsupported molecules are often directly applicable without any reactivity loss. For example, to obtain 1M solution, 1 mole of onium salt (200 g) is dissolved in 1 litre of solvent without any problem, but it is not possible to dissolve 50 kg of PEG₅₀₀₀ in the same volume.

Small molecules with a simple structure are present on the support part. As a result, reaction monitoring is highly facilitated and routine experiments such as NMR ¹H, NMR ¹³C, mass spectrometry, UV spectroscopy, IR and elemental analysis can be performed. Additionally, onium salt supported products can eventually be analyzed using HPLC equipped with a mass spectrometry. As all other conventionally supported methods, the OSSOS strategy affords easy purification with simple washes (alkane or diethyl ether) for the supported product to demix or to precipitate. Additionally, the use of onium salt as a soluble support is less expensive than conventional resins and an easy scale-up is possible (such as choline chloride, a natural product). The cost of one mole of synthesized product is very reasonable (from €26 to €360 for one mole).

	Solid (resin)	Soluble Polymer (PEG)	Onium Salt
Analysis	HR-MAS NMR, FT-IR	NMR, MS, IR	NMR, SR, IR, HPLC, elemental analysis
Conditions	Heterogeneous (resin swelling)	Homogeneous (pseudo dilution)	Homogeneous (1M)
Recycling	Easy	Difficult	Easy
Purification	Filtration, washes	Precipitation, filtration, washes	Precipitation, filtration, washes
Product recovery	Easy	Difficult	Easy
Automation	Easy	Possible	Possible
Loading	0.1 to 1 mmol.g ⁻¹	< 0.2 mmol.g ⁻¹	2 to 10 mmol.g ⁻¹
Support price	> 8000€/kg	360€/kg	80 to 360€/kg
Price for 1 mole of product	80 000€	1800€	26€ to 320€

Due to the attractiveness of this method, several reactions have been developed using OSSOS (Pucheault and Vaultier 2009). In most cases, the operating conditions are very close to those optimized in the unsupported version. Multi-component reactions, acid-catalyzed reactions, reactions catalyzed by transition metal complexes are possible. Radical reactions (zard addition), of which the success depends mainly on the equilibrium between all reaction kinetics, were unsuccessful at a supported solid phase (10 reagent equivalents, 26% yield). However, in homogeneous phase, conditions are better. Using soluble polymers as supports, the yield obtained was

40% with three reagent equivalents. Then, using onium salts, with only 1.3 reagent equivalents, the yield increase to 85% is comparable to the result obtained with an unsupported reaction.

Conclusion

Ionic liquids are compounds with original physico-chemical properties compared to other molecules which are conventionally used in chemistry. When a process presents problems, these ILs properties can be a sophisticated and innovative solution. For around 10 years, the industrial community has been interested in these products and currently several processes which exceed expectations are under production or at the pilot stage. Only small numbers of processes use ionic liquids as a conventional solvent. Indeed, being a liquid matrix is another feature of their properties which makes them a liquid of choice. Finally, the use of these compounds makes a lot of sense economically, as ionic liquids are still expensive compounds. It is possible to find ionic liquids which cost around €100/kg, which is expensive for a solvent, even if it is recycled. This price appears more reasonable when ILs add value to the process.

References

- Boon, J.A., J.A. Levisky, J.L. Pflug and J.S. Wilkes. 1986. Friedel-Crafts reactions in ambient-temperature molten salts. *J. Org. Chem.* 51: 480–483.
- Burguete, M.I., F. Galindo, E. Garcia-Verdugo, N. Karbass and S.V. Luis. 2007. Polymer supported ionic liquid phases (SILPs) versus ionic liquids (ILs): how much do they look alike. *Chem. Commun.* 3086–3088.
- Chen, X., X. Li, A. Hu and F. Wang. 2008. Advances in chiral ionic liquids derived from natural amino acids. *Tetrahedron: Asymmetry* 19: 1–14.
- Davis, J.H. 2004. Task-Specific Ionic Liquids. *Chem. Lett.* 33: 1072–1077.
- Davis, J.H., K.J. Forrester and T. Merrigan. 1998. Novel organic ionic liquids (OILs) incorporating cations derived from the antifungal drug miconazole. *Tetrahedron Lett.* 39: 8955–8958.
- Dominguez, M.P. 2012. *Ionic Liquids in Biotransformations and Organocatalysis: Solvents and Beyond.* John Wiley & Sons, Inc., Hoboken, New Jersey.
- Fischer, T., A. Sethi, T. Welton and J. Woolf. 1999. Diels-Alder reactions in room-temperature ionic liquids. *Tetrahedron Lett.* 40: 793–796.
- Fuller, J., R.T. Carlin, H.C. De Long and D. Haworth. 1994. Structure of 1-ethyl-3-methylimidazolium hexafluorophosphate: model for room temperature molten salts. *J. Chem. Soc. Chem. Commun.* 299–300.
- Greaves, T.L. and C.J. Drummond. 2008. Protic ionic liquids: properties and applications. *Chem. Rev.* 108: 206–237.
- Hanioka, S., T. Maruyama, T. Sotani, M. Teramoto, H. Matsuyama, K. Nakashima, M. Hanaki, F. Kubota and M. Goto. 2008. CO₂ separation facilitated by task-specific ionic liquids using a supported liquid membrane. *J. Membr. Sci.* 314: 1–4.
- Haumann, M. and A. Riisager. 2008. Hydroformylation in room temperature ionic liquids (RTILs): catalyst and process developments. *Chem. Rev.* 108: 1474–1497.
- Hu, Y.F. and X. Peng. 2014. Effect of the Structures of Ionic Liquids on Their Physical Chemical Properties. pp. 141–174. *In: S. Zhang, J. Wang, X. Lu and Q. Zhou (eds.). Structures and Interactions of Ionic Liquids.* Springer, New York.
- John, S.W. 2007. Molten salts and ionic liquids—are they not the same thing? *ECS Transactions* 3: 3–7.
- Kadokawa, J.-I. 2013. *Ionic Liquids—New Aspects for the Future.* InTech, Rijeka, Croatia.

- Kogelnig, D., A. Stojanovic, M. Galanski, M. Groessl, F. Jirsa, R. Krachler and B.K. Keppler. 2008. Greener synthesis of new ammonium ionic liquids and their potential as extracting agents. *Tetrahedron Lett.* 49: 2782–2785.
- Kokorin, A. 2011. Ionic Liquids: Applications and Perspectives. InTech, Rijeka, Croatia.
- Lee, S.-g. 2006. Functionalized imidazolium salts for task-specific ionic liquids and their applications. *Chem. Commun.*: 1049–1063.
- Lozano, P., T. De Diego, D. Carrie, M. Vaultier and J.L. Iborra. 2003. Lipase catalysis in ionic liquids and supercritical carbon dioxide at 150 DegC. *Biotech Prog.* 19: 380–382.
- Lozano, P., T. Diego, M. Larnicol, M. Vaultier and J.L. Iborra. 2006. Chemoenzymatic dynamic kinetic resolution of rac-1-phenylethanol in ionic liquids and ionic liquids/supercritical carbon dioxide systems. *Biotech. Lett.* 28: 1559–1565.
- Luo, H., S. Dai, P.V. Bonnesen and A.C. Buchanan. 2006. Separation of fission products based on ionic liquids: task-specific ionic liquids containing an aza-crown ether fragment. *J. Alloys Compd.* 418: 195–199.
- Marchand, G., P. Dubois, C. Delattre, F. Vinet, M. Blanchard-Desce and M. Vaultier. 2008. Organic synthesis in soft wall-free microreactors: real-time monitoring of fluorogenic reactions. *Anal. Chem.* 80: 6051–6055.
- Miao, W. and T.H. Chan. 2006. Ionic-liquid-supported synthesis: a novel liquid-phase strategy for organic synthesis. *Acc. Chem. Res.* 39: 897–908.
- Ohno, H. and K. Fukumoto. 2007. Amino acid ionic liquids. *Acc. Chem. Res.* 40: 1122–1129.
- Ouadi, A., O. Klimchuk, C. Gaillard and I. Billard. 2007. Solvent extraction of U(VI) by task specific ionic liquids bearing phosphoryl groups. *Green Chem.* 9: 1160–1162.
- Parvulescu, V.I. and C. Hardacre. 2007. Catalysis in ionic liquids. *Chem. Rev.* 107: 2615–2665.
- Plechkova, N.V. and K.R. Seddon. 2013. Ionic Liquids Uncoiled: Critical Expert Overviews. John Wiley & Sons, Inc., Hoboken, New Jersey.
- Pucheault, M. and M. Vaultier. 2009. Task specific ionic liquids and task specific onium salts. *Top. Curr. Chem.* 290: 86–124.
- Riisager, A. and R. Fehrmann. 2008. Supported ionic liquid phase catalysts. *Ionic Liq. Synth.* (2nd Ed.) 2: 527–558.
- Riisager, A., R. Fehrmann and P. Wasserscheid. 2008. Supported liquid catalysts. *Handb. Heterog. Catal.* (2nd Ed.) 1: 631–644.
- Robinson, J. and R.A. Osteryoung. 1979. An electrochemical and spectroscopic study of some aromatic hydrocarbons in the room temperature molten salt system aluminum chloride-n-butylpyridinium chloride. *J. Am. Chem. Soc.* 101: 323–327.
- Stolte, S., J. Arning, U. Bottin-Weber, M. Matzke, F. Stock, K. Thiele, M. Uerdingen, U. Welz-Biermann, B. Jastorff and J. Ranke. 2006. Anion effects on the cytotoxicity of ionic liquids. *Green Chem.* 8: 621–629.
- Vaultier, M. 2008. Ionic liquids in Synthesis, 2nd Edition. Wiley–VCH Verlag, Weinheim, Germany.
- Vaultier, M., S. Gmouh and F. Hassine. 2003. Use of functionalized onium salts as a soluble support for organic synthesis, especially in ester preparation. *In: CNRS, U. Rennes1 (eds.). WO2005005345*, p. 190.
- Visser, A.E., R.P. Swatloski, W.M. Reichert, R. Mayton, S. Sheff, A. Wierzbicki, J.H. Davis and R.D. Rogers. 2001. Task-specific ionic liquids for the extraction of metal ions from aqueous solutions. *Chem. Commun.*: 135–136.
- Walden, P. 1914. Molecular weights and electrical conductivity of several fused salts. *Bull. Acad. Sci. St. Petersburg* 1800: 405–422.
- Wasserscheid, P. and T. Welton. 2008. Ionic Liquids in Synthesis, 2nd Edition. Wiley–VCH Verlag, Weinheim, Germany.
- Welton, T. 1999. Room-temperature ionic liquids. Solvents for synthesis and catalysis. *Chem. Rev.* 99: 2071–2084.
- Wilkes, J.S. and M.J. Zaworotko. 1992. Air and water stable 1-ethyl-3-methylimidazolium based ionic liquids. *J. Chem. Soc. Chem. Commun.*: 965–967.

11

Water as Solvent and Solvent-free Reactions

Emilie Genin and Véronique Michelet

In the field of chemistry and in close collaboration with the US Agency for Environmental Protection (“US EPA”), Paul Anastas and John Warner introduced the concept of “green chemistry” and promoted catalysis among 12 principles (Anastas and Warner 1998). One of the key principles of “Green Chemistry” is to limit the use of volatile organic solvents in industrial processes. Indeed, these solvents are often toxic, expensive and problems are inherent to their disposal and reprocessing. A major research effort has been devoted in recent years in developing new synthetic methods that are more environmentally friendly. Among the classical non-usual solvents, water seems to be the best choice because of its abundance and non-toxicity. Nevertheless, the development of solvent-free processes during reactions and/or purification remains an idealistic solution.

Water as Solvent

Introduction

The use of water in organic synthesis is very attractive for several reasons. The cost of water as a solvent has, of course, significant economic advantages, in particular for the sustainability of industrial processes. Water is a non-toxic solvent and therefore allows releases of persistent organic pollutants to be reduced. Finally, water can be very effective in organic synthesis because of its very specific intrinsic physico-chemical properties. These characteristics may lead to the discovery of new reactivity.

The viscosity of water decreases with increasing temperature. This common property is important for molecular organic chemistry since the viscosity of water affects the diffusion of all kinds of substrates and the amount of sedimentation in the

case of suspensions (insoluble substrates). Water is also the substance with the highest specific heat. This means that a sudden change in temperature, practically speaking, does not change the temperature of the water. This advantage is very important when using water as a solvent to control the reaction temperature, particularly in the case of industrial reactors. Water also has a very high surface tension, which decreases with the temperature or the use of surfactants. Furthermore, water has a very high dielectric constant (ϵ water = 80/ ϵ MeOH = 30). The solubility of organic derivatives in water essentially depends on the polarity of the products and their ability to form hydrogen bonds. Thus, a small polar molecule such as acetic acid is extremely soluble in water. By contrast, soaps and detergents consisting of a hydrophilic head and one long hydrophobic chain have limited solubility and tend to form micelles by coalescence.

Polar and ionic compounds are water-soluble as they are hydrophilic. However, oil or other nonpolar products have very limited solubility in water. Indeed, the less polar products tend to auto associate as micelles to limit interactions with water. This association, also known as the hydrophobic interaction is not due to mutual attraction of these less polar molecules but to the high density of the cohesive energy of water (DEC, Table 1).

Indeed, the energy density of water (550 cal/cm^3) is almost 3 times greater than that of methanol (208 cal/cm^3) and 10 times greater than that of hexane (52 cal/cm^3). The hydrophobic interaction is considered as a low interaction, because energy of 3 kJ/mol is theoretically sufficient for a transfer of a methylene group CH_2 from an apolar organic phase to an aqueous phase. However, such a transfer of a non-polar molecule is unfavorable because of the reorganization process of the water molecules surrounding the solute, and therefore a substantial reduction of entropy.

The effect of salt must also be taken into account when carrying out chemical reactions in aqueous media. Indeed, the addition of hydrophilic electrolytes allows for the internal pressure of the water to be increased. Thus, an aqueous solution of 3M sodium bromide has an internal pressure of about 75 cal/cm^3 whereas the internal pressure of pure water is 41 cal/cm^3 . Most electrolytes increase the internal pressure of water and thus decrease the solubility of a hydrophobic molecule. This observation explains, for example, the use of saturated aqueous solution of various inorganic salts (sodium chloride, ammonium sulfate, etc.) to improve the separation of organic products from water during a reaction treatment. However, the use of surfactants such as sodium dodecyl sulfate (or SDS) allows for homogenization of the reaction mixture when a chemical reaction is performed in pure water with non-soluble products.

Table 1. Physico-chemical characteristics of different solvents.

Solvent	DEC (cal/cm^3)	Internal pressure (cal/cm^3)
Water	550.2	41.0
Methanol	208.8	70.9
Acetone	94.3	79.5
Hexane	52.4	57.1

The internal water pressure acts on the activating volume of a chemical reaction (DV^\ddagger). The internal pressure of water accelerates nonpolar reactions whose activation volume is negative and slows down reactions, whose volume is positive. Thus, the Diels-Alder reaction between cyclopentadiene and butenone is two times faster in the presence of lithium chloride in pure water because the salt increases the internal pressure of water.

The specific physico-chemical properties of water can therefore provide some advantages over conventional organic solvents. In addition, its low cost and non-toxicity are particularly interesting for applications on an industrial scale.

The Pericyclic Reactions, Nucleophilic Additions and Radical Reactions

The Pericyclic Reactions

Historically, the beneficial effect of water in the pericyclic reactions was described in 1980 with the Diels-Alder reaction between cyclopentadiene and methyl vinyl ketone (Scheme 1) (Rideout and Breslow 1980). A significant acceleration was observed in water, compared to methanol or isooctane. The selectivity towards the *endo* isomer also proved to be better in water than in the other solvents. Asymmetric versions have been studied, but in general led to moderate to good enantiomeric excesses. The example of the reactivity of the cycloheptenone constitutes one of the best results, the *endo* compound being obtained with 90% enantiomeric excess.

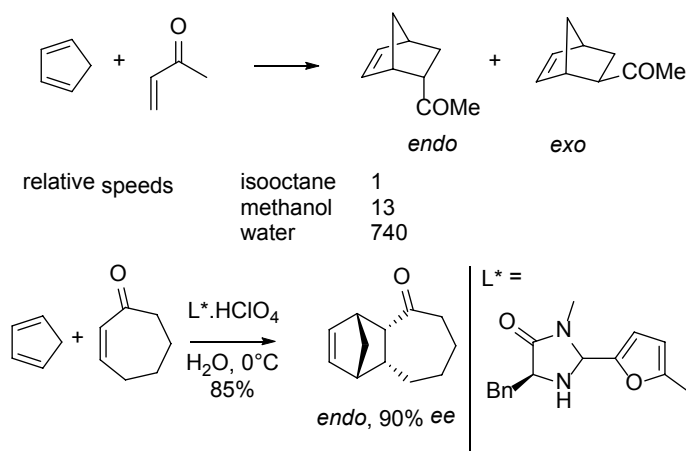


Figure 1. Diels-Alder reaction in water.

These reactions have been extended to hetero-Diels-Alder reactions and 1,3-dipolar cycloadditions and [4 + 3] cycloadditions (Scherrmann et al. 2005).

The Nucleophilic Additions

The nucleophilic additions in water include Barbier type additions (reaction between a halogenated compound and a carbonyl derivative in the presence of an

organometallic specie), the Michael and aldol reactions (Lubineau et al. 2004, 2005). The alkylation reactions and alkylation of carbonyl derivatives will be developed in the following paragraph. The use of water has been particularly beneficial in the case of Michael-type addition of methyl vinyl ketone (Fig. 2). The product resulting from a double addition reaction was observed as minor product in water, whereas it prevails in methanol. It is also important to note that no conversion was observed in organic solvents such as dichloromethane, THF or toluene. A particularly sophisticated asymmetric version was described in the presence of a chiral complex based on a silver complex. The enantiomeric excess for the quaternary-formed center was 83%. The aldol reactions of carbonyl compound have been extensively studied in water but have generally led to similar results to the reactions carried out in anhydrous media.

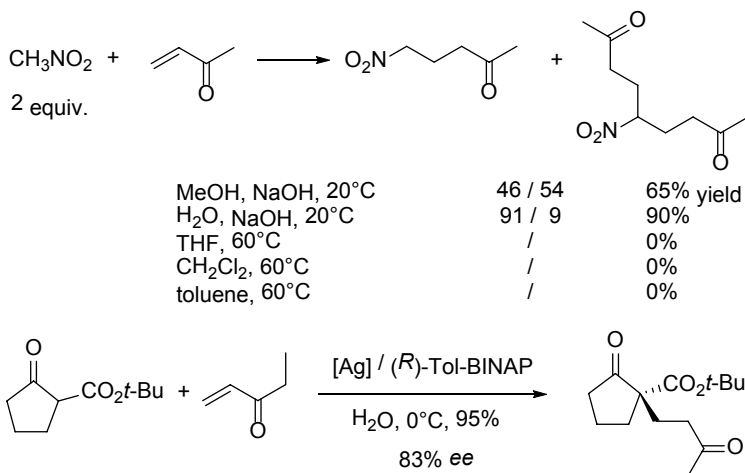


Figure 2. Michael type additions in water.

As industrial applications, the addition of β -diketones on glycoside derivatives are currently developed by L'Oréal for the preparation of the pro-xylan® anti-aging molecule.

The Radical Reactions

The use of water in reactions involving radicals is recent. It has been shown, for example, that the iodocyclization reaction of carbonyl iodo-functionalized derivative was more effective in water than in other organic solvents (Fig. 3). Other cyclizations have been described using water-soluble analogs of AIBN (azobisisobutyronitrile).

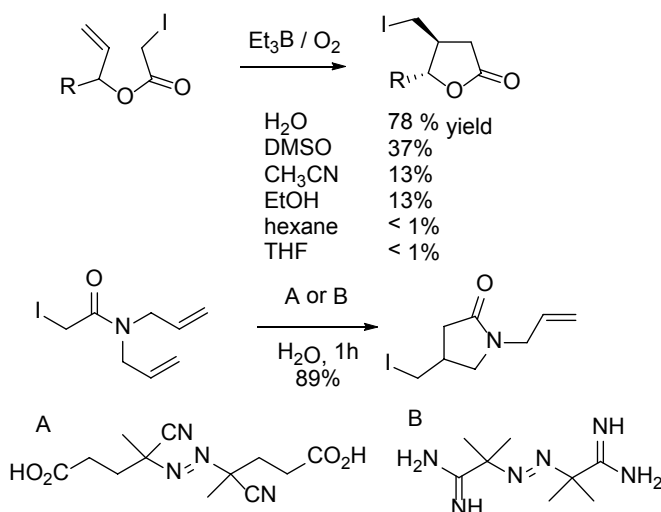


Figure 3. Radical reactions in water.

Catalysis in Water

Concepts, Advantages and Water-soluble Ligands

In the area of pharmaceutical derivatives, the production of a high value compound generally results in the production of waste and several very costly purification steps that may reach 50% of the cost of the whole process (Eissen et al. 2002; Chiusoli and Maitlis 2006). Catalysis represents one of the key points of modern chemistry: it allows the use of reagents in limited quantities (ideally equimolar), the saving of energy by increasing process efficiency and it also facilitates separation by increasing the selectivities of several reactions (Sheldon et al. 2007; Rothenberg 2008). Although heterogeneous catalysis allows an easy recovery of the catalyst by simple filtration, the effectiveness and selectivity of the heterogeneous methods are often lower. Conversely, homogeneous catalysis, which is particularly effective and selective and allows the use of milder conditions, induces a more delicate separation of the catalyst (Herrmann and Kohlpainter 1993; Thomas and Raja 2005). To overcome this drawback, the use of alternative and more environmentally friendly solvents, such as water (Li 2002a, 2002b), was envisaged and the concept of homogeneous catalysis in biphasic medium was developed to combine the advantages of homogeneous catalysis and the ease of separation of the catalyst (Cornils and Herrmann 1996; Cornils 1998). In this case, the reactants and products are soluble in the organic phase, while the catalyst is dissolved in water. During the reaction, the reaction mixture is vigorously stirred and/or heated to allow the catalyst/substrates interactions. At the end of the reaction, the catalyst is recovered and recycled by simple decantation (Fig. 4) (indexing aqueous phase extraction).

Due to their high coordinating properties, the main water-soluble ligands are phosphanes bearing ionic or neutral polar hydrophilic groups, such as

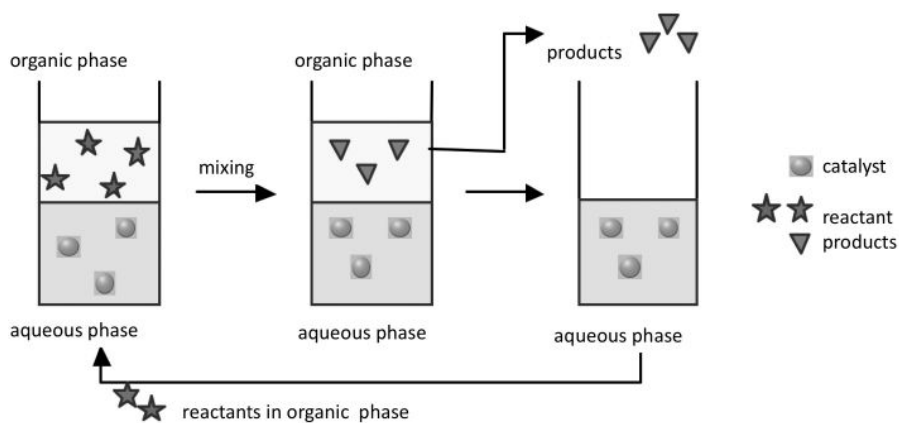


Figure 4. Concept of liquid/liquid separation in the presence of a water-soluble catalyst.

sulfonated phosphanes (SO_3^-), carboxylated (CO_2^- , CO_2H) and phosphorylated (PO_3^- , PO_3H_2) ones. Other phosphanes include amino functions (NH_2 , NR_4^+) and guanylated ($\text{RNHC(=NR')N}^+\text{R}_3$) ones (Leese and Williams 1999) or hydroxyl (implying aliphatic or glycosidic bonds) or polyether (Bergbreiter 2002). Soluble sulfonated phosphane ligands are by far the most commonly studied derivatives in literature (Pinault and Bruce 2003; Shaughnessy 2009). These phosphanes are commonly obtained by direct sulfonation reactions of the aromatic moieties of triphenylphosphane with oleum (concentrated sulfuric acid + 20% in weight of SO_3 acid) followed by treatment with sodium hydroxide (Fig. 5). This methodology allowed for the synthesis of the triphenylphosphinomonometal sodium sulfonate ligand (TPPMS) and its trisulfonated analogue, the TPPTS ligand (Shaughnessy 2006; Michelet et al. 2004). The highly acidic reaction conditions leads to the protonation of the phosphorous atom, which deactivates the aromatic ring and thus orientates the sulfonation reaction in *meta* position exclusively. This methodology has been used for many monophosphanes, diphosphanes and chiral phosphanes. The phosphanes bearing carboxylated groups (TPPTC) or phosphonate moieties (TPPMP) have also been described (Fig. 5). As regards water-soluble chiral phosphanes, the most numerous and representative phosphanes are also sulfonated phosphanes (Walsh et al. 2007). Several analogs of BINAP, NAPHOS (BINAS), BIFAP, and MeO-BIPHEP ligands were therefore synthesized (Fig. 5).

The Hydrogenation Reactions

The hydrogenation of olefins was firstly applied under homogeneous organoaqueous conditions using rhodium- and ruthenium-based water-soluble catalysts. The hydrogenation reactions of the $\text{C}=\text{O}$ double bonds has also been studied extensively in an aqueous medium, primarily using organometallic ruthenium complexes. For example, it was shown that the ruthenium-based systems are very effective for the hydrogenation of various aromatic aldehydes or α,β -unsaturated keto acids (Fig. 6). A water-soluble rhodium complex has also been described and was found to

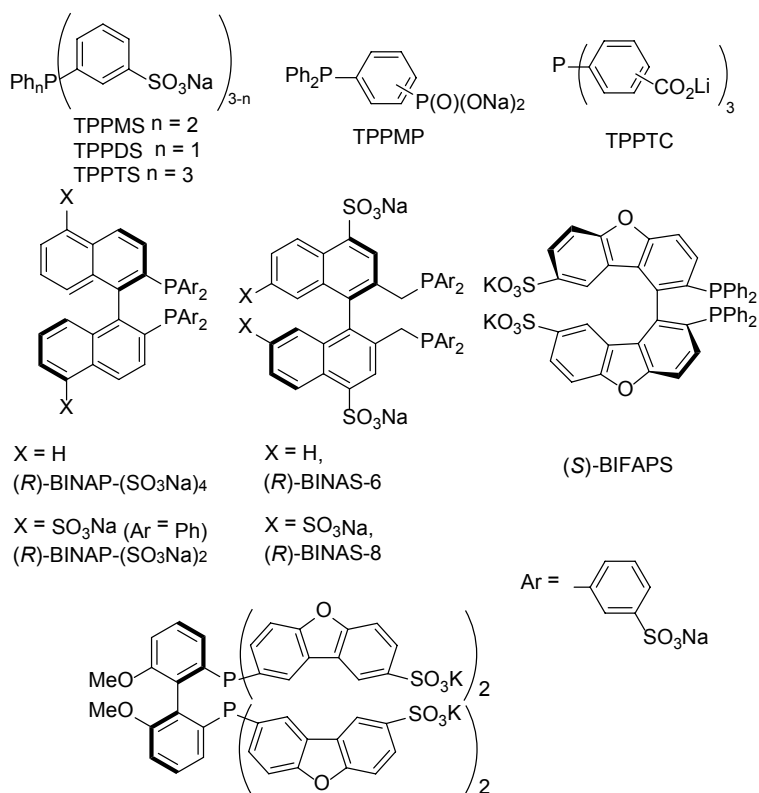


Figure 5. Examples of anionic water-soluble ligands.

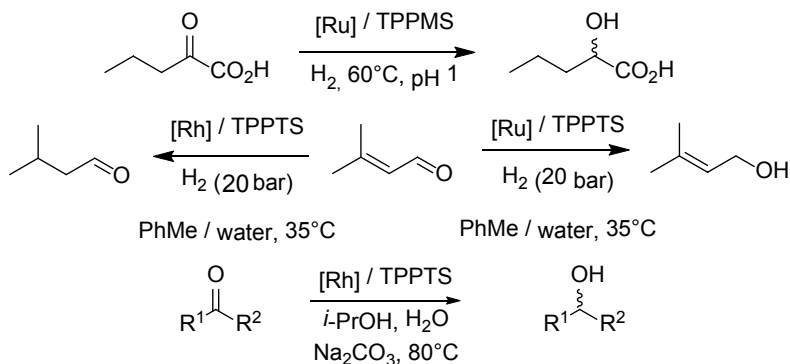


Figure 6. Examples of hydrogenation reactions.

be particularly efficient for the reduction of many aliphatic or aromatic aldehydes and ketones. The catalyst was easily recycled without loss of activity. Industrially, Rhone-Poulenc has developed highly chemoselective reactions of α,β -unsaturated aldehydes, key building blocks for the industrial synthesis of vitamin A and vitamin

E (Mercier and Chabardes 1994). Many studies have been conducted on the use of water-soluble chiral ligands in asymmetric hydrogenation reactions of prochiral substrates, such as α -actamidoacrylic esters, α,β -unsaturated acids, β -ketoesters or imines. Some catalytic applications leading to very good enantioselectivities are described in reviews (Sinou 2002; Pinault and Bruce 2003). It is important to note that the enantiomeric excess obtained under organoaqueous conditions is generally lower than those described in an anhydrous medium and depends heavily on the amount of water in the reaction medium.

In some cases, the lower enantiomeric excesses obtained in the aqueous medium have been improved by the use of new catalyst systems such as SAPC (Supported Aqueous Phase Catalyst). The hydrogenation of a precursor of naproxen was, for example, carried out with an enantiomeric excess of 96%, whereas it was only 70% under standard homogeneous organoaqueous conditions medium (Fig. 7) (Davies and Wan 1994).

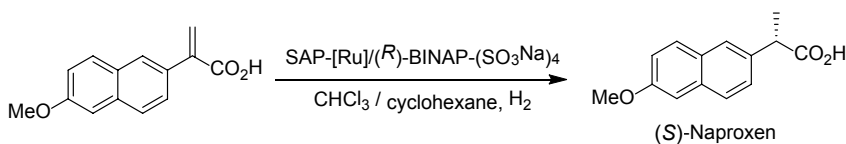


Figure 7. Synthesis of Naproxen.

Formations of C-C bonds C-C Starting from Carbonylated Derivatives

Barbier-Grignard type reactions are among the most useful and versatile reactions in organic synthesis. However, these reactions generally required strict exclusion of air and water, which leads to serious drawbacks in terms of Green Chemistry (use of an excess of desiccants and protection of functional groups such as hydroxyl and carboxylic acid groups). Furthermore, these reactions lead to the formation of a large amount of metallic waste, because they require a stoichiometric amount of organometallic species and halogenated derivatives, halides being generally used as a carbanion source. Although the preparation of arylmercuric chlorides in aqueous medium was described as early as 1905, and the production of tribenzylstannanes in water was described in the 1960s, the exploration of organometallic reactions in aqueous medium did not begin before the end of 1970. A major breakthrough in this area occurred in 1977 with the allylation reaction of carbonyl compounds in the presence of zinc by allyl bromide in a 95% ethanol and *tert*-butanol mixture, demonstrating the feasibility of the organometallic reactions in hydroxylated polar solvents.

Allylation reaction. The allylation reaction of carbonyl compounds is particularly attractive for the formation of C-C bonds in organic and medicinal chemistry because allylic alcohols and amines are useful intermediates for the synthesis of natural products and biologically active compounds. Among the nucleophilic addition reactions of carbonyl compounds, the allylation reaction is a key reaction that has shown the best results in an aqueous medium (Leseurre et al. 2010). Various

metals (Mg, Mn, Sm, Zn, Sn, In, Sb, Bi, Pb, Fe, Co) have shown some effectiveness in mediating this reaction. Zinc, tin and indium lead to higher activity. Some allylation reactions in organoaqueous medium also proved to be highly selective compared to the ones conducted in organic solvents (Lubineau and Canac 2002). The synthesis of α -methylene- γ -butyrolactones, obtained by allylation reaction of carbonyl compounds by 2-bromomethylacrylate in the presence of zinc, represents a significant illustration of this methodology (Fig. 8). Indeed, the reaction conducted in anhydrous THF led only to low yields. As with reactions in the presence of zero-valent metals, the allylation reaction of carbonyl compounds could be performed through the mediation of organostannanes in presence of a Lewis acid catalyst or in the presence of tin or indium metal salts. A major drawback in conducting this reaction is access to various allyl halides. In aqueous medium, the use of a palladium catalyst allowed, in the presence of indium or tin, to conduct the reaction from hydroxyl-, carboxylated- or methoxycarbonyloxy-functionalized allyl compounds (Fig. 8). The highly regio- and stereoselective allylation reaction of aldehydes has been described under organoaqueous conditions in the presence of allenes in place of allyl halides.

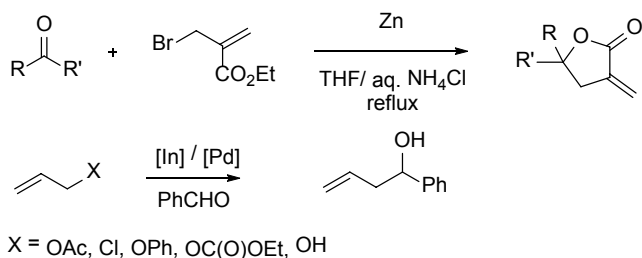


Figure 8. Examples of allylation reaction under organoaqueous medium.

The development of an asymmetric version of the allylation reaction in aqueous medium led to good enantiomeric excesses with different catalytic systems based on cerium, silver, indium or zinc. Asymmetric allylation of hydrazono esters in aqueous medium with allylsilanes in the presence of a catalytic amount of zinc fluoride and a chiral diamine ligand afforded the formation of (benzoyl)-4-hydrazino pentanoates with good enantiomeric excess (Fig. 9) (Hamada et al. 2003).

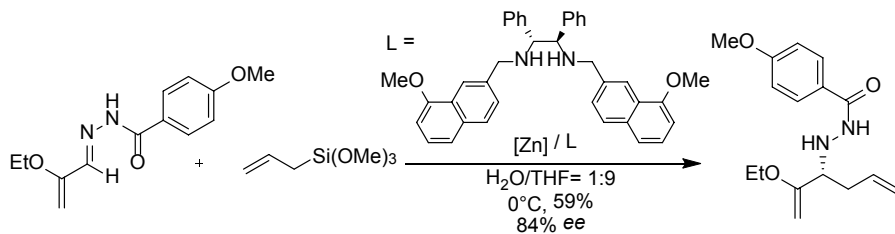


Figure 9. Asymmetric allylation under organoaqueous conditions.

Alkylation and arylation reactions. The activation of alkyl halides C-X bonds in water has long been neglected due to the instability of alkyl organometallic reagents in water. The double carbon-nitrogen bond of the imine derivatives proved to be a good radical acceptor. However, in theory, reactions involving free uncharged radicals are not affected by the presence of water. Zinc and indium organometallic species showed good activity for such reactions on N-sulfonimines, oxime ethers and hydrazones.

The addition of alkyl groups to aldehydes was the greatest challenge. In 2003, a Barbier-Grignard-type alkylation was reported in the presence of zinc and copper iodide in water with unactivated halides. Water also allows the alkylation of aldehydes with trialkylboranes in the presence of a nickel catalyst (Fig. 10). In 1998, the addition of arylboronic acid on aldehydes was discovered in the presence of a rhodium catalyst, resulting in the formation of secondary alcohols (Fig. 10). A wide

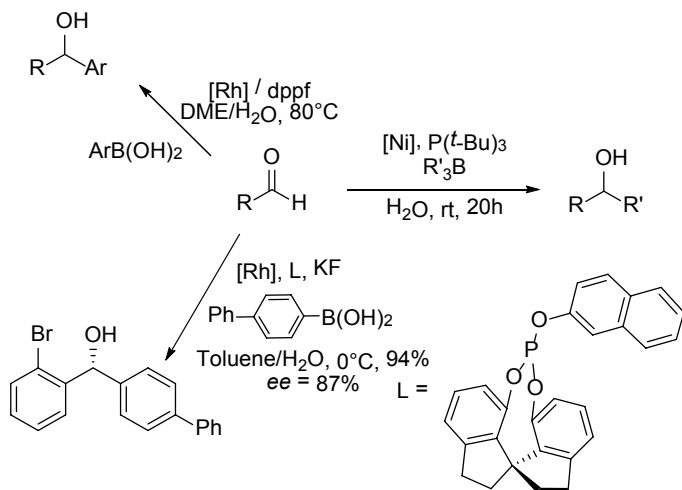


Figure 10. Alkylation and arylation reactions in organoaqueous medium.

variety of arylboronic acids and aldehydes may be used and many investigations on the catalyst and ligand were performed.

Examples of asymmetric arylation of carbonyl compounds (or derivatives) with boronic acids are rather limited. Enantioselective addition in the presence of a rhodium catalyst using a spiro monophosphite ligand (L) (Fig. 10) led, for example, to the desired alcohol having an enantiomeric excess of 87%.

Alkynylation reaction. The alkynylation reaction of carbonyl compounds and derivatives in an organoaqueous medium is of great interest (Herrerias et al. 2007) and proceeds via a C-H bond activation (Chen and Li 2006). Based on the efficiency of the ruthenium catalyst for C-H bond activation, the first alkynylation reaction of aldehydes with phenylacetylene in the presence of a Ru-In bimetallic catalyst in an aqueous medium was described in 2002 (Fig. 11). The same authors also reported

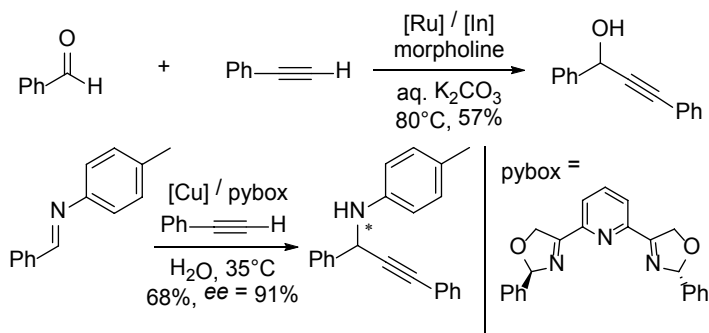


Figure 11. Alkynylation in organoaqueous medium.

the efficient addition of terminal alkynes to arylimines in the presence of a Ru-Cu catalytic system in water or under solvent free conditions (Wang and Li 2004). Silver and gold catalysts were also described as excellent catalysts for the coupling reactions of three components (aldehyde, terminal alkyne, amine).

The copper-catalyzed enantioselective alkynylation of imine (generated *in situ* from the amine and aldehyde) was developed in water in the presence of bis(oxazolonyl) pyridine tridentate ligand (pybox). Various propargylic amines may thus be obtained with good yields and enantiomeric excesses (up to 91%) (Fig. 11).

Cross-coupling reactions of allylic and vinylic derivatives (Tsuji-Trost, Sonogashira, Suzuki-Miyaura, Hartwig-Buchwald, Stille and Hiyama reactions). Coupling reactions constitute an area of very extensive research and have become increasingly important because of the efficiency of the catalytic systems that are fully in agreement with European global economic and environmental priorities (Alonso et al. 2008; Denmark and Sweis 2004; Shaughnessy and Devasher 2005). The Tsuji-Trost reactions (Trost and Lee 2000; Tsuji 2002; Pfaltz and Lautens 1999), the Suzuki-Miyaura (Miyaura and Suzuki 1995), Sonogashira (Chinchilla and Najera 2007; Sonogashira 2002; Doucet and Hierso 2007), Stille (Stille 1986), Hartwig-Buchwald (Muci and Buchwald 2002; Hartwig 1998, 1999, 2002) and Hiyama (Hatanaka and Hiyama 1991; Hiyama and Hatanaka 1994, 2002) cross-couplings have been widely studied in organoaqueous medium or water (Fig. 12). The use of water in these systems has allowed, on the one hand, for the recycling of the catalyst system when a water-soluble ligand is involved (Genet et al. 1999). On the other hand, the reaction conditions have also allowed, under mild conditions, for an easy and efficient access to water-soluble structures and bioactive molecules (Leseurre et al. 2010). Some examples are provided in Fig. 13.

Reactivity of alkenes and alkynes (metathesis and Mizoroki-Heck reactions, 1,4-addition reactions, hydroarylation, hydroformylation and cyclization reactions). The reactivity of alkenes in water or in organoaqueous medium is mainly based on the reactivity of an alkene on another alkene (polymerization) and on the addition of aryl or vinyl groups. Depending on the groups present on the alkene and the catalyst system used, various activities are observed. The addition of carbon monoxide is also possible. The alkynes can be hydrated in water or also undergo addition reactions.

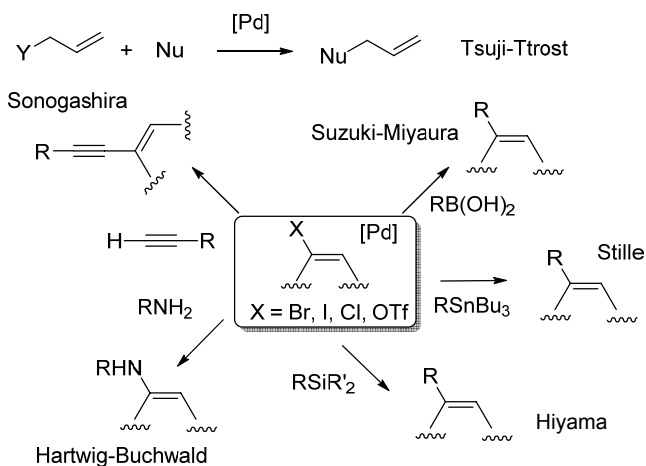


Figure 12. Cross-coupling reactions.

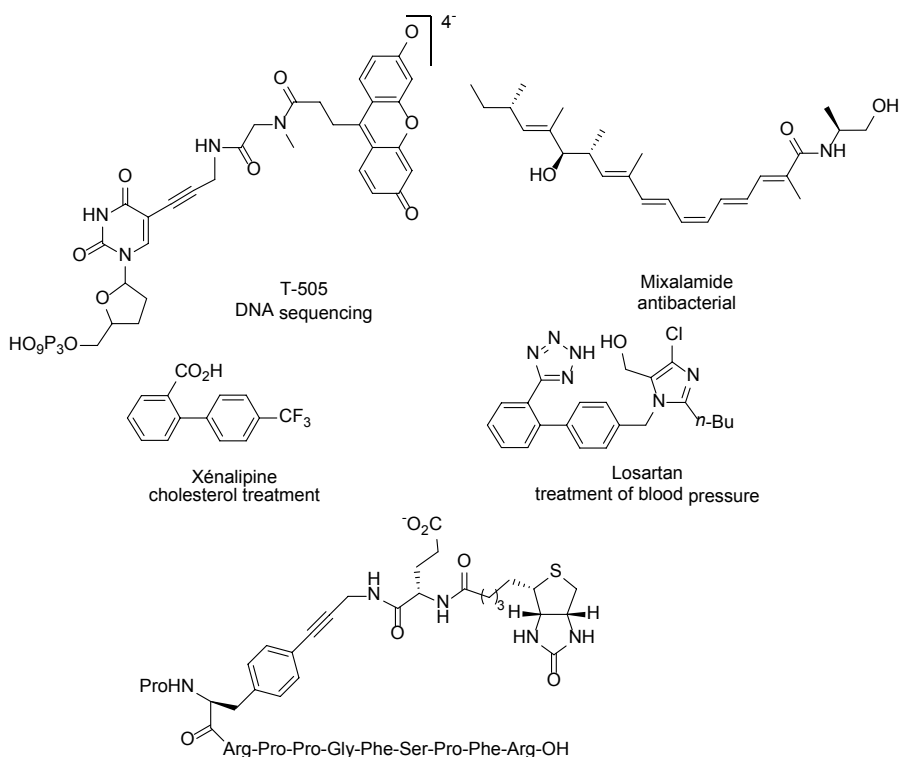


Figure 13. Examples of biomolecules implying cross-coupling reactions in organoaqueous medium or in water.

The polymerization of cyclic functionalized alkene such as norbornene derivatives has been particularly efficient in an aqueous medium using palladium catalysts or water-soluble ruthenium catalysts (indexing polymerization). Depending

on the reaction conditions and the metal used, the selectivity of the reaction is different, thus providing access to a range of different rubbers (Fig. 14). It may be noted that carbenes can be generated in water. The metathesis reaction has also been described extensively in water or in organoaqueous medium.

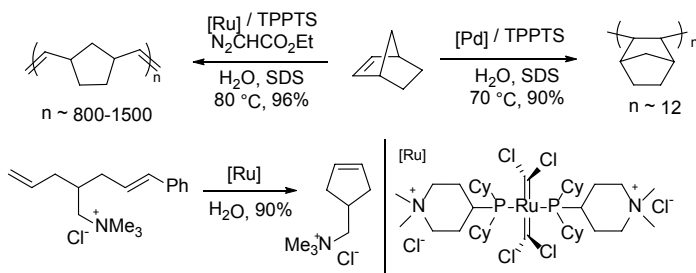


Figure 14. Synthesis of rubbers by polymerization reactions and examples of ring-closing metathesis.

The Mizoroki-Heck reaction (Heck 1979; Beletskaya and Cheprakov 2000) involves the coupling of an aryl or vinyl halide (or triflate) and alkenes in the presence of a catalytic amount of palladium and a base (Fig. 15). The efficiency of this reaction in pure water or organoaqueous mono- or biphasic phase was, for example, demonstrated during the preparation of variously substituted cinnamic acids. A recent extension of this reaction has been described in the presence of water-soluble rhodium complex and involves a boronic acid partner in place of the halide derivative. When the alkene is a Michael acceptor such as an enone type, the addition of the aryl unit is followed by the hydrolysis of the rhodium intermediate, the overall reaction being a 1,4-addition (Fig. 15). The addition of alkynes was also possible using boron derivatives (Fig. 15).

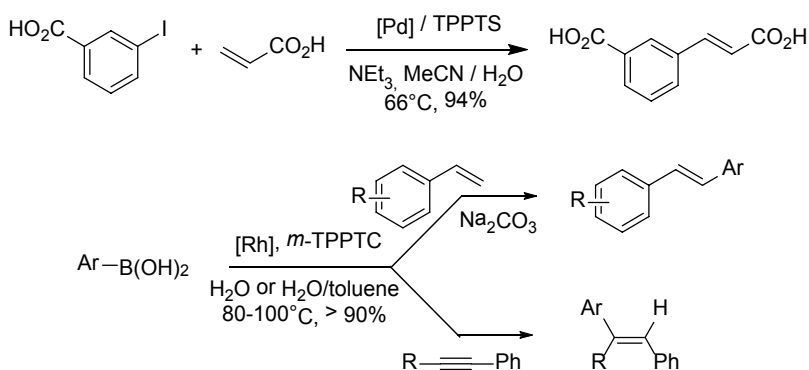


Figure 15. Mizoroki-Heck reactions & hydroarylation reactions of alkynes.

The telomerization of conjugated dienes catalyzed by rhodium or palladium complexes has also been developed in organoaqueous medium with the addition of dicarbonyl derivatives or polyfunctional alcohols. This highly regioselective reaction has been used by the Rhone-Poulenc company for the commercial synthesis

of a precursor of vitamin E (Fig. 16). Furthermore, allylamine was prepared in water by adding nitrogen nucleophiles to dienes. A telomerization reaction in the presence of nucleophiles such as alcohols is also possible. The latter methodology, applied to butadiene in the presence of ethylene glycol, leads for example to monotelomere used as a precursor of PVC plasticizers.

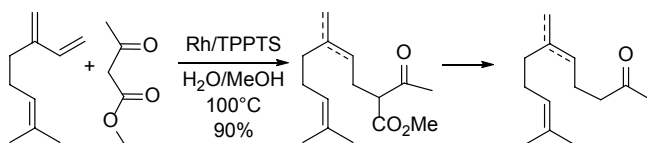


Figure 16. Synthesis of vitamin E precursor.

The hydroformylation reaction was discovered in 1938 by Roelen in the presence of a cobalt catalyst. This reaction has grown considerably through the introduction of rhodium catalysts. However the separation of catalyst and reaction products has long limited the use of hydroformylation in the industry (Franke et al. 2012; Gusevskaya 2014). In 1979, the use of a water-soluble phosphine, TPPTS (or TPPMS), made it possible to carry out the reaction in a biphasic medium. One important industrial application of this method uses homogeneous catalysis in water for the transformation of *n*-propene to *n*-butanal (Rührchemie/Rhône-Poulenc process) (Kohlpainter et al. 2001; Frey 2014). This application was established in 1984 and is still widely used, it is based on the use of a rhodium catalyst under biphasic conditions; the selectivity of the reaction is very satisfactory (94% of the linear aldehyde, Fig. 17). This reaction has also proved particularly effective for the synthesis of fluspirilen (neuroleptic) and its analogs (vasodilators, antiparkinson agents), tolterodine (used for incontinence treatment) and melatonin (natural substance acting on sleep). These structures are shown in Fig. 17.

The efficiency of the hydroformylation process in organoaqueous medium is generally limited to olefins bearing a limited number of carbon atoms (propene or butene). Indeed, the yield of the reaction decreases significantly in the case of longer-chain olefins due to the very low solubility of these compounds in water. Thus, many

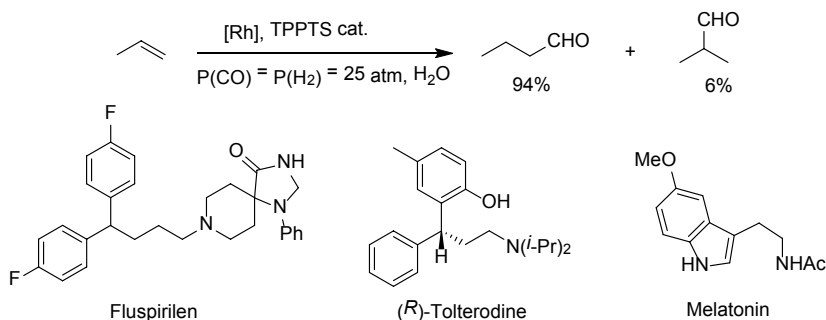


Figure 17. Industrial synthesis of *n*-butanal: Rührchemie process—Applications of the hydroformylation reaction.

alternatives have been proposed to facilitate the methods of mass transfer between the aqueous phase and the organic phase. The Supported Aqueous Phase Catalysis (SAPC), which consists of the immobilization of a hydrophilic organometallic catalyst supported on a silica or glass bead has proven effective for obtaining long-chain aldehydes. Thermo regulated catalysis that plays with the solubility of the organometallic complex (generally soluble at high temperature and insoluble at room temperature) is also an alternative. The use of co-solvents, amphiphilic phosphanes, surfactants or functionalized cyclodextrins was also particularly beneficial. A cumulative acceleration effect was observed, for example, in the hydroformylation of 1-dodecene in the presence of a surfactant and water-soluble ligands.

The hydroxycarbonylation reaction is an extension of the hydroformylation reaction and allows the synthesis of carboxylic acids *via* the coupling of a halogenated derivative with an alcohol or by adding formic acid to an alkene. This reaction has long been limited by the necessary high pressure of carbon monoxide and led to low yields. An important breakthrough in this area occurred by conducting the reaction in organoaqueous medium in the presence of Pd (II)/TPPTS ligand. Aryl, benzyl or allyl bromides or chlorides may be converted very efficiently to the corresponding carboxylic acids in the presence of base. This time, the alcohols are also used as reactants in the presence of sulfonic acid. This method was successfully applied to the synthesis of ibuprofen (Fig. 18).

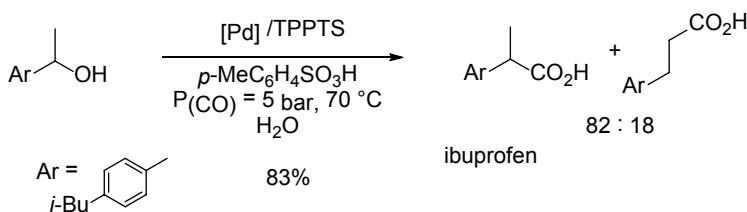


Figure 18. Synthesis of ibuprofen.

The hydroxycarbonylation under biphasic medium has also emerged as a significant alternative for the synthesis of phenylacetic acid. Originally, this acid was formed starting from the cyano compound, obtained from benzyl chloride. 1400 kg of salt was formed per kg of phenylacetic acid. The use of the Pd/TPPTS system in the presence of carbon monoxide and benzyl chloride as a precursor has prevented the formation and thus the destruction of a large amount of salts. This strategy also has a financial advantage as carbon monoxide is about six times less expensive than the cyano derivative.

Solvent-free Reactions

Introduction

Benefits of Solvent-free Reactions

Performing solvent-free organic syntheses has many advantages (Loupy and Haudrechy 1996; Nagendrappa 2002a, 2002b; Cave et al. 2001). The most obvious

is the simplification of experimental procedures. Indeed, these methods may be carried out on smaller volumes and the collection, purification and recycling of the reaction medium costs nothing. The purity of the products formed is often high, which facilitates purification steps (washing, extraction, chromatography, etc.). In some cases, these steps may even be omitted. In addition, solvent-free sequential reactions can be performed with excellent yields. Moreover, solvent-free processes often induce a significant enhancement in kinetics due to higher concentrations of reactants. Thus, reactions requiring several hours in diluted solution can be conducted in a few minutes under solvent-free conditions and some difficult or impossible reactions under standard conditions become feasible. Solvent-free techniques also offer the possibility of working at higher temperatures, without being limited by solvent boiling points, and also allow for the shifting of the equilibrium of a reaction generating volatile polar molecules (methanol, ethanol, water, etc.) by simply heating, without using a specific apparatus such as a Dean-Stark trap. Furthermore, the high concentration of the reaction medium may lead to noticeable changes in terms of molecular interactions between the reactants, which subsequently induce either an increase in selectivity or a singular selectivity (resulting from a mechanistic change). Thus, solvent-free processes are not only environmentally friendly but also provide efficient, safer and more economical procedures for industries (i.e., temperature and reaction time decreased, reducing the reactors size, process intensification, no costs related to purchase and solvent waste treatment).

However, we must not forget that the solvent plays a crucial role in classical organic synthesis by creating a homogeneous medium. By stirring it, the diffusion of the reactants is then facilitated and heat exchanges are more easily controlled. By contrast, solvent-free reactions are very different since the physicochemical properties of the reaction medium, as well as the associated kinetic and energetic parameters, constantly evolve during the process due to changes in the system's composition (Correa et al. 2003; Balland et al. 2002). Thus, special attention should be paid to potential hot spots before implementing a solvent-free process. Detailed fundamental research should be conducted on the heat of reactions released and its dissipation, in order to avoid any loss of control. In recent years, significant research efforts have been made in the field of process engineering, with a view to developing systems which compatible with solvent-free exothermic reactions or transformations involving highly viscous compounds and solids.

The Different Techniques Used

The implementation of solvent-free processes is obviously more or less complex depending on the physical state of the reactants and products under the operating conditions (Loupy and Haudrechy 1996; Nagendrappa 2002a, 2002b; Cave et al. 2001). The approach is relatively easy if at least one of the reagents is liquid, as it can play the role of solvent. The reactants can be introduced in stoichiometric proportions or the liquid may be used in excess and recycled if necessary. In the case of reactions involving both a solid and a liquid, the process occurs either in a solution or at the solid-liquid interface, depending on the solubility of the solid compounds in the reaction medium. In some cases, a phase transfer agent may be used in a catalytic

amount to enhance the reaction efficiency in a heterogeneous medium (solvent-free Phase Transfer Catalysis, i.e., PTC conditions). Similarly, a large number of reactions in the gas phase are described and used for many years in both industrial and academic scientific circles. In recent years, research has therefore focused on the development of new technologies to carry out reactions between solids and gases but also between solids (Kaupp 2006). A large number of major processes related to the petroleum industry, polymers and the production of raw materials (ammonia, methanol, etc.) involve reactions between a solid catalyst and a gas reactant. This type of transformation is generally carried out in a continuous flow reactor at a high temperature and possibly high pressure (Rothenberg 2008; Kaupp 2006). The reagents are injected at the inlet, the reaction takes place on contact with the catalyst, which is immobilized on a fixed structure in the reactor (catalyst bed) and products are recovered at the outlet. Although simple at first, the efficiency of these processes relies on the perfect understanding of their physicochemical properties (diffusion, adsorption, desorption, catalyst's structure, poisoning, etc.).

Reactions between solids remained unexplored until recently because they were considered as less efficient due to the difficulty in creating large contact areas between the reactants. However, it has been known for many years that it is possible to perform a chemical reaction by simply grinding two solid reactants in a mortar using a pestle. In the late 90s, a more sophisticated technology originally used in inorganic chemistry, called "ball milling", was adapted to organic synthesis in order to enable automated grinding and to make it more efficient (Kaupp 2006; Rodriguez et al. 2007). Ball mills consist of a drum containing steel balls which, once set in motion, transform a coarse solid introduced in the drum to a finely ground powder due to shocks or friction between the balls or against walls. Commonly, ball mills allow for the preparation of reagent particles with a diameter smaller than 10 nm and thus with a large contact surface suitable for chemical reactions. In laboratories, equipment conventionally used includes planetary and vibration ball mills, whereas horizontal rotary ball mills are preferred for industrial applications. A brief description of these devices is given below:

- a planetary ball mill consists of a central horizontal tray which can rotate at high speed (100–1000 revolutions/min), on which between one and eight cylindrical reactors containing grinding balls are fixed, these reactors turn around their own axes in the opposite way,
- a vibration ball mill is composed of one or two grinding jars, each containing one or more balls which can be agitated at a frequency of 10–60 Hz in three orthogonal directions. Some devices are equipped with heating and cooling, in order to control the temperature during the grinding,
- a horizontal rotary ball mill comprises a mill roll with a horizontal rotor inside. Unlike other apparatus, the reactor is fixed and only the reagents and balls are set in motion by the rotation of the rotor. Mills which are currently available have a cylinder capacity ranging from 0.5 to 400 liters and tolerate a maximum rotational frequency of 1800 rev/min, providing the opportunity to work under

vacuum or inert atmosphere. They are also equipped with a temperature control system. This technology saves considerable energy and is well suited for industrial applications.

By investigating reactions between solids in more detail, they can be classified into different categories. Some transformations, involving the reaction of two solids to form a third solid, actually take place in the solid state. However, it was shown in the early 2000s that, in most cases, the grinding of two intermediately solid reactants leads to a liquid phase due to the formation of a eutectic mixture with a melting point below the reaction temperature. Thus, the kinetics are similar to that of liquid-liquid solvent-free processes.

Whatever the precautions taken, some reactions involving solvent-free pure reagents are too violent or dangerous to use. Thus, an alternative method has been developed which involves the replacement of the solvents by recyclable mineral solid supports with a high specific surface (typically sand, silica, clay, alumina) (Loupy and Haudrechy 1996; Nagendrappa 2002a, 2002b; Cave et al. 2001). Each of the reagents is separately impregnated on a support and the reaction is subsequently carried out between the impregnated reagents without solvent. This technique allows a significant increase of the reaction yield by limiting the products decomposition, especially for highly exothermic reactions. As with a solvent, the solid support acts as a diluent which helps to limit thermal effects, but offers considerable advantages in terms of cost and safety. In addition, solid supports with acid-base properties (silica, alumina) can be used simultaneously as a reactant and a dispersant. However, the major drawback of this technique is that solvents are often required during the impregnation of the support and the isolation of the product.

Finally, these solvent-free reactions can be accelerated by combining them with conventional activation techniques such as sonication, microwave or light irradiations. Numerous examples of microwave assisted solvent-free organic synthesis have been described in recent years (Strauss and Varma 2006; Polshettiwar and Varma 2008).

A very large number of solvent-free reactions are currently identified. The objective of the next section is to present, through selected examples, the range of possibilities offered by this technology.

Oxidations and Reductions

Oxidation Reactions

The use of oxidation reagents (KMnO_4 , MnO_2 , CrO_3 , NaIO_4 , O_3 , iron-based derivatives, etc.) impregnated on a solid support (clays, silicas, aluminas, etc.), often combined with microwave activation, has been widely applied to the solvent-free oxidation of alcohols, amines, sulfides and enamines. Solvent-free oxidation reactions are now a key tool for manufacturers and they are involved in many “clean” processes which were implemented in recent years. Conventional chromium or manganese-based stoichiometric oxidants tend to be replaced by “clean” oxidants such as H_2O_2 or O_2 in combination with solid catalysts. For example, in the 90s, BASF developed an alternative method for the synthesis of citral (key intermediate

in the synthesis of the vitamins A and E), involving an oxidation step in the gas phase of an alcohol to an aldehyde, catalyzed by a silver catalyst supported on silica (Fig. 19).

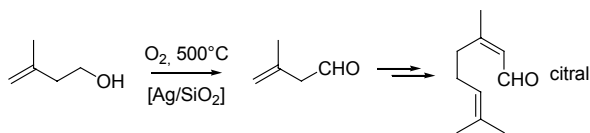


Figure 19. BASF process for the synthesis of citral.

This has also been applied to the industrial preparation of formaldehyde from methanol and should in the future be used in many syntheses (Sheldon et al. 2007). It is noteworthy that the combination of oxygen and a supported silver catalyst was already used on an industrial scale to produce ethylene oxide from ethylene gas. Furthermore, the use of zeolites or molecular sieves for the selective oxidation of substrates, such as alcohols, has been extensively studied since the late 60s (Fig. 20) (Guisnet and Ramôa Ribeiro 2006; Thomas and Raja 2005). These microporous materials, which display various structures, are now widely used in petrochemistry and have encouraged increasing interest in the field of fine chemistry. A process for the direct synthesis of phenol, named AlphO_x[®], has been developed by Monsanto in the United States and is an interesting alternative to the conventional industrial process via cumene. The benzene is oxidized in the gas phase and at high temperature in the presence of nitrous oxide and the zeolite Fe-ZSM-5. Solvent-free synthetic routes have also been implemented for the preparation of precursors which are widely used in industrial polymerization processes. The oxidation of cyclohexane or xylene with dioxygen leads, in one step, to adipic or terephthalic acid, respectively. Cyclohexanone oxime, which is the precursor of nylon 6, can be obtained through ammoximation from ammonia and oxygen by generating hydroxylamine *in situ*.

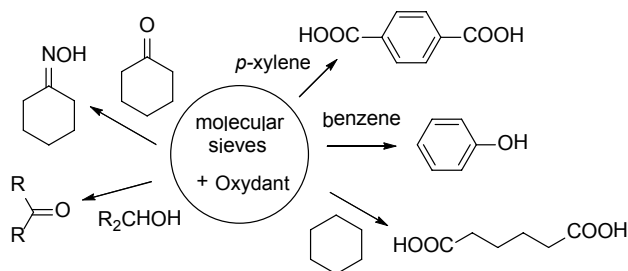


Figure 20. Oxidation reactions catalyzed by molecular sieves.

In addition, the oxidation of ketones and imines by grinding them with *meta*-chloroperbenzoic acid (m-CPBA) provides the corresponding esters or amides (Fig. 10–21) (Guisnet and Ramôa Ribeiro 2006; Thomas and Raja 2005). Thanks to the absence of the solvent, the products are quickly afforded in significantly higher yields than those observed under classical diluted conditions.

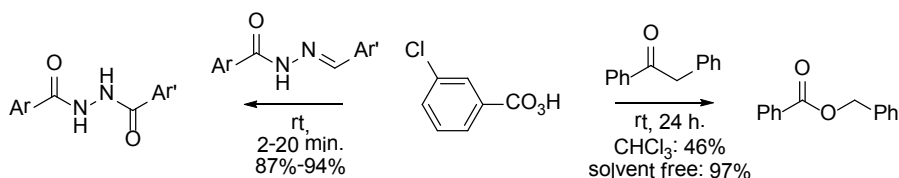


Figure 21. Oxidation reactions with *m*-CPBA in the solid state.

Another fundamental reaction in the petrochemical industry is the catalytic dehydrogenation of ethylbenzene to styrene, known to be highly endothermic and to display moderate conversions. Economic issues related to the production of styrene led companies ABB Lummus and UOP to introduce a new process for oxidative dehydrogenation named SMART[®] in 1995 (Fig. 22). The efficiency of this method lies in the fact that the dehydrogenation of ethylbenzene, in the presence of steam on a fixed bed, is coupled to the oxidation of the hydrogen generated into water. The combustion of the by-product (hydrogen gas) thus provides the energy necessary for the dehydrogenation. Benzene is also produced industrially by dehydrogenation of cyclic or acyclic hydrocarbons in catalytic reforming.

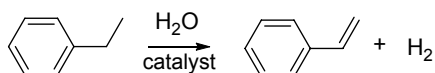


Figure 22. Dehydrogenation of ethylbenzene.

Reduction Reactions

Numerous examples have been described in literature to illustrate the feasibility of most conventional reduction reactions under neat conditions. Thus, the reduction of carbonyl derivatives, acid derivatives and carboxylic acids is performed by using either pure powdered borohydride (excess) or supported NaBH₄, which may optionally be associated with microwave activation. In some cases, a chemoselectivity can be observed and enantioselective reductions of ketones are possible using a reducing agent embedded in a chiral host (Fig. 23). However, the enantiomeric excess values often remain moderate (Loupy and Haudrechy 1996).

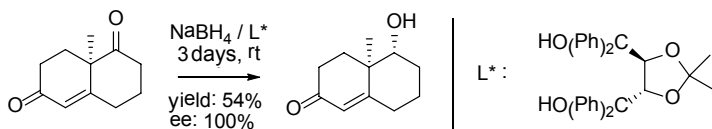


Figure 23. Asymmetric reduction of carbonyl derivatives in the solid state.

Reduction of nitrobenzene derivatives in the corresponding amine can also be carried out under neat conditions by impregnating reagents onto solid supports. In addition to obvious environmental considerations, an advantage of this solvent-free process lies in the observation of an unusual selectivity. Thus, the reduction of *para*-nitrobenzaldehyde with Na₂S in ethanol leads to the corresponding amine, whereas

the same reaction carried out on alumina under neat conditions selectively induces the reduction of the aldehyde (Fig. 24) (Loupy and Haudrechy 1996).

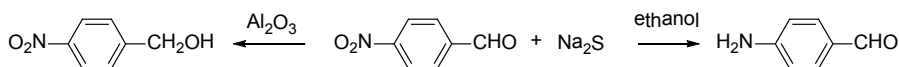


Figure 24. Unusual selectivity with the reduction of the nitrobenzaldehyde.

Furthermore, catalytic hydrogenation is a major reaction for industries, as it is involved in many processes ranging from petrochemistry to fine chemistry through the pharmaceutical industry. In the presence of a wisely chosen catalyst and dihydrogen (“clean” and abundant raw material), highly chemo-, regio- and stereoselective reductions are conducted. It was then found that the hydrogenation of alkenes, imines or ketones could be efficiently carried out without a solvent. Thus, when crystals of cinnamic acid doped with a complex of palladium (II) are maintained under an atmosphere of hydrogen, the chemoselective reduction of the carbon-carbon double bond was observed (Fig. 25). Since 2001, particular attention has been paid to enantioselective solvent-free hydrogenation processes. These conditions may make it possible to increase both the rate and the enantioselectivity of the reaction as shown by Zhang and coworkers with the hydrogenation of liquid ethyl acetoacetate in the presence of a chiral catalyst Ru*/SEGPHOS (Fig. 25) (Walsh et al. 2007).

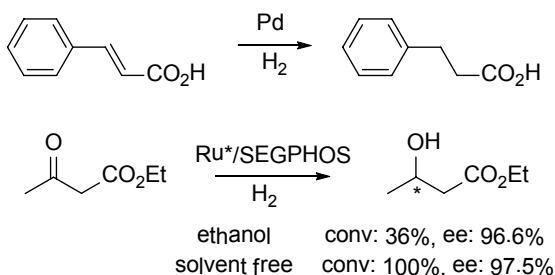


Figure 25. Solvent-free catalytic hydrogenation.

Substitution Reactions

Nucleophilic Substitutions

Many solvent-free aliphatic nucleophilic substitutions are known at present and generally a significant increase in the reaction efficiency was demonstrated.

The conversion of secondary and tertiary alcohols into the corresponding alkyl chlorides is performed in very good yields by simply maintaining the solid substrate under an atmosphere of hydrogen chloride (Fig. 26). Simple mixing the reactants (solid or liquid) is sometimes sufficient to perform the reaction. Thus, dithioacetals, valuable synthesis building blocks, are efficiently prepared in one step by reacting a thiol with a vicinal dichloroalkane, which usually displays a low reactivity, in the presence of a base (Fig. 26). This synthetic route is a particularly attractive alternative

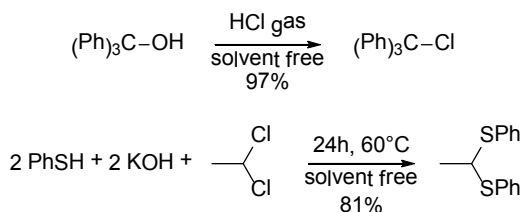


Figure 26. Solvent-free nucleophilic substitutions without any support or catalyst.

with respect to the classical route described by Corey and Seebach, which involves two steps and a tricky purification procedure (Loupy and Haudrechy 1996; Tanaka and Toda 2000).

Another important applications field is the alkylation of amines, imines, carboxylic acids, etc. In general, the solid substrates can be quantitatively alkylated by means of solid-gas (by using iodomethane vapor) or solid-solid techniques. One of the significant challenges of this reaction is the synthesis of ionic liquids, “clean” solvents, which have been used for numerous applications in recent years (Fig. 27). Efficient solvent-free alkylation methods of *N*-methylimidazole with halogenalkanes have been described either in microwave reactors or continuous flow. It is thus possible to prepare 16.5 kg of product per day (Strauss and Varma 2006). The solvent-free technique involving an alumina support is also particularly suitable for anionic reactions such as these substitutions. Indeed, the strength of bases such as KOH and KF is enhanced after impregnation on alumina, which allows various alkylations to occur under very mild conditions and with good yields (Fig. 27). Finally, the solvent-free CTP technique, involving, for example, a catalytic amount of ammonium salt, has been widely exploited for performing difficult substitution reactions under milder conditions with better yields, in a shorter time. For example, we can cite the alkylation with long chains alkylating agents (Fig. 27), which is known to be almost unreactive under standard conditions. This process is of interest in the fields of chemical detergents or liquid crystals. An extremely interesting reactivity can be observed with this technique by combining it with microwave irradiations. The products are quantitatively obtained in a few minutes at a several hundred gram scale (Loupy and Haudrechy 1996; Cleophax et al. 2000).

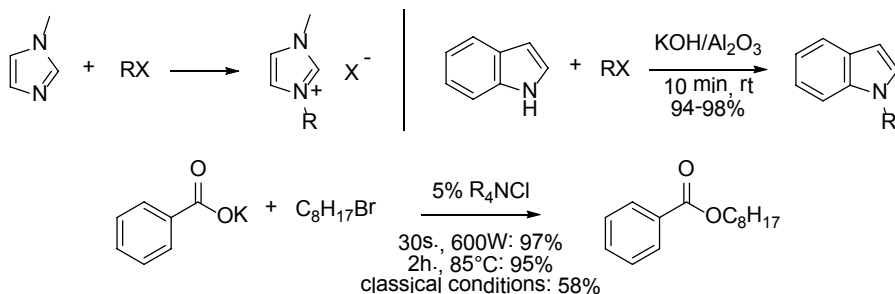


Figure 27. Examples of solvent-free alkylation reactions.

The scope of solvent-free nucleophilic aromatic substitution reactions could also be significantly expanded by applying this PTC method. These reactions, often involved in industrial processes, are known to be limited to substrates which are activated by the presence of electron-withdrawing groups on the aromatic ring. However, under neat conditions and at a high temperature, the nucleophilic substitution with non-activated aromatic halides occurs and provides the products with excellent yields (Fig. 28). For these reactions, a phase transfer agent which is thermally more stable than the ammonium salts is used, such as TDA-1, crown ether patented by Rhône-Poulenc (Loupy and Haudrechy 1996).

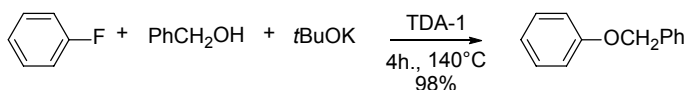


Figure 28. Examples of solvent-free nucleophilic aromatic substitutions.

Electrophilic Aromatic Substitutions

Solvent-free electrophilic substitutions, especially the Friedel Crafts reactions, are involved in many major industrial processes related to both petrochemistry and fine chemistry (Sheldon et al. 2007; Guisnet and Ramôa Ribeiro 2006; Rothenberg 2008; Thomas and Raja 2005). In addition to the limits in solvents use, industries, to the extent that this is possible, favor the use of recyclable solid acids such as zeolites to replace conventional corrosive and hazardous liquid acids (HF, H₂SO₄, AlCl₃, etc.) For example, a major breakthrough occurred in 1976 in this area with the report of the first alkylation process on zeolite developed by Mobil Badger for the synthesis of ethylbenzene (Fig. 29). This method, which was conducted in the gas phase at a high temperature, leads to very high yields and has the additional advantage of avoiding the formation of polyalkylation byproducts which is traditionally observed. Since then, many companies (Dow Chemical, Enichem, UOPs, etc.) have implemented similar methods, using different types of zeolite catalysts, to alkylate naphthalene derivatives or produce cumene, which is a key intermediate in the synthesis of phenol.

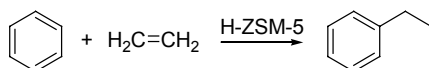


Figure 29. Mobil-Badger process for ethylbenzene production.

Zeolites are also widely used to perform Friedel-Crafts acylation reactions in the field of fine chemistry. In the 90s, the company Rhone-Poulenc has developed a continuous process in fixed bed which are strikingly efficient for the acetylation of anisole with acetic anhydride in the presence of zeolite beta catalyst (Fig. 30).

Compared to the previous process which operated with stoichiometric amounts of AlCl₃ and acetyl chloride in dichloromethane in a closed reactor, the Rhône Poulenc process (now Rhodia) is dedicated to the synthesis of *para*-acetoanisole and is much simpler. It also has the advantage of limiting water consumption and the

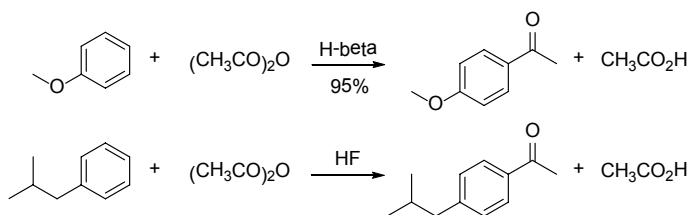


Figure 30. Industrial applications of solvent-free aromatic acylations.

amount of aqueous effluents. Acetylation product is isolated and has improved yield and purity due to the increased selectivity of the *para* isomer. This method is not only more environmentally friendly but also more economically viable. The same type of reaction has been used by the company Boots-Hoechst Celanese for the acetylation of isobutylbenzene to *para*-acetylisobutylbenzene (Fig. 30), a key intermediate in the synthesis of ibuprofen. The BHC procedure which provides this anti-inflammatory in three steps is often cited as a model of “clean” industrial process and has been rewarded twice. For the acetylation step, the hydrofluoric acid plays the role of both solvent and catalyst in order to optimize the selectivity and is subsequently recycled to 99.9% (Sheldon et al. 2007; Rothenberg 2008; Guisnet and Ramôa Ribeiro 2006). The feasibility of solvent-free bromination, nitration and azo coupling reactions of aromatic derivatives has also been demonstrated but these substitutions have not yet given rise to industrial applications (Kaupp 2005).

Isomerizations, Rearrangements and Cycles Formation

Isomerizations and Rearrangements

The *Z/E* geometric isomerization of unsaturated compounds can be performed with iodine under neat conditions by means of thermal or photochemical activation (Fig. 31). The position isomerization of aliphatic alkenes with a double bond has also been widely studied under solvent-free conditions with a supported reagent, using pure reagents or using the CTP method (Loupy and Haudrechy 1996). Thus, the natural essential oil safrole is isomerized by means of a basic catalysis to isosafrole, which is a precursor of piperonal (widely used in perfumery) (Fig. 31).

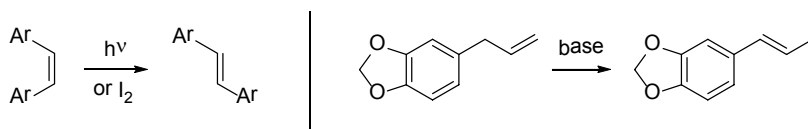


Figure 31. Examples of solvent-free isomerization reactions.

In addition, conventional transpositions can be carried out under solvent-free conditions with very good yields in rather short reaction times (Fig. 32). Thus, vicinal diols are dehydrated easily to ketones in the presence of either *para*-toluenesulfonic acid in powder or a solid acid catalyst (clays, zeolites, etc.), while a concomitant

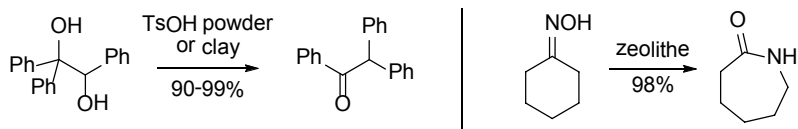


Figure 32. Examples of solvent-free transpositions.

pinacol rearrangement occurs. Similarly, the acid-promoted and industrially popular Beckmann rearrangement has been studied extensively (Sheldon et al. 2007; Guisnet and Ramôa Ribeiro 2006; Rothenberg 2008; Thomas and Raja 2005). The Sumitomo Chemical company, in the late 90s, developed a strikingly environmentally friendly and efficient vapor phase process for caprolactam synthesis, starting from the oxime and the zeolite MFI catalyst.

Pericyclic Reactions

The solvent-free [4 + 2] cycloadditions, especially Diels-Alder and hetero Diels-Alder reactions, are part of references, which have been widely described in literature on the subject. So, many cyclic adducts were prepared quite easily by simply mixing the diene and the dienophile. It was also reported that reactivities and selectivities are generally increased when these reactions are carried out under neat conditions by means of acid solid supports (silica, clays), allowing the activation of the dienophile through the complexation with Lewis acid sites at the surface of these substrates (Fig. 33). It is noteworthy that the hetero Diels-Alder reaction is one of the most efficient and straightforward synthetic methods for the preparation of heterocycles, which are compounds of interest in medicinal chemistry. Asymmetric versions of this reaction have been successfully adapted to solvent-free conditions and generally provide expected adducts with good yields and good enantiomeric excesses (Nagendrappa 2002a, 2002b; Loupy and Haudrechy 1996; Walsh et al. 2007). In addition, photochemical [2 + 2] cycloadditions can occur in the solid state under light irradiation (Fig. 33). These solvent-free reactions were accidentally discovered in the late nineteenth century when changes in properties of solids, such as anthracene or quinones, have been observed after prolonged exposure to sunlight (Nagendrappa 2002a, 2002b; Tanaka and Toda 2000).

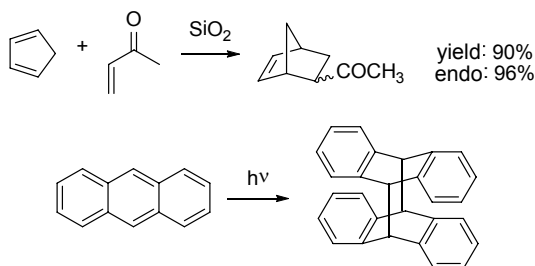


Figure 33. Examples of solvent-free [4 + 2] and [2 + 2] cycloadditions.

Finally, sigmatropic rearrangements or ene reactions can occur in the solid state at high temperatures (Fig. 34) (Nagendrappa 2002a, 2002b).

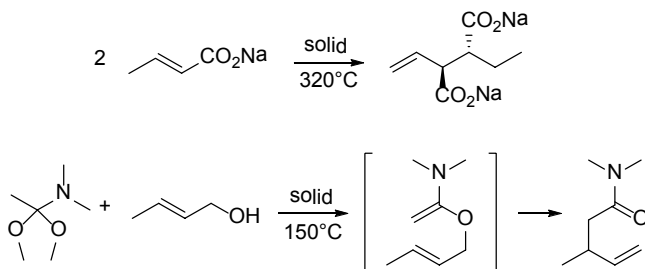


Figure 34. Examples of sigmatropic rearrangement and ene-reaction.

Cyclocondensations

Solvent-free di- or multi-component cyclocondensations have aroused growing interest in recent years in the field of heterocyclic chemistry (Fig. 35). Most of these reactions are performed under microwaves irradiations (Bougrin et al. 2005) by using conventional solvent-free techniques and, in most cases, a remarkable increase in reactivity is observed which allows adduct isolation with very good yields after only few minutes. These “clean” reactions gain increasing popularity because they are adaptable and suitable for a large scale production or parallel synthesis (Kaupp 2005).

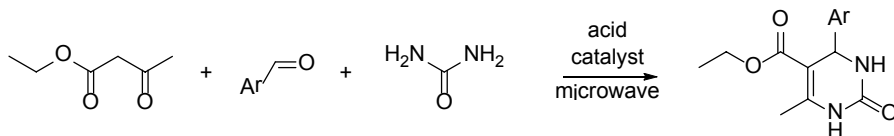


Figure 35. Example of solvent-free cyclocondensation.

Addition, Elimination and Coupling Reactions

Addition to Alkenes and Elimination

Most conventional electrophilic addition reactions to alkenes or alkynes can be performed in solvent-free conditions with good yield and selectivity, either by directly reacting pure reagents (often gas/solid) or by using solid acid catalysts (Kaupp 2005, 2006; Loupy and Haudrechy 1996). These reactions have been implemented in many industrial processes for large scale production of solvents or raw materials (Fig. 36).

For example, up to 6 million tons of cyclohexanol, intermediate in the synthesis of Nylon 6 via adipic acid, are produced per year. The traditional protocol, based on the oxidation of cyclohexane in the liquid phase, displays a moderate selectivity (70% to 85%) and a low conversion (< 10%) related to the formation of byproducts. Major industrial progress in this area occurred in 1990 with the launch of a new

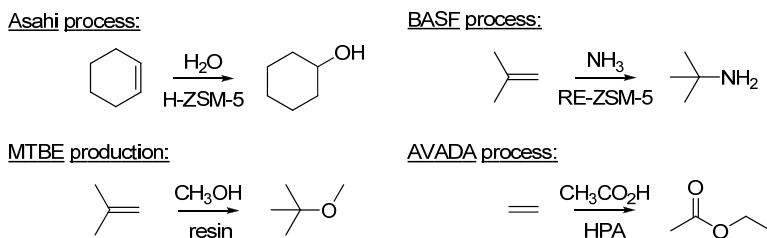


Figure 36. Examples of industrial processes involving an addition to alkenes.

process (the Asahi process), involving the hydration of cyclohexene in the presence of a zeolite. Cyclohexene, produced by partial hydrogenation of benzene, is reacted with a suspension of zeolite H-ZSM-5 in water leading to cyclohexanol with excellent selectivity and 10–15% conversion per pass. Similarly, zeolites catalyze the addition of ammonia to alkenes. This has been operated on an industrial scale by BASF to efficiently produce the *tert*-butylamine from isobutene. This fully atom economic method replaces the conventional synthesis based on the Ritter reaction, requiring the use of cyanide and hydrochloric acids and generating sodium formate (Sheldon et al. 2007; Chiusoli and Maitlis 2006). Another example which is widely cited is the production of methyltertbutylether (MTBE) which is used as a solvent and an additive to gasoline, by reacting a mixture of 2-methylpropene and methanol in excess with an acidic resin in fixed bed reactors (Chiusoli and Maitlis 2006). In 2001, the commercialization of the AVADA process that provides ethyl acetate in one step from ethene and acetic acid was a major breakthrough in the production of this solvent. This ideally economical and ecological process was awarded the Astra Zeneca prize in 2002 (Rothenberg 2008).

The solvent-free conditions are also compatible with radical reactions as illustrated by the addition of *a*-iodoesters to alkenes initiated by copper (Fig. 37). This protocol does not use any solvent since it involves the mixing of the reagents at high temperature directly followed by the product distillation.

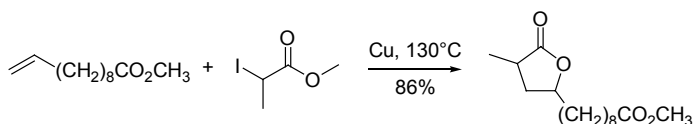


Figure 37. Example of a radical addition to an alkene initiated with copper.

In contrast, dehydration reactions and more generally eliminations can be performed by using conventional solvent-free techniques (Fig. 38). Once again, these methods are in many cases much more efficient than traditional approaches in dilute solution (Kaupp 2005; Loupy and Haudrechy 1996).

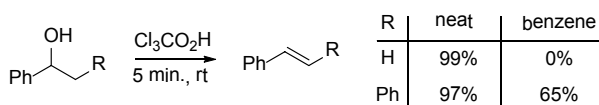


Figure 38. Example of solvent-free dehydration starting from an alcohol.

Reactivity of Carbonyl Derivatives

Acetalization and imine formation are very traditional reactions in organic chemistry. In standard conditions, the chemical equilibrium is generally shifted by removing the water produced using a Dean-Stark apparatus, which involves the use of a large volume of solvent (benzene, toluene or cyclohexane). By contrast, the conventional solvent-free techniques allow performing these reactions at several hundred grams scale very easily and efficiently, whatever the reactants' physical state. Water is continuously removed either by heating under reduced pressure or by adding a drying agent (MgSO_4 , clay, etc.) to the reaction medium (Kaupp 2006). A classically cited and very visual example is the condensation of 4-aminotoluene with *ortho*-vanillin (Fig. 39). When the two solid reagents are brought into contact at ambient temperatures, an orange liquid appears and then solidifies quickly, leading quantitatively to the product (Cave et al. 2001). Moreover, the formation of acetals has been extensively described to protect diols or carbonyl functions (Fig. 39) (Loupouy and Haudrechy 1996).

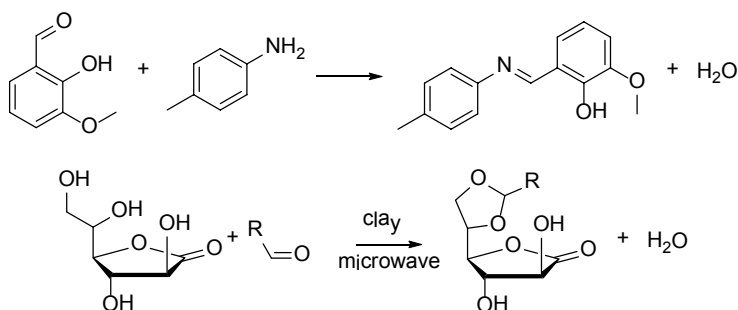


Figure 39. Examples of imine and acetal formation under neat conditions.

Both achiral and asymmetric aldol condensations, and more generally solvent-free additions of carbon nucleophiles (organometallic compounds, stabilized carbanions) to saturated or α,β -unsaturated carbonyl derivatives, have also been extensively studied (Fig. 40). An increase in yield and possibly in selectivity is often observed with respect to dilute conditions. The anions are generated by using either

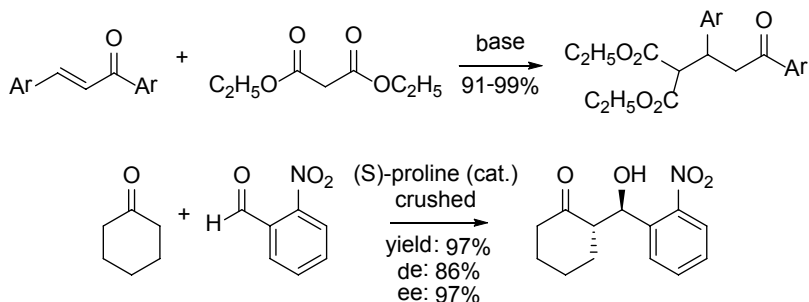


Figure 40. Additions of carbon nucleophiles.

a solid base (sodium hydroxide or alkoxide salt) or inorganic derivatives (clays, calcite, etc.) which then act as a support and a base simultaneously.

Similarly, solvent-free techniques often afford a great advantage in terms of reactivity for the Wittig reaction, which is one of the most powerful methods for the synthesis of alkenes. It has been shown that it is possible to prepare the phosphorus ylide and then react the olefin “one pot” in a few hours with an excellent yield (Fig. 41) (Rodriguez et al. 2007).

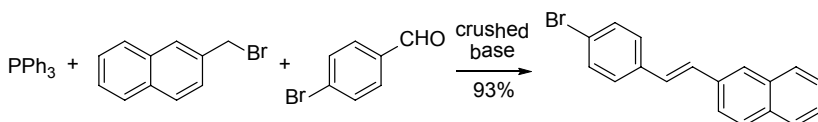


Figure 41. Example of solvent-free Wittig reaction.

Metal-catalyzed Coupling Reactions

Due to their high synthetic potential, the metal-catalyzed coupling reactions have attracted growing interest in the field of solvent-free chemistry since the early 2000s. In this context, BINOL is prepared with a much higher yield by the solid-state reaction of naphthol with a stoichiometric amount of iron chloride (Fig. 42). The beneficial effects of concentrated media have also been exploited for metal-catalyzed coupling reactions such as the Heck reaction and the Suzuki reaction (Fig. 42).

Feasibility for the production of a few hundred grams was recently demonstrated. Conventional methods and solvent-free procedures are sometimes complementary as illustrated by the reactivity of aryl halides in the Suzuki coupling. While the presence of an electron-withdrawing group on the aromatic ring promotes reactivity in the solution, the electron rich aromatic halides are the most reactive in the solid state (Rodriguez et al. 2007). Moreover, an increasing number of metal-catalyzed reactions (metathesis, Pauson-Khand, hydroformylation, allylic amination) are successfully developed at the moment, by focusing first on the achiral version and then the asymmetric one (Walsh et al. 2007).

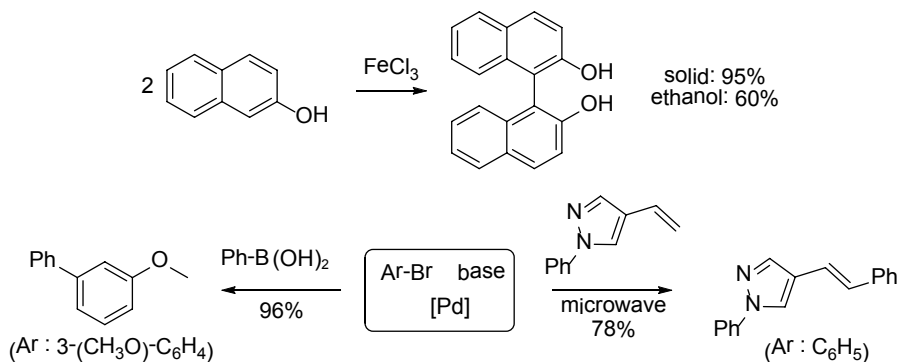


Figure 42. Examples of solvent-free metal-catalyzed coupling reactions.

Polymerization Reactions

Finally, solvent-free reaction conditions described above for additions were extrapolated to the production of polymers. The development of solvent-free polymerization processes has been the subject of intensive research in recent decades because of their huge industrial importance (Fig. 43).

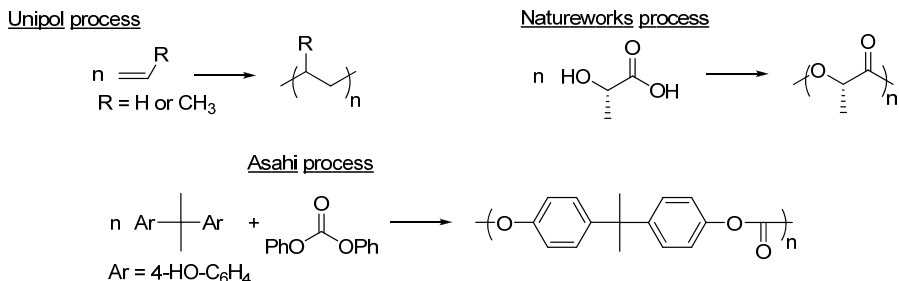


Figure 43. Examples of industrial processes involving an addition to alkenes.

Thus, following Unipol® process (Union Carbide), the polyethylene and polypropylene can be produced at a tens of tons scale by polymerizing in a fluidized bed ethene and propene, respectively. This method has the advantage of avoiding solvents while being compatible with different catalysts, depending on the desired polymer type and most of all it solves the tricky problem of the catalyst/product separation. Following Union Carbide, many industrial groups (BP, Elf Atochem, BASF, etc.) have developed similar processes. In addition, the Cargill Dow company has received the “Greener Reaction Conditions Award” in 2002 for the development of its solvent-free process for producing the polyester derived from the polymerization of lactic acid (NatureWorks® process) (Vink et al. 2003). Finally, a major breakthrough was made in the late 90s regarding the synthesis of polycarbonates when Asahi Chemical Industry has commercialized a process requiring no solvents or phosgene (Metzger 1998).

References

- Alonso, F., I.P. Beletskaya and M. Yus. 2008. Non-conventional methodologies for transition metal catalysed carbon-carbon coupling: a critical overview. *Tetrahedron* 64: 3047–3101.
- Anastas, P.T. and J.C. Warner. 1998. *Green Chemistry: Theory and Practice*. Oxford University Press, New York.
- Balland, L., N. Mouhab, J.M. Cosmao and L. Estel. 2002. Kinetic parameter estimation of solvent-free reactions: application to esterification of acetic anhydride by methanol. *Chem. Eng. Process* 41: 395–402.
- Beletskaya, I.P. and A.V. Cheprakov. 2000. The Heck reaction as a sharpening stone of palladium catalysis. *Chem. Rev.* 100: 3009–3066.
- Bergbreiter, D.E. 2002. Using soluble polymers to recover catalysts and ligands. *Chem. Rev.* 102: 3345–3384.
- Bougrin, K., A. Loupy and M. Soufiaoui. 2005. Microwave-assisted solvent-free heterocyclic synthesis. *J. Photochem. Photobiol.* 6: 139–167.

- Cave, G.W.V., C.L. Raston and J.L. Scott. 2001. Recent advances in solventless organic reactions: towards benign synthesis with remarkable versatility. *Chem. Commun.* 21: 2159–2169.
- Chen, L. and C.J. Li. 2006. Catalyzed reactions of alkynes in water. *Adv. Synth. Catal.* 348: 1459–1484.
- Chinchilla, R. and C. Najera. 2007. The Sonogashira reaction: a booming methodology in synthetic organic chemistry. *Chem. Rev.* 107: 874–922.
- Chiusoli, G.P. and P.M. Maitlis. 2006. *Metal-Catalysis in Industrial Organic Processes*. The Royal Society of Chemistry, Cambridge.
- Cleophax, J., M. Liagre, A. Loupy and A. Petit. 2000. Application of focused microwaves to the scale-up of solvent-free organic reactions. *Org. Process Res. Dev.* 4: 498–504.
- Cornils, B. 1998. Industrial aqueous biphasic catalysis: status and directions. *Org. Proc. Res. Dev.* 2: 121–127.
- Cornils, B. and W.A. Herrmann. 1996. *Applied Homogeneous Catalysis with Organometallic Compounds*. VCH, New-York.
- Correa, W.H., J.K. Edwards, A. McCluske, I. McKinnon and J.L. Scott. 2003. A thermodynamic investigation of solvent-free reactions. *Green Chem.* 5: 30–33.
- Davis, M.E. and K.T. Wan. 1994. Design and synthesis of a heterogeneous asymmetric catalyst. *Nature* 370: 449–450.
- Denmark, S.E. and R.F. Sweis. 2004. Organo silicon compounds in cross-coupling reactions. pp. 163–216. *In: A. de Meijere and F. Diederich (eds.). Metal-Catalyzed Cross-Coupling Reactions*. Wiley–VCH, Weinheim.
- Doucet, H. and J.C. Hierso. 2007. Palladium-based catalytic systems for the synthesis of conjugated enynes by Sonogashira reactions and related alkynylations. *Angew. Chem. Int. Ed.* 46: 834–871.
- Eissen, M., J.O. Metzger, E. Schmidt and U. Schneidewind. 2002. 10 years after rio-concepts on the contribution of chemistry to a sustainable development. *Angew. Chem. Int. Ed.* 41: 414–436.
- Franke, R., D. Selent and A. Börner. 2012. Applied hydroformylation. *Chem. Rev.* 112: 5675–5732.
- Frey, G.D. 2014. 75 Years of oxo synthesis—the success story of a discovery at the OXEA Site Ruhrchemie. *J. Organomet. Chem.* 754: 5–7.
- Genet, J.-P., M. Savignac and S. Lemaire-Audoire. 1999. Transition Metal Catalysed Reactions. pp. 55–74. *In: S.-I. Murahashi and S.G. Davies (eds.). Transition Metal Catalyzed Reactions, A Chemistry for the 21st Century Monograph*. Blackwell Science, Oxford.
- Guisnet, M. and F. Ramôa Ribeiro. 2006. *Les zéolithes : un nanomonde au service de la catalyse*, EDP Sciences, Les Ulis.
- Gusevskaya, E.V., J. Jiménez-Pinto and A. Börner. 2014. Hydroformylation in the realm of scents. *Chem. Cat. Chem.* 6: 382–411.
- Hamada, T.K. Manabe and S. Kobayashi. 2003. Catalytic asymmetric allylation of hydrazono esters in aqueous media by using ZnF₂-chiral diamine. *Angew. Chem. Int. Ed.* 42: 3927–3930.
- Hartwig, J.F. 1998. Transition metal catalyzed synthesis of arylamines and aryl ethers from aryl halides and triflates: scope and mechanism. *Angew. Chem. Int. Ed.* 37: 2046–2067.
- Hartwig, J.F. 1999. New carbon-heteroatom and carbon-carbon bond formation. *Pure Appl. Chem.* 71: 1417–1423.
- Hartwig, J.F. 2002. Palladium-catalyzed amination of aryl halides and related reactions. pp. 1051–1096. *In: E. Negishi and A. de Meijere (eds.). Handbook of Organopalladium Chemistry for Organic Synthesis*. Wiley-Interscience, New York.
- Hatanaka, Y. and T. Hiyama. 1991. Highly selective cross-coupling reactions of organosilicon compounds mediated by fluoride ion and a palladium catalyst. *Synlett.* 12: 845–853.
- Heck, R.F. 1979. Palladium-catalyzed reactions of organic halides with olefins. *Acc. Chem. Res.* 12: 146–151.
- Herrerias, C.I., X. Yao, Z. Li and C.J. Li. 2007. Reactions of C-H bonds in water. *Chem. Rev.* 107: 2546–2562.
- Herrmann, W.A. and C.W. Kohlpainter. 1993. Water-soluble ligands, metal complexes, and catalysts: synergism of homogeneous and heterogeneous catalysts. *Angew. Chem. Int. Ed.* 32: 1524–1544.
- Hiyama, T. 2002. How I came across the silicon-based cross-coupling reaction. *J. Organomet. Chem.* 653: 58–61.
- Hiyama, T. and Y. Hatanaka. 1994. Palladium-catalyzed cross-coupling reaction of organometalloids through activation with fluoride ion. *Pure Appl. Chem.* 66: 1471–1478.

- Hiyama, T. and E. Shirakawa. 2002. Cross-coupling reactions: organosilicon compounds. *Top. Curr. Chem.* 219: 61–85.
- Kaupp, G. 2005. Organic solid-state reactions with 100% yield. *Top. Curr. Chem.* 254: 95–183.
- Kaupp, G. 2006. Waste-free large-scale syntheses without auxiliaries for sustainable production omitting purifying workup. *Cryst. Eng. Comm.* 8: 794–804.
- Kohlpaintner, C.W., B. Cornils and R.W. Fischer. 2001. Aqueous biphasic catalysis: Ruhrchemie/Rhône Poulenc oxo process. *Appl. Catal. A: Gen.* 221: 219–225.
- Leese, M.P. and J.M.J. Williams. 1999. Palladium catalyzed coupling using guanidinium complexes on glass beads. *Synlett.* 10: 1645–1647.
- Leseurre, L., J.P. Genêt and V. Michelet. 2010. Coupling reactions in water. pp. 151–206. *In: P. Anastas and C.-J. Li (eds.). Handbook of Green Chemistry Series: Water as a Green Solvent.* John Wiley & Sons, Weinheim.
- Li, C.-J. 2002a. Developing metal-mediated and catalyzed reactions in air and water. *Green Chem.* 1: 1–4.
- Li, C.J. 2002b. Quasi-nature catalysis: developing C-C bond formations catalyzed by late transition metals in air and water. *Acc. Chem. Res.* 35: 533–538.
- Loupy, A. and A. Haudrechy. 1996. Effets de milieu en synthèse organique. Masson, Paris.
- Lubineau, A. and Y. Canac. 2002. Indium-promoted Barbier-type Allylations in aqueous Media: New access to 2-C- and 4-C-branched sugars. *Adv. Synth. Catal.* 344: 319–327.
- Lubineau, A., J. Augé and M.C. Scherrmann. 2004. Organic chemistry in water. pp. 27–43. *In: B. Cornils and W.A. Herrmann (eds.). Aqueous Phase Organometallic Catalysis: Concepts and Application, Second Edition.* VCH Verlagsgesellschaft gmbh, Weinheim.
- Lubineau, A., J. Augé and M.C. Scherrmann. 2005. State of the art: organic chemistry in water. pp. 40–46. *In: B. Cornils (ed.). Multiphase Homogeneous Catalysis.* Wiley–VCH Verlagsgesellschaft gmbh, Weinheim.
- Mercier, C. and P. Chabardes. 1994. Organometallic chemistry in industrial vitamin A and vitamin E synthesis. *Pure Appl. Chem.* 66: 1509–1518.
- Metzger, J.O. 1998. Solvent-free organic syntheses. *Angew. Chem. Int. Ed.* 37: 2975–2978.
- Michelet, V., M. Savignac and J.P. Genet. 2004. Triphénylphosphinotrimétasulfonate de sodium. *In: L. Paquette, P. Fuchs, D. Crich and P. Wipf (eds.). Electronic Encyclopedia of Reagents for Organic Synthesis.* Wiley, New York.
- Miyaura, N. and A. Suzuki. 1995. Palladium-catalyzed cross-coupling reactions of organoboron compounds. *Chem. Rev.* 95: 2457–2483.
- Muci, A.R. and S.L. Buchwald. 2002. Practical palladium catalysts for C-N and C-O bond formation. *Top. Curr. Chem.* 219: 131–209.
- Nagendrappa, G. 2002a. Organic synthesis under solvent-free condition: an environmentally benign procedure-I. *Resonance.* 7: 59–68.
- Nagendrappa, G. 2002b. Organic synthesis under solvent-free condition: an environmentally benign procedure-II. *Resonance.* 7: 64–69.
- Pfaltz, A. and M. Lautens. 1999. Allylic Substitution Reactions. pp. 834–884. *In: E.N. Jacobsen, A. Pfaltz and H. Yamamoto (eds.). Comprehensive Asymmetric Catalysis.* Springer, Berlin.
- Pinault, N. and D.W. Bruce. 2003. Homogeneous catalysts based on water-soluble phosphines. *Coord. Chem. Rev.* 241: 1–25.
- Polshettiwar, V. and R.S. Varma. 2008. Microwave-assisted organic synthesis and transformations using benign reaction media. *Acc. Chem. Res.* 41: 629–639.
- Rideout, D.C. and R. Breslow. 1980. Hydrophobic acceleration of Diels-Alder reactions. *J. Am. Chem. Soc.* 102: 7816–7817.
- Rodriguez, B., A. Bruckmann, T. Rantanen and C. Bolm. 2007. Solvent-free carbon-carbon bond formations in ball mills. *Adv. Synth. Catal.* 349: 2213–2233.
- Rothenberg, G. 2008. Catalysis: Concepts and Green Applications. Wiley–VCH, Weinheim.
- Scherrmann, M.-C., S. Norsikian and A. Lubineau. 2005. Solvophobic activation of organic reactions. pp. 341–401. *In: Atta-ur-Rahman and G. Jenner (eds.). Advances in Organic Synthesis.* Bentham Science.
- Shaughnessy, K.H. 2006. Beyond TPPTS: new approaches to the development of efficient palladium-catalyzed aqueous-phase cross-coupling reactions. *Eur. J. Org. Chem.* 8: 1827–1835.

- Shaughnessy, K.H. 2009. Hydrophilic ligands and their application in aqueous-phase metal-catalyzed reactions 109: 643–710.
- Shaughnessy, K.H. and R.B. DeVasher. 2005. Palladium-catalyzed cross-coupling in aqueous media: recent progress and current applications. *Curr. Org. Chem.* 9: 585–604.
- Sheldon, R.A., I. Arends and U. Hanefeld. 2007. *Green Chemistry and Catalysis*. Wiley–VCH, Weinheim.
- Sinou, D. 2002. Asymmetric organometallic-catalyzed reactions in aqueous media. *Adv. Synth. Catal.* 344: 221–237.
- Sonogashira, K. 2002. Sonogashira Alkyne Synthesis. pp. 493–529. *In*: E. Negishi (ed.). *Handbook of Organopalladium Chemistry for Organic Synthesis*. Wiley, NY.
- Stille, J.K. 1986. The palladium-catalyzed cross-coupling reactions of organotin reagents with organic electrophiles. *Angew. Chem., Int. Ed.* 25: 508–524.
- Strauss, C.R. and R.S. Varma. 2006. Microwaves in green and sustainable chemistry. *Top. Curr. Chem.*, vol. 266, *Microwave Methods in Organic Synthesis*. 199–231.
- Tanaka, K. and F. Toda. 2000. Solvent-free organic synthesis. *Chem. Rev.* 100: 1025–1074.
- Thomas, J.M. and R. Raja. 2005. Designing catalysts for clean technology, green chemistry, and sustainable development. *Annu. Rev. Mater. Res.* 35: 315–350.
- Trost, B.M. and C. Lee. 2000. Asymmetric allylic alkylation reaction. pp. 593–649. *In*: I. Ojima (ed.). *Catalytic Asymmetric Synthesis*, 2nd Ed. Wiley–VCH, Weinheim.
- Tsuji, J. 2002. Palladium-catalyzed nucleophilic substitution involving allylpalladium propargylpalladium and related derivatives. pp. 1669–1844. *In*: E. Negishi (ed.). *Handbook of Organopalladium Chemistry for Organic Synthesis*, J. Wiley, New-York.
- Vink, E.T.H., K.R. Rabago, D.A. Glassner and P.R. Gruber. 2003. Applications of life cycle assessment to NatureWorks polylactide (PLA) production. *Polym. Degrad. Stab.* 80: 403–419.
- Walsh, P.J., H. Li and C.A. de Parrodi. 2007. A green chemistry approach to asymmetric catalysis: solvent-free and highly concentrated reactions. *Chem. Rev.* 107: 2503–2545.
- Wang, M. and C.J. Li. 2004. Ruthenium-catalyzed organic synthesis in aqueous medium. *Topics Organomet. Chem.* 11: 321–336.

12

Electrochemical Processes for a Sustainable Development

André Savall and François Lapicque

Introduction

Electrochemical processes have been used for decades in diverse branches of industry such as synthesis of fine chemicals, mass production of certain metals such as aluminium or sodium, production of gas, e.g., hydrogen, chlorine or fluorine, deposition of metals or alloys, treatment of effluents or power production. Besides these various industrial applications, electrochemical techniques constitute the principle of numerous analytical techniques. At a more fundamental level, they are also used in the study of mass transfer phenomena in liquid media at the contact of a solid surface. The wide spectrum of applications results from two main characteristics of electrochemical systems:

- The electrochemical reaction is a heterogeneous process which thus presents numerous common points with the reaction taking place onto the surface of a catalyst. The electrochemical conversion consists of the sequence of physico-chemical processes, e.g., adsorption, reactions at the electrode surface (charge transfer) with possibly chemical reactions, and physical steps as transport and transfer phenomena.
- Electrical charges obey specific laws for transport phenomena—as Ohm's law—and the electrochemical reaction on the electrode surface follows Faraday's law (molar flows are proportional to the electrode current).

Before commenting electrochemical processes in a context of sustainable development, it has been preferred to present briefly electrochemical engineering. This discipline can be considered as partially derived from chemical engineering, the main developments of which date back World War II. Before this period, fundamental disciplines, e.g., physics, chemistry, physical chemistry and electrochemistry

were at the origin of the main scientific discoveries in this domain: it can be mentioned for example the progress accomplished in the understanding of transport phenomena through the works of Nernst, Einstein, Stokes, Planck or Maxwell, or the development of the electrochemical techniques by scientists such as Tafel, Volmer, Butler or Heyrovski. The development of processes was at this period more within the competence of engineers. Afterward, as for chemical engineering, with however some delay, the link between the fundamental disciplines and the phenomenological methods—involving tools such as residence time distributions and ideal reactor calculations—allowed in the seventies the real development of electrochemical engineering as a discipline for engineers and researchers. These last decades saw the diversification of the applications and the methods used, as explained farther.

Development and Diversification

The development of electrochemical engineering as well as that of chemical processes by action of the electron certainly benefits from scientific and technological progresses, but is also linked to the changes in the politico-economic world, as for instance the successful arrival of developing countries in the industrial production of big tonnage, the rarefaction of raw materials and the awareness of environmental problems (Lapicque 2004; Bebelis et al. 2013).

Energy

In answer to the rise in energy price caused by the successive oil crises, the adopted energy policy strongly varied from a country to another one: while the fast development of nuclear power plants favored the use of electricity over that of fossil energies, other European countries have more relied upon coal, gas or oil. So, the interest of the electron as energy vector is partially dependent on the policy chosen regarding energy. However, in every case, because energy becomes gradually rarer and more expensive, the efforts concern the reduction of its consumption in chemical as well as in electrochemical processes, both in research and in production. The moderate cost of the electron as reagent compared with that of the chemical reducers or oxidizers has stimulated research towards the development of new electrosynthesis processes.

Furthermore, this situation aroused numerous works to improve the performance of energy converters such as batteries, fuel cells and either solar cells. In particular, because electricity is not always produced when and where it can be used for various applications, it is often considered the dual installation of electrolyzers (producing hydrogen from water and using electricity, and more and more relying upon technology derived from that of fuel cells) and fuel cells (producing electricity from hydrogen and oxygen/air), to be operated at different periods of time, and allowing more reliable management of energy. Improvement of the technology of these two electrochemical reactors, increasing the production rate per surface unit (Arico et al. 2013) and limiting emissions as well as energy losses in conversion, corresponds to a green engineering approach. The domain of fuel cells and related renewable energy

has been largely reported in papers and textbooks for two decades, e.g., EG&G fuel cell Handbook, Hartnig and Roth 2010; Larminie and Dicks 2010; Rand and Dell 2008.

Industrial Production

Traditional productions performed by electrochemical processes—chlorine and aluminium for example—have tended for three decades or so to move towards the emergent industrial nations. Meanwhile, in the area of fine chemistry such as for the production of flavours or active drugs, electrochemical processes diversified thanks to the development of new synthesis routes involving selective electrocatalysts (Degner 1988). However one has to admit that few of these new routes gave rise to competitive industrial processes on one hand because of the cost and of stability of catalysts, on the other hand because of the investment cost of these new processes.

By contrast, two considerable improvements were achieved in the area of production by electrochemical route:

- Replacement of strongly toxic compounds—cyanides for example—either as reagent in certain organic syntheses (Chaussard et al. 1990) or as complexing agent (Ballesteros et al. 2011) in surface treatment processes, or hazardous metals such as cadmium in batteries;
- Introduction of microreactors: these devices working in the sub-millimetre-length scale are characterized by transfer rate clearly higher to those offered by conventional systems, both for mass transport to the electrode and for the heat released by the reaction and which must be evacuated. These promising devices, the realization of which was made possible by the progress accomplished in microtechnologies, in particular in Germany in the 1990's (Ehrfeld et al. 2000), make also possible to isolate intermediate species or toxic by-products.

As a matter of fact, “small” is not the only solution in view to enhancing performance and reliability; it is rather the optimization of the micro-structuration of reactors and the best control of the local variables which improve the efficiency (Matlosz 1995; Bouzek et al. 2010; Löwe et al. 2002).

Environment

Electrochemical techniques appear as promising ways for the environmental protection. Before of opening the concepts of clean processes, green engineering (Anastas et al. 2000; Anastas and Warner 2005) or green electrochemistry (Pletcher and Weinberg 1992), the electrochemical techniques were adapted and used for the treatment of waste and effluents (Rajeshwar and Ibanez 1997; Jüttner et al. 2000; Chen 2004). They have been applied for the abatement of polluting species by various techniques: (i) by direct reaction on the electrode, either for total oxidation of organic matter to CO₂, or disinfection of urban or rural waters (Bergmann et al. 2002), (ii) by indirect electrochemical regeneration of reactive species after chemical action on the pollutant. Several techniques of separation of pollutants were also proposed; let

us quote for example: membrane technologies (electrodialysis) (Strathmann 2010), mechanical separation (settling, flotation) after electrocoagulation (Canizares et al. 2009), or electrokinetic techniques by application of an electrical field to allow metal species in contaminated soils to migrate towards a limited volume.

Toward Clean Electrochemical Processes

Although still a current concern, pollution treatment responds to an urgent need to avoid the scattering of pollutants in the nature and damage hazard at environment. Pretty soon aroused the idea to integrate in the treatment approach, the possible recovery—or recycling—of valuable species after their separation from the effluent to be treated. In particular, water is more and more considered as a product and no longer exclusively either a solvent or a medium. Furthermore, in the selection of the technique to be developed, the technique to be retained has to be the source of zero secondary pollution. This principle of zero pollution is at present taken into account in the concept of clean processes which corresponds in a way to the maxim “prevention is better than cure”. The design of these clean processes includes aspects entirely related to reaction and transport/transfer phenomena. It also comprises process engineering to control all emissions of matter, e.g., greenhouse effect gases, polluting species—while ensuring optimal integration of energy, to limit the significance of heat emission: the multiple skills of engineers are to be employed for this purpose.

After introducing the scope of electrochemical processes, it was preferred to present a brief background section of electrochemical engineering allowing the reader to be introduced to the specificity of electrode reactions. Afterward two particular applications of electrochemical processes have been described. Amongst the various applications of electrochemical engineering, the area of environment—for remediation or waste treatment, and that of energy conversion—fuel cells, batteries, photovoltaic systems and their optimal combination—have been already treated in numerous books for a couple of years, are not analyzed and discussed here. We preferred to focus here on two less well-known applications, namely electrochemical synthesis and electrochemical generation of strong oxidants for disinfection, allowing various aspects of the area to be covered, namely materials, reactions and reactors, in the context of clean and safe engineering.

Backgrounds in Electrochemistry and Electrochemical Engineering

Physicochemical Backgrounds

Electrochemical Interface and Double Layer (Bard and Faulkner 1980; Girault 2004)

The surface of the electrode constitutes a border for the transfer of electrons: in the electrolytic medium, which can be an electrolytic solution, a molten salt or a conductive polymer, charges are transported by ions under the effect of the electric field. In the metal phase—electrodes, metallic connections—the current is transported by electrons, while charge transfer occurs on the electrode surface.

The surface of the electrode is generally charged, i.e., covered with a monolayer of ions and molecules of solvent (water for example): anions are preferentially adsorbed in most cases. This ion layer is stable on the electrode surface and is frequently called the inner Helmholtz layer. Farther from the surface, solvated counter ions—often cations—form the outer Helmholtz layer. Farther still in the electrolytic medium, anions and cations coexist, but the electroneutrality is not yet respected: this second region is called the diffuse Stern layer and constitutes a transition with the electrolytic bulk. The set of rigid and diffuse layers (double layer) of a thickness from a few to 30 nm depending on the ionic strength is the place of a very intense electric field (10^9 V m^{-1}).

Potentials and Current

Definition of Potential

The potential of a charge in a considered phase is proportional in the energy required to extract an electron from infinity and to transport it to the considered location. For Galvani potential, the considered location is the surface of the electrode while for Volta potential, it is about the edge of the double layer. The potential of electrode is defined as the difference between the Galvani potential and the Volta potential (Coeuret and Storck 1993). Although defined as a difference of potentials, it cannot be directly measured and a reference is actually required: for this purpose it can be used various electrochemical references formed by redox couples, e.g., H^+/H_2 couple for the standard hydrogen electrode (SHE) or AgCl/Ag for the silver chloride reference.

Definition of Current Density

The potential in the electrode phase can often be considered as constant for sufficient conductivity of the electrode phase κ_M . The current density in the electrode is expressed with the potential gradient in the metal phase Φ_M :

$$\vec{i} = -\kappa_M \overrightarrow{\text{grad}}\Phi_M \quad (1)$$

A similar relation is written in the electrolytic phase, of conductivity κ_s , with the solution potential Φ_s :

$$\vec{i} = -\kappa_s \overrightarrow{\text{grad}}\Phi_s \quad (2)$$

Therefore, the current density vector can be defined and calculated both on the electrode surface and in any location in the electrolytic solution.

Faraday's Law

Faraday's law relates the current intensity that flows through the interface metal-electrolytic medium to the conversion flux of considered electroactive species A. For the example of the reduction of A involving n_e electrons:



The current intensity I is given by:

$$I = n_e F R_A \quad (4)$$

where F is the Faraday's constant, equal to 96487 coulombs per mol and R_A the conversion rate of species A, in mol s⁻¹. Relation (4) can be expressed in terms of current density (i in A m⁻²) and of conversion flux density (N_A in mol m⁻² s⁻¹):

$$i = \frac{I}{S} = \frac{n_e F R_A}{S} = n_e F N_A \quad (5)$$

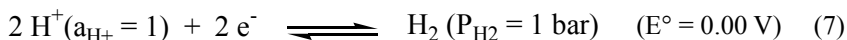
where S is the surface of the electrode. In case that two reactions or more occur at the electrode, the faradaic yield (or current yield) Φ_e is defined as the probability for an electron to be transferred for the desired reaction. For the example of reaction (3):

$$i = \frac{n_e F N_A}{\Phi_e} \quad (6)$$

Fraction $(1 - \Phi_e)$ of the current is consumed through other reactions such as the solvent electrolysis or degradation of product B formed.

Electrodes and Cells at Thermodynamic Equilibrium

Electrodes, electrode potential. The potential difference at the electrode (M)/solution(s) interface $\Delta\phi = \phi_s - \phi_M$ is not measurable in principle. However, by combining two electrodes 1 and 2 in an electrochemical cell the difference between the two interface potentials can be measured; this difference is commonly called cell voltage: $U_{cell} = \Delta\phi_1 - \Delta\phi_2$. To normalize the measurements of potential, the standard hydrogen electrode (SHE) based on the reaction:



was chosen as reference electrode and the potential difference U_{cell} was then defined as the potential of electrode (noted E) with regard to the SHE. According to IUPAC recommendations, the potential difference U_{cell} of an electrochemical cell is equal in absolute value and sign to the electric potential of metal connector of the right electrode (half-cell I) ϕ_I minus that of the left hand electrode, ϕ_{II} (Fig. 1). The limiting value of the potential difference at zero current in the cell is also called electromotive force E.

The electrode potential is actually the electromotive force of a cell in which the left-hand electrode is a SHE, with a potential equal to 0 V, and the electrode to be tested is on the right side. The electromotive force of the cell then represents measurement of the right electrode potential. Written for standard conditions ($P = 1$ bar, activity of species, $a_i = 1$), the standard electrode potential (E°) is a specific property of the redox couple involved at the electrode (Table 1). The electrode potential (E_0) measured at equilibrium, i.e., at zero current, depends in fact on the reactant activities according to Nernst equation. For the redox couple $\sum \nu_i O_i + n e^- \rightleftharpoons \sum \nu_i R_i$ where n is the number of electrons transferred, the Nernst equation is written in the form:

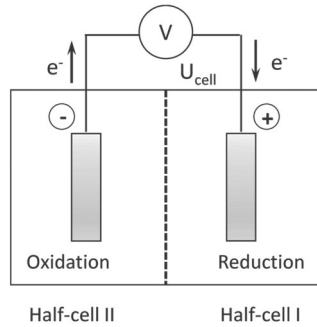


Figure 1. Electrochemical cell formed by two half-cells (I) and (II). In cases that the voltmeter reveals that $\phi_R > \phi_L$, reduction reaction (e.g., $A + e \rightarrow B$) occurs in half-cell I.

Table 1. Electrode reactions and standard electrode potentials E° . By convention, half reactions are written as reductions.

Electrode reactions	Standard potential E° (V) at 25°C vs. SHE
$\text{Li}^+ + e^- \rightleftharpoons \text{Li}$	-3.045
$\text{Na}^+ + e^- \rightleftharpoons \text{Na}$	-2.711
$2 \text{H}_2\text{O} + 2 e^- \rightleftharpoons \text{H}_2 + 2 \text{OH}^-$	-0.8277
$\text{Zn}^{2+} + 2 e^- \rightleftharpoons \text{Zn}$	-0.763
$\text{Fe}^{2+} + 2 e^- \rightleftharpoons \text{Fe}$	-0.409
$2 \text{H}_3\text{O}^+ + 2 e^- \rightleftharpoons \text{H}_2 + 2 \text{H}_2\text{O}$	0
$\text{Cu}^{2+} + 2 e^- \rightleftharpoons \text{Cu}$	0.340
$\text{Ag}^+ + e^- \rightleftharpoons \text{Ag}$	0.799
$\text{O}_2 + 4 \text{H}_3\text{O}^+ + 4 e^- \rightleftharpoons 6 \text{H}_2\text{O}$	1.229
$\text{Cl}_2 + 2 e^- \rightleftharpoons 2 \text{Cl}^-$	1.37
$\text{F}_2 + 2 e^- \rightleftharpoons 2 \text{F}^-$	2.87

$$E_0 = E^0 - \frac{RT}{nF} \sum v_i \ln a_i = E^0 + \frac{RT}{nF} \ln \frac{\prod a_{O_i}^{v_i}}{\prod a_{R_i}^{v_i}} \quad (8)$$

The electrode potential (E_0 vs. SHE) indicates on the oxidizing—or reducing—power of the redox couple for the considered activity conditions. The standard Gibbs free energy of the global reaction in the cell $\Delta_r G_T^0$ at temperature T is linked to the electric work by the relation:

$$\Delta_r G_T^0 = -nFU_{\text{Cell}}^0 \quad (9)$$

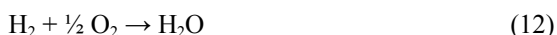
$\Delta_r G_T^0$ is calculated by the algebraic sum of the standard Gibbs free energy of formation of reactants and products in the half-reaction; in practice, by using data at 298 K: $\Delta_r G_{298}^0 = \sum v_i \Delta_f G_{i,298}^0$. If $\Delta_r G_T^0$ is negative, the reaction is exergonic and can occur spontaneously, as for batteries. In the opposite case—endergonic reaction—the reaction is possible only with a contribution of electrical energy from the external environment: this is the case for a device known as electrolyser or electrochemical cell. Equation 9 implies that the cell voltage—or the standard potential—of exergonic reactions is positive, as in Fig. 1.

Cell voltage. By definition, the reversible voltage of an electrochemical cell is an algebraic variable; $U_{0,Cell} = E_{0,c} - E_{0,a}$ in which $E_{0,c}$ and $E_{0,a}$ are the equilibrium potentials of the cathode and the anode respectively.

Let us consider the cell of Fig. 1 with an oxygen electrode on the right side and a hydrogen electrode on the left. According to IUPAC convention, the electrode reactions must be written:



the global reaction being:



The cell voltage under standard conditions is defined as follows:

$$U_{Cell}^0 = E_{O_2/H_2O}^0 - E_{H^+/H_2}^0 = 1.229 V \quad (13)$$

The potential difference U_{Cell}^0 being positive, according to Equation (9) the global Gibbs free energy $\Delta_r G_T^0$ of the cell reaction is negative and equal to $-237.160 \text{ kJ } (mol \text{ H}_2O)^{-1}$ at $T = 298 \text{ K}$. The global reaction is spontaneous and can deliver electrical work nFU_{Cell}^0 when carried out in a reversible H_2/O_2 fuel cell for example. The reversible heat $T\Delta_r S_T^0$ calculated from standard absolute entropy S_T^0 of the reactants in Reaction (12) by $T(S_{H_2O,liq}^0 - S_{H_2,g}^0 - 0.5S_{O_2,g}^0)$ is negative at $T = 298 \text{ K}$ ($-48.647 \text{ kJ } (mol \text{ H}_2O)^{-1}$). This heat released by the system cannot be exploited as electrical work.

If the same two half cells are arranged opposite, with the hydrogen electrode on the right, the cell voltage U_{Cell}^0 is negative and $\Delta_r G_T^0$ is positive (case of electrolyzers). The reversible heat $T\Delta_r S_T^0$ is positive and is taken up from the environment; thus the cell cools. This effect can be compensated if the cell is operated at an increased cell voltage generating the corresponding amount of heat in the system. The corresponding cell voltage is denoted as the thermoneutral voltage defined by:

$$-nFU_{th} = \Delta_r H_T^0 \text{ with } \Delta_r H_T^0 = \Delta_r G_T^0 + T\Delta_r S_T^0 \quad (14)$$

In fact, under real operating conditions ($I \neq 0$), the cell voltage U_{Cell} differs from the voltage at zero current because of irreversible phenomena: (i) the ohmic drop in the electrolytic medium—and the rest of the cell, and (ii) the existence of overpotentials at the two electrodes, as explained below.

Electrode Overpotentials (Diard et al. 1996; Newman 1991)

Definition. Electrochemical reactions are catalytic processes for which the control of the potential settles the current density crossing the electrode interface. The charge transfer can be of finite rate and various models have been proposed to predict the “additional cost in potential” required to allow the passage of the considered current density. For anodic reactions, overpotential η_a is equal to $(E_a - E_{0,a})$ and is positive. Conversely, cathode overpotential η_c defined as $(E_c - E_{0,c})$ is negative.

The classical model of Butler-Volmer. The most well-known model to describe the kinetics of charge transfer is that of Butler-Volmer, which can be applied for reactions assumed reversible and involving only one electron:



Assuming that the charge transfer is the rate-controlling step in the global conversion of A to B, the current density—proportional to the specific flux N_A —is given by the expression:

$$i = i_0 \left\{ \exp\left(\frac{\alpha n_e F}{RT} \eta\right) - \exp\left(\frac{(1-\alpha) n_e F}{RT} \eta\right) \right\} \quad (16)$$

Overpotential η appearing here can be positive—the oxidation rate of B is larger than the reduction rate of A—or negative, in the opposite situation. The coefficient of charge transfer α is comprised between 0 and 1, and i_0 is the exchange current density, i.e., the density of flow of electrons crossing the interface at equilibrium ($i = 0$); although the overall current is nil, the charge flow is not zero but depends on rate constant of the direct and inverse processes. For sufficient polarization, i.e., for absolute values of the overpotential larger than 30–50 mV, one of the two terms in the Butler-Volmer equation becomes negligible and the current density can be approximated by:

$$i \approx i_0 \exp\left(\frac{\alpha n_e F}{RT} \eta_a\right) \text{ for anodic processes} \quad (17a)$$

$$i \approx -i_0 \exp\left(\frac{(1-\alpha) n_e F}{RT} \eta_c\right) \text{ for cathodic processes} \quad (17b)$$

which is equivalent to the empirical Tafel's law:

$$\eta_a = a + b \log(i) \quad (18)$$

This relation being a simplified law does correspond to irreversible reactions.

Partial control by mass transfer rate. For sufficient current densities, mass transfer of species A can become a “slow” process in comparison with the charge transfer, and limit the global conversion. In this case, as for catalytic processes, a profile of concentration of A establishes in the vicinity of the electrode (Fig. 2). The additional difficulty for reaction $A \rightarrow B$ results in a new penalty in the potential, called concentration overpotential η_d . This overpotential depends on the relative importance of the concentration at the electrode surface (subscript s) compared with the concentration in the solution bulk (subscript b):

$$\eta_d = \frac{RT}{(1-\alpha)n_e F} \ln\left(\frac{C_{Ab}}{C_{As}}\right) \text{ for } A \rightarrow B \quad (19)$$

For calculation of the current density in such conditions, a generalized Butler-Volmer equation can also be used taking into account the kinetics for both charge and mass transfer, corresponding to overpotentials η_{ct} and η_d respectively.

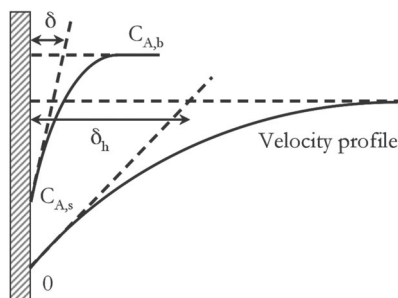


Figure 2. Profiles of velocity and concentration of electroactive species A near the electrode.

Complex Reactions and Electrocatalysis (Diard et al. 1996; Wendt and Kreysa 1999)

Numerous electrochemical reactions are complex, in a way that several electron exchanges can be involved together with adsorption/desorption stages and possibly chemical reactions bringing in for example water molecule or protons. The overall rate of the process is controlled by that of the slowest stage (rate-controlling step). The overall rate of a worked reaction can have very different orders of magnitude depending on the electrode material. For example the exchange current density for hydrogen evolution in acid medium can vary from hundreds of A m^{-2} to a few 10^{-9}A m^{-2} , respectively on Pt and Hg.

Some examples of electrocatalysis reactions are briefly given below.

- For hydrogen evolution, the catalyst has to allow the adsorption of hydrogen atoms formed by reduction of protons H^+ , but also to insure the easy desorption of the dihydrogen molecule: the existence of a maximum for the exchange current density has been demonstrated for an intermediate value of the adsorption energy of hydrogen atom on the considered metal, following the famous volcano-profile of this variation (Enyo 1983; Trasatti 1992).
- For oxygen evolution, the anodic reaction is catalysed by the electrocatalytic oxidation of the metal atoms of multiple valence which can be “overoxidized”. Decomposition of the oxide of higher valence leads to oxygen and to the oxide of lower valence. Maximum efficiency of the catalyst is obtained for an intermediate value of the heat of formation of the metal oxide of the higher valence (Trasatti 1992).

Tables 2 and 3 give typical values of the exchange current densities for hydrogen and oxygen evolution—respectively—on various electrodes. Knowledge of the exchange current density i_0 for a given reaction is to facilitate the selection of the suitable material for the considered reaction at the optimal rate. Moreover, the Tafel slope also given in the two tables indicates on the capacity of an electrode material to exhibit higher activity upon increase in the overpotential. Besides, electrode materials have to be selected also to minimize occurrence of side reactions.

Table 2. Values of the exchange current density at room temperature for hydrogen evolution in acidic and alkaline media (According to Tilak et al. 1982).

Material	Acidic medium		Alkaline medium	
	H ⁺ /M	<i>i</i> ₀ /A m ⁻² (Tafel slope, mV/dec)	OH ⁻ /M or wt%	<i>i</i> ₀ /A m ⁻² (Tafel slope, mV/dec)
C			40%	0.3 (148)
Cd	0.25	1.7 x 10 ⁻⁷ (135)	6	4 x 10 ⁻³ (160)
Fe	0.5	7 x 10 ⁻² (133)	0.1	1.6 x 10 ⁻² (120)
Hg	0.1	7.8 x 10 ⁻⁹ (116)	0.1	3 x 10 ⁻¹¹ (120)
Ni	0.25	6 x 10 ⁻² (124)	0.5	8 x 10 ⁻³ (96)
Pb	0.05	1.3 x 10 ⁻⁹ (118)	0.5	3.2 x 10 ⁻³ (130)
Pt	1	7 (30)	0.1	0.68 (114)

Table 3. Values of the exchange current density at room temperature for oxygen evolution in acidic and alkaline media (According to Tilak et al. 1982).

Material	Acidic medium		Alkaline medium	
	H ⁺ /M	<i>i</i> ₀ /A m ⁻² (Tafel slope, mV/dec)	OH ⁻ /wt%	<i>i</i> ₀ /A m ⁻² (Tafel slope, mV/dec)
Pt	1 (80°C)	1.3 x 10 ⁻⁷ (90)	30%	1.2 x 10 ⁻⁵ (46)
RuO ₂ + TiO ₂	1 (80°C)	1.3 x 10 ⁻⁴ (66)		
Beta-PbO ₂	H ₂ SO ₄	6 x 10 ⁻⁶ (120)		
Fe			30%	0.17 (191)
Ni			30%	2.3 x 10 ⁻³ (62)

Cell Voltage and Energy Yields (Coeuret and Storck 1993)

The actual cell voltage U_{Cell} under current operation is calculated from the various following contributions: the equilibrium potentials at the two electrodes (reversible potential), the charge transfer overpotentials at both electrodes, η_{ct} —which can often be expressed by Butler Volmer's law or Tafel law, concentration overpotentials, η_d , and the ohmic drop, proportional to the overall resistance of the electrochemical reactor, R_c . For electrolysis cells or reactors, U_{Cell} is negative and these contributions require the application of a more negative potential difference to allow the electrochemical operation. Relation (20) below gives the usual expression of the cell voltage:

$$U_{Cell} = E_{0,c} - E_{0,a} - \eta_{ct,a} - \eta_{d,a} - |\eta_{ct,c}| - |\eta_{d,c}| - R_c I \quad (20)$$

For current generators, the cell voltage is positive, but the existence of ohmic drop and the various overpotentials, contribute to reduce this value from the reversible cell voltage.

A Brief Introduction to Energy Considerations

Operation of the electrochemical cell consumes the power ($U_{Cell} I$). Power $U_{th} I$ is converted to chemical energy at constant temperature and the complement ($U_{Cell} - U_{th}$) I is degraded in heat—regardless of pumps and other ancillary devices required for operation of the overall process.

The specific energy consumption is often defined as the electrical energy consumed for the production of 1 kg of species B as follows:

$$E_s = \frac{U_{\text{cell}}Q}{M_w} = \frac{U_{\text{cell}}n_e F}{M_w \Phi_e} \quad (21)$$

if Q is the electric charge consumed in the considered production, M_w , the molecular weight of species B. The specific energy consumption varies typically from a few kWh kg⁻¹ to nearly 100 kWh kg⁻¹.

Transport and Transfer Phenomena in Electrochemical Systems

Mass Transport Flux and Current Density (Newman 1991; Girault 2004)

In the presence of an electric field, ionized species are submitted to an electric force the intensity of which is proportional to their charge and to the intensity of the local electric field. A viscosity force is generated by the velocity of charged particles in the environment of non-nil viscosity. The force balance corresponds to the limiting velocity of the charged particles, and thus to their mobility u' , which is defined as their velocity for a unit of electric field. In the case of diluted solutions, the mobility of the ions is linked to its diffusion coefficient D by the equation of Nernst-Einstein:

$$u' = \frac{D}{RT} \quad (22)$$

From the expression of Stokes for the viscosity force mentioned above, relation (22) leads to the conventional relation, valid only in very diluted media and for a given ion species:

$$\frac{D\mu}{T} = Cte \quad (23)$$

The flux density N_j of ion particles possessing charge z_j and present at local concentration C_j can be expressed by the sum of the specific flows of convection, diffusion and migration. For the case of diluted solutions, N_j is expressed by Nernst-Planck's relationship:

$$\vec{N}_j = C_j \vec{u} - D_j \overline{\text{grad}} C_j - \frac{D_j C_j}{RT} z_j F \cdot \overline{\text{grad}} \Phi_s \quad (24)$$

where \vec{u} is the local average velocity of the conducting fluid. The current density circulating through the electrolytic solution results from the specific fluxes according to Faraday's law:

$$\dot{i} = \sum_j z_j F \vec{N}_j \quad (25)$$

Besides, the electroneutrality relation

$$\sum_j z_j C_j = 0 \quad (26)$$

can be applied anywhere in the considered electrochemical system—except in the neighborhood of the double layer—and so, from the expression of the specific flow, the current density can be expressed as:

$$\vec{i} = -F \sum_j z_j D_j \overrightarrow{\text{grad}} C_j - \kappa_s \overrightarrow{\text{grad}} \Phi_s \quad (27)$$

where conductivity κ_s is defined by:

$$\kappa_s = F^2 \sum_j z_j^2 \frac{D_j C_j}{RT} \quad (28)$$

These relations are valid only in diluted media. For more concentrated media, it is advisable to use more complex transport equations (Newman 1991). Besides, for a zero concentration gradient, the expression of the current density simplifies to the Ohm's law given above.

Mass Transfer at Electrode Surfaces

The finite rate of mass transport phenomena for both reactants and products is expressed by the existence of concentration profiles for the various species, as explained above.

Transfer phenomena. Mass transfer phenomena result from momentum exchanges in the fluid in motion with reference to the electrode surface. The fluid velocity is nil on the electrode surface which is supposed motionless here. The velocity field establishes along the electrode surface, with a velocity profile hydrodynamic layer, as shown in Fig. 2.

An exception in this situation is the perfectly established laminar flow, with a parabolic velocity profile between two flat electrodes, for Reynolds numbers, Re , below approximately 2000 for established flows in a pipe or in ducts (NB. Re characterizes the inertial behavior of the flow compared with its viscosity). Higher Reynolds numbers caused by higher velocity or more important electrode gaps, correspond to turbulent flows. However, the hydrodynamic regime is rarely established because the electrode length is usually restricted in most electrochemical cells. Mostly, because of the entrance and outlet sections of the liquid, with local changes in cross sections of flow directions, the flow becomes established along the electrode, unless it is locally disrupted. Turbulence zones and dead volumes can be also encountered. Mass and momentum transfers present certain similarity. However, because the kinematic viscosity of the media is approximately 1000 times than the diffusivity of the electroactive species, the hydrodynamic layer is approximately 10 times larger than that of the concentration profile (Fig. 2).

Nernst film model and limiting current density. Mass balance in an elemental fluid volume can be expressed as follows:

$$\frac{\partial C_j}{\partial t} = \text{div} \vec{N}_j = \text{div}(C_j \vec{u}) - D_j \nabla C_j - \frac{D_j z_j F}{RT} \text{div}(C_j \overrightarrow{\text{grad}} \Phi_s) \quad (29)$$

In the neighborhood of the electrode surface, the local velocity of the fluid can be neglected. Furthermore, in the presence of an excess of supporting electrolyte—which has to be chemically inert but which must allow charge transport—the migration term of can be neglected. In permanent regime, the above balance reduces to:

$$D_j \nabla C_j = 0 \tag{30}$$

In the case of one-dimensional systems, the equation above leads to a linear concentration profile: this approximation corresponds to the Nernst film model, with thickness δ as shown in Fig. 2. For such assumptions, the current density related to the consumption of species A can be written as:

$$i = n_e F D_A \left(\frac{C_{Ab} - C_{As}}{\delta} \right) \tag{31}$$

Besides mass transfer flux can be expressed as the product of a mass transfer coefficient, k_L , and the concentration difference appearing in the above formula, as shown below:

$$i = n_e F k_L (C_{Ab} - C_{As}) \tag{32}$$

When the charge transfer is very fast compared with the mass transfer to the electrode, i.e., for high absolute overpotentials, the reaction rate is then controlled by mass transfer, so concentration C_A is zero on the surface of the electrode. In such a case the current density attains its limiting value i_L :

$$i_L = n_e F k_L C_{Ab} \tag{33}$$

In cases of low/moderate overpotentials, the current density depends on the kinetics of both charge and mass transfers. Figure 3 shows on an example the variation of the current density with the overpotential for the case of an oxidation process for arbitrary values of i_L .

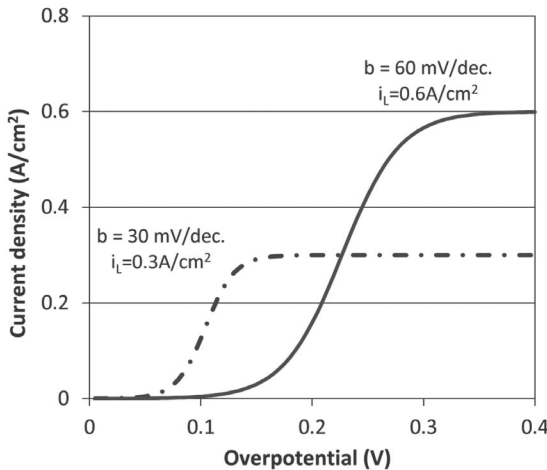


Figure 3. Typical profiles of current density vs. overpotential (case of oxidation reaction). Exchange current density $i_0 = 0.001 \text{ A cm}^{-2}$.

Mass transfer coefficient and existing correlations for its estimation. Identification of the two expressions for the current density leads to the expression of coefficient k_L , according to the film model. In fact, the mass transfer coefficient depends on the diffusivity of the considered species, and several variation laws can be encountered in literature depending on the considered model:

$$\begin{aligned} k_L &\approx D_j / \delta \text{ Film model} \\ k_L &\propto D_j^{2/3} \text{ Motionless free surface} \\ k_L &\propto D^{1/2} \text{ Penetration model} \end{aligned} \quad (34)$$

Determination of the value for mass transfer coefficient is an important stage in the study of electrochemical processes because it allows prediction of the maximal current density. Mostly electrochemical techniques are used for this purpose (Pickett 1979; Coeuret and Storck 1993; Ibl Dossenbach 1983). The rate of mass transfer is expressed in the form of dimensionless correlations, which are valid whatever the physicochemical system:

$$Sh = \frac{k_L d}{D} = a Re^n Sc^{1/3} \quad (35)$$

where Sh is the Sherwood number, Re the Reynolds number and Sc the Schmidt number. Sc compares the kinematic viscosity ν of the solution with the diffusivity of the electroactive species in this solution ($Sc = \nu/D$). Typically, k_L depends strongly on the average velocity of the fluid, u_m , on physicochemical parameters such as the solution kinematic viscosity and the diffusivity of the electroactive species, and on the electrochemical features of the cell, e.g., design and dimensions. Characteristic dimensions of the cell can be the electrode length and the hydraulic diameter d_h of the channel. Inert wire nettings inserted between both electrodes, or into the compartment of the working electrode allow the intensification of mass transfer: they act as so-called turbulence promoters. In reality, the liquid flow is disrupted locally by the presence of the grid without being turbulent, mainly because of the low dimensions of the wire netting (in the order of a few millimeters or below). In the case of electrochemical reactions carried out on the surface of a fixed-bed electrode, the diameter of particles d_p forming the bed also intervenes. As indicated by Equation 35 mass transfer coefficient is an increasing function of liquid velocity, taking into account the exponent n in the power function involved. Although local mass transfer coefficients can be considered, most correlations have been established with average velocity u_m of the fluid. Exponent n strongly depends on the flow regime, varying from 1/3 for established laminar flows to 0.8 for fully turbulent flows. In most cases, flow in electrochemical cells is not fully established and the dimensions seldom allows real turbulent conditions, so the electrolyte flow is usually disrupted, resulting in exponent n in the order of 0.5 (see Table 4).

An important exception is represented by micro-reactors, whose electrode gap is far lower than the millimetric scale: when the profiles of concentration in the neighborhood of both parallel electrodes interpenetrate—i.e., for a space inter-

Table 4. Literature examples of mass transfer correlations; d_h is the mesh dimension of the grid employed, d_p is the diameter of the particles in the fixed bed and d is the electrode gap (According to Pickett 1979; Coeuret and Storck 1993).

Flow regime with reference	Conditions of validity	Correlation
Established laminar flow (Lévêque)	$Re = \frac{u_m d_h}{\nu} < 2300$	$Sh = \frac{k_L d_h}{D} = 1.85 \left(Re Sc \frac{d_h}{L} \right)^{1/3}$
Laminar non-established flow (Pickett and Ong 1974)	$Re = \frac{u_m d_h}{\nu} < 2300$	$Sh = \frac{k_L d_h}{D} = 1.85 Re^{1/2} Sc^{1/3} \left(\frac{d_h}{L} \right)^{-0.05}$
Turbulent non-established flow (Pickett 1979)	$Re = \frac{u_m d_h}{\nu} > 2300$	$Sh = \frac{k_L d_h}{D} = 0.145 Re^{2/3} Sc^{1/3} \left(\frac{d_h}{L} \right)^{1/4}$
Turbulent (Chilton-Colburn)	$Re = \frac{u_m d_h}{\nu} > 2300$	$Sh = \frac{k_L d_h}{D} = 0.023 Re^{0.8} Sc^{1/3} d_h^{0.2}$
Flow through a stack of inert grids placed on the electrode surface (Letord-Quéméré et al. 1988)	$150 < Re_g = \frac{u_m d_g}{\nu} < 1500$	$Sh_g = \frac{k_L d_g}{D} = 1.25 Re_g^{0.46} Sc^{1/3}$
Fixed bed of active particles (Barthole-Delaunay 1980)	$10 < Re_p = \frac{u_m d_p}{\nu} < 50$	$Sh_p = \frac{k_L d_p}{D} = 1.31 Re_p^{0.54} Sc^{1/3}$
Laminar flow in sub-millimetric channel (Pickett 1979)	$\frac{DL}{u_m d^2} > 0.1$	$Sh = \frac{k_L d}{D} = 2.69$

electrode of 50–100 μm —the conventional theories for mass transfer are not applicable anymore and the Sherwood number reaches a constant value, independent of the average flow velocity, and so is it for mass transfer coefficients, which vary nevertheless with the reciprocal of the cell gap.

Mass transfer coefficients range is typically from 10^{-6} and 10^{-4} m s^{-1} depending on the cell configuration and the flow conditions.

Current Distributions in Electrochemical Cells

Distributions of potential or current density have a very important role in the operation of the electrochemical reactors. As a matter of fact, if it is possible to impose the potential of electrode or the global current in the cell by using conventional stabilized power supplies, factors such as the geometry of the cell and the kinetics of the various processes involved in the considered electrochemical conversion, can be the source of local potential differences. The spatial variation of potential in the cell corresponds to non-uniform distributions of current density. Therefore, the specific flux of production of electrogenerated species is not the same in all locations of the electrode surface.

- The non-uniform character of potential and current density distributions has important consequences in the operation of electrochemical processes.

- The uniformity of the potential of electrode is required in numerous production processes, in particular for electrosynthesis where the selectivity of the reaction is ruled by the electrode potential.
- Non-uniform distributions of current density result from local variations of ohmic drop.
- In galvanic processes, distributions of current density govern the distributions of deposit thickness. Too important variations must be avoided to prevent corrosion phenomena in zones covered by too thin deposits.
- In electrometallurgical processes non-uniform distributions result in too important growth at particular—favoured—locations: this irregular growth can modify the geometry of the cell in the case of low electrode gaps. Moreover, important changes in the hydrodynamics and the ohmic drop can be observed along time. On the contrary accelerated corrosion phenomena of the anode are observed in some locations: the operating costs of the global process are then increased because of the more frequent replacement of anodes.
- The use of the three-dimensional electrodes, e.g., fixed beds of conductive particles is often limited by too strong variations of the electrode potential.

The distribution of the current density and the electrode potential is a significant scientific domain for improving or modelling electrochemical processes as shown by the number of articles and chapters of works dealing with this problem (Ibl 1983; Newman 1991; Deconinck 1992). In a general way, current and potential distributions are influenced by four factors, which characterize the considered electrochemical process:

- The geometry of the cell, i.e., shape, dimensions and configuration of the electrodes and other components of the cell;
- The conductivity of the electrolytic medium and of the electrodes;
- The kinetics of charge transfer at the interface metal-solution—slow charge transfer processes correspond to high values of charge transfer overpotential η_{ct} ;
- The mass transfer rate, linked to overpotential η_d : this overpotential becomes significant for mass controlled operations.

Because of the non-uniformity of current distributions, the electrochemical conversion of the reactant can be hindered by three sorts of resistances. First of all, the ohmic resistance of the electrolytic solution—plus sometimes that of the electrode— R_{ohm} , which depends on the two first factors. Two more resistances related to occurrence of the electrode reaction have also to be accounted for: charge transfer resistance R_{ct} , defined as $(\partial\eta_{ct}/\partial i)/S$ and mass transfer—diffusion-resistance R_d , equal to $(\partial\eta_d/\partial i)/S$ if S is the electrode surface.

Equations to be Solved

Current density distribution can be calculated by using the continuity equation:

$$\operatorname{div}(\vec{i}) = 0 \quad (36)$$

where the current density is given by relation (27). When mass transfer by diffusion or convection is not rate-controlling, i.e., for current densities clearly lower than i_L , resistance R_d is little significant in comparison with the two others. Furthermore, in absence of chemical reactions, the chemical composition of the medium is uniform in the cell and Equation (36) simplifies to:

$$\nabla^2 \Phi_s = 0 \text{ (Laplace's Equation)} \quad (37)$$

$$\dot{i} = -\kappa_s \overrightarrow{\text{grad}} \Phi_s \quad (2)$$

The current—and thus the potential gradient—is zero on the surface of the insulating zones. Other boundary conditions depend on the operating conditions and involve the relation between the electrode potential and the current density, given for instance in the form of Butler-Volmer relation.

Wagner number, Wa , is frequently used to quantify the importance of the charge transfer resistance in comparison to the ohmic resistance of the cell:

$$Wa = \frac{R_{ct}}{R_{ohm}} \quad (38)$$

It can be shown that the distributions of potential and current density are more uniform for high values of the Wagner number, i.e., for low charge transfer rates and very conductive electrolytic media. This situation is looked for in galvanoplastic processes, so deposition baths contain generally additives allowing charge transfer to be significantly inhibited—and thus metal growth—together with a wide excess of supporting electrolyte support.

Electrochemical Reactor Design: An Introduction

General Aspects

Operation of electrochemical reactors can be described according to various criteria:

1. Chemical composition of the electrolytic solution: is the solution homogeneous, or does it exist significant changes in concentrations between the cell inlet and the outlet?
2. Flow conditions in the cell: for example, does the solution flow regularly along the electrode surface, or are there recirculation vortices which infer local turbulence phenomena? Furthermore, depending on the flow patterns, the composition of the liquid can be more or less uniform and this point is linked to the previous item. Models of ideal reactors—largely used in chemical engineering—e.g., agitated reactors of uniform composition and plug flow reactors—can be used to model the electrochemical cell. Alternatively more sophisticated models, e.g., with various zones, or in the presence of exchange phenomena, can be employed.
3. Operation along time: continuous or discontinuous runs of the reactor?
4. Electric connection and operating mode. For this last criterion, the cell can be operated with imposed current, corresponding to intensiostatic (or galvanostatic)

mode. Alternatively, it can be run at controlled potential, or even at controlled cell voltage. As a matter of fact, it can be preferable for fundamental studies to maintain constant the electrode potential for better control of the process selectivity. However, in industrial practice or at least for real application, cells are not provided with a reference electrode, so the potential difference at the two current connectors (cell voltage) is fixed.

The various combinations of operating conditions are treated in textbooks (Goodridge and Scott 1995; Wendt and Kreysa 1999) on electrochemical engineering and development of the model equations derives from chemical reaction engineering. These models are of a practical use for the design and the sizing of a cell for the production of interest. However, in these models, specific physical phenomena such as deactivation of the electrode or occurrence of side electrode processes, are only rarely taken into account and the results of the models must be confirmed even corrected by experiments.

A Frequently Used Example: The Filter-press Cell Operated Continuously at Limiting Current

This cell consists of two flat, parallel electrodes, separated by a thin gap to minimize the ohmic drop. For sufficient fluid velocity, liquid flow can be supposed to be of plug flow type. This case is the most simple, offering the maximal performance of the cell, the electrode potential of which must be fixed in a domain, so that the current density can attain its limiting value i_L everywhere on the electrode surface.

As for plug-flow chemical reactors, the mass balance is written with concern to species A contained in the volume element and which is consumed on the elementary surface dS in the cell:

$$\dot{V}C_A = \dot{V}(C_A + dC_A) + \frac{i}{n_e F} dS \quad (39)$$

NB. C_A refers here to the bulk concentration of species. Because the current density is equal to i_L on the electrode surface, and taking into account Relation (33), mass balance (39) resumes to:

$$\dot{V}dC_A = -k_L C_A dS \quad (40)$$

Integration of the above relation yields:

$$C_{A,out} = C_{A,in} \exp\left(-\frac{k_L S}{\dot{V}}\right) \quad (41)$$

Conversion rate of species A at the reactor outlet can then be deduced:

$$X_{out} = 1 - \exp\left(-\frac{k_L S}{\dot{V}}\right) \quad (42)$$

From the mass transfer correlations given above, it can be shown using Relation (42) that, in most of cell configurations, the conversion of A at the cell exit is low, usually far lower than 10%. Two important exceptions can nevertheless be given: i) fixed bed electrodes, for which the specific surface is very large in comparison with

that offered by flat electrodes in by filter-press cells, ii) electrochemical microreactors which offer very high area/volume ratio, in particular when the electrode gap is far below one millimeter.

Relation (42) allows the influence of the velocity—linked to the volume flow rate—on conversion X to be predicted. Increasing the velocity enhances mass transfer coefficients, however according to a power-law function whose exponent is below unity. Therefore increased solution velocity results finally in reduced conversion. When high conversion of species A (close to unity) is required, the electrolyte solution is recycled between the reactor and the reservoir and, as done in chemical reactor engineering, the conversion rate can easily be shown to increase with the recycling rate.

Electroorganic Synthesis

Electrosynthesis in Conventional Processes

Introduction

Electroorganic synthesis is generally described as an alternative way to other organic synthesis methods, the electric activation substituting itself for thermal, catalytic or even photochemical activations. From the second quarter of the nineteenth century, Kolbe studied the oxidation of carboxylic acids on the surface of platinum anodes, in neutral solutions to produce alkanes by dimerisation of the radicals produced by the decarboxylation. Afterward, syntheses diversified, with the help to some extent of the improvement in the understanding of phenomena involved in the electrochemical cell. In addition, the above diversification have still more benefited from the tremendous advance of organic synthesis, in particular in Germany and other European countries, then afterward in the United States, in Japan, in India, and nowadays throughout the world. It was then noticed that, in numerous cases, the electron brought in appropriate conditions allowed the use of strongly toxic reactants or the formation of undesired substances in the reaction medium to be avoided. Syntheses developed in the first half of the twentieth century were essentially addressed to low or moderate tonnage productions, for many in fine chemistry or in specialty chemistry as exemplified below:

- Anodic oxidation of hydrocarbons for the synthesis of alcohols, in particular carbinols, aldehydes and carboxylic acids;
- Ether synthesis by methoxylation;
- Synthesis of amines or other aminocompounds, and amides from nitrocompounds;
- Grignard synthesis for the formation of carboxylic acids, carbinols, aldehydes or even organometallic compounds.

Since then, syntheses strongly diversified, in particular by the development for example of stereoselective syntheses, dimerisations or electrochemical polymerizations.

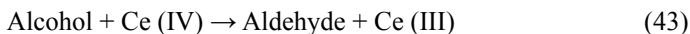
Cells used until the 1960's, were of a design directly deriving from that of agitated vessels in chemical industries. In most cases, the reactant (substrate) exhibiting only a low affinity for water or the electrolytic medium was dispersed in the form of droplets or solid particles in the electrolytic solution. This medium was frequently at this time a relatively concentrated solution of sulfuric acid. As described clearly in the book of Tilak (Tilak et al. 1982), the conversion of the electrochemical substrate consists of its dissolution or solubilization, followed by its conversion on the electrode surface: the maximal current density is proportional to reactant solubility C^* . The rise of the temperature allows, in addition to activation of electrode processes, to increase the substrate solubility and to lower the surface tension of the suspended entities, at the risk of favoring secondary reactions, such as formation of dimers or unsaturated species, at the anode.

By use of Relation (33) and assuming a mass transfer coefficient at a few 10^{-5} m s^{-1} , it can be shown that a solubility lower than 10^{-2} M corresponds to a current density lower than 100 A m^{-2} , and thus to a specific production rate below or in the order of $0.1 \text{ kg m}^{-2} \text{ h}^{-1}$. To mitigate the poor to-moderate solubility of the organic substrates, physico-chemical parameters of the reaction and the electrolytic medium can be optimised and, on the other hand, the design of the electrochemical cell can be improved. These solutions are discussed below.

Physicochemical Solutions

Various synthesis techniques can be considered to carry out electroorganic synthesis reactions, as briefly reminded below (Baizer and Lund 1983; Pletcher and Walsh 1993; Lund and Hammerich 1991):

- Indirect electroorganic synthesis, for reduction and oxidation reactions with a low solubility of the substrate. Conversion of the substrate to the desired product is achieved by action of an oxidizing/reducing agent, being mostly a metal salt. The regeneration of the redox agent is carried out on the surface of the electrode, as exemplified below for the case of aldehyde production:



- The electrochemical reaction is carried out to regenerate the Ce (IV) from a concentrated solution of Ce (III): high production rates can then be expected. The regeneration is achieved in a filter-press cell, whose design is suitable for electrochemical conversion of concentrated reactants; the filter-press cell is mounted in a flow rig, connected to the stirred reactor in which the chemical reaction occurs—here alcohol oxidation. The configuration is often called Ex-cell regeneration. For this particular example, the aqueous phase has to be treated upstream of the electrolytic cell to remove all dissolved organic compounds which could inhibit the electrode surface (Tzedakis and Savall 1997).
- It is possible to increase the “apparent” solubility of an organic species by use of surfactants. Addition of these compounds being electrochemically inert over

a certain concentration allows the formation of micelles or liposomes of organic compounds: these entities, with size is usually below one micrometer are dispersed in the continuous aqueous phase. However mass transfer rate of these entities—far larger than single molecules—by convective diffusion towards the electrode surface is clearly slower than that of dissolved molecules. As a result, the limiting current density is not increased in so spectacular a way.

- The adsorption of dissolved ions, in particular those of the supporting electrolyte on the electrode surface influences the adsorption of the solvent, e.g., water. In some cases, as for the cathodic hydrodimerisation of olefines, it is preferred that water does not adsorb on the cathode surface to avoid the side evolution of hydrogen. The synthesis of adiponitrile from acrylonitrile had been strongly improved since the first synthesis by introduction of large-size organic salts, the adsorption of which limits strongly that of water molecule, which is to favor undesired dimerization reaction (Lund and Hammerich 1991).
- As introduced by chemists at the end of the 1970's, phase transfer agents make it possible to introduce a redox species contained in the aqueous phase towards the dispersed globule of organic phase (Caubère 1982): these agents are often of amphiphilic nature. Upon use of such agents, the chemical reaction involved in the indirect electrosynthesis does not occur in the bulk of the electrolytic aqueous phase, but in the organic phase, which is a medium usually more favorable to the organic synthesis as can be predicted by Hammett's laws. However, because most of the redox organic reactions involve protons, it is likely that reactions in the presence of these transfer agents occur at the interface between the two phases.
- Finally, more and more electrosynthesis reactions are conducted in a mixed aqueous-organic medium (e.g., EtOH-H₂SO₄ 1M 50:50), or even in organic solutions. For that purpose, the solvent has to possess a dielectric constant high enough—e.g., acetonitrile, dimethylformamide or trimethylurea—so that the ions of the dissolved electrolyte, produced by solvation, can ensure the circulation of the electric current. The supporting electrolyte support is generally formed by salts of voluminous cations (quaternary ammonium or phosphonium ions) and of anions of smaller sizes which however can be polarized, e.g., sulfate, fluoroborate or iodide.

Reactors

Filter-press with turbulence promoters (Coeuret and Storck 1993). Most of electrochemical cells are of filter-press type to limit the importance of the ohmic drop in the inter-electrode gap. Furthermore, supplying the cell with turbulence promoters, in the form of polymer grids or other inert corrugated materials in direct contact with the electrodes allows mass transfer rates to be increased by the flow disruption, resulting in higher limiting current density values. In one configuration, the gap can be filled with a stack of wire nettings (grids), which behaves as an inert fixed bed whose porosity is higher than that of inert particle beds. Another alternative consists in inserting only inert grid close to the electrodes, the rest of the channel

formed by the two facing electrodes being empty. The global electrolyte velocity is generally slightly lower than that to apply in an empty channel, but the mass transfer coefficient of transfer is clearly enhanced.

Capillary gap cells. At the end of the sixties, BASF patented the principle of the capillary gap cell. The principle of the cell can be partly considered as the application of the above described technique, but with a very thin capillary space and filled with a single grid or wire netting. This configuration allows inter-electrode gaps below one millimeter: such a configuration is of great interest in electroorganic synthesis for the production of carbinols, methoxy compounds or of aldehydes, in particular in organic electrolytic media, for which the conductivity is generally clearly lower than that of a concentrated aqueous solution. Furthermore, the patented cell is provided with metal disks acting like bipolar electrodes: the cell is in fact a stack of metal disks drilled in their centers and separated from each other by a sheet of wire netting. The weight of the pile ensures the cohesion of the set, the constancy of the inter-electrode gap, even under the pressure of the radial fluid flow, from the central vein towards the peripheral region, outside of the stack. As a matter of fact, the stack is installed in a tank or in a column and the electric connections consists of two current leads fixed at the two extreme disks of the cell stack (Lund and Hammerich 1991).

In spite of the numerous works published or patented in the domain, few production processes are currently operated at the industrial scale. It is due to several factors, in particular the cost of the electrochemical cells, a consequence of the reduced number of equipment manufacturers, the relative efficiency of catalytic (conventional) processes, and the necessary separation of the end-product from the electrolytic solution downstream of the cell. It is likely that the big tonnage production is never ensured by electrosynthesis; on the other hand for specific productions, the recent progress in electroorganic synthesis should offer new means of production to the chemistry area.

New Trends in Electroorganic Synthesis

General Aspects

Electroorganic synthesis aims at producing organic compounds, with high yields and selectivity with reasonable costs of energy and investment. For the sake of green processes implementation of the electrosynthesis must be designed then carried out in a way to avoid formation of toxic compounds, even as intermediate species (Frontana-Urbe et al. 2010; Schäfer 2011). For this purpose, the following possibilities can be considered:

- Change reactivities: expensive, unstable and/or toxic reactivities, e.g., cyanides, phosgene, organochlorinated reagents are to be excluded, as well as superoxidizing reagents or reducing agents, e.g., borohydrides or silanes.
- Change the solvent and the supporting electrolyte: the solvent will be as often as possible one the reactants—as methanol in methoxylations—and, as discussed later, submillimetric reactors allow to strongly reduce the “salt” concentration, which facilitates greatly the separation stage of the key product from the

reacting medium after the synthesis. Ionic liquids, as for them, can exhibit the two functions of solvents and electrolytes, and are therefore considered as a tool for the development of clean technologies in electrosynthesis (Doherty et al. 2012). Nevertheless, long term stability of the ionic liquid employed in the process considered has to be evaluated, together with solutions for end-of-life of the particular compound (Schäfer 2011).

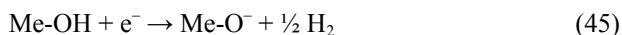
- Select the electrode materials, for both their intrinsic nature and by their chemical and electrochemical resistance, in a way that the solution going out of the cell is perfectly heavy metal-free, of course while avoiding the occurrence of undesired side reactions. An electrode material in full development from the end of the twentieth century is boron-doped diamond, due to its very broad “electrochemical window” in aqueous media and its particular catalytic properties.
- Make sure while examining the reaction mechanism that strongly toxic intermediate species could not be formed in the overall synthesis.

As presented by Fuchigami 2007 and by Schäfer 2011, several new electroorganic syntheses have been proposed, in full consistence with green chemistry and sustainable development: among these new methods, we present briefly here two methods which appear significant, promising and representative of electrosynthesis area.

Coupling Anodic and Cathodic Reactions

Most of the electrochemical processes have been designed to carry out a reaction at the cathode (or at the anode): the reaction which occurs at the counter-electrode (respectively anode or cathode) is hoped to be not detrimental to what takes place at the working electrode. It is however possible—and preferable—to take advantage of electron exchanges at the surface of the two electrodes, either for two independent reactions, e.g., chlorine generation at the anode and the alkali production at the cathode according to the well-known chlorine-alkali process, or with coupled, “paired” reactions (or so-called “convergent reactions”) which contribute mostly to the formation of a single product. In this second solution, the species generated at one electrode is (are) to be consumed through the reaction occurring at the other electrode.

An important example of synthesis by paired reactions is the organic methylation of compounds by substitution reaction. The alcoholate is first generated at the cathode after:



The methanolate formed then reacts chemically on the organic substrate in the solution bulk or at the vicinity of the anode surface to lead to the methoxycompound:



where X^- is an anion such as halogenide anion. MeO^- is an example of electrogenerated base, EGB, which reacts on intermediate species generated at the anode as described above. These electrogenerated bases—being anions, dianions or even anions

radicals—represent one of the best examples of coupled electrochemical reactions and, according to the envisaged synthesis (Utley and Nielsen 1991), nitrogen-containing compounds, e.g., diazo or amide anions, oxygenated compounds such as superoxide anion O_2^- , or carbon-based compounds such as carbanion radicals. It can be supposed at this level that the efficiency of this base is governed by stability of anions or radicals, but also strongly depends on the inter-electrode gap in the cell. An additional benefit of this synthesis technique is the increase in the solution conductivity by continuous generation of anions, what allows to avoid in some cases of the addition of supporting electrolyte (Paddon et al. 2002).

Two examples of synthesis obeying this principle are given below:

- Non-Kolbe electrosynthesis (Tajima et al. 2007) for methoxylate synthesis from carboxylic acid R-COOH:



The reactivity of methanol sometimes too low, can be largely enhanced by electrogenerated base—of piperidin type for instance. Piperidin reacts at the cathode and becomes active enough to react with methanol in an acid-base reaction:



The alcoholate formed reacts on the carbanion to form the ether, while the conjugated acid EGB' is regenerated at the cathode. These bases can be supported on silica for example, allowing easier separation of the key product after the synthesis stage.

- The synthesis of methoxyether of aldehydes (diacetal) from methoxycompounds, e.g., 4-methylanisole 4-methoxy-benzylaldehyde-dimethylacetal (Ziogas et al. 2000; Attour et al. 2008), by successive anodic oxidations to ether, aldehyde (in the form of diacetal), then to carboxylic acid (in the form of triester), each of the steps involving two electrons.

Electrosynthesis of Fluorinated Compounds

Chemical synthesis of fluorinated compounds, which exhibit great chemical stability, in particular in aggressive media, have to be carried out upon action of gaseous fluorine. The electrochemical way allows partial reduction in the potential hazard of toxicity and less significant emission in the synthesis (Fuchigami 2007). Nevertheless, the conventional synthesis route for monofluorinated compounds of oxygenated compounds such as THF or dioxan relies on the use of solvents such as acetonitrile or dichloromethane with Et₄NF, HF as supporting electrolyte: this electrolyte is an ionic liquid, exhibiting also a real toxicity. Recently Hasegawa et al. 2006 improved the synthesis by replacing the solvent by the oxygenated substrate itself and by limiting the concentration of the ionic liquid, which results in considerable increase in yield and selectivity in monofluorinated compounds.

Advanced Reactors for Electroorganic Synthesis

Should only one example of advanced reactors for electrosynthesis be given, the example would be in “microreactors” area, the main characteristics of which is the inter-electrode gap clearly below the millimeter (Rode et al. 2008; Rode and Lapique 2009). Design and manufacturing of these microreactors could greatly benefit from the progress of microtechnology (Löwe et al. 2002), which can be applied to numerous domains of industry or engineering sciences. In addition to the reduction of the inter-electrode gap, the possible local variation of sizes or operating parameters allows transfer intensification: this point will be discussed before the description of two types of electrochemical microreactors below.

Transfer Intensification

In the presence of submillimetric inter-electrode gaps, diffusion layers developing on both electrodes can partly overlap in the cell. In such cells, the mass transfer coefficient varies with the reciprocal of the channel thickness d , as explained above. Furthermore, for a cell provided with parallel flat plate cells, the specific electrode area, a_e , varies as $1/d$. The conversion rate in an electrochemical submillimetric reactor is an increasing function of the product ($k_L \cdot a_e$) as shown by relation (42): because this term varies as $(1/d^2)$, it can easily be understood that submillimetric reactors can be operated without recycling and offer almost total conversion.

The low thickness of the channel reduces the ohmic drop between the electrodes, and thus the energy dissipated by Joule effect and the often undesired effects of temperature rise on selectivity. It is also possible to reduce the concentration of supporting electrolyte. Furthermore, for electrochemical paired reactions, the anionic species generated at the anode increases the conductivity of the medium, so addition of supporting electrolyte can sometimes be avoided as expressed above.

Interdigitated Electrode Cells

Belmont and Girault 1994 developed the concept of microstrips of interdigitated coplanar electrodes as soon as 1994. Electrodes have been manufactured by successive depositions of conductive and insulating layers by screen-printing, on a plate substrate out of stainless steel or aluminium. Electrodes, with a geometrical arrangement according to two band series imbricated one in the other (Fig. 4), have a width far below the millimeter, with a fine insulating band being 0.25–1 mm wide. The length of every electrode is of the order of two centimeters and a plate contains up to 70 electrodes. These systems have been tested for the example of furane methoxylation in a MeOH medium, and or propylene epoxidation in an aqueous solution with the Br_2/Br^- redox couple: paired electrochemical reactions are involved in the two syntheses.

This technology is at the same time simple and attractive since the plate provided with its two strip series can be immersed into a tank of electrolytic solution to be treated in a discontinuous operation. Two drawbacks to be mentioned: (i) the electrode strips have to be manufactured in the electrocatalytic material which is

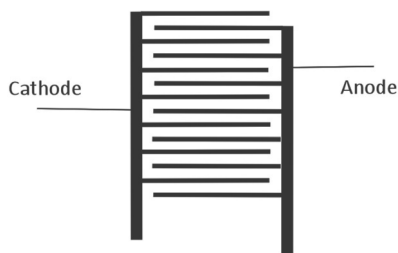


Figure 4. Interdigitated electrodes.

suitable to the considered electrosynthesis; (ii) distributions of potential and current density: because anodes and cathodes are not facing each other, these distributions can be far from homogeneous, which can be the source of uneven production rates and lower selectivity.

Microchannel Cells

This technology is of a simple implementation: sub-millimetric channels are formed by two flat electrodes separated by spacers, whose thickness defines that of the channel. The thickness can be as low as 80 μm (or below), as achieved by Ziogas et al. 2000 for the synthesis of anisaldehyde dimethyl acetal. Attour et al. 2008 have proposed a model predicting the cell operation for this synthesis: the model relies upon a criterion analogous to Wagner's criterion for potential distribution, and the number of transfer units (NTU) largely used in chemical engineering. In more refined technologies the single broad, thin gap is replaced by multiple parallel channels with diameters between 10 to several hundreds of micrometers (Jähnisch et al. 2004; Iken et al. 2012; Scialdone et al. 2014). The Institute of Microtechniques of Mainz (IMM) produces and markets multi-purpose cells, the electrode material of which can be easily changed (glassy carbon, steel, nickel for example). Derived designs of the simple microchannel cell have been proposed, in particular by IMM: design and sizing can be carried out by electrochemical reactor simulation by varying the conductance of mass transfer and the specific electrode area (a_v), depending on the targeted performance in terms of conversion and selectivity.

Other microreactors have been also proposed, in particular by the groups of Kenis (Christian et al. 2006; Yeom et al. 2005) or of Alkire in the USA in particular for on-site production of small quantities of hydrogen.

Microstructured Electrochemical Reactors

The various microreactors described above operate in a global way, in spite of their low dimensions. An approach, probably more complex with concern technology, consists in searching the optimal strategy of distribution of electric variables (Matlosz 1995). For example, if we consider a reactor allowing the almost complete conversion of the substrate, it is logical that the current density to be applied for optimal current (faradaic) efficiency is not the same at the cell inlet that near the outlet: therefore,

besides the intensification of transfer allowed by the sub-millimetric dimensions of the cell, microstructuring—by means of segmented electrodes for example—makes it possible to control locally the cell parameters and inlet variables for its optimal operation in terms of current yield and selectivity in the key-product (Rode et al. 2004, 2008). Microstructuring of the cell design has also been largely investigated in the area of energy conversion (see for instance Kolb et al. 2013; Schneider et al. 2010): interestingly, because of the similarity of the physical laws involved, the advances in design and modelling obtained for one application can usefully be employed for other applications.

Electrochemical Processes for the Production of Powerful Oxidants and for Disinfection

Electrosynthesis of Powerful Oxidants

Strong oxidizing agents such as ozone, hydrogen peroxide, peroxy-compounds, Ag^{2+} , etc. find numerous applications in synthesis, pollution abatement and surface treatment. Electrochemical techniques are particularly suitable for the production of some of these oxidants. When carried out in aqueous media, these processes require corrosion-resistant anode materials which have in addition to limit oxygen release. Most often, these anodes are constituted by noble metals (massive Pt and its alloys or platinum coated titanium) or by insoluble oxides (PbO_2 , SnO_2) deposited on a titanium substrate (dimensionally stable anode or DSA). Besides, since 1995 new techniques have been developed to prepare electrodes formed by a thin layer (≈ 1 micrometer) of synthetic diamond doped with boron (BDD) deposited on a substratum made either of silicon or a refractory metal (Nb, Ti). Diamond has received great attention because of its interesting properties and features: wide electrochemical window as shown on Fig. 5, weak adsorption capacity and very high chemical resistance even in strong acid environment.

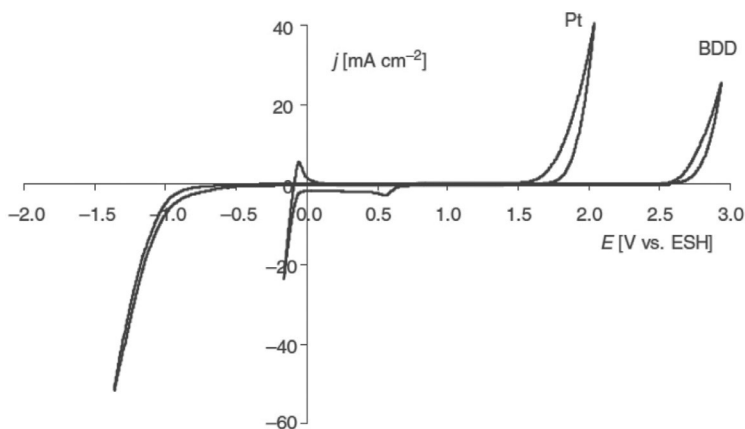


Figure 5. Polarization curves on polycrystalline BDD and on platinum in 1M sulphuric acid. Scan rate 50 mV s^{-1} ; temperature 25°C (According to Kapalka et al. 2010).

Depending on the applied potential, the oxidation reaction at BDD electrodes can follow two mechanisms (Panizza and Cerisola 2005): (i) direct electron transfer in the potential region of water stability before oxygen evolution (as for example the case of Ag^+ oxidation; see below), and (ii) indirect oxidation via electrogenerated hydroxyl radicals, in the potential region of oxygen evolution (water decomposition):



Hydroxyl radicals are well known for their very high oxidizing power ($E^\circ = 2.80$ V). Applications of BDD in electrosynthesis of powerful oxidants like ozone and peroxocompounds as well as in waste waters depollution through total mineralization of organics or in disinfection are under development.

Production of silver(II)

The cation Ag^{2+} is used as oxidising agent in nuclear industry for the dissolution of plutonium dioxide in nitric acid media and for degradation of contaminated organic substances. The reaction is carried out in 6 M nitric acid to stabilize the Ag^{2+} cation by complexation with the ion NO_3^- :

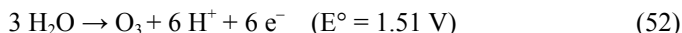


Massive platinum produces exceptional results in the regeneration of silver (II), but Ti (or Nb)-based DSA with a platinum coating also presents interesting potentialities (Arnaud et al. 1999). The Ag^{2+} generation rate on Nb/BDD anodes evaluated in a filter press reactor was similar than the one obtained on platinum coated titanium electrodes on condition however to impose a current intensity lower than the oxidation limiting current of the Ag^+ oxidation, otherwise concurrent reactions occur when hydroxyl radicals are produced according to Eq. 49 (Racaud et al. 2012).

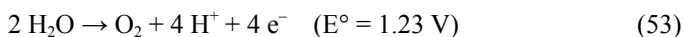
Production of Ozone

Ozone is a powerful agent, the action of which does not produce toxic products. This reactant can be obtained by oxidation of demineralised water on $\beta\text{-PbO}_2$ or BDD anodes plated on a solid polymer electrolyte (SPE) like Nafion (Kraft 2008):

Anode: catalyst PbO_2 (or BDD)

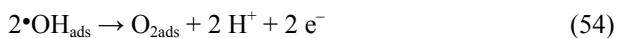


Competing reaction (thermodynamically more favorable):



In this electro-catalytic ozone production, the formation of adsorbed hydroxyl free radicals (on PbO_2 or BDD) as well as adsorbed oxygen is very important and

the following reaction steps, which occur after water discharge (Eq. 49), are usually considered (Wang and Chen 2013):



The gas mixture obtained ($\text{O}_2 + \text{O}_3$) can contain a weight concentration of ozone up to 14% after electrochemical production with current yield ranging from 15 to 20%. Recent tests conducted at pilot-scale (Kraft) showed that ozone production on BDD plated on SPE (Fig. 6) exceeds the performance of lead dioxide anode (current yield 24%). On the other hand, if Pt is used as the cathode material, the overvoltage for hydrogen production can be lowered, minimising the cell voltage. This technique is well adapted to small on-site preparation of ozone for the production of drinking water (up to $50\text{ m}^3\text{ hour}^{-1}$).

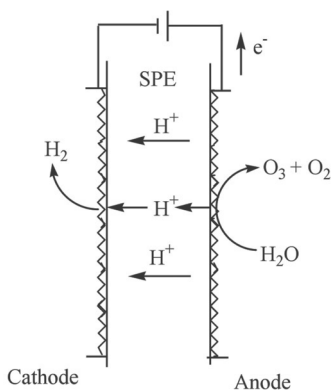
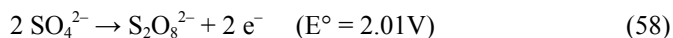
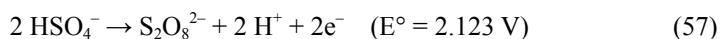


Figure 6. Schematic view of a BDD-SPE electrode reactor for ozone production in deionised water. The two electrodes can be made with a grid of Nb covered by a layer of BDD (adapted from Kraft 2008).

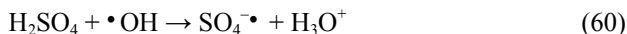
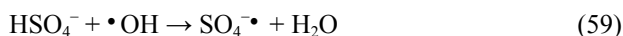
Electrosynthesis of Peroxo Compounds

BDD is particularly effective for the preparation of oxidizing agents for various applications in pollution abatement and in synthesis. Production of peroxodisulfuric acid (Serrano et al. 2002), peroxodiphosphate and peroxomonophosphate (Weiss et al. 2008) can be considered with this anode. Oxidation of sulphuric acid on BDD anode forms peroxodisulfuric acid according to the global scheme:



The diamond anode limits very strongly oxygen evolution; according to Serrano et al. 2002, HSO_4^- and H_2SO_4 , the main species at equilibrium in sulphuric acid

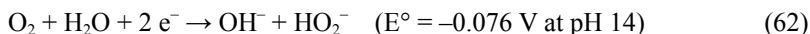
solution at concentration higher than 2 M, react with hydroxyl radicals to form sulphate radicals as follows:



The current efficiency is constant to a maximum value of 95% at 9°C (Serrano et al. 2002).

Electrosynthesis of Hydrogen Peroxide by Oxygen Reduction

Two-electron reduction of oxygen to produce hydrogen peroxide is a much researched topic. Indeed, the process is suitable for on-site peroxide generation, especially in the pulp and paper industry, in reason of its flexibility and the absence of transportation and storage. For most applications this industry uses alkaline peroxide in dilute solutions (ca. 3% w H₂O₂), such as can be obtained by the controlled two-electron electro-reduction of oxygen:



Considering the low solubility of oxygen in water (10 mg L⁻¹ at equilibrium with air at 25°C) the process uses a simple cell configuration in which a single alkaline electrolyte flows with oxygen gas through a perforated trickle-bed electrochemical reactor to intensify the triple contact between the catalyst (graphite), the electrolyte and oxygen or air (see Fig. 7). The current efficiency can reach 78% under 2000 A m⁻² (Gupta and Oloman 2006).

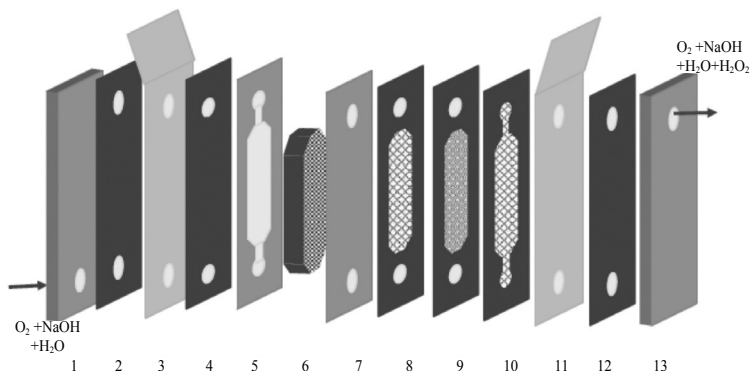
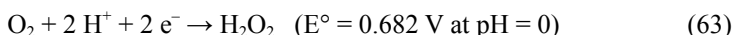


Figure 7. Configuration of a perforated trickle-bed electrochemical reactor for the synthesis of alkaline peroxide. 1, 13: carbon steel cell body; 2, 5, 12: gaskets; 4: Grafoil sheet (compressed graphite sheet with SS insert); 9: perforated anode (Grafoil); 10: nickel mesh anode; 7: diaphragm (microporous polyalkene); 8: nickel mesh anode; 3, 11 SS current feeder; 6: graphite felt (3.2 mm thick). Adapted from Gupta and Oloman 2006.

However, peroxides under alkaline conditions show poor stabilities and are not useful in disinfection applications. There is a need to design electrocatalysts that are stable and provide good current and energy efficiencies to produce hydrogen peroxide under acidic conditions. In this objective, Rhodes et al. 2011 at Lynntech have designed an electrochemical cell having a gas diffusion electrode (GDE) as the cathode and a platinized titanium anode (Fig. 8). The GDE comprises mainly an electrically conductive substrate in carbon fibers coated with a cathodic electrocatalyst layer containing a quaternary ammonium compound. The electrocatalytic layer which should be hydrophobic includes PTFE and a perfluorinated sulphonic acid polymer. In this catalytic layer, oxygen is reduced as follows:



The cathode and anode compartments are separated by a cation-exchange membrane (Nafion). The anode compartment is fed with deionized water. On the anode made of titanium plated with platinum, oxygen evolution takes place by water oxidation (reaction 53) and hydrated protons are transported towards the cathode by migration inside the sulphonic acid polymer. In summary, no chemicals are needed in the process; apart from deionized water; oxygen is produced at the anode. Hydrogen peroxide is pure and can therefore be used in disinfection applications. High concentrations of the order of 8–14 wt% can be generated by this method with stable production over 1000 hours.

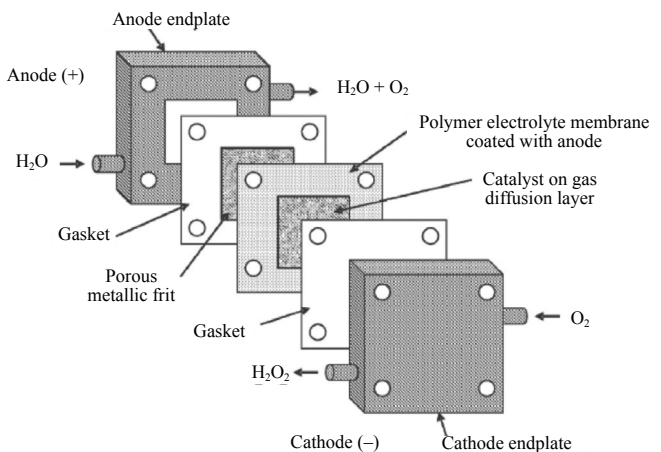


Figure 8. Expanded view of the Lynntech cell used to produce hydrogen peroxide under acidic conditions by catalytic oxygen reduction in a GDE (from Rhodes et al. 2011).

Chlor-alkali Electrolysis Using an Oxygen-diffusion Cathode

Chlorine is one of the most important products of the chemical industry. Chlorine production is continuously increasing in reason of the demand of major polymers (PVC), drugs, fine chemicals... As a strong oxidant chlorine is also currently used in disinfection.

Electrochemical chlorine production is currently one of the most energy-intensive and costly processes in the chemical industry, with power accounting for around 50% of the costs incurred during its production. For economic reasons all new chlor-alkali plants are based on the membrane cell process (Fig. 9a). In the edge of the 2000s the membrane technology had reached the maturity and any improvement could be then hoped only by the development of a new system to replace the release of hydrogen on steel or nickel by the reduction of oxygen in a gas diffusion electrode (Fig. 9b). Substitution of the hydrogen-evolving cathode in chlor-alkali cells with an oxygen-consuming cathode reduces the cell voltage by a theoretical value of 1.23 V as well as eliminates hydrogen, a low-value by-product. Such energy saving depends on the use of highly dispersed catalysts for the oxygen reduction reaction (ORR) in the gas diffusion electrode to minimize overpotential.

The idea of operating the chlor-alkali electrolysis with oxygen depolarized cathodes is by no means new (Moussallem et al. 2008). Extensive efforts in the 1970s and 1980s clearly demonstrated technical feasibility of membrane-type chlor-alkali electrolysis with oxygen diffusion cathode (ODC) even at pilot scale. But the achieved savings in cell voltage of 0.8–0.9 V was judged insufficient for an economic change to the new ODC technology (Moussallem et al. 2008). Huge progress, mainly in Japan and Germany, has been made during the 1990s not only at the laboratory scale but also in pilot electrolyzers and even industrial scale. The frequently used catalysts for oxygen reduction in sodium hydroxide solution are carbon supported platinum and silver either supported on carbon or as pure metal (see Moussallem et al. 2008 and references therein).

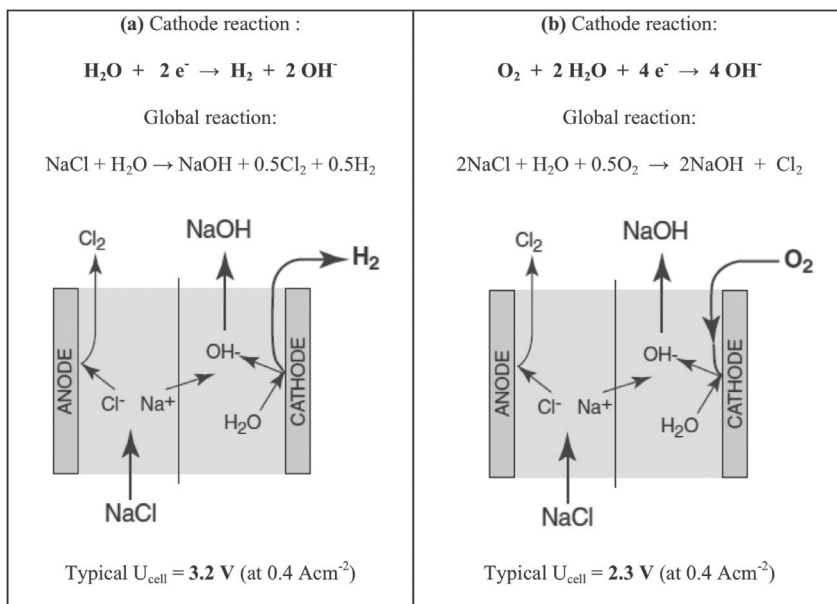


Figure 9. Chlor-alkali electrochemical membrane cell. (a) Conventional membrane cell; (b) Membrane cell with oxygen-diffusion cathode (ODC). The membrane is a solid polymer electrolyte (Nafion).

The role of the catalyst is to decrease the rate of peroxide generation (Eq. 63) and to favour the discharge of oxygen O_2 involving 4 electrons (Fig. 9b). Peroxide is a rather troublesome by-product which may destroy the microporous structure of the gas diffusion electrode.

The first industrial-scale chlor-alkali facility with ODC technique has been put into operation by Bayer in Ürdingen by spring 2011 (20,000 t/y). The porous catalyst system is made from silver catalyst particles supported on a PTFE-coated metal support (<http://www.rsc.org/chemistryworld/News/2009/November/19110901.asp>).

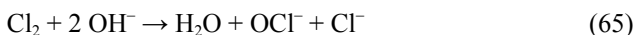
Electrochemical Disinfection

Disinfection by electrochemical techniques is of large interest because it is able to propose an alternative to conventional processes of water treatment relying on chemical agents such as metals (Cu, Ag), Cl_2 , HOCl, ClO_2 , chloramines, O_3 , H_2O_2 , $KMnO_4$, organic disinfectants. A common method for drinking water disinfection is the direct addition of chlorine or hypochlorite that is able to eliminate the most harmful microorganisms. But in spite of its efficiency chlorination, when used alone, has a limited action against some resistant microorganisms. Furthermore, chlorine could induce potentially toxic products such as chloroform. Thus, alternatives to simple chlorination for drinking water disinfection have been proposed (see references in Martinez-Huitle and Brillas 2008).

On-site production of chlorine by electrochemistry presents the major advantage to require neither transport nor storage with regard to the standard method. Active chlorine species such as Cl_2 , HOCl, OCI^- , are widely recognized as key oxidants responsible for inactivating cells in electrochlorination. These species can be produced by anodic oxidation of chloride on Ti-RuO₂ plate for example:



For cells operating without separator, hydrolysis of chlorine forms hypochlorite:

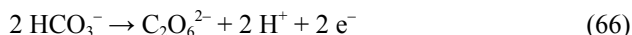


There are two types of electrochlorination procedures: (i) the synthesis of free chlorine from brine in an electrolytic generator (Fig. 9a) and (ii) the direct oxidants production from the water to be treated by electrolysis. In what follows the second case is considered. Recent investigations showed that the particular efficiency of the electrochemical process cannot be explained by the only action of the active forms Cl_2 , HOCl, OCI^- , in particular when the concentration of Cl^- ions becomes very low. Some researchers have pointed out that the disinfecting efficacy of this method is much higher than that of direct chlorination and have attributed the higher disinfecting power of electrochlorination to the oxidant role of reactive oxygen species (ROS) such as hydroxyl radical ($\bullet OH$), atomic oxygen ($\bullet O$), hydrogen peroxide, and ozone, which can be formed in small quantities from water by discharge at the anode (Martinez-Huitle and Brillas 2008). Some reactions involved in the formation of ROS are given by Eqs. 49, 54, 55, 56 and by the coupling of hydroxyl radicals which forms hydrogen peroxide.

The disinfecting power of the electrolysis was even demonstrated in the absence of chloride anions, what is particularly interesting since active chlorine can be in disinfection the source of harmful by-products.

The effectiveness of the electrochemical disinfection with BDD anodes has been verified by means of batch galvanostatic experiments: suspensions of *E. coli*, coliforms and enterococci in 1 mM Na₂SO₄ were tested by Polcaro et al. 2007. Under all the experimental conditions shown on Fig. 10 the population of bacteria was appreciably reduced. At BDD anodes appreciable amounts of ROS and other oxidising species (persulphate) are generated from the oxidation of ions present in the solution.

It has been also possible to disinfect waters (i) in a chloride-free phosphate buffer medium using a BDD electrode (Jeong et al. 2006) or (ii) hydrogen carbonate containing respectively *E. coli*, *Saccharomyces cerevisiae* or *Liegiella pneumophila*. This last bacterium is particularly sensitive to percarbonate which can be easily synthesized on a BDD electrode (Furuta et al. 2004):



It was suggested that the formation of peroxycarbonate is initiated by the reaction of hydroxyl radicals on hydrogen carbonate anion (Saha et al. 2004).

The disinfection by electrochemical technique has numerous advantages in the drinkable water treatment, water of swimming pool, treatment of water in cooling towers and medical equipments (Kraft 2008; Polcaro et al. 2007). Few equipments are at present available but it is necessary to take into account the fact that processes not appealing to active chlorine are relatively recent and have wide margin of progress.

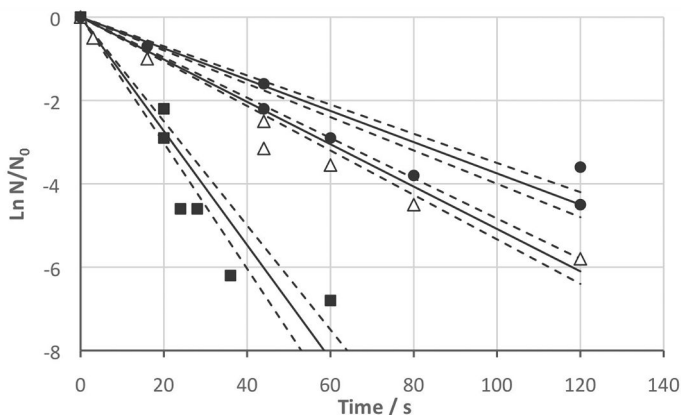


Figure 10. Survival ratio as a function of time during the electrolysis for *E. coli* (■), coliforms (Δ) and enterococci (●) during batch experiments at $i = 10 \text{ mA/cm}^2$ at Reynolds number Re of 1×10^4 . Initial concentrations: *E. coli* 6.4×10^2 CFU/ml, coliforms 2.3×10^3 CFU/ml, enterococci 4.4×10^3 CFU/ml. Full lines represent the least squares regression lines for the data and, dotted lines represent the standard error of the regression. Adapted from Polcaro et al. 2007.

References

- Anastas, N.D. and J.C. Warner. 2005. The incorporation of hazard reduction as a chemical design criterion in green chemistry. *J. Chem. Health Safety* 9–13.
- Anastas, P.T., L.B. Bartlett, M.M. Kirchoff and T.C. Williamson. 2000. The role of catalysis in the design, development, and implementation of green chemistry. *Catal. Today* 55: 11–22.
- Arico, A.S., S. Siracusano, N. Brioguglio, V. Baglio, A. Di Blasi and V. Antonucci. 2013. Polymer electrolyte membrane water electrolysis: status of technologies and potential applications in combination with renewable power sources. *J. Appl. Electrochem.* 43: 107–118.
- Arnaud, O., C. Eysseric and A. Savall. 1999. Optimising the anode material for electrogeneration of Silver (II). *Institution of Chemical Engineers Symposium Series* 45: 229–238.
- Attour, A., S. Rode, A. Ziogas, M. Matlosz and F. Lapicque. 2008. A thin-gap cell for selective oxidation of 4-methylanisole to 4-methoxybenzaldehyde dimethylacetal. *J. Appl. Electrochem.* 38: 339–347.
- Baizer, M.M. and H. Lund. 1983. *Organic electrochemistry, Introduction and Guide*. Marcel Dekker, Inc., New York.
- Ballesteros, J.C., E. Chainet, P. Ozil, Y. Meas and G. Trejo. 2011. Electrocrystallization of copper from non-cyanide alkaline solution containing glycine. *Int. J. Electrochem. Sci.* 6: 1597–1616.
- Bard, A.J. and L.R. Faulkner. 1980. *Electrochemical Methods*. Wiley and Sons, New-York.
- Barthole-Delaunay, G., A. Storck, A. Laurent and J.C. Charpentier. 1982. Electrochemical determination of liquid–solid mass transfer in a fixed-bed irrigated gas–liquid reactor with downward cocurrent flow. *Int. Chem. Eng.* 22: 244.
- Bebelis, S., K. Bouzek, A. Cornell, M.G.S. Ferreira, G.H. Kelsall, F. Lapicque, C. Ponce de Leon, M.A. Rodrigo and F.C. Walsh. 2013. Highlights during the development of electrochemical engineering. *Chem. Eng. Res. Des.* 1998–2020.
- Belmont, C. and H.H. Girault. 1994. Coplanar interdigitated band electrodes for electrosynthesis; Part 1, Ohmic drop evaluation. *J. Appl. Electrochem.* 24: 475–480; Part 2, Methoxylation of furan. *J. Appl. Electrochem.* 24: 719–724.
- Bergmann, H., T. Iourtchouk, K. Schops and K. Bouzek. 2002. New UV irradiation and direct electrolysis—Promising methods for water disinfection. *Chem. Eng. J.* 85: 111–117.
- Bouzek, K., V. Jiriny, R. Kodym, J. Krystal and T. Bystron. 2010. Microstructured reactors for electroorganic synthesis. *Electrochimica Acta* 55: 8172–8181.
- Canizares, P., C. Jimenez, F. Martinez, M.A. Rodrigo and C. Saez. 2009. The pH as a key parameter in the choice between coagulation and electrocoagulation for the treatment of wastewaters. *J. Hazard. Mater.* 163: 158–164.
- Caubère, P. 1982. *Le transfert de phase et son utilisation en chimie organique*, Masson, Paris [in French].
- Chaussard, J., J.-C. Folest, J.-Y. Nedelec, J. Perichon, S. Sibille and M. Troupel. 1990. Use of sacrificial anodes in electrochemical functionalization of organic halides. *Synthesis* 5: 369–381.
- Chen, G. 2004. Electrochemical technologies in wastewater treatment. *Sep. Purif. Technol.* 38: 11–41.
- Christian, Mitchell M., D.-P. Kim and P.J.A. Kenis. 2006. Ceramic microreactors for on-site hydrogen production. *J. Catal.* 241: 235–242.
- Couret, F. and A. Storck. 1993. *Eléments de génie électrochimique*, 2nd Edition, Techniques et Documentation, Lavoisier, Paris.
- Deconinck, J. 1992. *Current Distributions and Electrode Shape Changes in Electrochemical Systems*. *Lectures Notes in Engineering*, Vol. 75, Springer Verlag, Berlin.
- Degner, D. 1988. Organic Electrosyntheses in Industry. pp. 1–95. *In: Topics in Current Chemistry*, Vol. 148, Springer-Verlag, Berlin Heidelberg.
- Diard, J.P., B. Le Gorrec and C. Montella. 1996. *Cinétique Electrochimique*, Hermann, Paris [in French].
- Doherty, A.P., L. Diaconou, E. Marley, P.L. Spedding, R. Barhdadi and M. Troupel. 2012. Application of clean technologies using electrochemistry in ionic liquids. *Asia Pac. J. Chem. Eng.* 7: 14–23.
- EG&G Technical Services Inc. 2004. *Fuel Cell Handbook*, 7th Editions, U.S. Department of Energy-DOE, Morgantown, USA, pp. 7-1–7-49.
- Ehrfeld, W., V. Hessel and H. Löwe. 2000. *Microreactors: New Technology for Modern Chemistry*. Wiley-VCH, Weinheim.
- Enyo, M. 1983. Hydrogen electrode reaction on electrocatalytically active metals. pp. 241–300. *In: B.E. Conway, J.O'M. Bockris, E. Year, S.U.M. Kahn and R.E. White (eds.). Comprehensive Treatise*

- of Electrochemistry, Vol. 7: Kinetics and Mechanism of Electrodes Processes. Plenum Press, New York, London.
- Frontana-Uribe, B.A., R.D. Little, J.G. Ibanez, A. Palma and R. Vasquez Medrano. 2010. Organic electrosynthesis: a promising green methodology in organic chemistry. *Green Chem.* 12: 2099–2119.
- Fuchigami, T. 2007. Unique solvent effects on selective electrochemical fluorination of organic compounds. *J. Fluorine Chem.* 128: 311–316.
- Furuta, T., H. Tanaka, Y. Nishiki, L. Pupunat, W. Haenni and Ph. Rycken. 2004. Legionella inactivation with diamond electrodes. *Diamond. Relat. Mater.* 13: 2016–2019.
- Girault, H.H. 2004. Analytical and Physical Electrochemistry. EPFL Press, Marcel Dekker, Lausanne.
- Goodridge, F. and K. Scott. 1995. Electrochemical Process Engineering. A Guide to the Design of Electrolytic Plant. Plenum Press, New-York.
- Gupta, N. and W. Oloman. 2006. Scale-up of the perforated bipolar trickle-bed electrochemical reactor for the generation of alkaline peroxide. *J. Appl. Electrochem.* 36: 1133–1141.
- Hartnig, C. and C. Roth (eds.). 2010. Polymer Electrolyte Membrane and Direct Methanol Fuel Cell Technology. Woodhead Publishing, Oxford.
- Hasegawa, M., H. Ishii, Y. Cao and T. Fuchigami. 2006. Regioselective anodic monofluorination of ethers, lactones, carbonates, and esters using ionic liquid fluoride salts. *J. Electrochem. Soc.* 153: D162–D166.
- Ibl, N. and O. Dossenbach. 1983. Convective mass transport. pp. 133–237. *In: E. Yeager, J.O'M. Bockris, B.E. Conway and S. Sarangapani (eds.). Comprehensive Treatise of Electrochemistry.* Springer, New York.
- Iken, H., F. Guillen, H. Chaumat, M.R. Maizières, J.C. Plaquevent and T. Tzedakis. 2012. Scalable synthesis of ionic liquids: comparison of performances of microstructured and stirred batch reactors. *Tetrahedron Lett.* 53: 3474–3477.
- Jähnisch, K., M. Baerns, V. Hessel and H. Löwe. 2004. Chemistry in microstructured reactors. *Angewandte Chemie International Edition* 43: 406–446.
- Jeong, J., J.Y. Kim and J. Yoon. 2006. The role of reactive oxygen species in the electrochemical inactivation of microorganisms. *Environ. Sci. Technol.* 40: 6117–6122.
- Jüttner, K., U. Galla and H. Schmieder. 2000. Electrochemical approaches to environmental problems in the process industry. *Electrochimica Acta* 45: 2575–2594.
- Kapalka, K., G. Foti and Ch. Cominellis. 2010. Basic principles of the electrochemical mineralization of organic pollutants for wastewater treatment. pp. 1–23. *In: Ch. Cominellis and G. Chen (eds.). Electrochemistry for the Environment.* Springer, New York.
- Kolb, G., S. Keller, M. O'Connell, S. Pecov, J. Schuerer, B. Spasova, D. Tiemann and A. Zogas. 2013. Microchannel fuel processors as a hydrogen source for fuel cells in distributed energy supply systems. *Energy and Fuels* 27: 4395–4402.
- Kraft, A. 2008. Electrochemical water disinfection: a short review. *Platinum Metals Rev.* 52: 177–185.
- Lapicque, F. 2004. Electrochemical engineering. An overview of its contributions and promising features. *Chem. Eng. Res. Design* 82: 1571–1574.
- Larminie, J. and A. Dicks. 2010. Fuel Cell Systems Explained, 2nd Edition. Wiley, Chichester.
- Letord-Quemere, M.M., F. Coeuret and J. Legrand. 1988. Mass Transfer at the Wall of a Thin Channel Containing an Expanded Turbulence Promoting Structure. *J. Electrochem. Soc.* 135(12): 3063–3067.
- Löwe, H., M. Küpper and A. Zogas. 2002. Reactor and methods for carrying out electrochemical reactions. Patent number WO 0015872, DE 19841302.
- Lund, E. and O. Hammerich. 1991. Organic Electrochemistry, 4th Edition. Marcel Dekker, Inc., New York, Basel.
- Martinez-Huitle, C.A. and E. Brillas. 2008. Electrochemical alternatives for drinking water disinfection. *Angewandte Chemie International Edition* 47: 1998–2005.
- Matlosz, M. 1995. Electrochemical engineering analyses of multisectioned porous electrodes. *Journal of Electrochem. Soc.* 142: 1915–1922.
- Moussallem, I., J. Jörissen, U. Kunz, S. Pinnow and T. Turek. 2008. Chlor-alkali electrolysis with oxygen depolarized cathodes: history, present status and future prospects. *J. Appl. Electrochem.* 38: 1177–1194.
- Newman, J.S. 1991. Electrochemical Systems, 2nd Edition. Prentice Hall, Englewood Cliffs.

- Paddon, C.A., G.J. Pritchard, T. Thiemann and F. Marken. 2002. Paired electrosynthesis: microflow cell processes with and without added electrolyte. *Electrochem. Comm.* 4: 825–831.
- Panizza, M. and G. Cerisola. 2005. Application of diamond electrodes to electrochemical processes. *Electrochimica Acta* 51: 191–199.
- Pickett, D.J. and K.L. Ong. 1974. Influence of hydrodynamic and mass transfer entrance effects on the operation of a parallel plate electrolytic cell. *Electrochim. Acta* 19(12): 875–82.
- Pickett, D.J. 1979. *Electrochemical Reactor Design*, 2nd Edition. Elsevier, Amsterdam.
- Pletcher, D. and F.C. Walsh. 1993. *Industrial Electrochemistry*, 2nd Edition. Chapman and Hall, London.
- Pletcher, D. and N.L. Weinberg. 1992. The Green potential of Electrochemistry. 1. Fundamentals. *Chemical Engineering* 99(8): 98–103; The Green potential of Electrochemistry. 2. Applications. *Chemical Engineering* 99(11): 132–138.
- Polcaro, A.M., A. Vacca, M. Mascia, S. Palmas, R. Pompei and S. Laconi. 2007. Characterization of a stirred tank electrochemical cell for water disinfection processes. *Electrochimica Acta* 52: 2595–2602.
- Rcaud, C., A. Savall, P. Rondet, N. Bertrand and K. Groenen Serrano. 2012. New electrodes for silver (II) electrogeneration: comparison between Ti/Pt, Nb/Pt, and Nb/BDD. *Chem. Eng. J.* 211–212: 53–59.
- Rajeshwar, K. and J. Ibanez. 1997. *Environmental Electrochemistry: Fundamentals and Applications in Pollution Abatement*. Academic Press, San Diego.
- Rand, D.A.J. and R.M. Dell. 2008. *Hydrogen Energy Challenges and Prospects*. The Royal Society of Chemistry, Cambridge.
- Rhodes, C.P., C.L.K. Tennakoon, W.P. Singh and K.C. Anderson. 2011. Cathodic electrocatalyst layer for electrochemical generation of hydrogen peroxide. US 7,892,408 B2.
- Rode, S., S. Altmeyer and M. Matlosz. 2004. Segmented thin-gap flow cells for process intensification in electrosynthesis. *J. Electrochem. Soc.* 34: 671–680.
- Rode, S., A. Attour, F. Lapique and M. Matlosz. 2008. A thin-gap single-pass high conversion reactor for organic electrosynthesis. Part 1. Model development. *J. Electrochem. Soc.* 155(12): E193–E200.
- Rode, S. and F. Lapique. 2009. Microstructured reactors for electrochemical Synthesis. pp. 459–480. *In: V. Hessel, A. Renken, J.C. Schouten and J. Yoshida (eds.). Micro Process Engineering, Vol. 1. Wiley–VCH, Weinheim.*
- Saha, M.S., T. Furuta and N. Yoshinori. 2004. Conversion of carbon dioxide to peroxycarbonate at boron-doped diamond electrode. *Electrochem. Comm.* 6: 201–204.
- Schäfer, H.J. 2011. Contributions of organic electrosynthesis to green chemistry. *Comptes Rendus Chimie* 14: 745–765.
- Schneider, I.A., S. von Dahlen, A. Wokaun and G.G. Scherer. 2010. A segmented microstructured flow field approach for submillimeter resolved local current measurement in channel and land areas of a PEFC. *J. Electrochem. Soc.* 157: B338–B341.
- Scialdone, O., A. Galia, S. Sabatino, G.M. Vaiana, D. Agro, A. Busacca and C. Amatore. 2014. Electrochemical conversion of dichloroacetic acid to chloroacetic acid in conventional cell and in two microfluidic reactors. *Chem. Electrochem.* 1: 116–124.
- Serrano, K., P.A. Michaud, Ch. Comninellis and A. Savall. 2002. Electrochemical preparation of peroxodisulfuric acid using boron doped diamond thin film electrodes. *Electrochimica Acta* 48: 431–436.
- Strathmann, H. 2010. Electromembrane processes: basic aspects and applications. pp. 391–429. *In: E. Drioli and L. Giorno (eds.). Comprehensive Membrane Science and Engineering*. Elsevier, Amsterdam.
- Tajima, T., H. Kurihara and T. Fuchigami. 2007. Development of an electrolytic system for non-Kolbe electrolysis based on the acid-base reaction between carboxylic acids as a substrate and solid-supported bases. *J. Amer. Chem. Soc.* 129: 6680–6681.
- Tilak, B.V., S. Sarangapani and N.L. Weinberg. 1982. Electrode materials. pp. 195–249. *In: N.L. Weinberg and B.V. Tilak (eds.). Technique of Electroorganic Synthesis, Part III. Wiley-Interscience, New York.*
- Trasatti, S. 1992. Electrocatalysts of hydrogen evolution. Progress in cathode activation. *In: H. Gerischer and C.W. Tobias (eds.). Advances in Electrochemical Sciences. VCH Verlag, Weinheim.*
- Tzedakis, T. and A. Savall. 1997. Electrochemical regeneration of Ce (IV) for oxidation of p-methoxytoluene. *J. Appl. Electrochem.* 27: 589–597.

- Utley, J.H.P. and M.F. Nielsen. 1991. Electrogenerated bases. *In*: E. Lund and O. Hammerich (eds.). *Organic Electrochemistry*, 4th Edition. Marcel Dekker Inc., New York.
- Wang, Y.-H. and Q.-Y. Chen. 2013. Anodic materials for electrocatalytic ozone generation. *International Journal of Electrochemistry* 2013: Article ID 128248, 7 pages.
- Weiss, E., C. Sáez, K. Groenen-Serrano, P. Cañizares, A. Savall and M.A. Rodrigo. 2008. Electrochemical synthesis of peroxomonophosphate using boron-doped diamond anodes. *J. Appl. Electrochem.* 38: 93–100.
- Wendt, H. and G. Kreysa. 1999. *Electrochemical engineering, sciences and technology in chemical and other industries*. Springer Verlag, Berlin.
- Yeom, J., G.Z. Moszgai, B.R. Flaschsbart, E.R. Choban, A. Asthana, M.A. Shannon and P.J.A. Kenis. 2005. Microfabrication and characterization of a silicon-based millimeter scale, PEM fuel cell operating with hydrogen, methanol or formic acid. *Sensors and Actuators B* 107: 882–891.
- Ziogas, A., H. Löwe, M. Küpper and W. Ehrfeld. 2000. Electrochemical microreactors: a new approach for microreaction technology. pp. 136–156. *In*: W. Ehrfeld (ed.). *Microreaction Technology: Industrial Prospects*, Proceeding of IMRET 3. Springer Verlag, Berlin.

13

Photocatalytic Engineering

Jean-Marie Herrmann and Eric Puzenat

Historical Recall

Although old references mention photo-assisted phenomena, mainly in homogeneous phases, heterogeneous photocatalysis actually originated in the sixties in various catalysis laboratories in Europe. In England, F.S. Stone first studied the photo-adsorption/desorption of oxygen on ZnO (Barry and Stone 1960) before studying the photocatalytic oxidation of CO on the same solid (Romero-Rossi and Stone 1960). He subsequently switched to titania under rutile phase for oxygen photo-adsorption (Bickley and Stone 1973) and selective isopropanol oxidation in acetone (Bickley et al. 1973). This last reference was the first one to mention OH° radicals as oxidizing agents formed by the neutralization of surface OH^- surface anions by photo-holes h^\cdot . In addition, this simple and selective reaction was and still is a direct and simple test to demonstrate some photo-activity of solids. Simultaneously, in Germany, K. Hauffe was also studying the photocatalytic oxidation of CO on ZnO (Doerfler and Hauffe 1964a,1964b) and, actually, this reference was the first one to include the term “photocatalysis” in its title, according to the Chemical Abstracts database. In the same decade, while studying the sintering and the electrical properties of ultra-pure oxide powders for nuclear applications, Juillet and Teichner in Lyon (France) obtained erratic results on titania anatase which puzzled them until they realized that titania was photosensitive to daylight, especially on sunny days (Juillet and Teichner 2003). They demonstrated photo-adsorption and photodesorption of oxygen and subsequently decided to use the photo-activated oxygen species to perform mild and selective oxidations of light alkanes in the gas phase (Formenti et al. 1970; Djeghri et al. 1974). In fact, whereas photocatalysis was developing behind closed doors in Europe, there was a great stimulus and impact from Japan, with the re-publication, in English, of a previous work by Fujishima and Honda (1972) on the *photo-electrolysis* of water using a UV-irradiated titania-based anode in the review “Nature”. This paper acted as a “catalyst” for the globalization of photocatalysis. Unfortunately,

newcomers in the field of photocatalysis have never read this article and improperly cite it as the starting point for photocatalysis, which is clearly incorrect.

At the end of XXth century, heterogeneous photocatalysis appeared as a new emerging “Advanced Oxidation Process” (AOP), as illustrated by the reports by Blake (1994, 1995, 1997, 1999, 2001), with more than 2000 publications registered on the subject. Presently, more than 1000 articles are published yearly. Heterogeneous photocatalysis is simultaneously able to be efficient in Green Chemistry, in Fine Chemicals and in emerging “Advanced Oxidation Processes” (AOP) (Herrmann 1999, 2000, 2006, 2012). Photocatalysis is based on the double aptitude of the photocatalyst (essentially titania) to simultaneously **adsorb** reactants and **absorb** efficient photons ($h\nu \geq E_G$).

Fundamental Principles of Heterogeneous Photocatalysis

When a semiconductor catalyst SC of the chalcogenide type (oxides (TiO₂, ZnO, ZrO₂, CeO₂, etc.), or sulfides (CdS, ZnS, etc.) is illuminated with photons whose energy is equal to or greater than their band-gap energy E_G ($h\nu \geq E_G$), there is **A**Bsorption of these photons and creation within the bulk of electron-hole pairs, which dissociate into free photoelectrons in the conduction band and photoholes in the valence band (Fig. 1).

Simultaneously, in the presence of a fluid phase (gas or liquid), a spontaneous **A**Dsorption occurs and according to the redox potential (or energy level) of each adsorbate, an electron transfer proceeds towards acceptor molecules, whereas a positive photohole is transferred to a donor molecule (actually the hole transfer corresponds to the cession of an electron by the donor to the solid).

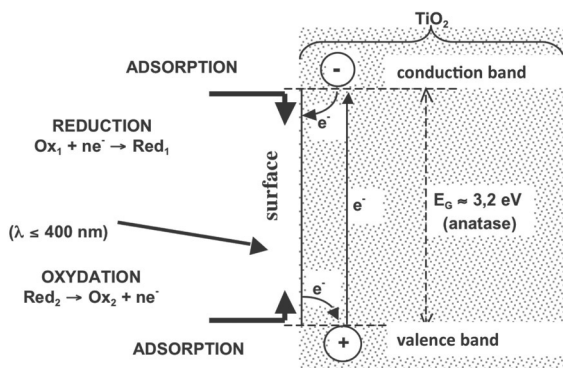
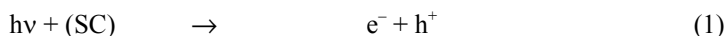


Figure 1. Energy band diagram of illuminated titania.

Each ion formed subsequently reacts to form the intermediates and final products. As a consequence of reactions (1–4), the photonic excitation of the catalyst appears as the initial step of the activation of the whole catalytic system. Therefore, the efficient photon has to be considered as a reactant and the photon flux as a special fluid phase, the “electromagnetic phase”. The photon energy is adapted to the absorption by the catalyst, not to that of the reactants. The activation of the process goes through the excitation of the solid but not through that of the reactants: *there is no photochemical process in the adsorbed phase* but only a true heterogeneous photocatalytic regime, as demonstrated below.

The photocatalytic activity (or the quantum yield defined further) can be strongly decreased by the electron-hole recombination, described in Fig. 2, which corresponds to the degradation of the noble photoelectronic energy into trivial heat.



(N: neutral center; E: energy (light $h\nu' \leq h\nu$ or heat))

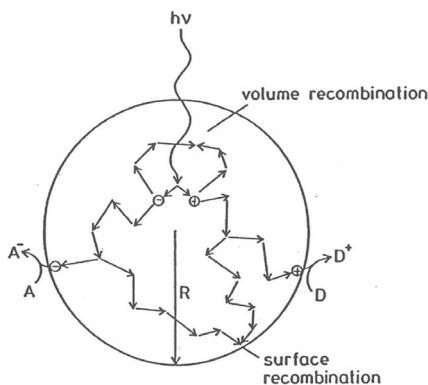


Figure 2. Fate of electrons and holes within a spherical particle of titania in the presence of acceptor (A) and donor (D) adsorbed molecules.

Photocatalysts

Various chalcogenides (oxides and sulfides) have been used: TiO_2 , ZnO , CeO_2 , ZrO_2 , SnO_2 , Sb_2O_4 , CdS , ZnS , etc. As generally observed, the best photocatalytic performances with maximum quantum yields are always obtained with titania. In addition, anatase is the most active allotropic form among the various ones available, either natural (rutile and brookite) or artificial ($\text{TiO}_2\text{-B}$, $\text{TiO}_2\text{-H}$). Anatase is thermodynamically less stable than rutile, but its formation is kinetically favored at lower temperatures ($< 600^\circ\text{C}$). This lower temperature for the synthesis of anatase could explain its higher surface area and its higher surface density of active sites for adsorption and for catalysis. In all the systems described in the present paper, the catalyst used was titania (Degussa TiO_2 P-25, $50 \text{ m}^2/\text{g}$, mainly anatase), unless otherwise stated.

Influence of Physical Parameters Governing the Photocatalytic Activity

The number of physical parameters which govern the photocatalytic activities of all the solids is equal to five and all the results are summarized in the five diagrams of Fig. 3.

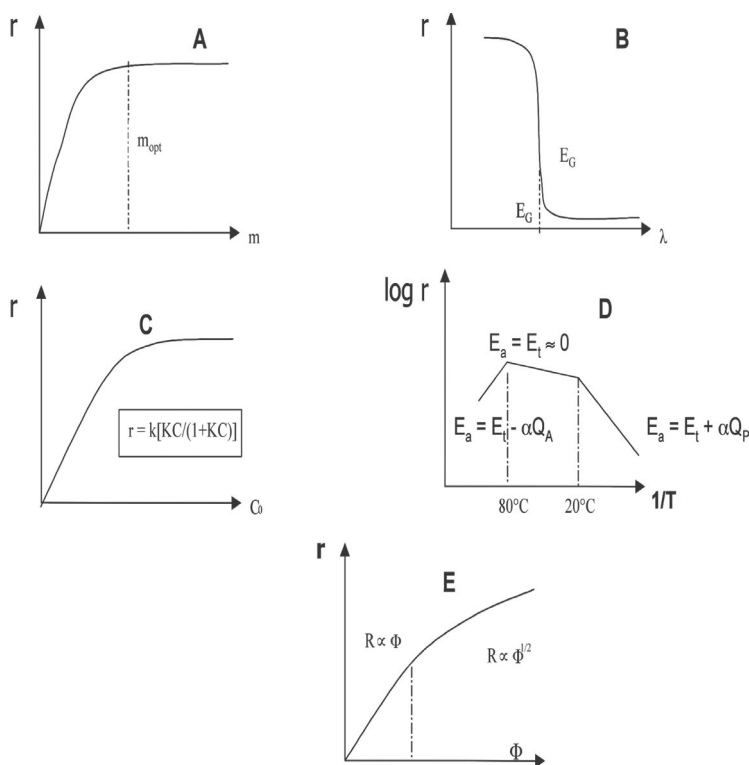


Figure 3. Influence of the different physical parameters which govern the kinetics of photocatalysis: reaction rate r ; (A): mass of catalyst m ; (B): wavelength λ ; (C): initial concentration c of reactant; (D): temperature T ; (E): radiant flux Φ .

Mass of Catalyst

Either in static, in slurry or in dynamic flow photoreactors, the initial rates of photocatalytic reactions were always found to be directly proportional to the mass m of catalyst (Fig. 3A). This indicates a true heterogeneous catalytic regime. However, above a certain value of m , the reaction rate levels off and becomes independent of m . This limit depends on the geometry and on the working conditions of the photoreactor. These limits correspond to the maximum amount of TiO_2 in which all the particles—i.e., all the surfaces exposed—are totally illuminated. For higher quantities of catalysts, a screening effect of excess particles occurs, which masks part of the photosensitive surface. For applications, this optimum mass of catalyst has to be chosen in order (i) to avoid an unuseful excess of catalyst and (ii) to ensure a total

absorption of efficient photons. These limits range from 0.2 to 2.5 g/L of titania in slurry batch photoreactors.

Wavelength

The variations of the reaction rate as a function of the wavelength follows the absorption spectrum of the catalyst (Fig. 3B), with a threshold corresponding to its band gap energy. For TiO₂ having $E_G = 3.02$ eV, this requires: $\lambda \leq 400$ nm, i.e., near-UV wavelengths (UV-A). In addition, a check must be performed in order to confirm that the reactants do not absorb the light to conserve the exclusive photoactivation of the catalyst for a true heterogeneous catalytic regime (no homogeneous or photochemistry in the adsorbed phase). Since the solar spectrum contains 3–5% UV-energy, photocatalysis can be activated by solar energy (“Helio-photocatalysis”; see below).

Initial Concentrations and/or Partial Pressures

Generally, the kinetics follows a Langmuir-Hinshelwood mechanism confirming the heterogeneous catalytic character of the system with the rate r varying proportionally with the coverage θ as:

$$r = k \theta = k (KC/(1+KC)) \quad (6)$$

where k is the true rate constant; K is the constant of adsorption at equilibrium and C is the instantaneous concentration.

For diluted solutions ($C < 10^{-3}$ M), KC becomes $\ll 1$ and the reaction is of the apparent first kinetic order, whereas for concentrations $> 5 \times 10^{-3}$ M, ($KC \gg 1$), the reaction rate is maximum and is of the zero apparent order (Fig. 3C).

In the gas phase, similar Langmuir-Hinshelwood expressions have been found including partial pressures P instead of C . Actually, the photocatalytic reactions are of the redox type with two reactants, the oxidizing agent being generally oxygen. In actual fact, the reaction rate is proportional to both coverages, that of the reactant θ_R and that of oxygen θ_{O_2} .

$$r = k\theta_{O_2}\theta_R = k[K_O P_{O_2}/(1 + K_O P_{O_2})] [K_R C_R/(1 + K_R C_R)] \quad (7)$$

Generally, θ_{O_2} is maximum or at least constant. Consequently, θ_{O_2} , close to unity, is integrated in k , which explains the formalism presented above.

Temperature

The influence of temperature on a photocatalytic reaction rate is complex. Due to the photonic nature of the activation of the solids, the photons replacing the phonons, a photocatalytic reaction does not require heating and can occur at room temperature. The true activation energy E_t , relative to the true rate constant k_t ,

$$k_t = k_0 \exp(-E_t/RT)$$

is nil. However, the apparent rate constant varies with temperature exhibiting a complex non constant apparent activation energy E_a , which gives a complex non-linear Arrhenius plot presented in Fig. 3D. This behavior can be easily explained within the frame of the Langmuir-Hinshelwood mechanism described above. k_a has to be related to the thermodynamic adsorption constant K , which is a function of T , according to Van't Hoff's law:

$$K = K_0 (\exp[-\Delta H_{(ads)}/RT])$$

with $\Delta H_{(ads)}$ = adsorption enthalpy of the reactant. This enthalpy is always negative since adsorption, a spontaneous phenomenon, is always exothermic. It is often expressed by Q , its absolute value:

$$Q = |\Delta H_{(ads)}| = -\Delta H_{(ads)}$$

Three domains can be distinguished:

1. Around room temperature, the apparent activation energy E_a is often very small, around 5–6 kcal/mole (≈ 20 –24 kJ/mole). In the medium temperature range ($20^\circ\text{C} < t^\circ < 80^\circ\text{C}$), the apparent activation energy $E_a = \partial \ln r / \partial (1/T)$ results from a combination of the true activation energy E_t and of the enthalpy of adsorption.
2. At very low temperatures ($-40^\circ\text{C} < t^\circ < 0^\circ\text{C}$), the activity decreases and the activation energy E_a becomes positive (Fig. 3D). The slope $\partial \log r / \partial (1/T)$ increases with $(1/T)$. The decrease in temperature promotes adsorption, which is a spontaneous exothermic phenomenon. The coverage tends to unity, whereas KC becomes $\gg 1$.

At the same time, the lowering in T also promotes the adsorption of the final reaction product P , whose desorption tends to inhibit the reaction. As a result, there appears a term $K_p C_p$ in the denominator of Eq. (6). If P has a high enthalpy of adsorption, it becomes a strong inhibitor, when one achieves: $K_p C_p \gg KC$ and the Langmuir-Hinshelwood equation becomes:

$$r = kq = kKC/(1 + KC + K_p C_p) \approx k KC/K_p C_p \quad (8)$$

where K_p is the adsorption constant of final product P . The result is an apparent activation energy E_a equal to: $E_a = E_t + \Delta H_{A\cdot} - \Delta H_{P\cdot}$, i.e., to the algebraic sum of the true activation energy E_t (theoretically equal to zero) and of the enthalpies of adsorption $\Delta H_{A\cdot}$ and $\Delta H_{P\cdot}$ of reactant A and of the inhibiting final product P , respectively. Since $\Delta H_i\cdot$'s are always negative, one generally writes: $\Delta H_i = -Q_i$, Q_i being the heat of adsorption, which is counted as positive.

$$E_a = E_t - Q_A + Q_p \approx 0 - Q_A + Q_p = -Q_A + Q_p \quad (9)$$

If product P is the strong inhibitor, this means that $Q_A < Q_p$ and in Eq. (9) E_a tends asymptotically to Q_p . Such a relationship was actually verified for photocatalytic reactions involving hydrogen, mainly alcohol dehydrogenation (Pichat et al. 1982), carried out on bifunctional Pt/TiO₂ photocatalysts. E_a was found equal to + 10 kcal/mol (+ 42 kJ/mol), which is just equal to the heat $QH_{2(ads)}$ (or to the opposite of the

enthalpy $\Delta H[H_{2(ads)}]$ of the reversible adsorption of H_2 on platinum, measured by microcalorimetry (Herrmann et al. 1987).

$$E_a = E_t - \Delta H[H_{2(ads)}] = 0 + QH_{2(ads)} = +10 \text{ kcal/mol (42 kJ/mol)} \quad (10)$$

3. At “high” temperatures ($q^\circ C \geq 70\text{--}80^\circ C$) for various types of photocatalytic reactions, the activity decreases and the apparent activation energy becomes negative (Fig. 3C). The exothermic adsorption of reactant A becomes disfavored and tends to limit the reaction. As a result, the Langmuir-Hinshelwood equation becomes:

$$r = k\theta = k KC/(1 + KC) \approx k KC \quad (11)$$

with an apparent activation energy equal to:

$$E_a = E_t + \Delta H_A \quad (12)$$

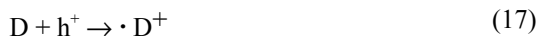
As the temperature increases, the adsorption of reactant A becomes limited and E_a , which is now negative, tends to $-Q_A$

$$E_a = E_t + \Delta H_A \approx 0 + \Delta H_A = -Q_A < 0 \quad (13)$$

As a consequence of Fig. 3D, the optimum temperature is generally comprised between 20 and $80^\circ C$. *This explains why solar devices which use light concentrators instead of light collectors require coolers* (Mehos and Turchi 1993). This absence of heating is attractive for photocatalytic reactions carried out in aqueous media and in particular for environmental purposes (photocatalytic water purification) (Herrmann et al. 1998). There is no need to waste energy by heating water which possesses a high heat capacity. This explains why photocatalysis is cheaper than incineration.

Radiant flux

It has been shown that for all the photocatalytic reactions studied the rate of reaction r is proportional to the radiant flux ϕ (Fig. 3E). This confirms the photo-induced nature of the activation of the catalytic process, with the participation of photo-induced electrical charges (electrons and holes) to the reaction mechanism. However, above a certain value, estimated to be ca. 25 mW/cm^2 in laboratory experiments, the reaction rate r becomes proportional to $\Phi^{1/2}$. This can be demonstrated as follows: The five basic equations are:



and, in accordance with the principles of heterogeneous catalysis, the rate limiting step is the reaction in the adsorbed phase (Eq. 18). Therefore

$$r = r_{18} = k_{18} [A^-] [D^+] \quad (19)$$

In an n-type semiconductor such as titania, the photo-induced holes are much less numerous than electrons (photo-induced electrons plus n-electrons): $[h^+] \ll [e^-]$. Therefore holes are the limiting active species. Thence:

$$r = r_{18} = r_{17} = k_{17} [D] [h^+] \quad (20)$$

At any instant, one has:

$$d[h^+]/dt = r_{14} - r_{15} - r_{17} = 0 = k_{14} - k_{15}[e^-] [h^+] - k_{17} [D] [h^+] \quad (21)$$

Thence:

$$[h^+] = \frac{K_{14} \Phi}{k_{15}[e^-] + k_{17} [D]} \quad (22)$$

and

$$r = \frac{k_{17} [D] k_{14} \Phi}{k_{15}[e^-] + k_{17}[D]} = \frac{k_{14} k_{17}[D] \Phi}{K_{17}[D] + k_{15} [e^-]} \propto \Phi \quad (23)$$

From the above equation, it can be seen that the reaction rate is directly proportional to the light flux.

In the case of high fluxes, the instantaneous concentrations $[e^-]$ and $[h^+]$ become much larger than $k_{17}[D]$. Therefore Eq. (22) becomes:

$$[h^+] \approx \frac{K_{14} \Phi}{k_{15}[e^-]} \quad \text{with } [h^+] \approx [e^-] \quad (24)$$

Thence

$$[h^+]^2 \approx k_1 \Phi / k_2 \quad (25)$$

The reaction rate r becomes

$$r = r_{18} = r_{17} = k_{17}[D] (k_{14}/\Phi k_{15})^{1/2} \propto \Phi^{1/2} \quad (26)$$

indicating that r has become proportional to $\Phi^{1/2}$ and that the rate of electron-hole formation becomes greater than the photocatalytic rate, which favours the electron-hole recombination (Eq. 15). In any photocatalytic device, the optimal light power utilization corresponds to the domain, where r is proportional to Φ . This constitutes the right challenge of chemical engineering to design photoreactors consuming all the efficient photons invested.

Photocatalytic Quantum Yield

In photochemistry, the quantum yield is the number of converted molecules per incident photon. In heterogeneous photocatalysis, it corresponds to a doubly kinetic magnitude and is defined as the ratio of the reaction rate in molecules converted per second (or in mols per second) to the incident efficient photonic flux in photons

per second (or in Einstein per second (an Einstein being a mol of photons)). This is a kinetic definition, which is directly related to the instantaneous efficiency of a photocatalytic system. Its theoretical maximum value is equal to 1. It may vary on a wide range according (i) to the nature of the catalyst, (ii) to the experimental conditions used (concentrations, T, m, etc.), and (iii) especially to the nature of the reaction considered. We have found values comprised between 10^{-2} % and 70%. The knowledge of this parameter is fundamental. It enables one (i) to compare the activities of different catalysts for the same reaction, (ii) to estimate the relative feasibility of different reactions, and (iii) to calculate the energetic yield of the process and the corresponding cost.

New Concepts in True Heterogeneous Photocatalysis: Stoichiometric Threshold, Turnover Number and Turnover Frequency

Turnover Number <TON> and Stoichiometric Threshold

The notion of turnover number <TON> in heterogeneous catalysis has to be taken into account. Its definition is the same as in enzymatic or homogeneous catalysis, i.e., it is the number of molecules converted per active site in a given time (Herrmann 2012). It is only possible to determine it in heterogeneous catalysis if the nature and number of active sites have been carefully identified and quantified. It is easy for noble metal-based catalysis since every surface metal atom can be considered as an active site. As an upper limit of the number of active sites n_{sites} at the surface of titania, one can conventionally choose the maximum value of the surface density of titanol groups Ti-OH, equal to 5×10^{18} OH/m² or 5 OH/nm². Therefore, one gets: $n_{\text{sites}} = 5 \times 10^{18}$ OH/m² \times S_{BET} \times m_{cat} .

For demonstrating the **true catalytic nature** of a photocatalytic reaction, the conversion has to be carried out beyond a certain percentage corresponding to the **stoichiometric threshold <ST>**. It is defined as the minimum number of molecules that have to be converted to be greater than the maximum number of potential active sites, initially present at the surface of a mass m of titania photocatalyst used in the reaction. For example, if a photoreactor contains 1 g of titania Degussa P-25 (with $S_{\text{(BET)}} = 50$ m²/g), which is fully illuminated and respects the laws mentioned above, a given photocatalytic reaction could be declared as “truly catalytic” only if the number of converted molecules is higher than $n_{\text{min}} = (5 \times 10^{18}) \times m \times S_{\text{(BET)}} = 2.5 \times 10^{20}$ molecules, i.e., 4.2×10^{-4} mol. In the case of a weak adsorption of reactants such as alkanes, the number of sites can be assimilated to the ratio of the total surface area exposed to the area occupied by one single molecule in the conditions of a Langmuir monolayer adsorbed.

Actually, a true catalytic system should work with ratios n/n_{min} of several orders of magnitude. For example, ratios n/n_{min} as high as 10^3 could be obtained in alcohol dehydrogenation (Pichat 1982). <TON> and <ST> are related by the following equation:

$$\langle \text{ST} \rangle = m.d.S.\langle \text{TON} \rangle$$

The test for the respect of the stoichiometric threshold is particularly important for dealing with a true photocatalytic process.

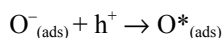
Turnover Frequency <TOF>

As in enzymatic and homogeneous catalyses, the turnover frequency <TOF> is the number of molecules converted per second and per active site (Boudart and Djéga-Mariadassou 1982). It is only possible to determine it in heterogeneous catalysis if the nature and number of active sites have been carefully identified and quantified. It is easy for noble metal-based catalysis since every surface metal atom can be considered as an active site. In that case, Boudart estimates that correct values should range between 10^{-2} and 10^{+2} sec^{-1} with a correct mean value around 1 sec^{-1} (Boudart and Djéga-Mariadassou 1982). Low values of ca. 10^{-3} sec^{-1} can be incorrect because of large analytical errors. On the other hand, <TOF> higher than 10^{+3} sec^{-1} can become limited by diffusion (Boudart and Djéga-Mariadassou 1982). In heterogeneous photocatalysis, <TOF> is much more difficult to be determined. As an upper limit of the number of active sites n_{sites} , one can choose the maximum value of the surface density of titanol groups Ti-OH, equal to $5 \times 10^{18} \text{ OH/m}^2$ or 5 OH/nm^2 [21]. Therefore, one gets: $n_{\text{sites}} = 5 \times 10^{18} \text{ OH/m}^2 \times S_{\text{BET}} \times m_{\text{cat}}$.

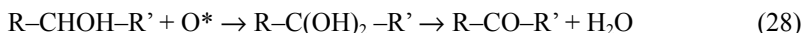
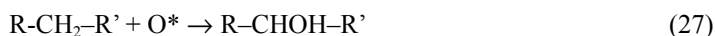
Nature of True Photocatalytic Reactions

Selective Mild Oxidation Reactions in Dry Media

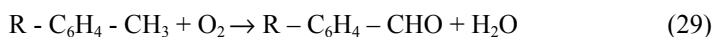
Historically, the first photocatalytic reactions were performed in dry gas phase (Formenti et al. 1970). Electrical photoconductivity measurements indicated the formation of two ionosorbed oxygen species, O_2^- and O^- at steady state (Herrmann et al. 1981). However, *in situ* photoconductivity measurements (Herrmann et al. 1979) indicated that only species O^- could be the precursor of an active species for oxidation by reaction with a hole:



This activated dissociated species is strongly electrophilic and able to insert into a C-H bond, thus creating an alcohol intermediate, able to be oxidized as a transient gem-diol, which spontaneously dehydrates into a final carbonyl-containing molecule:



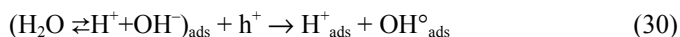
This O^* species is not cracking and responsible for an optimal selectivity in mild oxidation reactions. Both gas and liquid phase oxidations using air as the oxidizing agent mainly concern the mild oxidation of alkanes, alkenes and alcohols into carbonyl-containing molecules (aldehydes and ketones). Aromatic hydrocarbons (Pichat et al. 1986) such as alkyltoluenes or o-xylenes were 100% selectively oxidized on the methylgroup into alkylbenzaldehyde:



Pure liquid alcohols were also oxidized into their corresponding aldehydes or ketones. In particular, the oxidation of isopropanol into acetone was chosen as a photocatalytic test for measuring the efficiency of passivation of TiO₂ or ZnO-based pigments in paintings against weathering. The ensemble of these reactions constitutes a *réservoir* of applications in fine chemistry (pharmacy, perfume, etc.) according to the principles of Green Chemistry: atom economy, absence of solvents, energy savings with the working conditions at ambient temperature (Anastas and Warner 1998).

Total Oxidation Reactions in Presence of Water (humid air or aqueous phase)

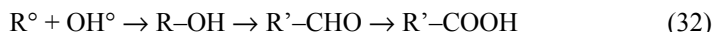
By contrast with the selective mild oxidation reactions in dry gaseous or liquid organic phases, the selectivity turns in favor of total oxidative degradation as soon as water is present. This was ascribed to the photogeneration of stronger, unselective, oxidizing species, namely OH° radicals originating from water via the OH⁻ groups of titania's surface:



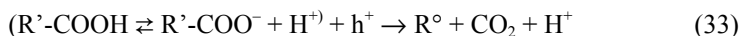
OH° radicals, known as the second best oxidizing agent after fluorine, are nucleophilic and generate water by abstraction of a hydrogen atom from reactant RH.



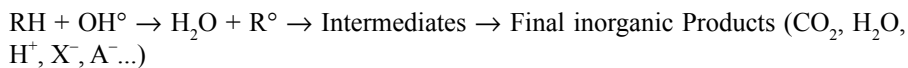
Radicals R° undergo attacks by radicals OH°, leading to the formation of increasing numbers of oxidized intermediates:



Holes h⁺, already responsible for the OH° radical formation, are also responsible for the appearance of CO₂, according to the "photo-Kolbe" (Kraeutler and Bard 1978).



Therefore, the overall total oxidation can be summarized as:



The consequence of the absence or presence of water in the medium is a double aptitude for anatase to act both in fine and in environmental chemistry.

Environmental Applications

Photocatalytic Treatment of Water

There are two stages involved in water treatment for potabilization: **detoxification** and **disinfection**. Detoxification involves (i) the inerting of inorganic pollutants and (ii) the degradation and mineralization of organic compounds. Disinfection of water

involves the inactivation or even the total degradation of micro-organisms (bacteria, virus, spores, etc.).

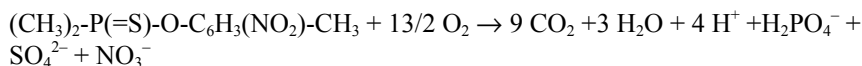
Detoxification

Inorganic pollutants

Many toxic inorganic anions are photocatalytically oxidized into harmless or less toxic compounds by using TiO₂ as a photocatalyst (Herrmann 1999, 2006). For example, SO₃²⁻, HSO₃⁻, S₂O₃²⁻, S²⁻ and HS⁻ are oxidized in SO₄²⁻, whereas PO₃³⁻ is oxidized in PO₄³⁻. NO₂⁻ and NH₄⁺ ions oxidized in NO₃⁻, whereas cyanide CN⁻ anions are oxidized in OCN⁻ before hydrolysis into NO₃⁻ and CO₃²⁻ (Frank and Bard 1977). At the same time, heavy metal cations (Ag⁺, Hg²⁺, Pd²⁺, Au³⁺, Rh³⁺, Pt⁴⁺, etc.) are reduced by photoelectrons before depositing on TiO₂, without any screening of the surface (Herrmann et al. 1986, 1988).

Organic Pollutants

Owing to the water adsorbed at the surface of titania and to its oxidation by photo-holes, the formation of unselective, strongly oxidizing OH[°] radicals enables the degradation of practically all the organic pollutants (common organic compounds, pesticides, dyes, explosives, solvents, hydrocarbons, fuels, medication, etc.) in CO₂ and H₂O. The only exceptions are fluorinated compounds and, strangely, cyanuric acid C₃H₃N₃O₃, resulting from degradation of triazinic compounds. This is because of the redox potential of the reaction and also because of the oxidation state of carbon, which is already at level +4 inside this molecule. Complex molecules such as pesticides, containing hetero-atoms are totally mineralized in CO₂, H₂O, plus in innocuous inorganic anions as described above. In particular, the highly dangerous organophosphorus compounds, now prohibited in agriculture, are totally mineralized. For example, phenitrothion disappears, according to stoichiometry (Kerzhentsev et al. 1996):



In this study, it was shown that the degradation reaction of phenitrothion initiated via the attack by OH[°] radicals of the weak point of the molecule, i.e., the thio-group –(P=S)– oxidized in –(P=O)–, thus forming phenitro-oxon, is significantly more toxic than its parent compound. This is why this insecticide was used as a “homicide” in warfare gases, alongside other organo-phosphorus compounds such as sarin. This ability of photocatalysis to destroy organo-phosphorus compounds has inspired some researchers to design photocatalytic gas masks for the US army (see Fig. 4) in case of chemical war (Hoffmann et al. 2004), which has recently become a geopolitical problem. It appears that a serious process intensification is still necessary.

Another example in line with “Green Chemistry” (Anastas and Warner 1998) in water photocatalytic decontamination is total mineralization into CO₂ and innocuous inorganic anions (Cl⁻, SO₄²⁻, NO₃⁻) of complex molecules such as dyes, which are not

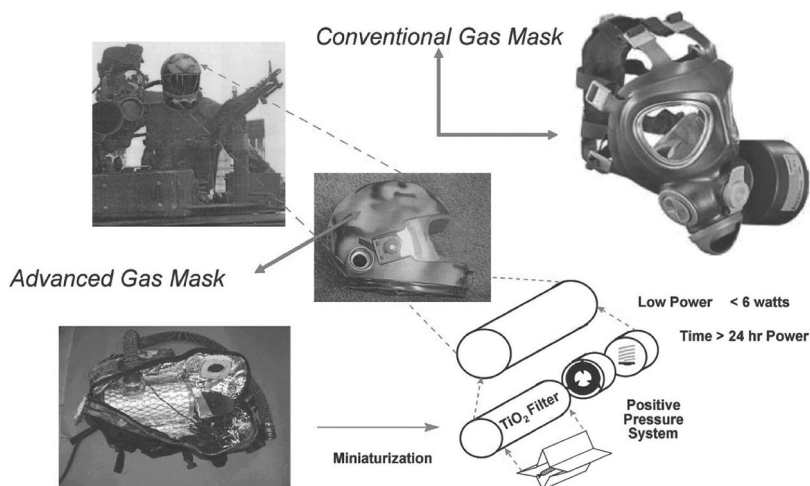


Figure 4. Description of a photocatalytic gas mask (Hoffmann et al. 2004).

only decolorized but also totally destroyed. Currently, half of all dyes used worldwide are azo-dyes (i.e., containing the $-N=N-$ azo group). Among them, Congo Red is a particularly recalcitrant industrial dye and is a printers' "nightmare", as they cannot eliminate its intense red color using ordinary physico-chemical means. Its developed formula is given in Fig. 5.

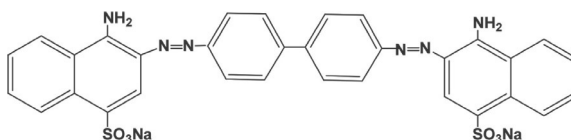
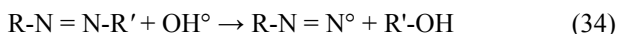


Figure 5. Developed formula of Congo Red azo-dye.

Whereas the mass balance of element nitrogen could not be established by analyses in the aqueous phase, by using an air-tight batch slurry photoreactor connected to an air-tight gas chromatograph, an evolution of N_2 in the gas phase could be evidenced and quantified. It just corresponded to mol fraction of the $-N=N-$ azogroups. The total mass balance in nitrogen was found to be equal to 100%, as illustrated by the kinetics curve in Fig. 6.

Whereas the double aromatic rings of biphenyl and naphthalene groups are totally mineralized in CO_2 and H_2O , both azo-groups are mineralized in di-nitrogen, according to both reactions:



The 100% selective degradation of $-N=N-$ azogroups in gaseous N_2 constitutes an ideal example of water decontamination with a typical "environmentally friendly" reaction (Lachheb et al. 2002). Similar results were obtained for all the other azo-

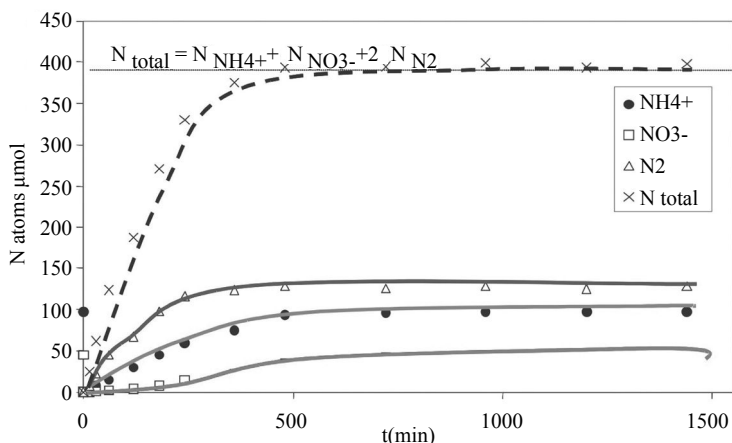


Figure 6. Kinetics of appearance of nitrogen-containing final products in Congo Red degradation.

dyes tested. This is the first example, to our knowledge, of a nitrogen evolution during the aqueous photocatalytic degradation of complex N-containing pollutants.

Warning: Erroneous and Misleading Photocatalytic Normalized Tests based on Dye Decolorization

Many tests and recent papers are based on dye decolorization, which is easy to perform with a UV-visible spectrophotometer. However, these tests, which all claim titania's activation in the visible, can represent the most "subtle pseudo-photocatalytic" systems, hiding the actual non-catalytic nature of the reaction involved. This was quantitatively demonstrated with the apparent photocatalytic "disappearance" of indigo carmine dye (Vautier et al. 2001). Visible light excites the adsorbed dye molecules at an energy level higher than that of the conduction band of titania, thus inducing a spontaneous electron transfer to titania, which destroys the regular distribution of conjugated bonds within the dye molecule and causes its decolorization. Once transferred to titania, the electron will participate in an additional iono-sorption of molecular oxygen as O_2^- . This is a photo-induced stoichiometric reaction, irrelevant to photocatalysis. As a consequence, all misleading photocatalytic reactions, exclusively based on dye decolorization, should be banished.

Potabilization of Water

Water potabilization obeys two imperatives: (i) detoxification (described above) and (ii) disinfection. The latter one has been evaluated with the photocatalytic degradation of bacteria such as *Escherichia coli* or *streptococcus faecalis*. Figure 8 shows two electronic micrographs of *E. coli* cells, of the order of one micrometer, before and during the attack by nanoscopic particles ($d \approx 32$ nm) of TiO_2 photocatalyst (P-25 Degussa, now Evonik). Strangely, the "supramolecular reactant" to be destroyed is two orders of magnitude larger than elementary grains of the photocatalyst.

Figure 7 perfectly illustrates the size inversion between the catalyst grain and the reactant. The result is improved efficiency of a suspended photocatalytic bed in a slurry photoreactor in comparison with a fixed bed for the degradation of such micro-organisms. From a Chemical Engineering point of view, the issue to be considered is the design of a slurry photoreactor which is compatible with a non tedious easy final filtration of the catalyst, for its future recycling.

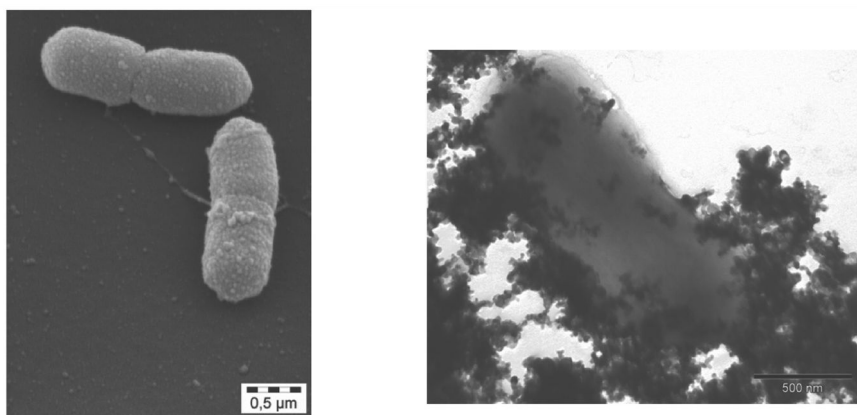
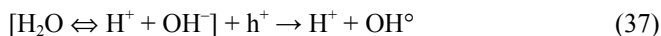


Figure 7. Micrographs of *E. coli* Bacteria before and during the attack by UV-irradiated Degussa P-25 TiO₂ nanoparticules.

Photocatalytic Air Treatment

All pollutants destroyed in the aqueous phase can also be degraded when they are present in the air, especially all the VOCs, since they follow the same reaction mechanisms, provided a certain level of humidity is present, as this is necessary to maintain a certain level of hydration of titania's surface, with hydroxyl groups, which are precursors of OH° radicals (Herrmann 2006).



Inner Air Treatment

The inner air treatment in confined atmospheres with air (re)-circulation through a filter supporting titania enables one to eliminate volatile organic compounds (VOCs), odors, toxic gases in offices, workshops, submarines, clean rooms in electronics, hospitals, etc. For chemical engineering reasons, the photocatalyst has to be used in a fixed bed, or should be deposited on a photo-inert support. The optimal option would be the use of a fluidized bed but the homogeneous distribution of UV-photons would be problematic under such conditions. Anyway, since no chemical engineering studies have yet been attempted, this would be a good challenge. We opted for a

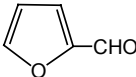
flexible support, paper, on the fibers of which commercial titania was merely bound using a UV-transparent silica binder. This was performed by Joseph Dussaud from AHLSTROM paper company. Other photocatalytic devices can equip kitchen ventilations, air conditioning systems in rooms or in cars. Some air purification devices are being considered for the electronics industry, which requires a “molecular” purity of the ambient atmosphere for improved performance of their nano-scale components. It is noteworthy that silicon which contains VOCs is destroyed, the organic part being mineralized as CO₂ and H₂O, whereas Si is converted in silica, which remains at the surface of titania, without causing photocatalysis issues, since it is transparent to UV-light. Most products sold are produced in Japan. In addition, it has been shown that the addition of activated carbon to titania in the aqueous phase created a strong interaction between both solid phases, with a kind of synergy: activated carbon adsorbs a great quantity of pollutants which are subsequently transferred to titania under the action of a driving force corresponding to an intense concentration gradient between activated carbon and “self-cleaning” titania (Matos et al. 2001). Such synergy exists in (humid) air treatment and enables one to absorb pollution peaks. Under these conditions, UV-irradiated titania-based photocatalysis could be successfully applied to the elimination of air pollutants, VOCs, solvents, odors, chemicals, etc.

Case Study of Odor Elimination

Odors are generally highly diluted VOCs that conventional physico-chemical processes cannot treat efficiently (Le Cloirec 1998). By contrast, photocatalysis can easily destroy odors at low concentrations and under low flow rates, at room temperature, especially when titania is associated with activated carbon AC* (Matos et al. 2001).

A practical example in air purification has been successfully applied to the removal of odors in confined atmospheres, in particular in domestic refrigerators (Guillard et al. 2004). Some common domestic odors, listed in Table 1, have been successfully eliminated at +4°C.

Table 1. Formulas of some common domestic odors.

Name	Formula	Origin
Butadione	CH ₃ -CO-CO-CH ₃	Odor of rancid butter
Dimethyldisulfide	CH ₃ -S-S-CH ₃	Odor of cabbage
Furfural		Odor of burnt milk
Valeric acid	CH ₃ -(CH ₂) ₃ -COOH	Odor of corporal perspiration
2-heptanone	CH ₃ -CO-(CH ₂) ₄ -CH ₃	Odor of strong cheese

A patented mini-photocatalytic reactor for the elimination of odors and bacteria has been inserted in the air recirculation circuit of a domestic refrigerator (Guillard et al. 2004). It is described in Fig. 8. The photocatalytic degradation of the odor molecules is performed by UV-irradiated TiO_2 which is deposited on a special paper Ahlstrom® and associated with activated carbon AC*, present as black dots on the photograph, introduced in order to promote ab- and adsorption of odors, in particular in case of pollution peaks. To avoid heating in a refrigerator, UV-A light is provided by UV-leds. The device was commercially name « Biolyse », although there is no bio-systems at all. According to Fig. 2D, because of the photo-activation process, the low temperature at 4°C is not detrimental but favors the adsorption of odors on the biphasic catalyst. This anti-odor domestic refrigerator prototype has been validated, patented and industrially produced in a first series at 40,000 exemplaries, followed by a second one of 70,000 units.

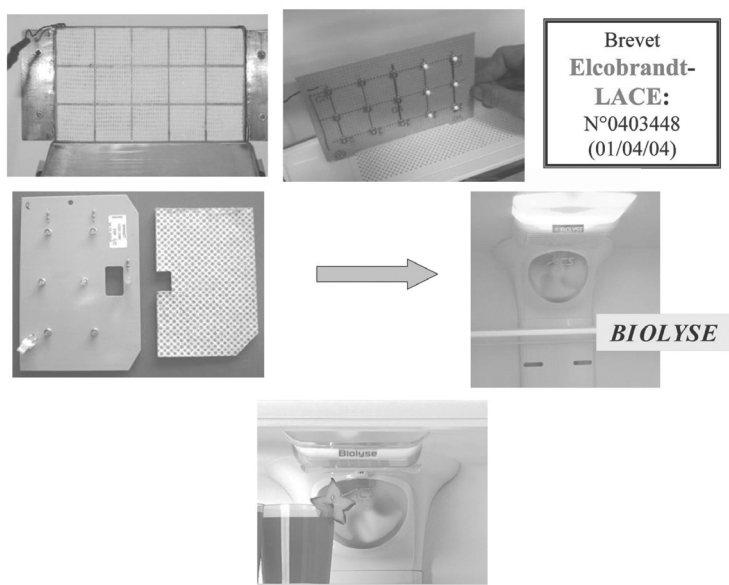


Figure 8. Mini-photocatalytic reactor for the elimination of odors and bacteria inserted in the air recirculation circuit of a domestic refrigerator (French Patent N° 0403448, 01/04/04 by C. Guillard, J.M. Herrmann, J.P. Chevrier, C. Bertrand and E. Philibert).

The disinfection aptitude of titania-based photocatalysis evidenced in water was confirmed in air disinfection. For instance, Virus H5N2, a model virus close to H5N1, responsible for the avian flu, could be photocatalytically de-activated in a dynamic photoreactor with a single pass of contaminated air at a flow rate of $50 \text{ m}^3/\text{h}$ with an efficiency of 99.93%. This has been done in a specialized P3 medical laboratory of the medical school of the Lyon-1 University (Guillard et al. 2008).

Outer Air Treatment

Objectively, the photocatalytic treatment of outer air can only be performed outside at a very short distance from the emission sources, particularly those of toxic gases and/or of odors. The advantage of photocatalysis is that it is able to operate at low concentrations and under low flow rates, where the other physico-chemical processes are inefficient, as illustrated by Fig. 9 by Le Cloirec 1998.

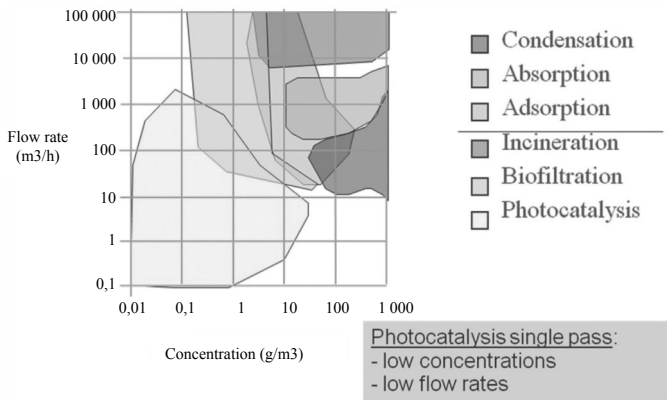


Figure 9. Operational field of photocatalysis. Diagram of the flow rate as a function of the concentration.

The outer air treatment must also be associated with water and solid waste treatment, because of their emissions of strong odors. Kinetics and efficiencies can be greatly improved by associating deposited titania with activated carbon AC*. Titania photocatalysts destroy the odors using solar UV-photons in day time, whereas activated carbon traps odors during the night or during a pollution peak. On the next day, the pollutants accumulated on AC* are spontaneously transferred to titania under the action of a driving force constituted by a strong concentration gradient between AC and self-cleaning titania (Matos et al. 2001). This concept has been applied by Joseph Dussaud from Ahlstrom paper company to industrially prepare special papers supporting TiO₂ + AC* under the shape of large sheets of media to cover aqueous or solid sources of odor emissions. This system was successfully applied, mainly in catering industries. This was done by covering water treatment ponds or lagoons with rafts on which large sheets of Ahlstrom papers were settled. Figure 10 illustrates the covering of ponds of used water from olive oil industrial mills in Mèze in the south of France.

While the bio-treatment of waters which are highly loaded with polyphenols is operating, the strong odors emitted by the aqueous phase are adsorbed by both phases TiO₂ and AC*. In day light, these odors are eliminated by titania, whereas at night, AC* continues to adsorb odors, which will be transferred to titania in day time for the reasons explained above.

Another example is given for a mustard factory close to Dijon (France), where Ahlstrom paper sheets are fitted on metallic cables above the ponds; see Fig. 11.

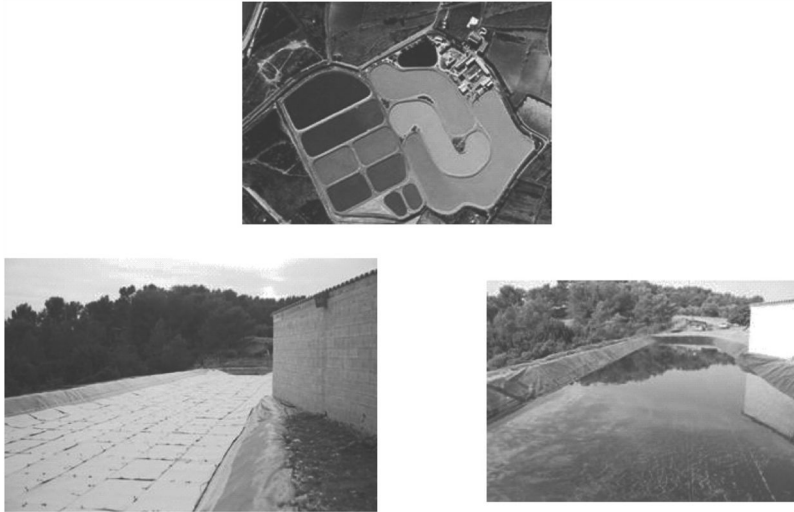


Figure 10. Elimination of bad odors emitted by a used water pond in an olive oil mill in Mèze (France). Top: aerial view of the basins; below right: uncovered pond; below left: pond covered by floating rafts supporting Ahlstrom papers covered by $(\text{TiO}_2 + \text{AC}^*)$ photocatalyst.

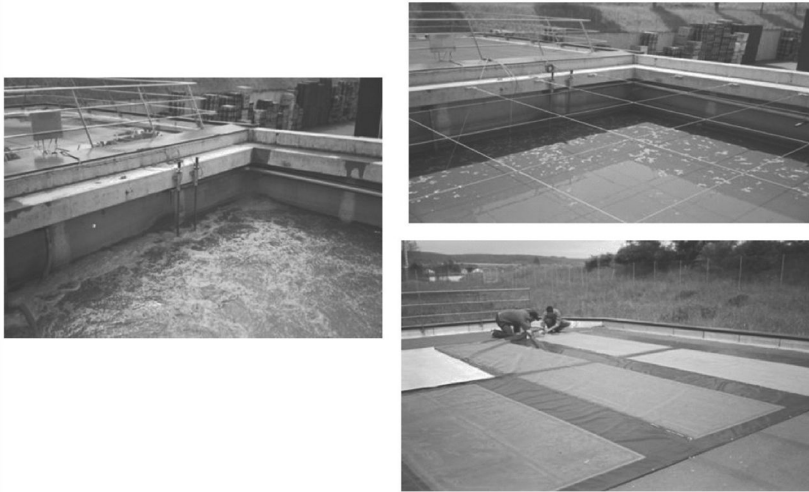


Figure 11. Elimination of strong odors emitted by biologic treatment basins in food industry (presently mustardery close to Dijon) (by courtesy of Mr.J. Dussaud, Ahlstrom Co 2007).

The same system for odor removal was also applied to solid wastes. For example, sludge produced at paper mills has to be stored in warehouses before disposal in agricultural fields for plowing, which happens only twice a year. During storage, fermentation occurs, producing bad odors, in particular odors which contain sulfur. This sludge is stored in special warehouses, whose covers and windows are made of Ahlstrom paper covered with titania associated with AC^* Fig.12. It is noteworthy

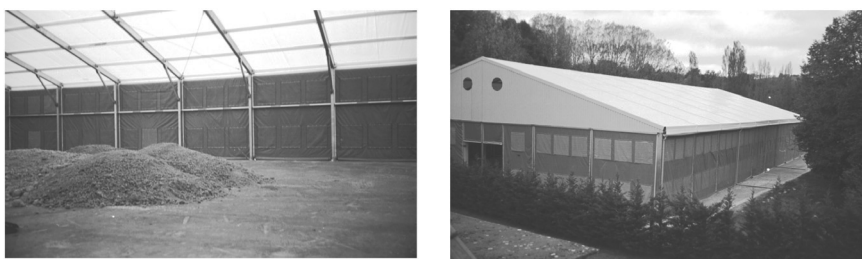


Figure 12. (right): Drying sludge of paper mills stored in a warehouse whose walls and windows are constituted of special Ahlstrom paper supporting titania; (left): outside view with sunlight activation) (by courtesy of Mr.J. Dussaud, Ahlstrom Co 2007).

that this system is efficient enough that the communities surrounding these factories have abandoned legal proceedings.

Solar Photocatalysis: “Helio-photocatalysis”

The various types of photocatalytic reactions described above, performed under artificial UV-light, can also be performed under natural solar light. The most effective photocatalysts are anatase samples which absorb only ca. 3% to 6% of the overall solar energy at the earth’s surface, depending on the altitude and latitude of the localization, as well as on the climate. We have named it “*Helio-photocatalysis*” in order to distinguish it from a potential helio-thermocatalysis, which would be based on heating by the concentrated infra-red beams of the sun and which has never before been demonstrated.

Validation of the Results of “Helio-photocatalysis” at the Pilot Scale

All selected reactions, performed under artificial UV-light and validated at the laboratory scale, could be reproduced at the solar platform in Almeria (PSA), Spain, using solar energy at the pilot scale, with an extrapolation factor equal to 12,500, corresponding to the ratio of the volume of the pilot photoreactor (250 L) to that of the lab microreactor (20 cm³).

All the kinetic laws established in the lab were observed and confirmed, with, in particular, identical behaviors of the physicochemical parameters (mass of catalyst, efficient wavelength, concentrations, temperature, radiant flux) described in Fig. 3. The reactions were performed in a Compound Parabolic Collector (CPC) photoreactor at PSA. The CPC photoreactor used at Plataforma Solar de Almeria (PSA) in Spain is described in Fig. 13 with the collector having an inclination angle of 37° corresponding to the latitude of Almeria. The CPC collector, which is the irradiated part of the system, corresponds to a plug flow reactor. It is connected to a tank via a recirculation pump and the ensemble corresponds to a batch reactor. Since the elimination of pesticides follows a first order of kinetics, the C_{A0} concentration at the inlet and C_A at the outlet of the collector are related by the following equation:

$$C_A/C_{A0} = \exp(-kt) \quad (38)$$

Because of the recirculation, C_{A_0} varies with time as:

$$-V_2 (dC_{A_0}/dt) = Q (C_{A_0} - C_A) \quad (39)$$

where V_2 is the volume of the tank, and Q is the flow rate. Combining Eqs. (38) and (39),

$$\text{one gets: } -V_2 (dC_{A_0}/dt) = Q [C_{A_0} - C_{A_0} \exp(-kV_1/Q)] = QC_{A_0}[1-\exp(-kV_1/Q)] \quad (40)$$

where V_1 is the volume of the tank, and Q is the flow rate.

The integration of the differential equation (40) gives:

$$[C_{A_0}]_{\text{final}} = (C_{A_0})_{\text{initial}} \exp[-(1-\exp(-kV_1/Q))(Q.t/V_2)] \quad (41)$$

If the flow rate Q is high and if V_1 is not too important, Eq. (41) can be simplified as follows:

$$\exp(-kV_1/Q) \approx 1-kV_1/Q \quad (42)$$

Therefore $[C_{A_0}] = [C_{A_0}]_{\text{initial}} \exp[(-kV_1/Q) \times (Q/V_2) t]$

$$= [C_{A_0}]_{\text{initial}} \exp(-k(V_1/V_2) t) \quad (43)$$

The residence time t_R in the CPC collector is equal to:

$$t_R = [V_1/V_T] t = [V_1/(V_1 + V_2)] t = [r/(1 + r)] t \text{ with } r = V_1/V_2 \quad (44)$$

Therefore Eq. (43) becomes :

$$C_{A_0} = [C_{A_0}]_{\text{initial}} \exp[-(1 + r)/r] k t_R] \quad (45)$$

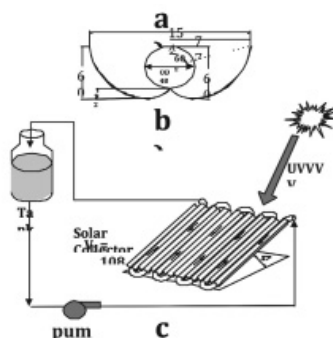


Figure 13. Picture and scheme of the CPC photoreactor at PSA.

By determining ratio r from the geometry of the reactor, one can calculate the apparent first order reaction rate constant k .

The solar photocatalytic degradation of pollutants in the CPC photoreactor has been successfully applied at PSA on various pollutants, as exemplified by the total mineralization of 2,4-D (2,4-dichlorophenoxyacetic acid), a well-known herbicide. In Fig. 14, the temporal variations of 2,4-D, 2,4-dichlorophenol (2,4-DCP), the main intermediate formed, Cl^- anions produced and the total organic carbon (TOC) are

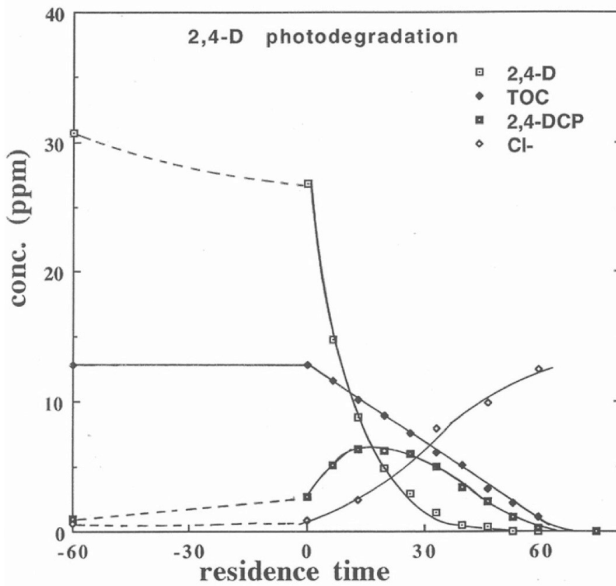


Figure 14. Kinetics of (i) herbicide 2,4-D and TOC disappearance, (ii) of Cl⁻ anion formation and (iii) of 2,4-DCP appearance and disappearance.

represented. After an adsorption period of one hour in the dark, 2,4-D disappears following a first order of kinetics. Cl⁻ anions follow a sigma shaped curve in agreement with the consecutive reaction scheme:



giving

$$[Cl^-] = 2 C_0 [1 - k_2 / (k_2 - k_1) \exp(-k_1 t) + k_1 / (k_2 - k_1) \exp(-k_2 t)] \quad (47)$$

The TOC decreases linearly to zero within one hour, with an apparent zero kinetic order. That could be interpreted by assuming a saturation of surface sites by all the intermediates.

$$-d[TOC]/dt = + d[CO_2]/dt = k \sum \theta_i = k \sum K_i C_i / (1 + K_i C_i) \approx k \theta_{sat} \approx k \quad (48)$$

where θ_i represents the surface coverage of the i^{th} intermediate and θ_{sat} the overall coverage at saturation.

The kinetics of 2,4-D disappearance were repeated at two different dates with two different solar UV-radiant fluxes obtained during a partly cloudy day and with a bright sunny day. It can be seen in Table 2 that both rate constants of 2,4 D and of TOC disappearance, independently of their units, are quite proportional to the mean solar UV power flux. This means, according to Fig. 14, that the CPC photoreactor is working in optimal conditions with respect to solar irradiation and can also work with diffuse UV-light.

Table 2. Evidence for the proportionality between the mean radiant flux and the rate constants of herbicide 2,4-D disappearance ($k(2,4-D)$) and of TOC elimination ($k(TOC)$) on two different days (partly cloudy and bright sunny).

$\Phi(UV)$ (W/m^2)	$k(2,4-D)$ (min^{-1})	$k(TOC)$ (ppm/min)
31	6.79×10^{-2}	0.1575
38.2	8.72×10^{-2}	0.203
$\Phi_1/\Phi_2 = 0.81$	$k_1/k_2 = 0.78$	$k_1/k_2 = 0.78$

These experiments were compared with initial studies performed in a laboratory microphotoreactor working with artificial light and confirmed the same kinetics, same reaction pathway and same quantum yields. Only two points of apparent divergence were observed: (i) the optimum concentration in titania for the CPC pilot plant was 0.2 g/L instead of 2.5 g/L for the batch microreactor, and (ii) the TOC disappearance at PSA was faster than the measured CO_2 evolution in laboratory experiments. This was ascribed to the CPC photoreactor design with a recirculating tank which promotes the production of the final products detrimentally to that of the intermediate ones.

Validation of Fixed-bed Solar Photocatalytic Reactor Using Deposited Titania

Although slurry photoreactors can be estimated as the most efficient ones, they have a significant drawback: the final tedious filtration of titania particles. To overcome this obstacle, titania can be deposited on photo-inert supports. A successful attempt was made by depositing titania on a special Ahlstrom paper using amorphous silica as a binder to anchor the photocatalyst particles on inorganic fibers. Such a photocatalytic material has been used in an adapted solar photoreactor called Cascade Falling Films Photoreactors (CFFP) described in Figs. 15 and 16.

To test the efficiency of the CFFP solar reactor, photocatalytic reactions were calibrated against a slurry CPC photoreactor with the same surface of sun collector

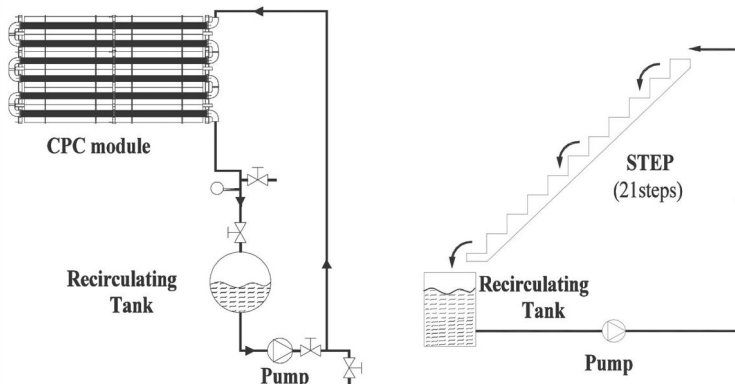


Figure 15. Comparative diagrams of CPC slurry reactor and Cascade Falling Films Photoreactors (CFFP).

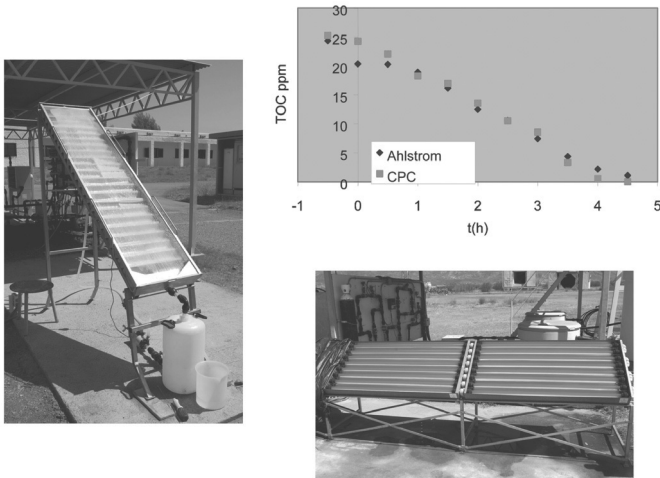


Figure 16. Photographs of CPC (slurry) and of CFFP (fixed bed) photoreactors. Comparison of their performances by following the TOC disappearance in the reaction of 4-chlorophenol total degradation.

as shown in the photographs in Fig. 16. Surprisingly, the results were similar in the total degradation of 4-chlorophenol, as indicated by the Total Organic Carbon (TOC) disappearance (Fig. 16).

Solar Water Potabilization by Helio-photocatalysis

These two types of photoreactors were studied in order to produce drinking water for remote isolated human communities in arid countries. Two European contracts were entered into regarding North Africa (AQUACAT Program) and Latin America (SOLWATER Program). The slurry photoreactor appeared as redhibitory since the final tedious filtration of the photocatalyst was not compatible with a robust and simple design. The concept of a deposited catalyst on the special Ahlstrom paper, efficient for both detoxification and disinfection, was conserved, but the use of CFFP reactor had to be abandoned because water evaporation was too high, which is a drawback in countries where water is so scarce. Eventually, a final prototype was elaborated, which is presented in Fig. 17. The fixed bed of titania deposited on Ahlstrom paper is placed along the focal axis of a CPC collector inside glass tubings positioned in series, either on a glass fin or on a co-axial glass tubing. This ensemble is settled on a fixed rack, whose plane is inclined with an angle equal to the latitude of the working location, in order to get the maximum solar irradiation around noon. The photoreactor reactor looks like a plug flow reactor but since it is connected to a reservoir of several hundred liters, the ensemble acts as a batch reactor (Levenspiel 1972). The photovoltaic panel seen on the photographs has been added just to run a small dc-electrical pump for a permanent circulation of water to be potabilized. The oxygen necessary for the oxidation of impurities comes, if air is present, to the top of the reservoir. Permanent recirculation allows for the maintenance of potabilization of water, especially in the case of disinfection, by inhibiting the regrowth of ambient

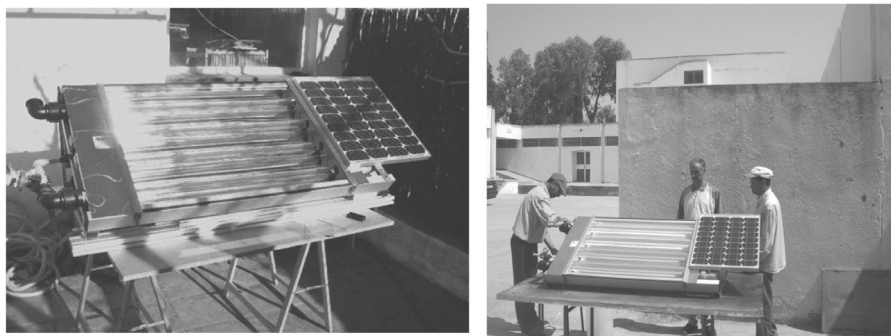


Figure 17. Photographs of the Aquacat and Solwater prototypes for solar photocatalytic potabilization of water in arid counties.

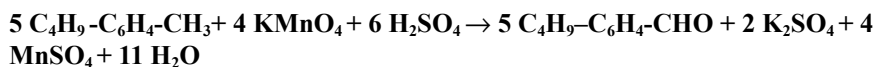
micro-organisms. This prototype, which is quite autonomous and robust, was produced in several exemplaries and exported to different countries involved in both programs (Morrocco, Tunisia and Egypt for Aquacat and Mexico, Argentina and Peru for Solwater). The highest quantum yields were obtained in Peru since the prototype was settled close to Cuzco at a very high altitude of ca. 4000 m.

Use of Photocatalysis in Reasoned Agriculture

Photocatalysis can be utilized in reasoned agriculture to clean polluted waters. This has been demonstrated in a winery in Burgundy, where polluted waters, resulting from the rinsing of nebulizers, tanks and tractors used in vineyards, were treated by photocatalysis in the CFFP reactors described above, irradiated either in sunlight during day time or in workshops with artificial UV-irradiation provided by UV-A lamps after their storage in elevated reservoirs (Fig. 18). Most commercial pesticides used in vine treatment could be successfully destroyed below a limit compatible with the discharge to the sewage or the local river.

Photocatalysis at Work in Fine Chemistry

Photocatalysis can be useful in fine and ultrafine chemistry, especially in non aqueous organic phases, for limited productions of high added value products. This is the case in the perfume industry. For example, the synthesis of an important intermediate, 4-tertio-butyl-benzaldehyde (4-TBA), is made via the stoichiometric oxidation of 4-tertio-butyl-toluene (4-TBT) by permanganate KMnO_4 , in an ultra-acidic medium according to the reaction:



A large number of (in)organic side products are generated, such as manganese and potassium sulfates. In addition, the aqueous ultra-acidic medium must be



Figure 18. Treatment of vine pesticide-containing rinsing waters in a Cascade Falling Film photoreactor, working either in sunlight during day time (right) or with UV-lamps in a workshop in periods of intense vine treatments (left).

neutralized eventually. A “green” alternative is offered by photocatalysis in pure liquid organic phase (Pichat et al. 1986):



Such a reaction obeys all the principles of green chemistry: absence of solvent, no additives, no heating, conservative use of energy, permanent control of conversion (stopping irradiation immediately stops the reaction), “atom economy”, 100% selectivity with no loss of carbon atoms, cheap catalyst, use of natural oxygen from the air as the unique oxidizing agent, no solid nor liquid waste. The only limitation of the process is the control of conversion below 10% with a periodic withdrawal of 4-TBA from the reaction mixture since the spontaneous oxidation of 4-TBA in 4-TB-benzoic acid occurs at higher concentrations of 4-TBA. In line with “green” or sustainable chemistry, one can estimate the E-Factor, defined by Sheldon as the ratio of the mass of wastes to the mass of the desired final product (Sheldon 2000). The E-factor can vary from 0.1 in heavy chemistry to several hundred in ultra-fine chemistry (pharmacy, perfumes, etc.). Currently, the E-factor for photocatalysis is 12 times smaller than that of the industrial stoichiometric reaction and in addition, if the water formed in the photocatalytic reaction is not considered as a waste, its E-factor tends to infinity.

Such an alternative reaction is directly involved in Chemical Engineering. For a possible adoption by industry, a real “intensification” and optimization of the process is required.

Academic Photocatalytic Engineering

The previous paragraphs have concerned the description of photocatalysis since its origin as well as the different types of “photocatalyzable” reactions with, in

particular, those directly applicable in “Green” Chemistry and in Environmental Catalysis. Different photoreactors have been proposed, depending on the reactional problems to be solved. Photocatalytic engineering was in progress at the same time as the fundamental studies presented above. A recent outcome has been established by H. de Lasa, B. Serrano and M. Salaiques in 2005. Their book, entitled *Photocatalytic Reaction Engineering*, is directly addressed to Chemical Engineers and concerns kinetics, different types and designs of photoreactors, light source interactions between light and solid photocatalysts, energetic efficiency, modeling in air and water treatment and detailed content.

Classification of Photocatalytic Reactors

Photocatalytic reactors can be classified according to their design, based on three fundamental characteristics:

- catalytic bed: slurry or fixed bed
- irradiation: polychromatic UV-lamps or sun
- number and positions of light sources.

Concerning fixed beds, several photo-inert supports have been proposed: glass (Aguado and Anderson 1993; Fernandez et al. 1995), glass fibers (Hofstadler et al. 1994; Serrano and de Lasa 1997), glass beads (Al-Ekabi and Serpone 1988), glass wool, quartz (Fernandez et al. 1995), membranes (Aguado and Anderson 1993; Chester et al. 1993), silica gel (Matthews and McEvoy 1992), stainless steel (Fernandez et al. 1995), concrete (Hadj-Aïssa et al. 2011), activated carbon (Uchida et al. 1993), optical fibers (Peill and Hoffmann 1995), zeolithes and special papers (Guillard et al. 2008).

It has to be noted that fixing a deposit of titania on a support generally implies a thermal treatment (i) to get a perfectly crystallized anatase, and (ii) to create strong bonds between titania and its support. Hard conditions such as calcination at 500°C induce migration of cations from the support solid phase into the first layers of titania, forming a kind of doping, which kills the photocatalytic activity (Herrmann 2012). This was demonstrated by the doping of TiO₂ by Cr³⁺ and Fe³⁺ cations originating from a stainless steel support or by its contamination by Na⁺ and Si⁴⁺ cations originating from an ordinary glass (Fernandez et al. 1995).

Conversely, overly mild synthesis or deposition conditions can lead (i) to improperly crystallized supported TiO₂, whose performance levels are very poor, and (ii) to a weakly bonded catalyst, whose loss in the reaction medium is highly probable.

The advantages and drawbacks of slurries and of fixed beds are presented in Table 3.

Design of Solar Photocatalytic (or “heliophotocatalytic”) Reactors

Solar or heliophotocatalytic reactors are mainly used as slurry reactors, except those working with fixed beds on Ahlstrom paper in the paragraphs described above. There are two types of solar reactors: one using a light concentrator (of the parabolic type)

Table 3. Comparison between slurry and fixed bed photocatalytic reactors.

Type of reactors	Advantages	Drawbacks
Slurry	<ul style="list-style-type: none"> • Uniform distribution of the catalyst • Large developed surface of the catalyst by volume unit of the photoreactor • Small mass transfer limitation • Poor fouling of the catalyst • Good stirring of the particles which favors gas, solid and liquid interactions • Limited flow losses • Excellent interactions between the catalyst and micro-organisms for water disinfection and the bactericide activity of TiO₂ 	<ul style="list-style-type: none"> • Tedious or even redhibitory final post-operative filtration of the powder catalyst • Strong light diffusion
Fixed bed	<ul style="list-style-type: none"> • Operation in continuous regime • Beneficial effect of an adsorbing support for concentrating trace pollutants previously to their transfer to TiO₂ (see activated carbon/ TiO₂) • Absence of tedious final filtration of the catalyst for its recovery and re-use 	<ul style="list-style-type: none"> • Loss of photonic efficiency induced by light attenuation by a fixed bed • Small mass transfer limitation • Poor fouling of the catalyst • Possible leaching of TiO₂ layers • Weak bactericide activity of immobilized TiO₂ confronted to micro-organisms

and the other one using a light collector without concentration (“one sun reactor”). As mentioned above, the first one is inherited from initial solar thermal fluidic experiments. Their comparison is summarized in Table 4.

Table 4. Comparison of heliophotocatalytic reactors with and without light concentrators.

Type of solar heliophotocatalytic reactor	Advantages	Drawbacks
Solar heliophotocatalytic reactor without light concentration	<ul style="list-style-type: none"> • Small optical losses • Utilization of both direct and diffuse (on cloudy days) light • Simple design • Low investment cost • Radiative domain in which reaction kinetics are proportional to radiant fluxes ($r \propto \Phi$) • No thermal effect on the reaction medium, especially water to be treated (no need for coolers) 	<ul style="list-style-type: none"> • Large size of the reactor • Important pressure loss by friction
Solar heliophotocatalytic reactor with light concentration	<ul style="list-style-type: none"> • Reduced volume of the photoreactor • Small size of the solar concentrator 	<ul style="list-style-type: none"> • Exclusive use of direct light • Possible excess of photons, for which the reaction rate becomes: $r \propto \Phi^{1/2}$ • Loss in quantum yield • Energetic efficiency not adapted to small or trace concentrations • Heating of the reaction medium • Need for coolers to avoid working in temperature domains where $\partial r / \partial T < 0$

Personal Free Remarks

Concerning photocatalysis, titania remains the best photocatalyst because of its double aptitude for simultaneously **adsorbing** reactants and **absorbing** efficient photons. Curiously, titanium is located at the top left of the periodic table of transition elements. Among the commercial photocatalysts, titania Degussa (now Evonik) P-25, with a modest but constant specific area of 50 m²/g, permanently remains the best one, although it does not have a pure structural composition since it is composed of 80% anatase and 20% rutile. Perhaps, its double aptitude, discussed above, is the result of its preparation mode in a flame reactor.

Any attempt at modifying titania catalysts, either by noble metal deposits or cation- and/or anion-doping, was unsuccessful. In the present text, many chemists, mainly from material science backgrounds, have prepared a tremendous number of new solids. To valorize their “babies”, they illuminate them and claim that they are good or even excellent photocatalysts, even working in the visible light. As part of this reasoning process, they are helped by a fallacious reaction, which is, in reality, an apparent pseudo-catalytic one: the decolorization of dyes. Once illuminated in UV or visible light in the presence of titania, the dye gets excited at an energy level possibly higher than that of titania’s conduction band. Therefore, a spontaneous electron transfer from the dye to titania, which decolorizes the dye in a stoichiometric process (not catalytic at all), ceases as soon as saturation has been reached. At high dye concentrations, higher than the stoichiometric threshold, no dye decolorization occurs!

For all studies in photocatalytic engineering, the reaction chosen should have been carefully submitted to all the criteria described above. In contrast to selective mild oxidation reactions such as that of 4-TBT (see above), the photocatalytic reactions of total oxidation are rather complex. A typical example can be given by the photocatalytic total degradation of formaldehyde H-CHO, which could be considered as a simple bimolecular reaction. Actually it involves 12 elementary steps (Fig.19) (Herrmann 2012).

Conclusions and Perspectives

Because of the theme of the present book, this chapter is rather focussed on environmental photocatalytic applications but for a wider vision of the photocatalytic engineering, the reader is invited to also read the book by de Lasa et al. (de Lasa et al. 2005) which is mentioned above.

Objectively, photocatalysis is not adapted to large mass productions because of (i) the low quantum yield, which is fundamentally smaller than unity (< 1), and (ii) the high corresponding photonic fluxes to be provided. By contrast, in fine chemistry (pharmacy, perfumes, etc.), its high selectivity, combined with a strong process intensification, enables one to envisage new innovative processes with a correct, new and environmentally friendly concept. Applications of photocatalytic engineering are to be addressed to niche applications as a priority.

Concerning helio-photocatalysis, environmental applications have been proposed according to local needs: potabilization of water and conservation of its potability,

Reaction mechanism of formaldehyde photocatalytic degradation

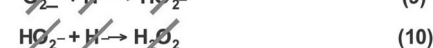
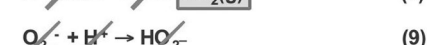
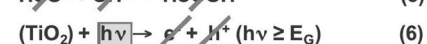


Figure 19. Reaction mechanism of the photocatalytic degradation of formaldehyde.

odor elimination, self-cleaning building materials (glass, concrete, metals, etc.). The fundamentals of photocatalysis could be helpful for atmospheric chemistry, where the fate of atmospheric volatile organic pollutants (VOCs) under sunlight could be influenced by photocatalytic processes after adsorption on aerogels. In particular, a few percents of aerial TiO_2 has been quantitatively detected in the smog of Los Angeles or in the sand dust which is produced in the Sahara desert and then moves to the Atlantic ocean or the north of Europe.

Acknowledgements

The authors would like to thank their past and present collaborators, in particular Mrs C. Delbecque, as well as Drs Sixto Malato and Julian Blanco for their help in performing experiments in the field of “helio-photocatalytic” engineering at PSA. The authors would also like to especially thank Mr. Joseph Dussaud from Ahlstrom Company for his innovative solutions aimed at solving real environmental problems. As the initial chapter (published in French) (Dunod, Paris 2010), the present chapter is dedicated to our late young colleague Sylvain Miachon (1968–2009).

References

- Aguado, M.A. and M.A. Anderson. 1993. Degradation of formic acid over semiconducting membranes supported on glass. Effects of structure and electronic doping. *Solar Energy Mat. and Solar Cells*. 28: 345–361.
- Al-Ekabi, H. and N. Serpone. 1988. Kinetic studies in heterogeneous photocatalysis. 1. Photocatalytic degradation of chlorinated phenols in aerated aqueous solutions over TiO_2 supported on a glass matrix. *J. Phys. Chem.* 92: 5726–5731.

- Anastas, P.T. and J.C. Warner. 1998. *Green Chemistry: Theory and Practice*. Oxford Press, New York. By permission of Oxford University Press. p. 30.
- Barry, T.I. and F.S. Stone. 1960. The reactions of oxygen at dark and irradiated zinc oxide surface. *Proc. Royal Soc.* 255: 124–144.
- Bickley, R.I. and F.S. Stone. 1973. Photoadsorption and photocatalysis at rutile surface. I: Photoadsorption of oxygen. *J. Catal.* 31: 389–397.
- Bickley, R.I., G. Munuera and F.S. Stone. 1973. Photoadsorption and photocatalysis at rutile surfaces. II: Photocatalytic oxidation of isopropanol in acetone. *J. Catal.* 31: 398–405.
- Blake, D.M. 1994, 1995, 1997, 1999 and 2001. Bibliography of work on the Photocatalytic removal of hazardous compounds from water and air. NREL/TP-430-22197, National Renewable Energy Laboratory, Golden Co.
- Boudart, M. and G. Djéga-Mariadassou. 1982. *Cinétique des réactions en catalyse hétérogène*. Masson, Paris, New York.
- Chester, G., M. Anderson, H. Read and S.A. Espulgas. 1993. Jacketed Annular membrane photocatalytic reactor for wastewater treatment: degradation of formic acid and atrazine. *J. Photochem. Photob. A: Chem.* 71: 291–297.
- Djehgri, N., M. Formenti, F. Juillet and S.J. Teichner. 1974. Photointeraction on the surface of titanium dioxide between oxygen and alkanes. *Faraday Disc. Chem. Soc.* 58: 185–193.
- Doerfler, W. and K. Hauffé. 1964a. Heterogeneous photocatalysis I. The influence of oxidizing and reducing gases on the electrical conductivity of dark and illuminated zinc oxide surfaces. *J. Catal.* 3: 156–170.
- Doerfler, W. and K. Hauffé. 1964b. Heterogeneous photocatalysis II. The mechanism of the carbon monoxide oxidation at dark and illuminated zinc oxide surfaces. *J. of Catal.* 3: 171–178.
- Fernandez, A., G. Lassaletta, V.M. Jimenez, A. Justo, A.R. Gonzalez-Elipe, J.M. Herrmann, H. Tahiri and Y. Ait Ichou. 1995. Preparation and characterization of TiO₂ photocatalysts supported on various rigid supports (glass, quartz and stainless steel). Comparative studies of photocatalytic activity in water purification. *Appl. Catal. B: Environmental* 7: 49–61.
- Formenti, M., F. Juillet and S.J. Teichner. 1970. Photo-oxydation ménagée de paraffines et oléfines sur anatase à température ambiante. *C.R. Acad. Sci. Paris* 270: 138–141.
- Frank, S.N. and A. Bard. 1977. Heterogeneous photocatalytic oxidation of cyanide and sulfite in aqueous solutions at semiconductor powders. *J. Phys. Chem.* 81: 1484–1488.
- Fujishima, A. and K. Honda. 1972. Photolysis-decomposition of water at the surface of an irradiated semiconductor. *Nature* 238: 37–38.
- Guillard, C., J.M. Herrmann, J.P. Chevrier, C. Bertrand and E. Philibert. French Patent No.: 0403448, 01/04/2004.
- Guillard, C., T.H. Bui, C. Felix, V. Moules, B. Lina and P. Lejeune. 2008. Microbiological disinfection of water and air by photocatalysis. *C.R. Chimie* 11: 107–113.
- Hadj-Aïssa, A., E. Puzenat, A. Plassais, J.M. Herrmann, M. Haehnel and C. Guillard. 2011. Characterization and photocatalytic performances in air of cementitious materials containing TiO₂. Case study of formaldehyde removal. *Appl. Catal. B: Environmental* 107: 1–8.
- Herrmann, J.M. 1999. Heterogeneous photocatalysis: fundamentals and applications to the removal of various types of aqueous pollutants. *Catal. Today.* 53: 115–129.
- Herrmann, J.M. 2000. Photocatalytic degradation of pesticides in water in contact with modified titania. Extension to Helio-photocatalysis. *Entropie.* 228: 39.
- Herrmann, J.M. 2006. Photocatalysis. pp. 73–106. *In: Arza Seidel (ed.). Kirk-Othmer Encyclopedia of Chemical Technology*, Vol. 19, 5th Edition. John Wiley & Sons, Inc., Hoboken, New Jersey.
- Herrmann, J.M. 2012. True heterogeneous photocatalysis. *In: S. Lacombe and N. Keller (eds.). Environmental Science and Pollution Research*, Springer, special issue. *Environ. Sci. Pollut. Res.* 19: 3655–3665.
- Herrmann, J.M., J. Disdier, M.N. Mozzanega and P. Pichat. 1979. Heterogeneous Photocatalysis: *in situ* photoconductivity study of TiO₂ during oxidation of isobutane into acetone. *J. Catal.* 60: 369–377.
- Herrmann, J.M., J. Disdier and P. Pichat. 1981. Oxygen species ionosorbed on powder photocatalyst oxides from room-temperature photoconductivity as a function of oxygen pressure. *J.C.S. Faraday Trans. I.* 77: 2815–2826.

- Herrmann, J.M., J. Disdier and P. Pichat. 1986. Platinum photoassisted deposition on powder TiO_2 using various Pt complexes. *J. Phys. Chem.* 90: 6028–6034.
- Herrmann, J.M., J. Disdier and P. Pichat. 1988. Photocatalytic deposition of silver on powder titania. The consequences for the recovery of silver. *J. Catal.* 113: 72–81.
- Herrmann, J.M., J. Disdier, P. Pichat, S. Malato and J. Blanco. 1998. TiO_2 -based solar photocatalytic detoxification of water containing organic pollutants. Case studies of 2,4-dichlorophenoxybenzoic acid (2,4-D) and of benzofuran. *Appl. Catal. B: Environmental* 17: 15–23.
- Herrmann, J.M., M. Gravelle-Rumeau-Maillot and P.C. Gravelle. 1987. A microcalorimetric study of metal-support interaction in the Pt/ TiO_2 system. *J. Catal.* 104: 136–146.
- Hoffmann, M.R., W. Balserski and J. Moss. 2004. Advanced air filtration and gas mask devices based on semiconductor photocatalysis. *Book of Abstracts, 2nd NIMS International Conf. Kanagawa, Japan.* 43.
- Hofstadler, K., R. Bauner, S. Novall and K. Heisler. 1994. New reactor design for photocatalytic wastewater treatment with TiO_2 immobilized on fused silica glass fibers: photo-mineralisation of 4-chlorophenol. *Environ. Sci. Tech.* 28: 670–674.
- Juillet, F. and S.J. Teichner. 2003. private communications.
- Kerzhentsev, M., C. Guillard, J.M. Herrmann and P. Pichat. 1996. Photocatalytic pollutant removal in water at room temperature: case study of the total degradation of the insecticide fenitrothion (phosphorothioic acid,O,O-dimethyl-O-(3-methyl-4-nitrophenyl)ester). *Catal. Today* 27: 215–223.
- Kraeutler, B. and A.J. Bard. 1978. Heterogeneous photocatalytic decomposition of saturated carboxylic acids on TiO_2 powder. Decarboxylative route to alkanes. *J. Am. Chem. Soc.* 100: 5985–5992.
- Lachheb, H., E. Puzenat, A. Houas, M. Ksibi, E. Elaloui, C. Guillard and J.M. Herrmann. 2002. Photocatalytic degradation of various types of dyes (Alizarin-S, Crocein Orange G, Methyl Red, Congo Red, Methylene blue) in water by UV-irradiated titania. *Appl. Catal. B-Environ.* 39: 75–90.
- de Lasa, H., B. Serrano and M. Salaiques. 2005. *Photocatalytic Reaction Engineering.* Springer Science, New York, USA.
- Le Cloirec, P. 1998. *Les Composés Organiques Volatils (COV) dans l'Environnement,* Lavoisier, Paris.
- Levenspiel, O. 1972. *Chemical Reaction Engineering.* John Wiley, New York, p. 175.
- Matos, J., J. Laine and J.M. Herrmann. 2001. Effect of the type of activated carbon in the photocatalytic degradation of aqueous organic pollutants by UV-irradiated titania. *J. Catal.* 200: 10–20.
- Matthews, R.W. and S.R. McEvoy. 1992. Destruction of phenol in water with sun, sand and photocatalysis. *Solar Energy* 49: 507–513.
- Mehos, M.S. and C.S. Turchi. 1993. Field testing solar photocatalytic detoxification on TCE-contaminated groundwater. *Environ. Prog.* 12: 194–199.
- Peill, N.J. and M.R. Hoffmann. 1995. Development and optimization of a TiO_2 coated fiber-optic cable reactor: Photocatalytic degradation of 4-chlorophenol. *Env. Sci. Tech.* 29: 2974–2981.
- Pichat, P., J. Disdier, M.N. Mozzanega and J.M. Herrmann. 1982. Pt content and temperature effects on the photocatalytic H_2 production from aliphatic alcohols over Pt/ TiO_2 . *Nouv. J. Chim.* 6: 559.
- Pichat, P., J. Disdier, J.M. Herrmann and P. Vaudano. 1986. Photocatalytic oxidation of liquid (or gaseous) 4-tert-butyltoluene to 4-tert-butylbenzaldehyde by O_2 (or air) over TiO_2 . *Nouv. J. Chim.* 10: 545–551.
- Romero-Rossi, F. and F.S. Stone. 1960. *Actes 2° Congr. Intern. Catalyse, Paris, Tome II,* p. 1481.
- Serrano, B. and H. de Lasa. 1997. Photocatalytic Degradation of Water Organic Pollutants. *Kinetic Modeling and Energy Efficiency.* *Ind. Eng. Chem. Res.* 36: 4705–4711.
- Sheldon, R.A. 2000. *CR Acad. Sci. (Paris), série IIC (Chimie/Chemistry)* 3: 541–551.
- Uchida, H., S. Itoh and H. Yoneyama. 1993. Photocatalytic degradation of propylamide using TiO_2 supported on activated carbon. *Chem. Lett.* 12: 1995–1998.
- Vautier, M., C. Guillard and J.M. Herrmann. 2001. Photocatalytic degradation of dyes in water. Case study of indigo and of indigo carmine. *J. Catal.* 201: 46–59.

14

Biocatalysis and Bioprocesses

Jean-Marc Engasser

Introduction

Industrial biocatalysis uses enzymes to carry out transformations of raw materials and precursors into products of interest (Matsuda 2007). The biocatalysts are either isolated enzymes (generally produced by microbial fermentations), or living cells containing the enzymes catalysing the targeted reactions (Aehle 2005).

Over the last forty years the industrial potential of enzymes and cellular biocatalysts has been strongly improved through molecular biology. Techniques of protein engineering now allow the construction of tailor-made enzymes with improved catalytic properties for the production process. Moreover, with methods of cell engineering, it is possible to construct cells with intensified metabolic pathways for biomolecules biosynthesis or with novel biosynthetic capacities.

Enzymes and living cells, especially microorganisms, have been traditionally used for the production of food, fermented beverages and ingredients. Progress in molecular biology triggered the wider exploitation of biocatalysis for the production of chemicals, pharmaceuticals and materials (Straathof and Adlercreutz 2002). Today biocatalysts are used in several hundred industrial processes (Liese et al. 2006) producing a large variety of molecular architectures ranging from small molecules, such as ethanol or lactic acid, to high molecular weight macromolecules, such as polysaccharides or glycosylated proteins.

Biocatalysts have become particularly strong participants in the development of sustainable processes (Anastas and Crabtree 2009).

They have competitive advantages for transforming renewable agricultural resources into fuels, chemicals and materials. They are used both in the initial stages of biomass hydrolysis and in the final stages of bioproducts synthesis. Due to their remarkable selectivities, enzymes have also gained importance for green chemistry (Fessner and Anthonsen 2009). With enzymes it is often possible to simplify the

process flowsheet for producing multifunctional and chiral molecules, and therefore to reduce both the consumption of reactants and energy and the production of wastes.

The strong emergence of industrial biocatalysis also benefited from major progress in bioprocess engineering (Shuler and Kargi 2002). Novel technologies of bioreactors and biomolecules purification have been developed that improve product quality and process productivities (Antolli and Liu 2012). Basic knowledge was also gained in the kinetics and thermodynamics of bioconversion processes (Dutta 2010), leading to more efficient operation of bioreactors. Simultaneously, biochemical engineering witnessed spectacular progress in multi-scale modeling at the level of biomolecules, cells and bioprocesses (Blanch and Clarck 1997). As a result, enzyme and cell engineering can rely on molecular modelling of structure-activity relationships and in simulating cellular metabolism. Moreover, the design and optimization of bioreactors and bioprocess can also be accelerated by the use of process simulators that integrate bioconversion models, production cost evaluations, and, more recently, environmental impact evaluations.

This chapter presents an overview of the tools, methodologies and industrial applications of biocatalysis and bioprocesses (Fig. 1). The first part briefly describes biocatalysts of industrial interest and techniques of enzymatic and cellular engineering. It outlines key advantages of biocatalysts for sustainable products and processes. The second part reviews the progress in bioprocess engineering. It describes the technologies and operations of bioreactors for the scale-up of bioconversions. It details bioprocess modelling (Sablani et al. 2007) and simulation advances, and, on some selected examples, illustrates their uses for process design and optimization.

Biocatalysts	Bioprocesses
Enzymes Cells: microbial, animal, plant Enzyme and metabolic engineering	Bioconversions Bioreactors Extractions-Purifications
Modeling – Simulation	
Bioinformatics Enzymes structure-activity Cell metabolic fluxes	Bioprocess models Cost evaluation Environmental evaluation

Figure 1. Biocatalysis and bioprocesses toolbox.

Biocatalysis and Biocatalysts Engineering

Enzymes and Enzymatic Bioconversions

Enzymes structure and catalytic properties. Enzymes are proteins that catalyse chemical reactions in living organisms (Bommarius and Riebe 2004). Their structure entails a cavity or tunnel-shaped active site, which binds the reaction substrates (Fig. 2). Substrates can then react to be transformed into products. It is the precise geometry and composition of the active site that is responsible for the generally high

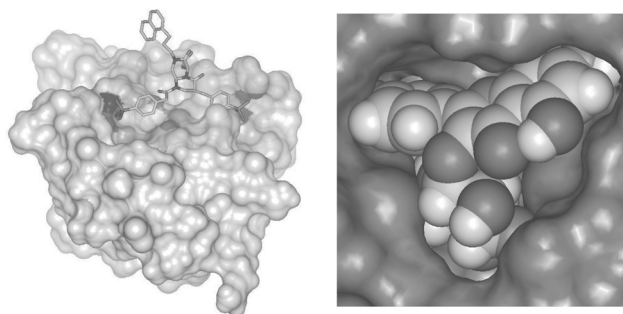


Figure 2. Enzyme's three dimensional structure with an active site for the binding of a reaction substrate.

chemio-, regio- and enantio-selectivities of enzymes. In industrial processes, enzyme catalysts are often relatively fragile, as they progressively lose their active structure, especially when exposed to high temperatures or organic solvents.

Enzyme catalysed reactions. The international classification of enzymes, based on the type of catalysed reaction, distinguishes:

- i) Oxidoreductases, that accelerate oxidation and reduction reactions,
- ii) Transferases, enact the transfer of chemical groups between molecules,
- iii) Hydrolases, that promote reactions involving water,
- iv) Isomerases, capable of rearranging the molecular structure of substrates,
- v) Lyases that facilitate the transfer of chemical groups with the formation of double bonds,
- vi) Ligases, involved in other synthetic reactions.

Within this classification the main industrially used enzymes are indicated in Table 1. On the basis of the number of applications, hydrolases and oxidoreductases are the dominant industrial enzymes (Fig. 3).

Table 1. Enzymes used for industrial biocatalysis.

Oxidoreductases	
	dehydrogenase, reductase, oxidase, monooxygenase, dioxygenase, laccase, catalase
Transferases	
	glycosyltransferase, transaminase
Hydrolases	
	protease, peptidase, lipase, amidase, acylase, esterase, amylase, glucoamylase, lactonase, phosphorylase
Lyases	
	decarboxylase, nitrilase, aldolase, fumarase, hydratase, aspartase
Isomerases	
	Amino acid racemase, glucose isomerase, xylose isomerase

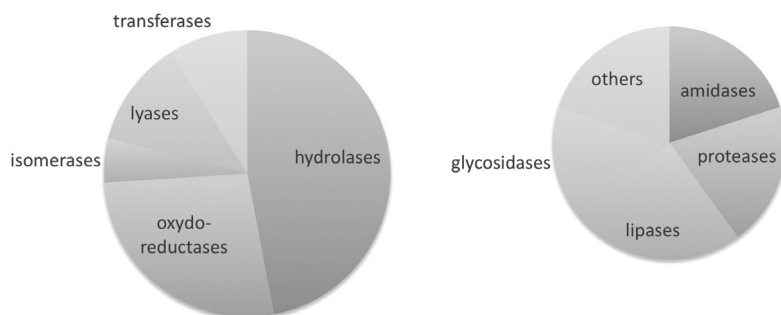


Figure 3. Enzymes uses in industrial biocatalysis.

Enzymes mainly catalyse reactions in aqueous media. But several of them are also active in non-aqueous media such organic solvents, ionic liquids and supercritical fluids. In organic media, for example, which are used to increase the solubility of hydrophobic substrates, hydrolases perform reverse synthetic reactions with the elimination of water.

Enzyme Engineering

Enzyme engineering techniques, namely site-directed mutagenesis and directed evolution, are now classically used to improve catalytic properties of enzymes by changing the amino acid sequence of their primary structure.

Site-directed mutagenesis performs targeted modifications of one or several amino acids at the active site or another location in the protein structure. Selecting the mutation is often directed from the understanding of the enzyme structure-activity relationship. It may also rely on recent advances of molecular modelling, based on the theories of molecular dynamics and quantum mechanics, to simulate the initial enzyme-substrate docking and the reaction of the intermediate formed complex. Molecular modelling can also assist in the *in silico* design of enzymes with modified activities or selectivities.

Another technique for improving industrial enzymes is directed evolution. It reproduces, in the laboratory, the natural mechanisms of genetic evolution. It consists in introducing random mutations in the gene coding for the enzyme by recombination of parent genes. This technique of gene shuffling rapidly yields gene banks of second generation that are then screened for the selection of enzymes with improved catalytic performances. The recombination process can be repeated several times, the daughter proteins produced by the first evolution serving as parents for the following evolution.

With site-directed or random mutagenesis it is possible to obtain improvements, sometimes spectacular, in enzyme properties, such as specificity, selectivity, activity and stability in aqueous or organic media. For some enzymes, novel catalytic activities were also reported through structural mutations.

Cellular Biocatalysts

Besides enzymes, industrial biocatalysis also uses whole cells to carry out bioconversions, generally called fermentation processes. Inside cells several enzymes or entire metabolic pathways may contribute to the synthesis of biomolecules. Cellular biocatalysts are exploited to produce both small molecules. For example, amino acids, organic acids, alcohols, lipids, antibiotics, macromolecular peptides, proteins and polysaccharides. They are also efficient catalysts for industrial scale oxidoreduction reactions involving NADH or NADPH cofactors for electron transfer.

For fermentation and bioconversion processes (Vogel and Haber 2007), most versatile cells are the microorganisms (Fig. 4, Table 2). Bacteria, yeasts and fungi have the advantages of rapid growth on relatively simple nutritional media and of efficient synthesis and excretion of a large diversity of molecules. Animal cells are also being exploited in industrial cultures for the production of therapeutic proteins, like monoclonal antibodies. Even though they have lower growth rates and higher nutritional requirements compared to microorganisms, animal cells have the unique capacity of protein glycosylation, which is often a prerequisite for biological activity. Plant cells can also synthesize active metabolites and recombinant proteins. But their industrial interest remains limited by low productivity in culture and their reduced capacity to excrete biomolecules.

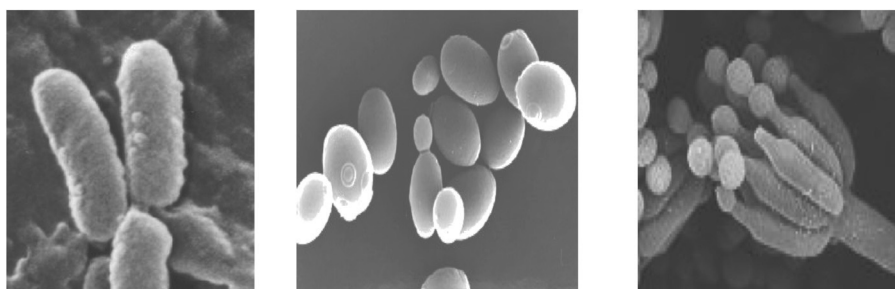


Figure 4. Microorganisms (bacteria, yeasts, fungi) used in industrial biocatalysis.

Table 2. Microbial cells used for industrial fermentations and bioconversions.

Bacteria	
	Escherichia coli, Corynebacterium, Bacillus, Lactobacillus, Streptomyces, Streptococcus
Yeasts	
	Saccharomyces cerevisiae, Pichia
Fungi	
	Penicillium, Aspergillus

Cellular and Metabolic Engineering

Novel tailor-made cellular biocatalysts can be constructed through genetic engineering techniques. The simplest consists in introducing genes coding for heterologous proteins not present in the native cell. Thus bacteria, yeast, fungi and

animal cell have been engineered to synthesize and excrete novel enzymes and therapeutic proteins. Oxidoreduction enzymes have also been overexpressed in the bacteria and yeasts, and the recombinant cells used for industrial scale oxidation and reduction reactions.

A more elaborate approach is metabolic engineering that targets the modification of entire cellular pathways, either to accelerate the production of an existing metabolite, or to produce novel molecules. This is achieved by amplifying the expression of enzymes already present or introducing enzymes constitutive of new production pathways. It may also involve the elimination of metabolic reactions leading to undesirable byproducts.

With the recently gained knowledge on the regulation of cellular metabolism, a more rational approach of metabolic engineering can now be pursued. It is based on the identification of the kinetic bottlenecks either for the production of precursors and energetic intermediates by the central metabolism, or for the synthesis of the desired product by its specific producing pathway. It may further imply the construction of kinetic models of cell intracellular metabolism and their applications to predict metabolic changes induced by modified expressions of intracellular enzymes.

Biocatalysis for Sustainable Processes

Biocatalysis for the Transformation of Renewable Agricultural Resources

Biorefineries. Biorefineries are integrated industrial facilities that process agricultural resources, or biomass, into a wide spectrum of bio-based products and bioenergy. The concept of biorefinery was introduced in the 90s based on the model of oil refineries that transform crude oil into fuels and chemicals.

Biorefineries facilities have been developed on a variety of renewable raw materials: whole plants (cereals, oil plants, sugar beets, potatoes), trees, algae. They integrate a wide range of transformation processes combining mechanical, thermal, chemical and biochemical operations. In biorefineries, agricultural resources are first separated into molecular intermediates: starch, sugars, proteins, lipids, cellulose, hemicellulose, lignins and other phenolic compounds. In a second stage, these intermediates are transformed into products of interest by additional conversion and purification operations. Biocatalysts are initiators of bioresource transformations.

Biorefineries are designed for the simultaneous production of a wide range of molecules of interest as fuels, chemicals, materials and food. They cover low-cost commodities (fuels, solvents) produced in high tonnage, intermediate value chemicals (polymers, surfactants, ingredients) and high value-added products like pharmaceutical and nutritional actives (Yang 2007).

Enzymatic hydrolysis of agricultural resources. Enzymes are particularly efficient catalysts for the initial transformation of agricultural resources. Enzyme cocktails, containing cellulases, proteases, xylanases, oxidases, and lipases advantageously replace chemical hydrolysis or solvent extraction processes with higher energy consumptions and wastes production. The starch industry now currently uses amylases and glucoamylases to hydrolyse starch in glucose syrups. In the future

lignocellulosic fractions of plants and wood are also expected to be hydrolysed on a large scale by cellulases.

Microbial production of bio-based precursors. Microbial biocatalysts have strong potential for the production of chemicals starting from agricultural biomass components. Based on microbial transformations, industrial flowsheets are being elaborated to convert biomass into intermediate chemicals with two to six carbons. These intermediates are mainly organic acids, alcohols, or amino acids naturally synthesized and excreted by microorganisms. With metabolic engineering it is possible to introduce in cells the pathways for the production of additional non-natural metabolites. In a second step the produced intermediates are then used as building blocks for the production of chemical commodities and specialties (Fig. 5).

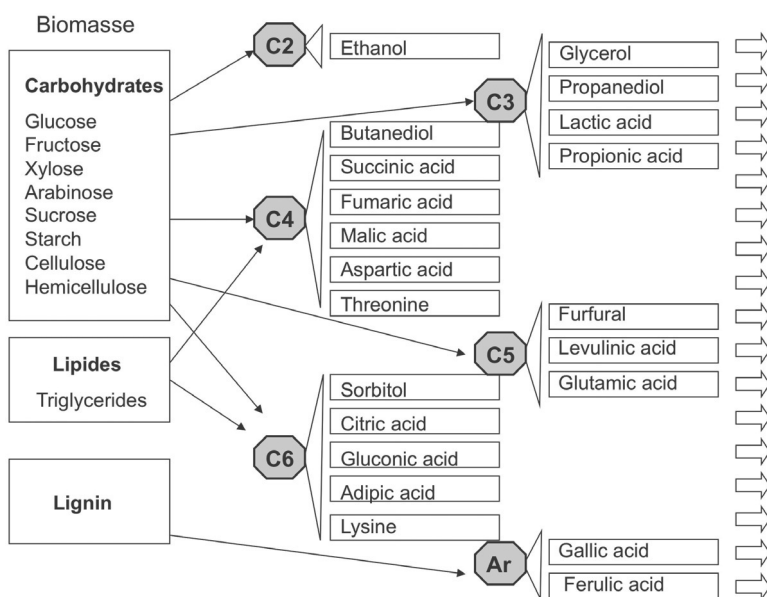


Figure 5. Intermediates production schemes from biomass.

Production of biopolymers by enzyme and microorganisms. Biocatalysts are also efficient for the production of biodegradable biopolymers (Loos 2011) following several process strategies (Fig. 6). Some polymers are naturally produced by microorganisms, for example proteins, polysaccharides (xanthane and dextrane) and polyesters (polyhydroxybutyrate). For the production of a broader range of bio-based macromolecules, a promising approach is the enzymatic or chemical polymerization of precursors or monomers derived from biomass. Some monomers, like sugars, amino acids, fatty acids or phenolic compounds, are directly extracted from agrosources. Others are produced by chemical, enzymatic, or microbial conversions of these precursors into di- or multifunctional monomers, such as acids (succinic), hydroxy acids (lactic acid), polyols (glycerol, propanediol, and sorbitol).

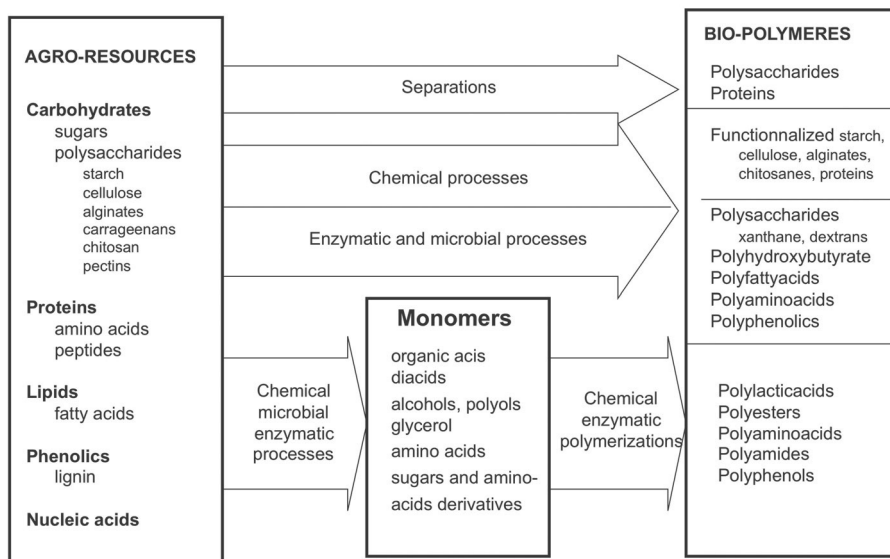


Figure 6. Biopolymers production schemes through biocatalysis.

These monomers are then polymerized to new families of polymers (polyesters, polyamides and polyphenolics), carrying a diversity of functional properties.

Polymerization steps can also be efficiently catalysed by enzymes, for instance using lipases and proteases for opening ring polymerization or condensation polymerization, oxidases for radical polymerizations of vinyl or phenolic compounds, or glycosidases for polysaccharides synthesis. With enzymes it is also possible to selectively functionalize polymers like proteins and polysaccharides (starch, cellulose).

Biocatalysis for Green Chemistry

Green chemistry is an additional area of high potential for biocatalysis (Illanes 2008; Grunwald 2009). Due to their high selectivity and mild operating conditions, enzymes can significantly reduce chemical process environmental impact in terms of energy and chemicals consumptions as well as waste production. An increasing number of enzymes, in particular hydrolases and oxidoreductases, are being used for organic synthesis (Drauz et al. 2012) in aqueous and non-aqueous media (Carrea and Riva 2008) (Table 3). Biocatalysts are particularly efficient for the synthesis of chiral building blocks and their transformations into active drugs (Gotor et al. 2008). Taking advantage of their regio- or enantioselectivity makes it possible to avoid the tedious protection-deprotection steps required by chemical synthesis (Faber 2011). An illustrative example is the DSM enzymatic process for the antibiotic Cephalexin production. This novel process, which includes only two enzymatic steps, replaces the traditional thirteen step chemical process. From an environmental point of view, the shift from a chemical to an enzymatic production results in a near 50% reduction of energy consumption and effluents generations.

Table 3. Enzymatic reactions for organic synthesis.

Products	Precursors	Enzymes
amines	amides ketones	protease, amidase transaminases
alcohols	esters aldehydes	esterase, lipase reductase
aldehydes	alcohols carboxylic acids	alcohol dehydrogenase, monooxygenase reductases
ketones	alcohols	alcohol dehydrogenase
epoxides	alcenes	epoxidase
diols	diketones	alcohol dehydrogenase
carboxylic acids	nitriles ketones	nitrilase oxygenase
esters	acids, alcohols	esterase, lipase
amides	carboxylic acids	protease
amino acids	amides keto acids nitriles	amidase transaminase nitrilase
Hydroxy acids	amides, esters cyanohydrins carboxylic acids	hydrolase nitrilase oxygenase

Bioprocess Engineering

Bioprocess Engineering Challenges

A competitive utilization of a biocatalyst on an industrial scale requires an efficient bioconversion process. This is the field of bioprocess engineering (Doran 2013) or biochemical engineering (Katoh and Yoashida 2009; Dumont and Sacco 2009). Generally, biotechnological process design has to meet several criteria:

- i) A production target. Depending on the applications, production scales are from hundreds of kg to millions of tons.
- ii) Product composition and quality specifications. A particularly important criterion is the product purity level, which is much higher for pharmaceuticals than for chemical commodities or fuels.
- iii) Cost competitiveness, regarding both facilities investments and operation. Depending on the product specificities, biotechnological production costs span from less than 1 € per kg, for example for ethanol, to millions of €/kg for therapeutic proteins.
- iv) Environmental efficiency, in terms of energy and water consumption or pollutant emissions.

Selection of Bioprocess Flowsheets

Bioprocess design starts with the selection of the sequence of unitary operations transforming raw materials into the final product. Central in the flowsheet is

the biotransformation generally catalysed by a single enzyme or cell. But the transformation may also involve a combination of conversion reactions:

- i) Consecutive steps of enzymatic conversion, as for example the liquefaction and saccharification of starch by alpha amylase and glucoamylase;
- ii) Consecutive steps of enzymatic bioconversion and microbial fermentation, illustrated by the transformation of starch into ethanol;
- iii) Consecutive chemical and enzymatic reactions, such as chemioenzymatic processes for the synthesis of chiral compounds.

Upstream of the central bioconversion step are operations of raw materials pre-treatment (extraction, ion-exchange and filtration) or media thermal sterilization. The downstream part of the process mainly consists of separation and purification operations. Many of these operations are similar to the one used for chemical processes design: centrifugation, adsorption, precipitation, crystallization, extraction, evaporation, distillation, drying, spray drying, ... But bioprocesses often include additional operations more specific to biomolecules, such as membrane separation (microfiltration, ultrafiltration, nanofiltration, reverse osmosis, dialysis, electrodialysis) and chromatography operations (ion exchange, gel permeation, hydrophobic and affinity).

Bioprocess Optimization

On the basis of a selected flowsheet, the optimal design of a production facility includes several steps:

- To choose the equipment technologies for the unit operations.
- To select their operation modes, which may be either batch, continuous, or fed-batch. Often an overall bioprocess combines operations carried out in both batch and continuous modes, which implies precise operation scheduling.
- To optimize the operation variables for the individual operations. For instance the temperature and pH, flow rates, substrates and biocatalyst concentrations, operation time or residence time.

The equipment sizing and optimization is first carried out for each of the individual operations. The following sections describe in more detail the bioreactor technologies and operations. Other upstream and downstream operations are dealt with in other biochemical engineering books.

The final bioprocess optimization requires a global approach integrating unit operations interdependences. For instance, the bioreactor operation and efficiency influences upstream operations, by determining the required quantities and flow rate of raw materials. At the same time, the achieved product and by-product concentrations at the end of the bioconversion strongly influences the downstream operations design.

Models and Simulators for Optimal Bioprocess Design

A major challenge for bioprocess engineering is to develop simulation models that can guide process optimization. Several process engineering software, in current use in chemical industry (SuperPro Designer, Schedule Pro, Aspen, Prosim, Pro II), have been extended to biotechnological processes. Simulators (Fig. 7) are expected to carry out mass and energy balances, first at the level of individual unit operations. Then for the entire process, to determine the consumption of raw materials, chemicals and energy, together with the production of by-products and waste. Simulators perform equipment sizing by determining volumes of tanks or columns, surface areas of filters, membranes and heat exchangers. They also evaluate the investment and operational costs of production facilities. Models supporting the simulations may be based on process engineering fundamentals such as fluid mechanics, mass and heat transfer, or reaction kinetics.

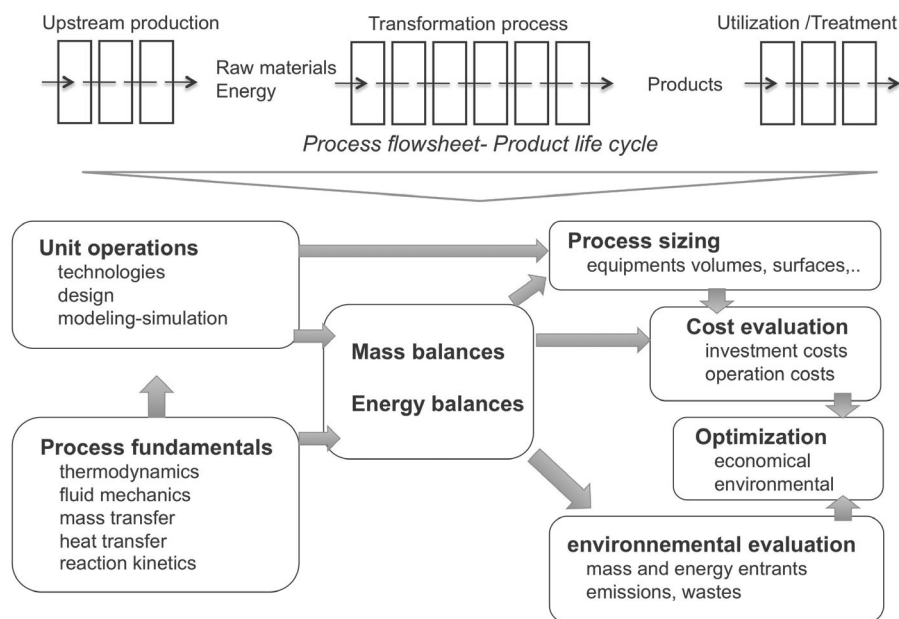


Figure 7. Bioprocess simulators organisation.

Recently, simulators have been completed to provide additional evaluations of process environmental impacts. Environmental evaluations can be extended to the product global Life Cycle Assessment (LCA) that, in addition to the production process, also considers the production of raw materials and energy vectors, the distribution and the final utilization of the product (“from cradle-to-grave analysis”) (Fig. 8). Most frequently evaluated are the consumptions of primary energy, non-renewable resources and water as well as the impact from air emissions such as the global warming potential of greenhouse gas, the formation of photochemical oxidants and air acidification, the impact related to water emissions (eutrophication, DCO), the production of solid waste, and more globally, the human and environmental toxicity.

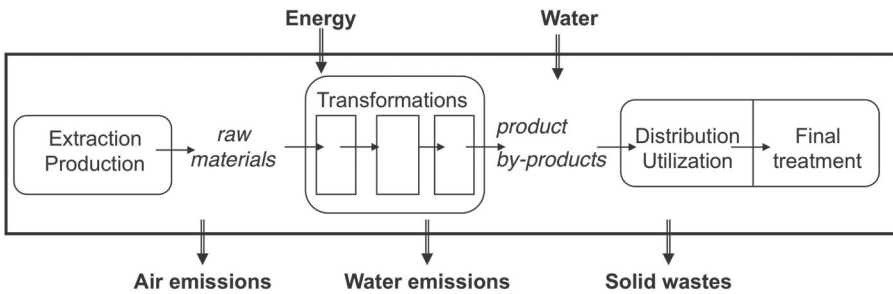


Figure 8. Product Life Cycle Assessment.

Bioreactors Technologies and Operations

The bioreactor can be considered as the heart of the bioprocess. It determines the composition, the structure and the quantity of produced products. Its productivity, selectivity and conversion yield have a major influence on production cost and environmental impacts. Bioreactor design and optimization is a central task of bioprocess engineering (Liu 2013).

Several reactor configurations are used on an industrial scale for catalytic enzymes and cells (Fig. 9). The proper choice of reactor technology depends on the reaction and product characteristics and the technical targets to achieve. Reproducibility and sterility issues must also be considered. A comparative review of available technologies and operation mode of bioreactors is presented below. Possibilities for intensification of reactor productivities are also discussed.

Biocatalyst in solution		Biocatalyst immobilized	
Operation mode			
batch	fed-batch	continuous	
Stirred tank		Tubular reactor	
Membrane bioreactor		Fixed bed Fluidized bed	

Figure 9. Bioreactors technologies and operations.

Reactors with Soluble and Immobilized Biocatalysts

Bioreactors can be classified in two categories, depending on the soluble or immobilized state of the biocatalyst.

Firstly, the reactors with the biocatalyst in solution. Enzymes and cells are in an isolated shape in solution, and reactors are configured in mixed tanks of cylindrical pipes.

Secondly, reactors with the biocatalyst immobilized on solid supports. There are many techniques for enzyme and cell immobilization (Fig. 10): adsorption, reticulation, attachment by covalent bonds and inclusion inside polymers (alginate,

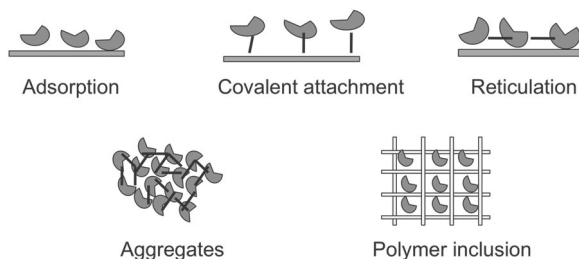


Figure 10. Enzymes immobilization techniques.

acrylamide). The techniques differ by the nature and cost of the support (organic or mineral) and the quantity of fixed biocatalyst (Guisan 2006). With enzymes and cells immobilized inside particles (generally a few mm in diameter), bioreactor configurations are stirred tanks with the particles in suspension or in a column reactor. The most frequently used technology is the continuous fixed bed reactor with a compact bed of catalytic particles inside a column or tube. An alternative is the fluidized bed configuration in which catalytic particles are brought into a fluidized state by an upstream flow inside the column.

Biocatalyst immobilization presents several advantages: a continuous operation with retention of biocatalyst, a possible stabilization of enzymes; an operation at high enzyme or cell densities leading to higher productivities. But performances of the bioreactors can be reduced by substrate and product diffusional limitations in the biocatalyst microenvironment. Moreover, in the case of fixed reactors, support fouling can occur at long operating times.

Bioreactors Operation

For catalysts in either soluble or immobilized form, a key design choice is the reactor operating mode, which may be batch, continuous or semi-continuous.

a) Batch mode

In a batch reactor, substrates and the biocatalyst are introduced initially and biotransformation is prolonged until achieving the desired substrate conversion yield. Batch operation has the advantage of simplicity and robustness. It is particularly well adapted to processes exposed to high risks of microbial contamination. Its productivity, however, may be limited by the inhibition of the enzyme or the metabolic deviations of the cell at the initial high substrate concentrations. Product accumulation in the reactor may also inhibit the rate of bioconversion.

b) Continuous mode

In a continuous operating mode, the substrate solution or suspension is continuously introduced and the products withdrawn. The biocatalyst is fed continuously, or added initially and then retained inside the reactor, as in a fixed bed. Continuous operation, which is generally designed to run at a steady state, has the advantage of possible higher productivities due to the reduction of service

times between during consecutive operations. It can be stabilized at favourable low substrates concentrations and reduced accumulation of inhibitory products. But the continuous mode is more exposed to risks of microbial contamination, and thus less used for biotransformations with strong sterilization constraints (Whittall and Sutton 2012). Maintaining a sufficient long steady-state may also be problematic because the enzyme denaturation is too fast or due to cell metabolic instabilities.

c) Semi-continuous or fed-batch mode

A third mode, frequently used with microbial fermentation, is the semi-continuous mode, more generally called the fed-batch. Part of the substrate is added initially and the remaining is progressively introduced during the course of the bioconversion, whereas the product is only discharged at the end. The substrate addition flow rate can be modulated to control the concentration of substrate during the bioconversion, and avoid the initial excessive substrate concentrations. In addition, by providing precise concentration profiles of limiting substrates, fed-batch operation makes it possible to control the time course of cell transition from an initial phase of cellular growth to a second phase of intense metabolites production.

Flow Optimization in Continuous Reactors

When selecting the continuous mode, a key design variable is the internal flow of the reactive medium, which is strongly dependent on the geometry of the reactor vessel. In the case of a tubular geometry, the flow of medium is more of a plug flow type, in which substrate conversion progresses all along the reactor. Under steady-state a decreasing substrate concentration gradient and an opposite increasing product concentration gradient are established between the inlet and the outlet of the reactor. In a well-stirred tank, on the contrary, the entering substrate is almost instantaneously mixed with the internal solution. Substrate and product concentrations are then uniform and equal to the outlet stream concentrations. The proper choice between plug flow and stirred tank essentially depends on the enzyme kinetic characteristics, and more precisely on the influence of substrate and product concentrations on the rate of reaction (Fig. 11). When the bioconversion rate increases with substrate concentration and/or is inhibited by the product, the plug flow operation is more efficient. In the opposite, for a reaction inhibited by excess substrate, it is better to rapidly dilute the feed in a stirred tank, equal conversion yields are obtained for plug flow and stirred tank when the reaction rate remains constant with the varying substrate concentrations. For a microbial fermentation with an initial cellular growth phase, which can be considered as an autocatalytic reaction, a stirred tank may be preferable in terms of productivity.

Methods of Bioreactors Intensification

The cost competitiveness of a bioprocess requires sufficiently high bioconversion efficiencies for the bioreactor. With enzymatic or microbial bioconversions, the

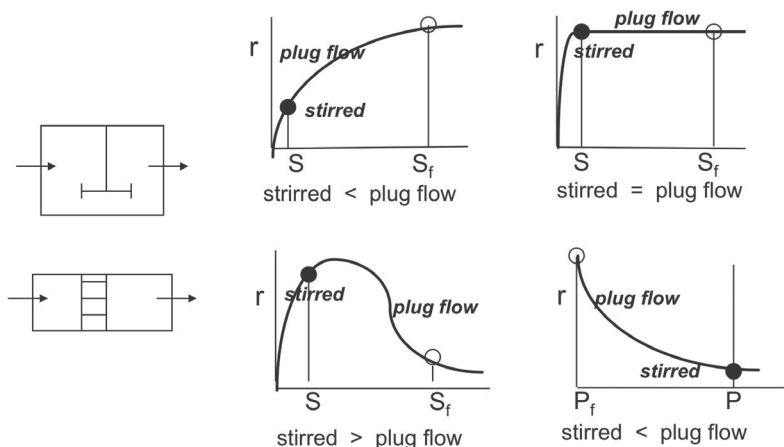


Figure 11. Compared productivities of continuous stirred and plug flow reactors.

generally suggested threshold values are around 100 g/l for final product concentration, 100 g/l/day for the volumetric reactor productivity, 90 to 95% substrate conversion yield to product, and from 100 to 1000 g product formed per g of catalyst used. Where necessary, several techniques can be used, alone or in combination, to improve these performance criteria for a biocatalytic process:

- i) The operation under high excess of solid substrate. Increasing the initial substrate concentration is the main approach to increase the final product concentration. In the case of a substrate with relatively low solubility in the reaction medium, bioconversion can be carried out with an initial excess of solid substrate. During the course of the reaction the solid substrate then progressively dissolves and is then transformed.
- ii) The use of membrane bioreactors to retain the biocatalyst (Fig. 12). Coupling the reactor with an ultrafiltration or a microfiltration module allows a continuous operation of the reactor with retention of the soluble biocatalyst inside the reactor. With a membrane bioreactor, it is also possible to continuously eliminate an inhibitory product and to operate at high biocatalyst densities. Main limitations are the permeation flux reduction due to polarization and membrane fouling effects. Membrane bioreactor technology is particularly well adapted for continuous oxidoreduction reactions implying cofactor regeneration. An ultrafiltration membrane is then used to retain the two enzymes catalysing the bioconversion and the cofactor recycling reactions, and the NADH cofactor grafted of a soluble polymer. Membrane bioreactors are also useful for the controlled hydrolysis of biopolymers, such as proteins. By the correct selection of the UF membrane cut off, the size of the hydrolysed products in the permeate stream can be precisely controlled.
- iii) The use of oxygen-enriched air enrichment in fermentors. Because of the very low solubility of oxygen in aqueous media, around 7 mg/l under normal aeration conditions, the concentrations of microbial or animal cells in fermentors are

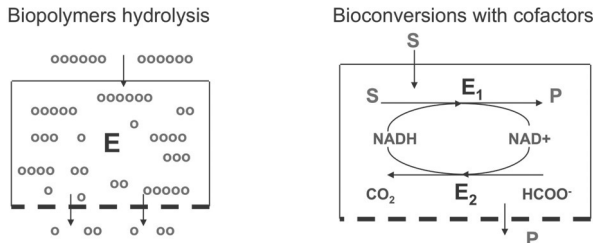


Figure 12. Enzymatic membrane bioreactors applications.

generally limited by the oxygen supply. By enriching the inlet air with oxygen it results in a higher oxygen solubility and transfer rate in the medium, therefore higher bioreactor productivity.

iv) The *in situ* elimination of products.

Depending on the nature of the product, the bioreactor can be coupled to different separation techniques to continuously remove the formed product: precipitation or crystallization, evaporation or distillation, adsorption on ion exchange resins or molecular sieves and extraction by a water immiscible solvent. The *in situ* elimination of an inhibitory product can substantially increase the bioreactor productivity. A coupled reaction-separation technology is also recommended to increase the substrate to product conversion yield of reversible reactions.

Enzymatic and Cellular Bioreactors Modelling

Simulators based on kinetic and thermodynamic modelling of the biocatalytic reaction are powerful tools for bioreactors design and optimal operation.

This section outlines the modeling approaches developed in bioprocess engineering, and summarizes the main kinetic laws encountered to simulate the dynamics of bioconversions.

Bioprocess Modelling Methodology

Bioreactor models are designed to simulate its dynamics behaviour and predict its technical performance for a given set of operational conditions (Fig. 13). Models take into account the reactor geometry or configuration, the state of the biocatalyst (soluble or immobilized), and the various operating variables, namely the concentrations of substrates and biocatalyst at the beginning of the reaction or at the inlet of the reactor, the temperature, the medium flow rate, the time of reaction or the residence time. Final reactor performances are the concentrations of products and by-products; possibly the distribution of molecular weights in the case of polymers, the substrates to product conversion yield, and the volumetric productivity.

For the elaboration of a knowledge-based kinetic model, the first step is identifying the biological or physicochemical processes that are likely to control the rate of reaction and the final conversion yield. In a homogeneous reaction medium containing soluble enzymes or dispersed cells, the time progress of the

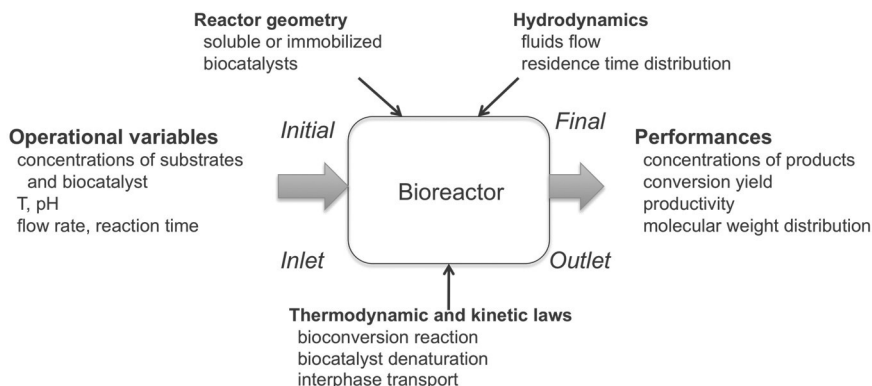


Figure 13. Factors governing bioreactors behaviour.

bioconversion is controlled by the reaction kinetics and possibly by the rate of biocatalyst denaturation (kinetic control regime). With reversible reactions, the final substrate to product conversion yield is limited by the reaction equilibrium state under the operating conditions (thermodynamic control). Bioreactor modelling is more complex in a heterogeneous reaction medium containing several phases, such as liquid media containing immobilized biocatalyst carriers or solid substrate particles, or liquid media with air bubbles. Under these conditions, it is also necessary to account for possible rate limiting solute transports between the phases.

A second step of bioreactor modelling is the choice of kinetic and thermodynamic laws to represent the identified rate limiting processes. For the bioconversion itself, models can use the classical laws of enzyme and microbial reactions and of biocatalysts denaturation. On the other hand, the rate of limiting interphase transport processes are generally expressed using equilibrium distribution constants between the phases and mass transfer coefficients in the flowing reaction medium.

As a final step, based on the set of laws describing the kinetic process limitations, the time course of the bioconversion reaction is then predicted by the resolution of the equations expressing the mass balances of the involved substrates, products and biocatalyst. Parameters in the laws are obtained from literature or from previous measurements, or identified by fitting the model to experimental data.

Laws of Enzyme Kinetics

Enzymatic reactions of industrial interest have relatively similar kinetic behaviour. Laws describing the dependence of reaction rates in a function of medium composition are more or less complex depending on the number of involved substrates and products. Most frequently expressions used to describe the rate of enzymatic reaction, generally expressed in g (or mole) of substrate transformed per minute and litre of medium, as a function of the concentrations of substrate, product and biocatalyst are given in Table 4. With soluble enzymes, the reaction rate is always proportional to the concentration of the active enzyme. The basic kinetic

Table 4. Laws for enzyme kinetics.

Michaelis-Menten $r_s = \frac{V_{\max} C_E C_S}{K_m + C_S}$	Inhibition by excess substrate $r_s = \frac{V_{\max} C_E C_S}{K_m + C_S + C_S^2 / K_I}$	r_s substrate reaction rate V_{\max} maximal rate K_m Michaelis constant K_I inhibition constant by substrate
Inhibition by product competitive type $r_s = \frac{V_{\max} C_E C_S}{K_m (1 + C_P / K_P) + C_S}$	non-competitive type $r_s = \frac{V_{\max} C_E C_S}{(1 + C_P / K_P)(K_m + C_S)}$	K_p product inhibition constant C_s substrate concentration C_p product concentration C_E enzyme concentration
Enzyme denaturation $r_d = k_d C_E$		r_d enzyme denaturation rate k_d denaturation constant
Temperature effect on maximal activity $V_{\max} = A \exp(-E_a / RT)$	Temperature effect on denaturation rate constant $k_d = A_d \exp(-E_{ad} / RT)$	A pre-exponential factor for reaction E_a activation energy for reaction A_d pre-exponential factor for denaturation E_{ad} activation energy for denaturation

law is the Michaelis-Menten relation that describes the kinetic evolution from a first order kinetic to a zeroth order kinetic at increasing substrate concentrations. It can be completed to represent the inhibition by excess of substrate or by inhibition by products. On the other hand, the rate of enzyme denaturation is simply proportional to the concentration of active enzyme. An increase in temperature increases both the maximal reaction rate and the rate of enzyme denaturation. These phenomena are well described by Arrhenius-type laws that contain activation energies for both the reaction and the enzyme denaturation. For each considered bioconversion reaction the different kinetic parameters must be adjusted.

Laws for Cellular Kinetics

Laws for cellular kinetics are relatively identical for microbial, animal and plant cells. They describe the rates of cell growth, consumption of substrates (carbon and nitrogen sources, oxygen) and metabolites production. Most frequent rate expressions are given in Table 5. Volumetric rates are generally proportional to the concentration of cells expressed per g dry mass cell or per million of cells. The laws for cell growth are generalizations to several substrates and products of the laws of enzyme kinetics. Usually the rate of substrates consumption is simply related to the rate of cell growth, the rates of metabolites production, and possibly substrate consumption for cell maintenance. The rate of metabolite production, on the other hand, may be more complex, depending on the cell growth rate and on the medium composition.

Laws for the Transfer of Substrate between Phases

In multiphase reaction systems, the model also involves kinetic laws for the interphase transfer of compounds (Table 6). For the various encountered situations,

Table 5. Laws for microbial kinetics.

<p>cellular growth</p> $r_x = \mu C_x = \mu_{\max} C_x \left(\frac{C_s}{K_s + C_s} \right) \left(\frac{C_o}{K_o + C_o} \right) \dots \left(\frac{1}{1 + C_p / K_p} \right) \dots$	<p>r_x growth rate μ specific growth rate μ_{\max} maximal specific growth rate K_s Monod constant pour sugar substrate K_o Monod constant for oxygen substrate K_p product inhibition constant C_s sugar substrate concentration C_o oxygen substrate concentration C_p product concentration C_x biomass concentration</p>
<p>nutrients consumption</p> $r_s = q_s C_x = Y_{s/x} \mu C_x + m_s C_x + Y_{s/p} q_p C_x$	<p>r_s substrate consumption rate q_s specific substrate consumption rate $Y_{s/x}$ conversion yield substrate/biomass m_s maintenance constant for sugar substrate $Y_{s/p}$ conversion yield substrate/product</p>
<p>metabolites production</p> $r_p = q_p C_x = Y_{p/x} \mu C_x + m_p C_x$	<p>r_p product production rate q_p specific product production rate $Y_{p/x}$ stoichiometric coefficient product/biomass m_p non-growth associated specific product production rate</p>

Table 6. Kinetic laws for interfacial transfer.

<p>solid substrate dissolution</p> $r_{dis} = k_{dis} A_{sol} C_{sol} (C_s^{sat} - C_s)$	<p>r_{dis} dissolution rate k_{dis} dissolution rate constant A_{sol} solid specific surface area C_{sol} solid particles concentration C_s^{sat} solute saturation concentration C_s solute medium concentration</p>
<p>substrate transport between medium and biocatalyst surface</p> $r_s = k_s A (C_s^m - C_s^s)$	<p>r_s substrate transport rate k_s substrate transport coefficient A particles external surface area C_s^m medium substrate concentration C_s^s surface substrate concentration</p>
<p>oxygen transfer between air and medium</p> $r_o = k_l a V (C_o^{sat} - C_o)$	<p>r_o oxygen transfer rate k_l oxygen transfer coefficient a specific air surface area V medium volume C_o^{sat} saturated oxygen concentration C_o medium oxygen concentration</p>

the transfer rate is generally expressed as the product of the interfacial surface area, the mass transfer coefficient and the substrate concentration difference expressing the departure from equilibrium.

Examples of Bioprocess Simulation and Optimization

The final section of the review presents three examples of using bioprocess engineering approaches to simulate and optimize bioconversion processes. A first example is the use of life cycle assessment methodology (Curran 2012) to evaluate the environmental effects of the ethanol production from agricultural resources. A second example illustrates the use of a simulator coupling a kinetic model and a cost evaluation to optimize an enzymatic starch hydrolysis reactor. A third example outlines the intensification of an enzymatic synthesis of sugar esters based on the use of an integrated process modelling.

Life Cycle Assessment of Bioethanol from Sugar Beets

The methodology of life cycle assessment evaluates the main environmental impacts of a process or product (Horne et al. 2009). It is illustrated for the production of ethanol, a biofuel, from sugar beet. The life cycle (Fig. 14) considers the steps of beet culture and transport, ethanol production (sugar extraction, fermentation, distillation and dehydration), co-products processing (pulp pressing and drying, vinasses concentration), and the combustion of ethanol. On the basis of classical yeast fermentation for the conversion of sugar into ethanol, the results obtained for the mass inventory and some of the environmental impacts are summarized as follows:

- Mass inventory (Table 7). With an agronomical yield of 75 T beets par ha of cultivated land, the process gives a production of 5.3 T of ethanol and 8.5 T of co-products. It also generates 290 T of liquid effluents.
- Environmental inventory. The primary energy consumption of the ethanol life cycle, which takes into accounts the energies for beets and ethanol production, for entrants (fertilizers) production, and the energy sources (fuel, natural gas, steam) are evaluated near 50 MJ/kg of ethanol. On the other hand, the emission of green-house gases, calculated from the emissions of CO₂ and N₂O during beet production and transformation, and the life cycle of mass and energy entrants, is found to be almost 5.5 kg CO₂ eq/kg ethanol. It is close to the amount of CO₂ captured by beet for photosynthesis.
- Distribution of environmental impacts along the cycle (Fig. 15). When calculating the respective contributions of the life cycle steps, ethanol production and by-

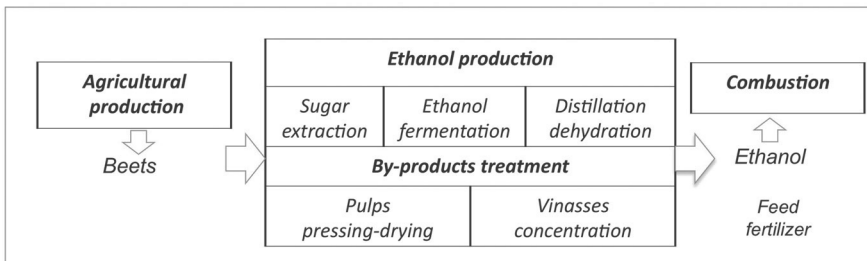
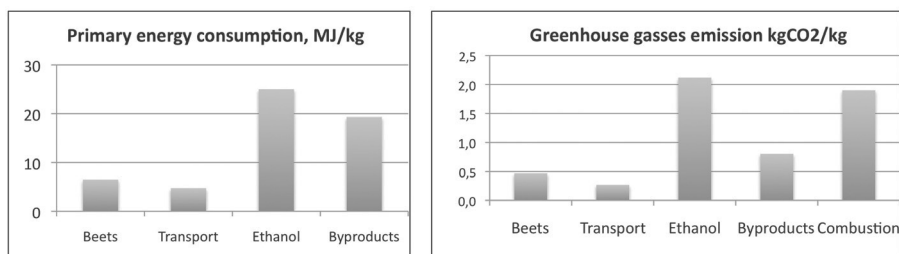


Figure 14. Life Cycle Assessment of ethanol from sugar beets.

Table 7. Mass inventory and environmental impacts of bioethanol from sugar beets.

Mass inventory per ha land			Environmental impacts per kg ethanol	
Inlet			water	56 kg/kg
	fertilizers	430 kg	primary energy	50 MJ/kg
	pesticides	7 kg	liquid wastes	54 kg/kg
	water	300,000 kg	green-house gases	
Outlet			emission	5,5 kg CO ₂ eq/kg
	ethanol	5,370 kg	beets capture	5,6 kg CO ₂ eq/kg
	beet pulps	3,330 kg	net	-0,1 kg CO ₂ eq/kg
	vinasses	5,240 kg		
	liquid wastes	290,000 kg		

**Figure 15.** Environmental impacts distribution between ethanol life cycle steps.

product processing are assessed to be the main contributors to both primary energy consumption and CO₂ emission.

- d) Allocation of environmental impacts between ethanol and the by-products. To compare the environmental impacts of ethanol with the corresponding impact of a fossil fuel, the LCA methodology suggests allocating the environmental loads between the main product ethanol and the generated by-products. The often used allocation method by substitution subtracts the respective impact from the total impact saved through using the by-products. Considering the substitution of beet pulp by soya protein for animal feed and the substitution by concentrated vinasses of nitrogen and phosphorous fertilizers, the primary energy consumption allocated to ethanol is reduced from 50 to 35 MJ/kg ethanol, and the emission of CO₂ from 5.5 to 3.5 kg CO₂ eq/kg ethanol.

When comparing the environmental impact of ethanol and gasoline, the bioethanol fuel has much reduced CO₂ emission impact. The energetic benefit is less favourable as the 35 MJ/kg requirement is larger than the combustion energy of 27 MJ/kg ethanol. This can be improved by saving energy through internal recycling of heat between the unit operations of ethanol production and byproduct processing.

Optimization of an Enzymatic Starch Hydrolysing Process

An enzymatic process, using a glucoamylase, is widely used to transform maltodextrins into a glucose syrup obtained by a previous enzymatic liquefaction

of starch. This example shows how a simulator, coupling kinetic modelling and cost evaluation, can guide the choice of the bioreactor technology and the operational temperature.

a) Kinetic simulation of the bioconversion in the reactor

For the hydrolysis of maltodextrins by glucoamylase, the kinetic model entails a Michaelis type of rate expression as a function of maltodextrins concentration, with an additional competitive inhibition term by the produced glucose, and a first order kinetic law for the thermal denaturation of the enzyme. After an initial identification of kinetics parameters for an industrial liquid concentrate of glucoamylase, the model adequately describes the time variation of the concentrations of maltodextrins, glucose and active enzyme at a given temperature (Fig. 16).

b) Optimal operating mode for bioconversion

The established kinetic model can be used to compare the performances of different reactor operating modes: either using the enzyme in a soluble mode, the reactor being operated batch-wise or continuously in a plug flow tubular equipment or in a stirred tank, or using the enzyme in an immobilized form in a fixed bed reactor, the enzyme being adsorbed inside porous particles (Cao 2005). For each of the operating modes the enzyme concentration and the temperature are optimized to minimize the cost of the bioconversion process.

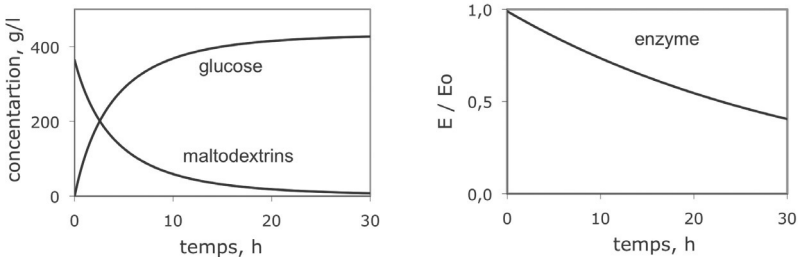


Figure 16. Kinetic model for maltodextrins hydrolysis by glucoamylase.

Results obtained for the sizing and production cost for an annual capacity of 20,000 T of transformed maltodextrins are summarized in Table 8. When the enzyme is used in a soluble form, the optimal temperature is between 40 and 55°C depending on the operating mode and internal flow. The lowest cost, around 63 €/ton is obtained for the batch operation, assuming a 10 €/l concentrate enzyme cost. The much higher production cost of the continuous stirred tank reactor is due to the strong inhibition by the formed glucose.

With an immobilized enzyme technology (Buchholz et al. 2005) the optimal operating temperature is found much lower at around 25°C. This is necessary for a one month operation of the fixed bed reactor. For an immobilization support cost around 20 €/kg the bioconversion cost near 60 €/kg is only slightly smaller than the lowest cost with the soluble enzyme. Under these conditions, on an industrial scale, it is the simplest batch technology with the soluble enzyme which is generally used.

Table 8. Bioreactors performances for maltodextrin saccharification by glucoamylase.

		Optimal temperature	Reaction/residence time	Reactor volume	Enzyme consumption	Bioconversion cost
Soluble enzyme						
	Batch	51°C	34 h	240 m ³	37 m ³	63 €/T
	Continuous stirred tank	42°C	160 h	1050 m ³	130 m ³	140 €/T
	Continuous plug flow	54 °C	23 h	150 m ³	53 m ³	69 €/T
Immobilized enzyme						
	Fixed bed	25°C	1.5 h	28 m ³	35 m ³	59 €/T

Simulation and Intensification of an Enzymatic Reactor for the Production of Sugar Esters

Enzymes such as lipases and esterases can be used to produce novel multifunctional molecules combining sugars and fatty acids. The obtained sugar esters are biodegradable surfactants with the appealing properties for food and cosmetic formulations. Whereas chemical synthesis esterifies all the hydroxyl groups on the sugar, the enzymatic synthesis is more selective and only produces mono and diacylated sugars on the primary hydroxyls. Moreover the enzymatic reactions take place at a lower temperature, which reduces secondary reactions and improves product quality. However, to become economically competitive, enzymatic process must achieve sufficiently high levels in terms of conversion yield, sugar esters concentration and productivity. This example illustrates the use of bioprocess engineering methods to intensify a lipase catalysed process for fructose palmitate synthesis in a methyl-2 butanol-2 medium.

a) Choice of bioreactor technology

For the choice of the bioreactor technology, the first barrier to overcome is the reduced lipase life-time, limited to a few hours, in a non-aqueous organic media. Lipase immobilization considerably increases the life-time up to several weeks under operating conditions of 60°C. Thus a stirred vessel with immobilized lipase particles in suspension was selected as the reactor technology.

A second barrier to the esterification process is the medium accumulating the water liberated by the reaction. This limits the final conversion yields of the acid and sugar substrates at under 20%. The limitation can be overcome by coupling the reaction with continuous water elimination. In practice, the bioreactor is equipped with a dehydration loop consisting of the evaporation of the reaction medium and its dehydration by passing through a fixed bed of molecular sieves. Moreover, due to the low solubility of sugars in the organic media (a few g per litre), the lipase reaction is preferably carried out with an initial high excess of solid sugar in the medium.

b) Bioconversion process modelling

Based on this reactor technology, a kinetic model of the esterification process is established. It contains kinetic laws for the three potentially rate limiting steps

(Fig. 17): the sugar dissolution, the reversible esterification of the sugar by the fatty acid (described by a Michaelis-Menten law generalized for two substrates and two products), and the elimination of water by the dehydration loop (simply described by a rate proportional to the evaporation flow rate and the water content of the medium). This model adequately describes the kinetics, over 20 hours, of conversion of fructose into fructose monopalmitate and dipalmitate. It accounts for the initial rapid accumulation of water in the medium, followed by its progressive decrease during the course of the reaction (Fig. 18).

c) Optimal bioreactor operation

The model is then used to simulate the possibility of process intensification by increasing the initial sugar concentrations of fructose and lipase particles (Fig. 19). It shows that substantial increase in fructose esters concentrations

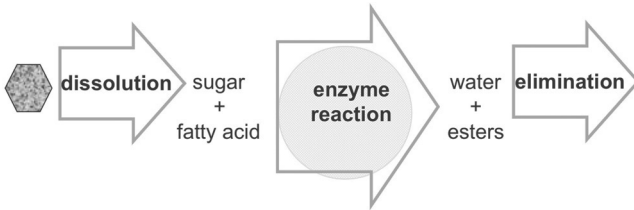


Figure 17. Rate limiting processes of lipase catalysed sugar acylation.

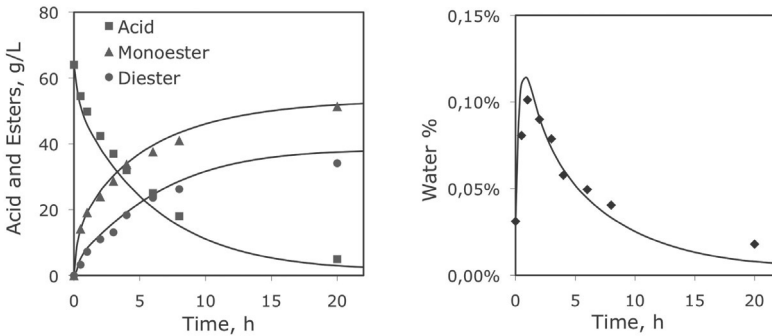


Figure 18. Kinetic model for the lipase catalysed production of fructose palmitate in non-aqueous medium.

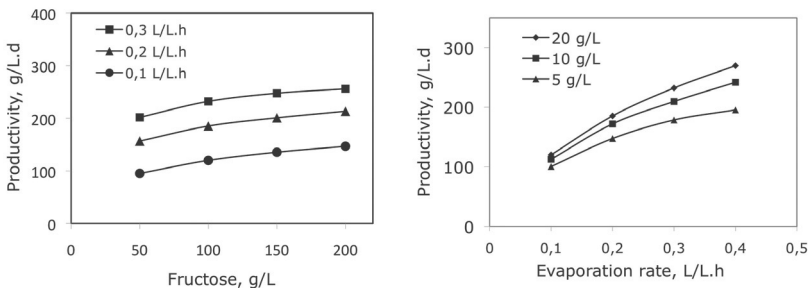


Figure 19. Simulation of the effects of fructose concentration and medium evaporation rate on the bioreactor sugar ester productivity.

can only be achieved by simultaneously increasing the medium evaporation and dehydration rate. With this operation strategy, at an initial 200 g/l fructose concentration and 20 g/l enzymatic particles, and an evaporation rate of 0.2 l/l.h, the enzymatic process yields up to 230 g/l fructose palmitate after 20 hours of reaction time. Reaching this level of productivity greatly improves the industrial competitiveness of the lipase-catalysed sugar ester production process.

References

- Aehle, W. (ed.). 2005. *Enzymes in Industry: Production and Applications*. Wiley-VCH, Weinheim.
- Anastas, P.T. and R.H. Crabtree. 2009. *Handbook of Green Chemistry*. Wiley-VCH, Weinheim.
- Antolli, P.G. and Z. Liu. 2012. *Bioreactors: Design, Properties, and Applications*. Nova Science Publishers, New York.
- Blanch, H. and D. Clarck. 1997. *Biochemical Engineering*. Marcel Decker, New York.
- Bommarius, A. and B. Riebe. 2004. *Biocatalysis: Fundamentals and Applications*. Wiley-VCH, Weinheim.
- Buchholz, B., V. Kasche and U. Bornscheuer. 2005. *Biocatalysts and Enzyme Technology*. Wiley-VCH, Weinheim.
- Cao, L. 2005. *Carrier Bound Immobilized Enzymes: Principles, Applications, and Design*. Wiley-VCH, Weinheim.
- Carrea, G. and S. Riva. 2008. *Organic Synthesis with Enzymes in Non-Aqueous Media*. Wiley-VCH, Weinheim.
- Curran, M.A. (ed.). 2012. *Life Cycle Assessment Handbook: A Guide for Environmentally Sustainable Products*. John Wiley & Sons, Inc., Hoboken, NJ, USA.
- Doran, P.M. 2013. *Bioprocess Engineering Principles*. Elsevier, Oxford, UK.
- Drauz, K., H. Gröger and O.L. May. 2012. *Enzyme Catalysis in Organic Synthesis: Third, Completely Revised and Enlarged Edition, 3 Volume Set*, Wiley-VCH, Weinheim.
- Dumont, F.E. and J.A. Sacco. 2009. *Biochemical Engineering*. Nova Science Publishers, New York.
- Dutta, R. 2010. *Fundamentals of Biochemical Engineering*. Springer, Berlin.
- Faber, K. 2011. *Biotransformations in Organic Chemistry*. Springer, Berlin.
- Fessner, W.D. and T. Anthonsen. 2009. *Modern Biocatalysis: Stereoselective and Environmentally Friendly Reactions*. Wiley-VCH, Weinheim.
- Gotor, V., I. Alfonso and E. Garcia-Urdales. 2008. *Asymmetric Organic Synthesis with Enzymes*. Wiley-VCH, Weinheim.
- Grunwald, P. 2009. *Biocatalysis: Biochemical Fundamentals and Applications*. Imperial College Press, London (distributed by World Scientific).
- Guisan, J.M. 2006. *Immobilization of Enzymes and Cells*. Humana Press, New York.
- Horne, R.T., T. Grant and K. Verghese. 2009. *Life Cycle Assessment: Principles, Practice and Prospects*. CSIRO Publishing, Collingwood.
- Illanes, A. (ed.). 2008. *Enzyme Biocatalysis: Principles and Applications*. Springer Science + Business Media B.V.
- Katoh, S. and F. Yoashida. 2009. *Biochemical Engineering: A Textbook for Engineers, Chemists and Biologists*. Wiley-VCH, Weinheim.
- Liese, A., K. Seelbach and C. Wandrey. 2006. *Industrial Biotransformations*. Wiley-VCH, Weinheim.
- Liu, S. 2013. *Bioprocess Engineering: Kinetics, Biosystems, Sustainability, and Reactor Design*. Elsevier, London.
- Loos, K. (ed.). 2011. *Biocatalysis in Polymer Chemistry*. Wiley-VCH, Weinheim.
- Matsuda, T. 2007. *Future Directions in Biocatalysis*. Elsevier B.V., Amsterdam.
- Sablani, S.S., A.K. Datta, M.S. Rahman and A.S. Mujumda. 2007. *Handbook of Food and Bioprocess Modelling techniques*. Taylor & Francis, CRC Press, Boca Raton, Florida.
- Shuler, M. and F. Kargi. 2002. *Bioprocess Engineering: Basic Concepts*. Prentice Hall, Upper Saddle River.
- Strathof, A. and P. Adlercreutz (eds.). 2002. *Applied Biocatalysis*. Taylor & Francis, Amsterdam.

- Vogel, H. and C. Haber. 2007. *Fermentation and Biochemical Engineering Handbook*. Noyes Publications, Westwood, New Jersey.
- Whittall, J. and P.W. Sutton. 2012. *Practical Methods for Biocatalysis and Biotransformations 2*. John Wiley & Sons, Ltd.
- Yang, S.T. 2007. *Bioprocessing for Value-Added Products from Renewable Resources*. Elsevier B.V., Amsterdam.

15

Catalysis Contribution to a Sustainable Chemistry

Philippe Kalck and Philippe Serp

Introduction

During the industrial development, including the twenty-year period after World War II devoted to rebuilding the industrial and the economical framework, all the objectives of the chemical industry were aimed at manufacturing essential products and power production. Coal was the main raw material and the components related to the process energy, selectivity in the required products as well as the waste treatments were considered to be a secondary priority. Among the various factors that addressed these environmental issues and required from chemistry, it took into account the concept of sustainable development and the first oil crisis in 1973 where the crude oil price abruptly doubled, played a crucial role. It is important to also underline the significant progress performed in the synthetic pathways and the progressive awareness of the environmental issues, which led to the increasingly stringent legislations that we know today. These last aspects are closely intertwined and most of the time the binding legislation is just anticipating the progress that we can expect from the chemists.

Today, around 85% of all the products we are using involve a catalyst, at least in one step of their manufacture. As catalysis considerably decreases the activation energy of a reaction so that it becomes possible to adjust the conditions to support a given pathway, it can combine efficiency and selectivity to save energy. Thus, the atom economy, i.e., realizing the full conversion of the reactants into the expected products, and significantly decrease or even remove the pollutants are just two positive aspects currently due to catalysis. Under these conditions, catalysis provides effective and usually, elegant solutions to Sustainable Chemistry. It is operating not only in the chemical industry but also in energy, transport, medical care, health, nutrition and water quality. Rather than addressing all the aspects and contributions

of catalysis, we will focus on a number of representative examples, so as to illustrate the atom economy for the diastereoselective synthesis of menthol, or in the field of energy the large scale production of ammonia and acetic acid in which the process energy is particularly efficient. We will also describe the fuel cells to store and produce energy, and for the mobile sources of transporting the catalytic converters in the field of de-pollution. Finally, we will show how it is possible to use renewable raw materials such as biomass to produce the CO/H₂ syngas, from which we can produce the major intermediates of chemistry.

Selectivity and Atom Economy

Diastereoselective Synthesis of (-)-menthol

Menthol is largely known for its peculiar aroma and its refreshing flavour. It is a nutritious aroma and a perfume present in many daily products including toothpaste, chewing-gum, fizzy drinks, pastries and even cigarettes. This additive is produced worldwide at around 30,000 T/year and its production increase is around 10%/year (in 2012) (<http://www.leffingwell.com/menthol1/mentinfo.htm>). Two-thirds are obtained by extraction from the *mentha arvensis* plant in India (9,700 T), China (2,100 T), Brazil (450 T), Taiwan (300 T), then cooling the extract and crystallization, achieving 82% purity.

Today three industrial pathways produce (1*R*,3*R*,4*S*)-menthol from the 8 isomers of 5-methyl-2-(1-methylethyl)-cyclohexane-1-ol. They are operated by Symrise, Takasago and BASF.

A synthetic pathway was initially performed by Symrise through the Haarmann and Reimer process (Fleischer et al. 1972) in which thymol, synthesized from *m*-cresol, is hydrogenated on a heterogeneous catalyst to provide after distillation the racemic mixture of (+/-)-menthol (Etzold et al. 2009); then a reaction with benzoic acid gives menthyl benzoate, which is selectively crystallized: (-)-menthol is obtained after deprotection reaction, whereas the unwanted isomer is recycled and racemized. A new process (Gatfield et al. 2002) resorts to the hydrolysis of menthyl benzoate with recombinant *Candida Rugosa* lipase leads to (-)-menthol with an enantiomeric excess of 99.9%. The initial capacity of 3,600 T/year has been doubled in 2012 in the Holzminden plant in Germany.

The second process, from Tagasago Int., involves an asymmetric synthesis on a 3,000T/year scale in Japan and Germany. It was designed by S. Akutagawa and his team based on the Nobel Prize winner Ryoji Noyori's discovery that a rhodium-catalysed asymmetric allylic isomerization can achieve (-)-menthol with a 98.5% enantiomeric excess (Fig. 1) (Akutagawa 1992, 1999a, 1999b). By pyrolysing turpentine oil to produce β -pinene, then myrcene can be obtained. Addition of diethylamine in the presence of lithium or butyllithium results in the formation of *N,N*-diethylgeranylamine.

In this asymmetric catalysis the C = C double bond is shifted so that a chiral carbon atom is created, with the simultaneous formation of the enamine. The asymmetric induction is due to the introduction in the coordination sphere of the rhodium metal centre of the atropisomeric ligand (*R*)-BINAP or (*S*)-BINAP, containing a

C_2 axis (Fig. 2) (Noyori 1994). The $[\text{Rh}(\eta^4\text{-C}_8\text{H}_{12})\{(S)\text{-BINAP}\}]^+[\text{ClO}_4]^-$ complex transforms *N,N*-diethylgeranylamine into (*R*)-citronellal-(*E*)-enamine at 40°C , with just 0.75% of the (*S*) isomer. In the industrial process the reaction kinetics and a high enantioselectivity must be made compatible and thus the reaction is performed in batch reactors at 100°C , for 18 hours and with a substrate/catalyst ratio of 8,000. In these conditions, the whole conversion provides a 97.6% enantiomeric excess (Akutagawa 1999a, 1999b).

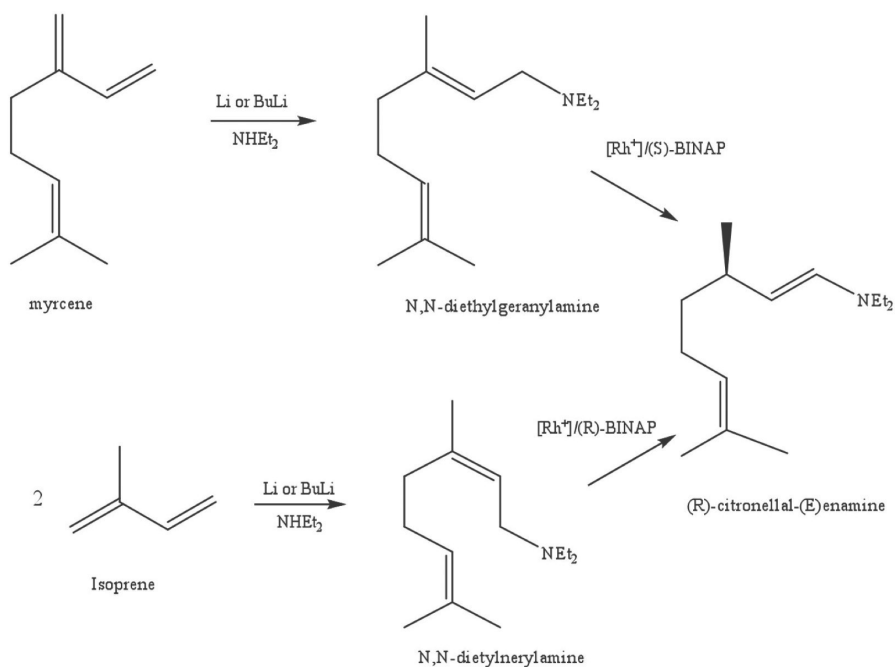


Figure 1. Chemical pathways to transform myrcene or isoprene into (*R*)-citronellal-amine.

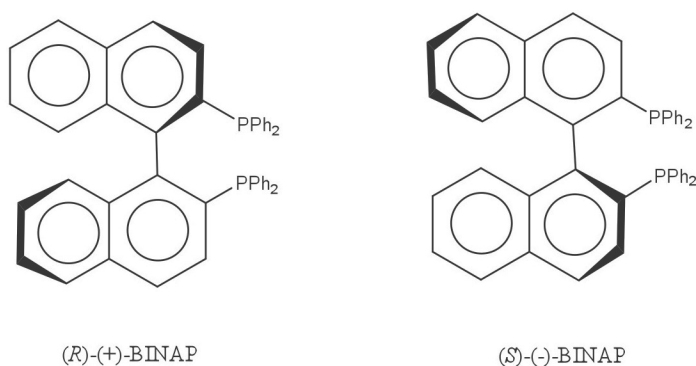


Figure 2. Spatial representation of (*R*) and (*S*)-BINAP ligands.

It is interesting to note that on the bench scale, the $[\text{Rh}(\eta^4\text{-C}_8\text{H}_{12})(\text{BINAP})]^+$ complex gives rise to 100 catalytic cycles, whereas the profitability is reached beyond 50,000! Elimination from the substrate of triethylamine, cyclooctadiene (C_8H_{12}) and mainly the geranylamine isomer in which the two $\text{C}=\text{C}$ bonds are conjugated achieves a turnover number (TON) of 8,000. Then, using the $[\text{Rh}(\text{BINAP})_2]^+$ complex, or better the Tol-BINAP ligand in which the two phosphorus atoms bring a tolyl- instead of a phenyl substituent, lead to achieve a TON of 80,000. From a batch of 7 tons of geranylamine dissolved in 3 m^3 of THF and 6.71 kg of $[\text{Rh}(\text{Tol-BINAP})_2]^+[\text{ClO}_4]^-$, distillation under reduced pressure can recycle the THF and separate the enamine; a further addition of *n*-heptane to the brown-orange residue precipitates the rhodium complex. The loss in catalyst is therefore limited to 2%, so that the TON of 400,000 is largely beyond the threshold of the economic rate of return.

Finally, the (*R*)-citronellal-(*E*)-enamine is hydrolysed in an acidic medium to lead to (*R*)-citronellal, which is further cyclized in the presence of ZnBr_2 . The resulting isopulegol is crystallized at -50°C from heptane solutions, providing an enantiomeric purity of 100%. The classical hydrogenation of (–)-isopulegol on Raney Nickel provides (–)-menthol (Fig. 3).

Concerning the *N,N*-diethylnerylamine, we must resort to the (*R*)-BINAP or (*R*)-(Tol-BINAP) ligands to obtain the (*R*)-citronellal-(*E*)-enamine. The achievement is quite the same as for the previous pathway.

The third and more recent industrial process, from BASF, starts from citral, since 2004 the Company produces around 40,000 t/year. This C_{10} building block for flavours, fragrances and vitamins is manufactured from isobutene, formaldehyde and air.

Citral is a mixture of the two (*Z*)- and (*E*)-isomers, i.e., neral and geranial, which can be independently hydrogenated into (*R*)-citronellal. BASF designed a catalytic system involving the (*S,S*)-chiraphos ligand to transform geranial or (*R,R*)-chiraphos to hydrogenate neral into the expected (*R*)-citronellal (Heydrich et al. 2009). The enantiomeric excess can be better than 91%. Careful analysis of the catalytic system formed in the reaction conditions show that the addition of Chiraphos to the $[\text{Rh}(\text{acac})(\text{CO})_2]$ precursor generates the $[\text{Rh}(\text{chiraphos})_2]^+\text{acac}^-$ resting state and that it is

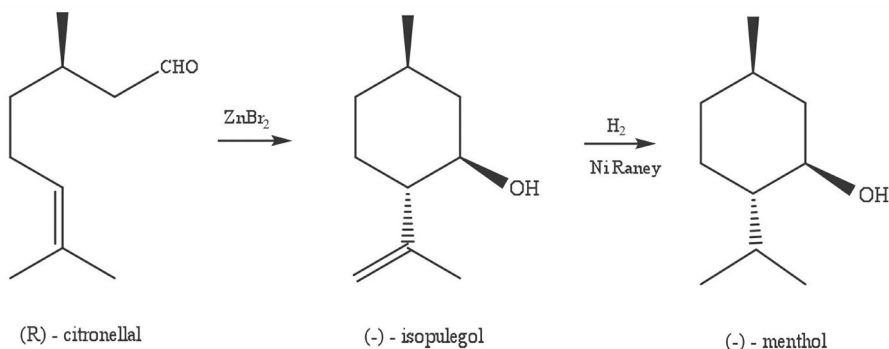


Figure 3. Reaction pathway to produce (–)-menthol.

necessary to introduce *ca.* 1,000 ppm of CO into the hydrogen charge to produce $[\text{Rh}(\text{H})(\text{CO})_2(\text{chiraphos})]$ and from it, the 16 electron $[\text{Rh}(\text{H})(\text{CO})(\text{chiraphos})]$ active species (Fig. 5) (Jäkel and Paciello 2010).

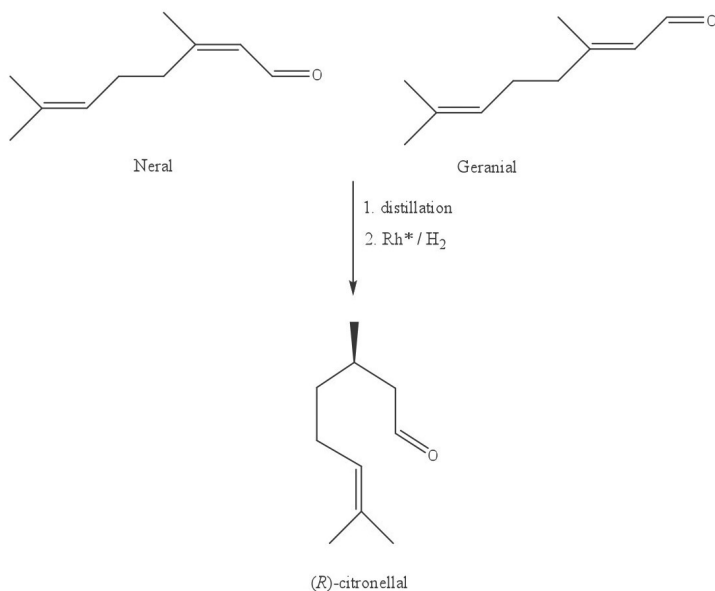


Figure 4. The two isomers of citral, neral (Z)-isomer and geranial (E), their separation by distillation and their asymmetric hydrogenation into (R)-citronellal.

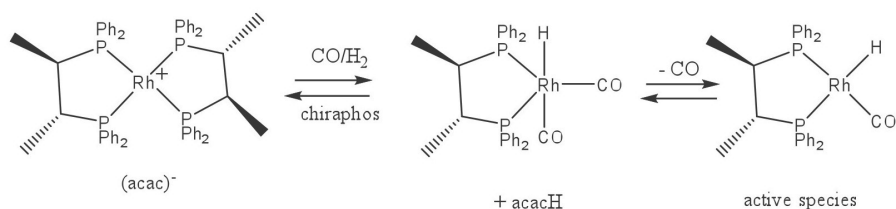


Figure 5. Generation of the active species starting from $[\text{Rh}(\text{acac})(\text{CO})_2]$, by coordination of chiraphos under CO/H_2 pressure.

Energy

Ammonia Synthesis

The large scale synthesis of ammonia is an interesting example to describe since it takes into account almost all of the set of problems to solve the use of catalysts on an industrial level. In fact, without nitrate fertilizers, we would be confronted with the same famines today as in the Middle Ages. The ammonia synthesis was discovered by Fritz Haber in 1908 and then developed on an industrial scale by Carl Bosch at BASF Co. Haber in 1918 and Bosch in 1931 received the Nobel Prize (Erisman et al.

2008). Their first osmium catalysts were operating at 300 bar and at high temperature, producing several tons per day of NH_3 . Still at BASF, Mitasch examined around 2,500 catalytic mixtures in 6,500 tests, before discovering the potassium-promoted iron catalysts, which is still operating today (Farrauto and Bartholomew 1997)!

Currently, the “Haber-Bosch” process produces around 160 million T/year (Rafiqul et al. 2005) in 80 countries, in plants where the capacity varies from 600 to 3,300 T/day. The energy consumption for this annual production is significant since it corresponds to 1% of the world’s energy. This process has been largely improved over time but remains one of the most energy-greedy industrial processes. From NH_3 , the industry synthesises nitric oxide and then nitric acid by oxidation on platinum/rhodium wires. By combining the two components ammonium nitrate is sold as a staple fertilizer. This represents around 85% of the NH_3 usage, the rest being dedicated to synthetic textiles and manufacturing explosives. All of these fertilizers directly contribute to life on our planet. Studies have shown that starting from 1.81 billion inhabitants at the beginning of the XX Century we would have reached only 3.5 billion in their absence, whereas in 2013 we have a population of around 7 billion (Fig. 6).

Whereas, on a global level, the ammonia synthesis contributes to water pollution and it will be necessary to include a “Nitrogen economy” in the future. This mature technology has a bright future and still offers real prospects in terms of energy efficiency, particularly for the existing plants. The block diagram shown in Fig. 7 summarizes all the reaction sequences to produce NH_3 .

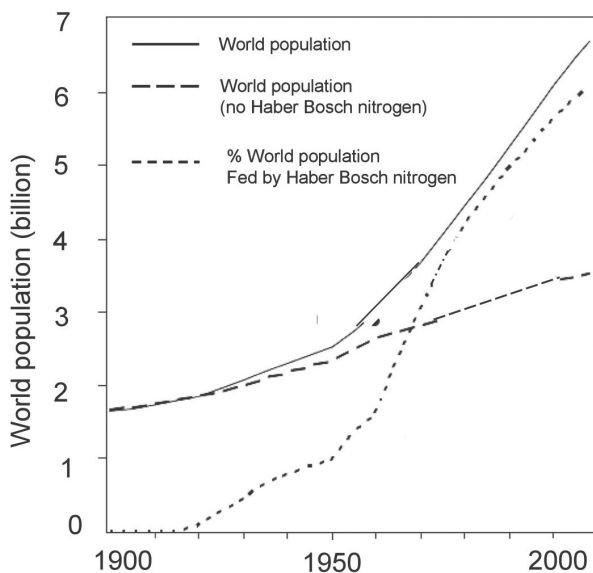


Figure 6. The world population over the XX Century and its use of nitrogen. From the total world population (solid line), an assessment has been made for the number of people who would have survived without the active nitrogen from the Haber-Bosch process (long dotted line), or expressed in a percentage of the global population (dotted-line) (adapted from Erisman et al. 2008).

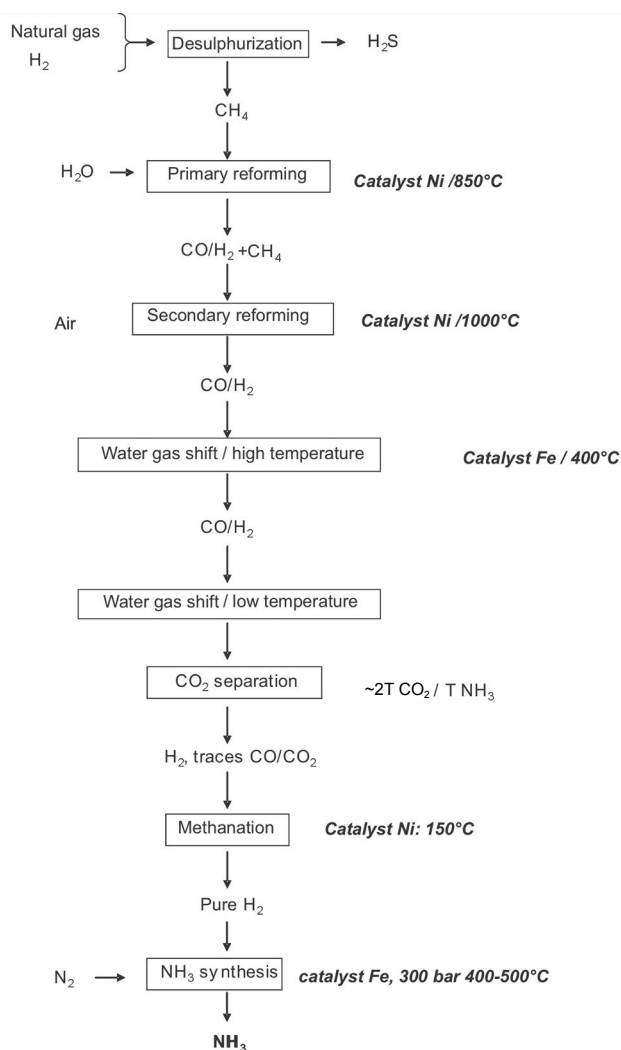


Figure 7. Reaction sequences to produce NH_3 .

The NH_3 plants usually have a 1,000 to 1,500 T/day capacity, but the more recent ones can attain 3,300 T/day. Most of the time, they are embedded into other plants such as urea reactors that allow to CO_2 valorisation produced in the process. Three main processes are used in the NH_3 manufacturing industry:

- The water vapour reforming from natural gas that is the most classically encountered.
- The partial oxidation of heavy naphtha feedstock.
- Gas synthesis (H_2 , N_2 , CO , CO_2 , H_2O , and various trace inert gases) by coal gasification. Although the latter process is not used anymore in Europe and the

USA for economic and environment reasons, the price increase of natural gas results in a desire for coal revival. The generation of upstream pure hydrogen from the converter entails numerous steps for converting natural gas into CO/H₂ through vaporeforming, performing the Water-Gas-Shift reaction (CO + H₂O → CO₂ + H₂) to transform CO into hydrogen with the co-production of CO₂, separating CO₂ through its adsorption in ethanolamine and further use in the synthesis of urea or in fizzy drinks. The CO and CO₂ traces are removed by the methanation reaction until they are as low as 10 ppm. From natural gas, the co-production of CO₂ is 2 T for 1 T of NH₃, whereas it is 16.5 T starting from coal! The energy loss diagram for the various steps of the process is shown in Fig. 8.

The energy consumption to produce 1 T of NH₃ is 30–35 10⁹J, mainly due to reforming; the third is devoted to the combustion of natural gas to reach the required temperature of 850°C and 1,000°C. Significant energy gains can be obtained by combining the installation of a pre-reformer, a gas turbine, the use of a pre-heater (CH₄, H₂O, air) and higher pressures, and a lower steam/CH₄ ratio. For example, the energy gain is 35 10⁹J/T_{NH₃} when a gas turbine is installed. Highly sensitive energy gains could be acquired using specific solvents such as methyl-diethanolamine (up to 14 10⁹ J/T_{NH₃}) to adsorb CO₂ and a Process Survey Adapter for the purification step of the synthesis gas (11 10⁹J/T_{NH₃}).

The overall reaction of ammonia synthesis is shown below:



It is a strongly exothermic equilibrium reaction which requires operating at a low temperature, and if possible, at a high pressure. However, activating the nitrogen molecule is the limiting step because of the high energy of dissociation of the N-N bond, which is 945 kJ/mol, much higher than that of the C-H bond in methane (439 kJ/mol). Thus, at 1,000°C in a 3H₂/N₂ mixture the percentage of NH₃ is only 0.1%. Therefore, the industrial production of NH₃ requires the presence of an effective catalyst. Conversely this balance can produce hydrogen cleanly since the co-product is nitrogen and is thus considered in applications for fuel cells.

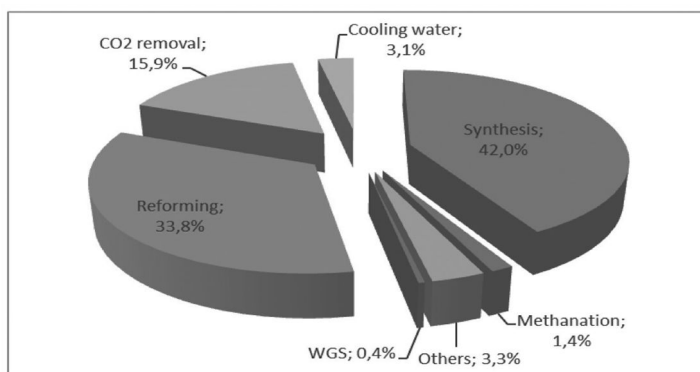


Figure 8. Loss in energy efficiency in an ammonia plant.

The first generation of catalysts developed by BASF used iron as a catalyst. It is melted down and contains two structuring agents such as alumina and CaO and an electronic promoter K_2O . Today conventional compositions consist of 78–82% iron, 11–14% $FeO + Fe_2O_3$, 1.5 to 3% Al_2O_3 , from 0.1 to 0.65% K_2O , 0.1 to 4% CaO, 0.3 to 0.6% MgO and 0.2 to 0.7% of SiO_2 . Such a catalyst has an average lifetime of 10 years (Farrauto and Bartholomew 1997). In the reactor, the $N_2/3H_2$ mixture is preheated, compressed and the reaction is conducted at $400^\circ C$ and 300 bar on two successive catalytic beds at space velocities from 7500 to 15000 h^{-1} . The mixture flows in a radial flow reactor provided with a catalyst bed containing fine iron particles (1.3 to 2.5 mm in diameter). In the new generation of reactors, an internal heat exchanger uses the heat from the reaction to preheat the gas mixture. The conversion rate is 15% NH_3 . The mixture leaving the reactor is quenched at $0^\circ C$ to condense the major part of NH_3 produced. The uncondensed gas, containing 3 to 4% of NH_3 , is recycled.

During the last 30 years new catalytic systems were investigated (Farrauto and Bartholomew 1997; Schlögl 2003; Szmigiel et al. 2002) and a ruthenium catalyst on graphite promoted by alkali or alkaline earth shows a much higher activity (about 100 times) decreasing the temperature and hence the process pressure. The disadvantages are: i) an inhibition of ruthenium by NH_3 that needs to stay at low conversion, and ii) methanation of the graphite support. Recent processes achieving productivity as high as 1850T/day associate in multistage reactors iron catalysts in the first fixed bed and the ruthenium catalyst in the following beds. Energy consumption is reduced by about $0.5 \cdot 10^9 J/T_{NH_3}$.

Currently, nitride catalysts free from noble metal and possessing good stability are explored. Thus, bi-metal nitrides $FeMo_3N$, Co_3Mo_3N and Ni_2Mo_3N are stable and active catalysts under industrial conditions (Jacobsen 2000).

Acetic Acid Synthesis

The global production of acetic acid is about 9 million tons per year and the main application is the manufacture of vinyl acetate (VAM) for artificial fibres and resins (see Fig. 9).

Most of the acetic acid production is carried out by the carbonylation of methanol in homogeneous phase catalysed by metals of column 9 (cobalt, rhodium, iridium). This contribution of about 80% has grown steadily over the years at the expense of the oxidation of naphtha and especially acetaldehyde. The availability and cost of raw materials ($CH_3OH \sim 160 \text{ €/T}$, $C_2H_4 \sim \text{€ } 450/T$) for a barrel of oil at US \$ 50 ~ makes the carbonylation of methanol the most cost effective method, particularly after the two oil crises.

This reaction was discovered by BASF in 1913 when exploring the reactivity of methanol (Weissermel and Arpe 2000). The first process was started in 1960 when the nickel-molybdenum alloys were discovered (Hastelloy®). In fact, the cobalt catalyst requires an iodide promoter at high temperature in aqueous medium that causes corrosion precluding the use of stainless steel. Working conditions are $250^\circ C$ and 680 bar CO. However, as the selectivities were 90% compared to CH_3OH and 70% compared to the CO the acetic acid yield was 70%, as many secondary products

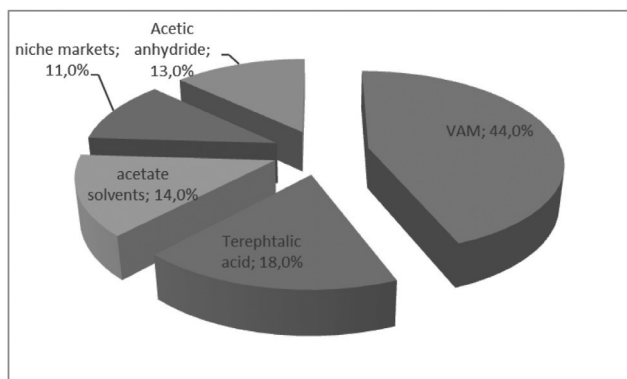
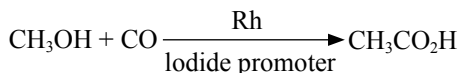


Figure 9. Main applications of acetic acid.

are formed, which requires a series of five distillation columns to obtain a pure product of 99.8%. This cobalt process was moved by the rhodium discovered in the 60s by Monsanto (Haynes 2006). Even though at the time the rhodium was 1,000 times more expensive than cobalt, its great reactivity and low sensitivity to hydrogen have led to a lower process cost. Carbonylation conditions are 190°C and 30 bar and the selectivity based on methanol and CO are respectively 99.5% and 90%.

Catalysis can be summarized as follows:



The iodide-promoter activates the methanol,



The rhodium catalyses the reaction $\text{CH}_3\text{I} + \text{CO} \longrightarrow \text{CH}_3\text{COI}$ leading to acetyl iodide, immediately hydrolysed to give CH_3COOH and regenerating HI, but also catalyses the displacement of the water-gas-shift reaction, $\text{CO} + \text{H}_2\text{O} \rightleftharpoons \text{CO}_2 + \text{H}_2$, which explains the presence of hydrogen in the medium and the loss of selectivity to CO. The main by-product formed in the amount of about 0.5% is propanoic acid, which requires a final distillation column to separate it from the acetic acid.

Besides the cost of rhodium, which reached € 300,000/kg in 2008, the weak point of the process is related to a minimum content of 14% water in the reactor to stabilize the rhodium, which has as a direct consequence the use of a very large distillation column to separate water from the acetic acid. The flow sheet of the process shows a third distillation column located immediately after the separator to recycle the light fractions. Separating the catalyst from the reaction products is carried out by an adiabatic expansion leading to a gas phase directed towards the distillation columns and an Rh-containing liquid phase recompressed to the reactor (Fig. 10).

Research to reduce energy costs has focused on catalytic systems that operate at low water content. Thus, since the 80s, Celanese uses lithium iodide to stabilize the rhodium and reach a water content of about 4 w/w%. The use of this technology has increased from a production capacity of 270,000 T/year in 1978 to 1.2 million T/year

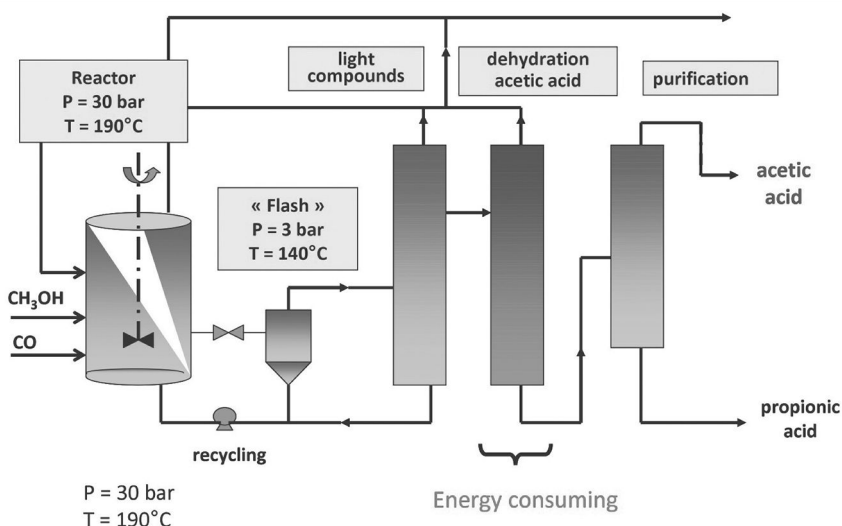


Figure 10. Flow Sheet of the Monsanto Rh process.

in 2001 (Torrence 2002) at the Celanese Clear Lake platform (Texas, USA). For its part, BP Chemicals has developed a new system combining ruthenium and iridium also giving a content of 2 to 5 w/w % water. This is interesting because this bimetallic catalyst selectivity versus CO can reach a value of 94%, which corresponds to a 70% reduction of CO_2 emissions. The highest kinetics than in rhodium and the low water content, which combines the first two distillation columns in Fig. 7 into a single one results in a reduction of the process cost by 30% (Haynes 2006; Jones 2000). It appears that even for such a chemistry process of a major intermediate, it is possible to achieve substantial progress. Research is continuing to try to produce acetic acid directly from synthesis gas (CO/H_2) without going through the manufacture of methanol, or by oxidative carbonylation of methane in the presence of superacid catalysts.

Fuel Cells

Introduction

A fuel cell is a complex system in which the chemical energy of a compound, that is, a fuel which is stored independently, is converted directly into electrical energy. The production of electricity is due to the electro-oxidation of the reducing fuel at one electrode (anode) coupled with the electro-reduction of an oxidant at the other electrode (cathode). Unlike traditional means of energy production, its performance does not depend on the Carnot cycle. Sir William Grove is often considered as the inventor of the fuel cell in 1839, where it uses the reverse electrolysis of water to generate electricity and water from hydrogen and oxygen (Fig. 11).

Francis T. Bacon in 1953 built a hydrogen-oxygen cell with an alkaline electrolyte and porous electrodes of nickel and nickel oxide. This prototype demonstrated the

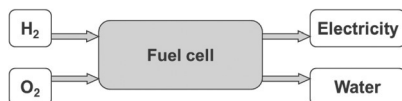


Figure 11. Schematic representation of a hydrogen fuel cell.

interest of fuel cells for spaceship applications. Then, the first prototype vehicles with an onboard battery appear in the United States and subsequently cell technology would benefit from the work on electric and hybrid vehicles. One of the key moments in the development of the fuel cell is the first oil crisis in 1973: for the first time the need to be independent in terms of energy appears. This is actually the early 1990s when the batteries were experiencing a revival. This is due to several key factors:

- Worsening environmental problems related to the greenhouse effect.
- Technological advances (better performing membranes for Polymer Exchange Membrane Fuel Cell catalysts, reforming).
- The first prototypes of vehicles or stationary installations were developed.
- The batteries have an advantage in terms of pollution if they use hydrogen, emissions are virtually zero and the noise is very low (good urban insertion). Finally, the batteries have the advantage of high efficiency.

Currently, there are six main types of fuel cells:

- AFC (Alkaline Fuel Cell)
- PEMFC (Polymer Exchange Membrane Fuel Cell)
- DMFC (Direct Methanol Fuel Cell)
- PAFC (Phosphoric Acid Fuel Cell)
- MCFC (Molten Carbonate Fuel Cell)
- SOFC (Solid Oxide Fuel Cell).

These cells (Table 1) differ according to the nature of the electrolyte and hence the level of operating temperature, architecture and application areas where each type can be used. In addition, each cell has different requirements in terms of fuel.

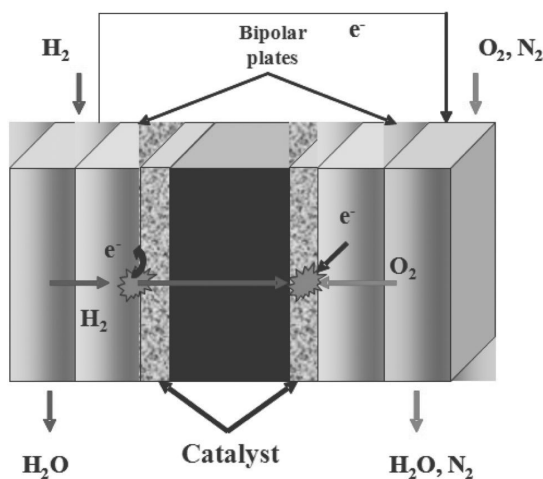
Structure of the Fuel Cell

The heart of the cell in an elementary cell comprises several elements: two electrodes, the anode and the cathode, the electrolyte and the bipolar plates to provide a diffusion layer surrounding the electrodes (Fig. 12). The exact arrangement of these elements and the nature of the constituent components depend on the type of cell, but their role remains the same.

The electrodes are the site of electrochemical reactions: at the anode oxidation and reduction at the cathode. These reactions usually have very slow kinetics, which depends more on the state of the electrode surface and the ease with which the reactions are carried out. For hydrogen (or other fuel) oxidation, a catalyst is required.

Table 1. Different kinds of fuel cells.

Type of cell	AFC	PEMFC	DMFC	PAFC	MCFC	SOFC
Electrolyte	KOH solution	Proton conductive polymeric membrane	Proton conductive polymeric membrane	Phosphoric acid	Molten Li_2CO_3 and K_2CO_3 in a LiAlO_2 matrix	ZrO_2 & Y_2O_3
Ions in electrolyte	OH^-	H^+	H^+	H^+	CO_3^{2-}	O^{2-}
Temperature	60–80°C	60–100°C	60–100°C	180–220°C	600–660°C	700–1000°C
Fuel	H_2	H_2 (pure or from reforming)	Methanol	H_2 (pure or from reforming)	H_2 (pure or from reforming)	H_2 (pure or from reforming)
Oxidant	O_2 (pure)	air	air	air	air	air
Application field	space	car, mobile phone, cogeneration,	mobile phone	cogeneration	cogeneration, centralized electricity production	cogeneration, centralized electricity production
Development	used	prototypes	prototypes	mature technology	prototypes	prototypes

**Figure 12.** Structure of a PEMFC.

It is the same for oxygen reduction: its role is to facilitate electronic exchanges (the slow step) and is specific to the reaction and the temperature level of the cell.

The electrolyte varies depending on the cell type: KOH for AFC ion batteries, exchange membrane for PEMFC and DMFC, phosphoric acid for PAFC, molten carbonates for MCFC and solid oxides for SOFC. It allows the ionic species (not electrons) to pass from the anode to the cathode. These electrolytes determine the operating temperature of the cell.

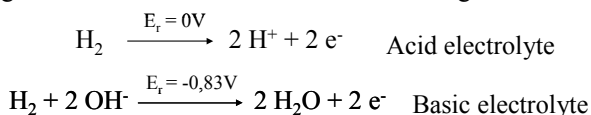
The bipolar plates (Cunningham et al. 2007) are joined to the anode and cathode materials. They have several roles: channelling gas from the outside, collecting the

current and managing the water flow. Usually in graphite, these plates must not only be current conductors, but also provide a homogeneous distribution of gas to the electrodes and participating in managing the water that has to be evacuated or supplied (for PEMFC). They must be resistant to environmental stresses cells (acidic or basic) and be impermeable to the reacting gases, as it may cause a chemical short-circuit.

To these critical components that make up the heart of the cell the accessories are then added that are needed for proper operation. These are tanks and pumps for fuel and water, the air compressor, the humidifier, the heat exchangers to cool the cell, the inverter for converting the DC output of the cell.

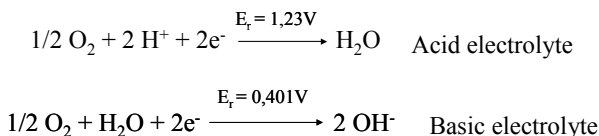
The Reactions

The fuel, usually hydrogen, sometimes methanol, is fed to the anode. The cathode is supplied with oxygen, or simply air, oxygen enriched or not. In a hydrogen-oxygen cell, the hydrogen oxidation occurs at the anode according to:

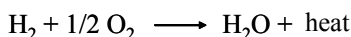


It is an easy and catalysed reaction. The hydrogen reacts by releasing two electrons circulating in the electric circuit connecting the anode to the cathode.

At the cathode, there is the difficult cathodic oxygen reduction (rate determining step) that is also catalysed:



The result is therefore:



This reaction is exothermic: at 25°C, the free enthalpy of the reaction is -237 or -229 kJ/mol, depending on whether the water formed is liquid or gaseous. This corresponds to a theoretical voltage of 1.23 and 1.18 V. Also this voltage depends on the temperature.

From the outset, Sir William Grove realized that the reaction occurs only when there is a triple contact point between the electrolyte, the reactants and the catalyst. Both redox reactions occur in the so-called “triple point” (Fig. 13) area. In this area are the electrolyte, through which the ionic species are moving, the electrodes, or more exactly the catalyst with an electron supply or removal and the gaseous reactant supply. This zone that can be seen as a two-dimensional space is essential for the proper functioning of the cell.

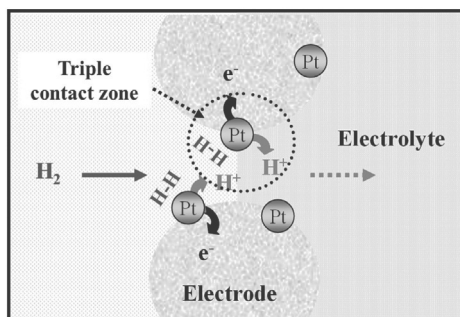


Figure 13. Schematic representation of the triple contact zone.

The Catalysts

One of the main obstacles to the achievement of fuel cells at an affordable cost is the price of the catalyst. The main blocking point is that on the cathode the oxygen molecule is reduced by protons and electrons to form water, which requires the relatively strong chemical bond between oxygen atoms to be broken and therefore requires a catalyst (especially as the temperature is low). Platinum and other precious metals are among the most effective catalysts for this operation. Much research is done to find other catalysts but so far no real breakthrough has been made. Thus, designing a cheaper catalyst is likely to contribute significantly to commercialising a technology based on alternative energy (Heo et al. 2008).

Oxygen Electroreduction

This is the most important reaction in the fuel cell. This reaction determines the rate in hydrogen/air fuel cells and this is where the most significant improvement opportunities reside.

In acid electrolytes the reaction takes place at high potential ($E_r = 1.229$ V) and most metals can be dissolved (Maillard et al. 2009), resulting in the use of noble metals. In basic electrolytes the potential is lower ($E_r = 0.401$ V) and more metals or non-metals can operate. Unfortunately, for “non-catalytic” reasons, the acidic medium is often preferred. For example, carbon-containing fuels produce CO_2 during the electro-oxidation and it reacts with bases to produce carbonates, which precipitate and decrease the performance of the cell. The presence of CO_2 in the air has the same effect when using H_2 . Today, most cells contain an acid electrolyte. Theoretically a potential difference of 1.229 V should be obtained (H_2/O_2), but in practice, we get 1.05 to 1.15 V. This is due to the fact that after the dissociation of O_2 it can produce hydrogen peroxide.

The most active catalysts for this reaction are platinum-based or platinum-based alloy. Precious metals are distributed onto carbon electrodes with a very high specific surface area (acetylene black). For basic electrolytes, silver can also be used for the good activity/cost compromise it represents. The influence of particle size on Pt activity is in the sense of an increase in dispersion of the catalyst. However, for Pt

particles < 1.4 nm—a drop in activity was noted. One of the major problems of Pt catalysts is particle sintering at high potential (Schmittinger and Vahidi 2008). On electronically conductive graphitic supports, platinum may be oxidized resulting in reduced activity, and in addition the support itself may also be oxidized (Maillard et al. 2009). Significant works are devoted to the search for stable systems. Results were obtained using Pt-V, Pt-Cr, Pt-Co-Ga, and Pt-Fe-Co alloys (Antolini 2003). Higher catalytic activities were obtained either by reducing the sintering or by modifying the electronic effects. In terms of performance, significant progress has also been obtained moving from Pt black (Pt divided mixed electrode material) to Pt supported on high surface area graphitic supports. For basic electrolyte cells (less studied), the choice of catalyst is more a compromise between the catalytic activity and the catalyst cost.

The most appealing supported homogeneous catalysts are based on metals (Fe, Co) chelated by macrocycles (Kiros et al. 1993). These molecules have structures similar to certain enzymes that are active in the decomposition of H_2O_2 . These structures favour interactions between O_2 and the metal. The stability of these systems, however, is still their weak point. Finally, the use of metal-free nitrogen doped carbon nanostructure as a stable catalyst for the oxygen electroreduction has been recently reported, opening an interesting perspective (Gong et al. 2009).

Hydrogen Electrooxidation

The 2 e-oxidation of hydrogen is less complex than the 4 e-reduction of O_2 , since the potential at the anode is constant. The catalysts are selected on the same basis, especially for their stability: for acidic environments Pt and its alloys are preferred and in basic media a wider choice is possible (Raney Ni). Pt is by far the most active in both environments. Hydrogen must be pure, otherwise CO (Igarashi et al. 1995) and CO_2 produce carbonates that precipitate in basic medium and damage the electrodes in acid medium. Pd/C* and Pt/C* systems, which are stable and present low loadings, are most often used. In basic medium non-noble metals may be preferred. If H_2 is obtained by reforming (presence of CO), much more CO tolerant Pt-Ru systems are preferred. The rate-determining step is dissociative adsorption followed by ionization. The development of catalysts with high specific surface areas and large dispersions is essential. For Pt/Ru systems, the strength of the binding of adsorbed CO decreases with the percentage of Ru. Sensitivity to CO decreases with temperature. Besides CO, sulphur can also be poisonous. Today, the option of feeding the cell with conventional fuels (gasoline, diesel) that could be converted into H_2 is studied. It will then be free from CO and sulphur compounds.

Methanol Electrooxidation

For transport, the fluid path is preferred for several reasons, including the infrastructure. Methanol does not turn easily in a fuel cell, but it is much more reactive than hydrocarbons. Other compounds such as ethanol, formaldehyde or formic acid may be envisaged. However, ethanol is not very reactive and the two others are toxic. As methanol can be directly oxidized (there is no need to turn it into H_2), the system is

attractive (Wasmus and Kuver 1999). Unfortunately, the performance is significantly below an H_2 fuel cell due to a much slower reaction rate. The opportunity to work in basic media (much faster rate) is excluded because of carbonate co-products from CO_2 . Until 1990, 3M H_2SO_4 was used at a working temperature of $60^\circ C$. With new electrolytes it is now possible to work at $100^\circ C$, and with Pt/Ru systems the activity could be multiplied by 10 (Antolini et al. 2008). However, the problem of catalytic activity still remains the crucial point.

Conclusion

The advantages of the fuel cell are numerous. In addition to reducing CO_2 emissions, necessary to control the greenhouse effect, the fuel cell contributes to improving the quality of life in the city, thanks to silent vehicles using an electric motor and the elimination of local polluting emissions (NO_x , particles ...). Cars with a fuel cell, fuelled by hydrogen stored on board, are potentially the only zero-emission vehicles. The problems associated with the production, storage and distribution of hydrogen remain. Currently, the interest in the industry and governments vary depending on the cell type and the technological advances made on their components. This interest is also highly dependent on specific applications for each type of cell. PEMFC that can be used in stationary, portable and mobile products can benefit from some synergy.

Use of Biomass as an Energetic Vector

Today, biomass constitutes globally 14% of the total energy consumed according to the International Energy Agency, although the percentages may fall 7–10% depending on the source (Fig. 14). Awareness has occurred over the last forty years, since the report of the Club of Rome in 1972, for using renewable resources as rationally as possible, instead of fossil-based raw materials.

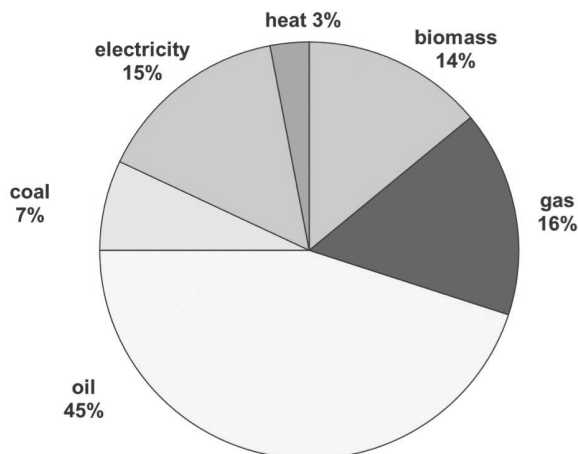


Figure 14. Raw materials for the worldwide energy consumption.

Longstanding developed chemicals were obtained or extracted from biomass, from pulp to biodegradable plastic or sophisticated molecules (Field et al. 2007). We will focus our attention on the most modern catalytic processes that attempt to encourage researchers to produce energy vectors such as hydrogen or CO/H₂.¹ Moreover, we find a concern in chemists from the early twentieth century that had been side-lined because of the performance obtained in petrochemicals. Today, catalytic processes based on hydrogen or synthesis gas are among the most strategic because they contribute to food, transport and the chemical industry (Fig. 15).

Figure 15 shows a steam reforming or partial oxidation of natural gas, light oil fractions, coal or biomass leading to synthesis gas (CO/H₂) or hydrogen. From there, the applications in the synthesis of large intermediates are classical including hydrogen for fuel cells. Even though the amount of carbon stored annually by plants is more than 5 times the 8 10⁹ T/year of carbon emitted into the atmosphere by burning fossil fuels, the proportion of arable land devoted to biomass for energy should not allow a substantial increase (Field et al. 2007).

Biomass in its broadest sense includes products from forests and crops, and waste. The main methods for producing fuels from these resources are in decreasing order of importance:

- The gasification leading to synthesis gas (CO/H₂)
- The liquification and pyrolysis leading to biofuels
- The hydrolysis followed by a fermentation of a reformer for the transesterification of triglycerides to the biodiesel.

Gasification of biomass is intended to produce a gas mixture containing predominantly CO/H₂ but also gives CO₂, CH₄, organic vapours, aromatic and poly-aromatics, water vapour, H₂S, traces of HCN, HCl and NH₃ and solid residues. Small

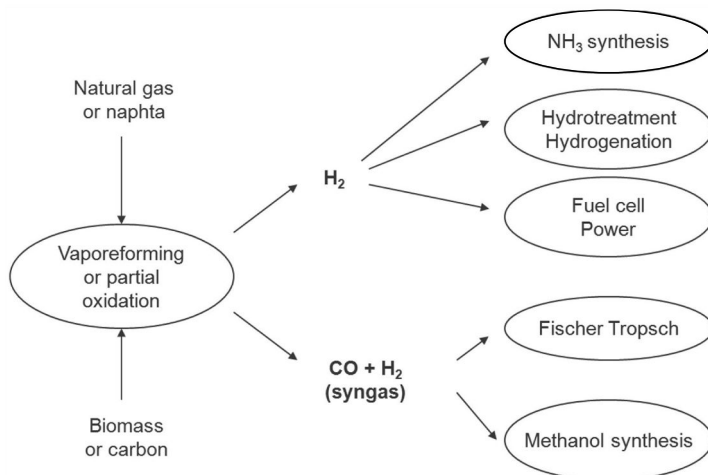
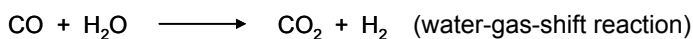
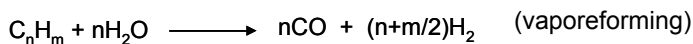


Figure 15. Hydrogen-based strategic catalytic reactions.

¹While maintaining a neutral CO₂ balance.

amounts of gaseous products incorporating alkali metal, alkaline earth metal or other elements such as Fe, Ti, Si, Al, or P are also present (Yung et al. 2009). The relative levels of these products also depend on the origin of the starting substrate. It needs to operate at a high temperature (500–900°C) in the presence of an oxidant (air, oxygen, water, optionally in the presence of CO) and a catalyst. The use of oxygen overcomes the presence of large amounts of nitrogen and gives the syngas a 2.5 times greater heat capacity than with air. The main catalytic reactions are:



The main criteria for selecting a catalyst is related to its low cost, ability to remove the tar, reform the methane, not lead to sintering, and to be resistant to attrition (Sutton et al. 2001).

The two main sources of catalyst deactivation are coking from hydrocarbons and native carbon generation, and sulfidation mainly due to H₂S. All contaminants also have a negative effect on the catalytic activity.

The performance of rhodium and platinum are both excellent for removing tars and for steam or dry reforming, but given their cost, nickel is preferred. It is deposited on a mesoporous alumina, and a promoter is often added (noble metal, transition metal, or alkali) to act on various parameters such as sintering, the conversion of tars, acceleration of a catalysis step, or the limitation of coking.

If the conventional steam reforming, used in existing facilities that start with methane, involves tubular reactors assembled in bundles containing deposited nickel, the biomass reforming reactors are more complex. The most commonly used are fixed bed reactors, but recent studies have shown that the use of fluidized bed reactors achieves higher conversions and a significant decrease in coking. In addition, the implementation of a reactor provided with a filter bed consisting of a cheap material such as dolomite and placed upstream of the fluidized bed will increase the lifetime of the nickel catalysts by decreasing the level of tar and impurities.

Moving to the development stage for these processes, it is still necessary to improve the ability of the catalyst charge to resist poisoning, coking and attrition. Nevertheless, it should be remembered that the cost per gigajoule produced from biomass (expressed for hydrogen produced) is still 3.5 times higher than that obtained from natural gas or coal. To avoid higher shipping charges of raw materials, small units would be preferable, and to improve efficiency of such small reactors, based on rhodium or platinum, highly active catalysts are currently being studied.

Environmental Catalysis

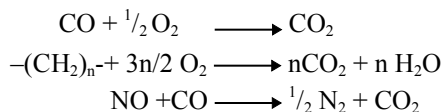
Since the 60s, the steady increase in the number of motor vehicles per year, which today reached 50 10⁶, has led to a huge number, close to 1 billion in 2009 when it had already reached 500 million in 1988. The vast majority of these vehicles are

based on the combustion of gasoline or diesel petroleum products and contributes to substantial environmental problems due to the emission of primary pollutants such as carbon monoxide, unburned hydrocarbons, nitrogen oxides but also the production of secondary pollutants such as ozone from photochemical reactions between volatile organic compounds and nitrogen oxides. These pollutants represent about 1% by volume of the exhaust gases leaving a petrol engine and their relative composition is as follows: 85% CO, 9.5% of NO_x, unburned hydrocarbons 5% and in addition emitted particles (Farrauto and Bartholomew 1997).

The oil contains sulphur and nitrogen impurities, which are today well eliminated in the refinery and provides a gasoline containing only traces of these heteroatoms. However, in the engine cylinder fed by the combustion, temperatures can reach 1,400°C so that nitrogen from the air results in the formation of nitrogen oxides by reaction with oxygen. In addition, CO and hydrocarbons arise from incomplete combustion.

To address the environmental issues and awareness that has occurred in recent decades, laws have gradually tightened and we have to remember the date 1970, the year in which the U.S. Congress passed the “Clean air Act Amendments”, imposing a program of emission control of motor vehicles. Europe adopted a similar attitude about 20 years later and the standards are much stricter. The State of California decided since the late 90s that releases should be zero CO, NO_x and unburned particles, ahead of the same technology.

From 1970, a catalytic system was invented that reduce by 90% the emissions of CO, NO_x and unburned in the presence of 10% water, 10 to 60 ppm of CO₂, other poisons such as zinc and phosphorus and at temperatures between 350 and 1000°C, at volume rates between 10⁴ and 10⁵ h⁻¹ for lifetimes of about 100,000 km. The reactions, generally referred as redox are:



The reality is more complex, since hydrogen can be generated by the water gas shift reaction ($\text{CO} + \text{H}_2\text{O} \rightarrow \text{CO}_2 + \text{H}_2$) and participates in the reduction of nitrogen oxides. Thus, between 1970 and 1973 more than 30 scientists examined the activity of 15,000 catalytic formulations, which helped to focus the catalytic system (tolerant to nitrogen oxides) on the platinum-palladium couple, which is used to reduce the emissions of hydrocarbons and CO by 90%.

The most commonly used definitions for exhaust gas are as follows: A/E: Ratio Air/Fuel: mass of air consumed by the motor relative to the fuel consumed by the engine.

λ = real A/E ratio divided by the stoichiometric A/E ratio.

In 1979, new standards for NO_x reduction led to the complete re-examination of the strategy. The first proposed solution was to couple two reactors in series, the first to reduce NO_x possibly leading to the co-production of NH₃; and the second after the

addition of air to convert hydrocarbons and CO to CO₂. However, a rich mixture is required in the engine compartment, which generates a lot of the unburned and CO, which results in excessive consumption.

The second solution, which has been adopted, is the 3-way catalyst. However, it requires work in a very narrow window for λ (Fig. 16) parameter that must be maintained close to 1.

It is also essential to properly adjust the engine intake and have a λ probe to analyse online oxygen. It is also understood that the carburettor was replaced by injection. It should be noted that the catalyst must be steady and this requires driving a distance of about 2 km in the urban cycle to then reach 90% conversion of pollutants. The catalytic converter comprises a support, an active phase, promoters and an external layer called a washcoat. The support should meet many constraints, such as: a high dispersion of the active phase, good mechanical strength, a low charge loss and a low thermal inertia. The solution adopted is to use a monolith. This is an oval section reactor of approximately 25 cm long, containing many small parallel channels, which is usually made of cordierite, a magnesium aluminosilicate. The use of metal monoliths, in addition to the higher costs, results in lower thermal resistance and the risk the washcoat detaching. The active phase is composed of a mixture of palladium, platinum and rhodium to ensure all redox reactions. As promoters nickel can be added to improve the activity of Pd or Pt in reducing NO_x, lanthanum to stabilize the dispersion of platinum and yet ceria CeO₂ to avoid sintering of the alumina porous surface, the formation of aluminate and also promote the water gas shift reaction. Finally, an essential component of the catalytic converter is the washcoat, consisting of a layer of alumina of high specific surface area for adequate dispersion of the active phase, which can increase in the developed surface of the support.

These three-way catalysts are very sensitive to the presence of poisons in the hydrocarbon so that their performance can very quickly be affected even annihilated. Lead in particular has a deleterious effect on precious metals forming inactive alloys and it is one of the reasons for its use as an anti-knock was prohibited. Phosphorus and zinc react with the washcoat at about 600°C by reducing its specific surface area, as well as sulphur resulting in the formation of SO₃, which is adsorbed onto the ceria. Beyond these poisonings, there are various deactivations related to sintering,

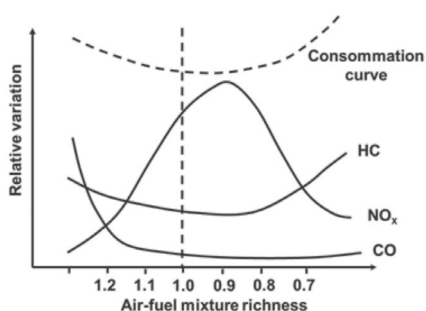


Figure 16. Lean mixture/rich mixture.

volatilization of metals to coking, attrition, thermal or mechanical shocks that cause cracking and delamination of the washcoat.

Nowadays to deal with more and more stringent laws, the effort is focused on reducing the previous initial period for optimal catalyst performance. Several solutions are being explored to improve cold starting. The first approach is to increase the temperature of the gas entering the catalytic converter either by bringing the catalyst closer of the engine, or by incorporating a pre-catalyst in the engine output. The second approach is to minimize the loss of heat from the gas outlet isolating the exhaust. A third approach is to rapidly increase the temperature of the catalyst either by electrical heating, or by installing a small upstream gas burner. All these explored measures require that the catalyst has excellent heat resistance.

Beyond these measures, legislation is moving towards an even stronger reduction of unburned hydrocarbons so that the possibility of installing a specific adsorbent is widely explored. When the catalyst is in a thermal regime, controlled desorption of hydrocarbon allows their conversion and therefore their disposal of the exhaust gases.

A different strategy is to develop lean-powered engines. Thus, the lower amount of hydrocarbons than the stoichiometry with respect to oxygen allows for lower fuel consumption and therefore lower CO₂ emissions. In contrast, if the three-way catalysts keep all their effectiveness for reducing CO and hydrocarbons, they do not have the capacity when medium rich in oxygen to convert nitrogen oxides. In this way, research for new catalytic systems is needed, and recently systems with cobalt, copper, iridium have been described.

In conclusion, it is important to note that, contrary to an industrial process where operating conditions are optimized and fixed, the choice was made by the manufacturers to produce very flexible converters. Indeed, it should take into account the size of the vehicle and therefore the engine, the driving style of the person, the local climate, etc.... Although the 3-way catalyst is already evolving to reflect new legislation, it is worth noting the superb work in developing an efficient catalytic reactor.

References

- Akutagawa, S. 1992. A practical synthesis of (–)-menthol with the Rh-BINAP catalyst. pp. 313–323. *In*: A.N. Collins, G.N. Shelldrake and J. Crosby (eds.). *Chirality in Industry, the Commercial Manufacture and Applications of Optically Active Compounds*. John Wiley & Sons, Chichester.
- Akutagawa, S. 1999a. Isomerization of carbon-carbon double bonds. pp. 813–830. *In*: E.N. Jacobsen, A. Pfaltz and H. Yamamoto (eds.). *Comprehensive Asymmetric Catalysis*. Springer-Verlag, Berlin.
- Akutagawa, S. 1999b. Asymmetric isomerization of olefins. pp. 1461–1469. *In*: E.N. Jacobsen, A. Pfaltz and H. Yamamoto (eds.). *Comprehensive Asymmetric Catalysis*. Springer-Verlag, Berlin.
- Antolini, E. 2003. Formation of carbon supported PtM alloys for low temperature fuel cells. *Mater. Chem. Phys.* 78: 563–573.
- Antolini, E., T. Lopes and E.R. Gonzalez. 2008. Effect of alloying degree in PtSn catalyst on the catalytic behaviour for ethanol electro-oxidation. *J. Alloys and Compounds* 461: 253–262.
- Cunningham, B.D., J. Huang and D.G. Baird. 2007. Review of materials and processing methods used in the production of bipolar plates for fuel cells. *Intern. Mater. Rev.* 52: 1–13.
- Erisman, J.W., M.A. Sutton, J. Galloway, Z. Klimont and W. Winiwarter. 2008. How a century of ammonia synthesis changed the world. *Nature Geoscience* 1: 636–639.

- Etzold, B., A. Jess and M. Nobis. 2009. Epimerisation of menthol stereoisomers: kinetic studies of the heterogeneously catalysed menthol production. *Catal. Today* 140: 30–36.
- Farrauto, R.J. and C.H. Bartholomew. 1997. *Fundamentals of Industrial Catalytic Processes*. Chapman and Hall, London.
- Field, C.B., J.E. Campbell and D.B. Labell. 2007. Biomass energy: the scale for the potential resource. *Trends Ecol. Evol.* 23: 65–72.
- Fleischer, J., K. Bauer and R. Hopp. 1972. Ger. Offen to Haarmann and Reimer GmbH, DE 2109456 A.
- Gatfield, I.-L., J.-M. Hilmer, U. Bornsheuer, R. Schmidt and S. Vorlová. European Patent to Haarmann and Reimer GmbH, EP 1223223 A1 (17 Jul. 2002, priority DE 10100913, 11 Jan. 2001).
- Gong, K., F. Du, Z. Xia, M. Durstock and L. Dai. 2009. Nitrogen-doped carbon nanotube arrays with high electrocatalytic activity for oxygen reduction. *Science* 323: 760–764.
- Haynes, A. 2006. Acetic acid synthesis by catalytic carbonylation of methanol. *Topics in Organomet. Chem.* 18: 179–205.
- Heo, P., H. Shibata, M. Nagao and T. Hibino. 2008. Pt-free intermediate-temperature fuel cells. *Solid State Ionics* 179: 1446–1449.
- Heydrich, G., G. Gralla, M. Rauls, J. Schmidt-Leithoff, K. Ebel, W. Krause, S. Oelenschläger, C. Jaekel, M. Friedrich, E.J. Bergner, N. Kashani-Shirazi and R. Paciello. 2009. World Patent to BASF SE WO2009068444 A2 (4 June 2009).
- Igarashi, H., T. Fujino and M. Watanabe. 1995. Humidity dependence of the oxidation of carbon monoxide adsorbed on Pt/C and PtRu/C electrocatalysts. *J. Electroanal. Chem.* 391: 119–123.
- Jacobsen, C.J.H. 2000. Novel class of ammonia synthesis catalysts. *Chem. Commun.* 1057–1058.
- Jäkel, C. and R. Paciello. 2010. The asymmetric hydrogenation of enones—access to a new L-menthol synthesis. pp. 187–205. *In*: H.-U. Blaser and H.-J. Federsel (eds.). *Asymmetric Catalysis on Industrial Scale*, 2nd Ed. Wiley–VCH, Weinheim.
- Jones, J. 2000. The Cativa® process for the manufacture of acetic acid. *Platinum Metals Rev.* 44: 94–105.
- Kiros, Y., O. Lindström and T. Kaimakis. 1993. Feasibility study of a mini fuel cell to detect interference from a cellular phone. *J. Power Sources* 45: 219–227.
- Maillard, F., P.A. Simonov and E.R. Savinova. 2009. Carbon materials as support for fuel cells electrocatalysts. pp. 429–480. *In*: P. Serp and J.L. Figueiredo (eds.). *Carbon Materials for Catalysis*. John Wiley & Sons, Hoboken (NJ).
- Noyori, R. 1994. *Asymmetric Catalysis in Organic Synthesis*. John Wiley, New York.
- Rafiqul, I., C. Weber, B. Lehmann and A. Voss. 2005. Energy efficiency improvements in ammonia production—perspectives and uncertainties. *Energy* 30: 2487–2504.
- Schlögl, R. 2003. Catalytic synthesis of ammonia—a never ending story? *Angew. Chem. Int. Ed.* 42: 2004–2008.
- Schmittinger, W. and A. Vahidi. 2008. Prevention of fuel cell starvation by model predictive control of pressure, excess ratio, and current. *J. Power Sources* 180: 1–14.
- Sutton, D., B. Kelleher and J. Rohross. 2001. Review of literature on catalysis for biomass gasification. *Fuel Process. Tech.* 73: 155–173.
- Szmigielski, D., H. Bielawa, M. Kurtz, O. Hinrichsen, M. Muhler, W. Rarog, S. Jodzis, Z. Kowalczyk, L. Znak and J. Zielinski. 2002. The kinetics of ammonia synthesis over ruthenium-based catalysts: the role of barium and caesium. *J. Catal.* 205: 205–212.
- Torrence, P. 2002. Synthesis of acetic acid and acetic acid anhydride from methanol. pp. 104–136. *In*: B. Cornils and W.A. Herrmann (eds.). *Applied Homogeneous Catalysis with Organometallic Compounds*. Wiley–VCH, Weinheim.
- Wasmus, S. and A. Kuver. 1999. Methanol oxidation and direct methanol fuel cells: a selective review. *J. Electroanal. Chem.* 461: 14–31.
- Weissermel, K. and H. Arpe. 1997. *Industrial Organic Chemistry*. Wiley, Weinheim.
- Yung, M.M., W.S. Jablonski and K.A. Magrini-Bair. 2009. Review of catalytic conditioning of biomass-derived syngas. *Energy and Fuels* 23: 1874–1887.

This book has been edited by Martine Poux, Patrick Cognet and Christophe Gourdon from the Laboratoire de Génie Chimique/ENSIACET, Toulouse. It presents an ensemble of methods and new chemical engineering routes that can be integrated in industrial processing for safer, more flexible, economical and ecological production processes in the context of green and sustainable engineering.

Different methods for improving process performance are dealt with, including:

- eco-design and process optimization by systemic approaches
- new technologies for intensification
- radical change of industrial processes via the use of new media and new routes for chemical synthesis.

These various methods are fully illustrated with examples and industrial cases, making this book application oriented.



6000 Broken Sound Parkway, NW
Suite 300, Boca Raton, FL 33487
711 Third Avenue
New York, NY 10017
2 Park Square, Milton Park
Abingdon, Oxon OX14 4RN, UK

K21572

